In The Name Of God

Cranfield University

College of Aeronautics

Department of Aerospace Technology

Ph.D. Thesis

Academic Year 1995/1996

Mohammad Ali (F) Vaziry-Zanjany

Aircraft Conceptual Design Modelling Incorporating Reliability and Maintainability Predictions

Supervisor : Professor John P. Fielding

March 1996

Abstract

A computer assisted conceptual aircraft design program has been developed (CACAD). It has an optimisation capability, with extensive break-down in maintenance costs. CACAD's aim is to optimise the size, and configurations of turbofan-powered transport aircraft.

A methodology was developed to enhance the reliability of current aircraft systems, and was applied to avionics systems. R&M models of thermal management were developed and linked with avionics failure rate and its maintenance cost prediction methods. The impact of the environmental control system, and engine-provided bleed flow was also modelled and incorporated into CACAD. The program showed the ARINC 600 & 408A flow rates to the avionics bay, and to the deck instruments may both profitably be increased by 50%. This keeps the direct operating cost (DOC) increase at bay for long-range passenger aircraft, and offers a reduction of up to 1% in DOC for the short to medium range passenger aircraft.

A methodology was developed to model all aspects of future high risk technologies, with special consideration given to reliability, maintainability, and development cost (R,M&D) predictions as applied to variable camber wings (VCW). Many aspects of VCW were modelled. These included different types of drag saving due to chord-wise, as well as span-wise camber variation. Models were also derived for mass, maintenance cost, and extra development cost increments for wing trailing edge devices, flight control, and hydraulic systems. On incorporation into CACAD, a reduction in DOC of up to 3.5% was predicted. The VCW technology were evaluated for DOC improvements, against a number of existing, future, and derivative aircraft, under different sensitivity conditions. R,M&D predictions were shown to be decisive in addressing the feasibility of a new technology.

The R&M predictions of the whole study shows that, long range, low to medium capacity derivative transport aircraft are most appropriate for the VCW technology,

and the short to medium range, low to medium capacity aircraft are most suitable for reliability enhancement projects of aircraft advanced systems.

Acknowledgement

The Author wishes to express his gratitude to I.R. of Iran Ministry of Culture, and Higher Education and Iran Aviation Industry Group, specially his excellency Dr. Torkan, Minister for Transport Industry for providing full financial support for this research program. I also wish to acknowledge College of Aeronautics, and Royal Aeronautical Society for providing extra fund needed to present some of this research work at the respective conferences, and journals.

I am deeply grateful to my supervisor Professor John P. Fielding for his continued support, invaluable advice, timely suggestions, appropriate directions, supply of information, and above all, his rich judgement of the trend of the progress in the aeronautical sciences.

Special thanks to Dr. R.I. Jones, Professor D. Howe in the department of aerospace technology for their advice, and supply of literature and information. I also wish to thank Dr. P. Pilidis for giving advice, and guidelines on engine bleeding, and letting the Author use the Turbomatch engine performance simulating program.

The Author wished to thank all members of the Department for their co-operation and specially my colleagues in conceptual design group, including Mr. R. Wilson for providing necessary debates on different issues relating to this research work.

The Author also wish to express his gratitude to Dr. Greff from Daimler-Benz Aerospace Airbus Germany, Mr. D.H. Jagger, Future Programs British Aerospace Airbus UK, Mr. Paul Simpkin from Rolls-Royce Commercial Aero Engines UK, and Mr. John Langley, Maintenance Cost Study, Airbus Industrie France, for their supply of information, comments, and guidance.

Finally I wish to thank my wife Maryam for her continuous moral support, and hard work at home, leaving me free to do my research work. She made my life at Cranfield a wonderful experience.

Preface

This thesis is submitted for the degree of Doctor of Philosophy at Cranfield University, UK. Some of the work described in this thesis has been presented at conferences, or is being refereed by Journals. The supporting papers are as follows :

1. Fielding, J.P. and Vaziry-Z.,M.A.F. "Avionics Reliability Enhancement Modelling for Aircraft Conceptual Design" AIAA 95-3906, 1st AIAA Aircraft Engineering, Technology, and Operation Congress, Los Angeles, September 1995.

2. Fielding, J.P. and Vaziry-Z., M.A.F. "Avionics Reliability Enhancement Modelling for Aircraft Conceptual Design" is submitted for publication in AIAA Journal of Aircraft.

3. Fielding, J.P. and Vaziry-Z., M.A.F. "Avionics Reliability Modelling for Ultra-high Capacity Aircraft" R&M Software Based Systems, Aerotech 95, I Mech E, Birmingham, October 1995.

4. Fielding, J.P. and Vaziry-Z., M.A.F. "Reliability Enhancement Modelling for Ultra-high Capacity Aircraft" is submitted for publication in Journal of Aerospace Engineering Part G of the Proceedings of the Institution of Mechanical Engineers.

5. Fielding, J.P. and Vaziry-Z.,M.A.F. " Reliability and Maintainability Implications of Variable Camber Wing" is accepted for publication in the Aeronautical Journal of Royal Aeronautical Society.

6. Vaziry-Z.,M.A.F. and Fielding, J.P. "Computer Aided Conceptual Aircraft Design (CACAD) For Transport Aircraft" College of Aeronautics Report Number 9608, Cranfield University, April 1996.

Notation

Due to extensive use of notations, abbreviation, and nomenclatures, they are presented in a form of Appendix A in the thesis. They are tabulated, and each term is defined, its unit is given, and if it is an input data, its value is also included.

List of Tables

List Of Figures

Table of Contents

CHAPTER 3

Reliability Enhancement Modelling Of Advanced Aircraft Systems Application : Avionics

CHAPTER 4

Reliability, Maintainability, and Development Cost Predictions of Future Technology

Application : Variable Camber Wing

1. Chapter 1

Introduction

1.1 General

Reliability, and maintainability have always been important subjects for consideration by aircraft designers, mostly at the detail design stage. The only consideration given by the conceptual designer was to avoid placing delicate components, such as avionics, too near to vibration and heat sources, such as the engines [1].

Reliability (R) means, few failures for long periods of aircraft operation. By quantification, reliability is the probability of a system or component that remains serviceable over a particular period of time. Unreliability of a system is the frequency at which it fails and requires corrective maintenance action [2]. It is the failure rate of a system. Maintainability (M) means simply the ease by which a defective aircraft can be repaired. Maintainability may be quantified as the number of maintenance man-hours (MH) required to fix a system every time it fails. Therefore R&M are bundled together and measured in MH per flight hour (FH).

It seems from the published literature, that aircraft conceptual design and R&M were linked in mid-seventies, when there was a need for maintenance cost justification for either Departments of defence or airlines as selecting criteria between manufacturers. This need led to the new requirement to assign quantified targets for R&M of each aircraft system at the preliminary design stage. Both requirements meant the establishment of R&M prediction methods for each aircraft system. The methods made use of correlation analysis to develop models which relate historical maintenance data to the design/performance parameters of aircraft. The first of such work was published by the Northrop Corporation in 1975 [3]. Later Maddalon

correlated such historical maintenance data, not with aircraft but with system design parameters [4]. The Vought corporation also developed reliability prediction models under contract with US Naval Air System Command in 1980 [5]. Cranfield University under the auspices of Fielding pursued a research campaign in this field at two levels of the conceptual, and the detail preliminary design. They were able to develop separate prediction equations for reliability and maintainability for different systems of fighter and transport aircraft based on the latest historical R&M data, using more advanced methodology in the late eighties [6,7]. In the detail preliminary design phase, both qualitative, and quantitative techniques were rigorously applied to novel aircraft design projects carried out every year. Qualitative methods such as fault tree analysis [8], failure mode and effects and criticality analysis (FMECA), zonal analysis [9] were used along with quantitative methods such as aircraft maintainability prediction via time synthesis [10]. Reliability block diagram analysis based on MIL-STD-756 was used in conjunction with the methodology proposed by Serghides [11], and maintainability prediction procedure was based on modified version of MIL-HDBK-472 (procedure 3). The details of above methods are elaborated in [7].

In brief the above work established a foundation for predicting base values for R&M of an aircraft being initially sized at the conceptual design phase. These base values were then analysed against the evolutionary trends and continuous reliability improvement of system equipment. Along with the end user's R&M requirement in view, a set of ambitious but realistic targets may be produced for the R&M of every aircraft system. These targets may then be pursued in the detail/preliminary design of each system using the above mentioned qualitative, and quantitative methods. If the targets are not met, the proposals are made to enhance the reliability of certain critical pieces of equipment, or to add to the redundancy of the system.

1.2 Back Ground To Present Research Work

Enhancing the reliability and maintainability of aircraft systems at the conceptual design phase is a highly desirable characteristic in the design of any modern aircraft. Predicting extra maintenance and development costs associated with future

technologies at the conceptual phase is essential and cost effective. Previous conceptual design techniques, allowed an aircraft be sized and optimised, and then later in preliminary phase, work was done towards :

- improving the system reliability, which may require further increase in the system mass, and or it may necessitate an increase in wing area or engine size

- reducing extra maintenance cost, or development cost, of a new technology which may jeopardise all the benefits of it.

This approach may be useful, but is often too late and too costly to implement, once the aircraft sizes are frozen, along with its budgeting.

Historically aircraft conceptual design methods were aimed toward fulfilling performance-dominated mission parameters with fuel, and or, take-off mass being the objective function, until the cost of maintenance and aircraft market price became so pronounced that the objective function changed to direct operating cost (DOC). Therefore the first idea behind the research work in this thesis was to integrate R&M modelling into the aircraft sizing process at the conceptual design phase, so that an aircraft may be sized with inherently higher reliability. The R&M of a new technology should be allowed to play their role as much as other major aerodynamic and mass aspects in the sizing process. At the end of the day the success of a high technology new aircraft configuration is shaped by its R&M effects. This idea was re-enforced by Sobeisky from NASA Langley Research Centre [12], who envisaged that conceptual design of transport aircraft will have to include not only the present modules of geometry, aerodynamics, propulsion, mass properties, economic analysis, and performance, but also new modules of thermodynamics, stability and control, reliability, maintainability, supportability, and structure.

1.3 Research Objectives and Thesis Outlines

To put the above idea into action, three major tasks were envisaged and this thesis is the report of the computational execution of these tasks.

Task 1 : The first task was to establish a moderately state-of-the-art computer assisted transport aircraft design synthesis with extensive maintenance cost

breakdown, covering all major aircraft systems, and major sections of structure. It embodies an explicit optimiser, which though simple, is adequately accurate in finding global minimum DOC. The program was written in simple FORTRAN 77 language, and is run with a conventional PC. A literature survey, program description, and its validation are given in Chapter 2, and detailed formulation, with tables of results are shown in Appendix B.

Task 2 : The second task was to devise a methodology that will give guidelines on system reliability enhancement modelling. This methodology was developed and applied to avionics systems, with long history of unreliability. The reliability improvement of which not only proves the applicability of the methodology, but on integration in aircraft sizing and optimisation process, may offer an aircraft with inherently higher avionics reliability. This will lead to higher aircraft dispatch reliability, and safety. Chapter 3 describes the literature survey for this task, chain of modelling, and the analysis and discussions of the results that were obtained. Appendix C presents the detailed formulation, and graphs, and tables of results.

Task 3: To accomplish the third task, a novel state-of-the-art air transport technology was studied. The variable camber wing (VCW) was chosen as suitable technology and was based on the latest design principles and experimental work pursued by MBB, and Cranfield in recent years. It was found that the latest advances in VCW technology have yet to be modelled into a conceptual design synthesis, let alone its R&M prediction modelling. Therefore efforts were devoted to model all aspects of VCW design including its R&M implications. Chapter 4 presents the historical development of VCW, and a literature survey, along with the descriptions of aerodynamic, mass, and R,M&D modelling, with analysis and discussions of results. Appendix D includes the detailed formulation, and graphs, and tables of results.

Chapter 5 presents a general analysis of the whole results of the above mentioned ideas along with shortcomings, and Chapter 6 presents some generalised conclusions, and proposals for further work.

Chapter 2

Computer Assisted Conceptual Aircraft Design (CACAD)

2.1 Introduction

For the implementation of R&M modelling in transport aircraft sizing and costing process, there was a requirement for a computer-aided design tool that not only sizes and optimises a jet transport aircraft but must be sufficiently comprehensive to accommodate detailed structural, systems, performance, and R&M design improvement modelling in its modular structure. Computer Assisted Conceptual Aircraft Design (CACAD) was thereby developed to provide the necessary tool for the R&M study. It designs and optimises a subsonic turbofan powered transport aircraft from 100 to 400 passenger capacity, for short to long range missions. Advancing the state-of-the-art of conceptual design may not have been the prime objective in the making of CACAD. It is a conventional design synthesis, by giving priority to simplicity of the design sequence. The majority of the design relationships used in CACAD are purposely taken from MVO [13,14], a computational design work developed by Royal Aeronautical Establishment RAE so that not to repeat their twenty five years of experience in aircraft conceptual design (published). However the program architecture, the design sequence, the algorithm of constraint solution, and the optimisation part of CACAD are the work of the Author.

2.2 Methodology in CACAD

The design departs from the traditional wing loading versus thrust to weight ratio optimisation, and sizing process. The latter method was found to be not suitable for R&M and future technology studies, and also is not adaptable for any type of current optimisation techniques. Beside the fact that it cannot easily optimise an aircraft when more than four independent variables (IV) are involved.

The chosen methodology involves a FORTRAN program that reads a general aircraft data file, and mission oriented data files. It then uses Roskam's class one design procedure [15] to arrive at a reasonably accurate take-off mass. It then sets the initial values for independent variables, and by doing so, it can go through the design relations with appropriately nested iterations and sizes the whole aircraft, covering mass, aerodynamics, and dimensions etc. The sized aircraft is then tested through constraints. The changes in wing area (wing loading), and engine thrust (thrust to weight ratio) take place to fulfil the constraint equations. The successful aircraft is then evaluated for DOC. The optimiser then applies appropriate changes to independent variables (IV) and the whole process is repeated for several successful aircraft, from which the lowest DOC produced aircraft shall be chosen for the output file.

2.3 Historical Development

Manual performance of the conceptual design, and initial aircraft sizing processes although being transparent, and flexible, does not offer the designer the speed by which he can relate sizing of various aircraft parameters, to geometry, performance, aerodynamic, and propulsion system. The iterative nature of the aircraft design process, and the large number of design disciplines involved, makes the process of defining, and sizing of aircraft a tedious task. Manual operation requires duplicating the calculations, and this must be repeated many times if for a particular aircraft, many configurations are to be evaluated. This led to methods of design and trade studies, performance evaluations, and sensitivity analysis which were restricted to a small number of options, that could be calculated by a finite number of people. As a

result countless numbers of hours of research were dedicated to developing parametric data bases that could be applied to new aircraft designs.

From the early Seventies, when computer use became more available, they were used to execute stand-alone programs of different departments of aeronautics. Computer power, and the numerical methods advanced, together with graphical capabilities. Computer systems became more user-friendly, and thus the design project quality improved considerably. Trade-off and sensitivity analyses, with more design parameters can be carried out quickly, with a more optimum design being achievable.

Accumulation of data from several transport aircraft designed, manufactured and operated from the mid-Fifties, led aeronautical engineers to develop reasonably accurate empirical equations for the prediction of geometry, performance, aerodynamics, propulsion, mass, and cost of aircraft. The methods have now been incorporated into computer systems.

Since the early Seventies, several computer assisted conceptual design systems were developed into a user-friendly software using the above developments. They are for public use, or for use in private companies. Most of them have been under continuous improvement. Of such codes, a few shall be briefly described below. A more detailed description is found in [16].

Salguero developed BIZJET to design and optimise aircraft suitable for business operations [17], and Jenkinson developed GATEP [18] to size a twin-engined propeller driven aircraft for commuter operation at Loughborough University. CASTOR is an improved version of GATEP. The Royal Aeronautical Establishment (presently Defence Research Agency) developed MVO [13] from the early Seventies, and since then a number of derivatives were developed for military purposes. The latest civil version by Collingbourne, designs and optimises passenger aircraft from 100 to 350 seats for short to long ranges [14].

Delft University of Technology offers ADAS [19,20] which is an extensive computer program system for aircraft design ranging from propeller driven to jet passenger of up to Boeing 747 size. CAPDA is another computer assisted aircraft design system developed by Berlin Technical University for experienced designers [21]. CPDS is a

very advanced system for complete design of subsonic and transonic commercial aircraft used in Boeing Commercial Aircraft [22].

Roskam developed AAA [23] in Kansas University, a software program that provides a powerful framework to support the iterative and non-unique process of aircraft preliminary design. AAA incorporates methods, statistical data bases, formulas, and even relevant illustrations and drawings from 8 volumes of "Aeroplane Design" [15]. It is commercially available for public purchase.

ACSYNT [24] is perhaps the most sophisticated and complete computerised design synthesis and includes several levels of structural analytical methods in addition to the usual aerodynamic, flight profile, etc. This has made the code able to perform a whole range of preliminary design process from configuration definition to preliminary structural analysis.

Together with advanced, and more capable optimisers, the present computer systems have profoundly enhanced the speed, and accuracy of conceptual design of aircraft. It is now possible to integrate some levels of the detail design stage as well as to add disciplines such as thermodynamics, structure, maintainability, reliability, and supportability.

2.4 Aircraft Design Relations

The design relations of CACAD synthesis are suitable for high-subsonic-speed transport aircraft in the preliminary stage of development, and it are integrated with an explicit optimiser. The relationships in the design synthesis are applicable to conventional transport aircraft with moderate sweep back on the wings, and wings of moderate to high aspect ratio. The engines are installed on the rear fuselage in two and/or on the wings in pairs or fours. The wing planform is assumed to be trapezoidal with constant span-wise thickness to chord ratio. The relationship between Mach number, thickness to chord ratio, sweep angle, and cruise initial C_L is taken from the work of Corning [25] for super critical airfoils.

The trimmed $C_{L\ max}$ is the work of Collingbourne [14] for high lift devices of conventional type. Most of the design relations are standard, and where a special method has been adapted they are justified appropriately. Appendix B presents the

design relations, their justifications and their sources. The cruise phase is divided into 5 sectors so that when a new technology such as variable camber wing (VCW) is integrated in CACAD, its impacts on sector-wise cruise fuel consumption become possible for modelling.

Fuselage is sized for the maximum number of passengers, while the payload is considered for the design number of passengers, and the mass of freight. The fuselage mass, and size is influenced by the amount of selected cabin differential pressure. It also caters for the effects of engines, mounted in its aft section, if that option has been chosen.

The furnishing mass include passenger and crew seats, galleys, toilets, floor and wall coverings, insulation, flight deck furnishing, catering, water systems, and miscellaneous cabin items. The method is suitable for short to medium capacity transport aircraft.

Wing flaps are sized for take-off or landing, whichever demands more. The gust load factor is based on the requirements of The Joint Airworthiness Requirements for an equivalent sharp-edged gust of 15.24 m/s at an altitude of 6090m for an aircraft mass at the end of the mission, during descent.

The wing mass allows for load relief from wing weight, the fuel content, and the weight of any wing mounted engine. It offers individual predictions for the skins, ribs, spars, engine support structure, undercarriage attachments, wing tips, and joints. The fuel tank volume allows the tank to be extended up to fuselage centre line.

Fin area is based on fuselage stability, as well as for the case of an outboard wing-mounted engine failure and includes spillage, as well as wind-milling drag.

Undercarriage mass is found as function of aircraft rate of descent. The masses of systems are found by a single relationship with options for relationships for each individual system.

Fuel mass for cruise is determined for an equivalent climb to cruise lost range along with stage length for constant speed, and height. There is a provision for diversion and hold. Diversion speed shall be decided for maximum range, with no compressibility drag.

The Mach critical drag is found with assumption that compressibility drag coefficient does not exceed 0.002.

Engines are sized through the constraints described in next section. Engine sfc at cruise, diversion, and hold together with engine mass/thrust ratio are supplied by the user from engine references most suitable for the class of aircraft under consideration [26]. Therefore there is no magic module in CACAD to determine engine sfc, thrust at different altitude, and Mach number.

2.5 General Layout of CACAD

CACAD is laid down in a FORTRAN 77 routine and all its terms are determined in such a sequence as to allow each computed known item help to determine the next item. Figure 2-1 shows a general flow diagram of CACAD. It shows the interaction between the main design synthesis module, constraints module, and optimisation routine. Figure 2-2 shows the generalised flow chart of the sequences of the operations within the main design synthesis module, along with all the iterations involved.

2.6 General Features of CACAD

This is an explicit optimisation of jet transport aircraft initial sizing with an extensive maintenance cost module, aimed at making it suitable for the incorporation of Reliability and Maintainability (R&M) models for further trade off investigations.

Most of the equations were from [13] and [14], and its predecessors [27to31], but many are taken from [15, 32to34,1,25]. At present it optimises to produce minimum Direct Operating Cost (DOC), and includes equality and inequality constraints. It incorporates conventional high lift devices, and includes updated relations to include advances in wing design and material selection from 1970 to 1993, with the provision of means to specify the degree of improvement in the technology of the wing design. Figure 2-3 shows the main elements of CACAD which are briefly described as follows:

The general data file contains more than 200 items of data ranging from geometry to performance, and coefficients of empirical equations, all updated to 1993 values .

Mission oriented data files consists of conventional items of aircraft mission data such as number of passengers, stage length, cruise speed and altitude, number of engines etc. They are so chosen to be able to produce aircraft resembling present flying jet transports.

Independent Variables are those aircraft parameters, the variation of which independently influence aircraft sizing process. They consist of wing gross area, total engine mass, aspect ratio, thickness to chord ratio, sweep at 1/4 chord, taper ratio, flap length span ratio, rear spar chord ratio, forward spar chord ratio, flap deflection at take off, and landing

Geometry consists fuselage outside diameter, length, pressurised cabin length, wing root chord, tip chord, mean aerodynamic chord, geometric mean chord, wing sweep angles, location of spars, flap sizes, location of under wing engines, ampennage areas, areas of all major surfaces, CG of aircraft, and other major components, fuel tank sizes. Control surface sizing such as aileron, elevator, and rudder are not included.

Structural mass estimation includes airframe mass consisting of fuselage, wing leading edge (LE), wing trailing edge (TE), flap, wing trailing edge aileron, wing box (ribs, cover, spars, engine fittings, landing gear fittings) horizontal tail plane, vertical fin, landing gears, furnishings.

System mass estimation includes avionics, electrical power, hydraulic, fuel, flight controls, and air-conditioning & pressurisation systems, along with anti-ice, oxygen, and fire extinguishing systems, etc.

Fuel mass estimation includes cruise, diversion, hold, allowances for taxi, initial climb , landing, and contingency fuel. The above masses together with payload, and crew mass make up the Take Off Mass . Almost all mass relations are painstakingly made functions of independent variables.

The aerodynamics consists of a series of relationships for untrimmed and trimmed C_{Lmax} at approach and take-off, being the function of almost all independent variables. Wherever appropriate, operating lift coefficient for cruise, diversion , hold, approach and take off are also included. Drag coefficient estimation includes all flight

conditions ,covering compressibility in cruise, along with single engine failure spillage and wind milling drag etc.

Performances include speed, and Mach number corresponding to cruise, diversion, single engine flight, approach, take-off, critical gust, maximum controllable, maximum operational, vertical descent, and stall.

The equality & inequality design constraints include standard constraints such as approach speed limit, take off distance limit, climb out gradient with one engine inoperative, engine failed height requirement, cruise thrust height requirement, throttle limit at approach (miss approach), fuel tank volume limitation, aspect ratio sweep limit, body angle limit, and buffet boundary limit.

The objective function was chosen to be DOC which is an acceptable engineering criterion for industry, as well as airlines. Its module was developed further to demonstrate the benefits and penalties of reliability and maintainability enhancement models of any conventional system or systems resulting from application of new technology. It considers performance, structures, and systems together with R&M implications when operated in the aircraft design synthesis. It covers standing costs of the aircraft, influenced by aircraft price, spares, maintenance material and labour, all broken down into engine and airframe major and minor sections [6,7]. It also includes cost of fuel, flight deck crew, landing fee, interest, insurance, etc.

Optimisation routine is of the explicit type and iterates through the independent variables (except wing area and engine mass) to search for a successful aircraft and its DOC value. It then compares the DOC of the successful aircraft and finds the minimum DOC aircraft. It has all possible features for rejecting independent variable values that do not conform to present design practices. The particulars of the optimum aircraft are later saved in an output file.

2.7 Maintenance Breakdown Module

Most references in aircraft cost analysis [35to37,4,15] offer correlation equations that determines maintenance cost for airframe, engine, and perhaps avionics. They do not go further than that. It is imperative to know how much each individual system maintenance, and spare parts cost are influenced when a new technology is installed

in an aircraft, and or an existing aircraft system reliability is enhanced,. How much development cost affect the price of aircraft. Therefore to account for the above requirements, two approaches were adopted to sub-divide maintenance cost into labour, and material, as well as spare parts holding, in CACAD.

In the first approach, Serghides equations [7] were used to predict the share of maintenance labour cost of each airframe system. The price of an individual system from [14] was used to predict the cost of maintenance material of each airframe system. For further break down of structural maintenance labour, MIL-HDBK-472 [93] was used to rank each major section of structure, such as wing box, wing LE, wing TE flap etc., so that the cost of maintenance labour contributed by each section be estimated.

In the second approach Cranfield work [38] was used to break-down airframe maintenance labour and material cost. For a more detailed break-down of structural maintenance material, and labour down to their main constituents, a new set of criteria was developed. Surface area, price, and a set of internal, and external factors were used for this purpose. The detailed description of each approach, together with the formulation involved are included in Appendix B section B4.

2.8 Constraints Module & Optimisation

In this section constraints considered in CACAD and the solution methods using constraints are described. The explicit optimisation developed for CACAD is also briefly presented.

2.8.1 Constraint module

CACAD sizes gross wing area, and engine mass (combination of thrust mass ratio, and engine thrust) through constraint equations. All detailed relations associated with following constraints are described in section B3 of Appendix B.

1. Approach conditions

The first constraint is the approach condition in which stall speed should not exceed approach speed divided by 1.3. The stall speed is found from the C_{Lmax} approach module, and highest landing mass from the take-off mass

module. Approach speed is specified by the user in the mission data file. A constraint module algorithm was developed to vary the wing area to bring this equality constraint to zero. The way it is programmed is given in the CACAD listing, Appendix E.

2. Take-off run requirement

A maximum take-off distance is specified in the input data and an inequality constraint ensures that engine thrust is sufficient to accelerate the aircraft to its take-off speed within this distance.

3. Climb-out gradient with one engine cut

The amount of gradient required for such an event is laid by the Airworthiness authorities. This is different for two, three, and four engine aircraft. The inequality constraint ensures that there is enough thrust to climb the aircraft for the prescribed gradient, as well as taking care of windmilling, and spillage drag of the failed engine.

4. Cruise thrust requirement

Thrust requirement for Cruise is a constraint that ensures there is sufficient thrust at the start of cruise and to still maintain a given climb gradient.

5. Engine-failed height requirement

This constraint ensures that there shall be sufficient thrust for the case when one engine becomes in-operative, and the aircraft remains above a certain height with a certain climb gradient potential.

6. A missed-approach

This constraint ensures that when an aircraft is approaching and the landing decision is reversed, the aircraft is able to climb out with one engine inoperative.

CACAD evaluates the engine thrust required for all the above constraints. It then changes the initially chosen engine thrust to the highest among the above constraints. This will then automatically fulfil all the rest inequality constraints related to engine thrust.

7. Fuel Volume Limitation

Fuel volume is found from an empirical relationship. This is then compared with mission fuel load found for the aircraft whose wing area and engine thrust has already been sized with earlier constraints. If there is shortages of fuel tank capacity, then CACAD increases the fuel tank by extending it toward fuselage centre line. When this is done and still there is shortage of fuel tank volume, CACAD abandons any more effort and stops and prints an alarm.

8. Aspect Ratio / sweep requirement

This constraint is for stability and control considerations. The constraint prescribes a limit that restricts the optimum solution to an aspect ratio/sweep range applicable to existing transport aircraft. CACAD ensures that an aircraft whose wing area, and engine thrust is sized for the above constraints is rejected, if it violates this requirement.

9. Buffet Limitation

Reference [39] is used to evaluate the buffet C_L capability of a supercritical wing. Then the highest C_L produced by CACAD at the initial cruise condition must be 1.3 times less than the buffet limit already computed. CACAD shall reject the aircraft if it exceeds this value and print an alarm.

2.8.2 Explicit Optimisation

There are a variety of methods to optimise a non-linear objective function such as DOC, and at the same time fulfilling a set of non-linear equality, and inequality constraints. Numerical optimisation can be a powerful tool for the design engineer. If applied properly, vast savings in time and analysis effort can be realised. However modules being integrated for design are increasing both in size, and complexity. Unfortunately, there is no perfect optimisation algorithm, and users are encouraged to try more than one method in comparative fashion [40]. Pant [41] has spent a great deal of time trying to prove that gradient-based techniques are not suitable for conceptual design optimisation. He had to investigate a number of the latest state-of-

the-art optimisation stochastic techniques, such as simulated annealing, Monte-carlo method, and generic algorithms. The question of which optimisation method would yields the right answer, let alone which ones are hard to use, or should not be used, is still the subject of active research amongst mathematicians. Those mathematicians who propose optimisation methods tailored to help aircraft designers but lack adequate aircraft design analysis, and those designers who have embarked upon research in mathematics of optimisation without a rich mathematical background, both group may develop methods being always open to challenge. Perhaps an independent research effort devoted solely to optimisation of conventional transport aircraft design synthesis by a joint group of mathematician, and aircraft designers working shoulder to shoulder may yield successful results, publishable eventually in standard text books.

An enthusiastic aircraft design researcher who wishes to remain in the field, and develop a conceptual design tool for transport aircraft for the investigation of R&M modelling must have a realistic view of optimisation. Bypassing optimisation is not possible, nor spending a great deal of time and drifting away from research objectives and falling into the traps of different optimisation techniques is a solution. For this purpose an explicit optimisation technique known to mathematicians as the Global Search (Brute Force) [40] method was developed, that solves the constraints, and optimises the DOC. This may sound very primitive, but due to knwledge base constraint solver algorithm, it works very quickly, perhaps faster than conventional optimisers. The procedure with its definitive path leads to a global minimum. The accuracy of the method is high enough that may be used for validation, and calibration of available optimisation techniques for design synthesises that contain not more than 10 independent variables.

2.8.2.1 *Optimisation Procedure*

The module works in conjunction with the constraint solver. The independent variables are given a set of ranges that are reasonable. Through a set of do loops, they are initiated from their extreme values. Wing area, and thrust although part of independent variables, stay out of do loops. They are initialised through a class-one design module so that they acquire a value close to the final value.

1. The constraints are solved by varying the wing area for constraint 1, and the engine thrust for constraints 2 to 6. A knowledge based algorithm will decide which way the wing area and thrust may be changed. If other constraints are met, a successful aircraft is produced for which a DOC module is operated, and its value is computed.

2. The do loops assign a new set of independent variables that are the same as the previous values, except for one of them with a step higher than its previous value. The wing area, and thrust of the previous aircraft is retained as initial value. This makes the design of the new aircraft with lowest number of iterations, hence taking very little time. The wing area, and thrust needs little variation to fulfil the constraint and another successful aircraft is produced whose DOC is compared with previous one. If found smaller, then the particulars of this aircraft are stored temporarily for the comparison with the next successful aircraft.

3. The process of do loops continues, but because their variation is close to the previous setting, the design cycle become faster every time faster, with fewer iterations.

The above procedure leaves no possibility of IVs unexamined, therefore it sweeps through all the possibilities, and the final minimum DOC is bound to be global. By working through this procedure a few times, and tuning the steps of do loops, the areas of local minimum are also detected for any further analysis.

2.8.2.2 *Advantages & Disadvantages*

This method is simple, easy to work with, and fast enough for up to 10 variables. Its accuracy is simply varied by the steps of do loops. It is most suitable for those who know the detail of their design sequence.

The prime advantage of this explicit optimisation method for conceptual design of aircraft is its ability to yield virtually no residual value in constraint equations. This is a significant benefit if there is a requirement of a feasibility study for modelling integration that have few kilograms of mass, and few counts of drag, and few Pounds of cost implications. Using conventional optimisation, if successfully implemented, due to their inevitable residual values, such small changes in aircraft parameters are

not reflected in the final design, but in most cases an opposite effect is detected. For example increasing the mass of a certain system by a few kilograms, must yield a slightly heavier and costlier aircraft. But an aircraft is designed with a few kilograms lower mass.

The disadvantage with this method is the way it varies the wing area, and thrust to solve the constraint equations. It requires considerable skill in the knowledge of aircraft design, and the class of aircraft under consideration. It can work with up to 20 variables, but is fast if the number of variables are less than 10. On the other hand, it allows a quick sensitivity study on the role of each variable over the objective function. It helps the designer to exclude some IVs or reduce the range, or to reduce the step size of those IVs which are important factors for the objective function.

2.9 Validation and Discussion of Results

A variety of modern and advanced transport aircraft designed by European (Airbus), and American (Boeing) are flying today which are obvious choices for the validation of a developed conceptual design synthesis. CACAD was allowed to run for missions as close as possible to those of the following aircraft :

I) Airbus family of A330, and A340 were chosen as the latest state-of-the-art in transport aircraft. CACAD also simulated Airbus A310, and A300-600, to cover the medium range, and medium capacity class.

II) For the short range, low capacity operation, the Fokker F100 was chosen as an aircraft with rear fuselage mounted engines.

III) Among the Boeing products, the B767 family of -200A, and -300Q aircraft was chosen not only for validation of CACAD, but for further study of VCW benefit for derivative aircraft, elaborated in Chapter 4. Another Boeing product the B757-200A was considered the least underivative aircraft amongst Boeing products for CACAD validation.

IV) CACAD capability for futuristic projects was tested for UHCA, mainly to be further utilised in Chapter 3 for ASRE program. Tables of the results are presented in Appendix B.

2.9.1 A330 & A340 Analysis and Validation of the Results

These two aircraft have identical common wings, but with 45000 kg difference in take-off mass. The latter four engined aircraft flies 5500 km longer against the former twin. CACAD is a conventional code that designs and optimises a single aircraft with definite parameters such as wing gross area against a set of mission input data. It can not run with multi-mission data simultaneously and produces a set of optimum aircraft having an optimum common wing area. Therefore when trying to design aircraft resembling any of the above aircraft, CACAD must produce two aircraft with two different wings. The one that resembles A330 may have a lower wing area than the actual A330, and the other one may have higher wing area than A340.

The CACAD-designed A330 must be lighter in take-off mass, zero fuel mass, and empty mass than actual A330, which is an oversized wing area member of the family. An oversized wing member of any modern transport aircraft is always heavier than a similar mission aircraft with an optimum wing. The opposite is true for CACAD-designed A340. The following table show this in brief, and Tables B-4, and B-5 in Appendix B show in detail.

	CACAD	*A330*	*%diff*	*CACAD*	*A340*	*%diff*
Wing Area m²	342.1	363.4	+5.5	378.4	363.4	- 4.1
Take-off Mass, kg	204768.5	212000	+3.4	254164.36	244000	- 4.2

The above table not only shows the strength of CACAD designed aircraft against the latest European state of the art to within 5%, but demonstrates a justifiable differences within the context of derivative aircraft.

2.9.2 B767-200A & B767-300Q Analysis and Validation of Results

These two extreme members of the Boeing B767 family of aircraft were simulated through CACAD, primarily for reasons elaborated in Chapter 4, section for derivative aircraft, but presented here for verification of the results.

The Boeing B767-300Q is the longest range (extra 5500 km to 767-200A), stretched version of the family with extra 45 ton in take-off mass. Both aircraft have identical wings. The -300Q is the under-sized wing, and -200A is the over-sized wing. The latter must have take-off , zero fuel, empty mass higher than a similar mission aircraft

with an optimum wing. The case is vice-versa for the former aircraft. This phenomena is clearly seen in the following brief table when CACAD designed two aircraft for the two missions. The detail results are included in Table B-6 & B-7 in Appendix B.

	CACAD	B767-200	%d	CACAD	B767-300	%d
Wing Area m²	248.652	263.3	5.5	283.3	263.3	7.4
Take-off Mass	127180.8	136078	6	169971.84	181437	6.4

The above table not only show the strength of CACAD-designed aircraft against the two modern American transport aircraft to within 6%, but demonstrates a justifiable differences within the context of derivative aircraft.

2.9.3 A300-600 Analysis and Validation of Results

CACAD designed this class of aircraft with an error of less than 5% of Airbus A300-600. A class that was not originally assumed to have been designed for derivatives. Although the resemblance of these two aircraft may help the validation of CACAD, the differences deserve a brief analysis.

CACAD's empty mass, and zero fuel mass (airframe, and engine) are heavier than the A300. This may be due to the system, structure etc. mass estimation relationships within CACAD that might be over-estimating. But why then is CACAD's take-off mass lower or nearly equal to A300. This is due to the fact that CACAD's aspect ratio is around 9.8 as compared to the A300's very low 7.7. This reduces fuel consumption so much that when mission fuel is added to the zero fuel mass, it results in a nearly equal take-off mass with the snow-ball effects of both side balancing. Then what is the justification of CACAD's higher wing area? In CACAD, the driver behind the wing area sizing is either approach speed, which is the same for both aircraft, or C_{Lmax} at approach. The latter is a complicated module that is composed of a number of empirical relationships as functions of flap sizes, flap angle of deflection, wing TC, TR, AR, $\Lambda_{1/4}$. Therefore there is no guarantee that CACAD's flap configuration, and efficiency should be close to that of A300. The problem becomes more complicated when the cost consideration of manufacturing the flap aspects of DOC gets into the optimisation cycle, and perhaps an inferior CACAD flap results in higher wing area,

but with lower overall cost impact. The detail results are included in Table B-8 in Appendix B.

2.9.4 B757-200A Analysis and Validation of Results

B757 is a typical modern Boeing product that the Author believes to have been designed and optimised very close to the -200 version. The CACAD-designed aircraft, differs in certain parameters more than 5% with B757, but the following justification may prove the validity of CACAD.

CACAD fuselage length is 11% longer than that of B757. Investigation showed that the minimum seat pitch for the high density arrangement in CACAD is 13% longer than the value that would equalise the two aircraft's fuselage lengths. This led to the CACAD-designed aircraft having a higher fuselage mass, but due to a lower wing area the overall empty mass rose only 2.6%, which is within the acceptable limit. This is seen in zero fuel mass, and maximum landing mass being higher than B757 only within 1 or 2%.

The CACAD designed-aircraft has a much higher aspect ratio around 10 than B757's 7.82. This again, like previous section, led to large drag reduction causing the engines to become smaller, with 15% lower thrust and lower fuel consumption. Consequently, the CACAD-designed aircraft has higher zero fuel mass but lower take-off mass of 4.8% (still within a reasonable limit).

CACAD's wing area is lower than that of B757 by 9%. This is due to the fact that the C_{Lmax} module within CACAD may not produce a value that must match with every type of high lift devices designed by Airbus, or Boeing for their individual aircraft. In this case B757-200's C_{Lmax} is 2.5, and that of CACAD is 2.85. The following table shows [42] the disparity of C_{Lmax} at landing for different transport aircraft.

Model	*Airbus A320*	*RJ70*	*Boeing B737-300*	*Boeing B757-200*	*McDonnell MD81*
C_{Lmax}	2.8	3.5	3.3	2.5	3.0

The detail results are included in Table B-9 in Appendix B.

2.9.5 Fokker 100 Analysis and Validation of Results

Fokker 100 according to [43] has a redesigned transonic wing with substantial improved aerodynamic efficiency, especially at high speed. This aircraft has also the lowest empty weight per seat in its class, with extensively modernised systems, and considerable use of composite material.

CACAD's designed aircraft is within 5% of that of F100. Indeed CACAD capability in designing an aft fuselage mounted engine type aircraft is validated with adequate trust. There were modifications to some formulations to enable such a match. The fuselage mass estimate relation within CACAD allows for variation in the material used in fuselage construction. Due to extensive use of composite material, 25% reduction in J_{fus} (specific mass of fuselage), 10% reduction in mass of the wing, systems, and furnishing were applied to appropriate design relations. Presence of short leg undercarriage due to absence of engines underneath wings justifies a 10% reduction in landing gear mass applied to CACAD related relation.

The only significant difference in the CACAD-designed aircraft with that F100 is the sweep angle. Apparently the F100 wing section is 10 to 15% thinner than that of CACAD, this allows the F100 wing to have lower sweep angle of 17 against CACAD's 23. The optimiser part of CACAD must have found thicker, but more swept wing results in lower DOC than vice-versa. The thicker wing results in lighter wing, hence a great deal of cost saving in making the wing. In CACAD the highest cost density amongst structural members belongs to wings. The higher sweep lowers C_{Lmax} value to be reduced hence increases the wing area, but not to the extent that higher thickness to chord ratio reduces the wing mass. It must be noted that the F-100 was developed from the Fokker 28, and was constrained by earlier aircraft wing sweep. The detail results are included in Table B-10 in Appendix B.

2.9.6 A310-200 Analysis and Validation of Results

This was one of the early designs of Airbus Industries, and was an aircraft that CACAD has great difficulty in modelling. Although previous aircraft results proved that CACAD has a slightly over-estimate airframe mass relations, the A310 looks over-weight for CACAD. The aircraft designed by CACAD has 7.8% zero fuel mass, 8% empty mass, 10% maximum landing mass, lower than that of A310. Due to its

heavy airframe mass difference, and increased aspect ratio of the CACAD-designed aircraft's drag is much lower, making fuel consumption lower, hence take-off mass, is lighter by 10%, and engine thrust is lower by 30%. On the other hand, although C_{Lmax} for approach in the CACAD-designed aircraft has a reasonable value of 2.75, for the same approach speed, and with 10% lower landing mass, CACAD's area is astonishingly 3.1% higher than A310. Therefore the differences between A310-200 and CACAD is not justifiable. Although CACAD has its own weaknesses, the differences were wide enough to justify further investigation into the quality of Airbus A310 design. This aircraft seems to have an unusually high take-off mass, with an unusually low wing area i.e. very high wing loading. The following table show this phenomena with respect to other nearest aircraft.

Items of comparison	*A310-200*	*B757-200*	*MD81*
Empty mass kg/seat	367	307.4	227.9
Wing Loading kg/m²	648	563	552

According to Avmark quarterly report [44] Delta airline's operating cost of its fleet of A310 is so high to have decided to retire them at early age. The same reference compared A310 DOC per mile per seat to other aircraft.

Figure 2-4 shows the DOC value of A310-200 per mile per seat. It is 5 times higher than the highest-value aircraft. These indications are convincing enough not to judge CACAD lack of conformance with this particular aircraft as a shortcoming. The detail results are included in Table B-11 in Appendix B.

2.9.7 UHCA Analysis and Validation of Results

There are few data available for this futuristic aircraft in standard references such as [43], but some published articles in Aviation magazines such as [49], contain limited data. They were used to make the following comparison table.

Aircraft Item	*Boeing*	*Airbus*	*RMCS[157]*	*Cranfield A4*	*CACAD*
T/O Mass in ton	above 455	above 515	544	506.5	577
Empty Mass in ton	?	260	225	244	288
Fuselage Length m	79.2	76.2	77	69	77.23
Fuselage Diameter m	?	8.53/6.77	8.4	7.76/6.56	8.4
Span	79.2	77.1	85	75.15	80.32
Aspect Ratio	?	?	9.4	8.4	8.6

Although CACAD must be improved significantly in order to design and optimise an UHCA, but the configuration and mass values are reasonable enough to be used for ASRE in Chapter 3. The detailed results are included in Table B-12 in Appendix B.

2.9.8 DOC Values, Aircraft Pricing Analysis, and Validation

The actual references available are mostly figures related to aircraft operated by US Airlines. Avmark DOC values are mostly 55 to 63% lower than the CACAD predictions. The following table shows this in brief.

DOC	*F100*	*B757-200*	*A310-200*	*B767-200A*	*B767-300Q*	*A300-600*	*A330-300*	*A340-200*	*UHC A*
£/Hr	2012	2964	3345	3509	3674	4191	4651	5040	10478
$/Hr	3018	4446	5017	5263	5511	6286	6976	7560	15717
Avmark	1679	2415	15260	2975	3415	3942	-	-	-
%Diff.	55	54	!	56.5	61	62			

The following reasons may help to explain these differences. Firstly the aviation fuel price in America is nearly 50% lower than in Europe. The standing charge part of DOC in Avmark is based on average aircraft market prices than actual brand new price considered in CACAD. The aircraft in the Avmark report are not operated over their full stage lengths. The DOC methodology in CACAD is based wholly on the MVO [14]. This methodology was the subject of investigation and comparison with AEA [35] methodology by Rosa [46]. The result of this work shows that these methodologies produce approximately equal results.

Therefore DOC values found for aircraft designed and optimised by CACAD though conservative, but may be treated with adequate trust with a suitable factor. It is important to note that CACAD application in ASRE modelling feasibility investigation, and VCW technology implications of Chapter 3, and 4, does not require an exact matching of DOC with actual airlines in Europe, and America. It is the relative values of DOC of aircraft designed by CACAD with and without such models that count most.

The aircraft pricing module in CACAD predicts a value of $129 million US for the Airbus A340-200. According to [47] Airbus is pressing hard to sell this aircraft to Air India for $125 million US in a contest with Boeing B777. Avmark [48] prices this

aircraft for $107 million US. On the other hand, Avmark puts a value of $125 million US for the B777-200. Boeing is selling this aircraft with concession to Air India for $100 million. Therefore the topic of aircraft pricing has two categories which should not be confused with each other, but must be seen together.

One is the aircraft cost, which is driven by the size, technology and the number of aircraft produced. This cost is the sum of the research, development, test and evaluation cost, and production cost divided by the number of planned production aircraft. The second is the airplane market price which is driven by the aircraft cost and number of international and national issues, competition and emergence of new projects in the market. With the above considerations it is concluded that CACAD pricing is reasonably correct against market price of successful aircraft such as Airbus A330, and A340, slightly higher than less successful one such as F100, and strongly overestimates prices of less popular aircraft such as the A310.

2.10 Shortcomings of CACAD

CACAD program is listed in Appendix E (in a separate booklet), and is retrievable by Microsoft Word for Window Version 6.0. The program can be compiled, and run in any standard FORTRAN 77 software, installed in a conventional PC network, and also VAX and SUN Work Stations. Program has not yet been made into sub-routines. There are areas that require improvement to reduce number of iterations while optimisation process takes place. It lacks a graphical output capability to show general configuration of designed-aircraft.

2.11 Conclusions

1. CACAD was shown to be reasonably capable of designing, and optimising a transport aircraft ranging from 100 to 400 passenger from 2500 to 14000 km, and for aircraft either having their engines under the wings or mounted at rear of fuselage.

2. The optimiser module is accurate enough to be recommended for testing and calibrating other optimisation modules developed for aircraft design, with independent variable not exceeding 20.

3. CACAD is capable of accommodating new technologies that have aerodynamic, propulsion, mass, development cost, and maintainability implications.

4. The maintenance cost module of CACAD is detailed to the extent that R&M and development cost implications modelling of a new technologies can be integrated to it.

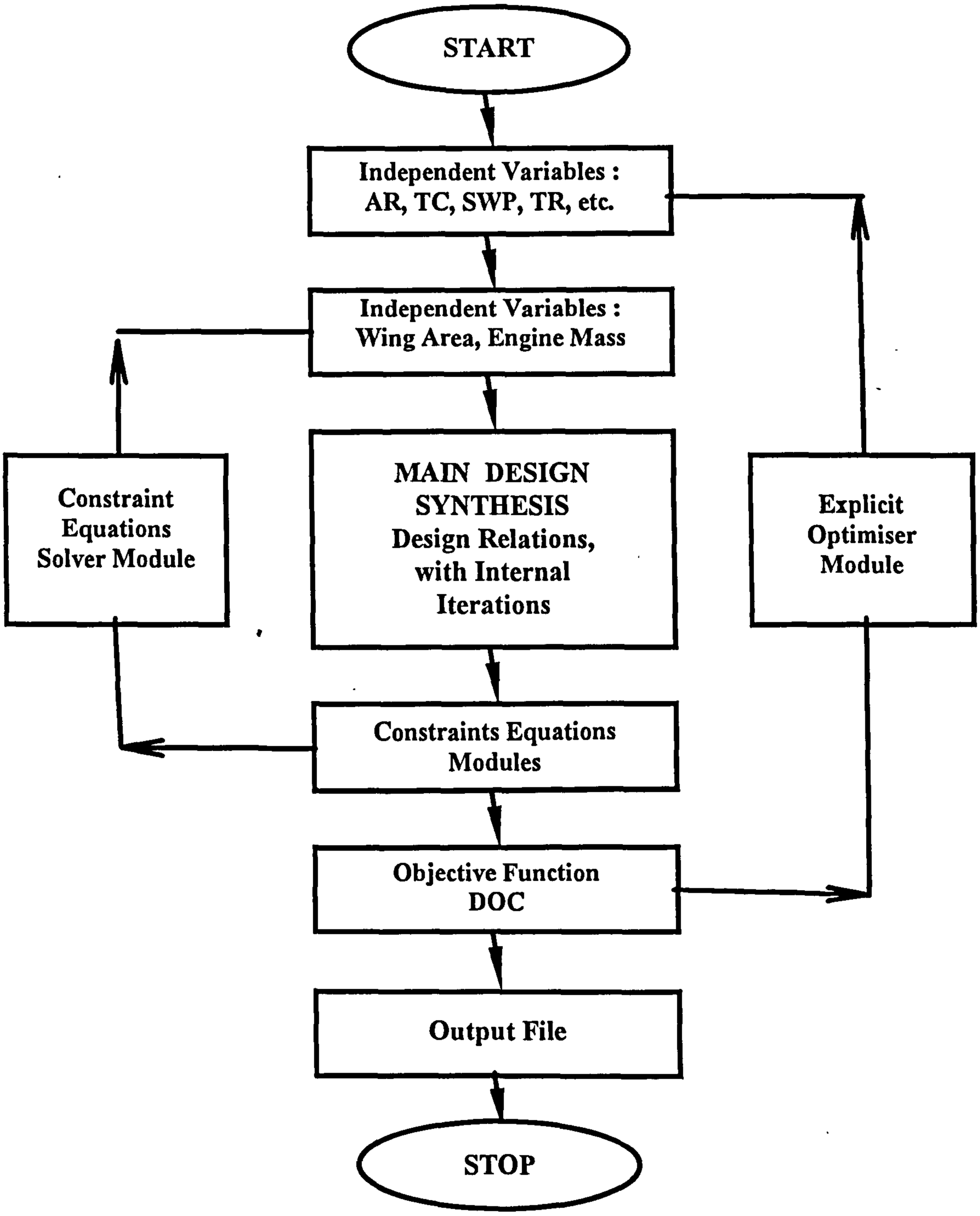

Fig. 2-1 : Flow diagram of major sections of CACAD

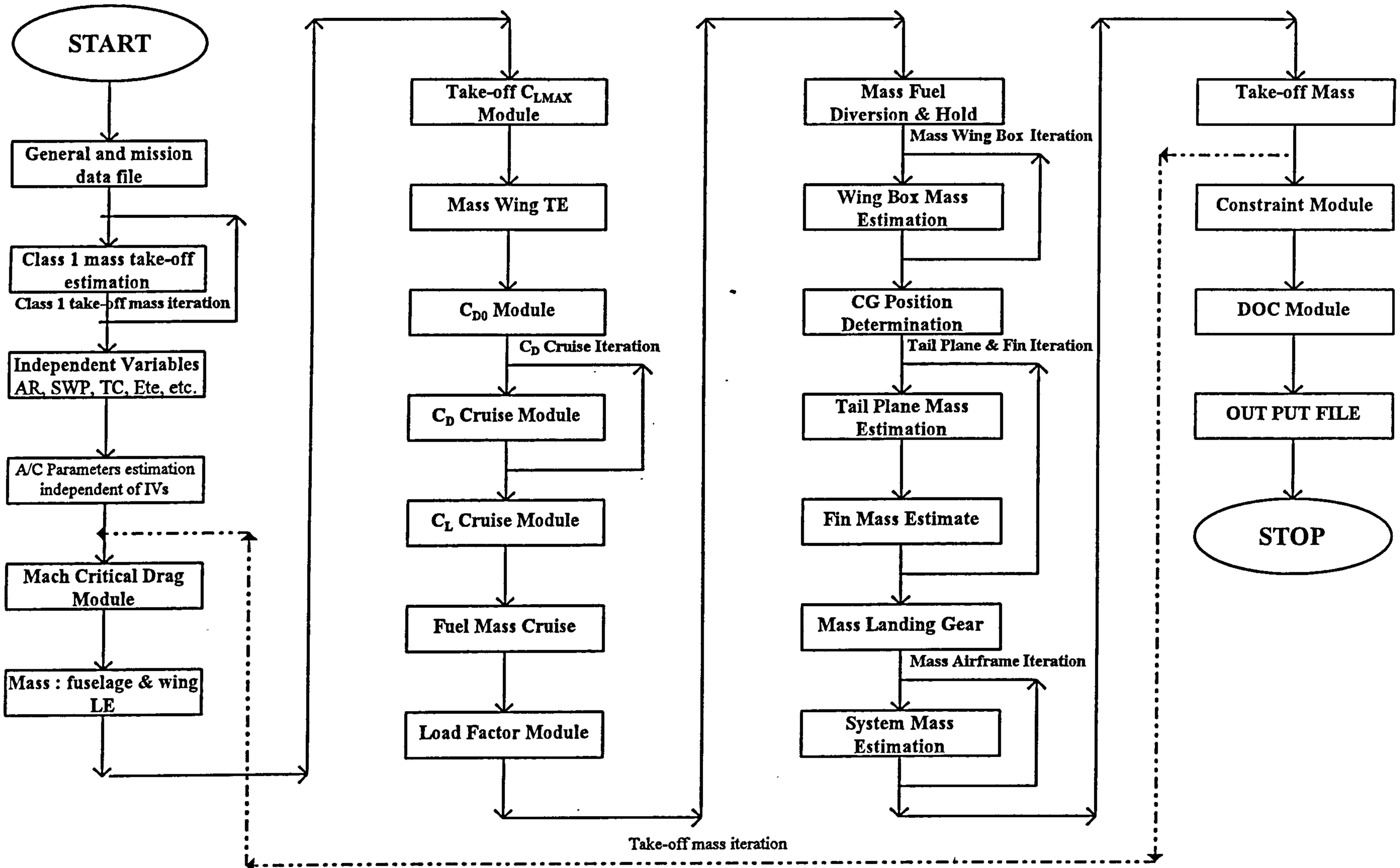

Fig. 2-2 - Flow diagram of modules of the main design synthesis in CACAD showing all possible iterations.

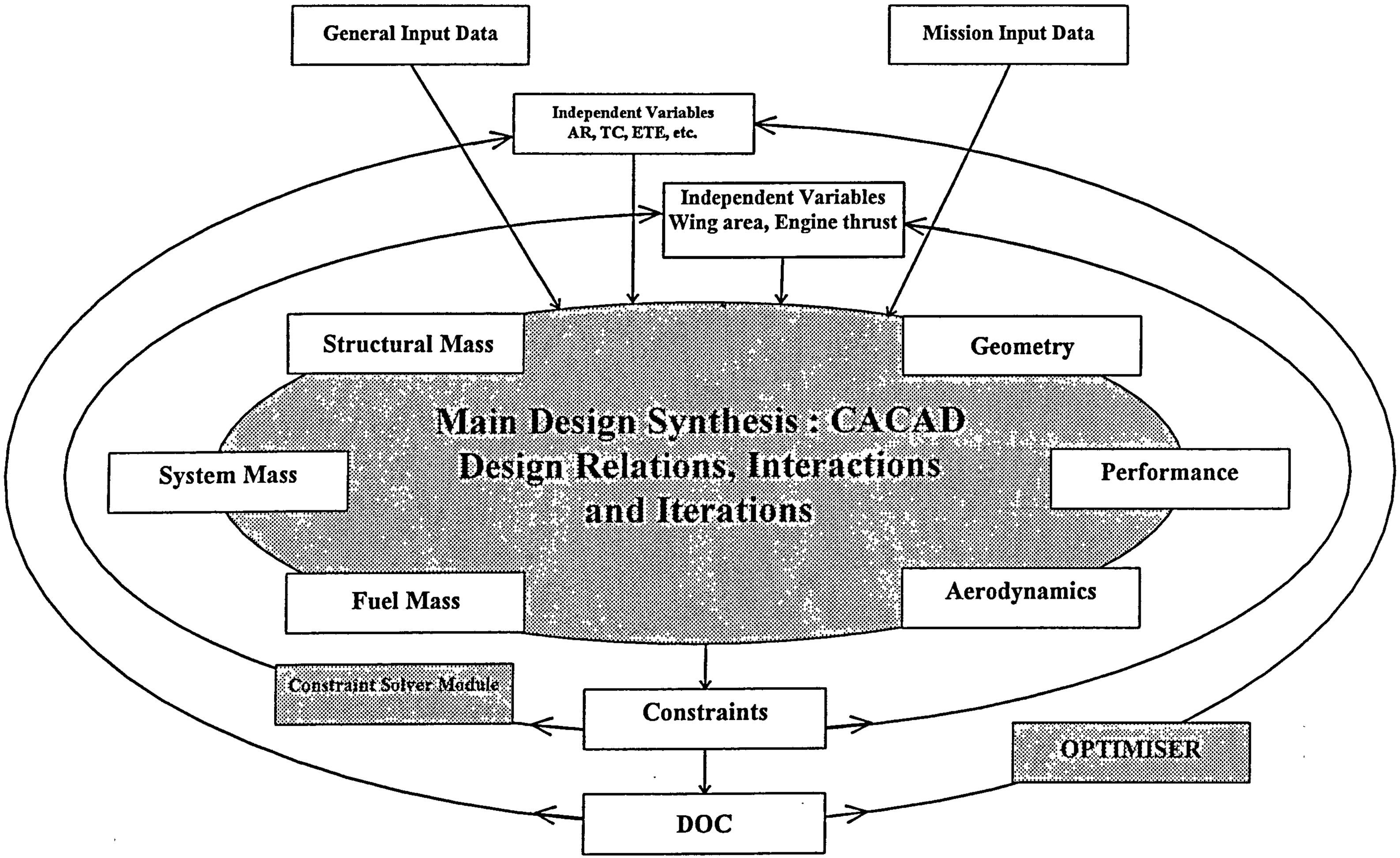

Figure 2-3 : The formation of CACAD main elements with respect to each other

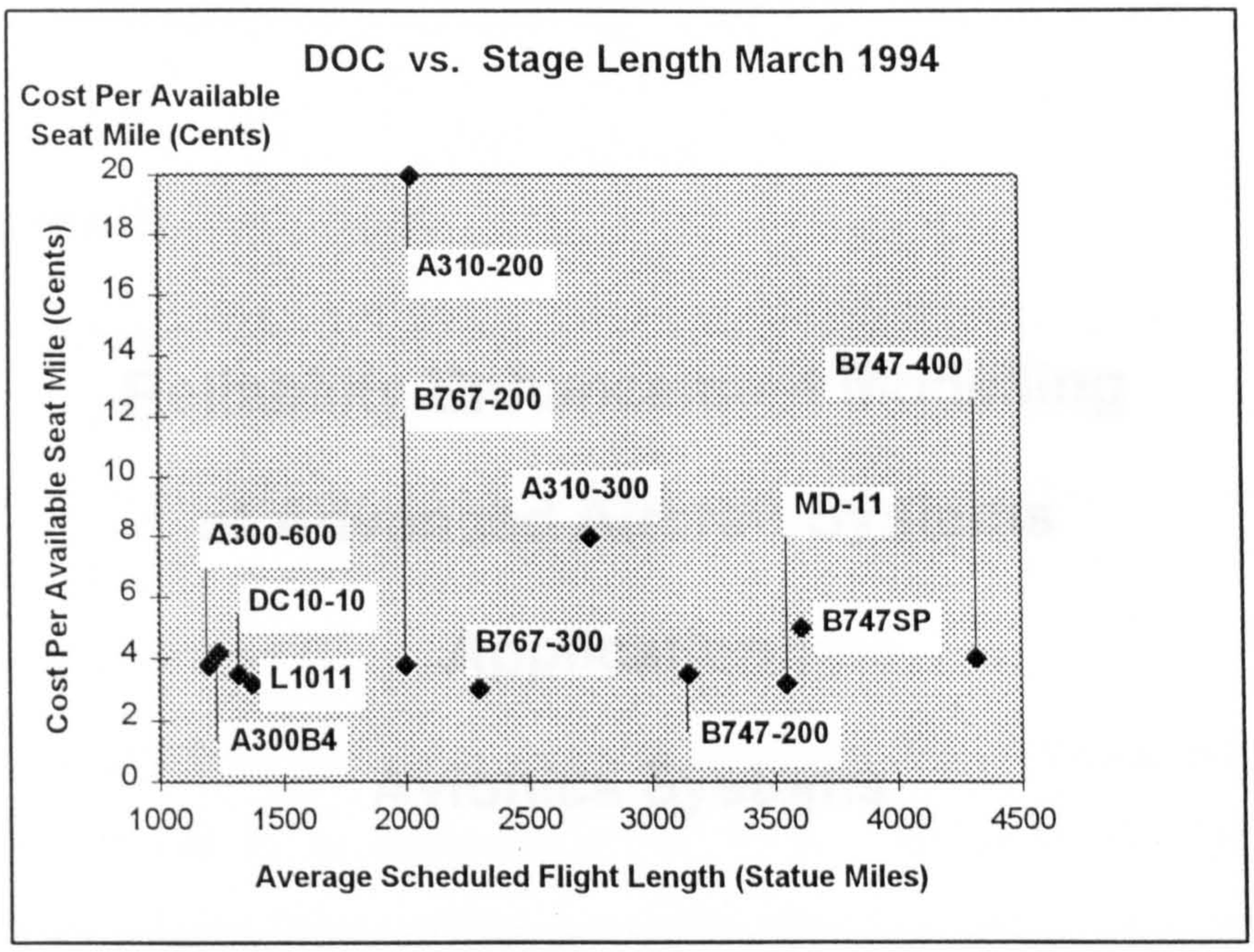

Figure 2-4 : Comparison of DOC of Airbus A310-200 with other transport aircraft [44].

CHAPTER 3

Reliability Enhancement Modelling of Advanced Aircraft Systems Application : Avionics Systems

3.1 Introduction

Statistical prediction equations were used to establish a base value for maintenance costs of existing state-of-the-art aircraft systems in CACAD. A wide range of reliability enhancing design solutions, supported by experimental results for aircraft system such as the avionics system were then investigated. A design solution was selected with the best combination of the following features : affordable, functionally efficient, minimum maintenance side-effects, adequately reliable, easily producable, with least mass, development cost, and complexity implications, and last but not the least, the design solution application must have predictable influences on other aircraft systems.

Such reliability enhancement measures(REM) were then modelled and integrated into the CACAD architecture. The dominant parameters of the design solutions and their influences on other aircraft systems were linked to the aircraft independent variables.

This integration was explored through optimisation and the aircraft sizing process to establish not only the possibility of such an REM, but also to search for the most appropriate combination of parameters that yielded a transport aircraft with a net reduction in DOC.

3.2 Research Objectives

Reliability Enhancement (RE) modelling of aircraft systems and incorporating them into CACAD is an effort to design an aircraft which is potentially capable of offering a greater facility to promote R&M of its systems. This will not only improve the safety of the aircraft, as a result of lower failure rate, but it may be possible to explore the conditions under which a net reduction in DOC is produced.

In general, reliability of an aircraft is enhanced by reducing its failure rate, which is directly proportional to its maintenance man hours. This is because, in a typical situation every genuine failure sends a part or the whole of a system, or a sub-system to the maintenance shop. Therefore the failure rate may be assumed to be equivalent to the number of times a system make a visit to maintenance shop. Total maintenance man-hours of a system is the product of its average failure rate and average maintenance man-hours spent at each visit to the maintenance shop (no fault-found situations also take maintenance man-hours, which is reflected in the average maintenance man-hours mentioned earlier).

The failure rate factor, which is the ratio of system failure rate before RE modelling to the system failure rate after RE modelling can be used to measure the amount of saving in the system maintenance man-hours.

Although an effective REM may reduce the system failure rate, it may well increase the complexity of the system. This may be due to more parts or complicated equipment added to the system. Such solutions may also reduce the accessibility of the system. These contribute to the increment of average maintenance man-hours, although the frequency of system visits to repair stations is reduced. Therefore REMs developed for aircraft systems must be such that while they contribute to lower failure rates, they impart minimum side-effects on system weight, complexity, and accessibility.

3.3 REM Methodology in General

There are common features in every major aircraft system. Major systems are defined as those aircraft systems that have a considerable share in the aircraft maintenance cost. The common features [50] are defined as Supply, Transmission, and User part of any system. The methodology is based on the fact that any improvement in system reliability may influence the operation, and/or improve the environmental condition of the common features of the system. Links are therefore established between the reliability-augmenting solution and the aircraft basic independent variables. This in turn opens the way to design an aircraft with an inherent potential for higher reliability. In Table 3-1, the major aircraft systems are divided into their common features and major components of each division are mentioned. The areas of aircraft conceptual design affected by any hypothetical reliability improvement are presented. Note that any improvement in system R&M must reduce the maintenance cost part of DOC. It may also be accompanied by penalties such as increases in wing area, engine size, and take-off mass. To understand how the generic Table 3-1 works, the following example is presented :

Consider reliability-improvement of the supply section of the fuel system. The supply section is primarily composed of fuel tanks, and fuel pumps. The hypothetical design solutions may include : - Either fuel tank sealant material might have been replaced with a more efficient but costlier material. - Or, the fuel tank material is changed to a one that cracks less, which might be heavier, or costlier. In both case, the mass and cost of the wing are affected by such REM, hence affecting the aircraft configuration when incorporating it into CACAD. If the fuel pump is undergoing an REM, then either the more reliable pump is likely to be heavier, and or costlier. It may be the latest state-of-the-art fuel pump design, which has made it lighter in weight. This might encourage the system designer to use two of them as redundant items to boost dispatch reliability. Most engineering methods to enhance system reliability, may produce higher system mass, cost, or size. It may also affect the mass, cost, size, and operation of the neighbouring system too.

3.3.1 Methodology Philosophy

R&M modelling incorporation into CACAD, according to the above methodology, shall in its first phase explore the design solutions that contribute to a more reliable system, i.e. lower failure rate, and a more maintainable system. It then must distinguish between those design solutions that are related to the architecture of the system, from those that are related with the system housing, or the system environment. The latter has a higher chance of being physically linked with the aircraft sizing process. Efforts must be devoted to search and recognise the experimental data to substantiate REM efforts. These may be already available, or it may be necessary to pursue such experiments, so as to produce fresh data that quantifies system R&M variation with environmental factors. Environmental causes are usually *temperature*, *humidity*, and *vibration*. Other environmental factors are less significant in jet transport aircraft.

It is worth mentioning that there are other remedies to boost aircraft operational reliability, and hence system safety. One example may be to increase system redundancy. This remedy may however increase system maintenance time, price, and system spares holding. It may also increase system mass, and space allocated. Finally the system's overall failure rate may not be reduced, or even increased. On the other hand boosting system redundancy if accomplished expertly, will reduce flight delays, work stoppages, and ground time. These are beneficial to DOC, by increasing the aircraft utilisation. Hence redundancy incorporation as an REM is also a matter of trade-off with both benefit and penalty consequences.

It may also be noted that, in most cases of enhancing the R&M of a system may involve the participation of other related systems. This requires quantifying the interactions between the systems. This is usually tedious work, and requires experimental data, that is often scarce and commercially sensitive.

3.4 REM Methodology Application to Avionics Systems

An investigation in 1974 [51] showed that 25% ($163 million) of total USAF maintenance cost ($650 million) was due to environmental causes, of which 54% was attributed to temperature (Figure 3-1), i.e. 14% of the whole of the annual maintenance

cost. The same study showed that nearly 39% of the maintenance cost was spent on avionics (Figure 3-2). Repeated investigation [51,52] showed that a great deal of avionics failures were environmentally related. The study in [52] also indicates that 41% of the maintenance man-hours on combat aircraft go to avionics along with 31% of the maintenance cost. There are more such examples and all show the gravity of avionics unreliability cost implications.

It is believed that, due to overestimation on engine performance deterioration, and / or engine vulnerability to bleed in the 60s, and 70s, and early 80s, environmental control systems were designed to give minimum cooling to the avionics system. This led to a situation in which it was not the reliability engineer or avionics design engineer who established the cooling capacity requirement for avionics as would be expected, but the airframe ECS engineer. Thus the design performed by a person who may know less about the cooling needs of a particular equipment than it's designer [53] .

The major environmental factors extracted from category II combat aircraft flight test report [51,52] resulted in following symptoms. With less severity, these may be generalised to cover transport aircraft as well :

- Cooling system capacity : insufficient flow of cooling air into the cockpit when the engine rpm fell below 84% in a hot-weather environment, and equipment over-temperature during high speed flight .
- Moisture : Emission of water into the cockpit during take off and low level operation in humid environments. Fog and moisture emission was so great that at times that it was a potential flight hazard.
- Temperature Control : Extremely poor distribution of cockpit temperatures with cool air temperatures as high as 130° F in pilot compartment, and 150-175° F in equipment compartment.

A detailed passenger aircraft DOC study in the College of Aeronautics at Cranfield University in 1976 showed that avionics constitute 11.5 % of the total maintenance cost [38] (see Figure 3-3). Surprisingly the same percentage was found for a Boeing 737-300 in a report published by an authority in Boeing [37] in 1990, (see Figure 3-4). A

recent confidential report on a medium-capacity jet military transport system maintenance man-hours showed that more than 21% of maintenance man-hours were devoted to avionics (Automatic Flight Control, Communication, Instruments, Navigation, Engine Indicating, ..) and 26.7% in a large capacity military jet transport [54].

Recently available data from airlines, [55to62], suggest that avionics has still among the highest failure rate producing systems. Figures 3-5, 3-6, and 3-7 give the state of reliability such as delay rate, PIREPS, and unscheduled removal rate produced by different systems in different transport aircraft.

The above findings were convincing enough to choose cooling of avionics as an effective REM, and also there appeared enough links with conceptual design scheme to modify CACAD to include the R&M disciplines.

Finally in this introductory section, It should be mentioned that beside numerous recommendations by the experts in the field that cooling can enhance avionics reliability, other alternative methods were also proposed by other experts such as passive cooling [63]. Pessimistic views warning against excessive reliability enhancement measures are dealt with in [64], and other views that avionics maintainability is more important than it's reliability are presented in [65].

3.5 Avionics System-Brief Description

Avionics (aviation electronics) in a typical modern jet passenger aircraft encompasses a wide variety of equipment and functions, such as radios, flight instruments, navigational aids, flight control computers, radar, and all electronic sensors [1]. They are usually cooled by air-conditioned air provided by the ECS.

The equipment that must indicate information to the pilot and accept pilot commands is avionics related flight instruments, and is housed in the flight deck; see Figure 3-8. The rest are installed in the avionics bay, the main compartment underneath flight deck (outside the pressurised cabin), and in other locations for technical, maintainability, and cost saving reasons, see Figures 3-9, and 3-10.

The major function of avionics equipment [15], is to enable the pilot to interface with the aircraft controls through the flight management systems (FMS), (Figure 3-11), a system that integrates propulsion controls, flight controls, and auto-pilot functions . An FMS comprises flight control computers, auto-pilot/auto-throttle controls (Figure 3-12), thrust management computer (Figure 3-13), inertial reference system (Figure 3-14), flight data acquisition system (Figure 3-15), communication and advisory systems (Figure 3-16), maintenance control, and display unit (Figure 3-17). Further description of these systems is beyond the scope of this dissertation (some description is included in every figure). The reader may pick any appropriate equipment name from the above figures and search through the related literature for more information.

3.5.1 History of Avionics Reliability Considerations

Reliability problems in avionics have been recognised since their introduction into aircraft in the 1920's . Since then avionics have been required to perform the compound functions of automatic flight control, navigation, fire control, automatic landing, performance monitoring, command and control and communication, data processing, radar control, automatic maintenance checkout, fuel management, bombing, electronic warfare, and display information, etc. Reliability of avionics received a major impetus during the post -World War II period. One of the first Advisory groups, established for this purpose in United States published its first report on Reliability of Electronic Equipment in 1957 [66]. Later these efforts resulted to the publication of MIL-STD-781B dated 1967. Since then most of the research work has concentrated on

- techniques of avionics systems reliability estimation to determine the relationship between estimated, demonstrated and actual field data
- cost-effective avionics reliability programs.
- avionics built-in test provisions for improving operational reliability.

A number of such works were published in [67]. Later more research was done on

- reliability growth.
- realistic evaluation of the causes of avionics unreliability.

- service failures affecting avionics reliability.
- reliability improvement warranty.
- avionics reliability and life cycle cost.
- avionics reliability modelling for fault-tolerant systems.
- software reliability

which are reported in [68].

From the mid 60's, the complexity and the amount of equipment and their power consumption and heat dissipation within the avionics system began to reach a formidable level. A lot of research was then diverted toward promoting reliability by highlighting environmental issues, especially the cooling system. Reference [69] contains a number of such works, of which the work of Groom from Boeing, and German from Royal Signals & Radar Establishment proved very useful for this thesis.

3.6 Avionics System Reliability Enhancement (ASRE) Modelling

More than 85% of the avionics system electrical power is consumed by avionics equipment in the equipment bay, and the rest by flight instrument on the flight deck. The method of cooling avionics in the flight deck may be considerably different to those of the bay. Also the flow requirements and failure rate variations with temperature are different in these two cases, therefore each was modelled independently.

Avionics REM requires extra bleed from the aircraft main engines which is cooled in the ECS and then supplied to the avionics systems. The bleed effects on engine performance, sfc, and thrust are modelled and affect the aircraft sizing process in CACAD. The ECS may increase in size and mass to handle the extra cooling flow. This requires ECS mass-prediction equations as functions of its output flow. Using experimental work, the avionics junction temperature in the compartment, and the avionics case temperature in the flight deck were linked to the ECS extra cooling flow rate. The failure rate changes of the avionics system with temperature, and it's

maintenance cost are also among the chain of models necessary to integrate ASRE in CACAD.

3.7 Modelling Incorporation Into the CACAD Flow Chart

The type of ASRE chosen, was to provide extra cooling to avionics beyond the minimum recommended by the regulatory authorities, to the extent that CACAD's explicit optimisation determines the optimum value. This required modelling of the effects of all participant systems. The flow chart in Figure 3.18 is an effort to demonstrate the key role of the participating systems and their relation with each other and with the CACAD design modules. Figure 3-19 shows the schematic diagram of ASRE associated with the flow diagram. In the subsequent sections, description of each model follows, along with typical results obtained. Where ever appropriate, and possible, some validation also accompanies the sections. Detailed formulation, and description, along with the results are included in the Appendix C.

3.8 Engine Bleed Modelling

For general study of bleed effects on engine performance, References [70,71] are useful. There are few published works available to report the bleed effect on the sfc, and the thrust of turbofan engines for different flight altitude, and Mach number. Hence a Code to simulate engine performance, called Turbomatch [72] established by Pilidis from the SME at the Cranfield University, was used for the above modelling.

3.8.1 Engine Bleed Modelling Justification

High energy air (high pressure and high temperature) is bled from the compressor section for the purposes of cabin air-conditioning & pressurisation, for ice protection of aircraft sensitive aerodynamic leading edges and for cooling of the avionics bay and the avionics in the flight deck. A medium capacity twin jet aircraft (200 PAX) usually requires 115 kg/min of air from its engines for air-conditioning purposes. For detail flow requirement refer to [73]. This is nearly 1 kg/sec of bleed from each engine. If the avionics power consumption is assumed to be 8 to 10 kW [74] and also assuming a minimum of 5 lb./min/kW (Arinc 600) [75] for cooling it, this will amount to 0.38

kg/sec i.e. 20% of the bleed from each engine go to the cooling of avionics systems. If enhancing the avionics cooling should require 50% extra bleed supply to the avionics systems, this means, extracting another 0.1 kg/sec of bleed from each engine (10% more bleed). Therefore the feasibility of engine bleed penalty-modelling for sfc increase and thrust reduction is justified.

3.8.2 Engine Bleed Position

Turbofan engines are bled from three ports in the compressor section. When the engine throttle is at the take off position, usually all bleed valves are turned off automatically. During the climb phase air is taken from LP compressor, during cruise from the IP compressor, and during descent and approach from the HP compressor. The cruise performance is likely to be the most adversely affected by compressor bleed, hence this flight phase was considered for bleed characteristics modelling. IP compressor bleed is normally used for bleed during cruise, hence this was used in the model.

3.8.3 General Flight Condition

Turbomatch was used to simulate a typical jet passenger aircraft engine resembling RB211 class characteristics while being bled. It was found that the rate of fuel, and the thrust penalty changes with altitude (in the ranges of 25000 to 35000 ft), and with Mach number (in ranges of 0.8 to 0.84), and in the bleed ranges up to 2 kg/sec were negligible, (see Figures 3-20, and 3-21). Therefore, to produce a general empirical equation between bleed flow rate and sfc increase / thrust reduction, an altitude of 35000 ft, and an average flight Mach number of 0.82 were selected as the common engine cruise flight condition. Fortunately those classes of engines which were considered suitable for the classes of aeroplanes selected by CACAD, published their thrust and sfc specification in cruise at about the same flight conditions as above .

It was also found that sfc/thrust penalty varies with engine configuration, i.e. engine major parameters such as mass flow rate, and compressor pressure ratio (CPR). They were less influenced by turbine entry temperature (TET), and engine by pass ratio (BPR). It was concluded that a generic universal empirical relation linking either sfc increase with bleed or thrust reduction with bleed is not achievable, and the rate of

variation is different within the class of transport turbofan engines. Therefore four possible configuration were considered; 15000 lbf , 30000 lbf, 52000 lbf, and 75000 lbf SLST class of engines resembling TAY 650, CFM56C2, CF6-80C2, and TRENT775 respectively. The tables of the bleed effect, correlation equations fitted to bleed characteristics curves are given in Appendix C, section C2.1.

3.8.4 Analysis of the Results and Validation

Bleed effect data from current engines, during their cruise phase is not readily available. Fortunately the bleed effect of two engines the Tay, and the Trent were supplied to the College of Aeronautics from a prominent company [76]. According to this reference, 2 lb./s (0.91 kg/s) bleed from the IP compressor of the Trent engine at maximum cruise setting would cause a 1.18% sfc rise. Turbomatch result for this type of engine is depicted in Figure C-3. According to this figure the penalty at the same bleed for the same condition is 1.15 to 1.2%. This is a reasonable validation of the Turbomatch modelling.

For the Tay engine at a bleed of 1 lb./s (0.45 kg/s) at 100% cruise setting, there would be a 3% sfc rise . The Turbomatch result for this type of engine gives a 3.1% sfc penalty. This is again reasonable validation against a real engine. It may therefore be stated that : *At maximum cruise setting, the Trent data and Turbomatch prediction line up very well. For Tay there is a 1% variation.* These results give considerable confidence in the modelling for high by pass ratio fan engines.

3.8.5 Turbomatch Bleed Prediction Validation Comment

A major penalty, the quantity of which decisively influences the feasibility of thermal avionics RE implementation, is the amount of sfc increase due to bleed. This increases the mission fuel load and quantitatively challenges the avionics maintenance benefit .

If the bleed effect on the engine sfc is underestimated an over-optimistic result would be deceptive. On the other hand, an overestimate would discourage research attempts to boost aircraft system reliability .

This part of the work may be open to review because of the controversy over the bleed-effect penalty variation with engine technology improvement. There is a great secrecy around this issue, but some actual experimental results from an older engine suggest that Turbomatch findings are an underestimate. Later models however , such as those in previous section show values nearer to the results from Turbomatch. Therefore, by considering the previous trend it is possible to suggest that, the advanced turbofan design is moving toward reduced bleed penalty effect. It might have even reached values lower than predicted by Turbomatch with latest GE90, and PW4000 engine or soon may arrive at lower values.

To avoid any uncertainty about the Turbomatch-predicted values of sfc penalty due to bleed, from any real modern engine, a 25% and a 50% rise in sfc penalty, was considered for sensitivity analysis. The details of this are presented later in this chapter.

3.9 ECS Mass Modelling

Current empirical equations for the prediction of ECS mass are not affected by output flow [1,15]. An extra supply of cooling flow to the avionics system may not influence ECS mass if any of these relations are used in CACAD. It was therefore necessary to establish a prediction equation for ECS mass as a function of its output flow rate. The procedure and the results are detailed in Appendix C. The relation is self-validating, as it is correlated with real transport aircraft ECS mass via the GD method [15].

3.10 Ram Drag Penalty

ECS consumes ram air for its heat exchangers and therefore any increase in its bleed output and mass will be accompanied by higher ram-air consumption, and hence produce an increase in the ram drag. Incorporation of the new technology elaborated in [77], may prevent such increase in ram drag. The use of air bearings in the cold air unit of ECS would enhance its life and reliability. This unit can continue producing cold air at cruise altitude where previously ram air temperature was adequate to by-pass the cold air unit. Using this new technology, bleed air is directly guided into the cold air unit, by-passing the secondary heat exchangers, hence avoiding the ram drag penalty attributed to them.

attributed to them. Surprisingly there should be some gain in engine performance, but this was not accounted for in the design synthesis due to lack of validated data.

3.11 Avionics Compartment

This section presents published data on state-of-the-art for packaging and cooling of those avionics within the bays, and compartments. There will be a justification for modelling the selected type. The procedure, and mathematical modelling, is described in Appendix C.

3.11.1 Arrangement and Packaging

Modular avionics packaging was an effort to standardise avionics modules and packaging. Arinc 600 establishes [75], the form factor, external design such as the size, the shape, and the environmental interfaces with aircraft for line replacement units (LRU), installed in civil aircraft, see Figure 3-22.

Arinc 600 also introduces the modular concept unit (MCU) as the basic unit of width for an LRU. Several attempts have been made to incorporate heat exchangers either within LRUs, Figure 3-23 i.e. conduction flow through and heat pipe [78], or within LRUs enclosures [53], Figure 3-24. This is done for the highest heat exchange rate for the lowest possible junction temperature and lowest pressure drop. These efforts may be very useful for a fighter aircraft where every little space saving is very helpful. For a transport aircraft, a simple conduction-cooled module LRU, within a simple MCU-size enclosure like the one in Figure 3-25 is an appropriate design. This offers the lowest cost of producibility, and maintainability, with the least limitation on the particle size of the cooling air.

Arrangement of modules within the enclosures may be such that the units with the lowest MTBF i.e. its failure-rate rises rapidly with temperature, be placed at highest cooled section of the enclosure. This is called thermal management priority within an MCU. The priority may be given to reliability-critical components, rather than temperature-critical components [79], avoiding the arrangement in the Figure 3-26 .

3.11.2 Methods of Cooling

Avionics LRUs within MCUs are arranged on avionics racks in every avionics compartment i.e. black boxes in the racks. There are several cooling techniques in which ECS cooling air is guided into the avionics racks to keep the LRU's junction temperatures within accepted limits. It is to be noted that, the performance of each method has been experimentally tested for military application, for a typical 5 W module. The results are quite reasonably applicable to the transport aircraft, especially when the main objective would be to model the rate at which junction temperature varies with flow rate increment [79].

(a) Conduction Cooling Air Rail : The MCU and the rack arrangement are shown in Figures 3-27, and 3-28 . In this configuration, the modules are serially mounted in an integrated rack tier. Since these modules are serially-cooled, the coolant temperature at the inlet to the rail heat exchanger is lower than the exit. If all the LRUs in the MCU have the same heat dissipation, then the maximum junction temperature occurs on the centre component of the last LRU. The performance of such an arrangement in the terms of ECS supply flow rate, supply temperature and avionics junction temperature are shown, for an average basis in Figure 3-29.

(b) Conduction Cooling Air Over Component : The arrangement for the MCU and the rack are shown in Figures 3-30, and 3-31. In this arrangement the LRUs are in parallel and the secondary air is passed between the modules. This air travels in a closed loop cycle the end of which is cooled through an interface heat exchanger supplied by ECS cool air. Since the modules are cooled in parallel the cooling air supply temperature is the same for all the modules in the tier. The thermal performance of this arrangement, on an average basis, is shown in Figure 3-32.

(c) Conduction Cooling Liquid Rail : In this arrangement a liquid coolant replaces the air in an exactly the same manner as in air rail method, to cool the MCU in

the avionics racks . The thermal performance of this arrangement, on an average basis, is shown in Figure 3-33.

The following two methods are more innovative, and look more unconventional than the previous three :

(d) Hollow Board : In this method the secondary air is guided through the hollow board of the LRUs, boosting the performance of the cooling of the electronic components, but adding complexity to the LRUs. The markedly improved thermal performance is shown in Figure 3-34.

(e) Heat Pipe Modules : Due to extensive research in this new cooling technique, [80] the method was also experimentally examined for its thermal performance included in [79]. The application of heat pipes in LRUs is shown in Figure 3-35. A heat pipe is a passive device typically consisting of a sealed container lined with a wicking material, and filled with just enough fluid to fully saturate the wick [81]. It operates with a closed vaporisation and condensation cycle. Heat dissipated from the components of the LRU is added to the evaporator section of the pipe, and vaporises the working fluid . The high temperature, and corresponding high pressure in this region causes the vapour to flow to the cooler end of the pipe, where the vapour condenses. The capillary forces in the wicking structure generate a positive pumping pressure that forces the working fluid back to the evaporator end. Because heat pipes use a phase change of the working fluid to transport heat, their effective thermal conductivity is much higher than the best solid conductors, together with rapid response time make them very promising in cooling the electronic systems Figure 3-36.

The following table shows the junction temperatures realised by say 3 lb/min/kW of ECS supply at 80 degree F for typical 5 watt modules for all above methods.

Airflow Rate	**Air Supply Temp.**	**Air Rail**		**Liquid Rail**		**Air over Component**		**Hollow Board**		**Heat Pipe**	
lb/min/ kw	*° C*	$T_{j\,max}$ *° C*	$T_{j\,avg}$ *° C*	$T_{j\,max}$ *° C*	$T_{j\,avg}$ *° C*	$T_{j\,max}$ *° C*	$T_{j\,avg}$ *° C*	$T_{j\,max}$ *° C*	$T_{j\,avg}$ *° C*	$T_{j\,max}$ *° C*	$T_{j\,avg}$ *° C*
3.0	26.6	112	82	110	100	121	112	72	58	88	64

3.11.3 Discussion and Selection of Cooling Method

It is necessary to make a selection among the methods described above. The one that is most feasible for the jet transport aircraft shall be used for avionics cooling modelling to be incorporated in CACAD .

Among the first three methods, the conduction air rail is not only functionally superior, but manufacturing costs are cheaper, with lower mass, and the least complexity. This method uses the smallest number of equipment, hence lowest failure rate, and leads to high reliability and maintainability. The last two methods, the hollow board, and the heat pipe, although offering a great deal of thermal superiority to the first three methods, their mechanical design still may be a challenge. Air leakage i.e. unreliability of operation, and difficult card removal i.e. poor maintainability, as well as the high cost of production make them unsuitable for this type of modelling. Even though their benefits are quantifiable, their penalties seems formidable and are hard to quantify.

The conduction cooling air rail method, which was eventually selected for modelling, had three variable parameters, ECS flow rate, ECS flow temperature, and LRU junction temperature. It required fitting a surface to known points to be able to establish a correlation equation . This was done, and the details are presented in Appendix C. The resulting equation was incorporated into CACAD.

3.12 Avionics In The Flight Deck

In this section the published data are presented for the state-of-the-art for packaging and cooling of avionics within the flight deck. Justification is given for the type selected for the modelling. The procedure of modelling and the derived equations are described in Appendix C.

3.12.1 Problem Description

The design trend in aircraft avionics equipment in the flight deck station is towards the use of light-weight high power density units. This may result in reduction in reliability and crew performance. If the temperature level in these units is controlled and made

uniform, the resulting improvement in reliability and crew performance will improve life cycle cost and ensures mission completion and increase the operational safety.

According to [82], a review of 5 different instruments indicated an MTBUR of 230 to 1600 hours, while their specification called for 4500 to 6000 hr. A high percentage of verified failures were thermally related such as capacitor and motor bearing failures. Current standards such as MIL-E-38453A [83], and ARINC 408A, Air Transport Indicator Cases and Mounting, 1975 [140], established minimum cooling limitations. The former allows a 40.6 °C touch temperature (case temperature) with 26.7 °C ground ambient (ECS supply temperature), and the latter puts the limit for ECS supply to a minimum of 8 lb/min/kW, with temperature at 37.8 °C so that the instrument's front face should be at 54.4 °C and its case at 65.6 °C.

3.12.2 Arrangement and Packaging

Although there is not a definite and universally accepted, or regulatory enforced configuration for the layout of instruments and navigation panels in a transport aircraft flight deck, a great deal of commonality exists between them. The trend shows that soon there shall be similar flight deck in every transport aircraft, for basic reasons such as ease of operation, ergonomic criteria, and pilot common-type rating. The Airbus A319, A320, and A321 have common flight decks instrumentation, but they in turn resemble the flight deck configuration of A330, and A340, which have identical flight deck systems.

Figure 3-37 presents the near-common flight deck instrumentation among A319, A320, A321, A330, and A340 aircraft, and Figure 3-38 shows another common flight deck between A300, and A310 aircraft. In all these aircraft there are 6 cathode-ray tubes (CRT), the first two, Figure 3-39, are placed in front of the pilot and the last two are in front the co-pilot. The flight deck in the Boeing 777 also look the same as in Figure 3-39. They are called electronic flight instrument systems (EFIS). One is deployed for primary flight display (PFD), and the other for navigation display (ND), see Figure 3-40. The last middle two CRTs are called electronic centralised aircraft monitors (ECAM). One is allocated for engine/warning display, and the other one for systems

information/reminder and warning display, see Figure 3-41. Among other major instruments are three multi-purpose control and display units (MCDU) enabling the pilots to have access to flight management system (FMS), and many other functions such as system maintenance data, coupled to a printer, called central maintenance system (CMS) see Figure 3-42. There are still many analogue instruments as backup, Figure 3-43.

3.12.3 Methods Of Avionics Flight Deck Cooling

Cooling air is guided through the flight deck by ECS ducting directly into the deck instrument compartment. Fresh air supply to flight crew is also exhausted to the back of instrument panel, through panel openings.

Three design schemes were studied by Boeing [82]. The first one considered a base configuration, apparently used as a conventional approach. In this, air enters the instrument bay, while cooling the instruments, and it is exhausted through an opening to the ambient temperature section of the nose fuselage, see Figure 3-44a.

The second proposal was called the suction type, in which air entered the avionics flight deck bay through holes around the instruments. It then expands as a jet into the space between the sides of the units and continues in the horizontal direction until it is evacuated by a general exhaust, see Figure 3.44b. The diameter of the expansion holes and the distance between the adjacent instrument walls are decisive in creating a fast non-uniform velocity profile of turbulent flow .

The third concept, called the pressurised panel, utilises the suction concept, assembled with a baseline panel but spaced apart to form a plenium Figure 3-44c. The supply air is from ECS duct is guided into the plenium, passes vertically up the plenium, turning 90 degrees into the jet holes. This method also facilitates the instrument-retaining method, and perhaps helps to reduce vibration, see Figure 3-45.

3.12.4 Discussion and Selection of Cooling Method

The thermal performance of each concept was experimentally tested for a typical heat release of 0.34 W/in^2. Results are presented in Figures 3-46, and 3-47. The last two

concept are apparently superior to the base-line, and the pressurised panel concept functions slightly better than the suction concept, but is heavier. Its performance is less susceptible to leakage , and the existence of double panel help keeps the instruments in place especially the big and heavy CRTs of modern decks. It was thought therefore to be superior to other types of cooling. Hence the pressurised panel thermal performance was used to formulate the empirical equation modelling purposes. The pressurised panel offers the highest thermal performance and its use in flight deck instrument cooling has been adapted by at least one major manufacturer; see Figure 3-48. The shortest possible back-spacing (the distance between the rear face of the instruments and flight deck instrument bay i.e. front pressure bulkhead) offers least disparity between units' individual temperatures and even offers slightly lower case temperature rise for the same airflow. Therefore the pressurised panel method with shortest back spacing was chosen. An empirical relation was developed to model the avionics case-temperature rise as a function of cooling flow rate. The formulation and the procedure for deriving it is given in Appendix C,section C4.2.

3.13 Avionics Systems Reliability Modelling

This section presents models of the reliability of the avionics system. It will describe how the avionics failure rate varies with system temperature. This will quantify the link between avionics reliability improvement, and the cooling modelling developed in previous sections .

3.13.1 Avionics Compartment Reliability Model

The precise relationship between operating temperature and failure rate for a particular system is revealed by part stress analysis, which calculates failure rates from the known system variables. Those include temperature, part quality, severity of the part operating environment, circuit complexity, and the experience of the manufacturer in making the device. Avionics reliability dependence on temperature is supported by MIL-HDBK-217 [132], according to which there exists a direct relationship between the reliability of temperature-sensitive electronic parts, and the part operating junction temperature. There might be other environmental stress factors, but temperature is one of the major

and better defined stress factors. Temperature and failure rate are exponentially related, with failure rate increasing dramatically with increasing part junction temperature .

Care must be taken while arranging electronic parts on LRUs, and locating LRUs in MCUs, that identical power dissipation parts may have different junction temperature and hence different reliability, emphasising the importance of part placement .

The temperature/failure rate characteristics of Figure 3-49 [83], consists of two curves one of which belongs to those components whose failure rate is much more sensitive to temperature, and the other one the least temperature-sensitive parts. The formulation and modelling procedure is given in Appendix C section C5.1, which is primarily based on Figure 3-49.

3.13.2 Avionics in Flight Deck Reliability Model

In the flight deck, the arrangement of equipment was chosen so that the case temperature of the avionics instruments can be controlled through pressurised panel cooling. A curve produced by the reliability group in one of the UK defence Establishment [84], is shown in Figure 3-50, which indicates the change in relative failure rate of military electronic equipment with its case temperature. There is no reason why this characteristics should be any different to that of civil avionics equipment. It has been derived from published failure rate data for the component parts, and is representative of component populations typical of many avionics equipment. Experiments and service experience has largely substantiated this characteristic pattern [84]. The shape of the curve below -30 degree C and above +80 degree C shown dotted is less certain, since it has been extrapolated from available information. The formulation and modelling procedure is given in Appendix C, which is primarily based on Figure 3.50.

3.14 Maintenance Cost Modelling

There are two areas in direct operating cost of an aircraft that are affected by avionics system reliability improvement. The first obvious one is the maintenance cost which is composed of maintenance labour, and maintenance material cost. Both are supposed to be reduced by ASRE. The other area is the standing charge, part of the aircraft DOC,

which in some literature, is called the depreciation cost. Two sections of this cost are affected by ASRE. The first is the depreciation cost of the avionics, in which the life duration element of it is increased due to enhanced avionics cooling and reduced failure rate. The other section is the spare parts holding cost, which is obviously reduced by reliability improvement.

3.14.1 Maintenance Man-hours (MHR)

As previously explained, the average MHR of any system is the product of failure rate (equivalent to number of visits a system makes to repair station) and MHR per visit. Any improvement in reliability must be accompanied by a reduction in failure rate factor (FRF). In section 3.13 failure rate (consequently FRF) associated with avionics system was linked with avionics temperature. This helped to determine the FRF change as a result of ASRE. Assuming that the amount of MHR per visit has not changed, then the total MHR change is directly proportional to FRF change. In CACAD, the base MHR allocated to avionics system corresponds to :

- 5 lb/min/kW bleed from engine to cool avionics bay (Arinc 600)
- 8 lb/min/kW bleed from engine to cool avionics deck (Arinc 408A)

Therefore every extra amount of cooling flow over and above the given figures will reduce system temperature, and hence cause a reduction in FRF. This will result in lower maintenance cost. A further discussion and formulation are presented in Appendix C.

3.14.2 Maintenance Material and Reliability Improvements

In CACAD, the maintenance material cost of any system is predicted as in standard text [14,32,34,1] is some function of the system price. Another approach is based on detailed research carried out in College of Aeronautics [38], which demonstrated that avionics make up 11.5% of the airframe maintenance, which was verified by [37], and in it, 67% goes to labour cost, and 33% toward the material. The latter approach was assumed for maintenance material of the base aeroplane before applying ASRE.

On the other hand, the total maintenance cost of avionics (labour and material) is a direct function of mean time between maintenance failure rate (MTBMF), which is directly proportional to average system failure rate [85]. The MHR cost element of it was proved to be directly proportional to system failure rate in the last section, hence the material cost element is also directly proportional to FRF. Any reduction in FRF was used to predict extra maintenance material cost in the avionics systems.

3.14.3 Avionics Spare Parts Holding Cost

Based on a spares provisioning equation derived by SABENA, presented in [85], the cost of avionics spare parts is the product of an average price of an avionics unit, and its inventory. The number of inventory items used, is decided mainly by the number of units being repaired per day, plus less importantly by the number of units sent to remote stations for emergency reasons.

The number of units being repaired per day is in turn proportional to the number of units failed per day, and the average repair time in days, for a unit. The number of units failed per day is directly proportional to flying hours per day, and inversely proportional to MTBUR. The latter is directly proportional to FRF. These chain of relationships were established in CACAD to determine the effect of change in FRF due to ASRE on spares holding. The complete description and formulation are presented in Appendix C.

3.14.4 Avionics Depreciation Cost

Depreciation of avionics equipment costs as part of aircraft DOC standing charges per flight is inversely proportional to the life of the system (refer to Equation B.225 to B230). The life of the avionics system can be defined as the product of the number of time the system undergoes overhaul, and system typical TBO. On the other hand TBO, is not chosen to exceed the average MTBMF of the system. MTBMF is inversely proportional to system maintenance failure rate. The latter is the product of average number of units in an avionics system, and typical unit failure rate. Typical unit failure rate improvement is shown by reduction in FRF due to ASRE. The above chain of

relations was established in CACAD and the detail formulations are described in Chapter C, section C6.3.

3.15 Special Application of ASRE to Ultra High Capacity Aircraft (UHCA)

It was apparent from the results of the work in the previous sections, that the higher the range and the capacity of a transport aircraft, the more vulnerable they are to engine bleed penalties, making ASRE futile. This is obvious that, due to increase in capacity and range, the amount of mission fuel increases so much that any contemplation of engine sfc is bound to inflict heavy losses on DOC, outweighing any benefits from maintenance cost reductions. Therefore, it was decided later that, an annexation to this chapter is necessary, in which new design solution is explored, and modelled, for future long range high capacity aircraft such as UHCA (or new large aircraft NLA).

In this section, in addition to the application of previous method, a new design solution is presented to boost avionics systems reliability of long range UHCA. The objective is to design an UHCA with a higher reliability potential, with reduced avionics failure rate, and enhanced overall safety, with the possibility of reduced engine penalty for a net reduction in DOC.

3.15.1 Introduction

Two alternative approaches were examined for UHCA, in one the avionics cooling was enhanced by using engine extra bleed air via the air-conditioning system. The second approach, which shall be dealt with in detail, uses an independent air-conditioning system for extra avionics system cooling, alongside the present conventional avionics cooling systems. The task was extended to determine the optimum cooling for maximum reduction in DOC.

3.15.2 Design Proposal 1

The extra cooling air is provided by the engine bleed system, in addition to what is bled for environmental control system (ECS). This method follows the exact methodology, and modelling of previous sections, hence does not require any further description.

3.15.3 Design Proposal 2

In this proposal, an auxiliary cold air unit (ACAU) was modelled, similar to electrically-operated off-the-shelf vapour cycle systems (air mass flow ranges from 15 to 25 lb./min, or 0.1 to 0.18 kg/sec) or an alternative future small boot-strap type in accordance with [86], that is modified to run with an electro-motor. The details of such equipment are presented in the mentioned reference.

The extra cooling flow rate provided by the ACAU shall be directed to the avionics equipment in the compartments and the instruments in the flight deck, joining the main stream of cooling flow provided by the standard ECS, see Figure 3-51, and 3-52 [85]. The type of cooling, cooling characteristics with respect to failure rate, maintenance cost variation with failure rate for both places of avionics systems, were elaborated in previous sections of this chapter. Figure 3-53 shows the schematic diagram of the design proposal 2.

3.15.4 ACAU Mass Estimation, Power Consumption, and Power-off Take Effects

- Mass Modelling :

The mass estimation relationship for the ECS which correlates with the ECS output flow rate, elaborated in 3.9 was modified to predict the mass of the ACAU. The formula, and its description is included in Appendix C, section C7.

In [85] a cold air unit that provides 37 lb/min of cooling flow was targeted at 72 kg, where as the developed equation C36 predicts 160 kg. If an electro-motor be included (used in typical ACAUs, and not in ECSs) and extra weight attributed to engine generator as a result of supplying higher power is also considered, then the above prediction may be treated reasonably conservative.

- Power Consumption Prediction :

It was assumed that the system is of the boot-strap type, and requires an electric motor to provide the net power requirement. The simple first law of thermodynamics was the basis to develop an equation to predict the power consumption of ACAU. This is

included in Appendix C. For a unit to provide 35 lb/min of cooling flow, equation C37 resulted in 15 kW net power requirement, and [30] shows 17 kW for 37 lb/min cooling flow, which gives confidence to the validity of the said equation.

- Power-off Take Effects on Engine Performance :

Engine generators are the main source of extra electric power supply to the ACAU. Typical high-bypass ratio turbofan engines are affected by extra power-off take in that fuel consumption increases, and thrust falls, which must be considered during the cruise phase of the flight. Apart from a few publications that give some insight into the effects of power off take in engine performance, to date there is no published literature to quantify such penalties during different phases of flight for a typical modern turbofan engine. Therefore, the TURBOMATCH code was again used to simulate engine performance while being power off-taken at various flight conditions. The empirical equation thus obtained from the data is presented in Appendix C, section C7. It was validated fairly well with actual data supplied from a prominent manufacturer [76].

3.15.5 Cold Air Unit Maintenance Cost Considerations

The design synthesis treats the ACAU as a small ECS on board, and for the optimum sizing, resulted in a value of £648.71 maintenance cost per 1000 flying hours for 15 hours flight duration. Reference [85] estimated maintenance cost of an auxiliary refrigeration system for the DC-10 as $900 per 1000 flying hours for 12 hours work per day (proposed for cooling avionics system while aircraft is on the ground) which matches with the above prediction. Although it may be claimed that cost escalation factor might have increased the above value, but since 1975 a lot of hard work has gone into increasing the reliability of such equipment [88].

3.15.6 Ram Drag Penalty

Considering design proposal 1, this penalty was dealt with in section 3.10. For design proposal 2, the vapour cycle system cold air unit consumes ambient air for its heat exchangers and therefore there is no need for ram air, and hence increase in ram drag. If cabin dump-air is guided to go through the cold air unit heat exchanger, condensation of

the refrigerant is made possible. For boot-strap type units, this method is also applicable.

3.16 Avionics Reliability Integration in CACAD

In this section the procedure of integrating ASRE in CACAD and its area of influence on the design cycle is briefly presented. Basically there are 11 items of modelling that are incorporated into different modules. They are divided into penalty, and benefit categories, see Figure 3-54.

3.16.1 The Integration Of Penalty Functions Into CACAD

a- Engine thrust Penalty Function : This influences the constraint package of CACAD, where the engine sizing for cruise is dealt with .The mass thrust ratio of the engine at cruise is increased when the thrust reduction due to bleed increment model is operated. Aircraft designed and optimised with a new engine specific mass will have higher engine mass to meet the same mission targets when supplying a higher cooling flow to the avionics systems .

b- SFC Increase Penalty Modelling : This shall influence fuel mass estimate module of CACAD, in which it simply replaces the sfc base value of the engine at cruise with a new sfc, where :

$$(sfc)_{with\ extra\ bleed} = (sfc)_{base} + [\Delta sfc = f(m_{ecs})]$$

the item in the bracket is the fuel penalty function (explained in C2.1). It also influences the values of sfc of the engine during diversion, and sfc during hold. Due to the above modelling integration in CACAD, the mission fuel consumption will increase when the optimiser searches for the most optimum extra bleed flow to the avionics system. Hence the aircraft designed and optimised at each bleed increment will carry a higher mission fuel load to meet the same mission targets .

c- System Mass Module : The new relation for ECS mass as a function of its out put flow is integrated into the CACAD system mass estimation module. This relation allows CACAD to allow for a heavier ECS at every bleed step,

- consequently producing aircraft with a higher system mass and hence higher zero fuel mass .

When the above penalties are implemented into CACAD, they collectively push the final design of optimised aircraft to be progressively larger and heavier at every bleed increment step.

Higher take-off mass contribute to higher aircraft prices that in turn push the depreciation cost part of DOCs to higher values. Higher mission fuel flow not only indirectly increases the take-off mass, but directly increases the fuel cost part of the DOC. Finally, the increase in system mass not only increases system price, but it also contribute to higher airframe and engine mass. This leads to higher maintenance material and labour cost elements of DOC, excluding avionics.

3.16.2 The Integration Of Benefit Functions Into CACAD

The following models together establish the benefit functions.

1- Avionics equipment bay junction temperature versus bleed flow rate.

2- Flight deck avionics deck case temperature versus bleed flow rate.

3- Avionics equipment bay failure rate versus its junction temperature.

4- Flight deck avionics deck failure rate versus its case temperature.

5- Avionics maintenance labour, material, spares holding, and standing charges versus avionics failure rate factor in the flight deck, and equipment bay.

They are integrated into objective function i.e. DOC . At every bleed increment, relations 1 & 2 determine the temperature drop, in avionics bay and flight deck. The calculated temperature drop is used in models 3 & 4 to establish the reduction in failure rate factors, which in turn are substituted in the models outlined in 5. They have been integrated into different sections of the DOC to determine the reduction in labour, and material cost of avionics together with the reduction of spares, and depreciation charges

.

3.17 CACAD Operation With ASRE Incorporated

In the design process, both penalty and benefit functions impart their influences on DOC simultaneously. CACAD takes each value of bleed increment separately and designs and optimises an aircraft for the minimum DOC and prints out the results. Thereafter it selects another incremental value of bleed, and repeats the whole process. This is then repeated for all types of aircraft defined in the mission input file. In this way, the user is provided, in one operation a series of aeroplanes whose various details such as geometry, masses, aerodynamic coefficients, prices, and DOC breakdown are stored in different output files. These output files are formatted so that they are retrievable by spread-sheet packages to facilitate tabulation and graphical representation of results.

CACAD with avionics reliability improvement modelling incorporated into it offers the user the following services :

- An optimised aircraft configuration with user-defined missions that has optimum potential for avionics reliability.
- A wide range of sensitivity analyses can be executed, such as aircraft range and capacity variation, fuel price and labour rate variation, and sfc improvement.
- Any other system reliability modelling once established can be incorporated into CACAD for the similar feasibility studies.
- Any type of fixed geometry, resembling either existing or future aircraft can be dictated to CACAD for avionics or any other system reliability enhancement study.

3.17.1 CACAD Operation with ACAU For UHCA

CACAD was modified to design and optimise a double deck fuselage passenger aircraft of long range, high capacity known as New Large Aircraft (NLA), or UHCA, whose specifications are elaborated in Chapter 2, and Appendix B.

ASRE modelling of the Design Proposal 2 consisted of installing an ACAU in the UHCA, in addition to its conventional cooling system. The above modelling were

incorporated into CACAD to simulate the presence of the ACAU. CACAD takes each value of extra cooling flow separately and with this, it designs and sizes an appropriate ACAU, estimates engine thrust and sfc penalties, and like previous sections, computes the amount of maintenance benefits. Finally it designs and optimises an UHCA for the minimum possible DOC, and prints out the results, thereafter incrementing the value of cooling flow and repeats the whole process.

3.18 Discussion of ASRE Simulations, and Validation

Four classes of passenger aircraft were chosen as follows :

(a) Low-capacity/short range, aft fuselage mounted of a class of aircraft similar to the Focker F100, with a class of engine similar to the Tay 650.

(b) Low to medium capacity, short to medium range, a twin aircraft of a class, similar to the Airbus A310, with a class of engine similar to the CF6-80C2.

(c) A medium-capacity, medium-range, a twin aircraft, of a class, similar to the Airbus A330, with a class of engine similar to the TRENT 775.

(d) A medium-capacity, long range, quadro aircraft, of a class similar to the Airbus A340, with a class of engine similar to the CFM56C2.

A separate mission file was established for each. Above missions cover nearly all present passenger aircraft flying today. The Airbus family class were preferred to Boeing family solely because the design formulation within CACAD matches closely to the European aircraft. The details about each class of aircraft is dealt with in Chapter 2. For each mission there are built-in thrust and sfc penalty functions, related to the engine class used, that is chosen by CACAD appropriately (see section C2.1).

3.18.1 Presentation of Results

CACAD was run for each mission, and the results of all four missions are treated together. Figure C.13 shows the DOC major breakdown for each mission . Note the percentage of fuel cost in every mission. Figure C.14 shows the mission fuel and mass take-off increase for each mission, at every bleed increment. Figure C.15 shows fuel mission increase for all missions together. Note that every point, in every curve

represents an optimised aircraft for the chosen value of bleed. The growth in engine size and wing area for every bleed increment step is depicted in Figure C-16 for each mission. Due to benefit functions operating inside CACAD, the percentage of standing charges, spares holding costs, and maintenance labour & material costs are progressively reduced with each bleed increment. The results are shown in Figure C-17.

The net effect on DOC, and hence the resultant percentage saving on DOC, is shown in Figure C-18 for all missions.

A sensitivity analysis based on maintenance labour rate cost variation, down to 25.0 £/hr, and up to 30 £/hr from a base value of 27.3 £/hr [14], was launched, and the resultant DOC variation for all steps of bleed flow increment is illustrated in Figure C-19 for all missions.

Another similar study, based on fuel price variation, down to 0.17 £/kg, and up to 0.21 £/kg from base value of 0.19 £/kg was done, and the resultant DOC variation for all steps of bleed increment is shown in Figure C-20 for all missions.

To model the most conservative DOC effect, and to remove any doubt on the validation of the bleed penalty effect on various engine sfc, the Author raised the sfc penalty by 25%, and the resultant DOC saving is shown in Figure C-21 (this excludes the Tay class which has already shown high rise in sfc).

3.18.2 Analysis of Results :

1. Short range low capacity aircraft such as those in F100 class have maintenance costs which account for a large portion of the DOC. This is because, they have a low mass, leading to a low initial cost, and therefore low depreciation charges. They also have mission low fuel mass, and hence costs, see Figure C-13a. This type of aircraft shows less penalty on mission fuel, and take-off mass due to higher bleed from the engines, as shown by the slope of the curves in Figure C-14a as compared with Figure C-14b,c,d. The F100 class also show least penalty in wing area enlargement and increase in engine size. This is also verified by the slope of the curves in Figure C-16a,b,c, and d.

Note : There is a sudden out-of-trend rise in the take-off mass slope, and a slight reduction in mission fuel mass slope at 1 lb/min/kW of extra bleed for the F100 class in Figure C-14a. The same pattern is observed in Figure C-16a. This is because every point in the diagram shows an aircraft designed and optimised at that bleed condition. At this particular bleed, a higher aspect ratio was selected by the optimiser resulting in higher wing mass hence take-off mass, and lower drag hence lower fuel consumption.

2. Long range medium-capacity aircraft, such as Airbus A340 class, being at the other extreme among the four selected classes of aircraft behaves in the opposite way. Aircraft price and hence standing charges, as well as mission fuel cost both make up higher percentages within the total DOC, pushing maintenance cost to a lower proportionate value, see Figure C-13b. It also shows a higher penalty on mission fuel, and take-off mass, due to higher bleed from the engines, as shown by the slope of the curves in Figure C-14b. This is further verified by the mission fuel mass penalty of all four aircraft together in Figure C-15 . The same trend is observed for wing area and engine thrust in Figure C-16b.

3. Due to the nature of avionics reliability enhancement measures, which consume fuel and require higher system and engine masses for reducing the maintenance cost, the DOC savings of a short-range low-capacity jet transport of the F100 class enjoy more savings from such ASRE than the long-range A340 class . This is verified by Figure C-18.

   Note : The other two aircraft namely the A310, and A330 always stay in-between .

3.18.3 Sensitivity Analysis

Labour rate and fuel price may vary among the airlines, and even countries of the world . In an extreme case, an airline may enjoy very low labour wages, but has to import fuel from abroad and has hard-currency difficulties. They will not welcome an aircraft which may consume more fuel to give lower avionics maintenance cost. In this type of study, the global economy is considered . Countries which are major users of transport

aircraft usually exhibit a predictable and uniform economic condition in which fuel price, and labour rate may vary within ±10% .

Having said that, the main objective of sensitivity analysis is different from that outlined above. It is conducted to consider future economic trend and its impact on the feasibility of undertaking such project work.

1. Labour rate variation is based on the quality of life. The Author has the opinion that in the next 25 years, this must increase, with growth in skill requirements, and higher sophistication in repair procedure of the future advance aircraft in the South Pacific, Western Europe, and North America. There are other arguments that suggest that China, and other countries where labour rates are low will get the chance to participate in highly skilled maintenance work, lowering the labour rate. Therefore a sensitivity analysis against labour rate of ±10% was conducted in CACAD.

   The results show that this has little impact on outcome of DOC saving in the different classes of aircraft; see Figure C-19.

2. Fuel prices may drop further, as more fuel resources are discovered in countries whose growth in population and their need of hard currency may force to flood the market with cheap oil. Internal conflicts, other regional conflicts among these countries, and world resources shortages, on the contrary, may result in lower fuel supply. Therefore a sensitivity analysis against fuel price increase of ±10% was conducted in CACAD. The results show that the impact of reduction in fuel price on long range aircraft is not so strong to increase DOC saving to the threshold of 1%, to make such ASRE modelling worthwhile, see Figure C-20.

3. Another benefit of sensitivity analysis is the ability to exaggerate the impact of a certain model on the sizing and costing process within CACAD. In ASRE, the main source of penalties is the effect of bleed on engine sfc. Although care was taken to establish a realistic prediction equations, it is always useful to exaggerate this in order to evaluate firmly the success of such modelling. A

25% under-estimation factor was incorporated into the cruise fuel estimation module (except for F100 class, as the bleed effect equation seems already an over-estimation). The results indicate that although DOC saving is reduced, the reduction is not so significant as to abandon this project for short to medium classes of jet transport aircraft, see Figure C-21

3.18.4 Discussion Of Results For UHCA

Results of design proposal 1 is shown in Figure C-22. The results were obtained for two options. The graph No.1 corresponds to the case when extra bleed is equally taken from each engine and the graph No.2 corresponds to letting all engines share the bleed requirements. Graph 3 in Figure C-22 shows the results of the application of design proposal 2 to UHCA. The saving in DOC is slightly higher than design proposal 1, but for following reasons the latter REM is superior to the former :

(a) The system requires electric power that in turn requires further shaft power-off take from the engines . This has less impact on fuel consumption than bleed, and engines are usually less sensitive to it .

(b) The system is fail-safe, due to conventional running of the avionics cooling system as an integral part of the ECS .

(c) The system is non dispatch-critical i.e. it does not prevent the flight in the case of system malfunction.

(d) The system is operational while the aircraft is on the ground using ground support equipment. This addresses the problems reported in [85] that so many passenger aircraft spend considerable hours a day parked on the ground while compelled to run their avionics systems.

(e) The mass estimation of the ACAU is conservative, power estimation is realistic and fuel penalty due to power off take is also realistic enough to strongly recommend such a scheme for UHCA.

3.18.5 Validation of Results

The validation of the results obtained from this chain of modelling integration in CACAD differs from usual validation procedures. This may be treated implicitly through the validation of each model used. The engine bleed model causes the size, the mass, and the fuel consumption to grow. The rate of growth was validated in section 3.8.5 with real engines namely the Tay, and the Trent. The growth of ECS mass with the rise in its output flow was validated with real transport aircraft whose ECS mass are tabulated within volume 4 of [15]. Flow supply to avionics compartment and flight deck and the associated temperatures of equipment in these areas are based on experiments conducted in Grumman, and Boeing reported in [79], and [82].

The avionics equipment temperature, and avionics reliability was also based on real life data reported in [84], [83], and [138] is widely accepted by Industry (quoted in those reports). The share of avionics in total maintenance cost is also important in validation of the economic feasibility of the results. A number of reports put the share of this system highest, after furnishing, and landing gear [55to62]. An independent report carried out by Cranfield University [38] was chosen to allocate the share of avionics in total maintenance cost. Recent references such as [47] allocate higher shares, and that of Boeing [37] give closer values to the one selected in ASRE.

The above validated models were integrated in CACAD whose ability to produce reasonable baseline transport aircraft was validated in Chapter 2. However final aircraft which is heavier, costlier to buy, but with lower DOC, higher dispatch reliability, and safety cannot be validated directly. Unless an airline or a manufacturer applies the instructions of this research work for a period of two years.

The latest report for defence of this work is about the F-15 fighter [87]. It underwent an avionics cooling enhancement program. Although no quantity was included (for obvious reasons), the field experience has shown the overall maintenance cost has dropped and fighter readiness has risen, which is equivalent to transport aircraft dispatch reliability. Apache Longbow high performance attack helicopters possess high output low weight military avionics. Two independent ACAUs operated with an

electro-motor replaces the conventional boot-strap air cycle machine to avoid engine bleeding, that adversely affected engine performance [88]. This has produced 20% higher cooling efficiency, with lower impact on engine performance due to power-off take effect.

3.19 CONCLUSIONS

1. The bleed penalty was only applied to a single engine, which is a gross over-estimation, as in real-life engines are going to share the extra cooling flow to the avionics systems (only in emergency cases is one engine bleed considered). Considering this sfc penalty exaggeration, high labour rate, and high fuel prices, it is concluded that there exists a definite minimum of 1% DOC saving for all classes of aircraft from low to medium range, low to medium capacity if designed for higher avionics reliability through higher cooling techniques. There will be higher saving with more realistic assumptions.

2. Due to the high percentage of fuel cost in the DOC of long-range aircraft, the bleed penalty effect on mission fuel mass, outweighs the benefits in avionics maintenance cost. Hence, due to high percentage of fuel cost in DOC, the rise in its saving is lower, or negligible for the long-range A340 aircraft class.

3. For UHCA, and for the same reason for an A340 class of aircraft, using an ACAU, to provide extra cooling to avionics equipment, proved an assured DOC saving.

4. Optimum aircraft are heavier than the non-optimum ones, when DOC is taken as the objective function for all missions, hence justifying the cost selection being superior to the classical take-off mass, or mission fuel mass objective functions.

5. Maintenance labour rate variation's impact on avionics RE is negligible . The reason lies within the fact that the labour cost contribution to total of maintenance material, depreciation, and spare parts holding cost is very small, *hence it is possible to conclude that any maintainability improvement, which is directed toward improving either removal and replacement time, and or repair*

time, if accompanied with any penalty side effects is bound to result in a cost penalty.

6. Fuel price reductions will make reliability improvements on any system including avionics, a more feasible project . The reason lies with the fact that, the majority of enhancement techniques require power either in the electric or pneumatic forms, that must be provided one way or another by the aircraft power plant . Even those systems that use ambient ram air will produce ram drags that must be coped-with by extra engine thrust, and fuel.

7. The sfc penalty sensitivity analysis shows that its impact on overall behaviour of the avionics RE feasibility for all missions is negligible, releasing the Author from the burden of finding such sensitive data from industry . This leads to the fact that only the base value of sfc of the engine is crucial in avionics RE modelling, not so much its behaviour while being bled.

Table 3-1

A generic presentation of REM and its areas of influence in CACAD

System Name	*Division*	*More Reliable Components*	*REM Implications on CACAD*
Fuel	Supply	Fuel Tank	Wing area or wing mass increase, cost increase
		Fuel Pump	Higher power consumption : SFC rise fuel mass increase, system mass and Cost increase
	Trans-mission	Fuel pipe lines, valves, sensors and switches	System mass increase, higher cost
	User	Engine	Engine is treated as an independent system
Hydr-aulics	Supply	Hydraulic Accumulator, Generator/Hydraulic Pumps	Higher power consumption : SFC rise fuel mass increase, System mass
	Trans-mission	Pipe lines, valves, sensors and switches	System mass increase, and system cost
	User	Actuators	System mass increase, and system cost
ECS	Supply	Bleed System, Air-conditioning Unit, Control Units	System mass, and cost increase, rise in aircraft drag
	Transmis sion	Air Ducting, Valves, Sensors, and Switches	System mass, and cost increase
	Users	Passenger, Avionics Equipment	Passenger comfort factor
Avio-nics	Supply	Electric Generators, Converters, Batteries	Higher power consumption : SFC rise fuel mass increase, system mass and cost increase
	Transmis sion	Wires, Busbars	no relation with CACAD
	Users	Avionics Black Boxes, Flight Deck Instruments	Subject of this Chapter.

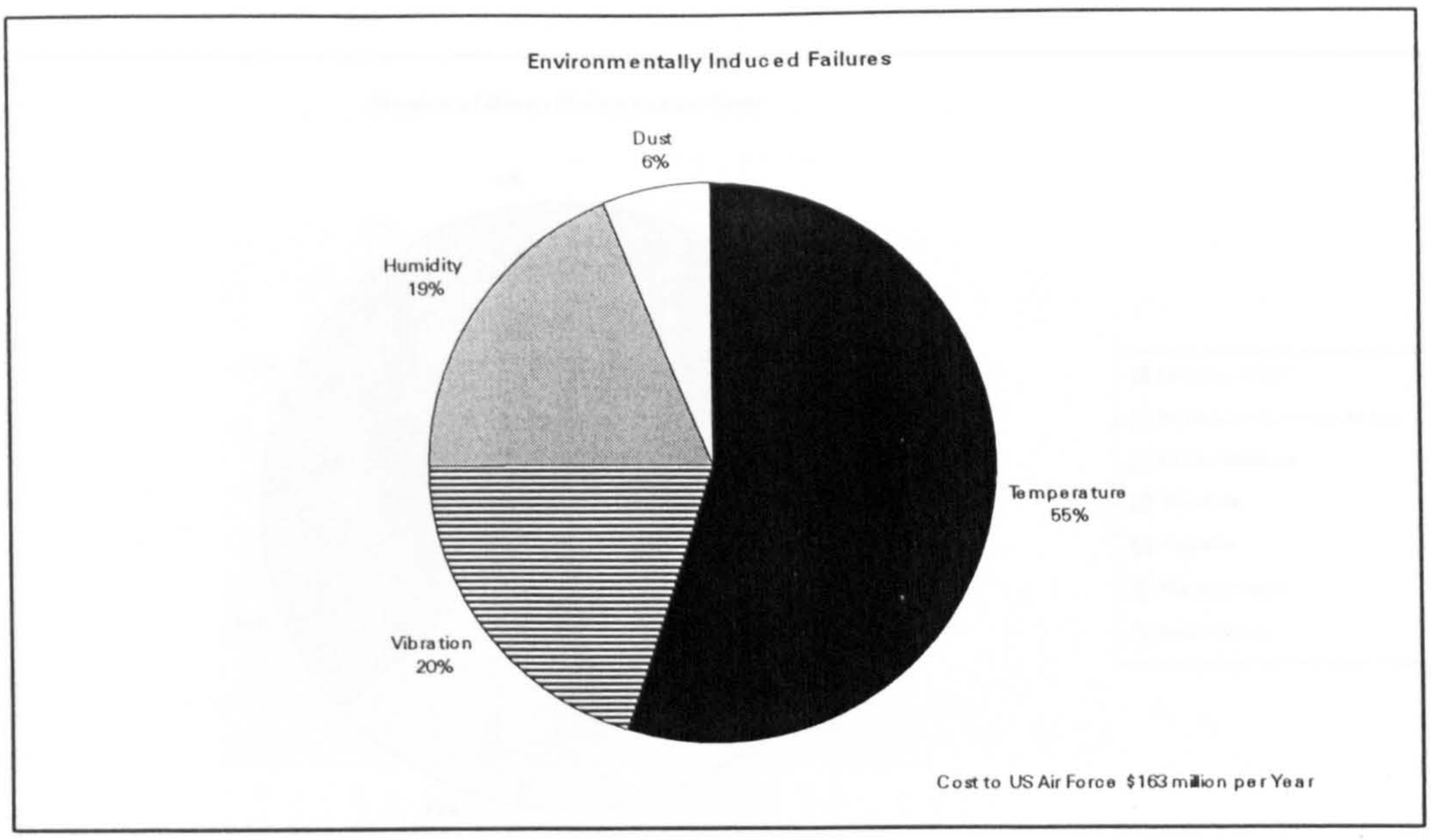

Figure 3-1 : The high share of temperature on environmentally induced failures among avionics equipment developed from [51]

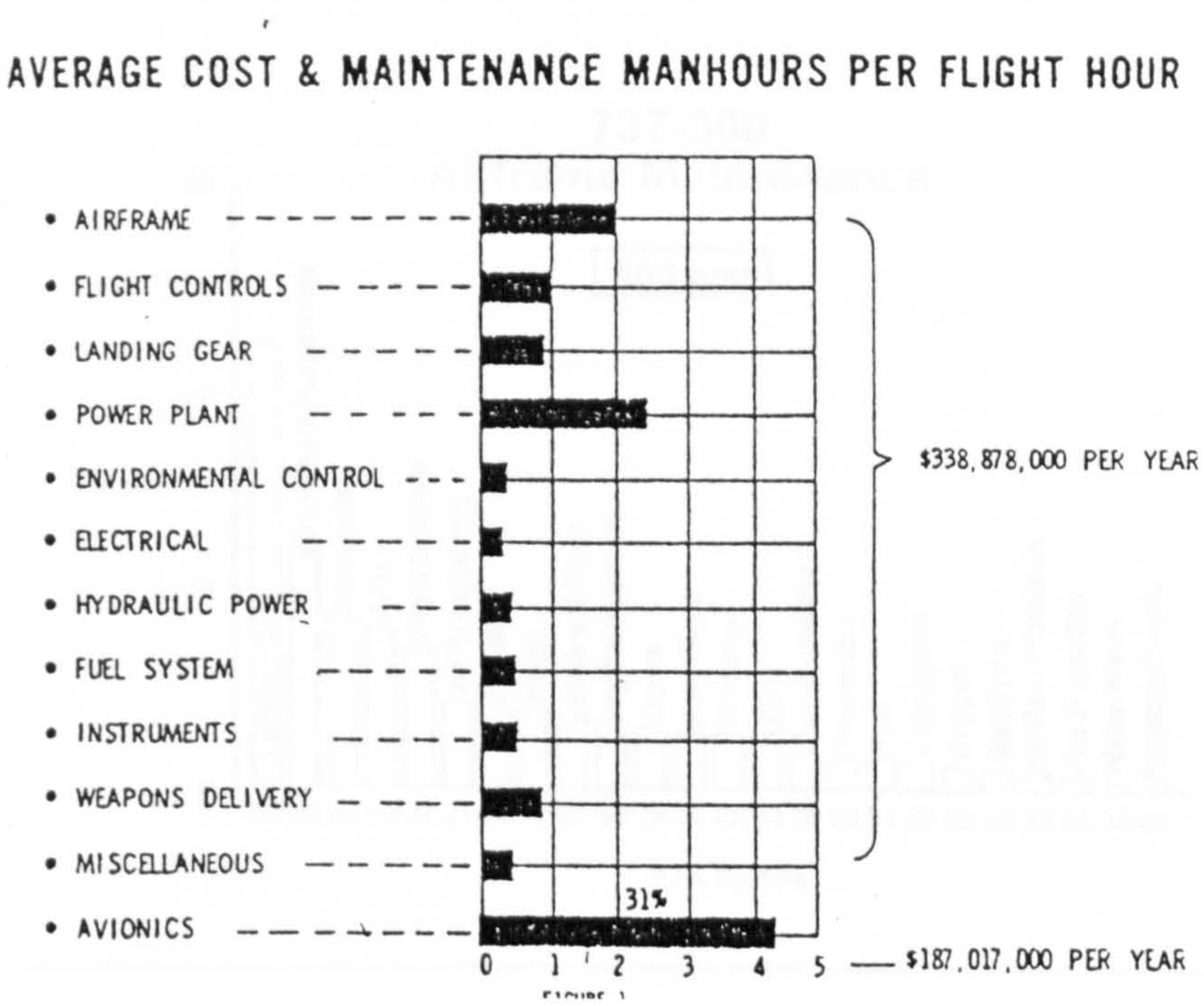

Figure 3-2 : Aircraft system maintenance cost distribution among USAF combat aircrafts [52]

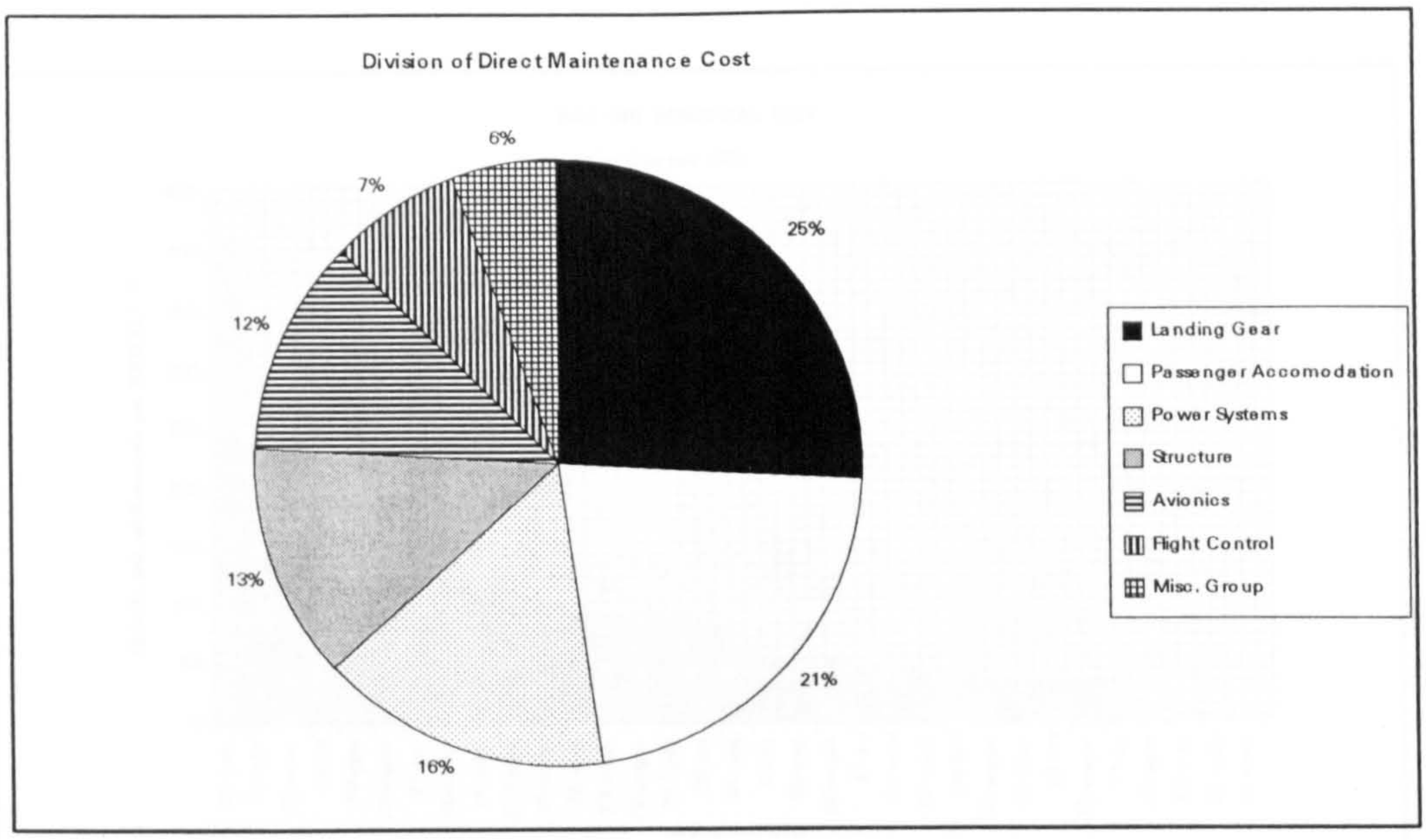

Figure 3-3 : Civil passenger Maintenance cost major break-down [38]

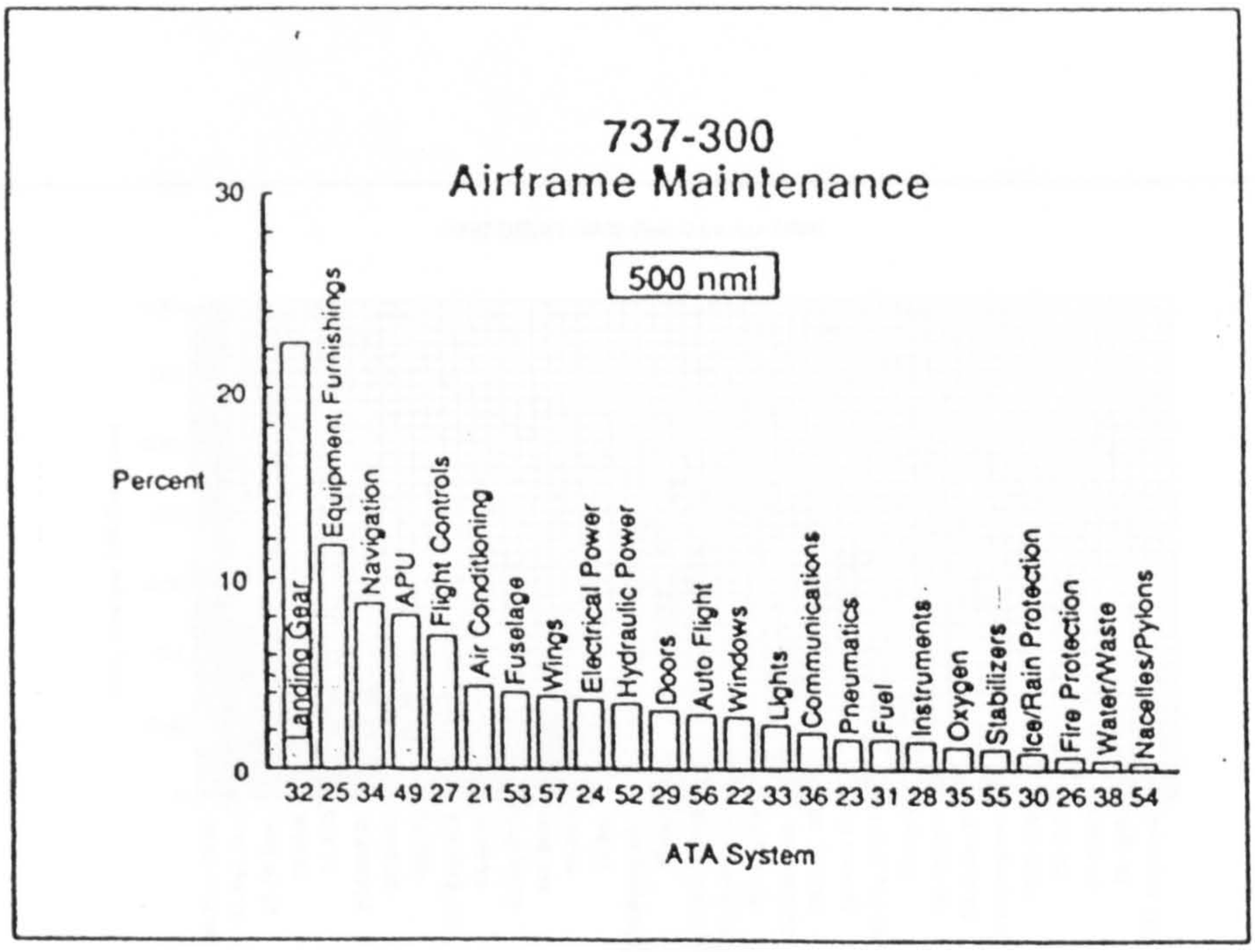

Figure 3.4 : Boeing 737-300 airframe maintenance cost break-down developed from [37]

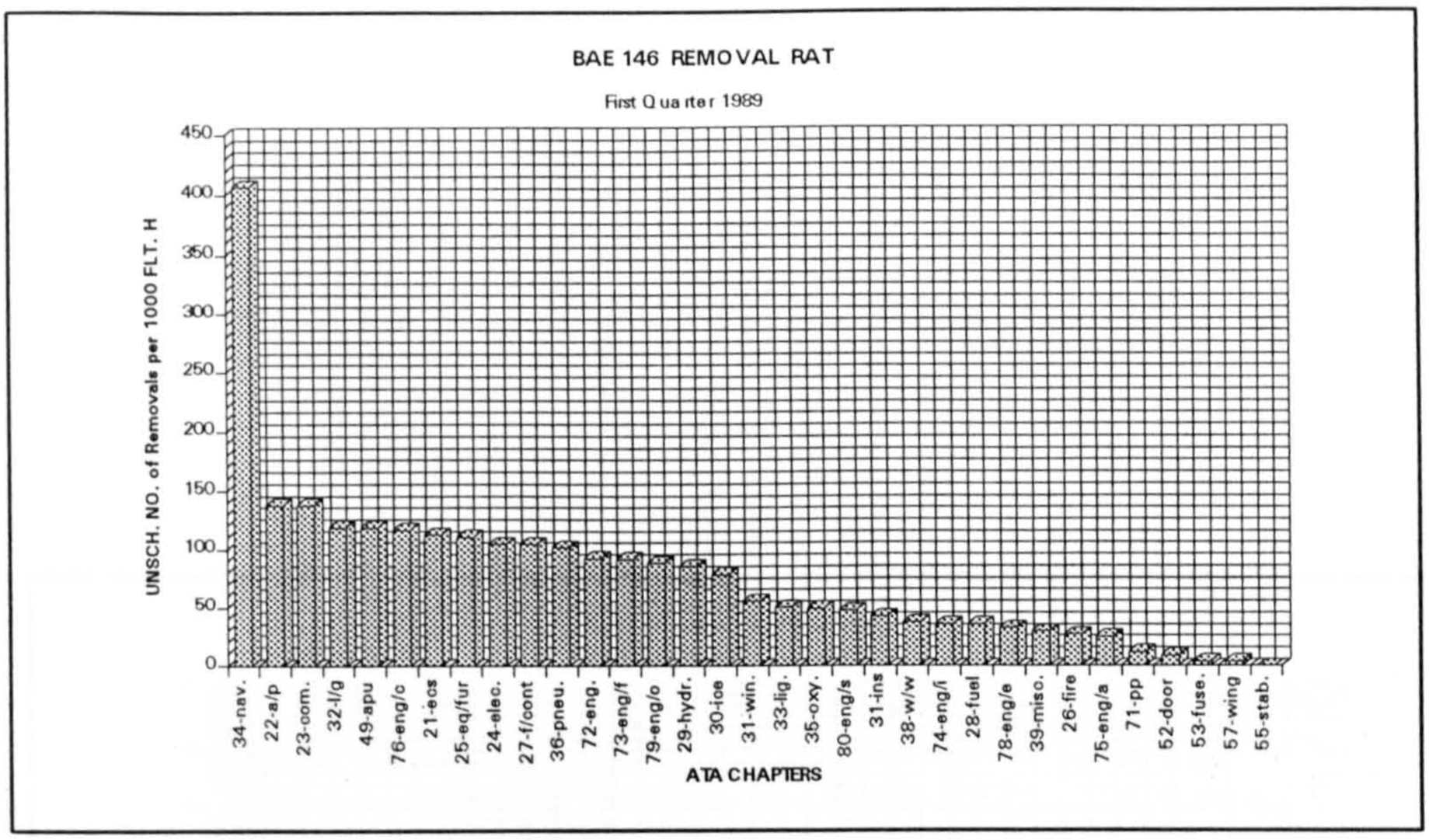

Figure 3-5 : BAE146, removal rate per ATA chapter break-down developed from [62]

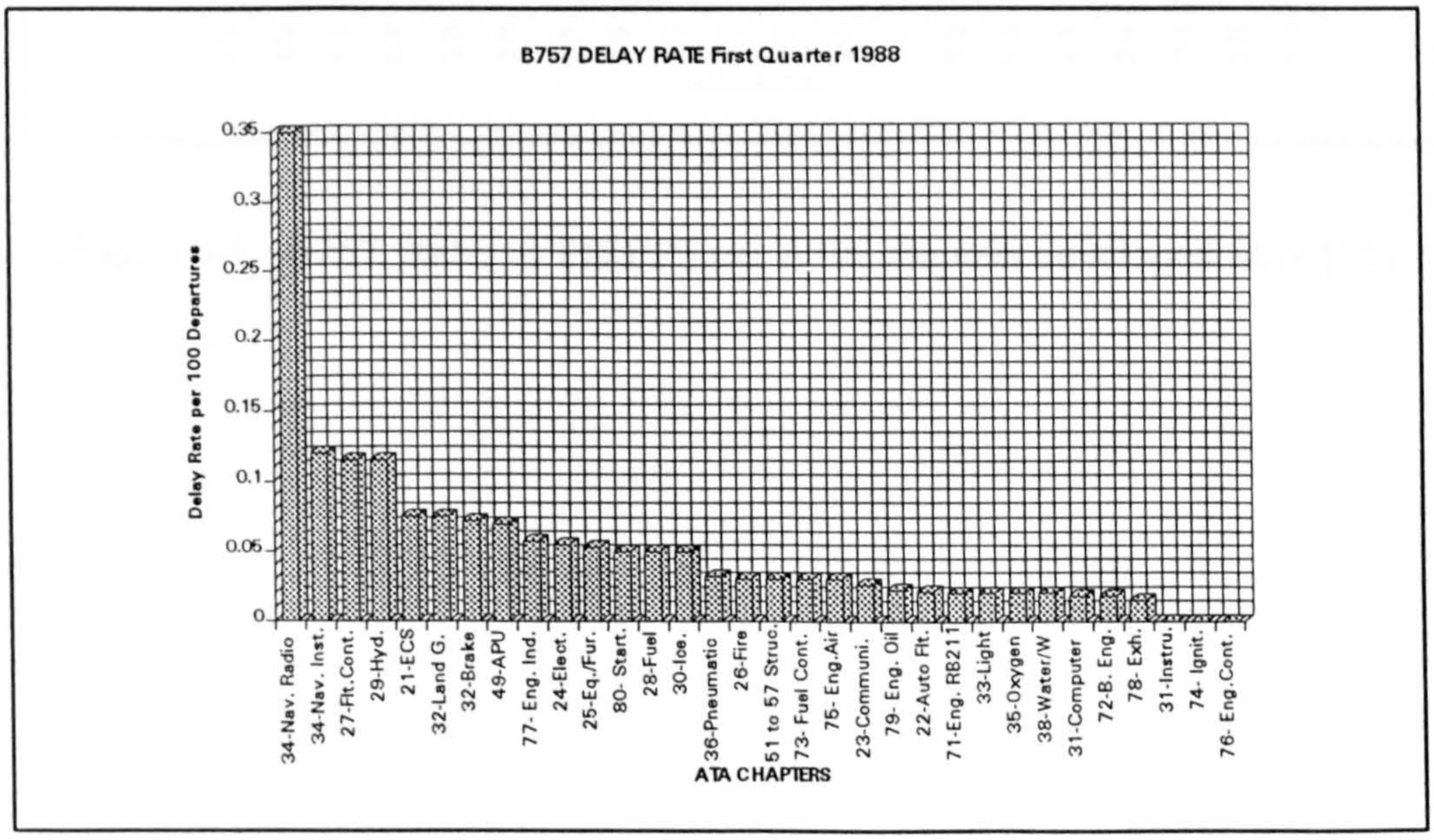

Figure 3-6 : B757, delay rate per ATA chapters developed from [57,58]

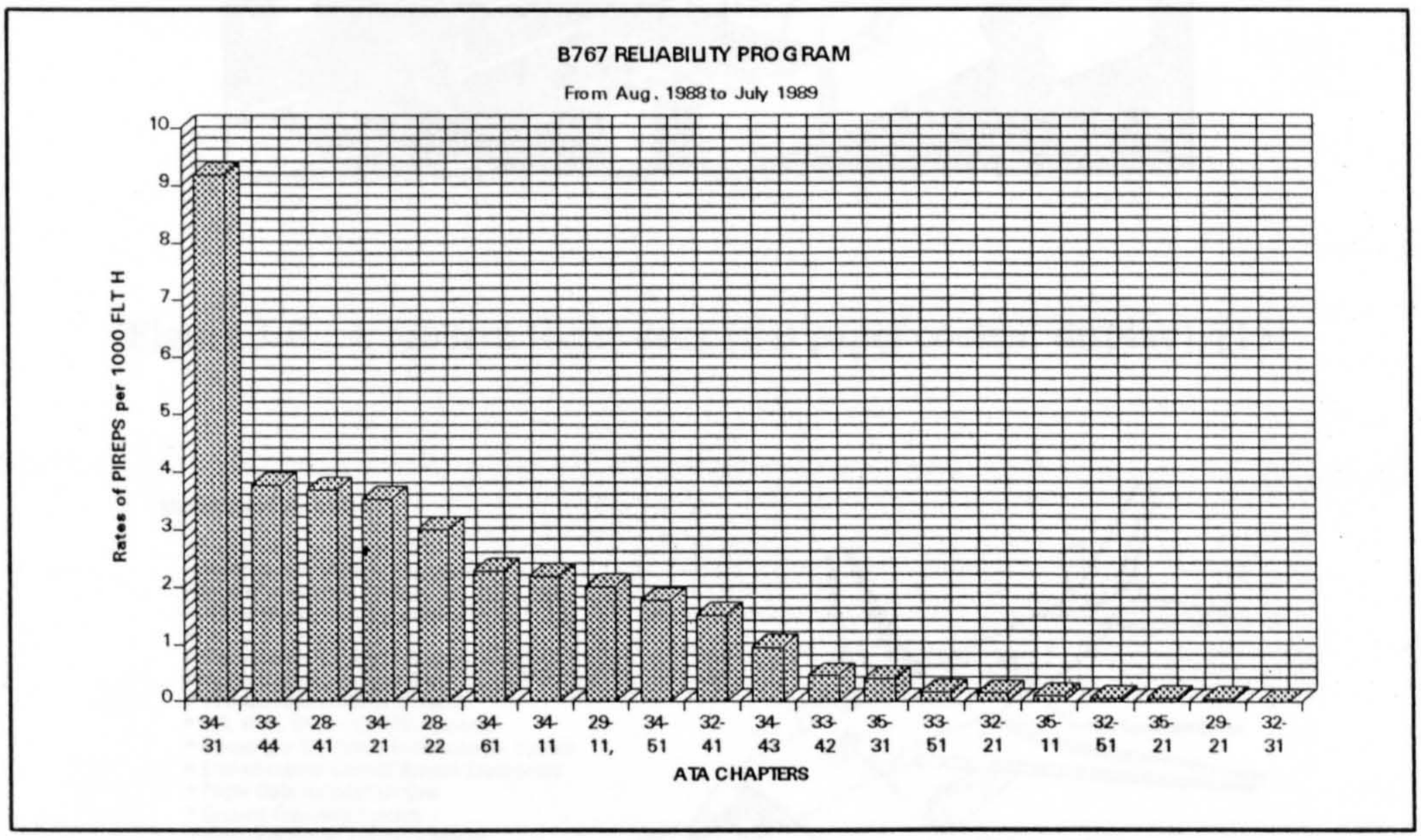

Figure 3-7 : B767, Rates of PIREPS per ATA chapters developed from [55]

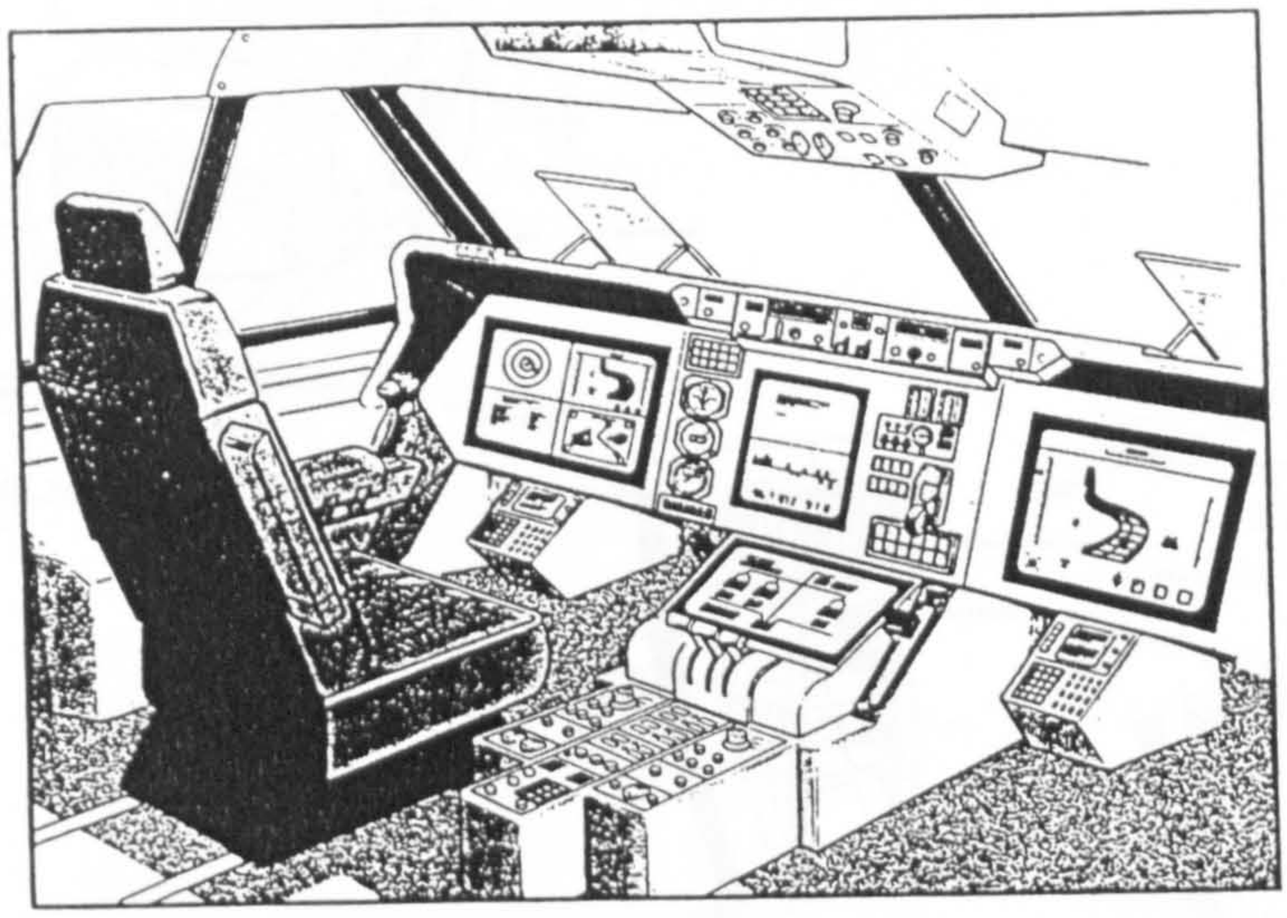

Figure 3-8 : A modern flight deck (flat panel cockpit display), [15]

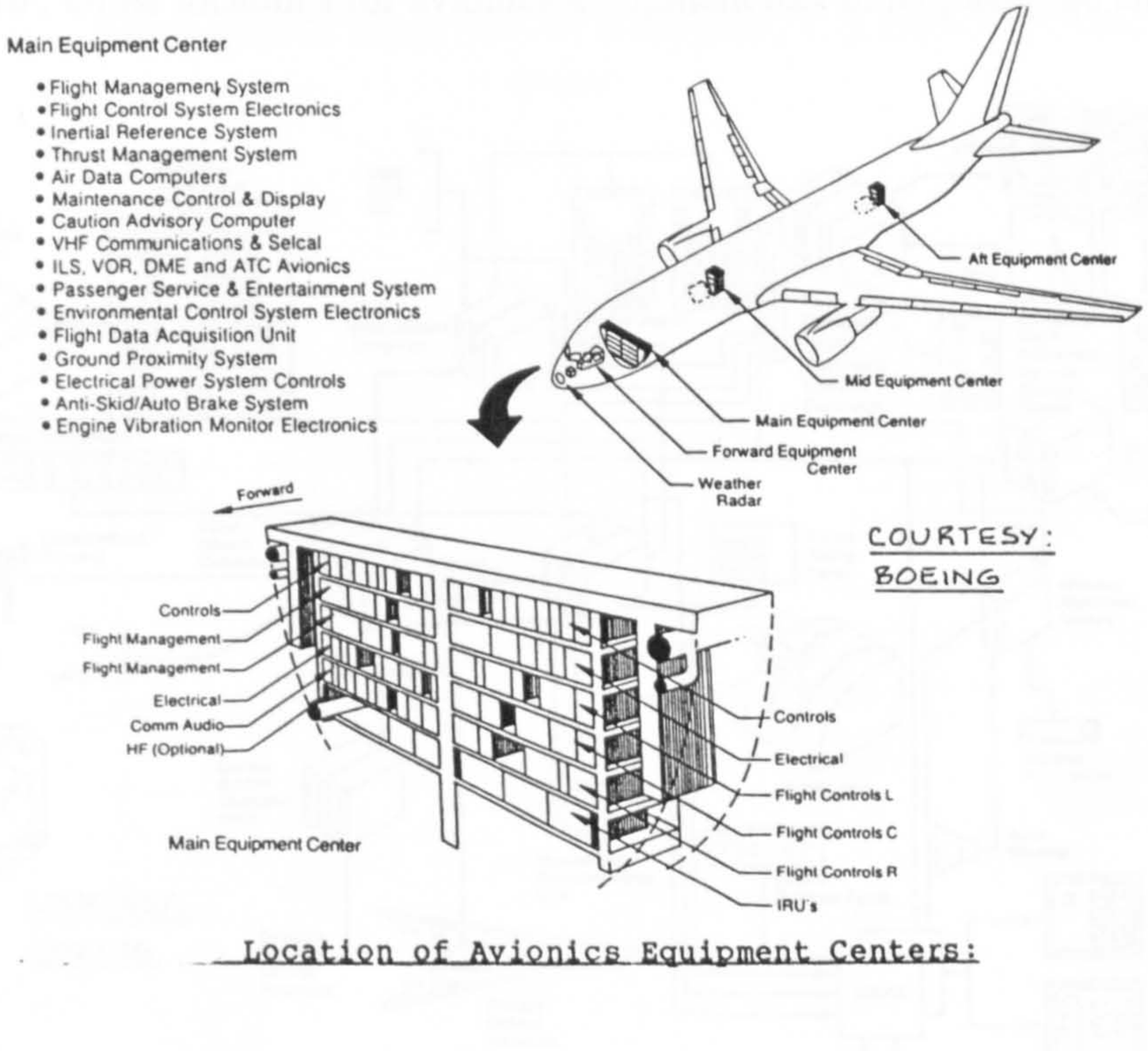

Figure 3-9 : Location of avionics bays in a typical jet passenger aircraft [15]

Features of Weather Radar

- Visual indication of storm conditions and areas of turbulence at ranges up to 320 miles
- Color-coded displays for levels of turbulence/precipitation
- Built-in test (BIT) capability to check system performance
- Meets requirements of ARINC 708 and FAA T50 C63b

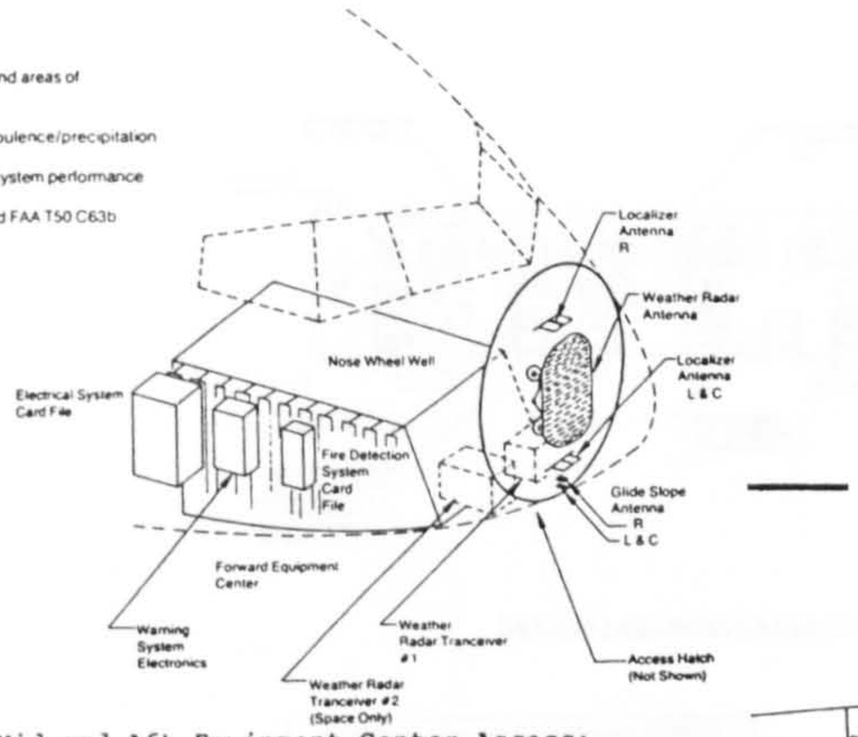

Mid and Aft Equipment Center Access: Boeing 767

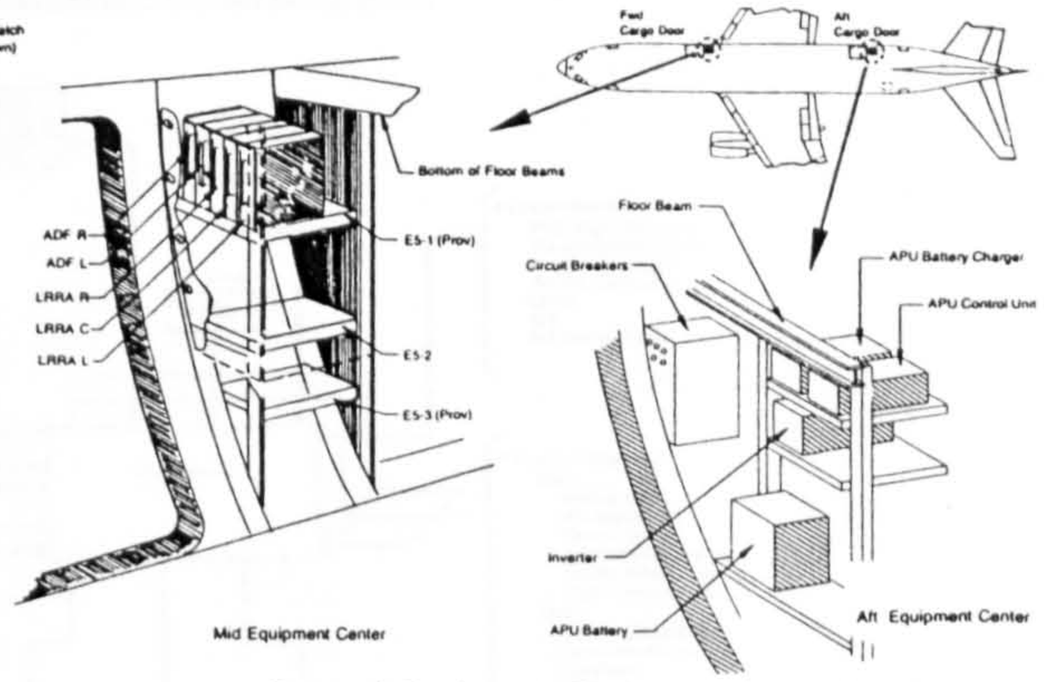

Forward Equipment Center, Radar and Flight Control Antennae Access: Boeing 767

Figure 3-10 : Other locations for avionics equipment bay in jet passenge aircraft [15]

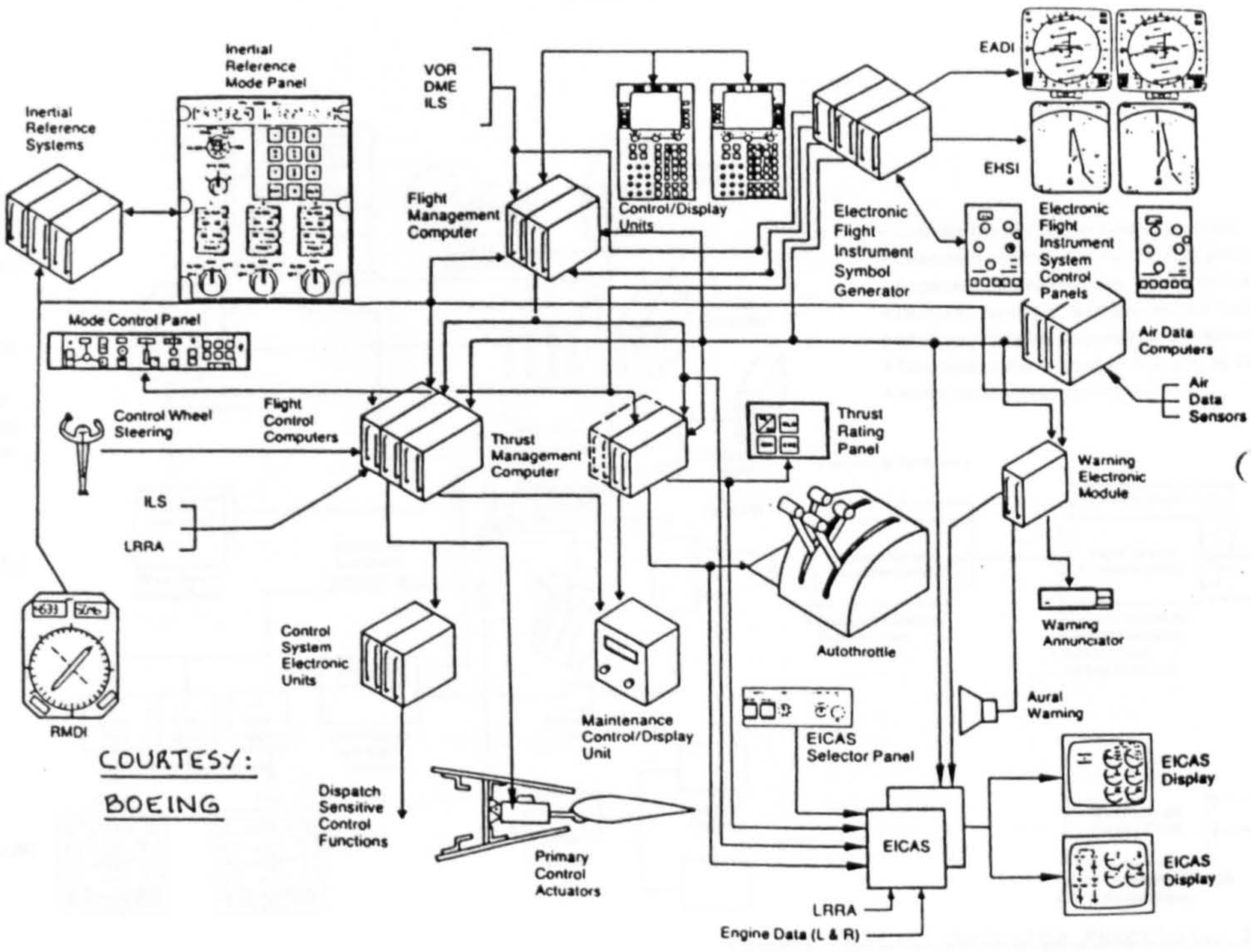

COURTESY:
BOEING

Figure 3-11 : Schematic diagram of FMS [15]

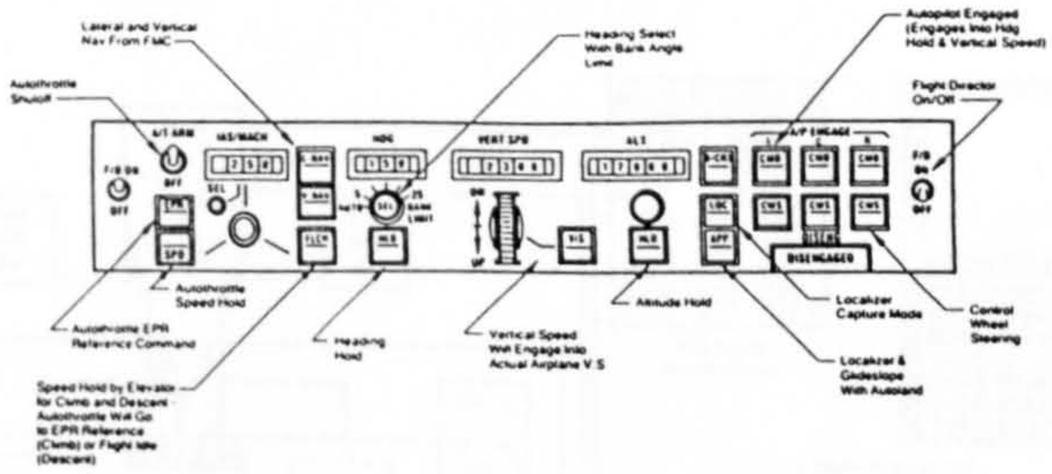

Autopilot/Autothrottle Control Panel:

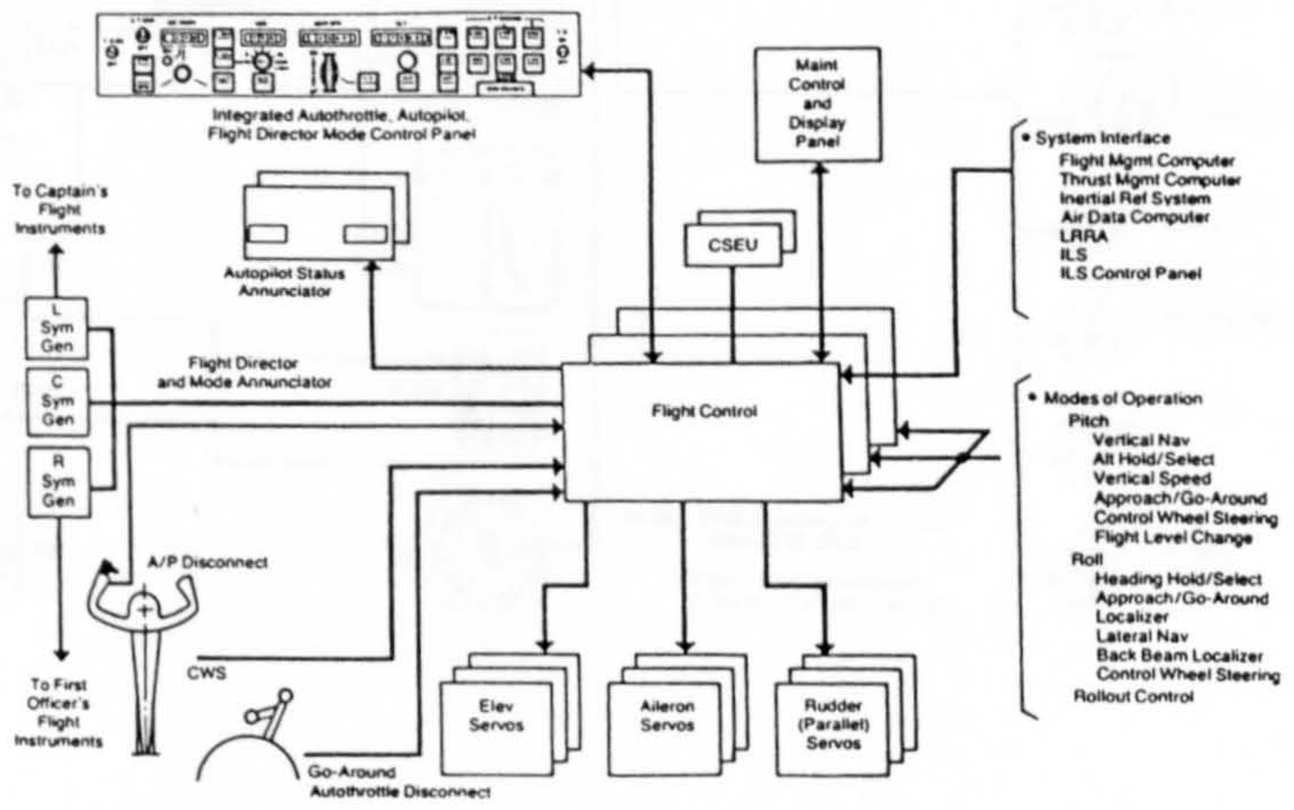

Figure 3.12 : Schematics of flight control computers, and auto-pilot, auto-throttle panel.

- Thrust rating
  - Thrust limit computation
  - Thrust derate
- Autothrottle control
  - Controls to thrust limit
  - IAS/Mach select
  - Autoland flare retard
  - Overspeed protection
  - Overboost protection

COURTESY : BOEING

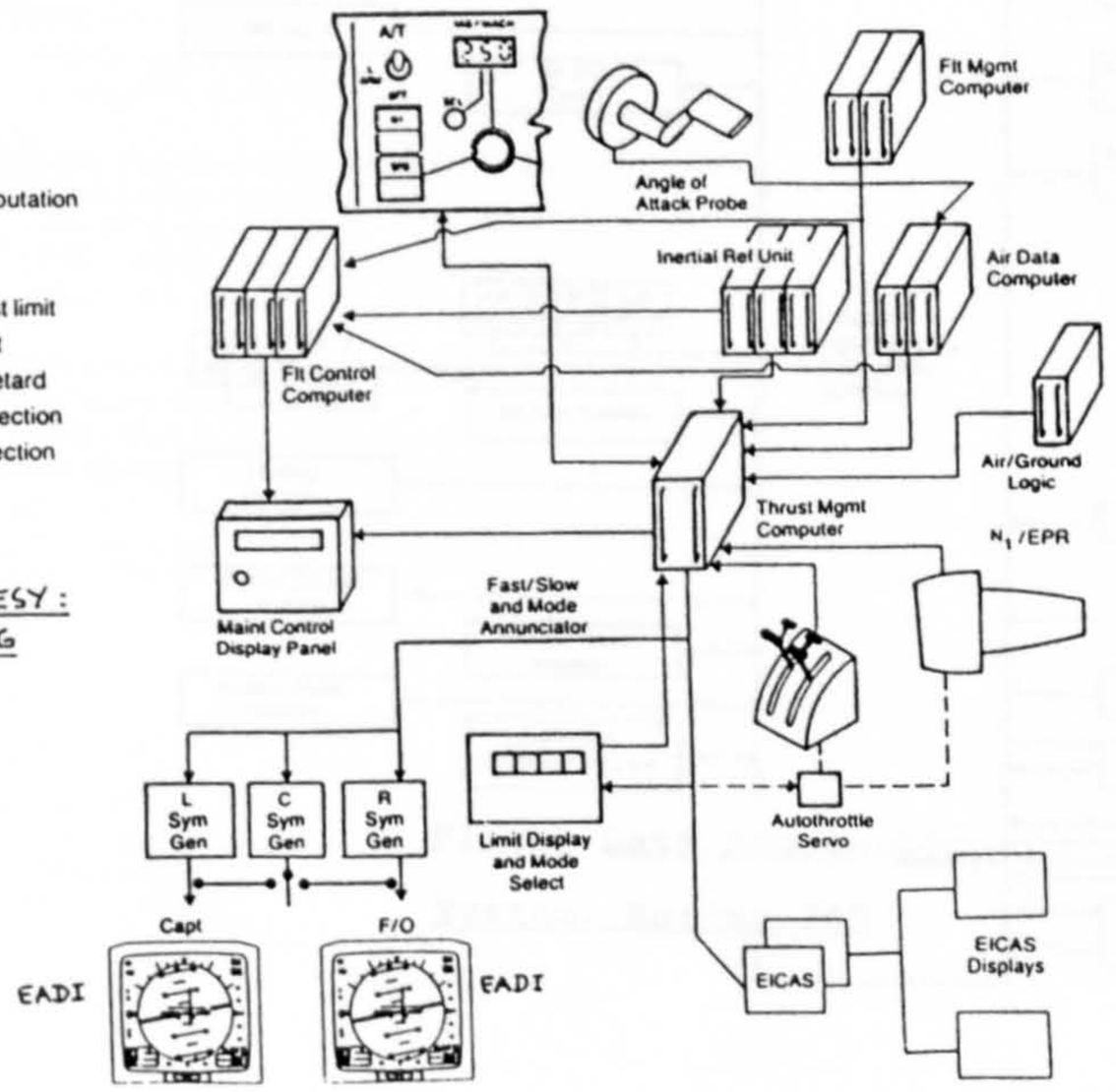

- Category IIIb and Rollout Guidance (Basic)
- Category II Achieved by LRU Deletion (Dual)
- Dispatch Sensitive Functions Separated in a CSEU Box
- Integrated Autopilot, Flight Director and Turn Coordinator
- Integrated Thrust Management and Autothrottle Functions
- Growth/Operational Changes Primarily by Software.
- Advanced Maintenance Capability

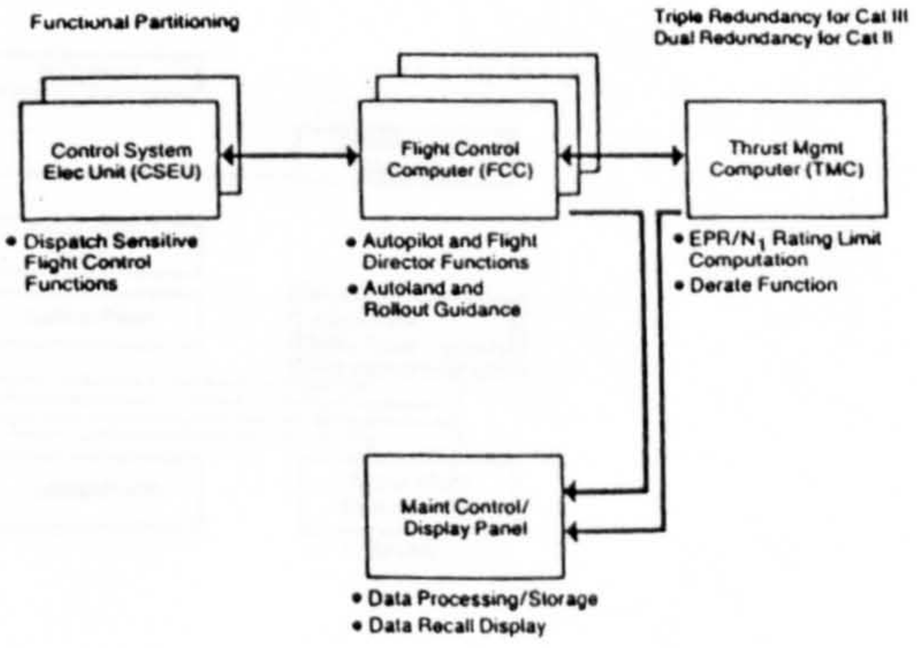

Flight Control Avionics Functions: Boeing 767

Figure 3-13 Thrust management computer functions schematics

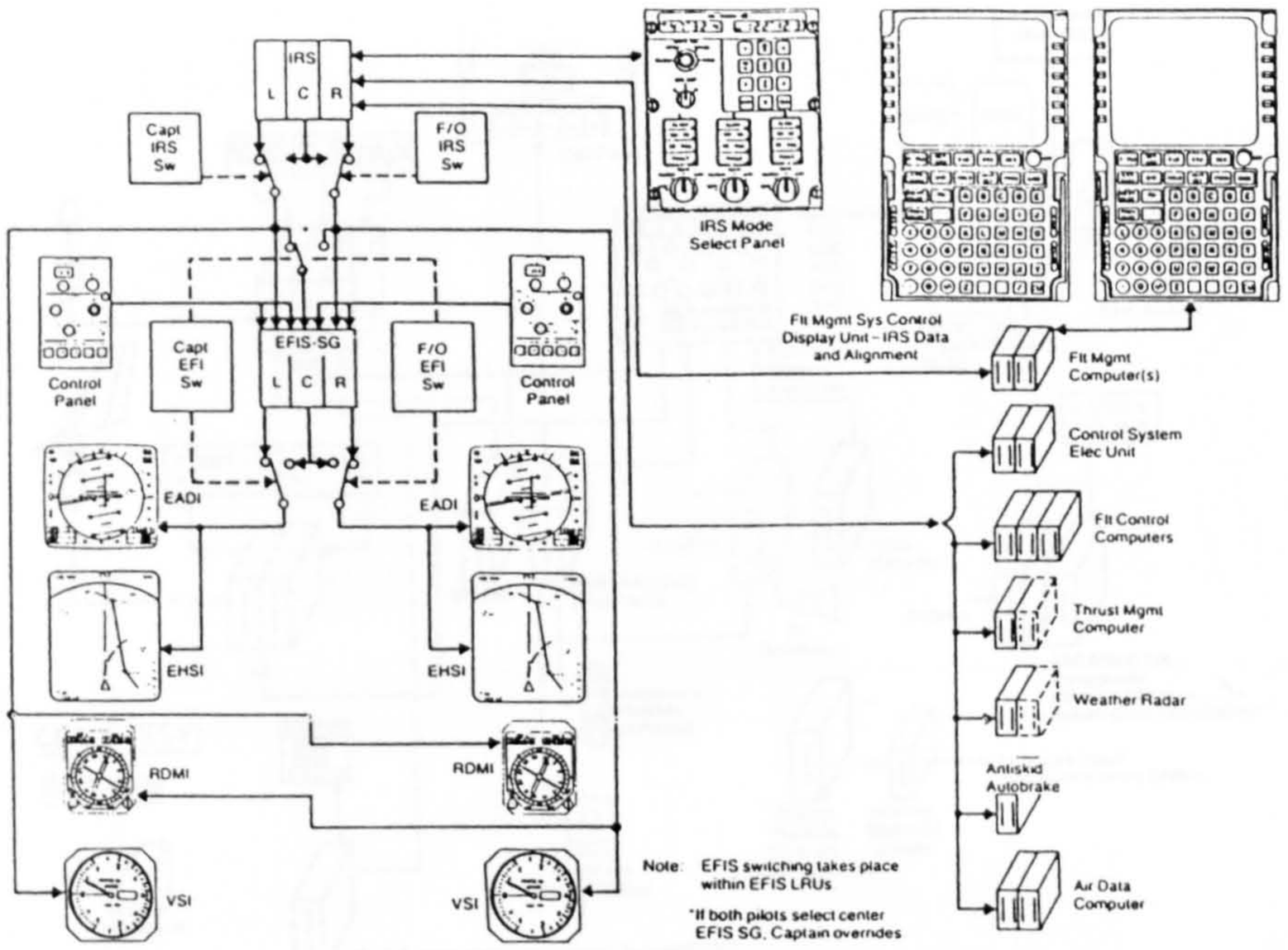

Figure 3-14 : Initial reference System schematic

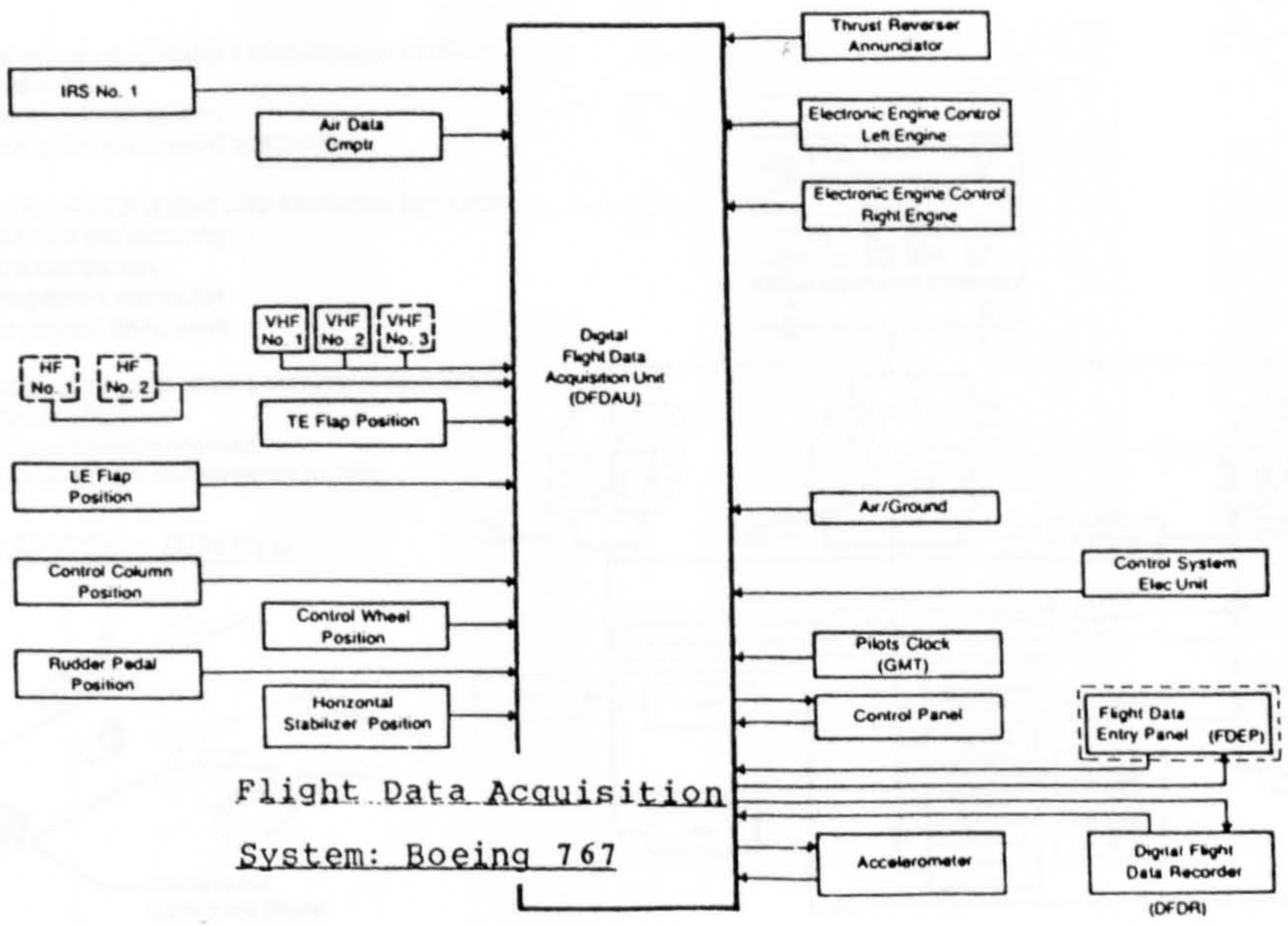

Figure 3-15 : Flight data acquisition system function diagram

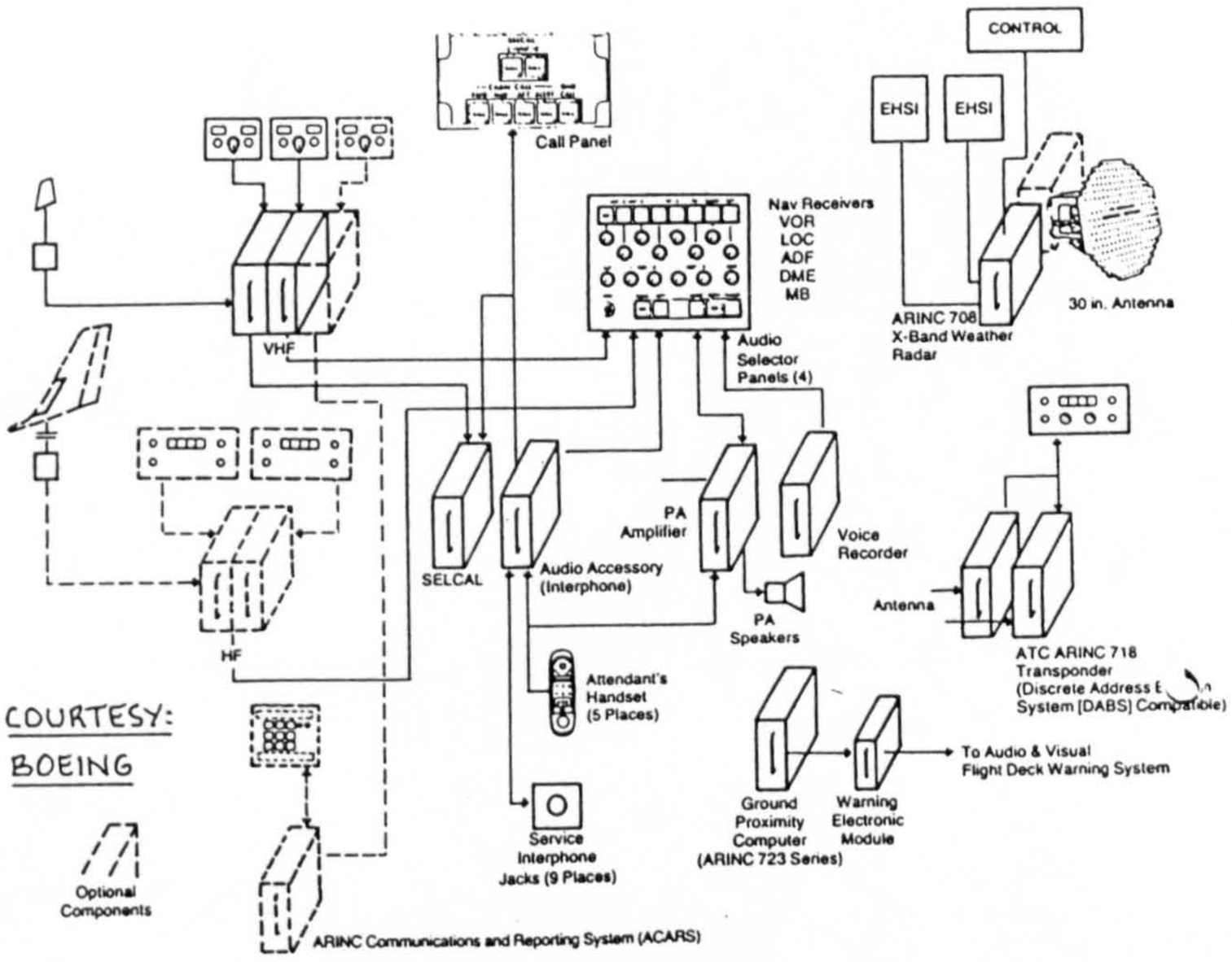

Figure 3-16 : Communication and advisory systems functional flow diagram

- Provides means to store and readout identification of LRU's which have failed in flight
  - •Flight squawk oriented system
  - •Designed for quick turnaround operation
- Provides means to readout faulted LRU interfaces following maintenace action for the following:
  - •Flight control computers
  - •Thrust management computer
  - •Flight management computers
- Provides means to display test and maintenance instructions to fault isolate to the LRU level
  - •Instructions are function oriented
  - •Designed for overnight maintenance activity

COURTESY: BOEING

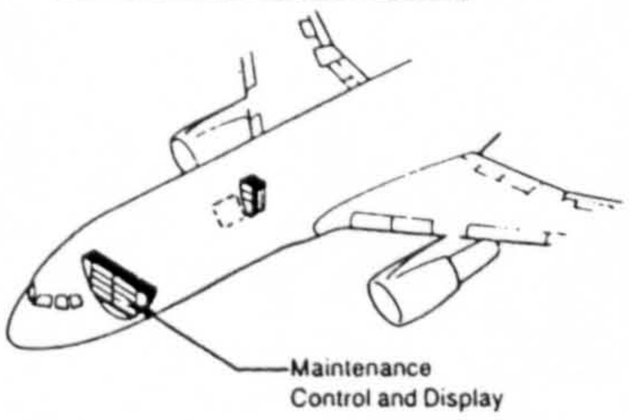

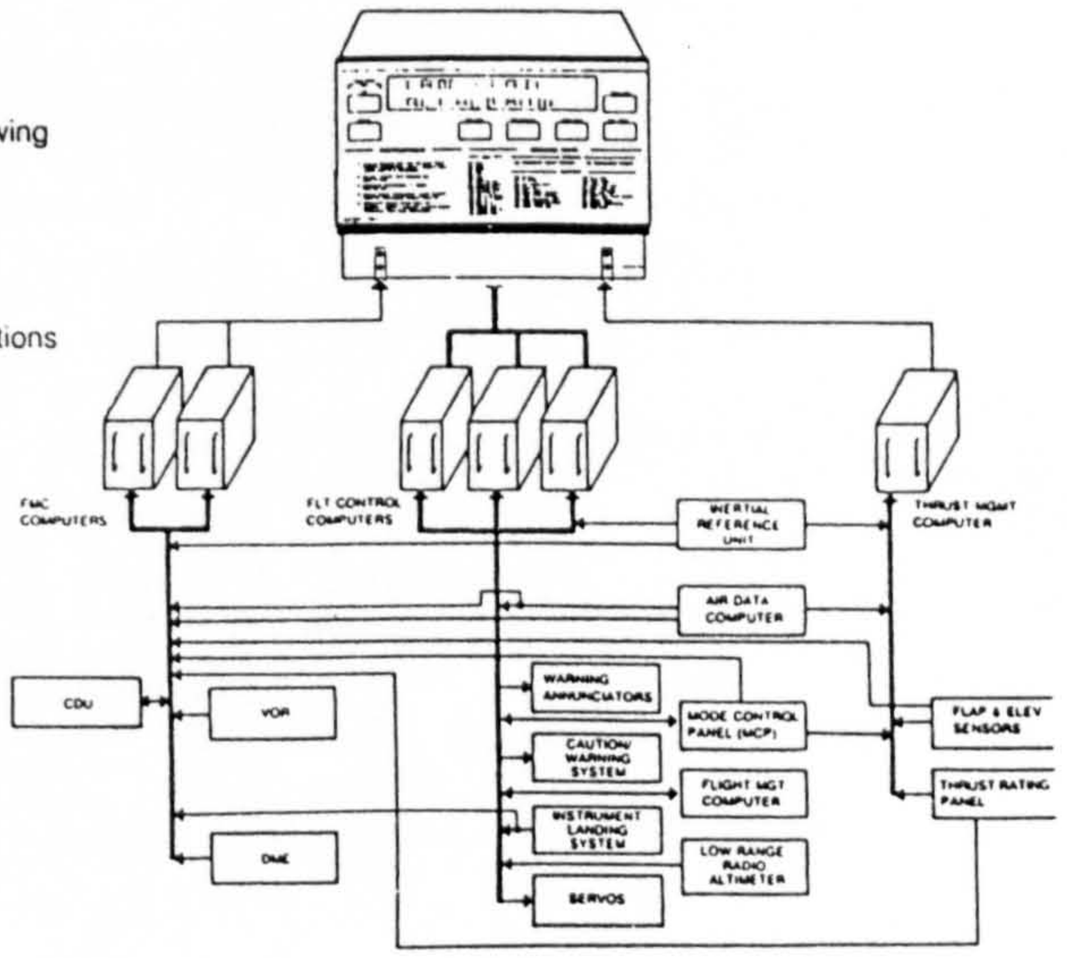

Figure 3.17 : Maintenance control and display panel diagram with brief functional description.

AVIONICS RELIABILITY ENHANCMENT MODELLING INTEGRATION INTO CACAD

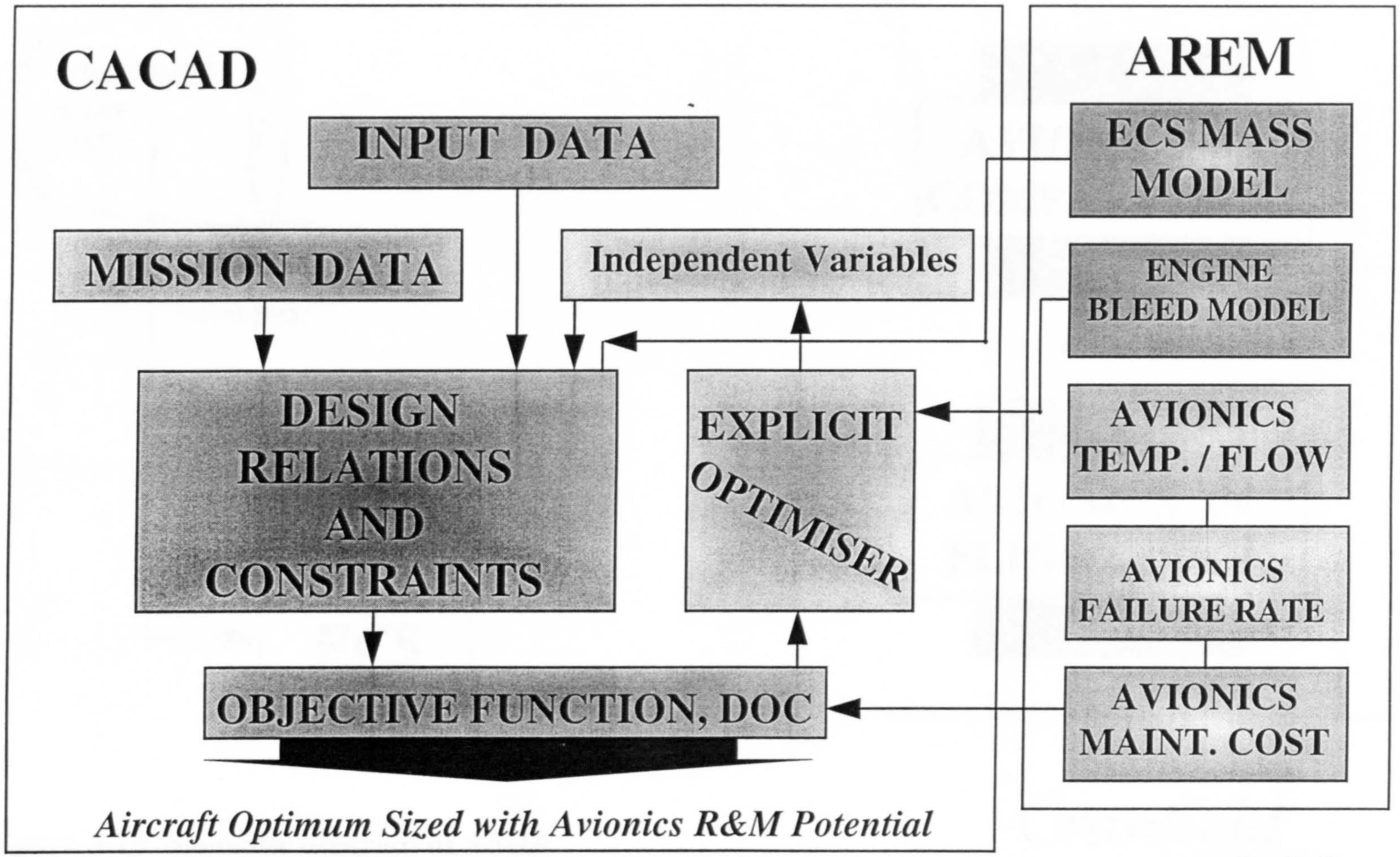

Figure 3-18, Flow chart of ASRE in CACAD

Cranfield UNIVERSITY

SCHEMATIC DIAGRAM OF COOLING FLOW AIR TO AVIONICS

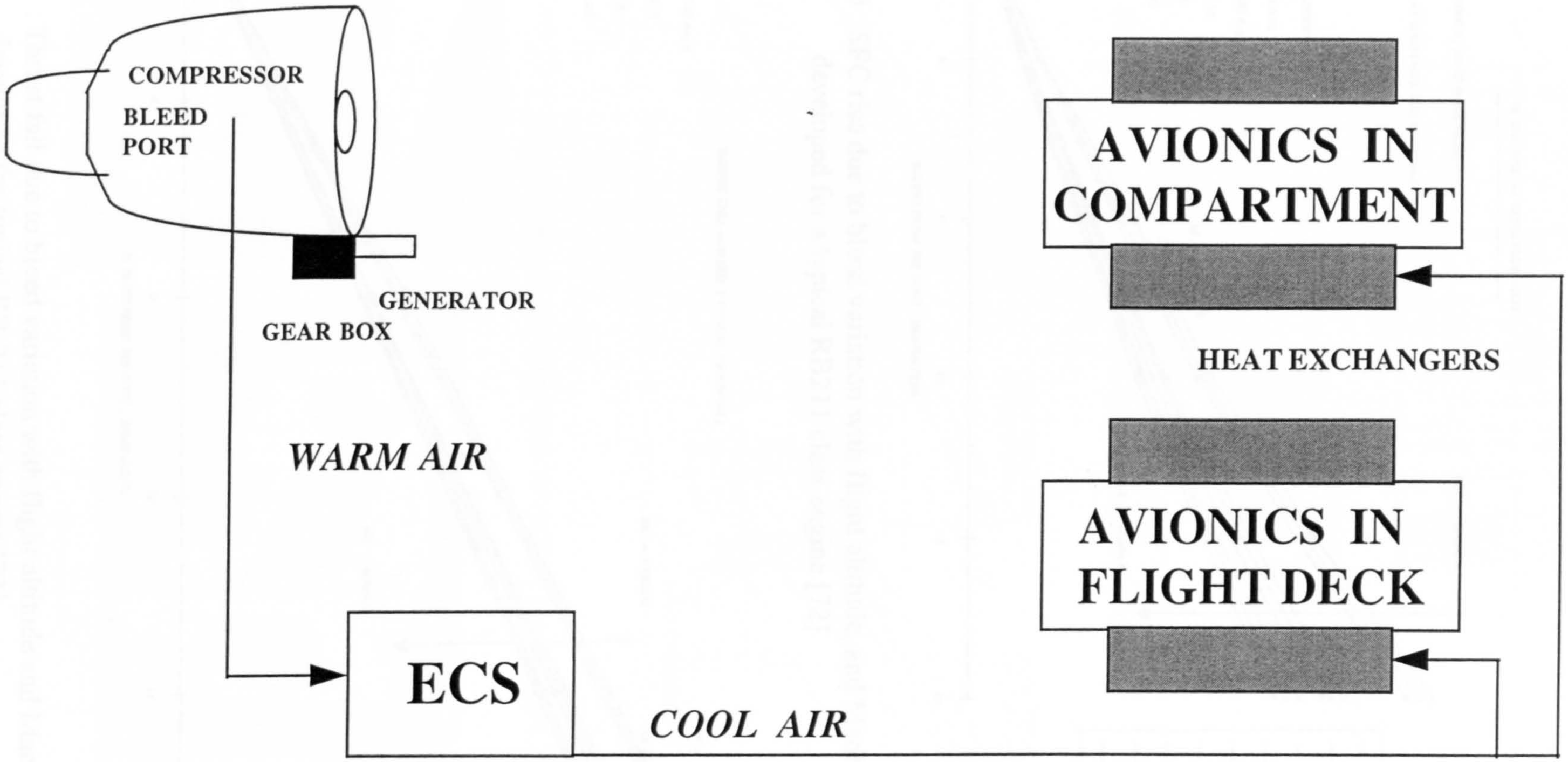

Figure 3-19 Shematic diagram of ASRE

Cranfield UNIVERSITY

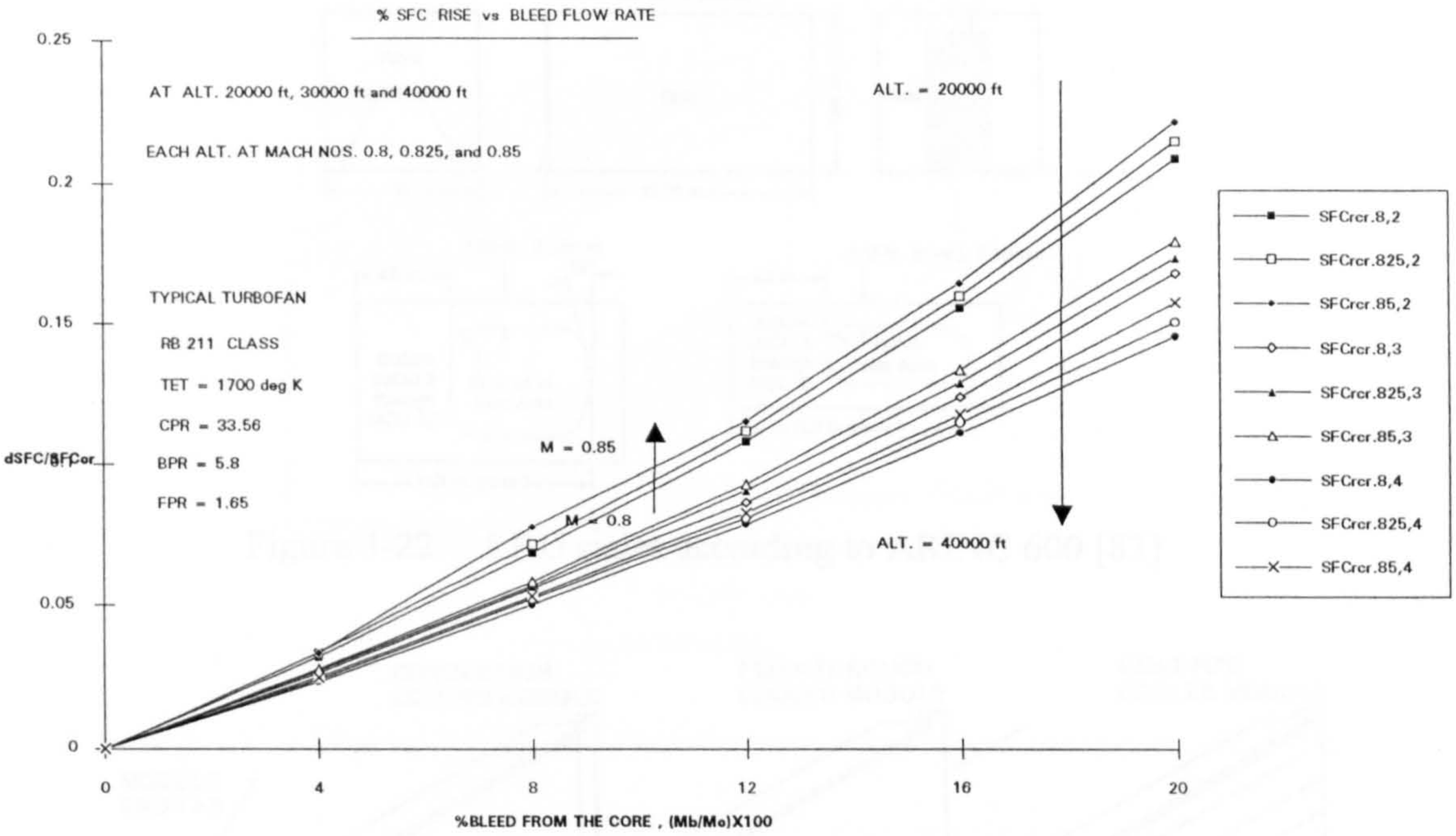

Figure 3.20 : SFC rise due to bleed variation with flight altitude, and Mach No. developed for a typical RB211 class engine [72]

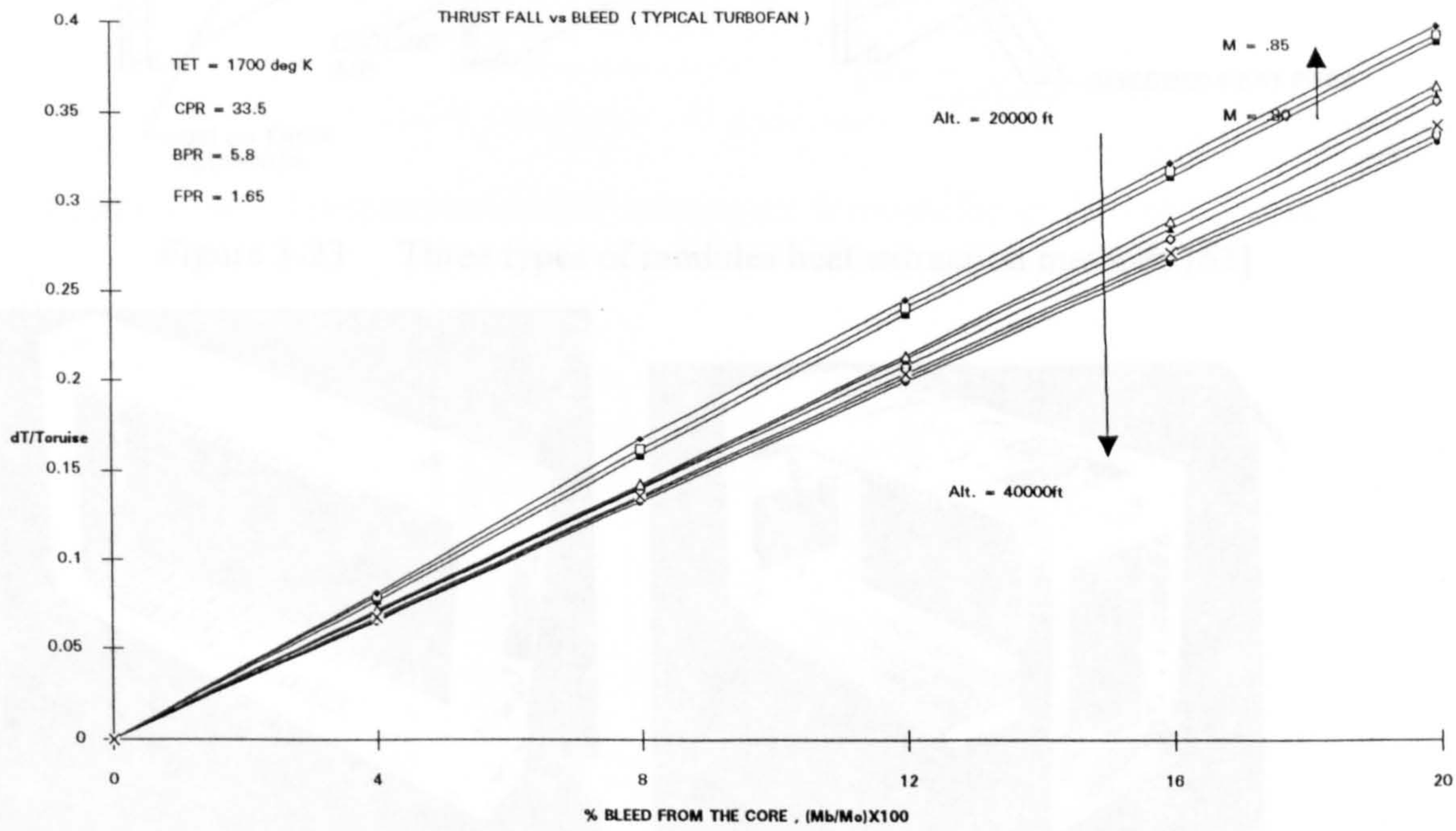

Figure 3-21 : Thrust fall due to bleed variation with flight altitude and Mach No. developed for typical RB-211 class engine [72]

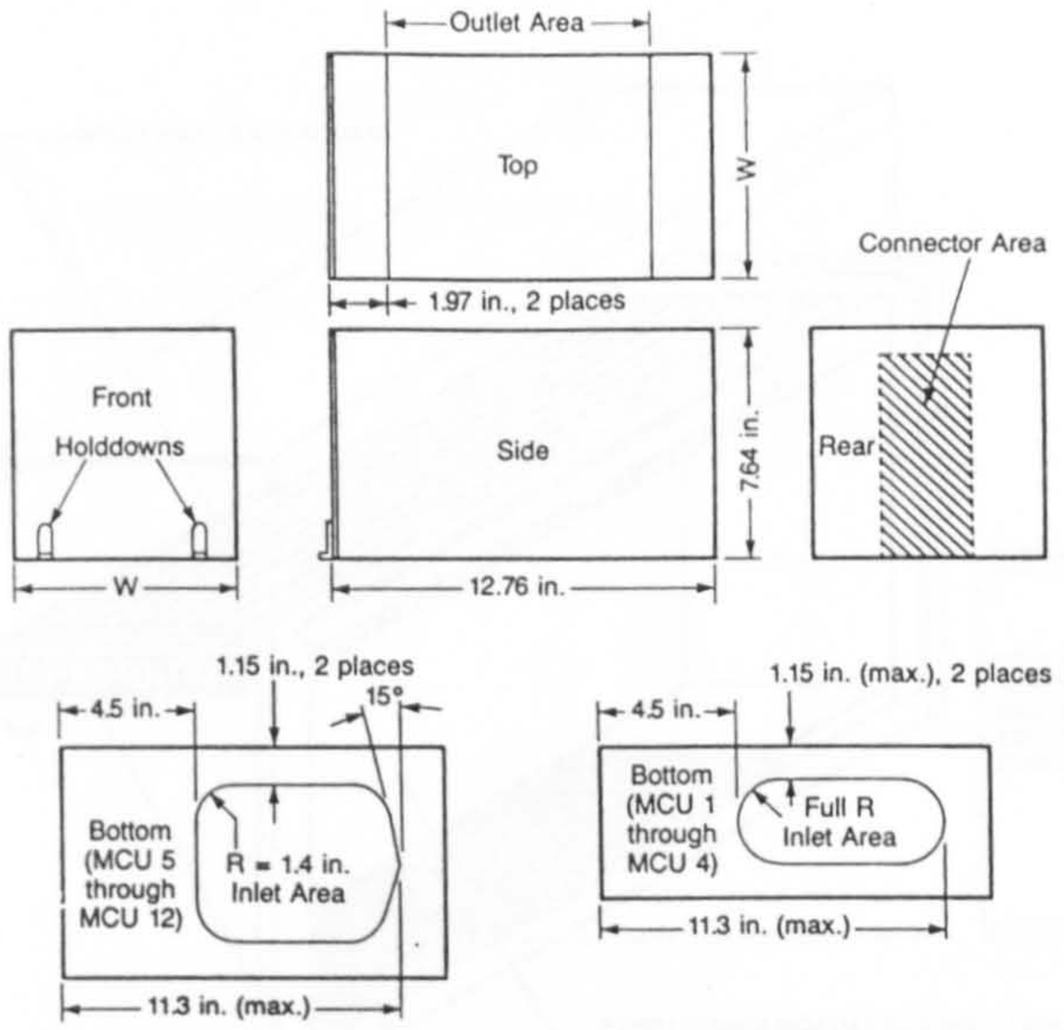

Figure 3-22 LRU sizies according to ARINC 600 [83]

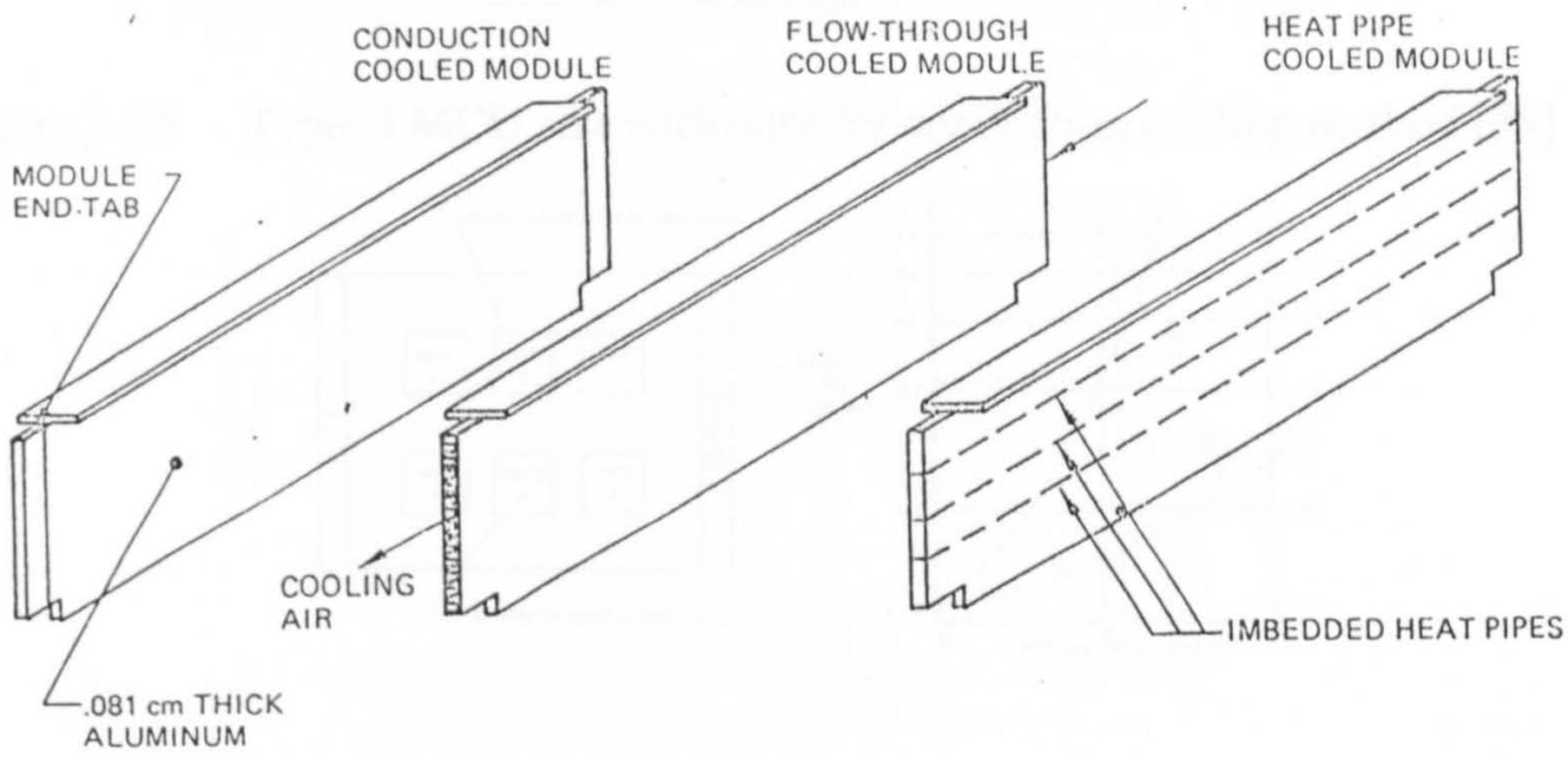

Figure 3-23 Three types of modules heat extraction methods [63]

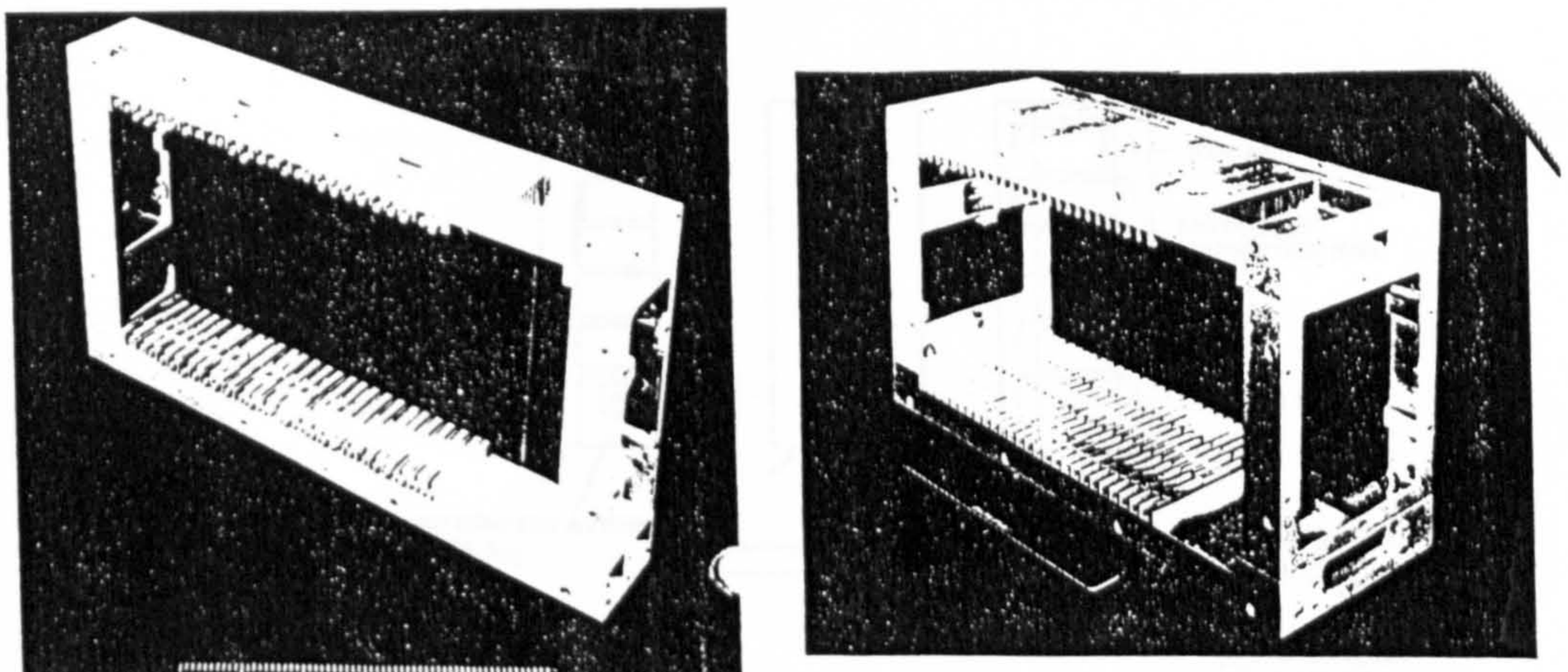

Figure 3.24 An advance heat exchanger frame for MCU [53]

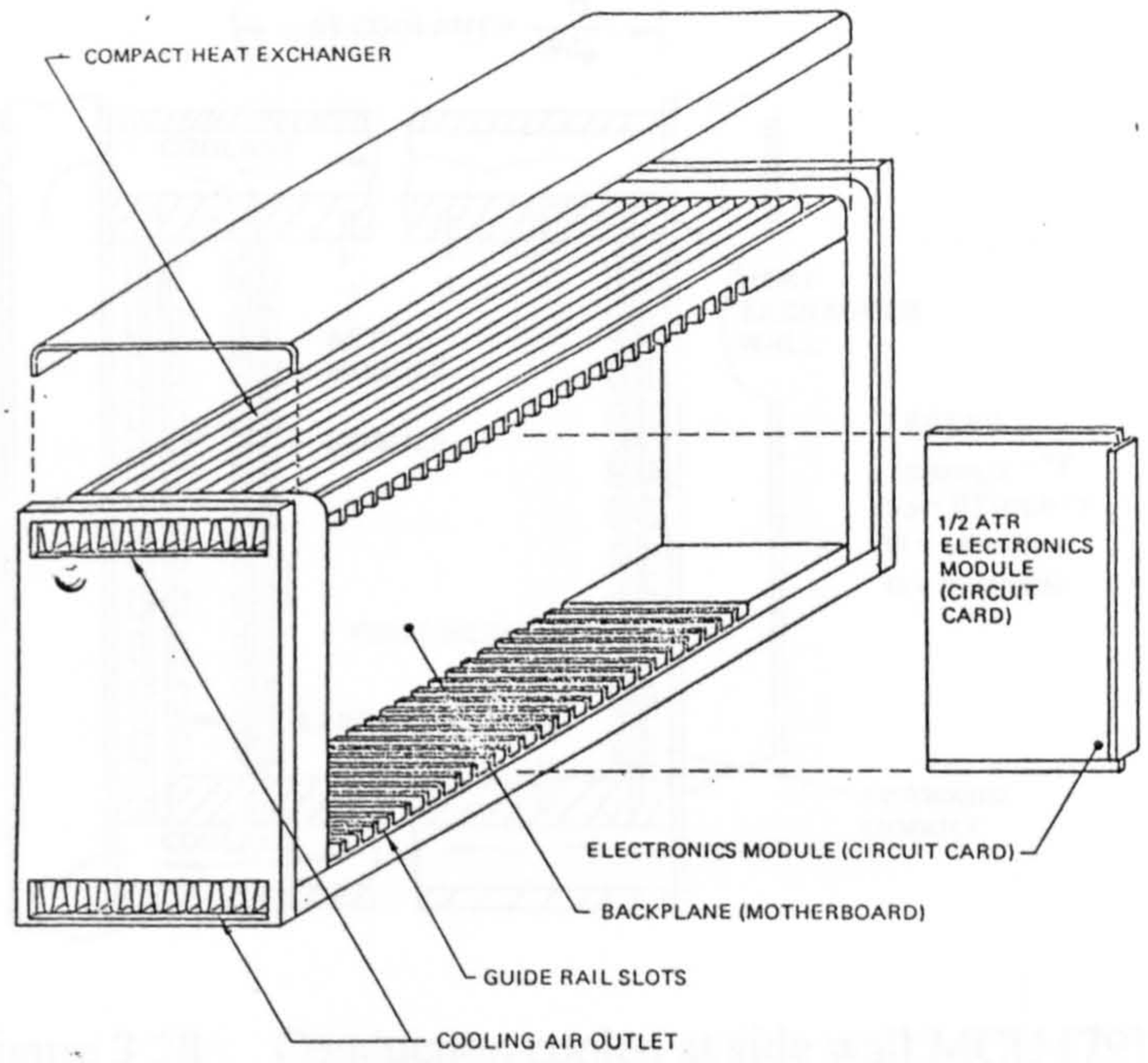

Figure 3-25 Typical MCU size enclosure for conduction cooling method [78]

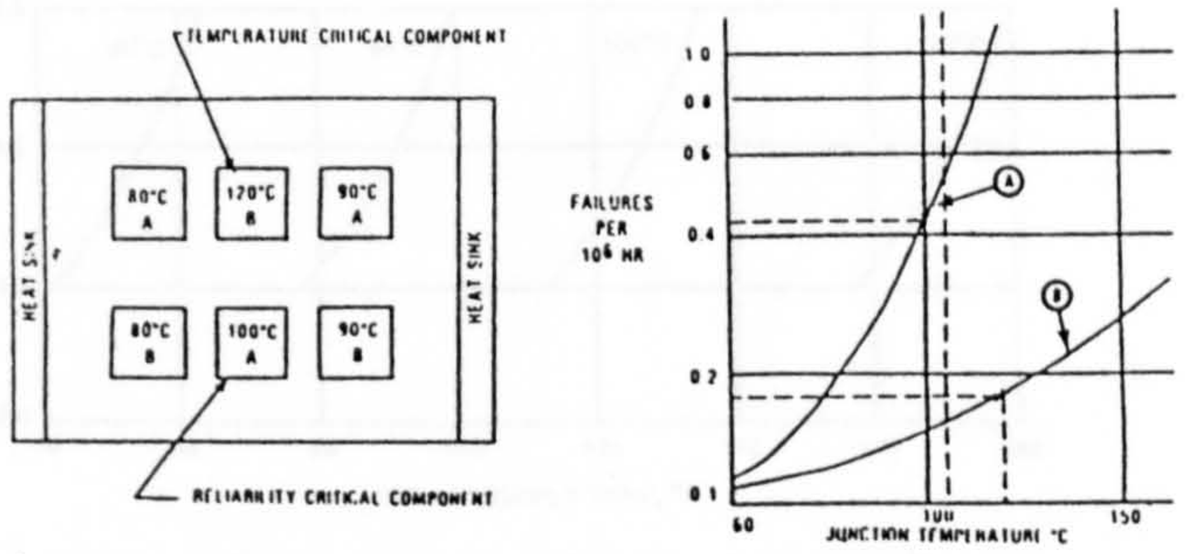

Figure 3-26 Temperature critical component & reliability critical component are placed on a same LRU [86]

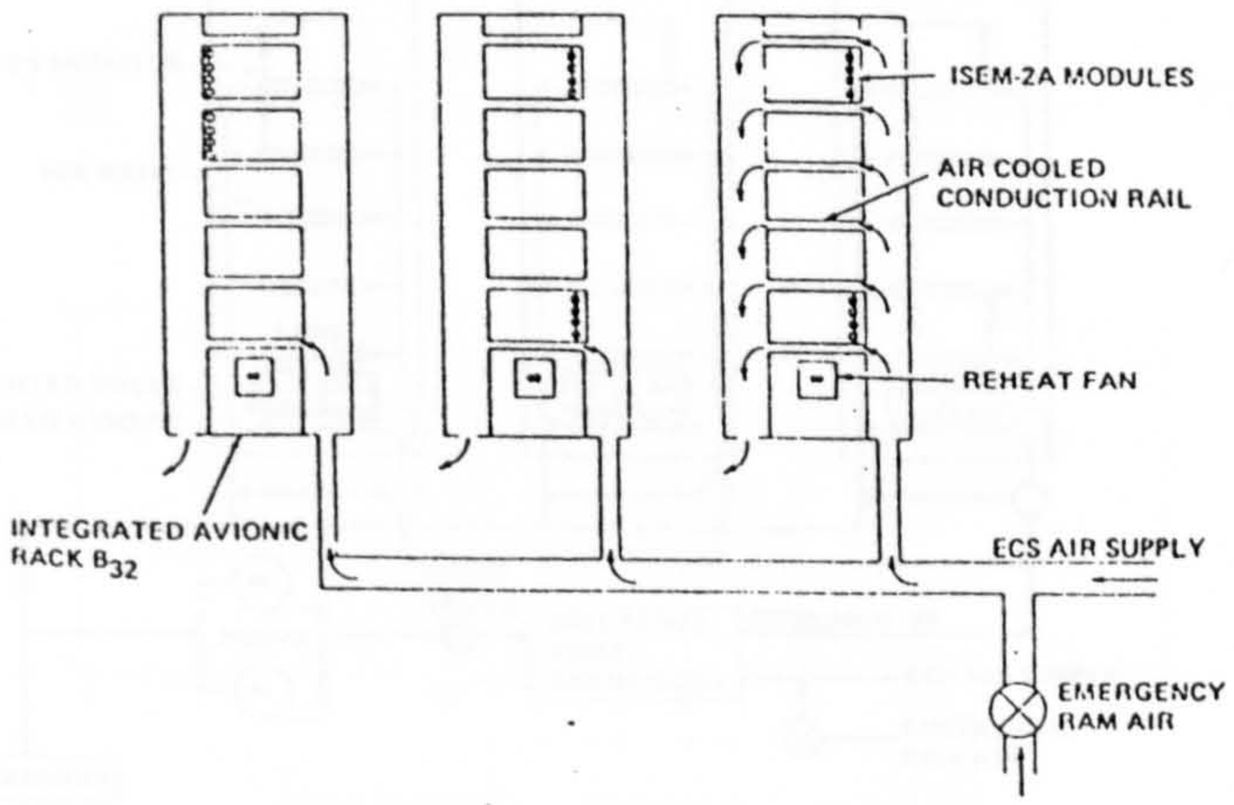

Figure 3-27 Typical coduction / air rail integrated rack configuration [79]

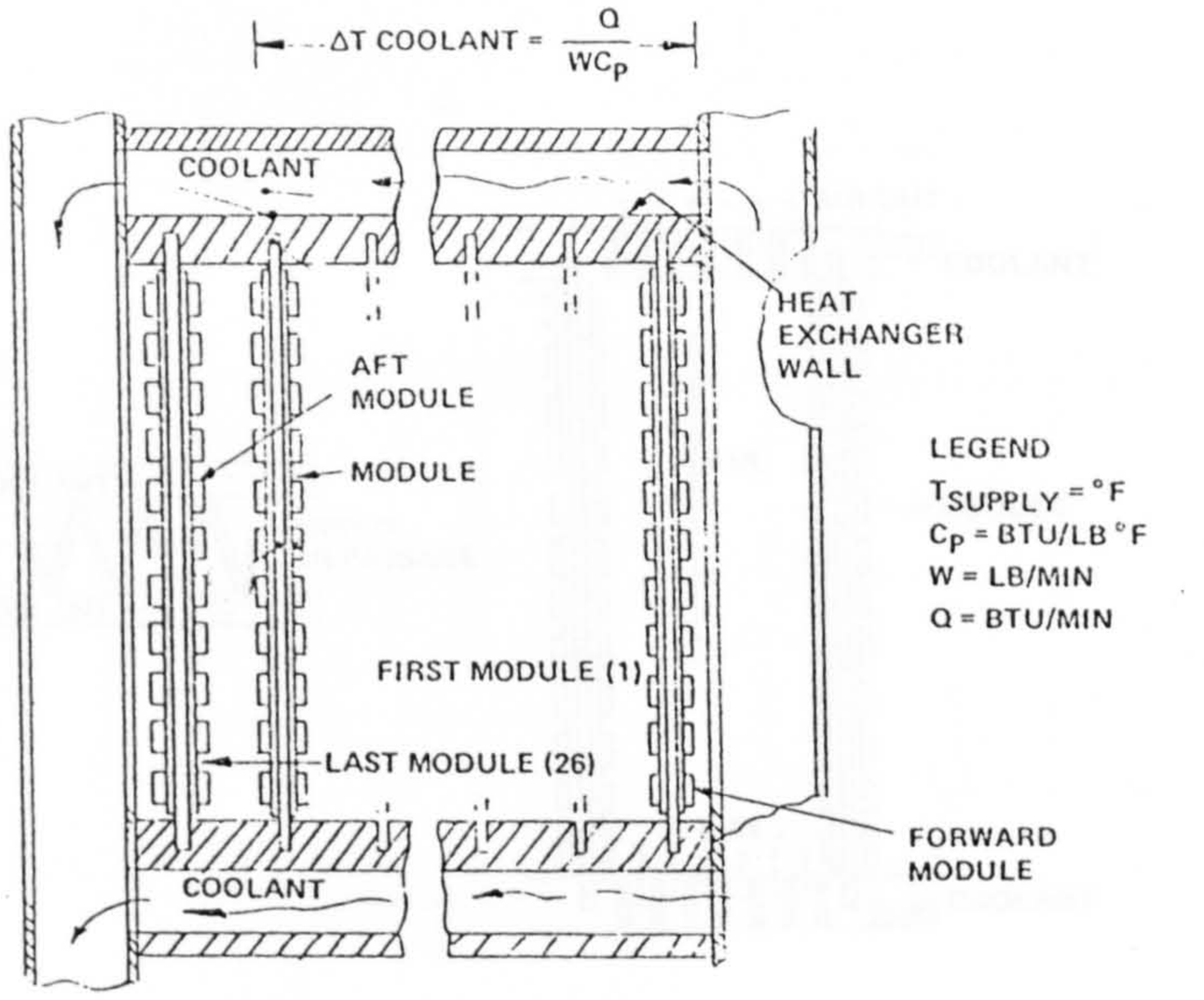

Figure 3.28 Conduction cooled at side wall MCU [79]

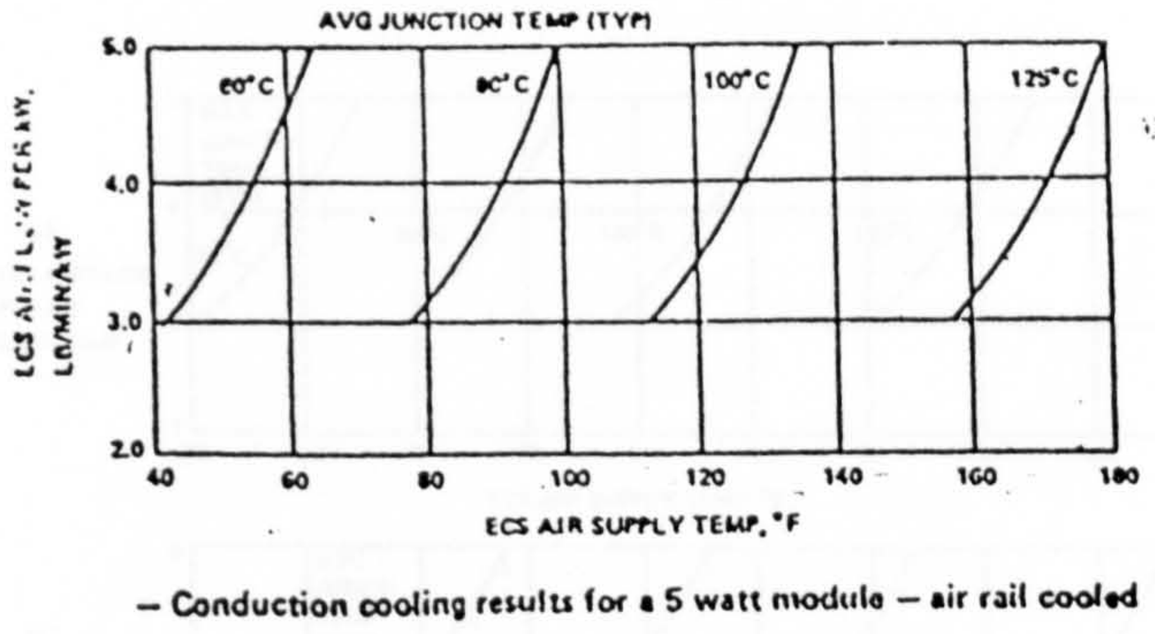

Figure 3.29 Conduction cooling thermal performance [79]

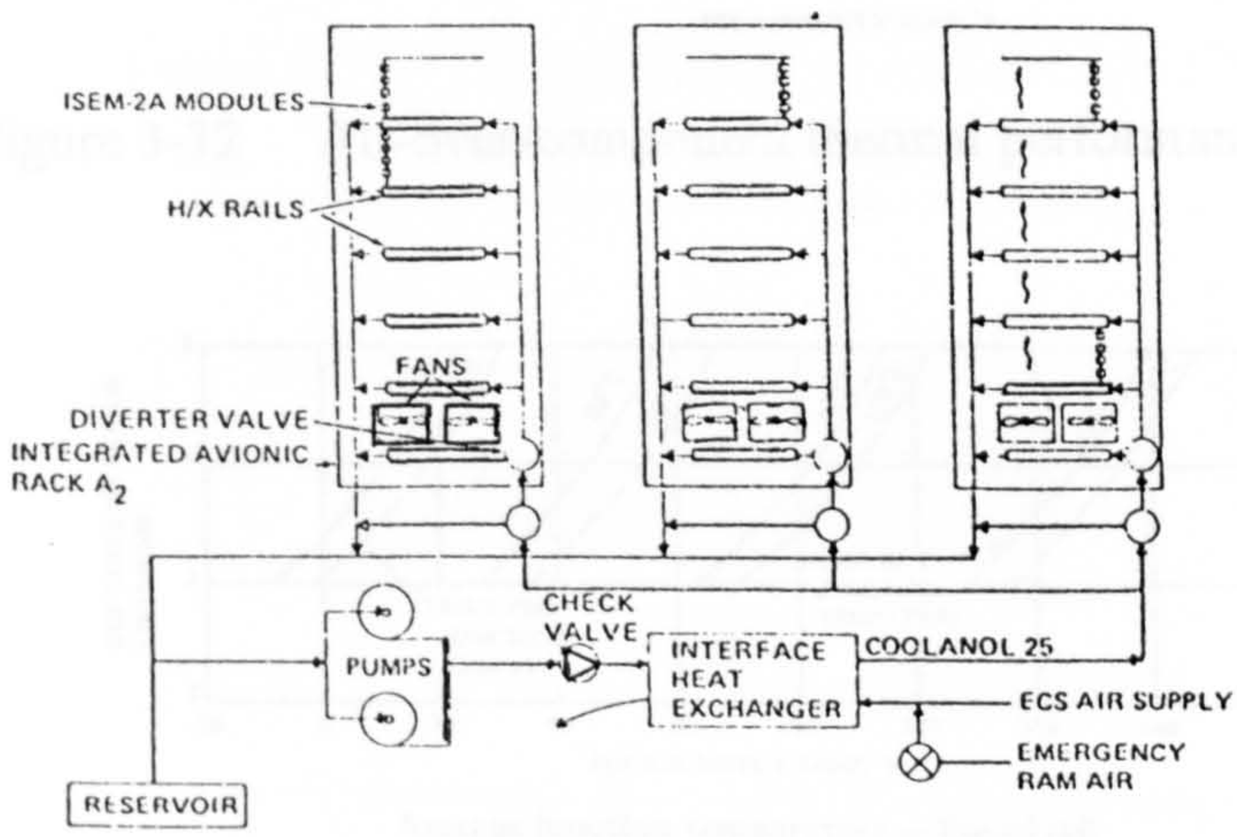

Figure 3.30 Typical air-over-componenet integrated rack arrangement [79]

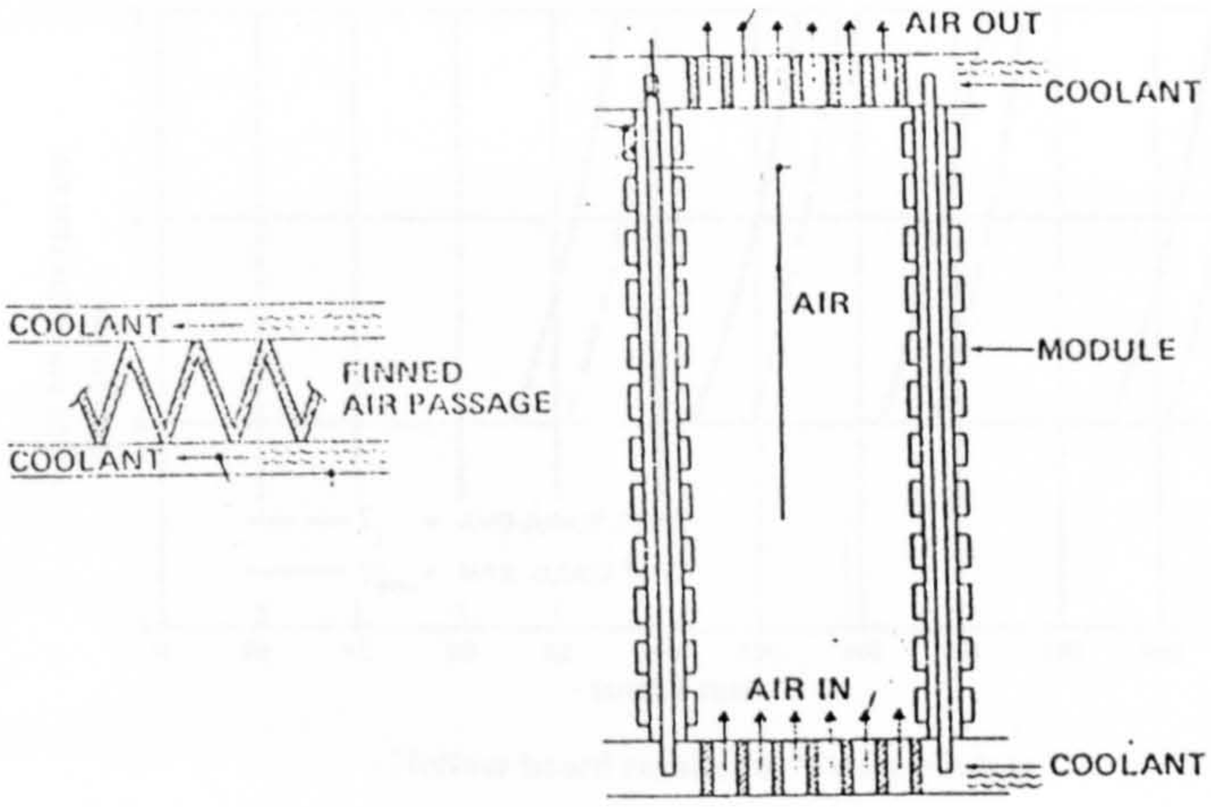

Figure 3-31 A close-up view of air-over-component arrangement at MCU level [79]

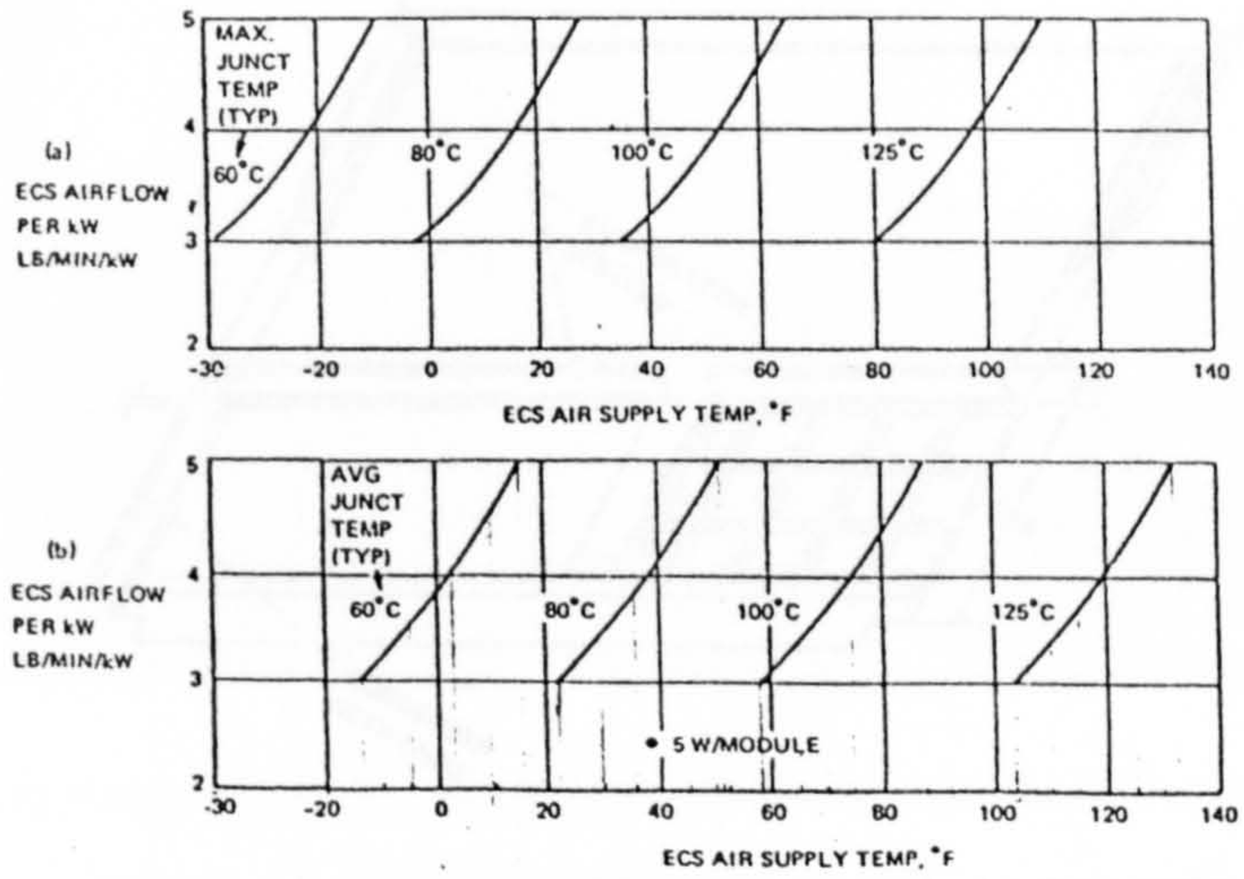

Figure 3-32 Air-over-component thermal performance [79]

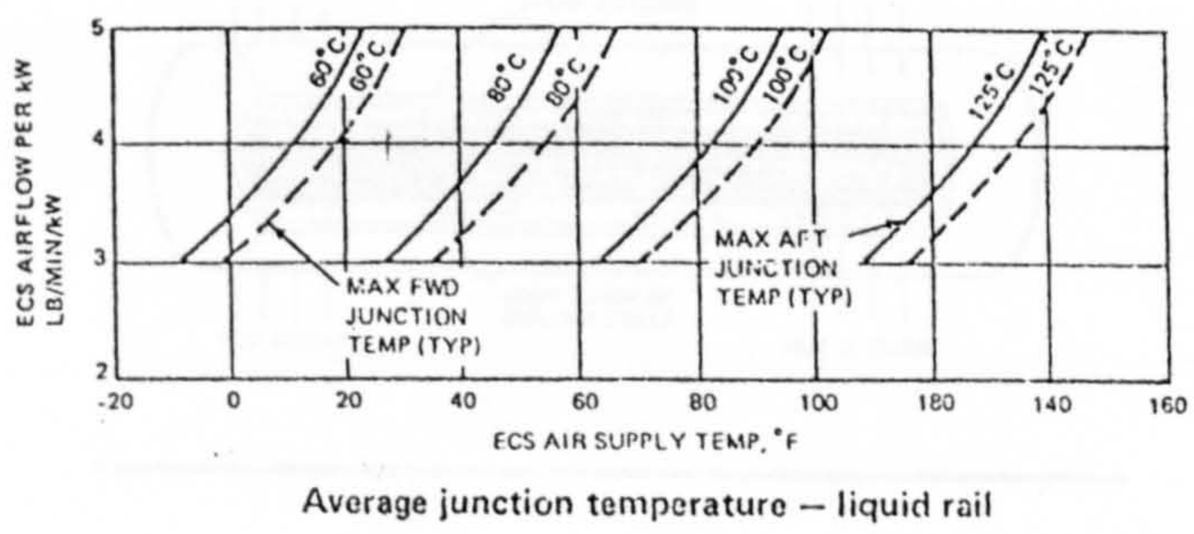

Figure 3-33 Liquid rail thermal performance [79]

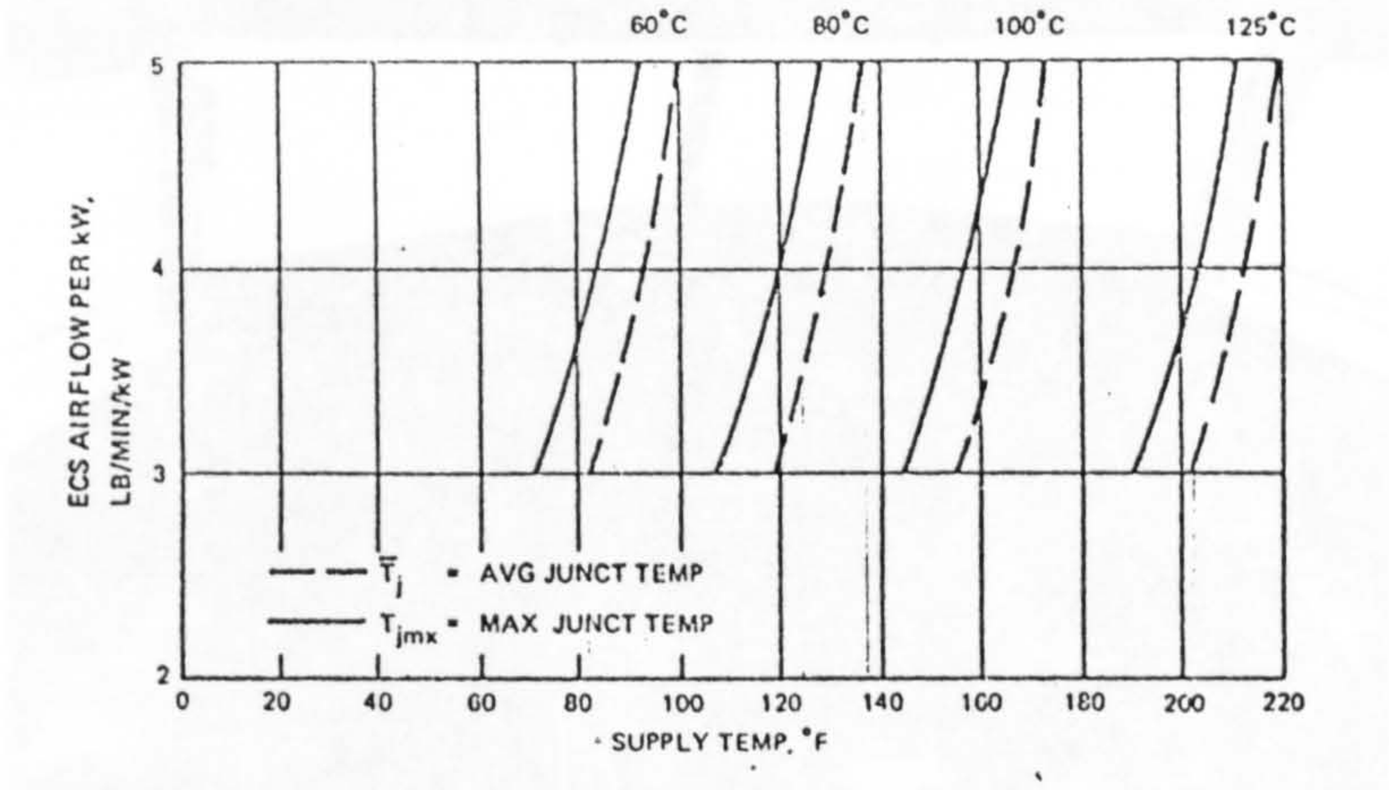

Hollow board results for 5 watt module

Figure 3-34 Thermal performance of hollow boerd module [79]

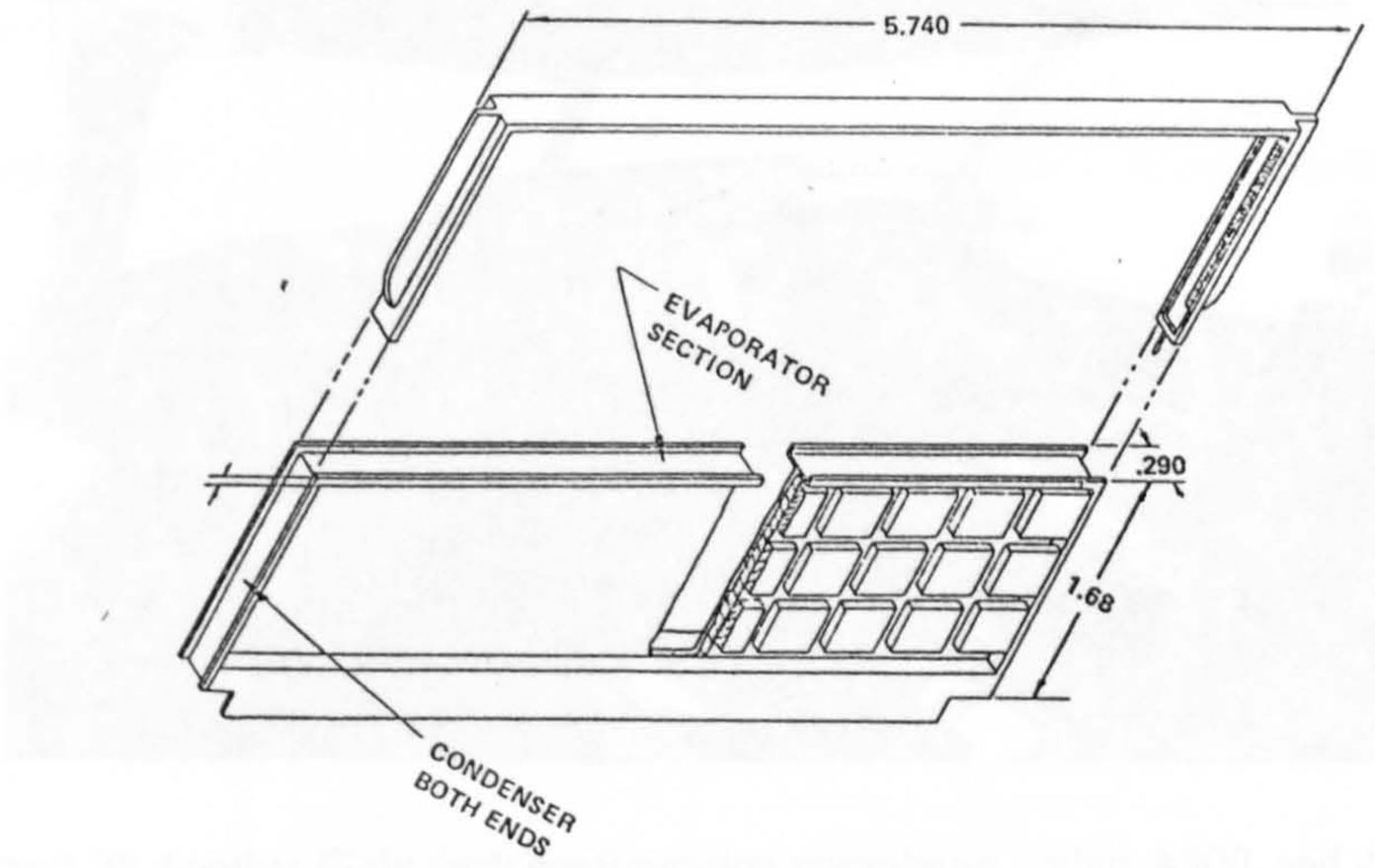

Figure 3-35 Typical heat pipe cooled LRU [79]

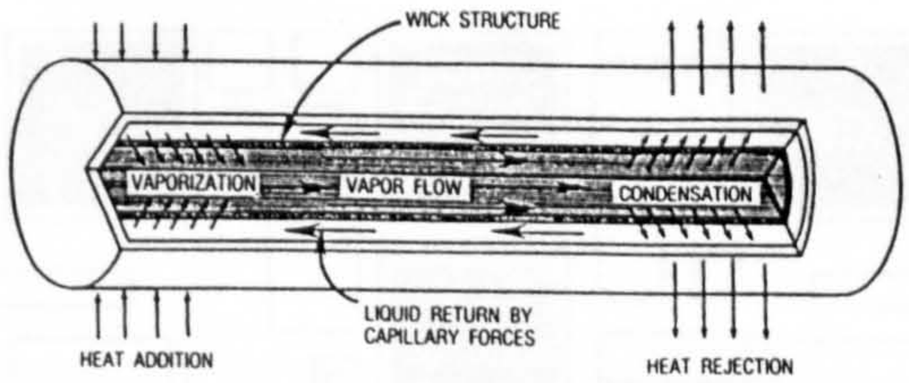

Figure 3-36 Internal configuration of a heat pipe [73]

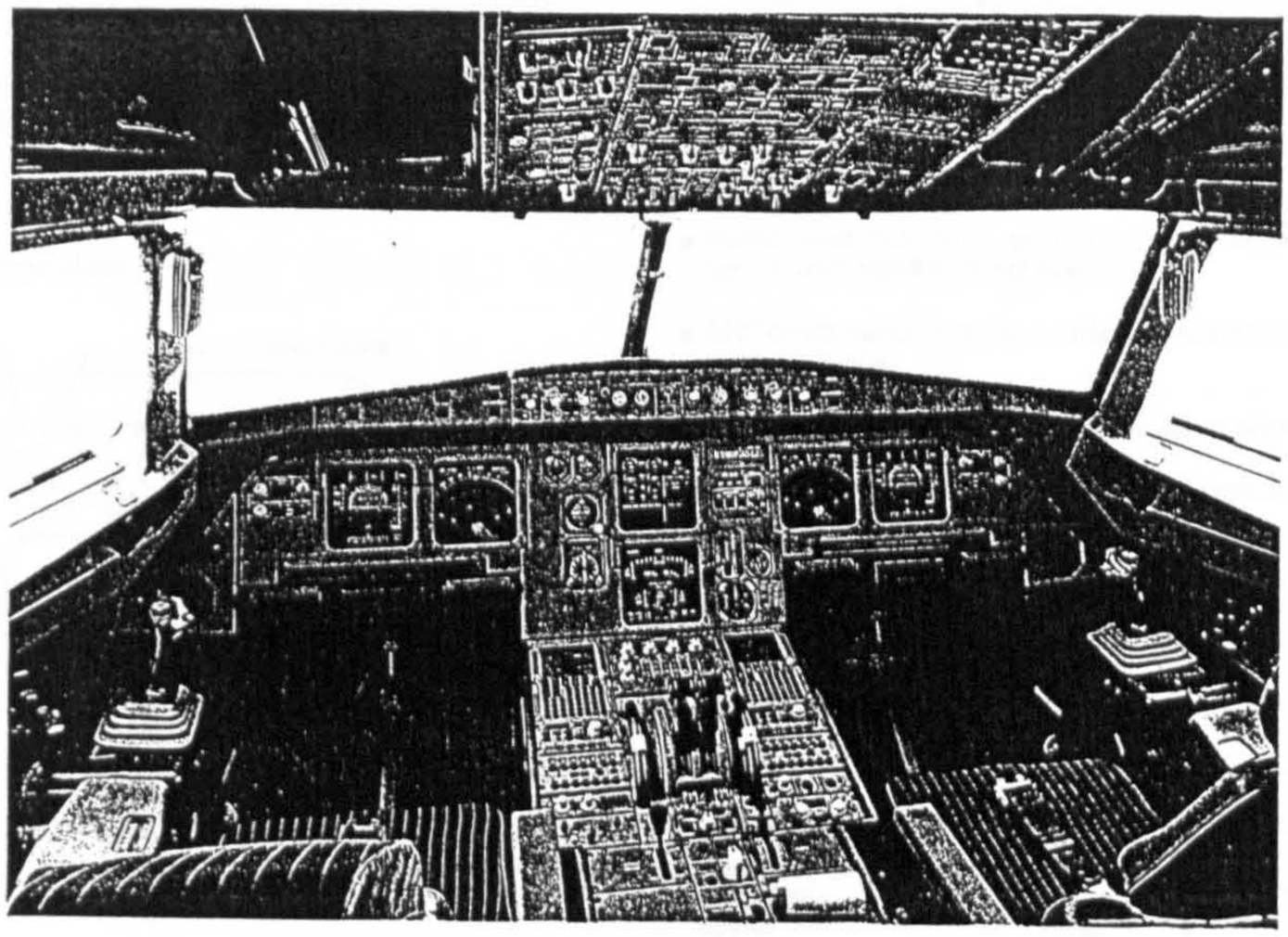

Figure 3-37 Typical flight deck resembling Airbus A319,320, 321, and A330, A340 [89]

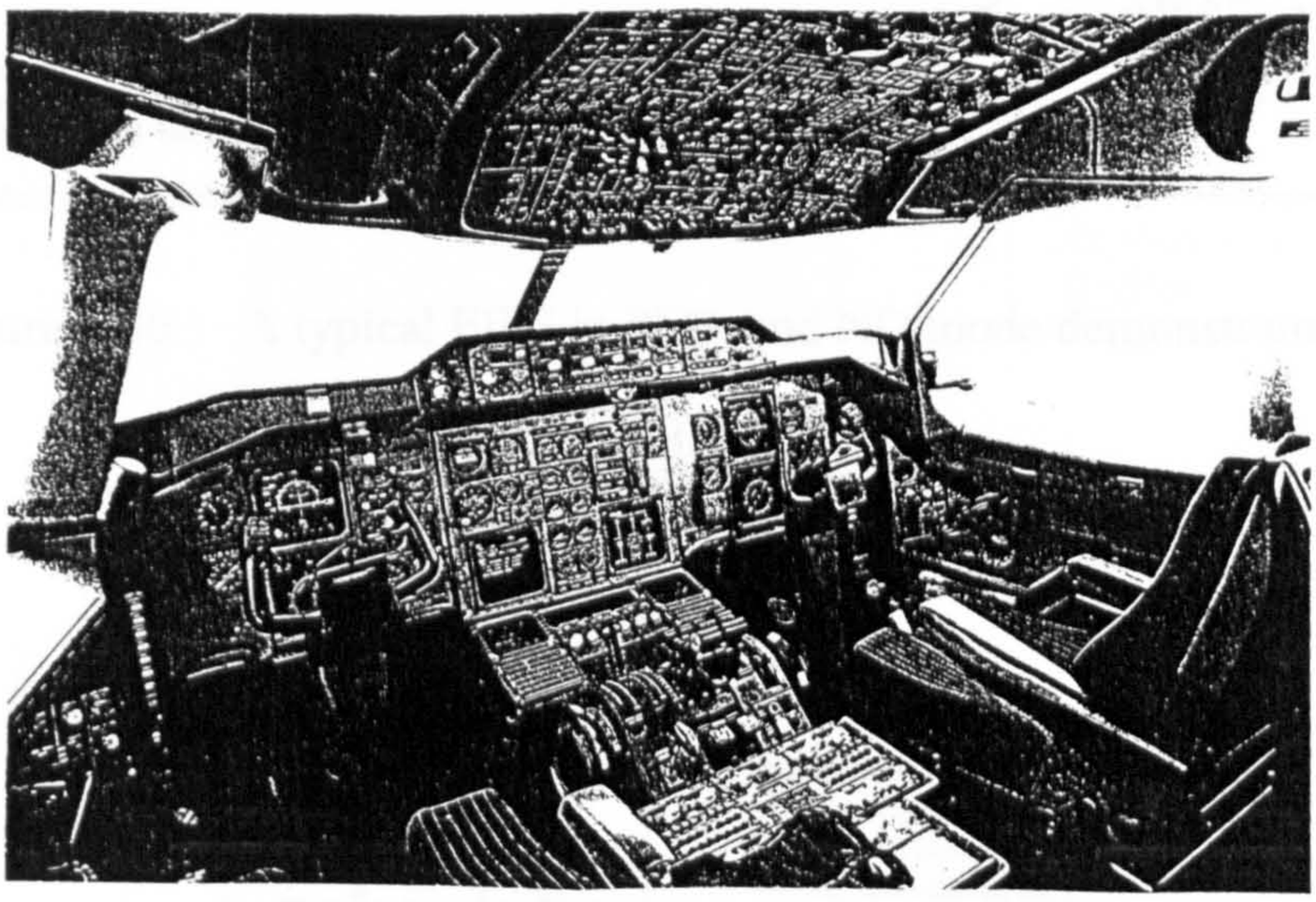

Figure 3-38 Another flight deck configuration resembling Airbus A300, and A310 [90]

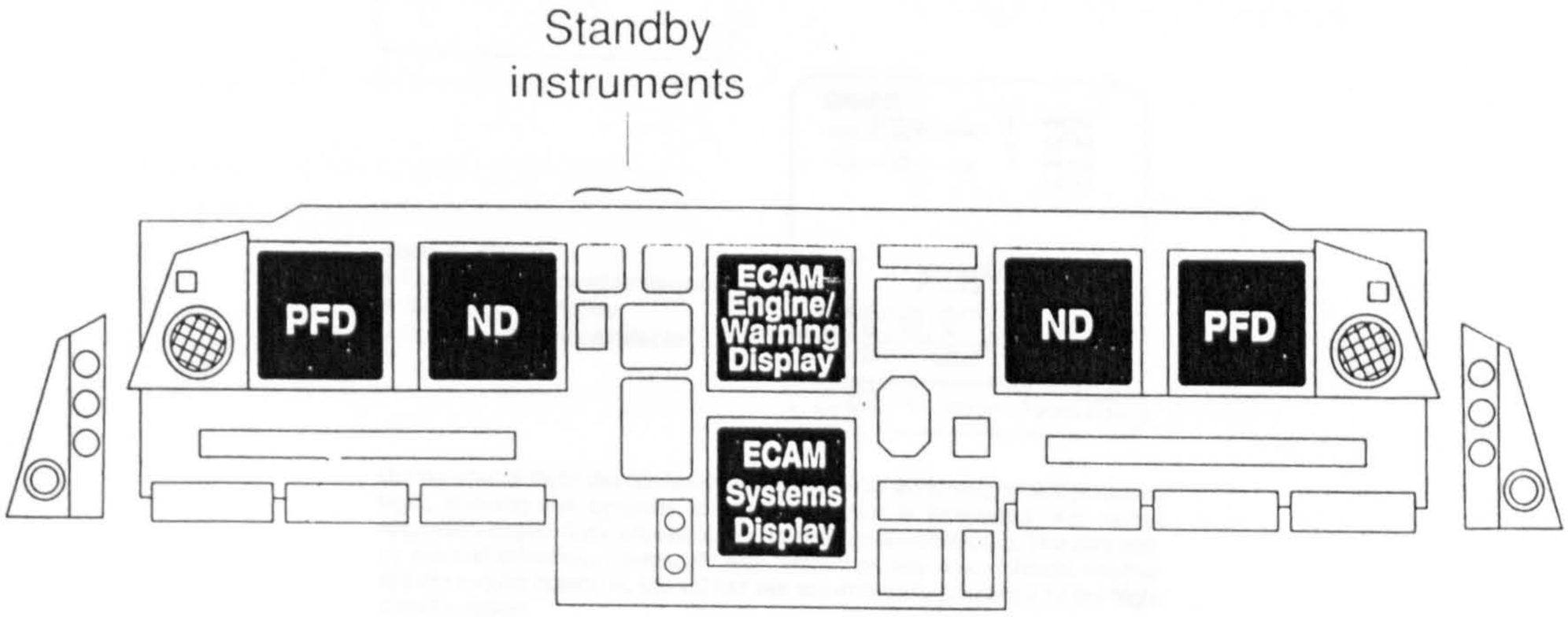

Figure 3-39 Front face of a typical flight deck, highlighting CRTs [89,90,91]

Primary flight display

The PFD provides clear and accurate information on a range of parameters including speed, altitude, attitude and heading of the aircraft.

Typical PFD climb configuration

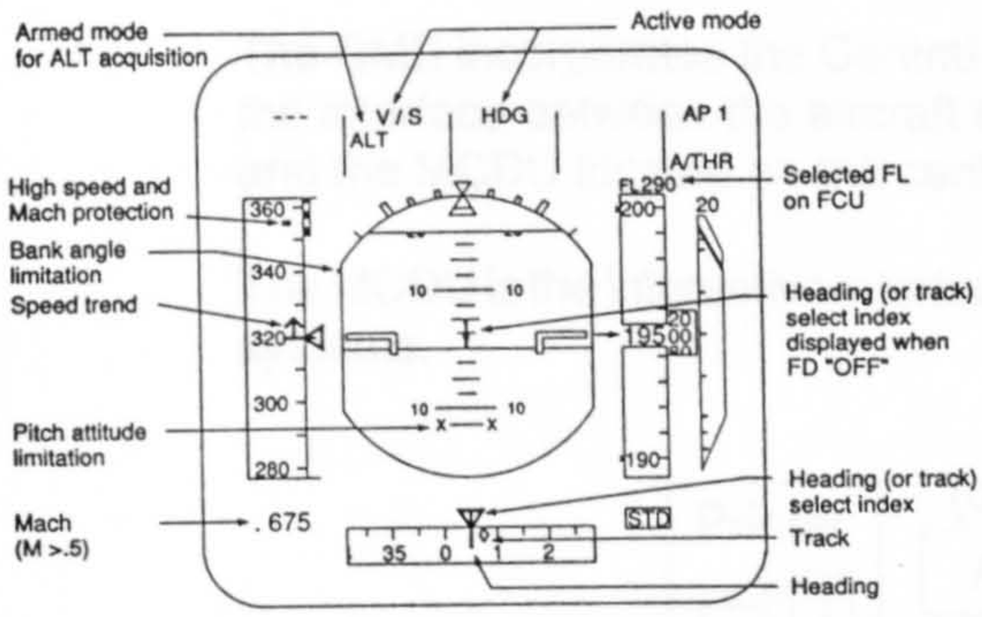

The PFD replaces the **six** electro-mechanical instruments used in older generation aircraft.

Moreover, by employing the power available from digital avionics, the conventional flight director is switched to the flight path vector for display on the PFD, making it possible to fly a non-precision approach to a higher level of accuracy than has hitherto been possible.

This feature has a beneficial effect on aircraft handling and pilot awareness.

Navigation display

The NDs are located inboard of each PFD and provide the pilot with essential data on the aircraft's position and course.

The ND has three selectable modes:

- **ROSE** mode (ILS, VOR, or NAV): heading up, aircraft symbol in screen centre, with weather radar available.
- **ARC** mode: heading up, horizon limited to a 90° forward sector, with weather radar available.
- **PLAN** mode : north up, display centred on selected waypoint.

Additional data from the flight management system is available in any mode.

ARC mode

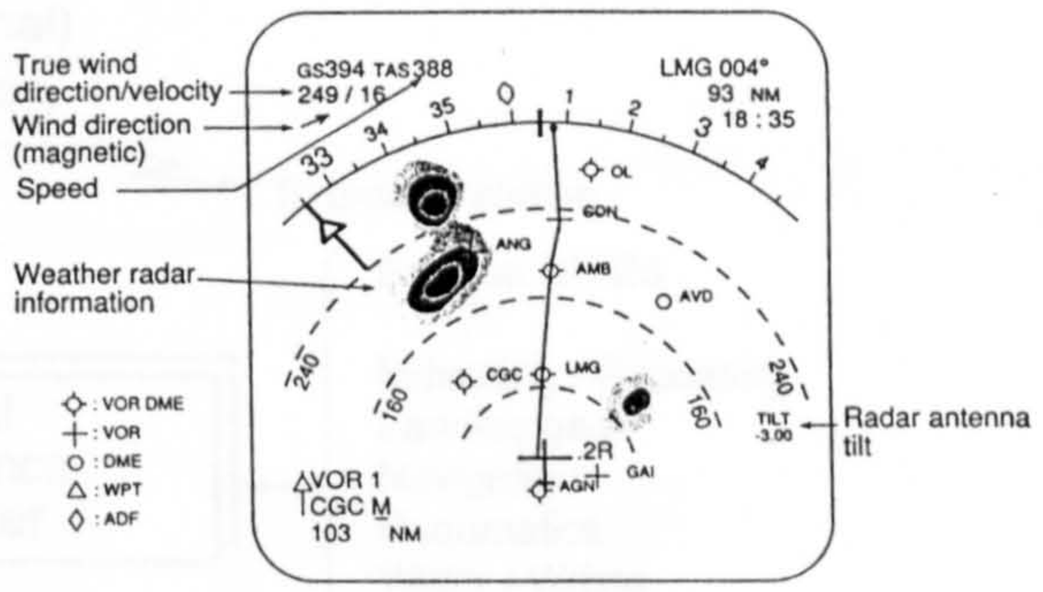

Figure 3-40 A typical EFIS in PFD, and ND mode demonstrator [91]

Electronic centralised aircraft monitor

Systems information is presented on two screens on the centre console by the Electronic Centralised Aircraft Monitor system. Sensors throughout the aircraft continuously monitor the systems and, if a parameter moves out of the normal range, automatically warn the pilot.

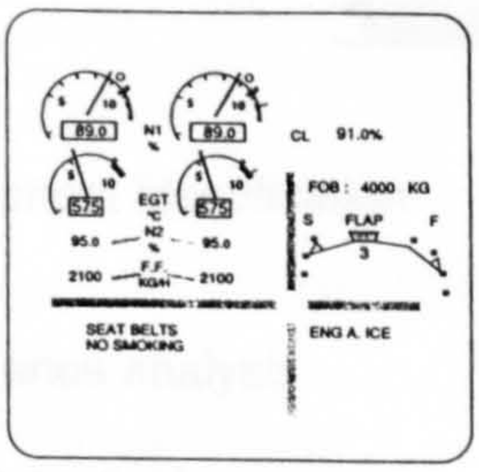

Engine/warning display

- Primary engine parameters
- Operational status (flap/slat setting, fuel volume, etc.)
- Memo and warning information (seat belts, anti-ice, etc.)

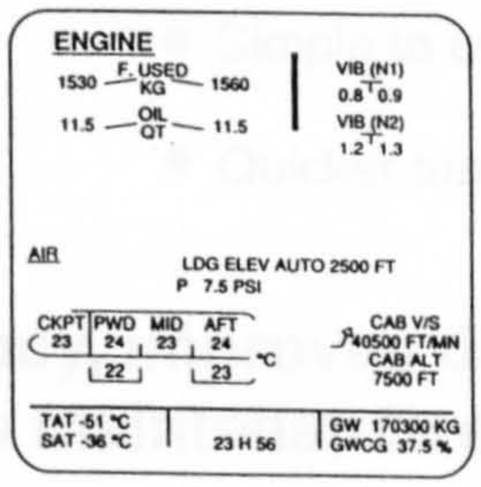

System display

- Flight-phase-related system data
- System malfunctions
- Fourteen displays available

During normal flight the ECAM presents displays according to the phase of flight, showing the systems in which the pilot is interested, e.g. some secondary engine data, pressurisation and cabin temperatures. The pilot can, by manual selection, interrogate any system at any time. Should another system require attention, the ECAM will automatically present it to the flight crew for action.

Figure 3-41 ECAM showing both possible modes [91]

Centralised maintenance system (CMS)

The CMS incorporates the Central Maintenance Computer (CMC), which is the interface between the aircraft systems, Built-in Test Equipment (BITE) and the MCDU located on the centre pedestal.

The MCDU is the interactive interface between the maintenance crew and the systems.

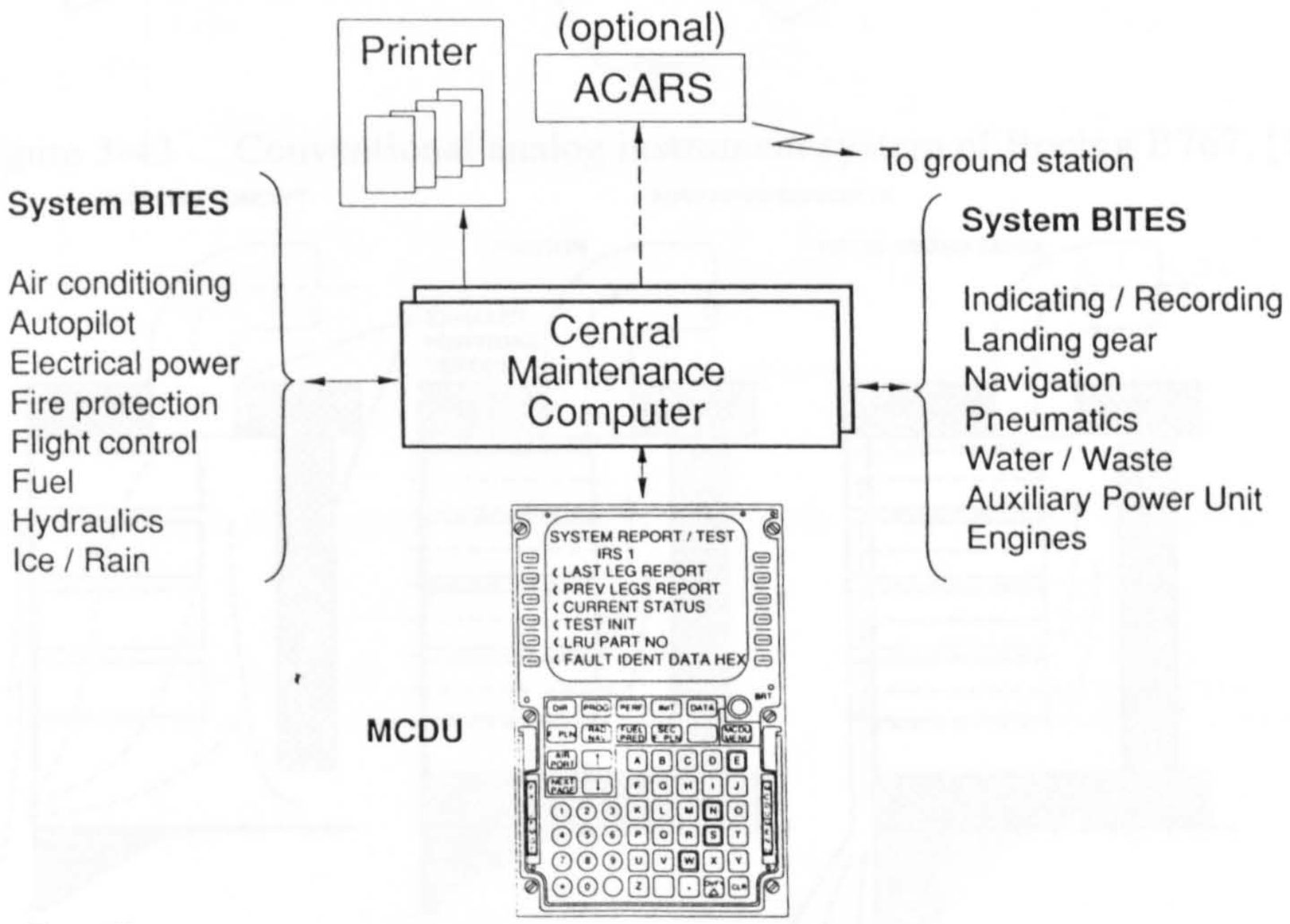

Functions

- Failed component identification
- Failure sequence analysis
- Diagnostic data display
- Data print-out and real-time reporting to ground capabilities

Benefits

- Unnecessary component removal minimised
- Improved troubleshooting
- Simple to use
- Quicker turnround

CMS - increases efficiency, improves dispatch reliability and reduces maintenance costs.

Figure 3-42 MCDU with peripheral description (91)

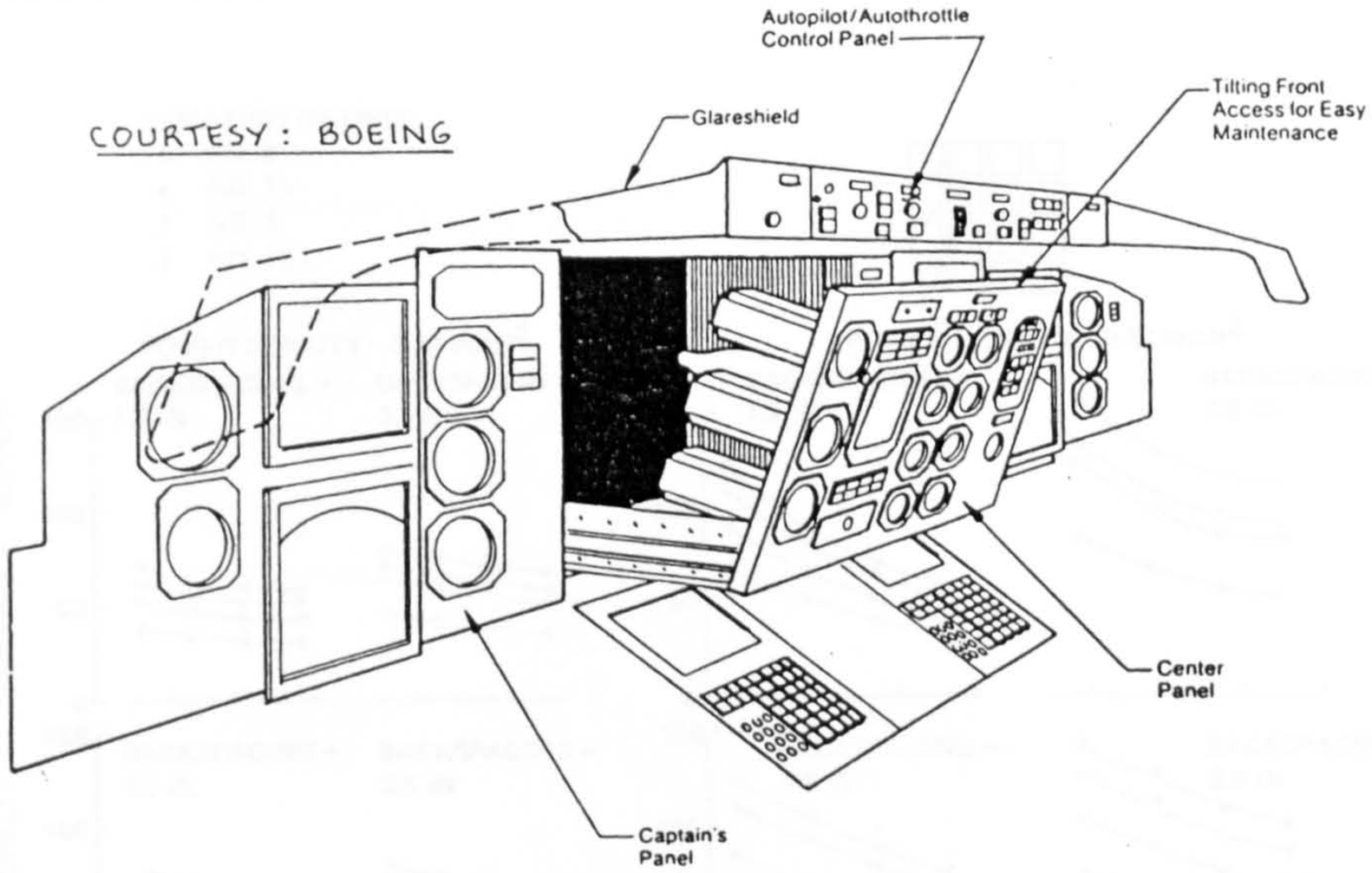

Figure 3-43 Conventional analog instrument system of Boeing B767, [15]

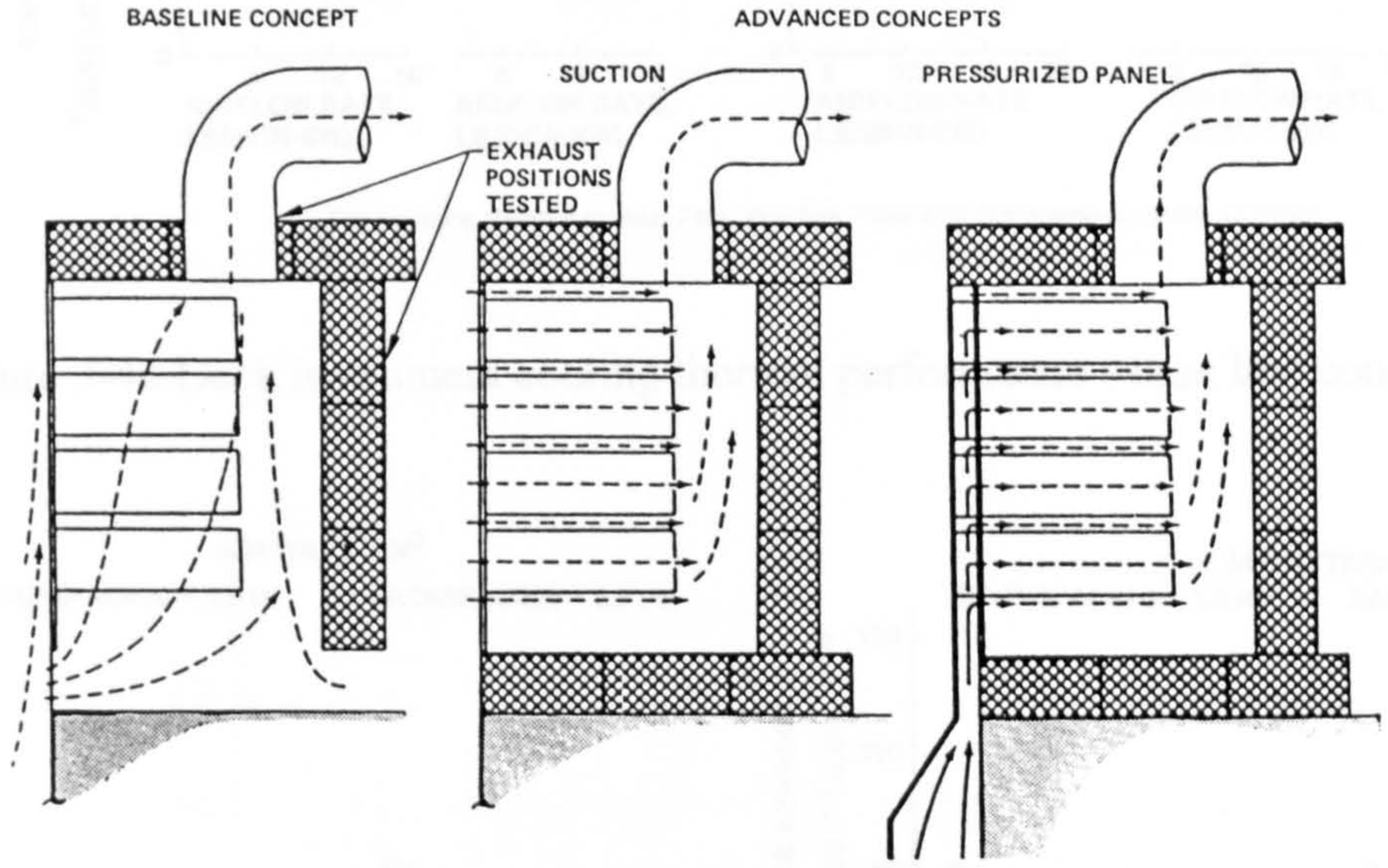

Figure 3-44 Deck instrument cooling concepts [82]

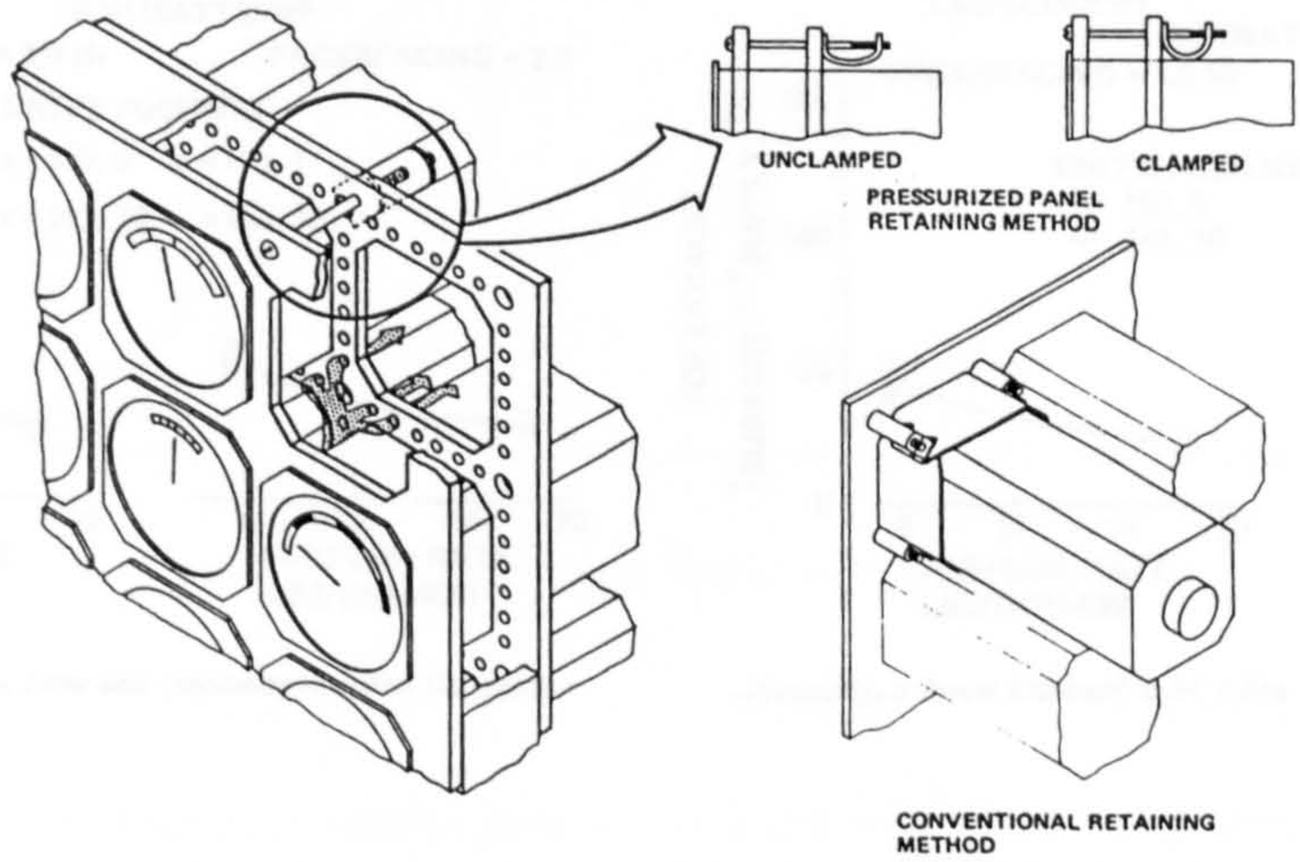

Figure 3.45 Pressurised panel retaining method compared with conventional one [82]

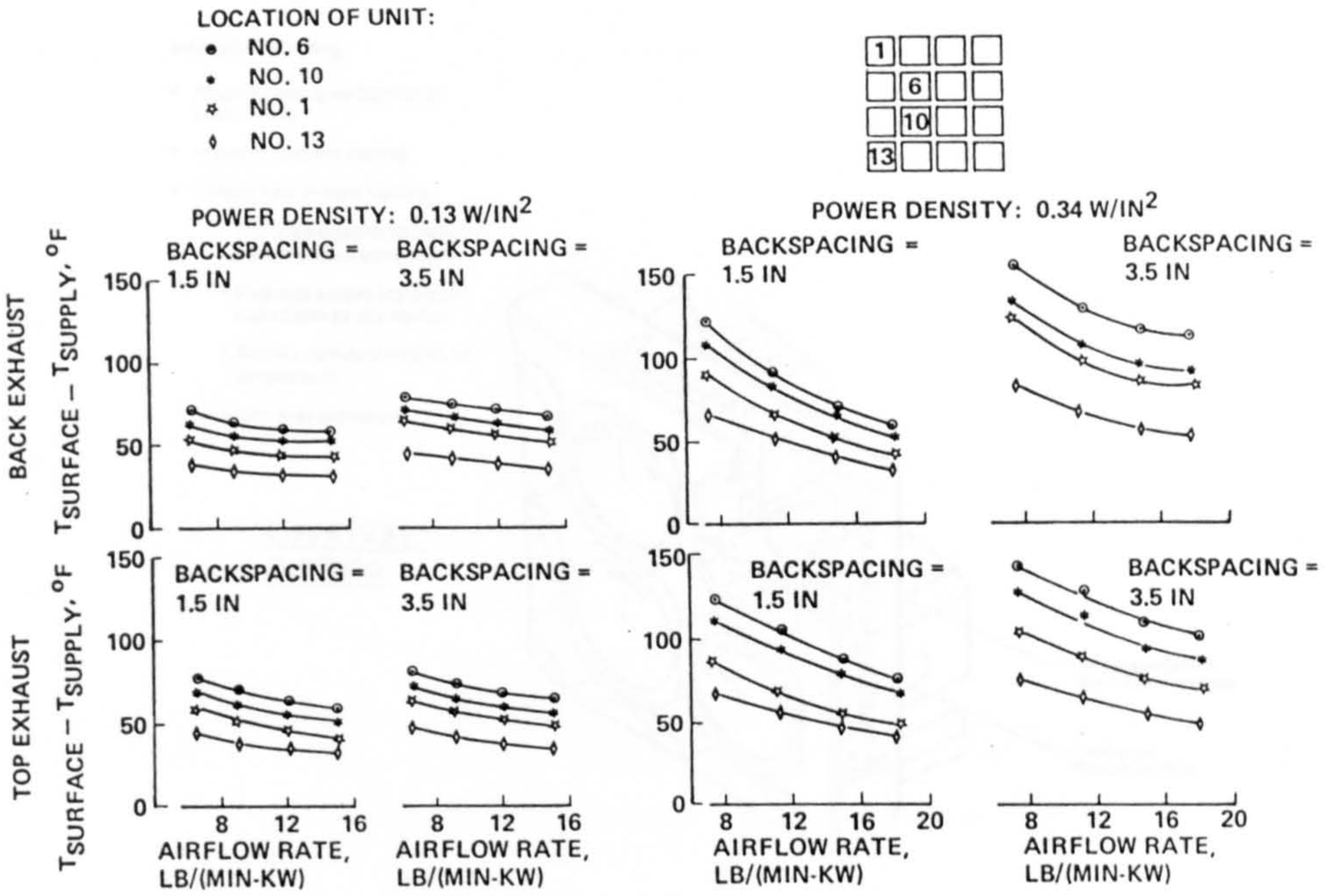

Temperature Related to Heat Flux, Position, Flow and Geometry–Baseline Concept

Figure 3-46 Deck instrument cooling thermal performance - base line concept [82]

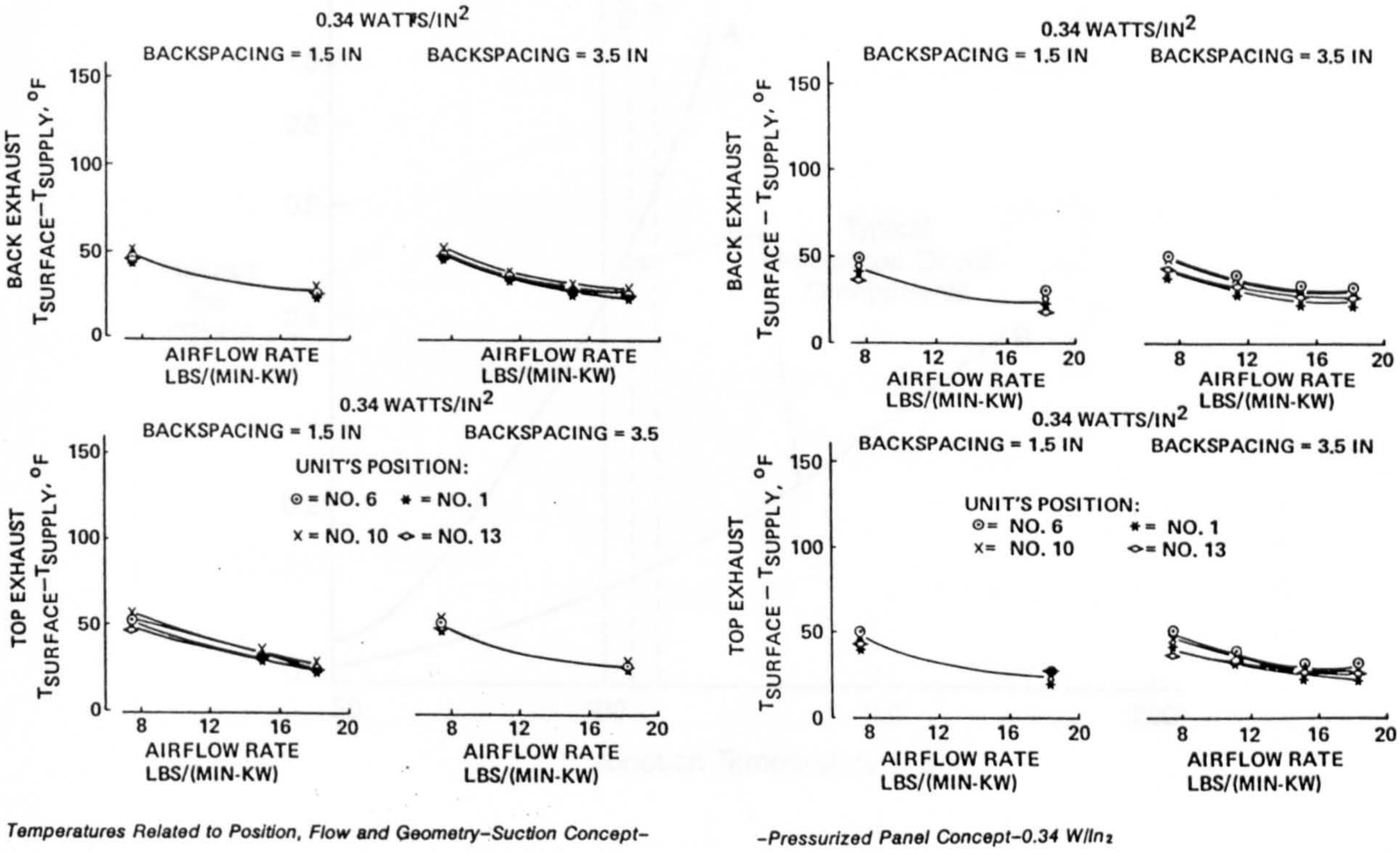

Temperatures Related to Position, Flow and Geometry–Suction Concept–

–Pressurized Panel Concept–0.34 W/in2

Figure 3.47 Thermal performance - a) suction concept, b) presserised concept [82]

Instrument Cooling

- Positive cooling for flight deck instruments
- Improved ground cooling
- Closed loop in-flight cooling
  - Reduced equipment contamination without using filters
  - Reduces system impact on main cabin air distribution
  - Permits control of cooling air temperature
  - Skin heat exchanger

COURTESY:
BOEING

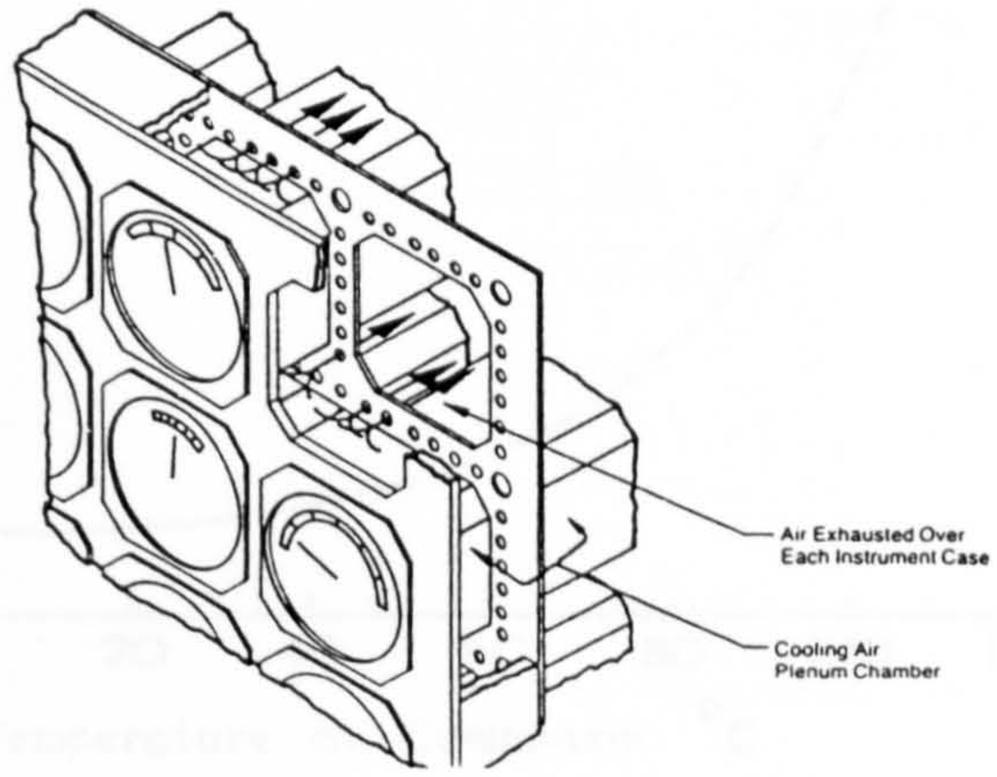

Figure 3-48 Cooling of flight deck instrument of Boeing B767, [15]

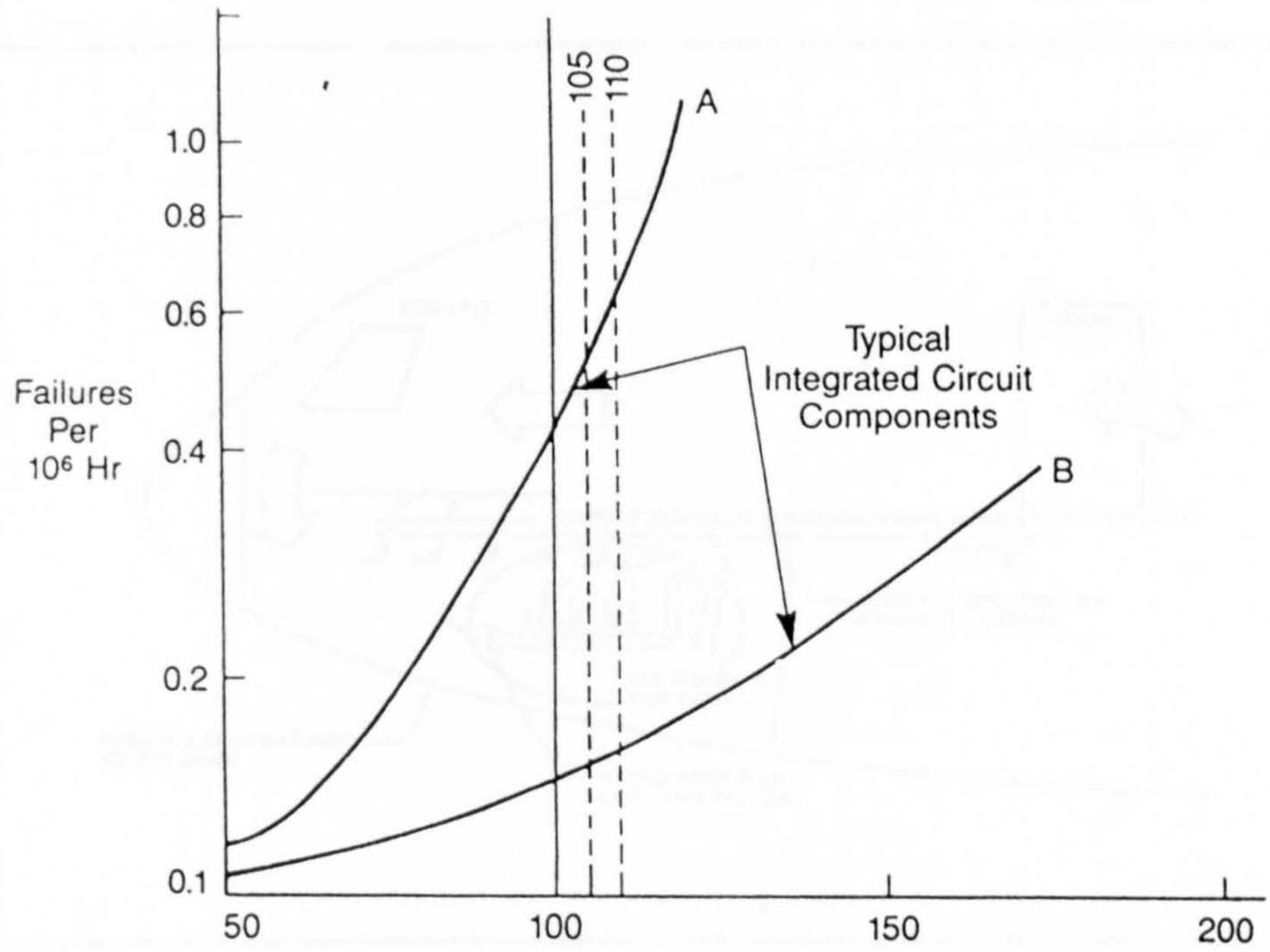

Figure 3-49 Failure rate versus junction temperature for two typically electronic components . A) Reliability sensitive to temperature B) Reliability less sensitive to temperature [83].

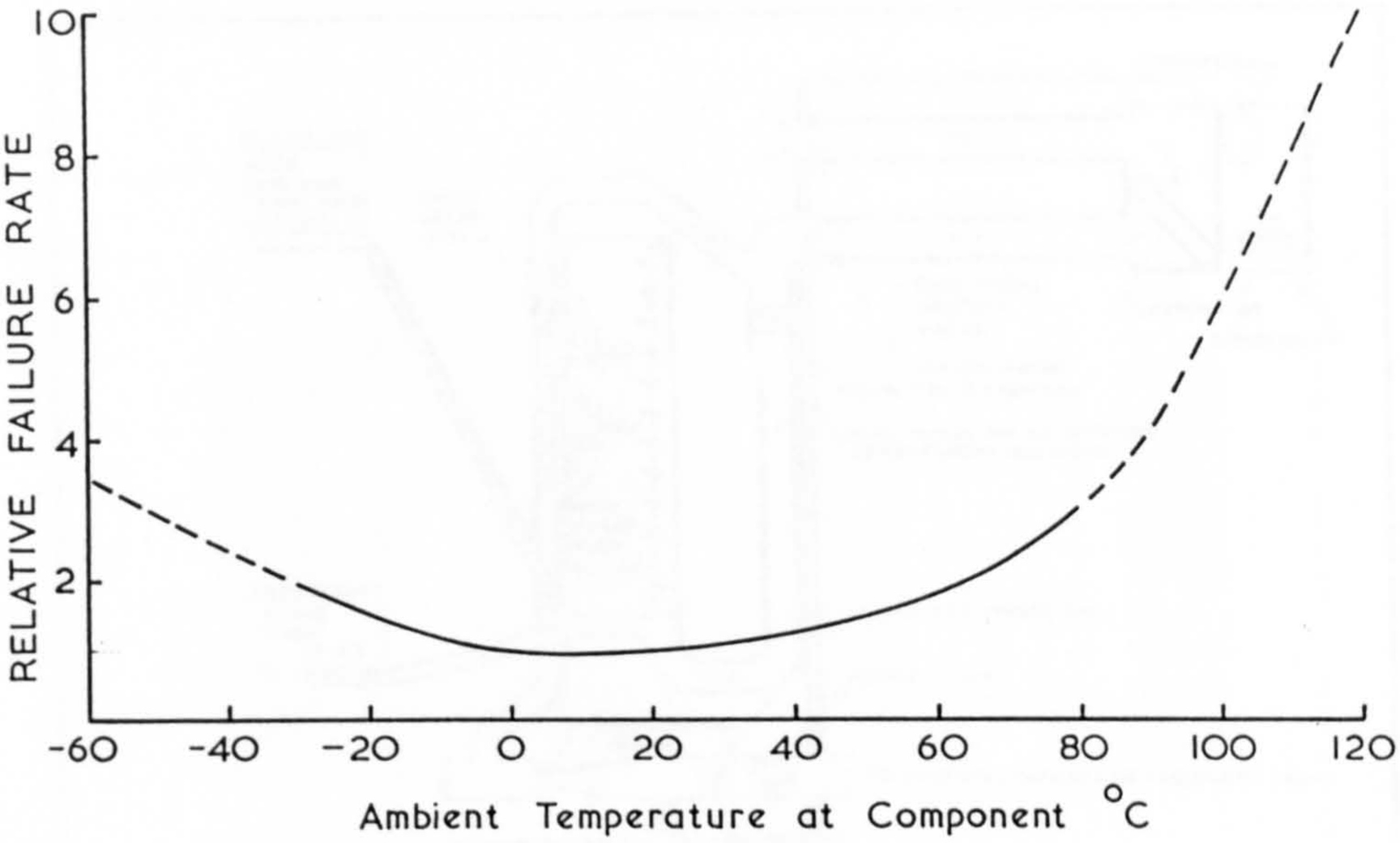

Figure 3-50 Relative failiure rate with temperature for electronic equipment [84]

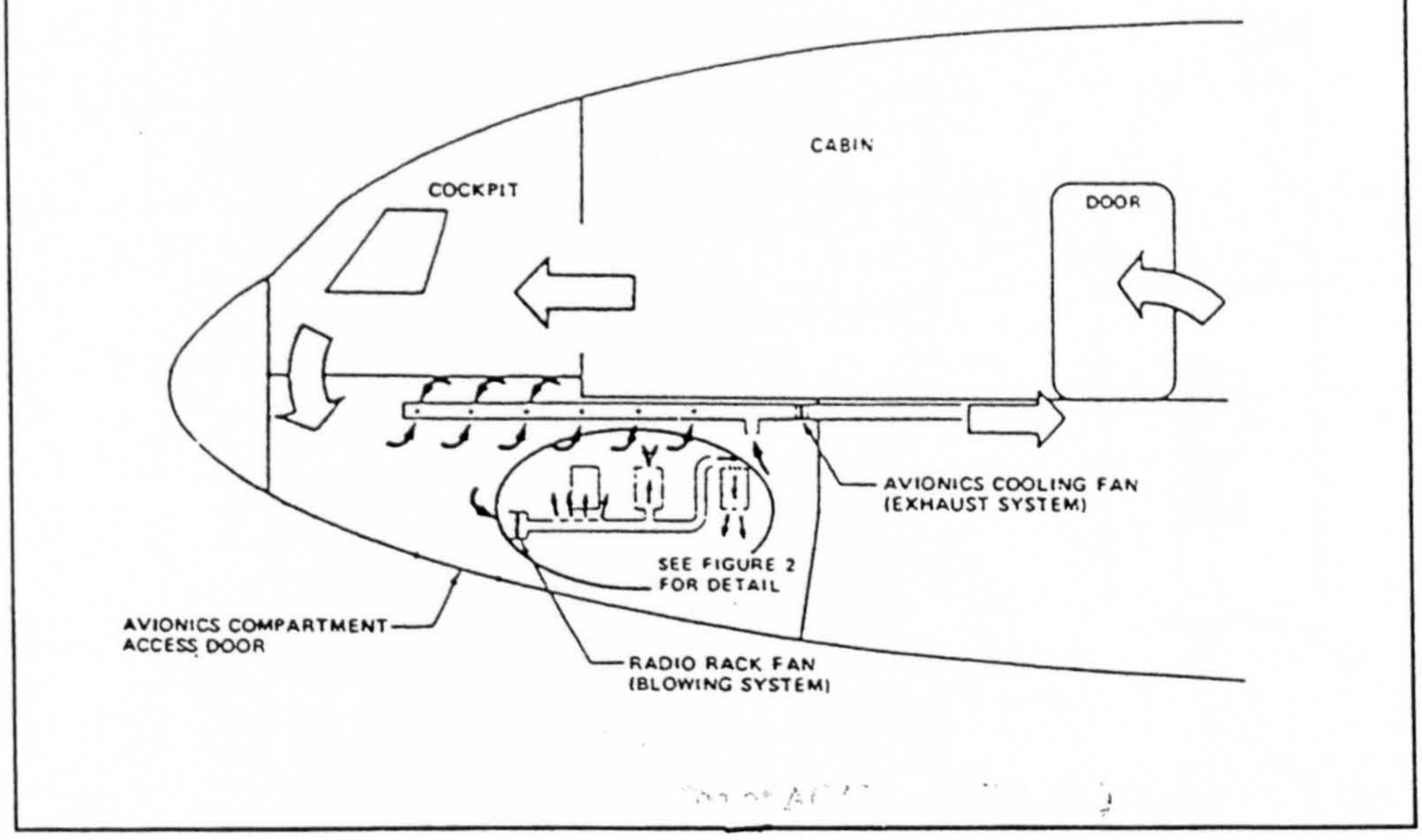

Figure 3-51 Typical location of ACAU in UHCA [85]

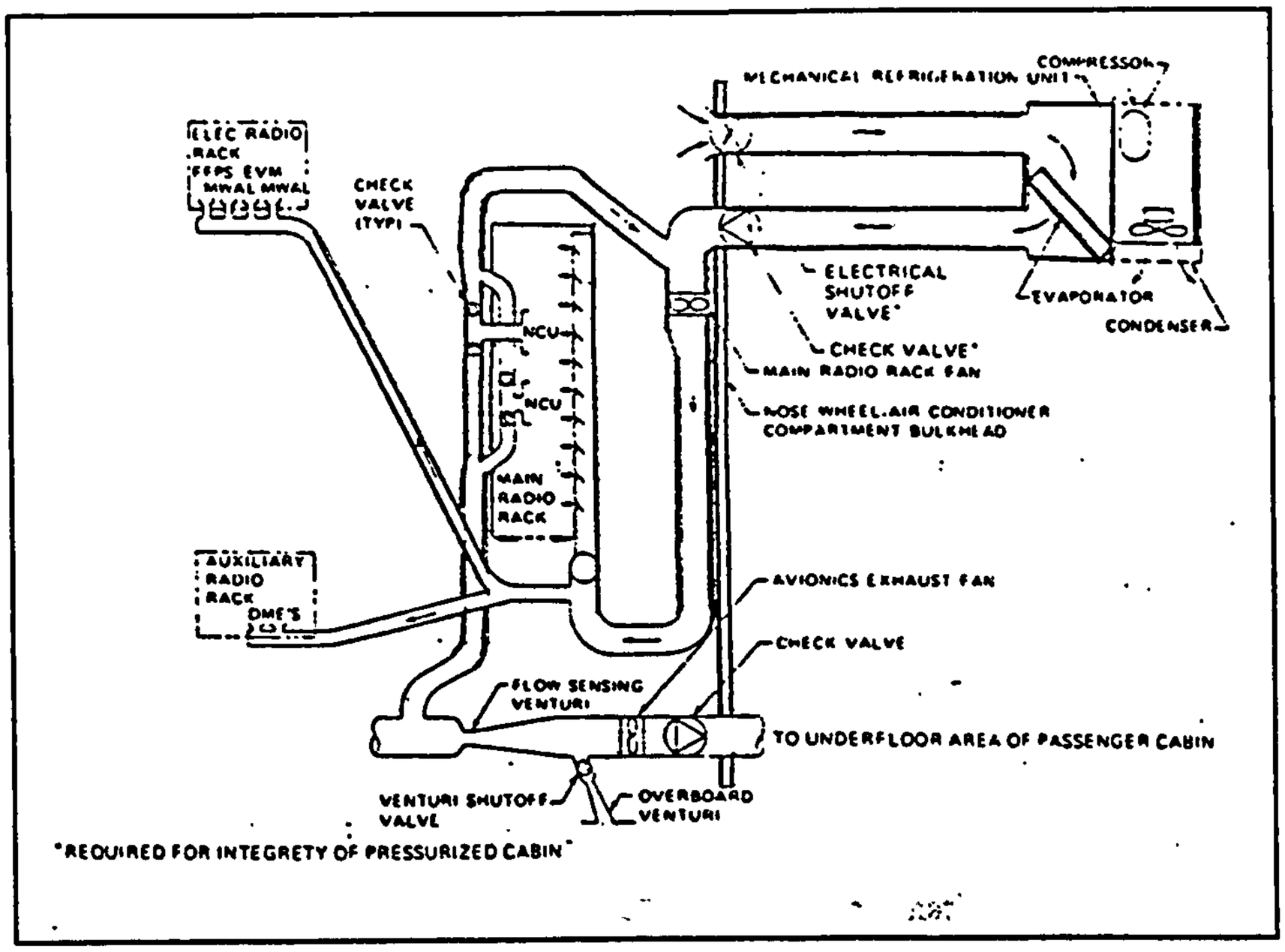

Figure 3.52 Typical vapour cycle ACAU schematic [85]

SCHEMATIC DIAGRAM OF DESIGN PROPOSAL 2
COOL FLOW AIR TO AVIONICS

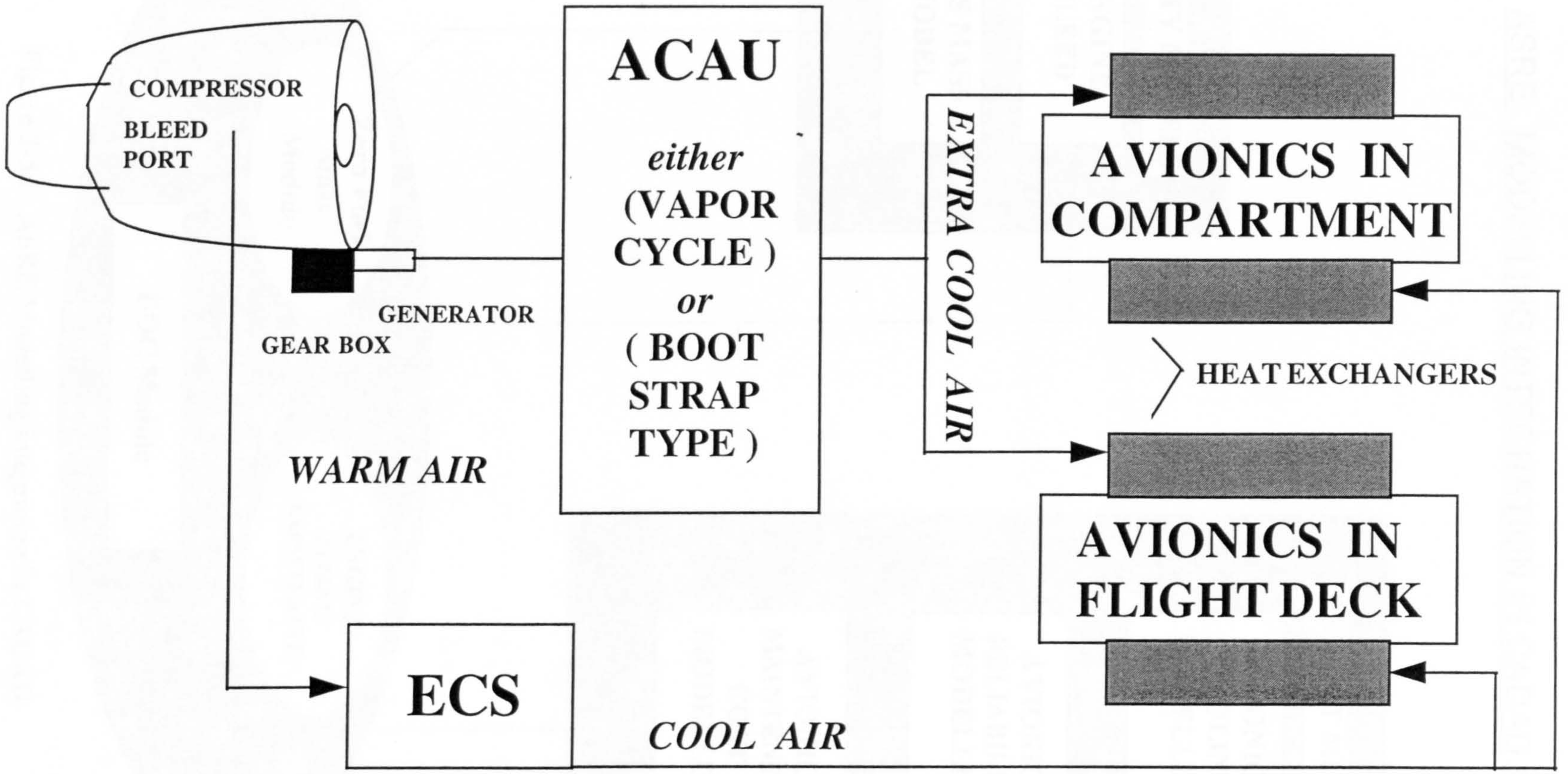

Figure 3-53 Shematic diagram of ASRE in UHCA

Cranfield UNIVERSITY

ASRE MODELLING INTEGRATION IN CADAD

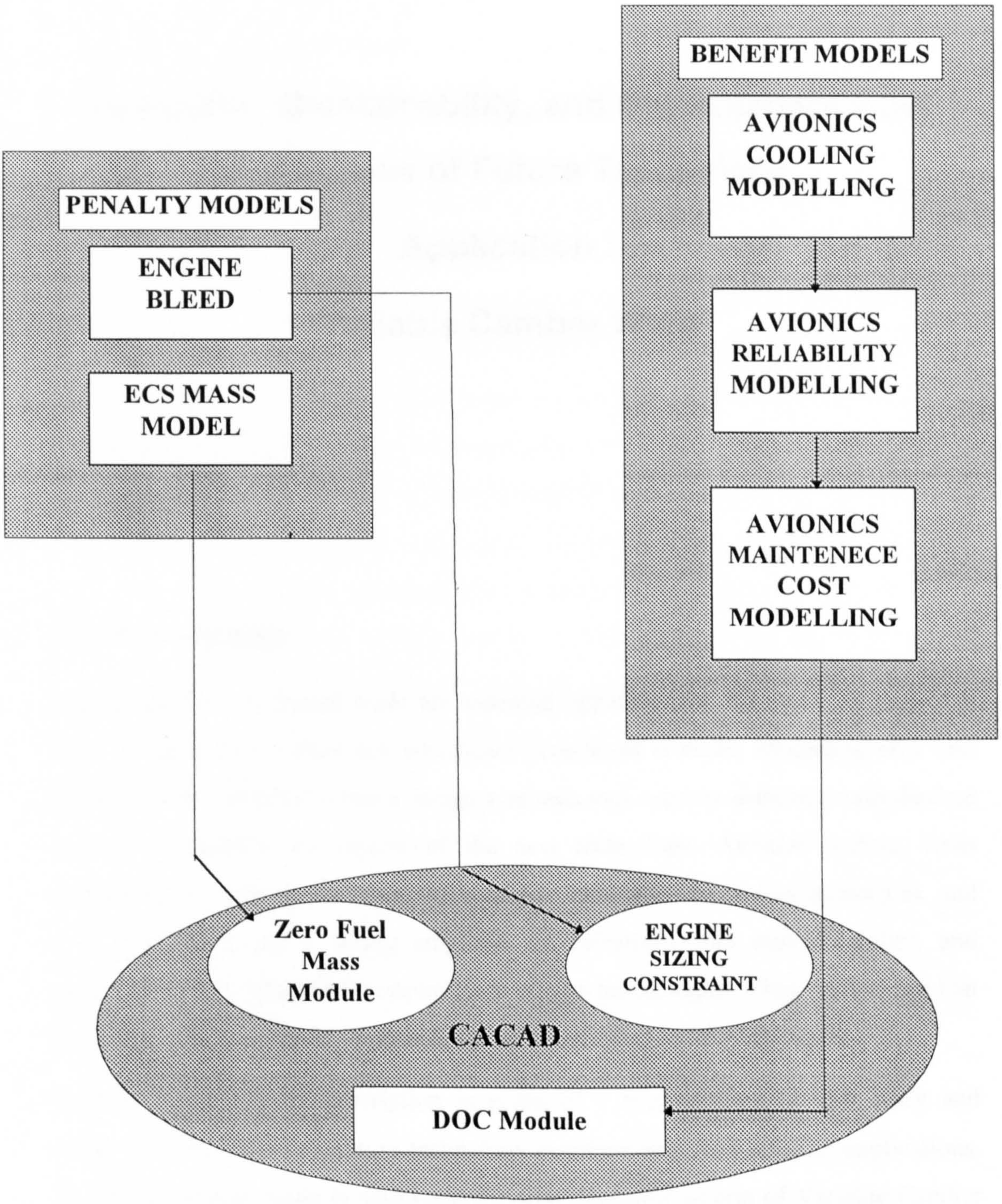

Figure 3-54 : ASRE Modelling integration in CACAD

CHAPTER 4

Reliability, Maintainability, and Development Cost Predictions of Future Technology

Application :

Variable Camber Wing

4.1 Introduction

Conceptual aircraft design tools are essential apparatus for the study of high risk future technologies, before any significant investment is made. Modelling of a new technology for integration into a design synthesis tool requires experimentally-backed data that quantifies all aspects of the new technology. Aviation sectors, from manufacturer to the airline users, maintenance industries, regulatory authorities, and even politicians, put a strong emphasis on reliability, and maintainability, and development cost (R&M&D) implications of new technologies. They wish to see that such aspects be accurately predicted, and to be reflected in DOC estimates.

In this chapter a brief description is given of a methodology for the study and evaluation of a high risk future technology together with its R&M&D implications. Due to investment made in aerodynamics, and structural aspects of Variable Camber Wing Technology (VCW) in Cranfield University, UK, and in MBB, Germany in recent years, and also reserving views expressed by the British Aerospace [135],

VCW was chosen as a typical high risk future technology. The historical development of VCW is reviewed, and the influences of VCW on all aspects of aircraft design are described, leaving the detail procedure, and formulations to be shown in Appendix D. The last sections of the chapter are devoted to the discussion and conclusions of results of VCW integration in CACAD.

4.2 Research Objectives

It is intended to develop a methodology that predicts R&M&D implications of introducing a high risk future technology into the design of jet transport aircraft. This shall be in addition to the usual modelling of aerodynamic, structural, propulsion, mass, and system changes associated with such a futuristic program. The methodology makes use of CACAD described in Chapter 2 to size and optimise a transport aircraft . Experimental results, and detail design studies that have already been carried out to defend such technologies were investigated and made into suitable models and incorporated in related modules of CACAD. The work was then extended to model maintenance cost prediction by investigating and quantifying the reliability, and maintainability aspects of new technology, using Airbus method [92], MIL-HDBK-472 [93], and already established maintainability prediction equations, and possibly actual failure rate analysis techniques. The methodology also predicts the extra development cost implication of a new technology by breaking such a cost into detailed sections, and sub-sections. It then investigates the cost effects of new technology on each element .

4.3 Methodology in General

Methods used to predict R&M&D should be such that they can be applied to any type of future technology. Every new technology be it a laminar flow wing, or use of new material in major structural parts of aircraft, and or perhaps new type of power-plant should result either in lower drag, lower take-off mass, or lower sfc respectively. At the same time, it may have mass penalty side effect, make extra use of system equipment, or extra use of engine bleed or power off-take, which may cause higher fuel consumption. The modelling of their experimentally-achieved benefits, and penalties and incorporating them into a design synthesis is considered to be a novel

research activity. It should advance the state of the art of feasibility studies, and sensitivity analysis of new technology application in aircraft design, before a significant investment is made.

On the other hand, new technologies may be associated with a combination of added equipment, added complexity, and added difficulty in accessibility. These must be investigated to the extent that the extra maintenance cost associated with the new technologies are quantified and incorporated into the DOC module of the design synthesis.

A new technology may also incur extra development cost on top of usual development costs. The usual development cost of an aircraft with a new technology on board may possibly decrease, compared to an equivalent conventional aircraft if the present prediction equations of [15], and [36] are used . This is due to the fact that the new aircraft will be more efficient and has a lower empty mass, lower fuel mass. A methodology was developed to allocate merit rise factor for every element of the sub-sections of the development costs so that, depending upon the nature of the new technology, the user is able to judge with reasonable degree of accuracy the extent to which extra development cost has occurred.

4.4 Methodology Application to VCW Technology

Among the most recently publicised new technology for use on future transport aircraft is VCW, laminar flow wing, and extensive use of carbon fibre composite material. VCW has been the subject of extensive research in both aerodynamic, as well as structural aspects in the College of Aeronautics at Cranfield University. Due to the availability of experimental results, the Author chose VCW as a suitable application bed for the above methodology. Modelling and incorporation of R&M&D aspects of VCW may also throw more light on this controversial topic, that has attracted opposing views of research scholars on both sides of the English Channel.

4.5 Introduction to VCW

In this introduction, a definition to VCW together with its design philosophy, and a historical overview of the subject is presented. The work performed at Cranfield, and MBB (presently Daimler-Benz Aerospace Airbus), will be assessed, with comparison

made of the R&M aspects, in addition to their obvious advantages and disadvantages. Finally, the type of technology and the assumptions that have been chosen for modelling will be discussed.

4.5.1 Definition and Design Philosophy of VCW

The application of VCW on jet transport aircraft is an attempt to produce a significant advance in aircraft efficiency during cruise, and thus offers considerable reduction in DOC. The fixed camber wing (FCW) geometry of present transport aircraft can be designed to give only one optimum lift coefficient, for which drag is minimum (L/D is maximum). This is allocated for the cruise phase of flight, where a large portion of the fuel is expended. During cruise, as fuel is consumed, aircraft mass is reduced considerably, implying a varying optimum lift coefficient throughout the cruise sector. To counteract this, a FCW aircraft should either increases the altitude of flight (cruise climb), with air traffic control limitations, and range, and time lost implications, or resolve to reducing the aircraft angle of attack with inevitable drag penalty. VCW, by way of varying the ordinates defining the airfoil section, offers different optimum lift coefficients appropriate to every stage of cruise, and even for other phases of flight; see Figure 4-1. This is achieved by extending and deflecting leading edge and trailing edge sections, keeping the wing box centre section between the wing spars unchanged. Traditionally leading and trailing edge sections were extended during take-off and landing phases of flight to vary the camber for high lift coefficient, and this is retained in VCW aircraft. Chordwise camber variation offers lower profile drag. Span-wise camber variation can lower the induced drag as well as wave drag, and prevents the increase of induced drag factor by maintaining lift distribution closer to an elliptic form, throughout the cruise range.

4.5.2 Historical development of VCW

Bats, birds, and insects made use of adaptive wings (variable camber included) for many thousands years. Before, and during 2nd World War, aircraft such as Albatross, Bristol, and Mustang used variable camber to enhance field (high lift devices) and manoeuvre performance . Famous post World War aircraft such as F-5, F-18, F-20, and X-29A, have all used camber variation for mainly manoeuvre enhancing device

[94to96]. For structural reasons camber changes were confined to LE, and TE portions of the wing.

Sail planes B-5, and B-6 [97], and fighter interdictor F-111(MAW) [98] are the typical examples of flexible surface deformation for camber variation. For transport aircraft applications, wind tunnel work reported in [99] showed optimistic drag saving, along with the Boeing investigation reported in [100]. They are typical late 70s design proposals for camber variation by flexible LE, and TE sections . Up to the mid 80s, VCW application using LE & TE sections was successful in military aircraft as manoeuvre enhancing devices.

4.5.3 Comparison of Cranfield and MBB Work

From the early 80s, MBB, and Cranfield University have conducted serious research work on different aspects of VCW. The aerodynamics, structural and system aspects, of VCW were the main areas of investigation. Intensive 2-D computational work, and 3-D wind tunnel works were carried out with airfoils specially designed for VCW. Actual prototype with flexible skins and non-flexible types, along with system incorporation, were developed and tested for strength and functional operation in both centres. The results of their work were published in references [101to118].

4.5.3.1 The Cranfield VCW Work

Cranfield pursued the aerodynamic philosophy of Professor Spillman who proposed a system whereby the leading edge and trailing edge segments of a wing are deployed in circular arcs resulting in both rotational, and chord extension incorporating some form of flexible material to take care of chordwise as well as span-wise variation of camber. Figure 4-2 shows the concept. The structural, as well as aerodynamic aspects of this concept was experimentally investigated under the auspices of Professor Fielding by Rao [109], Mackinnon [110], and Macci [103], and later through preliminary design projects by large number of students [103,104,119to124] which altogether created a treasury of information on VCW. The major considerations are as follows :

(a) The circular arc deployment of variable camber devices (VCD) ensures gradual, and smooth change of curvature from LE to TE, hence causing least drag penalty.

(b) Flexible skin camber variation is shown to be practically possible as it facilitates span wise camber variation with less drag associated with VCD splitting.

(c) Differential camber variation across the span not only offers a more elliptical lift distribution, it can also mean that low speed tip stall may be prevented by camber changes on the outer wing. These features lead to the idea that VCW requires less or not built-in twist with consequent drag saving benefits.

(d) The studies of [103to106] show that incorporation of high lift devices within the Cranfield VCD requires further practical design and development work.

(e) It is vital that the drag polar crossover point, for varying camber takes place at usual cruise lift coefficient, to produce an overall cruise drag saving. The Cranfield VCW offers the crossover point at higher lift coefficient, which requires further experimental work, see Figure D-14(c).

(f) There is further design work required to show practically, how the Cranfield VCD, along with high lift devices operate inside it, can be deployed on a swept, tapered, slightly twisted, and kinked wing of present transport aircraft.

(g) Cranfield VCW trailing edge system is composed of VCD as well as high lift devices in two different assemblies but the former is nested in the latter. The High lift devices in the Cranfield VCW however do not need to deflect as much as the equivalent system in FCW aircraft, with consequently lower weight. However the conceptual design mass estimation prediction equations treat it as a set of double moving surfaces at the TE of the wing. This makes the system to have higher mass penalty than that of the MBB design, because of all the elements involved.

(h) The Cranfield VCW requires a set of hydraulic actuators and their piping, in addition to hydraulic actuators necessary for usual high lift devices.

(i) In order to extend and deflect the camber varying surfaces on a circular arc basis (no matter how small), the Cranfield design philosophy requires a greater chordwise portion of the wing trailing edge section (more than usual

value of 30%), hence reducing the distance between the spars from the optimum value. This produces higher mass within the wing box in order to withstand the same flight loads.

(j) Due to the extra control surfaces, track mechanism, and actuators together with a potentially higher rate of failure associated with the flexible skin of VCD, the failure rate of the trailing edge system increases considerably. This will increase the cost of maintenance man-hours, and material to values higher than the trailing edge system of the present FCW.

(k) Cranfield VCD consists of moving camber varying surfaces, inside which high lift devices are nested, and out of which they extend, together with flexible skins made of fibre reinforced plastic, making it a novel design. This requires higher development costs, to guarantee a reliable service operation, along with higher certification cost.

4.5.3.2 *The MBB VCW Work*

Flexible skin camber variation allows a gentle change in curvature ensuring drag saving and seems most suitable for transport application, but perhaps due to reasons such as higher development cost, complexity, higher mass penalty, and tougher reliability standards of civil aircraft they were not pursued by MBB group, who were determined to apply VCW on the Airbus A330, and A340 aircraft .

MBB research scholars, who operated within Industry, were perhaps cost conscious, and pursued a design philosophy that was less innovative. They chose to vary the camber using the traditional high lift devices [109], Figure 4-3 shows the concept. Major considerations are as follows :

(a) Although chord-wise camber operation looks clear from given figures in the published literature, the differential camber variation across the span might need more justification, and illustration so that its complexity becomes measurable.

(b) MBB-designed VCW, when incorporated with an appropriate airfoil, demonstrated a suitable cross over point at usual transport aircraft cruise lift

coefficient, see Figure D-15 [114,fig4].This ensures drag saving during cruise, when the C_{Lcr} extreme values lies on either side of crossover point.

(c) In the MBB design philosophy, the Fowler motion for camber changes is established by the flap body, sliding underneath the spoiler trailing edge i.e. rubbing against it, see Figure 4-4 [112]. The rubbing action will need to be carefully designed so that it provides minimum friction and is not degraded by contamination such as dirt, and ice. The rubbing material is a potential maintenance cost hazard.

(d) The theoretical as well as experimental results indicate that flap chord lengths of more than 13% gradually degrade the drag saving of VCW. This may produce flap sizes smaller than what is optimum for take-off and landing. Hence implying a higher wing area or more complicated high lift devices in order to achieve the required approach velocity.

(e) The proposed system has undoubtedly superior qualities in maintainability, reliability, and lower development cost. It has features that offers no extra production cost factors to the existing trailing edge systems.

(f) The airfoil, specially designed for MBB variable camber wing apparently requires a small Fowler motion by the TE flap to change its camber, hence offering all the claimed benefits. If due to any reason camber operation ceases to commence, the consequences must be carefully studied, because two different operation by one system are lost.

4.5.4 Design Assumptions, and Aims

Assumptions under which the variable camber wing modelling was carried out for incorporation into CACAD are based on the design philosophy that has produced the most realistic experimental results. A design scheme was chosen that is technologically possible with the least extra cost of production, and having good R&M features. It is hoped that the feasibility study and the results of such an operation will become useful, and perhaps form a basis for any future consideration for the application of VCW technology in transport aircraft. These results together with a sensitivity analysis may offer a clearer picture to the leaders of future

programmes of transport aircraft. Listed below are the features of technology, and the assumptions that were chosen, for VCW modelling with, as many generic features as possible, incorporating features of both the MBB, and Cranfield concept :

(a) Camber variation by using the traditional high lift devices at the TE, similar to MBB design philosophy.

(b) Differential camber variation across the span, by using flexible skins at segment junctions.

(c) VCD system composed of inboard, and outboard flap. It also uses the aileron as flappernes ; see Figure 4-5.

(d) There will be independent actuators for the variation of camber across the span; see Figure 4-6.

(e) There shall be an allowance for the flap chord to rise to the maximum of 40% of the wing chord .

The aim of modelling of aerodynamics, mass, R,M&D for generic VCW configurations within CACAD is to establish :

- A transport aircraft configuration sized and optimised with VCW technology onboard, along with the effects of R&M&D implications.
- The quantitative contribution that each model offers to aircraft DOC, fuel, and drag module.
- VCW effects on overall configuration and cost of aircraft with different capacity, and range.
- Applying sensitivity analysis by variations of those parameters that are open to engineering judgement interpretations and possible experimental errors.

4.6 VCW Modelling Flow Chart

Before a detail variable camber wing modelling description is presented, it is useful to see these models in one picture and their relations with respect to CACAD. Figure 4-7 shows the models and differentiates them into penalty and benefit categories. It also demonstrates the link between these models with respective CACAD module.

4.7 Variable Camber Wing Modelling

VCW modelling sections of CACAD are composed of aerodynamic, mass, and R&M&D modules. Often the modelling produces reductions, or increments on parts of the aircraft that quantify the influences of VCW. Therefore a FCW aircraft design was chosen as a pre-requisite to the VCW design as a necessity, other than just for comparison purposes. For example there are certain disadvantages with FCW aircraft itself which are absent in VCW aircraft. These disadvantages are modelled and integrated into VCW aircraft synthesis in a positive manner. Under above heading, aerodynamic, and mass modelling are presented below, leaving the R&M&D modelling to a separate section.

4.7.1 Chord-wise Drag Saving In VCW

The main asset of variable camber wing technology is to employ chordwise camber change to arrive at a desirable C_L to match the requirement of cruise phase for optimum operation of aircraft, against existing methods which is either by changing angle of attack or flight altitude. This will save some cruise drag, if an appropriate airfoil section is used for wing design, and also the location of crossover point in the drag polar be at the usual cruise lift coefficient, see Figure D-15, in Appendix D. This primary drag saving is achieved whether or not the wing is made to acquire other drag savings elaborated in next sections [When the VCW is attached to the fuselage, it helps save further on upsweep drag, and wing fuselage viscous interference drag. When the span-wise camber change is employed the drag savings in sections 4.7.3 to 4.7.6, will be achieved].

The computational methods, and experimental works used to investigate the amount of drag saved during cruise, based on design principles of Cranfield, and MBB are reported in [105to107], and [109to114] respectively. Investigation of the theoretical and experimental results on 2-D, and 3-D wings with VCD for both design proposal shows that a drag saving of 5% may be possible during the cruise phase of the flight. In section D.7 the details of such works by MBB, and Cranfield are presented together with the amount of drag saved.

4.7.2 Rear Fuselage Upsweep Drag

This section deals with the drag saved due to the absence of angle of attack variation effects on rear fuselage upsweep. Rear fuselage upsweep causes an extra drag which is added to the fuselage's other drag components. It is defined by the cross flow concept [32,125], and is a function of fuselage planform areas of forebody A_I and aft swept body A_{II} . It is also a function of fuselage angle of attack α_f , and upsweep angle β (see Figure 4-8). It is a common practice to fly at an angle of attack at which the rear fuselage upsweep drag becomes minimum. The reduction in aircraft mass due to the fuel consumption during cruise, causes some reduction in the required C_L from the wing. In FCW aircraft where there is restriction on flight altitude, pilots usually have to change flight angle of attack until the wing produced C_L matches with aircraft required C_L. This gradually puts the rear fuselage upsweep at an angle different from the optimum one and hence the drag associated with upsweep rises.

In VCW aircraft, camber change can be used to reduce lift coefficient during flight, but maintains the fuselage at the optimum angle. This benefit has been modelled in CACAD for every cruise sector, the formulation and further description is given in Appendix D, section D.2. The study show that for an aircraft resembling the A340, the drag saving is approximately 0.9 counts (0.00008 to 0.00010) per every sector of cruise.

4.7.3 Wing Fuselage Viscous Interference Drag

This is the modelling of variable camber wing/fuselage viscous interference drag reduction due to the reduction of wing installation angle on fillet size in the wing-fuselage junction of a VCW aircraft.

Viscous interference is one of the components of the wing fuselage profile drag . According to [32], it occurs near the intersections of the wing and fuselage where there is a thickening of the boundary layers developed by the fuselage and wing. It also arises due to an increase in the local velocity near the intersection over the fuselage body. Both effects cause extra profile drag. This drag besides, other parameters, is approximately a function of wing/fuselage fillet circumference. In VCW, due to the reduction or absence of twist angle, the wing installed angle is

reduced, see Figure 4-9. This helps to reduce the fillet circumference value, and consequently the viscous interference drag. For this advantage to be modelled, the wing installed angle with and without twist is determined using a standard relation from [32]. The difference is used in conjunction with fuselage minimum drag incidence angle α_f (determined in previous section) to establish a new value for the circumference of the fillet. This will be lower for VCW. The formulation is given in section D3. For aircraft resembling the A340, this drag saving is very small, nearly 0.0857 counts. The origin of the formulation is from Hoerner, but no reference to experimental data. Due to negligible VCW gain over FCW, any further literature survey may not be justified.

4.7.4 Induced Drag due to Twist

This is the modelling of induced drag saving due to the reduction or absence of twist in VCW aircraft. The wing tips of the tapered FCW aircraft are usually twisted relative to the wing roots to reduce the angle of attack at the tip portion. This prevents tip stalling due to lower local incidence. The aircraft wing performance is assisted by twist during the approach when the angle of attack is high, and the control surfaces at outer wing must be fully operational.

There is a drag associated with twist which is the function of twist angle and aircraft lift coefficient [126]. When a VCW aircraft, approaches stall, the variable camber devices at the trailing edge of the outer wings are operated to produce negative camber, thus off-loading the tips, and preventing tip-stall. Hence the need for permanently twisting the wing is reduced or eliminated, and with it the associated induced drag. The formulation and description are given in D4. The drag saving for the VCW version of A340 type aircraft, varies from 3.8 to 4.5 counts. There is no experimental evidence recorded in standard texts for validation of the formulation used in section D.4, but an alternative relation in Hoerner [137] produces 6.4 counts of saving. This put above calculation on the safe side, being reasonably conservative.

4.7.5 VCW and Induced Drag Factor

In FCW aircraft, the lift distribution during the cruise phase departs from an elliptical distribution and pushes the centre of pressure towards the outer part of the wing,

hence increasing its moment arm from wing root. This tends to gradually increase the induced drag factor, which is a function of the location of the centre of pressure from wing root [128].

In VCW aircraft, however, variable camber devices are deployed in such a manner that the lift distribution is held elliptical, hence keeping the centre of pressure location unaltered . In CACAD, an empirical equation B90 [14] determines the average value of induced drag factor which varies from 1.1655 to 1.183 (refer to Appendix B tables of transport aircraft results). This value is validated by the figures given in [15, 32, 34, 1]. Therefore it is preserved for FCW design, and also as an average base value for VCW aircraft. The theory proposed by Garner [128] was used to establish the rate of variation of the induced drag factor with aircraft lift coefficient. This rate was used to determine the rise of this factor from its base average value, as the aircraft covers each cruise sector. The increment was used in negative form (benefit) for the VCW drag module. The detail formulation is given in section D5. For an aircraft like A340 in a VCW version, the induced drag factor was found to vary from 1.18175 to 1.16921. This variation is reasonable, because it falls within the Torenbeek given variation of 1.176 to 1.333. Also one of the formulae used (Equation D10) in section D5 is claimed to be very accurate by Torenbeek.

4.7.6 Mach Critical Drag and VCW

In a FCW aircraft, a typical variation of aircraft C_L with Mach number at certain angles of attack is depicted in Figure 4-10, where C_L reaches a peak value as Mach number approaches Mach critical lift, M_{CRL}. On the other hand C_D also increases rapidly with Mach number. When the increment in C_D reaches 0.002 ($[dC_D/dM]=0.1$), the Mach number is called Mach critical drag M_{CRD} [25]. At higher C_L this Mach number is reduced by ΔM_{CRD} and limits the flight speed. Aspect ratios beyond 8 have negligible effect on M_{CRD} [25]. Higher thickness chord ratios and lower sweep angles reduce Mach critical drag, and hence limit the flight speed.

For a FCW aircraft, the lift distribution along the span is such that section lift may exceed aircraft C_L (usually by 0.05 to 0.125, depending on range, and aircraft payload) in certain regions of the outer wing. The maximum section C_l will then

influence Mach-critical drag, therefore restricts the wing thickness to chord ratio. In VCW, on the contrary, the section C_ℓ may not exceed aircraft C_L due to the fact that twist is either absent or reduced considerably and lift distribution is maintained in an elliptical form. The above findings were quantified using the difference between section C_ℓ, and aircraft C_L. This difference is then favourably treated as a benefit and is subtracted from aircraft C_L reducing it for use in VCW Mach critical drag module.

On the other hand, C_L buffet onset is enhanced in VCW, producing higher Mach critical lift, see Figure 4-11 [109], hence allowing the aircraft to fly to a higher Mach number, and / or can have lower sweep, or higher thickness to chord ratio for the same flight Mach number. Both phenomena i.e. higher Mach critical drag, and Mach critical lift help VCW aircraft to be designed and optimised for higher thickness to chord ratio and/or alternatively lower sweep angle (whichever the optimiser finds most cost-effective with respect to DOC). A NASA report on VCW [100, page 60] also allows lower sweep, and higher thickness to chord ratio for VCW but with a slightly different argument for this subject.

This topic is further described with appropriate formulation in section D6. For the A340-200 class of aircraft, a FCW version produces an optimised thickness to chord ratio of 0.095, and a sweep $\Lambda_{1/4}$ of 27.76 degree. A VCW version is sized with an optimum value for thickness to chord ratio of 0.100, and sweep $\Lambda_{1/4}$ of 27.73, contributing a 0.5 to 0.75% reduction in DOC.

4.7.7 VCD Mass Estimation

Variable Camber Devices (VCD) must operate in similar ways to flaps, and aileron systems, when considering the MBB method. They extend to more than 90% of the wing net semi-span, divided into a number of sections . The inner-most wing, will act as an inboard flap segment, the middle section as an out board flap segment and the out board section will be flaperon segments (Figure 4-4).

The area of VCD / flap surfaces and hence their width and length act as independent variables in the aircraft design optimisation cycle, and the flaperon size is then determined accordingly. Therefore there is no need to establish a special module to size VCD.

The scheme of the system solution is given in Figure 4-3, where the camber variation is achieved by a small Fowler motion, in which the wheels of the flap carriage are guided by the two individual tracks in such a way that the flap body slides underneath the spoiler trailing edge. From the most deflected camber position the flap proceeds on its normal track into the high lift position. No mechanical additions beside the second track, nor additional drives related to VC are needed for chordwise camber change. For span-wise operation of VCD, there is perhaps a requirement for extra fittings, as well as extra actuators with further complications; see Figure 4-3.

The empirical solution to the estimation of the specific mass of flap systems in FCW aircraft incorporated in CACAD was taken from [14] which originated from Torenbeek. It has been investigated and found suitable for use with a modification to predict the specific mass of VCD for flap sections, and VCD for flaperon segments.

VCD operation during flight requires some extra mass in addition to the flap system to allow for extra fittings, and track and flexible skin, and higher cruise speed than approach speed, etc. As for outer flaperon section, the extra function of camber variation in addition to aileron operation, will add mass to the existing formulae for estimating the mass of the remaining of the trailing edge. The deflection behaviour of the flaperon in cruise requires the same sort of fittings and track mechanism as ailerons, but the Fowler motion will lead to increased mass. These extra masses seem mainly to be due to the VCD deflection angle. Therefore a relationship to predict the effect of deflection angle on flap system mass was used to predict the mass increment of VCD. In the similar manner, the deflection angle was used to predict the mass penalty of VCD flaperon over ailerons.

Equation B77 was used for the MBB design principle for the inner, middle, and outer sections of the VCD. One of the variables of the flap mass density within equation B77 is the flap deflection angle. By tracing the sensitivity of the equation to deflection, and given that the flaperons are less deflected than a conventional flap, a range of values were found to yield a mass density higher than usual ailerons but lower than flaps.

A typical value of FCW aileron mass density for a A340-200 class of aircraft is 30 kg/m^2 [14] and for a flap system covering 20% of the wing chord, 52.5% of the span,

at a deflection of 30 degree, on a wing with $\Lambda_{1/4}$ of 27 degree is 47 kg/m^2 (Equation B77). The modified mass estimation equation D27 yields 45 kg/m^2 for flaperon, and 60 kg/m^2 for VCD flap. These values seem reasonable, for the following argument :

The trailing edge surfaces of the same class of aircraft for FCW is 64.53 m^2 of which 45.92 m^2 is for flaps and 18.61 m^2 for the ailerons, with total mass of 2771 kg . In VCW for the same mission, the total trailing edge surface is 67.75 m^2 , of which 53.07 m^2 is VCD for inner and outer flaps, and 14.80 m^2 is flaperons, with a total mass of 3518 kg i.e. 26% higher than FCW. A mass increase of 2.3%, relative to wing mass.

The percentage of FCW trailing edge system with respect to take-off mass of typical aircraft resembling A340 is 0.011, and that of VCW version is 0.0144, an increment of 0.0034. Examining Table 2a of [129] gives some quantitative feel about mass increment of devices at LE, and TE of the wing as percentage of take-off mass.

Increment due to single slotted flap	0.003
Increment due to double slotted flap	0.006
Increment for LE slats	0.007

If we assume the additional mechanical complexities, and parts due to VCD to the TE of the wing resembles, converting single slotted flap to double slotted, and or less than installing a leading edge system, then the mass increment due to VCD operation in conjunction with flap operation when compared with above increments sounds reasonable, and conservative. Also Boeing in [100] used its long experience in aircraft design and development to predict 20% rise in the mass for a wing TE equipped with VCD. Their prediction is 6% lower than the above prediction. This may be due to the fact that, Boeing VCD, covers only 60% of the outer wing leaving the flap system un-modified, see Figure 4-11. It may also be due to Boeing's wing does not undergo span-wise camber change (at least they have not claimed so in [100]). MBB predicted that a TE system with only chordwise camber change capability, based on their design principle, may cause an extra mass of 0.5% relative to wing mass. This is a very optimistic value, compared to 2.3% due to our methodology, and Boeing's predictions. It may be concluded that the methodology developed in this Chapter, in

predicting the mass of VCD system is conservative, but can be trusted against probable risks.

4.7.8 VCW System Mass Prediction

The introduction of VCW in jet passenger aircraft is bound to expand the functions of aircraft systems, of which hydraulics, and flight control systems seem to be the most affected. The MBB method superimposes the secondary variable camber function with a primary function of the flap system. This is the most controversial part of the MBB design philosophy.

No matter which alternative design method, is used, when the question of mass is concerned, it is advisable to choose a reasonable but more conservative-oriented approach when the feasibility of new technology is under investigation. Most of the design proposals require enhanced hydraulic systems i.e. more actuators and hence more piping in the wing, though the design philosophy proposing no differential camber across the span claimed that no extra equipment is required. To reflect the addition of actuators, hydraulic pipe lines, and extra switches and relays in a highly empirical and statistical hydraulic mass estimation equation of the present texts is probably difficult. There is also no definite consensus about the number of such items and how they may vary with aircraft seats, and range.

A mass estimate equation for hydraulic systems is required that includes the number of system functions besides the usual parameters such as aircraft size and mass. Among standard texts, the Raymer relation, B175 was found most suitable. The validity investigation showed that this equation underestimated the transport aircraft hydraulic system mass by 4.7 times. Section D.9 was devoted to this investigation, together with a modification to the formulation.

Flight control systems by-&-large do not undergo mass increments as a result of VCW operation [109,112,118]. The main effect is the possible expansion of flight management software, and increased complexity in the electronic flight control system (EFCS). It is perhaps right to envisage, with a reasonable degree of confidence, that there is no additional mass for flight control system for conceptual design estimates. It is true that a flight control system's functions will increase as a

result of VCW, and according to Reymer this must be accompanied with some form of extra mass added to the system. The nature of the functions added to the system i.e. modifying the flap control computer program such that in addition to the conventional discrete high lift settings it will be flexibly start/stop the flaps in VC-regime. This does not entitle the system to a mass increment.

4.7.9 VCW Wing Box Mass Estimation

VCD, when installed at the TE of the wing usually occupies a higher percentage of chord (30 to 40%) than the conventional TE lift boosting devices (20 to 30%). This places a burden to the usual spar spacing which is usually 50% of chord for optimum wing skin mass. Normally, when wing spars are brought closer (less than 50%), the skin-stringer chord is less, and their bending-moment handling deteriorates and the skin must become thicker than optimum to compensate for. There is also the possibility of a reduction in fuel tank capacity.

Most available wing mass prediction equations do not take spar spacing into account, and few even reduce wing mass when the distance between the spars are reduced. Reference [14], from which wing mass estimate relations are taken from deals with the wing mass in relatively more detail, than any published literature. It consists of separate mass prediction equations for spars, ribs, skin, trailing edge flaps, trailing edge aileron, LE devices, undercarriage fittings, engine pylon fittings. When the spar spacing is reduced the mass of the skin is reduced; see equation B127. This is true when this distance is reduced from 0.75 down to 0.55. In VCW it is necessary to allow the distance to be further reduced. This makes this equation and most of the other open literature ones inapplicable for VCW. Boeing in [100, section 6.6.1] also elaborated the above problem but did not include a methodology to quantify it. Howe [129], recently developed the prediction equation B136 that takes into account the above short comings. This equation was used when VCW modelling was integrated into CACAD for estimation of the mass of wing skins. The detail formulation and description is given in section B2.14.

4.8 VCW R&M&D Cost Modelling

Although VCW technology offers a number of aerodynamic benefits, it also influences the TE of the wing, and perhaps hydraulic, and flight control system in a variety of ways. The obvious one is the extra mass, which was discussed in previous sections. Among other influences are perhaps, complexity increase, accessibility deterioration, increase in the number of parts, and pieces of equipment. It may also increase the number of functions of a few systems. These all add up to increase the maintenance cost. It may also impart some extra development cost. In the following sections the methodology by which these extra costs were predicted will be presented.

4.8.1 Maintenance Cost of VCD System

VCD are subjected to dual functions, low speed lift boosting operation and high speed camber change. This may be a major modification to the operation of the trailing edge system. It will take great skill by the designers to accomplish this with minimum increase in failure rate, ensure that the reliability of operation will remain as good as a conventional TE, with minimum maintenance characteristic deterioration. It is assumed that the camber variation takes place in chord as well as in the span-wise direction, based on MBB principle [109].

In CACAD, two major approaches were made to predict proportioning factors so that the known maintenance cost of airframes can be divided into its constituent parts i.e. different systems, and major sections of structure . The details of both approaches were discussed in section B3.1. In the first approach Sergheidis prediction equations [7] were used as proportioning agents, with a newly defined difficulty factor for distinguishing the VCW trailing edge system's extra maintenance cost over FCW one. The Airbus comparison method [92] was used to predict such a factor, the details, and formulation are given in Appendix D section D10. The second methodology discussed in section B3.2 contains such criteria that can be modified to include the influences of VCW, together with difficulty factors found by an Airbus comparison method. This involves surface area, mass, price, internal, and external conditions as proportioning agents to divide the known value of airframe structural maintenance cost into fuselage, horizontal tail & elevator, vertical fin & and rudder, wing box,

wing LE devices, and wing TE flaps & ailerons . The methodology then recognises the VCD extra maintenance cost over conventional TE flaps. The details are given in section D10.

The second approach, which is more reliable, was applied to an aircraft resembling the Airbus A340-200. The detail results are tabulated in Table D-10. The following extracts may be treated for validation of above methodology.

Items (Airbus A340-200 Class)		*FCW*	*VCW*
Aircraft	*Maintenance Cost £ per flight*	15051.43	14774.71
Engines	"	6943.52	6680.55
Airframe	"	8107.91	8094.16
Structure	"	1079.54	1175.19
Wing	"	438.51	483.65
Wing Box	"	201.66	185.68
Wing LE Devices	"	90.39	84.79
Wing TE Devices	"	146.82	213.18
Horizontal Tail	"	115.11	106.8
Vertical Tail	"	102.81	96.51

References [14], and [15] was used to predict maintenance cost of FCW aircraft, airframe, and engine. Approach two, discussed in Chapter 2 (2.7) and elaborated in Appendix B (B2.2), was used to arrive at the maintenance cost for an individual airframe systems, and structure as a whole. Structure is shown in the above table. A methodology was developed to predict sub-sections of structure maintenance cost (discussed in the same mentioned sections), some items of which are shown in the above table. It is clear that the VCW aircraft, being smaller, has lower overall maintenance cost. Moreover, had the extra maintenance cost of sections of aircraft affected by VCW technology not been predicted, this difference would have been much higher, and unrealistically boosting the benefits of the VCW technology. One of the major purpose of this section of the thesis was to quantify the maintainability of a high risk future technology. Maintenance cost of VCD has risen by 43% (146/213). It is interesting to repeat an argument once was used by Boeing in [100, section 7.5.2.2]. It seems certain that a conventional flap integrated with variable camber operation must have higher maintenance cost than its previous state. The

results show the same (43% rise). Now it is also probable that the extra complexity and equipment due to VC operation resembles less than or equal to operating leading edge devices, therefore the extra maintenance cost must be of the order of the latter system. This is verified by the figures in the above table (£68 extra maintenance cost of VCD, compares well with £85 for the LE devices).

4.8.2 Maintenance Cost of VCW System

If the hydraulic, and flight control systems of the FCW aircraft are assumed to have been replaced by systems that fulfil the same functions for VCW too, then the Airbus scheme for prediction of extra maintenance cost of both systems can be applied. There are no obvious influences of VCW on other systems of aircraft, and there is no report as such so far. For camber variation span-wise there are at least two actuators added to inboard devices, two to outboard devices, and a minimum of two flaperon devices on each of the wings. They are accompanied with number of switches, probes, filters, relays, piping, and wiring. These would add some difficulty in reachability, accessibility, and increase overhaul and repair time, along with higher inspection, and removal rate. All were considered when applying the Airbus comparison method, the details of which are given section D11.

The quantity of extra hydraulic, and flight control system maintenance cost for typical A340 aircraft for both versions extracted from Table D-10 are shown in following table along with four more typical systems :

Item	*FCW*	*VCW*	*Rise*
Hydraulics system maintenance cost in £/flight	465.44	518.43	52.99
Flight control system "	575.23	659.62	84.39
Air-conditioning system	237.67	232.82	-
Fuel system	126.55	124.33	-
Water waste system	102.84	100.77	-
Oxygen system	54.86	53.52	-

It is needless to repeat the same argument in the previous section, as it is clear that VCW version, being a smaller aircraft, has a generally lower system maintenance cost except for those systems that are affected by VCW technology. However the rise in the maintenance cost of these systems is either lower or of the order of adding a small system to the aircraft like water waste, or oxygen system.

4.9 Development Cost of VCW Technology

References [15], and [36] are two sources for prediction of the development cost of a jet transport aircraft at conceptual design level. The latter claims to produce more realistic results, but it was found to be more useful in fighter aircraft application. The former source might be rather optimistic in development cost estimation, but is more applicable to passenger aircraft having advance technology on board .

In the Wayne Burns [36] approach, f_{atf} is a factor related to military advanced technology features such as stealth, and vectored thrust ranging from 1 to 2, but for commercial transport, it is 0.9 ! On the other hand, Roskam uses f_{diff} as a judgement factor for consideration of advanced technology, being 1.0 for conventional passenger aircraft and 2.0 for the aggressive incorporation of advanced technology, such as laminar flow transport aircraft.

The objective of this study is to predict the extra development cost of VCW against FCW aircraft, and therefore the actual development cost is not a dominant factor. The Roskam relationships were selected as a basis to build a methodology to predict the extra development cost of VCW technology. In Roskam approach the f_{diff} coefficient is a very useful but it is a rather imprecise approach to inclusion of future technology. In order to be able to develop the methodology to predict extra development cost associated with the application of high risk future technology, all areas of development cost may be sub-divided. It is important that all items that are influenced by VCW technology be recognised and their quantitative impact on $(f_{diff})_{VCW}$ be realistically predicted.

Development cost consists of airframe engineering and design cost, development support and testing cost, prototype cost of flight test aeroplanes, test and simulation facilities cost, profit, and finance. The last three are assumed to be common whether or not VCW technology is introduced. The first three were investigated for possible areas of extra cost due to VCW. The details of the study are described and formulated in section D12.

4.10 VCW Technology for Derivative Aircraft

There are numerous combination of derivative aircraft, the most famous ones are as follows:

1. A common wing, but different payload & engines, with common fuselage diameter, but different length. Example : Boeing B767-200, and B767-300. Airbus A319, A320, A321. Airbus A340-200, and A340-300

2. A common wing, a common payload, an identical fuselage diameter and length. Different number of engines, and range. Example : Airbus A330-300, and A340-300.

A conceptual approach to aircraft design for an optimum configuration for the members of family is perhaps possible when trying the following procedure.

1. Range, payload and number of aircraft for each family member is decided. This is done by past experience i.e. replacing some ageing aircraft, and by studying the present market requirement, and finally by predicting the trend of air traffic in the next 25 years. Care must be taken for the variation of payload range so that they stay within a reasonable bound to be able to call them a family.

2. CACAD is prepared and run for each mission, keeping the fuselage diameter the same as the first step toward commonality. The DOC module shall be expanded to include the number of aircraft to vary for each mission.

3. A number of aircraft with different fuselage length, each with their own optimum wing area, are obtained to set the maximum and minimum boundary for the compromise wing area.

4. An integrated program is developed to include the saving in manufacturing cost of wing and fuselage, design and development of wing, and some saving in flight testing.

5. The integrated program varies the wing area for each member of the family to search for the minimum DOC for the highest produced aircraft member of the family.

6. The constraints must then be allowed to let each configuration .. acquire a feasible take-off length, and approach speed, and possibly single engine height failure, etc.

4.10.1 VCW Benefit for Derivative Aircraft

The under-sized wing member of the family has the problem of low altitude initial cruising, therefore it must cruise at lower altitude and spend a higher mass of fuel. VCW not only offers the aerodynamic benefits elaborated in previous sections to this undersized member of the family but it also offers an extra benefit. It allows the aircraft to climb to higher altitude for initial cruise by deploying camber to boost wing produced C_L to match aircraft required C_L. This shall save cruise fuel which saves DOC.

4.11 VCW Integration in CACAD

In this section the procedure of integrating the VCW modelling in CACAD is presented. Basically there are two series of models that are incorporated into different modules, and sub-modules of CACAD. There are the models that improve aircraft DOC i.e. aerodynamic benefit models. The other models are associated with VCW mass, and R&M&D implications which penalise DOC.

4.11.1 The Integration of the DOC Improvement Models of VCW in CACAD

There are basically three sets of improvement models. The first set is attributed to the chordwise camber deflection. These are drag saving during cruise, and aft body upsweep drag reduction due to elimination of the need to change aircraft angle of attack during the cruise. The second set are attributed to the camber variation span-wise that reduces the need for twist, or ideally eliminates it. The twist elimination saves some drag due to twist, and some drag due to the induced drag factor being prevented from rising during cruise sectors, and some drag due to wing-body viscous interference drag. The former and the latter sets of models are integrated into the drag estimation module of CACAD, causing reduction in cruise fuel consumption, as well as reducing thrust and engine mass requirement. There are related snow-ball effect on the entire aircraft sizing process. The third set concerns Mach-critical drag, which is

increased due to buffet improvement, as well as the wing local lift coefficient being prevented from exceeding aircraft lift coefficient in VCW aircraft. The latter model is integrated into the constraint module, and the former in the Mach-critical drag module.

4.11.2 The VCW Penalty Model Integration Into CACAD

The penalty functions are of two categories. The first ones are the effects of the mass penalty in wing trailing edge due to VCDs, and the hydraulic system mass penalty required to operate VCD chordwise as well as span-wise. When they are operated within the wing and system mass module of CACAD, they result in increases in the take-off mass, hence increasing DOC. The second category is the extra maintenance cost and development costs of VCW. These penalties are inserted in the DOC sub-modules for depreciation, as well as for maintenance cost. They result in further rises in DOC.

4.11.3 CACAD Operation With VCW

In the design process, CACAD designs and optimises a FCW aircraft for minimum DOC and produces the result as the base aircraft. Thereafter, all models of VCW are called into operation within CACAD, to design and optimises another aircraft with exactly the same mission and generates the results for a comparison study. The program is such that it operates again opening another mission file to make the study possible for different classes of aircraft. The results are retrievable in EXCEL so that all necessary graphs and tables are produced. Sensitivity studies are possible so as to vary the controversial parameters such fuel price, labour rate, maintenance factors, development cost factors, even twist, as the measure of aerodynamic maturity of the VCW technology, all at different ranges.

4.11.4 Derivative Design Integration with CACAD

A short-cut was made to avoid a great modification to CACAD. A class of aircraft similar to Boeing 767 family was selected as an appropriate derivative mission to evaluate, and quantify extra VCW derivative benefits. The following tasks were performed to arrive at the results.

1. CACAD was prepared to design and optimise an aircraft similar to the shorter range B767-200. It was also run to design and optimise aircraft for longer-range B767-300 flights. The results are tabulated in Table D-11 .

2. A common wing area equal to that of the B767 family was substituted in CACAD.

3. CACAD was run to simulate the undersized wing member of the family i.e. resembling B767-300Q. In this run the aircraft with FCW was designed to cruise at initial altitude corresponding to initial cruise lift coefficient determined from B767-300Q data [43]. When CACAD was operated for the VCW version of the B767-300Q, this restriction was removed, and an altitude appropriate to the best SFC cruise of the engine was selected. The results were tabulated in Table D-11.

4.12 Discussion of VCW Results

VCW models were integrated in CACAD, and the program was allowed to run for different Classes of transport aircraft. These included low, medium, and high capacity to ultra high capacity, short, medium to long range. The configurations included twin aft body engine, twin, and quadro under wing-engine aircraft.

4.12.1 Presentation of Results

1. A typical quadro A340 class aircraft was selected for the study of the effect of each VCW model on DOC. This aircraft, as will be shown later, is the most suitable existing transport aircraft for this technology. Figure D-17 shows a bar chart in which every bar shows its cumulative effect on DOC. The value on each bar indicate the share of each model in the DOC saving.

2. The saving in DOC for the other classes of aircraft mentioned above are shown in Figure D-18. The aircraft are arranged according to seat kilometres. The saving varies from a negative value of 0.8% for F100 class to as high as + 3% for UHCA. The reduction in take-off mass, and mission fuel mass are included in Figures D-19, D-20 for reasons of analysis.

3. A set of sensitivity analyses with respect to various ranges were carried out to cover future changing trends in the world market. Variations of range, fuel prices, labour rate, development cost factors, and maintenance cost factors were considered for quadro aircraft resembling A340 class. They are shown in Figures D-21 to D-24.

   Other types of sensitivity study were conducted using two classes of aircraft namely, A340-200 class, and UHCA. The variations of development cost, hydraulic mass penalty, Mach-critical drag benefit, and maintenance cost are carried out to examine the applicability of VCW, and the results are shown in Figures D-25, and D-26.

4. Detailed results of each aircraft parameters are given in Table D-10 for a typical class resembling the A340, and the results of incorporating VCW in derivative aircraft resembling B767 are tabulated in Table D-11 .

4.12.2 Comments On The Results

The discussion is conducted in the order of the results, presented in last section.

4.12.2.1 Analysis of the Impact of Each of the VCW Models

The effect of each VCW model on the performance, cost and mass of an aircraft resembling the Airbus A340 will be discussed. The sequence of incorporating VCW models was as follows (see Figure D-17) :

1. It was assumed that the wing TE is equipped with devices to vary the wing camber during cruise in chordwise as well as span-wise directions. The mass of the VCD was incorporated within CACAD, as the first penalty model. The DOC increased by 0.6%, which is a considerable value. Here any improvement in trailing edge design that can save mass produces at least 0.2 to 0.4% saving in DOC.

2. To allow chordwise and span-wise operations to be carried out successfully, the hydraulic system must be equipped to do so, implying an extra mass. Hence the mass increment prediction modelling of hydraulic system was made to operate within CACAD. A further rise of 0.28% was added to DOC. Together with VCD , the combined cost implication of the mass penalty

effect of VCW relative to FCW is 0.85% in DOC . This value can be reduced by reducing the number of actuators needed for span-wise operation of the VCDs.

3. If the technology of chordwise camber change during cruise is assumed to have been successful, and a 5% reduction in drag is achieved, then the saving in DOC is of the order of 1% . This along with the snowball effects of above mass penalties will cause a net reduction in DOC of 0.1% . This is a negligible benefit for VCW, if implemented only for chordwise camber variation. The maintainability and development cost implication penalties have yet to be included.

4. As a result of camber variation during cruise, the body upsweep drag shall be reduced, and if its drag prediction modelling is made to operate within CACAD then a further reduction of nearly 0.2% in DOC is achieved, resulting in net reduction of 0.3% . Such reduction in DOC for VCW technology in chordwise variation of camber is not a healthy improvement in terms of cost, and the risk of technology failures . It is believed by industry, that modifications that can be shown to produce to produce 1% DOC reduction may be considered for possible implementations. For a high risk technology a minimum of 5% fall in DOC is necessary [133].

5. Next, it was assumed that span-wise variation of camber is necessary. The first benefit would be to eliminate drag due to twist or reduce it, compared with a FCW aircraft. This model was made to operate together with the above models. A significant reduction in the net DOC of the order of 1.44% was achieved. This must be treated as a major drive in implementing span-wise differential camber variation .

6. The differential camber variation helps to maintain elliptical lift distribution. This in turn prevents the induced drag factor (1/Oswald efficiency factor) from gradual rise during cruise. Such benefit modelling was operated within CACAD. The impact on DOC was less than 0.1%. Although this is an inevitable benefit of span-wise camber variation, to develop the software that

continuously adjusts the TE surfaces may result in a rise in flight control system failure rate, which certainly outweighs its benefits in terms of DOC.

7. Another side-benefit of differential camber variation is a reduction in wing body viscous interference drag. The drag benefit is of the order of 0.08 count, which is so small that the benefit effect on DOC is only 0.03%.

8. The next major benefit as result of VCW introduction in CACAD is Mach critical drag benefit modelling. This has also been reported in [100]. It was possible to incorporate such a model to its full advantage i.e. influencing the sweep, and thickness to chord ratio selection module of CACAD. As a result, a rise in thickness to chord ratio of the order of 5%, and slight reduction in sweep angle was achieved, that results in a much better VCW aircraft. This pushed the saving in DOC up by 1.89%, to a net reduction in DOC of about 3.74%.

9. The introduction of development cost implication modelling in CACAD with reasonable prediction factors in every cost sub-section was brought into operation at this stage. Its penalty contribution to DOC was about 0.64% . This is a significant value, and may deserve a great amount of care by manufacturer to tackle the cost of RDT&E of VCW technology.

10. The integration of maintainability deteriorating coefficients in CACAD, was put into operation at this stage. It's contribution to DOC rise is about 0.23%. This small amount is an indication of a good design philosophy, and it is not an alarming value. It also gives advance warning that any complication in VCD configuration may result in higher maintenance cost. The net DOC gain falls to 2.87%.

4.12.2.2 *Analysis of the Results of VCW for Different Classes of Aircraft*

In this study a set of aircraft close to existing classes of transport aircraft were considered. All VCW models were integrated into CACAD. The program was operated to simulate VCW installation in aircraft resembling Fokker F-100, B757-200, B767-200, A310-200, A300-600, A330, A340-200, and UHCA . The aircraft were arranged according to the product of their seat, and range. Each aircraft was

designed for FCW, and then redesigned, and optimised for VCW. The DOC, take-off mass, and fuel mass saving of each aircraft were the subject of the following analyses, see Figures D-18, D-19, D-20. The details of the results are included in Table D-10, Appendix D. The coefficients of maintenance, and development cost used in following results are values developed in section 4.8, and 4.9.

1. The aircraft with short range, and low capacity such as Fokker F100 with 100 seat, and 2400 km range, right up to 190 seat, 5300 km range Boeing 757-200 show losses, if they are flown with VCW. The next set of aircraft are medium range, medium capacity from Boeing 767-100, a 220 seater, 6000 km range, to Airbus A330, a 336 seater, 8334 km range. They show a very modest benefit i.e. 0 to 0.4 % DOC saved. This is not encouraging enough to convince industry to take VCW technology on board such class of transport aircraft.

2. VCW technology starts to show significant benefit when the range of aircraft exceeds 10000 km . A distinct rise occurs from the Airbus A330 to the Boeing 767-300, and further rise to Airbus A340-200. The latter aircraft is typical of lower medium capacity, 260 seater, and very long range 14000km.

3. Range plays a higher role in pushing the cost benefit of VCW technology, than capacity. The major benefit of VCW is its ability to save the drag during cruise. Therefore to lower the capacity of the aircraft shall result in a smaller body, with its smaller proportion of maintenance cost, and the reduced drag of the fuselage, causing a higher proportion of fuel cost in DOC. This makes the application of VCW most ideal for low to medium capacity, but very long range aircraft. The UHCA showed higher DOC benefit but the slope of the benefit was reduced relative to the Airbus A340-200. This proves the fact that capacity rise is less influential than range increase, for DOC saving.

4. The reason the Boeing 767-200 stands away from the trend, lies with its cruise speed. It flies at Mach 0.85, 0.03 higher than neighbouring aircraft. This results in a lower depreciation cost (due to higher utilisation), making fuel cost a higher proportion in DOC. Hence VCW technology which is a

fuel-consumption reducer, causes an increased in DOC saving of this aircraft relative to those in its neighbourhood.

5. Figures D-19, D-20 show the trend of take-off mass, and mission fuel mass saving as a result of VCW technology integration in various transport aircraft. The DOC trend clearly show its conformance with fuel saving rather than take-off mass .

6. VCW incorporated in undersized wing derivative aircraft class resembling B767-300Q acquired extra fuel saving due to being able to fly at a more ideal altitude. This offered an extra 0.5% lower DOC in addition to other benefits of VCW.

4.12.2.3 *Range Sensitivity Analysis*

For this part of the sensitivity analysis, the Airbus A340-200 class was chosen, as it offers the highest suitability for VCW technology. This was proved by the results of the previous section. Range was varied from 8000 km to 14000 km. The lower range is the limit of VCW profitability, and the higher range is the amount sufficient for present long range high density air traffic routes.

%DOC variation with range is dominated with fuel consumption at cruise, which is the exponential function of the range. Therefore as it appears, it varies at slow slope and then changes rapidly to toward a steep slope in line with exponential nature of the equation. The reason that it starts to slightly decline from the steep slop at the extreme range lies with the all up mass element of the equation, whose growth is no more in line with the growth of mission fuel mass. Hence holding the slope from further increase.

For development cost, and maintenance cost sensitivity study to become possible, a single F_{diff} replaced all the F_{diffs} developed in section D12, and F_{difm} replaced all F_{difml} and F_{difmm} in section D11.

- Fuel Price Variation

Fuel price has influenced aviation development as well as air traffic prosperity for the past twenty years. The rise of the fuel prices was a great motive behind numerous research studies. Therefore the feasibility of VCW

as a fuel reducing technology must be evaluated against changing fuel prices. A 25% fluctuation in fuel price, keeping every other cost at current prices, was the assumption behind the following sensitivity analysis. Figure D-21 shows how fuel price variation affects DOC saving for different aircraft ranges. At shorter ranges, it changes DOC benefit by 0.15%, and at longer range, its influence rises to nearly 0.3%.

- Maintenance Labour-rate Variation

Maintenance labour has always been a controversial subject. Efforts directed toward reducing maintenance cost were partially motivated by the high cost of labour, although maintenance materials were not ignored. The temptation to do maintenance work in a cheaper labour environment has dominated the aviation scene. In the following investigation, labour rate that can influence, the maintenance cost implications of VCW technology was varied from 20 £/hr below the default value of 27.3 £/hr, to 35.0 £/hr. The results are shown in Figure D-22. For short to medium-range aircraft, the maintenance cost is a stronger player in DOC composition, while fuel cost is less dominant. Therefore the labour cost impact on DOC is significant in lower range aircraft, but quantitatively very modest. For longer-range transport aircraft the maintenance cost has a minor role compared with fuel cost, let alone the labour cost part of it. Therefore any change in labour rate shall not significantly affect the %DOC benefits of VCW for long range version.

- Development Cost Variation

The Development cost impact on DOC, shown in Figure D-23, is significant and its variation also heavily degrades the VCW net benefit. The effect is 0.65% at lower ranges to 0.45% of DOC saving at higher range. The impact is nearly doubled when the development intensity factor is raised another 33% to 1.6. It is clear that if a single rough value of F_{dif} had been assumed from [15] (a value between 1 and 2), it would have meant success or failure of a new technology just by one single coefficient. This gives support to the methodology described in 4.9, and elaborated in D12.

- Maintenance Cost Variation

Other than labour rate, maintenance costs are affected by extra maintenance material cost, increase in complexity, accessibility, and more number of parts due to VCW. Such factors were dealt with in detailed in sections 4.8.1, and 4.8.2. Here a factor F_{difm} is introduced to permit to carry out the sensitivity study, replacing those given in Tables D-3 to D-6. Maintainability cost implication factor F_{difm} reduces VCW benefits though not as much as development cost. Short-range aircraft are most affected due to a higher share of maintenance cost in DOC. It is as much as 0.35% DOC increase at low range, and 0.25% at long range for every 33% increase in the maintenance factor, see Figure D-24.

4.12.2.4 *Sensitivity Study for Two Classes of Aircraft*

In this type of sensitivity analysis two types of aircraft most suitable for VCW i.e. long-range medium capacity, resembling Airbus A340-200 class, and UHCA resembling A3XX were treated for further investigation. These sensitivity studies are a guide for aircraft design groups, to see the extent of their efforts makes a new technology cost effective.

An F_{dif} factor was introduced to replace the detail approach to extra development cost developed in section D12 . Its value was made to vary from 1 for no penalty to 1.5 for moderately and to 2 for aggressive VCW extra development cost. In the same way an F_{difm} factor is introduced and varied from 1.25 as reasonable to 1.75 as gross exaggeration of VCW extra maintenance costs. ΔC_L which is the difference between aircraft C_L and wing maximum outer section C_l , elaborated in sections D6. and 4.7.5 , is a factor to show the degree of Mach-critical drag benefit due to VCW. Its value is determined within CACAD, and is approximately 0.1. For this study it was reduced to its half value to lower the beneficial impact on VCW aircraft. N_f is a factor within hydraulic mass estimate defined in section D9. This is varied from 7 i.e. no extra mass of hydraulic system to 8 i.e. full extra mass. Having been able to vary the above factors for the said classes of aircraft, it was possible to establish different combinations to highlight the importance of each influencing factor in a feasibility

study of VCW technology. These are shown in Figures D-25, and D-26. The analysis of the results follows :

1. An ideal situation is defined by all VCW benefits, at their highest value. The VCD mass penalty is not ignored but, no hydraulic mass penalty is considered. Extra maintenance costs are considered at only a reasonable value. Column one of the series S1, shows 2.4%, and 3.6% DOC savings in VCW aircraft version of A340-200 class, and UHCA respectively. Then depending upon how much the cost of VCW development can be controlled, the reduction of DOC saving in the latter aircraft is 0.65%, and the former one 0.7% per 0.5 rise in intensity factor F_{dif}.

2. A less ideal situation, in which extra hydraulic mass due to VCW is introduced, is depicted in the S2 columns with the usual F_{dif} variation. A reduction in DOC of 0.3% takes place for both classes of aircraft. This reduction shows the extent of benefit that a Hydraulic design group's hard work can inject into VCW technology.

3. A great deterioration in DOC saving takes place when the Mach critical drag benefit factor is halved. This is depicted by S3 columns in both figures. A fall of 0.7% for A340-200 class, and 1.1% for UHCA is achieved. This is the extent of achievement when the related design group is able to successfully vary the camber span-wise for perfect elliptic lift distribution.

4. A further loss in DOC saving takes place when the maintenance implications of VCW rise from a reasonable value of F_{dif} 1.25 to 1.75 in both classes of aircraft. R&M group effort should save at least 0.3% in DOC for VCW technology. This is shown by S4 columns in both figures.

5. VCW technology for the most severe case produces a loss of 0.3 % in DOC for the A340-200 class, and a negligible saving of 0.5% for UHCA. This is shown by the last column of S4. This happens when all design group work efforts have failed.

4.12.2.5 *VCW for Derivative Aircraft, And Some Comments on Operational Flexibility of VCW*

The Boeing 767-300Q member of the B767 family designed by CACAD, when equipped with VCW From Table D-11 produced extra 0.48% DOC saving on the top of 2% saved previously (see Figure D-18). This was achieved due to the ability of this under-sized wing aircraft to fly to the higher cruise altitude appropriate with the pay load, and engine performance (see section 4.10.1, and 4.11.4) by way of deploying higher camber. This is one of the examples of the operational flexibility of VCW especially beneficial to derivative aircraft.

Time limitation did not permit the Author to carry out an investigation into the off-design performance of CACAD-designed different classes of aircraft discussed in section 4.12.2.2. However, it is reasonably possible to predict (lessons learned from derivative aircraft's results) a minimum of 0.2 to 0.3% extra DOC saving, when the said aircraft are flown with VCW at ranges and payloads other than design condition, as compared with an equivalent FCW aircraft. This is especially beneficial for the A340-200 class, if one chooses to fly with more passenger over a shorter route. The mission requires to climb to lower altitude than the ideal one, where C_L required is much lower than C_L produced by the wings. Thus aircraft has to fly at angles of attack much away from optimum, causing extra drag and higher fuel consumption. An equivalent VCW aircraft is able to match C_L required by decreasing its camber right from the beginning of the cruise phase. This may push DOC saved for the Airbus A340-200 class VCW aircraft up from 2.4% to 2.7%. This phenomena is much intensified with medium to long range executive aircraft. In this class, due to unschedule nature of the majority of the missions, the percentage of flights at ranges shorter than the design range is significant, and VCW can save a significant amount of fuel cost every year.

4.13 Validation of Results

Efforts were devoted to attribute the quantitative contribution of each model with either experimental results, or the results obtained by prominent experts of the field. For the whole VCW system integration in conceptual transport aircraft design modelling, there is not yet any published DOC report with a similar VCW design

philosophy. Out of the many publications that are referred to in this chapter only [100], and [109] have some figures pertaining to VCW integration in their design synthesises. These figures shall be explored for possible comparison with the results analysed in previous sections.

Boeing installed VCD at the trailing edge of the outer wings of two types of transport aircraft, both medium capacity (200 PAX), one twin short range (3700km), and the other a quadro long range (10200km). They produced a DOC penalty for the short range and an approximately 2% saving for the long range aircraft. They also produced a 3.1 to 4.2% fuel consumption benefit in their long range version [100]. MBB has not revealed the DOC savings in their publications so far, but they have mentioned a 6.8% fuel saving in their long range quadro [110,109,112]. In the following table the above results were put together along with the nearest results from VCW in CACAD :

Design proposal	*%Fuel saving*	*%DOC saved*	*Major particulars of aircraft*
Boeing	-	penalty	Twin short range (200 PAX, 3700 km)
"	3.1	2	Quadro long range (200 PAX, 10200 km)
MBB	4.3	?	Twin short range (? PAX, 3704 km)
"	6.5	?	Quadro long range (? PAX, 9250 km)
VCW in CACAD	-	Penalty	Twin short range (186 PAX, 5200 km)
"	3.7	0.4	Twin medium range (336 PAX, 8300 km)
"	6.0	2.0	Twin long range (210 PAX, 11230 km)
"	6.9	2.6	Quadro long range (264 PAX, 13700 km)

CACAD, and Boeing both reported a DOC penalty for the short range aircraft. The CACAD, and MBB results show that the higher the range of the aircraft the greater the fuel saving. The DOC savings of long range quadro aircraft for Boeing and CACAD are very close, taking into account that CACAD's quadro has a longer range, hence slightly higher DOC saving. The fuel savings of the MBB quadro, and CACAD are also very close. There are some major differences between Boeing and CACAD results on fuel saving in long range class.

It is very hard to give any justifications for this result but the following is a possible explanation :

- Boeing's VCD are heavy and occupy only 60% of the wing in the outboard region, hence its cruise drag reduction may not be as high as 5% claimed by MBB, and Cranfield work. Both effects do not encourage high fuel saving.

- Fuel prices considered by Boeing (7.8, 9.5, 15.8 Pence per kg) is much lower than CACAD (15.0, 19.0, 23.0 Pence/kg), but because Boeing has not considered (or has not revealed in their report) any extra development cost and extra maintenance cost in determining the DOC of their long range quadro, their DOC saving is as high as CACAD for the same range, and PAX.

4.14 VCW Conclusions

This section discusses the conclusions drawn from the results of each type of the study presented in the previous analysis section.

4.14.1 Impact of each VCW Model (A340-200 Class)

1. The model by model analysis is a useful tool, and it directs the attention to those models that are key penalties and benefits to the success of VCW technology.
2. The mass penalties, development, and R&M penalties have equal weight in DOC penalties.
3. The major benefits of VCW are cruise drag reduction (1% benefit for DOC), the elimination of twist due to camber variation span-wise (1.45%), and the Mach-critical / buffet margin expansion (1.85%).
4. This study shows that the introduction of camber variation during cruise only in the chordwise direction may not cause any net benefit for transport aircraft, therefore span-wise differential camber, may have to be implemented. A full exploitation of VCW technology may permit nearly a 3% reduction in DOC which is the minimum value that might be appealing to aircraft industries for long range transport aircraft.

4.14.2 VCW for Different Classes of Aircraft

1. VCW technology is perhaps feasible for transport aircraft whose design range exceeds 10000 km.
2. VCW technology offers more benefit to lower capacity aircraft in the long range category, hence the Airbus A340-200 class, and long range versions of the Boeing 777 class should benefit most.

3. Perhaps the class of aircraft that will most benefit will be long range executive aircraft. They not only benefit from its fuel saving advantages, but also have extra benefits from operational flexibility. It enables such aircraft if flying a short-range sector to fly at lower altitude with lower drag than if they were to fly with a fixed camber wing.

4.14.3 Sensitivities of VCW

1. The study shows that, any increase in fuel price would increase the benefits of VCW. However for longer-range aircraft, even a 25% reduction in fuel price does not render the technology unfeasible. Large increases in fuel price does not significantly help VCW suitability for short to medium range aircraft.

2. Due to the minor role of maintenance labour cost in the overall maintenance cost of medium to long range aircraft, even significant changes in labour rate do not significantly influence the %DOC saving of VCW technology.

3. Development cost is crucial to the profitability of VCW. The study shows that any negligence in development cost expenditure will critically penalise VCW, no matter how reliable, maintainable, and drag saving the technology achieves in real life.

4. The study indicate that the maintenance cost implication is important but was not decisive in the feasibility of VCW technology based on the MBB design philosophy. This conclusion gives advance warning that further complication in the VCD at TE of the wing may be uneconomical. This result may offer some lessons to the more complicated Cranfield design proposal.

4.14.4 Sensitivity Study Between UHCA, And A340-200 Classes Of Aircraft

1. The UHCA is less vulnerable to extra development cost intensity factor variation as compared to the A340-200 class. The reason lies with standing charge cost part of DOC, being more dominant than fuel cost. It does not vary considerably when F_{dif} is made to vary the depreciation cost.

2. The UHCA is more sensitive to the Mach-critical drag benefits of VCW, as compared with A340-200 class. This is due to fact that such benefits of the VCW affect the thickness to chord ratio which significantly reduces the wing weight, as well as wing area. These items significantly affect aircraft price, which is a dominant factor in the standing charge part of DOC for UHCA.

3. The impact of the hydraulic mass penalty, and the extra maintenance cost implication of VCW technology on both aircraft was not significant, and must be treated less critically when investment is allocated to the application of this technology.

4.14.5 VCW for Derivative Aircraft

Designing transport aircraft for an optimum future derivative type is perhaps an inevitable tasks in the present conceptual design practice in industry. An UHCA will be designed with a few versions, and therefore a common wing shall be adapted for all derivatives.

VCW offers a better performance, and further fuel saving for the vulnerable undersized wing member of the family. Assuming that the UHCA designed and elaborated in the previous sections be the derivative aircraft, the VCW can boost its already 3.1% DOC saving up to more than 3.6%. This makes the technology a serious candidate for further investigation for this class of aircraft.

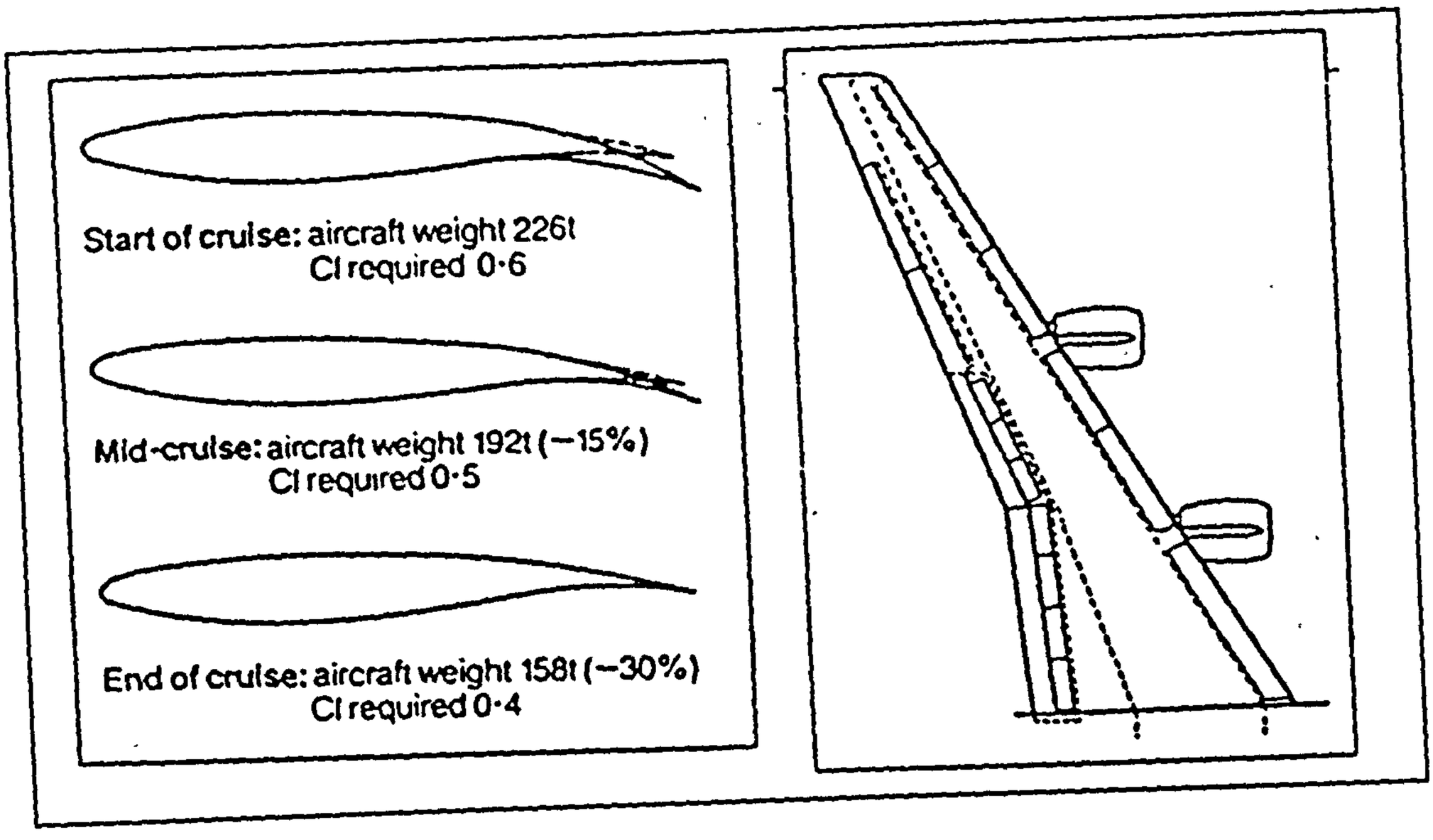

Figure 4-1 : Decreasing lift demand during cruise

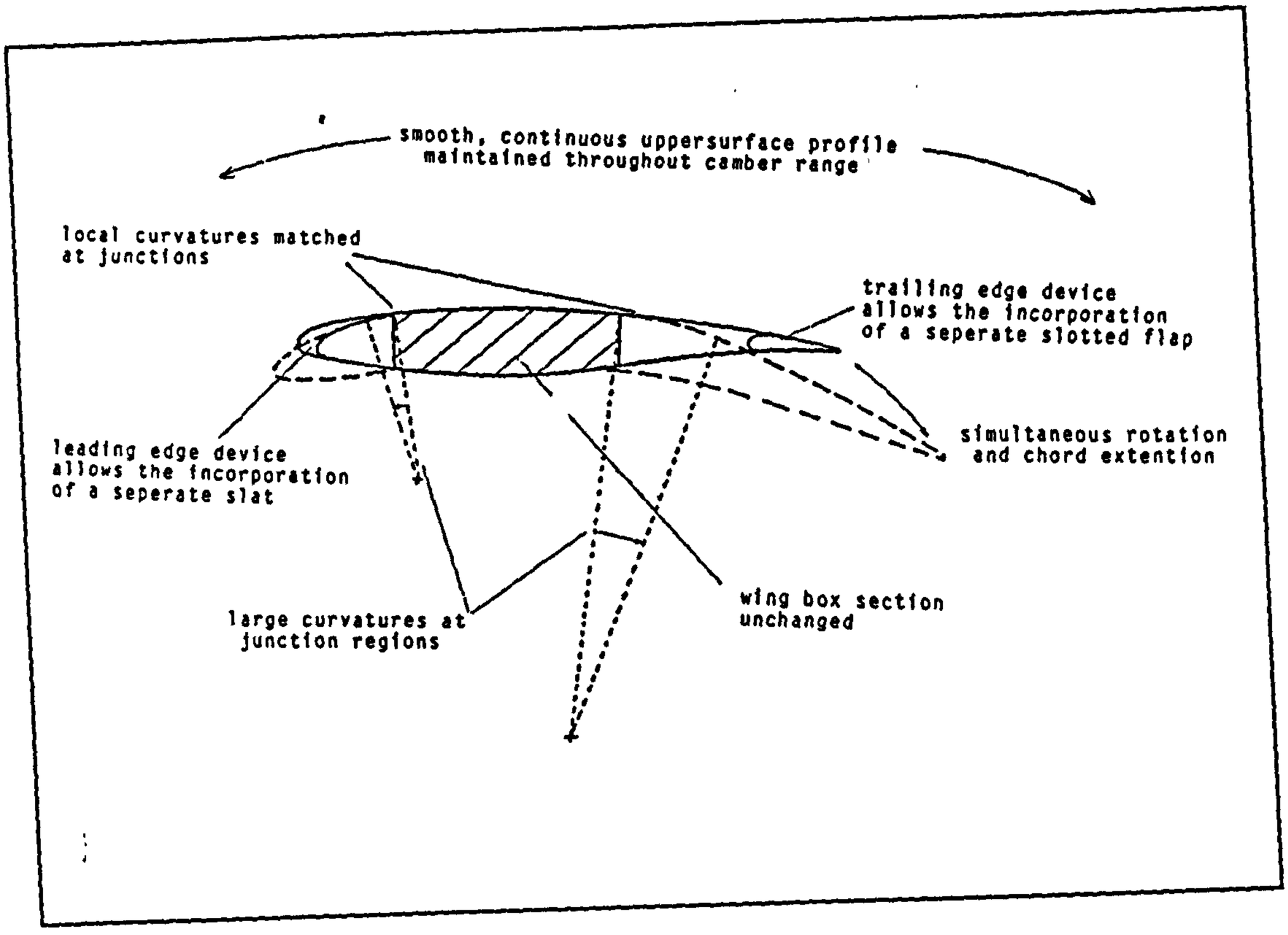

Figure 4-2 : Cranfield proposed variable camber system (Spillman)

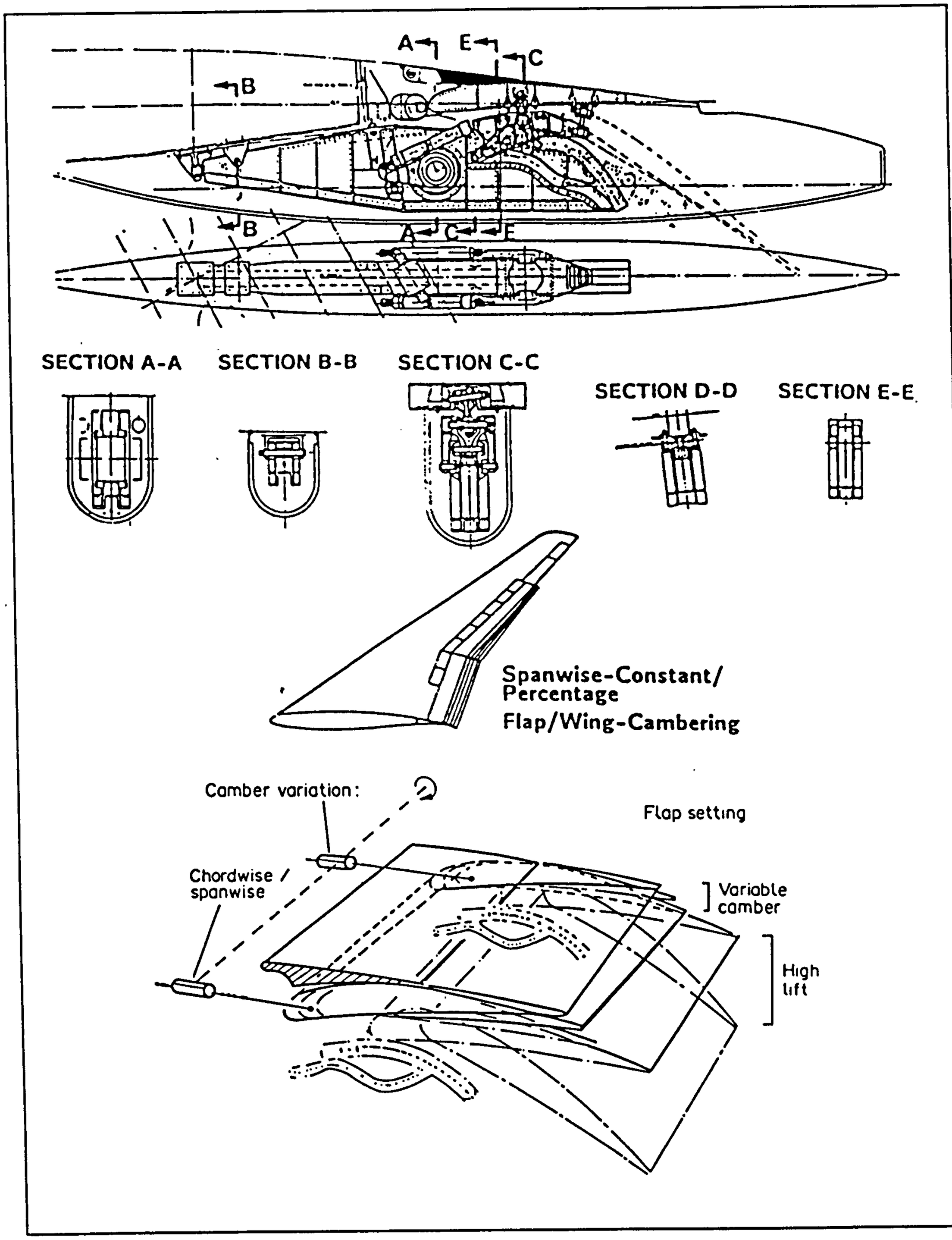

Figure 4-3 : Some features of the MBB design concept.

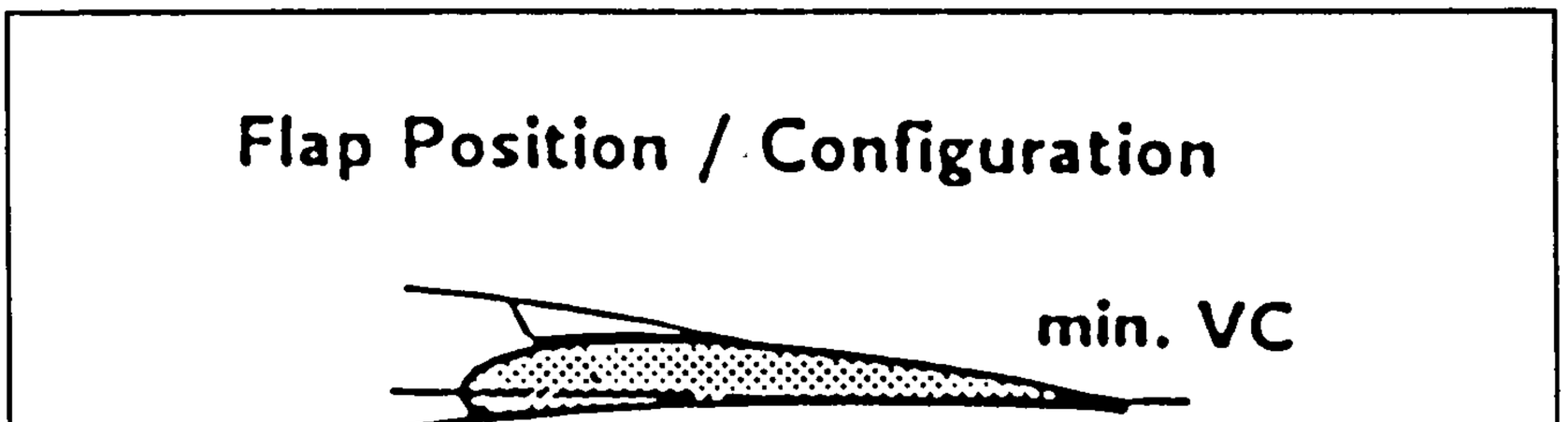

Figure 4-4 : The Fowler motion of the flap body, sliding underneath the spoiler trailing edge (rubbing against it) [109].

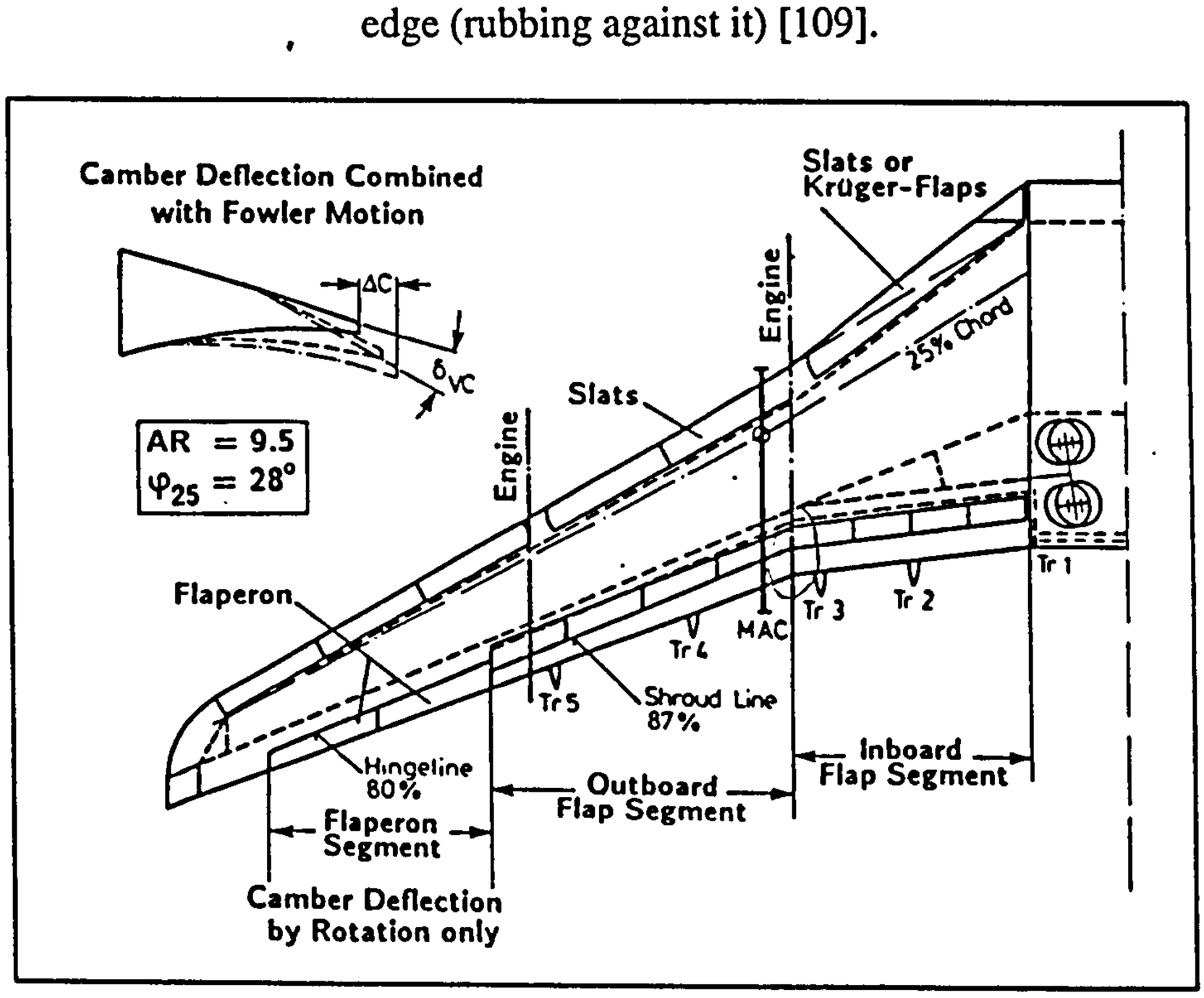

Figure 4-5 : Variable camber wing planform, and segmentation

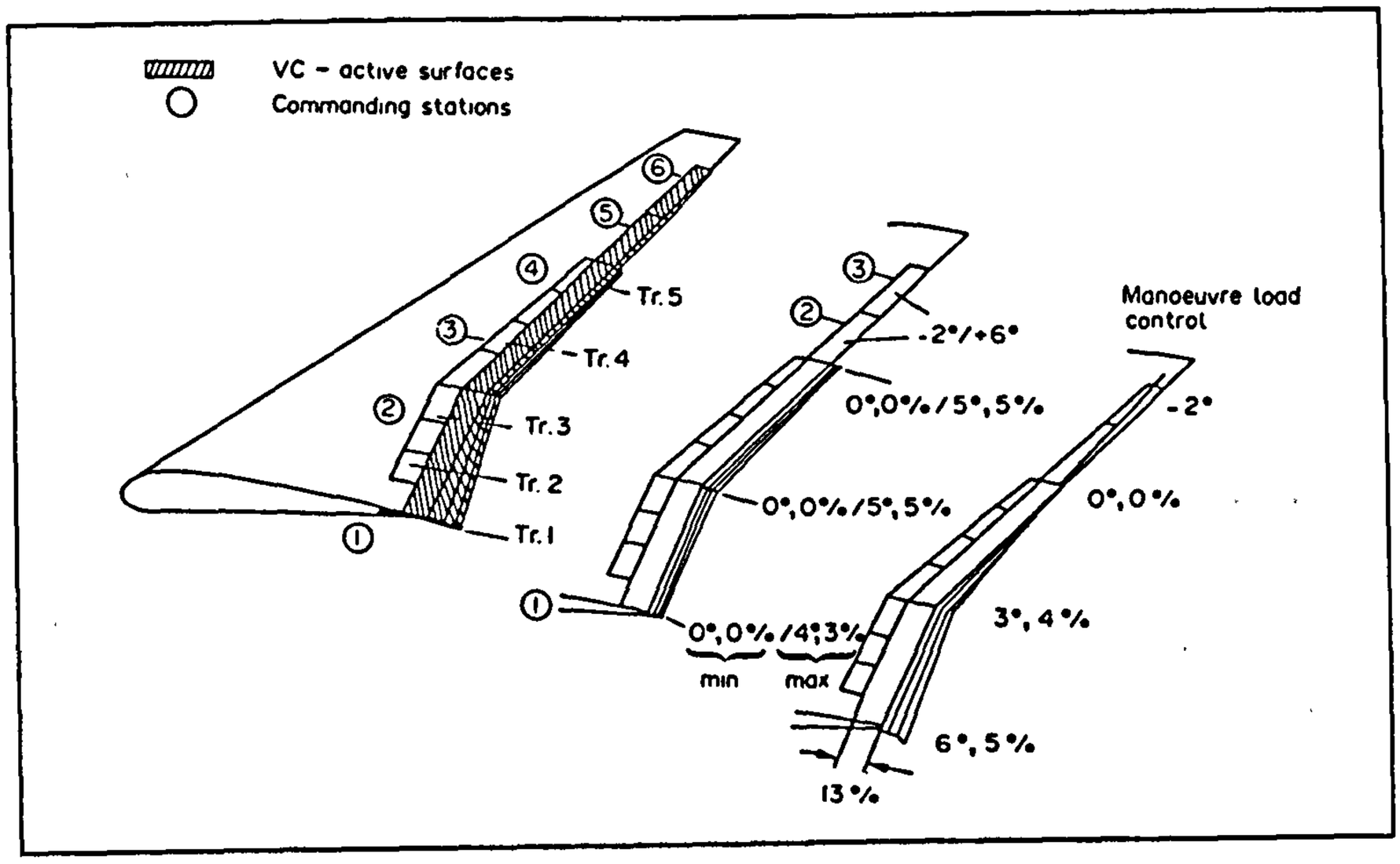

Figure 4-6 : Realisable variable camber configurations with commanding stations.

Figure 4-7. VCW Modelling integration in CACAD

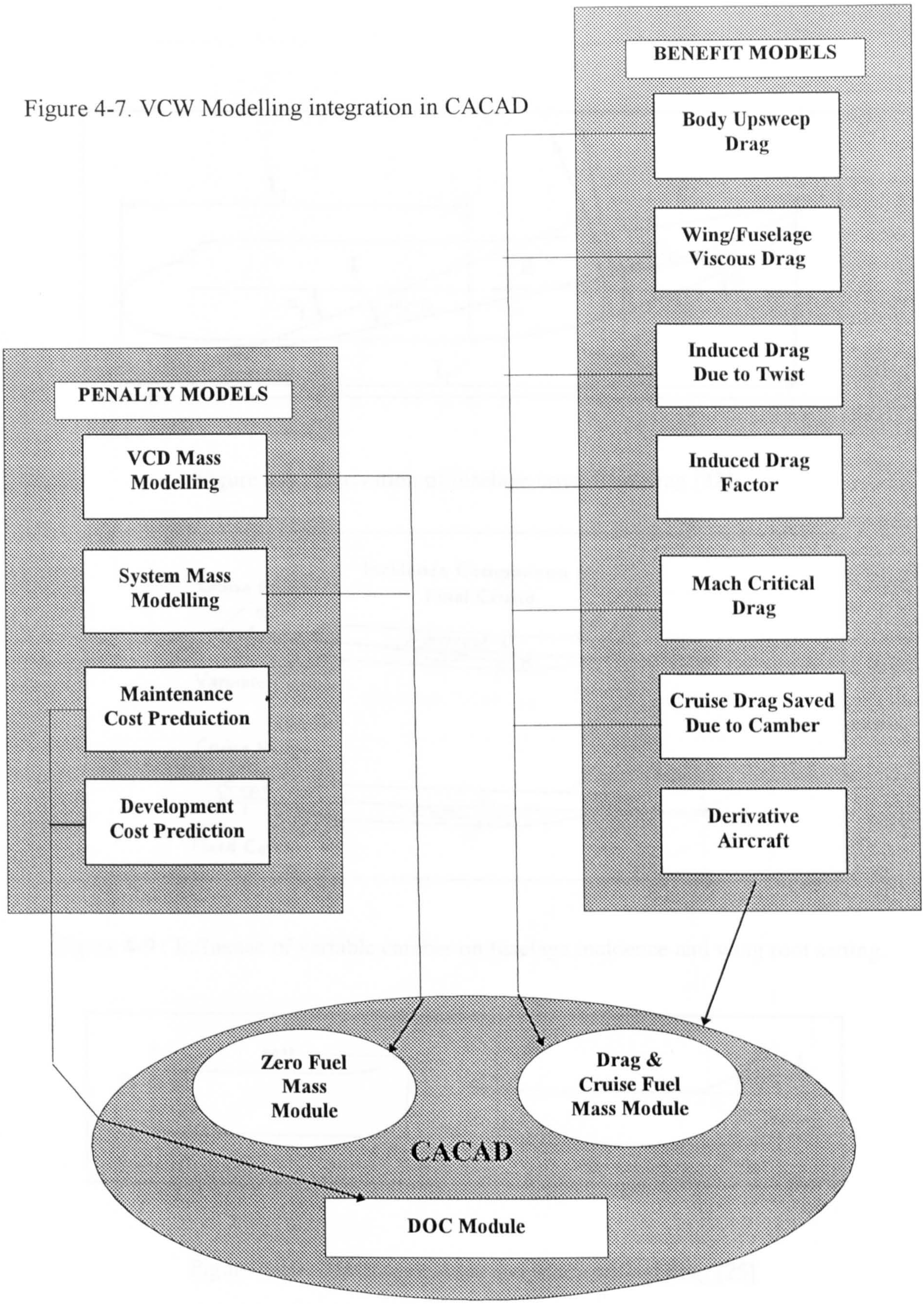

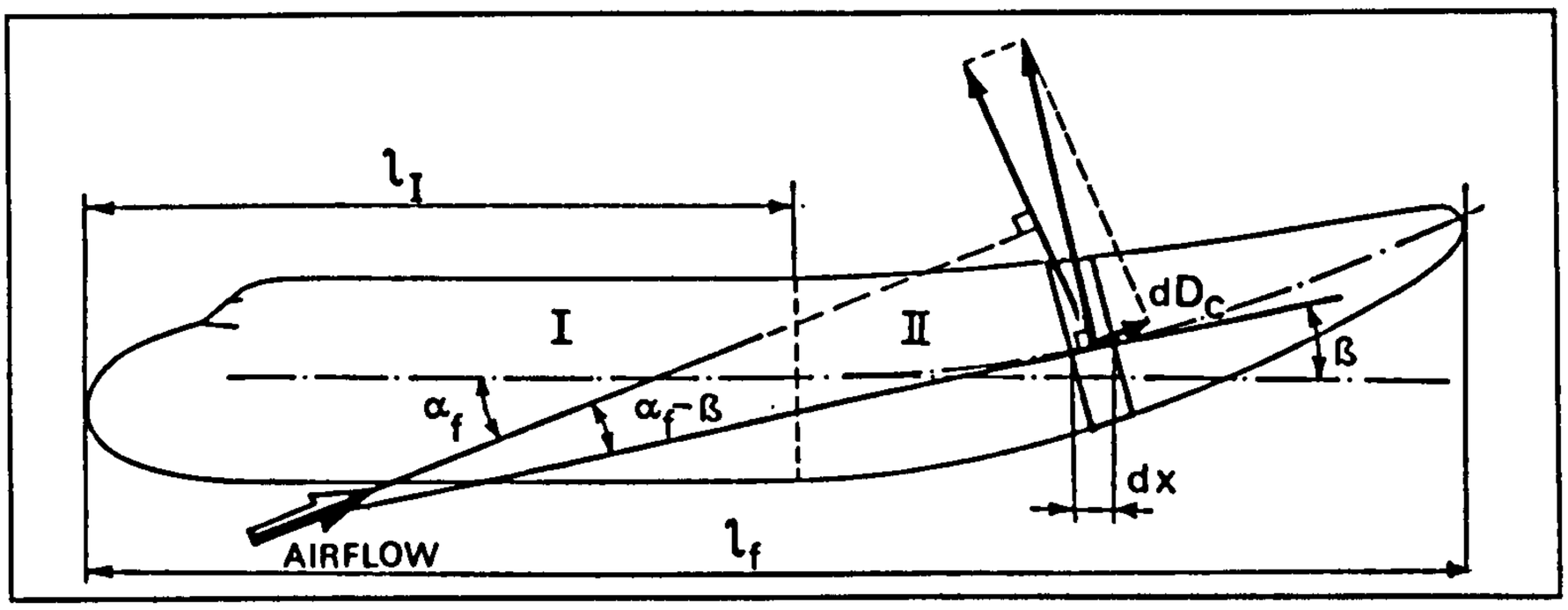

Figure 4-8 : Derivation of fuselage cross flow drag [32].

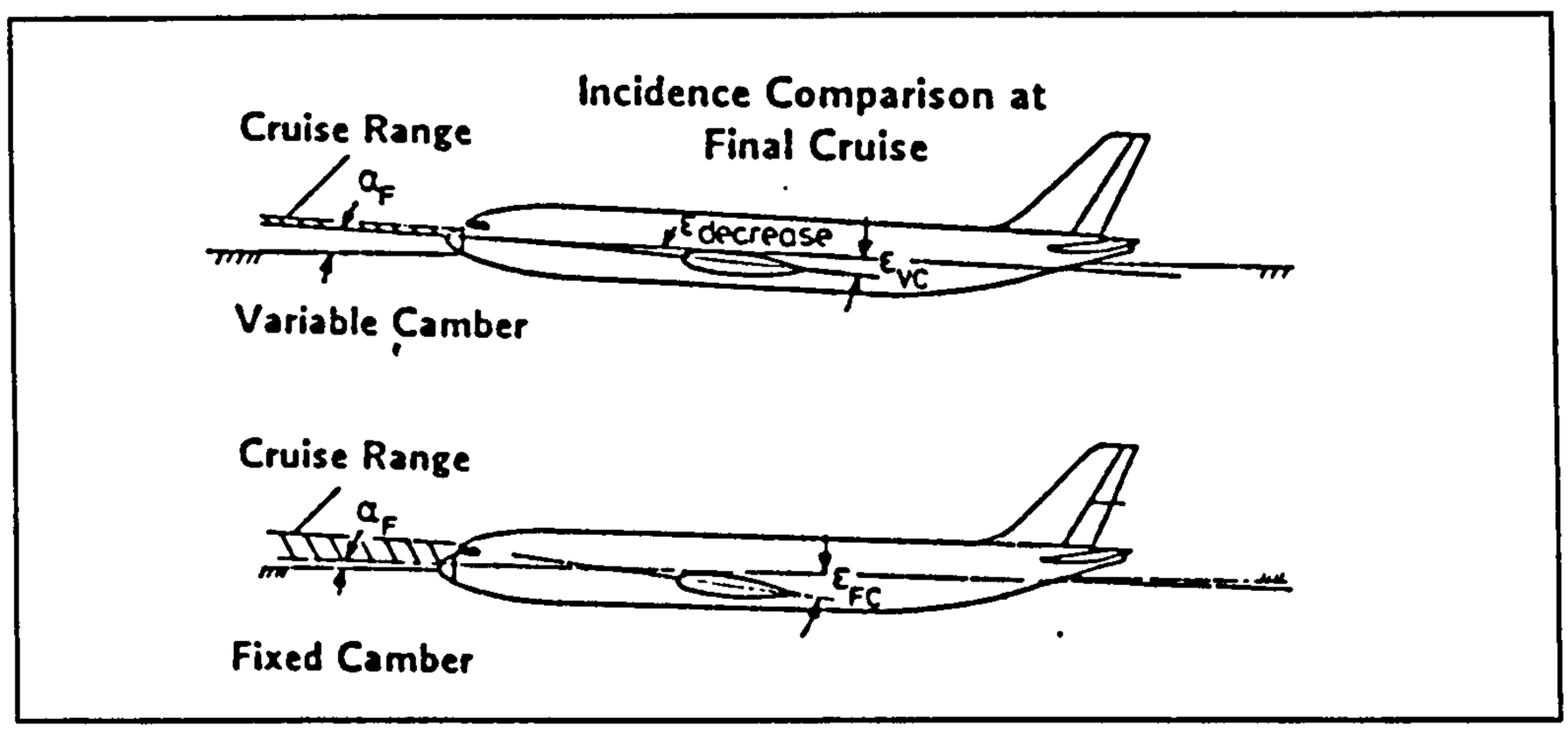

Figure 4-9 : Influence of variable camber on fuselage incidence and wing root setting.

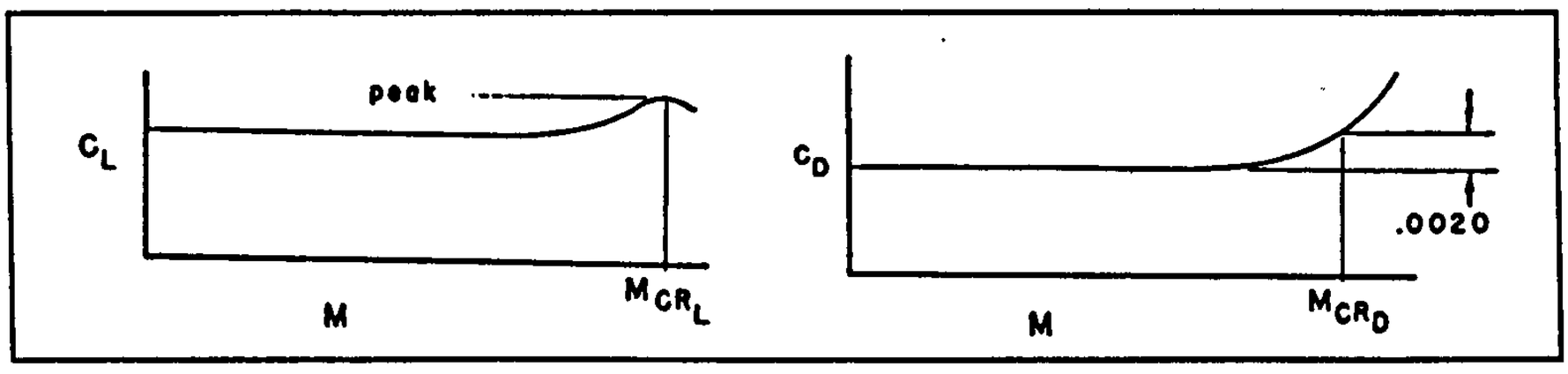

Figure 4-10 : Mach critical lift and Mach critical drag [25]

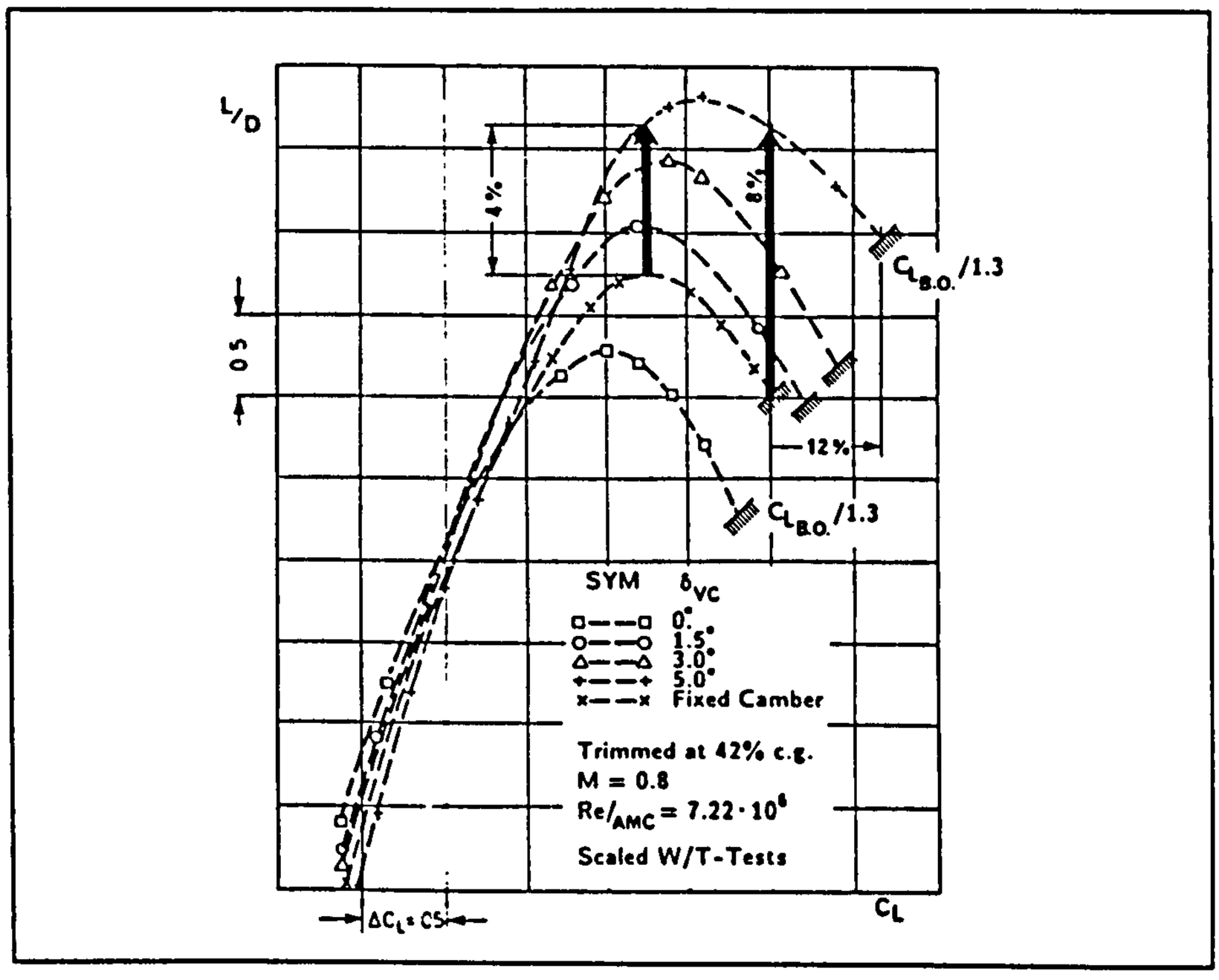

Figure 4-11 : VCW effect on scaled L/D (B.O. = buffet onset)

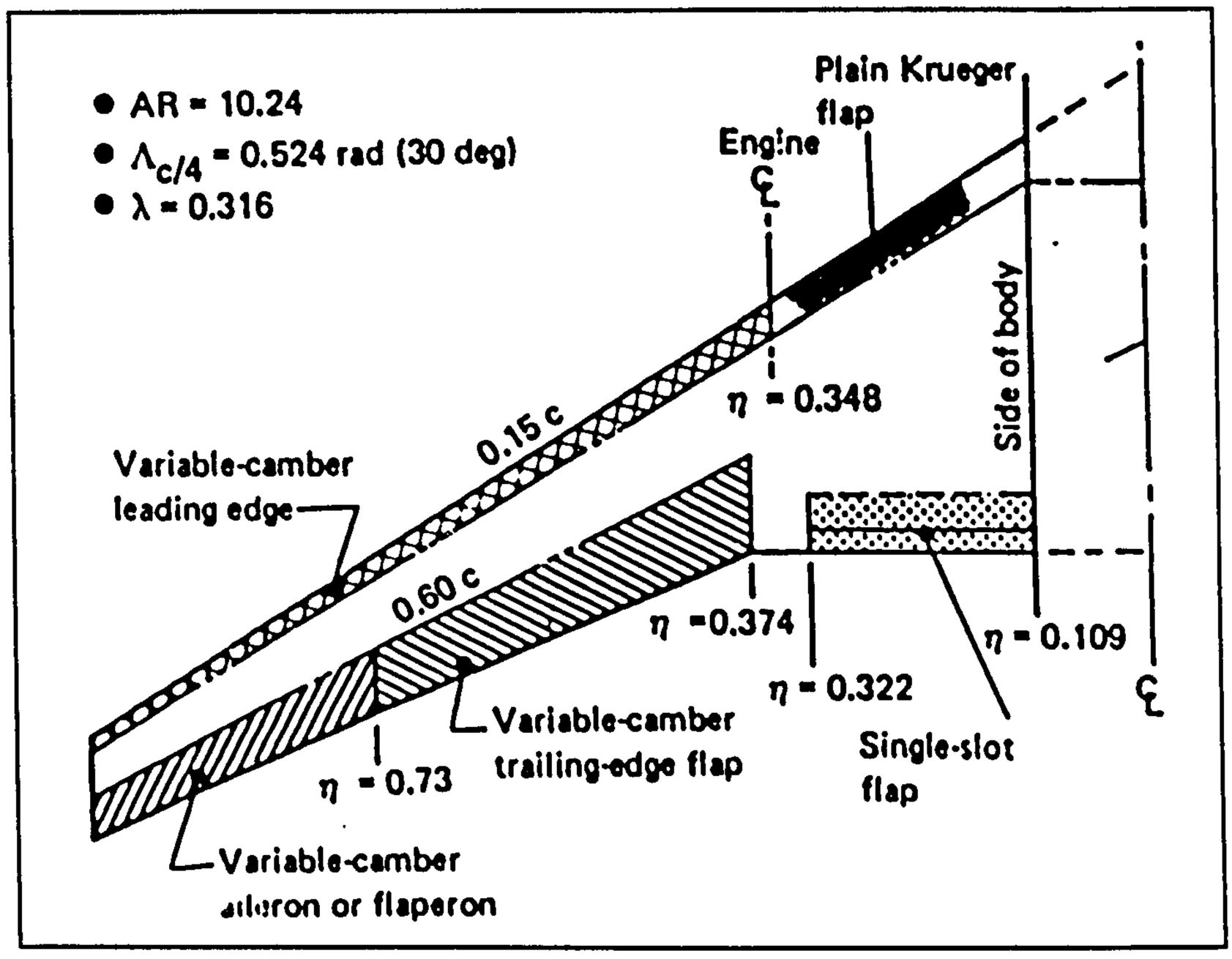

Figure 4-12 : Span-wise configuration of VCD proposed by Boeing [100]

Chapter 5

General Discussion of Results

5.1 Introductory Remarks

The whole spirit behind the present research work is to provide an appropriate place for R&M feasibility study and modelling, within the context of an aircraft conceptual design process. This is done by giving some elementary answers to the ways and means of R&M integration in aircraft design. It opens a field in the research area for those engineering features of R&M away from its statistical prediction aspects, and closer to the requirements of a real-life aircraft. A field that looks towards R&M from conceptual platform, but wishes to see R&M in the detail preliminary design stage. This research work has initiated a more refined engineering-judgement foundation for R&M, and development cost prediction of future high risk technology, besides the usual aerodynamic, mass, and performance aspects. On the whole, three major results were obtained :

- Conceptual design optimisation of transport aircraft CACAD : the results of which were discussed in Chapter 2.
- Reliability and maintainability enhancement modelling applied to avionics system, and further integration into CACAD. Its results were analysed in Chapter 3.
- The development of VCW modelling, and associated reliability and maintainability predictions, which were incorporated into CACAD. The results obtained were analysed in Chapter 4.

In this chapter, repeating the previous analysis of the results is avoided, instead a more generic analysis of the results will be presented.

5.2 Analysis of the Methodologies

The methodologies developed for R&M prediction encompasses two sub-methodologies. The first one is for R&M prediction when the aim is to enhance the reliability of an existing aircraft system, and to analyse the net benefit in terms of aircraft safety, dispatch reliability, lower maintenance cost and saving in the DOC. The second one is for R&M prediction when a new technology is intended to be employed to a transport aircraft development, so as to analyse net benefit in the entire cost of the risk undertaken. Both methodologies employed conceptual design optimisation as an appropriate apparatus for the implementation of R&M predictions. They also made use of the system maintenance cost prediction equations reported in [22], and [28], for establishing a base value for the share of each major system in the known airframe maintenance cost.

In the former methodology, in order to enhance reliability of an existing system, exploration of the engineering solutions were considered mandatory. This meant understanding, in depth, the detail engineering sources of the system unreliability, and choosing a REM with least maintainability side effect, and then modelling such measures, with their impact on different aircraft design disciplines. Thus the methodology relies on those experimental works that provides reliable evidence for improving the reliability of the system.

The latter methodology, that endeavours predictions of R&M implications of a future technology, also relies on the modelling of the experimental work that provide reasonable evidence of the benefits, and the penalties of a new technology. However the R&M prediction rests on engineering judgement. It is extremely expensive to base R&M&D implications on experimental results, especially when heavy investment is to be avoided. The methodology made use of the prediction equations based on the past actual development cost data reported in [1], and [25], for the development cost of a future aircraft program. It then extensively modified them to predict the impact of a new technology development cost. Hence it gives the engineering judgement a

horizon, as well as offering a methodology to apply to any high risk future technology. For R&M prediction, the methodology is a blend of past experience in maintenance cost predictions, and elaboration of the areas that might be degraded due to the maintainability aspects of a new technology.

5.3 General Discussion

There are a few general comments about the entire scope of the present work which may also be helpful for future research work in this area :

1. The share of the maintenance cost of the airframe in the total DOC must be correctly predicted, and be very close to what is occurring in the current transport aircraft. An over-estimation may justify the implementation of any REM with even heavy penalty. On the other hand, it may prevent the application of a new technology due to falsely showing heavy maintenance cost implications. In the following table CACAD has reasonably predicted this percentage :

Aircraft Type	Percentage of maintenance cost part of DOC	
	Actual [34]	CACAD
MD-80 / F100	15.7	15.8
757-200	14.8	15.1
767-300	13.4	12.4

Note : There are discrepancies between CACAD, and other type of aircraft. One of the obvious one is the number of engines. In real life, two similar mission aircraft one twin, and the other quadro have tremendous maintenance cost difference between airframe, and engine share of the total maintenance cost, see the following table. However, CACAD is not equipped to take care of this factor. It will take this research work away from its objectives if efforts were made to improve CACAD. Note the maintenance cost variation between the similar mission aircraft such as twin engine MD-81, and quadro BAe-146 (burden is not included).

Aircraft Type	*Total Maintenance Cost $/FH [34]*	*% Airframe share*	*% Engine Share*
	Short range, low capacity		
MD-81	184.48	63.2	36.8
BAe-146	551.21	43.8	56.2
	Range about 5 to 6000 nm		
B767-300	287.55	56	44
MD-11	369.64	53	47
B747-200	1072	40	60

2. The share of each individual system within the total maintenance cost of airframe system must also be predicted close to real life values. An overestimation of a certain system makes it a candidate for REM. A poorly developed REM with heavy side effects may appear beneficial. On the other hand a future technology may suffer from this, by its exaggerated maintenance penalty. It was shown that the avionics system is at present constituting a minimum of 11.5% of the total airframe maintenance cost. This is the lowest reported, to avoid the above problem.

3. Every model plays its important role in the net effect of a REM, or a future technology. However, there are usually one or two that become key to the success of the project. Any misjudgement or inaccuracy in the quantitative effect of such model may jeopardise the whole project. In case of ASRE, the failure rate variation with the supply temperature is an example. It may be possible to bleed the engine and make an accurate prediction of its penalties on engine performance. It is also possible to predict reasonably the benefit effects of failure rate on avionics maintenance cost. But the bridge between these two sets of models is the temperature effect on failure rate. This is the critical model in ASRE, and its validation is of utmost importance.

5.4 Short Comings

There are areas which deserve further study in order to attract a more serious investment in both, ASRE, and VCW toward detail design work.

1. The maintenance cost information in avionics system of the present all glass cockpit, and fly by wire aircraft of the latest Airbus, and Boeing family must be collected. The share of maintenance cost of each system within the overall maintenance cost may be reviewed. Aircraft such as A330, A340, A319, A320, A321, B777 have recently joined the airlines, and perhaps their sustained maintenance cost and system failure rate might be too ill defined to rely on. However, because of the heavy investment in their R&M features, a review of their individual maintenance costs with respect to overall airframe maintenance cost and also relative to their DOC, is mandatory.

2. Cooling systems of the latest state of the art commercial aircraft must be checked in detail. They might have been improved to the extent that they have increased the cooling flow rate beyond the regulatory limits.

3. Although ECS mass variation with its output flow has a less significant role in penalty analysis of ASRE compared with bleed effect, nevertheless it is still a subject that the Author wished to have had the actual data from the manufacturer. This is commercially sensitive data.

4. There is a possibility of higher electric consumption by flight control systems, and hydraulic systems, when camber variation is included in their software operation, and when the extra actuators are installed in the wing. This has not been modelled.

5. VCW effect may cause an extra drag penalty on propulsion installation drag [104]. This was not modelled, due to lack of available experimental data. However, due to the optimistic view reported in [103], and the recent findings at MBB, the effect is small at average cruise lifts, and can be alleviated through an optimised span-wise redistribution of camber deflection and pylon/nacelle design [136].

6. It is reported that there is an extra trim drag penalty associated with downwash change due to wing camber variation [104]. However a recent report in [136] indicated that there may not be any extra trim drag penalty, but there may even be some drag benefit (of the order of 1%). This was not modelled. The reason is partly due to the fact that above findings has not been reported publicly, and partly due to CACAD not being equipped with detail tail sizing modules.

7. There might be drag associated with differential camber variation across the span in variable camber device splitting . This was not modelled due to lack of experimental results.

8. The dimensioning load cases, and possible wing structural weight reduction also has not been modelled in-spite of choosing VCW design proposal that enables camber change across the span. This has been recommended by [103], and [136]. It is claimed that 24% root bending moment reduction at the manoeuvre case is possible. There have been views expressed by other experts of the field that such root bending moment reductions are possible in FCW aircraft using speed dumpers, etc.

Chapter 6

Conclusions and Further Work

6.1 Conclusions

Individual conclusion sections were presented for the operation of CACAD, ASRE in CACAD, and VCW in previous chapters. The following conclusions are more general in nature, and hopefully serve a wider scope of reliability, and maintainability incorporation into aircraft conceptual design.

1. Bleed and power-off take are two main sources of applying REM that require power supply. The study showed that, those REM for long range aircraft, if supplied with power off take, have higher chances of proving cost-effective. The turbofan engines are less power off-take sensitive than bleed off-take.

2. Bleeding long range aircraft's engines for any type of REM, applied to any aircraft system, may not result to an appreciable saving in DOC, unless labour cost jumps to a very high value, or fuel cost makes a drastic fall,

3. The results of ASRE in CACAD showed that, within the maintenance cost benefit, the share of spare part cost is more dominant than the labour, and the material cost. Therefore it is possible to conclude that those systems that have a higher share in the aircraft price system if undergoing REM, may have higher chances of feasibility success than those cheaper systems.

4. ASRE in CACAD resulted in 0.5 to 1.0% DOC improvement. If exploration for enhancing the reliability of other systems are carried out, it may produce

a total saving of the order of 2 to 3% in DOC. This, when compared with a high risk future technology, or engine improvement is worth pursuing.

5. R&M implication shows that any new technology that aims for a drag reduction of up to or less than 5%, with influences on the maintainability of other airframe sections, is bound to have difficulty in gaining anything higher than 2% increase in DOC.

6. In certain cases the VCW saved DOC of 3%, in which the development cost penalty was a dominant model. If this technology is successfully coupled with say laminar flow wing technology, a DOC gain of more than 5% may be achievable [134], because the combined development work such as common airfoil design, wind tunnel testing, and other computational, as well as experimental work saves development costs. These two technologies may produce intelligent wings of future transport aircraft.

7. R&M consequences of future technology are inevitable. Their quantitative impact may vary with the nature of a technology, but it is neither to be ignored nor be given a unrealistically difficulty factor. The old notion of not including them in the conceptual design feasibility study is behind us. The methodology used for the prediction of their impact is applicable to most technologies that are currently pursued.

8. Provided the labour cost for maintenance, design and manufacturing, as well as fuel cost vary within a reasonable bound of 10%, short to medium range transport aircraft are more suitable for REM. This is due to the maintenance cost having a relatively higher share in DOC. On the other hand new technologies that aim toward reducing drag, and hence fuel consumption are suitable to be implemented for medium to long range aircraft. This is due to firstly, fuel cost as a major player in DOC which would boost the benefit models, and secondly the maintenance cost lower share would reduce the R&M implications.

9. This research work indicated that statistical R&M prediction equations integration with conceptual design synthesis is possible and useful. However

this research work indicated that, for REM purposes, experimental work that produces the reduction of failure rate is required appropriate to any system.

6.2 Recommendations for Further Work

1. The conceptual design synthesis (CACAD) is equipped with a simple optimiser which could be replaced with a proven sophisticated state-of-the-art one. The accuracy of the new optimiser can easily be validated with present one. This may reduce the computational time of the design, when more number of variables are allowed to participate in the sizing process. It also saves time when more classes of aircraft are desired to be designed, one after the other. This is also true when simultaneously sensitivity analysis is to be carried out.

2. Integration of a graphical sub-routine would help to show an overall diagram of the optimised aircraft, and the aircraft that are equipped with REM, and or future technology. This is especially desirable when sensitivity analysis explorations are carried out, that changes the aircraft shape gradually. Graphics help the understanding of configuration changes.

3. REM for propulsion system is recommended for integration in CACAD. Since the maintenance cost of this section of the aircraft is considerable, its price share in the aircraft market price is significant, and there must be numerous experimental works available which decrease reliability enhancement for ETOPS projects.

4. Intelligent wings comprising of VCW system and laminar flow wing system may be modelled together for integration into CACAD, for all their aspects, including their R&M implications. Numerous sensitivity analyses can be conducted to widen the insight in their modes of applicability, and profitability.

5. CACAD can be extended to design executive aircraft, tactical cargo, and optimum derivative transport aircraft. This enables a widening of the applicability study of REM and future technology.

6. CACAD can be extended to estimate a VCW aircraft off-design performance, and DOC. This, when compared with equivalent FCW off-design, will quantify extra DOC saving. A sensitivity analysis may suggest, what class of aircraft, at what off-design range, may produce the highest extra benefit. This will eventually quantify the benefits of operational flexibility of VCW.

REFERENCES

1. Raymer, D.P. *Aircraft Design : A Conceptual Approach* AIAA Educational Series, 1989.
2. Punches, Ki *Airplane reliability in a nut shell*, IEEE, Transactions on reliability, Vol. R-32, No.2, June 1983.
3. Donna F. H., et all *Maintainability estimating relationships*, Northrope Corporation, Proceedings Annual Reliability, and Maintainability Symposium, 1975.
4. Maddalon, Dal V. *Estimating airline operating costs*, NASA Tech Mem. No. 78694, 1978.
5. Farguson, F.D. et all *Developemnt of Navy aircraft baseline reliability prediction models*. Vought Corporation, Feb. 1980.
6. J.P.Fielding, and V.C.Serghides,: *A Reliability and Maintainability Prediction Methodology for the Conceptual Aircraft Design Process* . Cranfield Inst. of Technology, Reliability Engineering and System Safety 20 (1988) 19-33, 1988.
7. V.C. Serghides, *Development of a Reliability and Maintainability Prediction Methodology for the Aircraft Conceptual Design Process*, M.Sc. Thesis, Cranfield Institute of Technology, 1985.
8. Fielding, J.P. *Fault tree analysis & FMECA,* COA lecture notes, 1968.
9. Fielding, J.P. *Reliability prediction methods for use in aircraft design*, Des 8930/1.
10. Schafer, T. et all *Developemnt of criteria and quantitative prediction of maintenance of Air Force equipment.* Aero-system Division. WP AFB, Ohio, September 1961.
11. Serghides, V.C. *T84 Basic military trainer aircraft R&M design*, M.Sc. Project thesis COA-DES, Cranfield University, 1985.
12. Consoli, R.D., Sobieski J.S., *Application of Advanced Multidisciplinary Analysis and Optimization Methods to Vehicle Design Synthesis*, General Dynamics, and NASA Langley Research Centre respectively, ICAS-90-2.3.4, 1990.
13. Peckham, D.H. *Multivariate Analysis Applied to Aircraft Optimisation - a First Progress Report* RAE, TM-Aero-1352, 1971.
14. Collingbourne, J. *Multivariate Optimisation Applied to the Initial Design of Transport Aircraft* RAE, TR-84044, 1984.
15. Roskam, J. *Airplane Design (8 Volume)* The University of Kansas 1991.
16. Pasaribu, H.M. *An approach to configuration design synthesis of subsonic transport aircraft using artificial intelligence techniques.* Ph.D. Thesis, Supervisor Fielding, J.P. Cranfield University, 1992.
17. Salguero, D.E. *A design synthesis program for business jet aircraft.* AIAA annual meeting and technical display, 12th. Washington D.C. January 28-30, 1976. AIAA Paper No. 76-216.
18. Jenkinson, L.R., Simos, D. A *computer program for assisting in the*

priliminary design of twin-engined propeller driven aircraft. Canadian Aeronautics and Space Journal, vol.30, No. 3, Sept 1988.

19. Bil, C. *Application of computer aided engineering to subsonic aircraft design in a university environment.* Proceedings of the 15th Conference of the International Council of Aeronautical Sciences. ICAS-86-3.1.1, pp. 108-118.
20. Bil, C. *Development and application of a computer based system for conceptual aircraft design.* Delft, Netherlands. Delft University Press, 1988.
21. Haberland, C et all *A computer augumented procedure for commercial aircraft preliminary design and optimisation.* Proceedings of the 14th Conference of the International Council of Aeronautical Sciences, ICAS-84-4.8.1, pp. 943-953. 1984.
22. Wallace, R.E. *A computerised system for the preliminary design of commercial airplanes.* AIAA, Aircraft Design, Flight Test, and Operations Meeting, 4th. LosAngeles, CA. Aug. 7-9, 1972. AIAA Papaer No. 72-793, 1973.
23. Roskam, J., Malaak,S.M., Anemaal,W. *AAA : Advanced aircraft analysis, a user-freindly approach to preliminary aircraft design,* ICAS-90-2.10.2, 1990.
24. Gregory, Thomas J. *Computerized preliminary design at the early stages of vehicle definition,* (NASA Technical Memorandum). - (NASA/TM X-62303)1990
25. Corning, G Professor *Supersonic and Subsonic, STOL, VTOL, Airplane Design.* Maryland University, College Park, Maryland, 1984.
26. Rolls Royce, Aero data. TS 1491 Issue 11 March 1994, Derby, England.
27. Peckham, D.H. *The Influence of Some Requirements and Design Standards on Subsonic Transport Aircraft Characteristics* RAE, TM-Aero-1074, 1968.
28. Perry, D.H *Multivariate Analysis Applied to Aircraft Optimisation, Some Proposals and Data for an Exploratory Study* RAE, TM-Aero-1237, 1970.
29. Piggott, B.A.M. Taylor, B. *Application of Numerical Optimisation Techniques to the Preliminary Design of a Transport Aircraft* RAE, TR-71074, 1971.
30. Purcell, A.G. *Fortran Program for Constrained Optimisation* RAE, TR-77142, 1977.
31. Edwards, B. *The Use of Computer Based Optimisation Methods in Aircraft Design* RAE, TM-Aero-1814, 1979.
32. Torenbeek, E. *Synthesis of Subsonic Airplane Design,* Delft University Press, 1976 .
33. Wood, Karl Dawson. *Aerospace vehicle design : volume II : spacecraft design,* Boulder, Colo : Johnson Pub. Co, 1964.
34. Nicolai, Leland Malcolm. *Fundamentals of aircraft design,* Dayton, Ohio : Nicolai : distributed by School of Engineering, University of Dayton, 1975.
35. AEA Association of European Airlines, G(T) 5656, 4th December 1989.
36. Wayne Burns, J (Vought Aircraft Corporation) *Aircraft cost estimation methodology and value of a pound derivation for preliminary design development applications.* 53rd Annual Conference of Society of Allied

Weight Engineers, Inc. Long Beach CA 23-25 May 1994.
37. Van Bodegraven,G. Boeing Commercial Aircraft, *Commercial Aircraft DOC*, AIAA 90-3224. Aircraft Design, Systems, and Operationss Conference Sept. 1990.
38. *Direct airframe engineering costs according to ATA 100 Chapters*, Addendum C, and B, College of Aeronautics Cranfield UK, May 1975.
39. Delta Method : *An empirical drag build up technique final report*. NASA-CR-151971, 1978.
40. Press, W.H. *Numerical Recipes in Fortran the Art of Scientific Computing*. 2nd edition. 1992.
41. Pant, R. and Kalker-kalkman, C.M. *On generating optimum configurations of commuter aircraft using stochastic optimisation methods*, submitted to the journal "engineering Optimisation" Oct. 1995.
42. Anonymous, *Table A3 narrow body jet transport - field performance and parameteric ratios*, Dept. of Aerospace Tech., Cranfield University, 1993.
43. Lambert, L.(ed.) *Janes all the world's aircraft* 1993-1994-1995 Editions. Janes Information Group.
44. *Quarterly aircraft operating costs and statistics*, Published by Avmark, Inc. 1994. 1st Quarter 1993.
45. Whitford, R. *Ultra - high capacity aircraft some design consideration* , AIAA 93-1108 Aerospace Design Conference, Feb.1993.
46. Rosa, M.R. *Performance & cost analysis of the A-94 Airline*, M.Sc. Thesis, College of Aeronautics, Cranfield University, 1995.
47. Dogfight, *Boeing and Airbus Industrie engaged in* .., Business India, Oct 23-Nov 5 1995.
48. Avmark International Ltd., *Semi-Annual Appraisal of Used Aircraft Values* Jan. 1995.
49. Aviation Week & Space Technology / November 21, 1994.
50. Qureshi, H. Late Ph.D. student in College of Aeronautics at Cranfield University who died during his write up stage: *Advanced Aircraft Systems*, 1994.
51. W.C. Savage, *Advance Environmental Control System*. US Airforce Flight Dynamics Lab., NAECON, 1974.
52. Zara, E. et al, *Advance Environmental Control For Avionic Systems*, Wright Patterson AFB, NAECON, 1977
53. Zentner, R.C. Kramer, T.J. *Development and Testing of Forced Air Cooled Enclosures for Higher Density Electronic Equipment* Boeing Aerospace Company, SAE840952, 1984.
54. Anonymous ; *Large, and medium transport aircraft arising, fault, and operational deffect rate*. Oct. 1990.
55. Britannica, *Reliability Program, B767*, July 1989.
56. British Airways, *REACT : Fleet reliability performance and engineering statistics, Concord*, Nov.1984.
57. British Airways, *C.P.R.Compenent performance report, B757*, Defect Analysis (S383), Feb.1988.
58. British Airways, *REACT : Fleet reliability performance and engineering statistics, B757*, April 1988 .
59. British Airways, *C.P.R.Compenent performance report, B747*, Sep. 1984.

60. British Airways, *REACT : Fleet reliability performance and engineering statistics, B737*, Nov. 1984.
61. British Airways, *C.P.R.Compenent performance report, B737*, Oct. 1984.
62. BAe 146, *In-Service Component Reliability Report*, March 1989 .
63. Leonard,C.T. *Passive Cooling for Avionics can Improve Airplane Efficiency and Reliability*, NAECON, 1987.
64. Leonard,C.T. , Pecht, M. *Failure prediction methodology calculations can mislead.* IEEE 1989.
65. Gehman, J. *Avionics maintenance more important than reliability.* The Rand corporation Santa Monica, CA. AIAA-89-2096.
66. AGREE, Advisory Group on Reliability of Electronic Equipment : *Report on reliability of electronic equipment.* US Government Printing Office, Washington D.C. 1957.
67. AGARD, *Reliability of avionics systems*, AGARD-CP-261, 1979.
68. AGARD, *Avionics reliability, its techniques & related disciplines.* AGARD-CP-261, 1979.
69. AGARD, *Avionics cooling and power supply for advanced aircraft.* P.W. Smith (ed.), AGARD-CP-196, 1976.
70. SAE Aerospace *Applied Thermodynamics Mannual, Part 31 : Aircraft Penalty Evaluation.*
71. K. Bauerfeind, Head of performance and control systems, MTU Gmbh, 8000 Munchen 50, : *Extraction of Auxiliary Power from Airbreathing Propulsion Systems.*
72. Palmer, J.R. *The turbomatch scheme for gas turbine performance calculations user's guide*. Cranfield Institute of Technology, Oct. 1983.
73. M.A.F. Vaziry-Z., *ECS Design for Business Jet E-92,* Project Thesis, Cranfield University, 1993.
74. Anonymous, B767, and A320 Electric power consumption chart.
75. ARINC Specification No.600-1, Aernautical Radio Inc., Annapolis, Maryland, June 1978.
76. Anonymous *Bleed and power off take effect on Trent and Tay engines* , Private communication with Rolls Royce, 15/12/94.
77. Crabtree, R.E. et al, *The Cabin Air Conditioning and Temperature Control System for the Boing 767,757 Airplanes* ASME-80-ENAs-5, 1980
78. Franklin, J.L. Kramer, T.J. *Thermal Design of Standard Avionics Enclosures* Boeing Aerospace Co., SAE Tech. Paper Series 820878, 1982.
79. Cirrito, V. *Thermal Design of Integrated Avionic Racks of Aircraft* Gruman Aerospace Corp., SAE Tech Paper Series 820871, 1982.
80. Mining, C.P. and Basiulis, A. *Improved reliability of electronic circuits through the use of heat pipe*, Highes Aircraft, IEEE 1985.
81. Peterson, G.P. *Heat removal key to shrinking avionics*, Aerpspace America, Oct. 1987.
82. Groom, K.D. Brooks, G.W. *Thermal Management of Flight deck Instruments* The Boeing Company, AGARD-CP-196, 1979.
83. Spitzer, C.R. *Digital avionic systems : principles and practices* - 2nd ed. New York : McGraw-Hill, 1993.
83.1 MIL-E-38453A, *Environmental Control, Environmental Protection, and Engine Bleed Air System, Aircraft, General Specification for*, 1971.

84. German, G. *Cooling of the Electronic Equipment in Relation to Component Temperature Limitations and Reliability* Royal Signals and Radar Establishment. AGARD-CP-196, 1979.
85. Boronow, W.S. *Cost Effectiveness of Refrigarated Air for Avionics Cooling on Wide Body Commercial Aircraft* ASME paper 75-ENAS-9, 1975.
86. Rogers, B.H. *Aircraft ECS for 21st centuary*, I.Mech.E. Sumposium, London, Sept. 1986.
87. Klass, P.J. Better *Cooling Aids Avionics Reliability*, Ohaio, Aviation Week & Space Technology, page 53 / June 20, 1994.
88. Nordwall B.D. *Apache Longbow to use vapor cycle cooling*, Aviation Week & Space Technology, page 64 / January 1, 1996.
89. Briefing, Airbus A321, AI / CM-T 316.00? Issue 3, May 1993
90. Briefing, Airbus A300-600, AI / CM-T 316.006 Issue 2, May 1993.
91. Briefing, Airbus A330, AI / CM-T 316.0015 Issue 3, May 1993.
92 Airbus Industrie, *Direct maintenance costs art or science?* Product Support Directorate, Maintenance Cost Gruop, AI/SE 21003, 1989.
93. MIL-HDBK-472, 24 May 1966 *Maintainability Prediction.* Department of defense Washington D.C. 20360.
94. Harris, R. and Bradfield, F. *Model experiments with variable camber wings.* ARC R&M No. 677, 1920.
95. Jones, E. et al *Lift and drag of the Bristol fighter with fairey variable camber wings.* ARC R&M No.1085, 1926.
96. Whitford R. *Design for air combat.* Jane's publishing company 1987.
97. Streather, R. *Variable geometry airfoils as applied to the Beatty B-5, and B-6 sailplanes*, ICAS-82-5.5.3, 1983.
98. Moxon, J. *Mission adaptive wings*, Flight International, 10th August 1985.
99. Ferris, J. *Wind-tunnel investigation of a variable camber and twist wing.* NASA TN D-8475, 1977.
100. Boeing Commercial Aircraft Company, *Assesment of variable camber wing for application to transport aircraft.* NASA CR 158430, 1980.
101. Spillman, J.J. '*Variable camber geometry for transport aircraft wings*' Proceedings of 'Aerotech 92' Conference 14-17 Jan. 1992 .
102. Spillman, J.J. '*The use of variable camber to reduce drag, weight and cost of transport aircraft*' Aeronautical Journal, January 1992 .
103. Macey, P. '*A feasibility study on the application of variable camber flaps on a military tactical transport aircraft*' M.Sc. Thesis, Cranfield Institute of Technology 1992-93 .
104. Lunn, J.D. '*Weight effects of variable camber wings*' M.Sc. Thesis, Cranfield Institute of Technology, 1992 .
105. Rao, A.J. '*Variable camber wings for transport aircraft*' Ph.D. Thesis . Cranfield Institute of Technology, 1987-88.
106. MacKinnon, A.V. Stollery, J.L. '*Wind tunnel tests on variable camber wing*' Coolege of Aeronautics Report No.9304, Cranfield Institute of Technology, March 1993.
107. MacKinnon, A.V. *An experimental study of a variable camber wing (VCW)*' Ph.D. Thesis, Cranfield Institute of Technology October 1993 .
108. Macci, S. *'Structural and mechanical feasibility study of a variable camber wing (VCW) for transport aircraft'* Ph.D. Thesis, Cranfield Institute of

Technology, August 1992 .
109. Greff, E. *'The development and design integration of a variable camber wing for long/medium range aircraft'* Aeronautical Journal November 1990 .
110. Szodruch J. and Hilbig R. *'Variable Wing Camber for Transport Aircraft'* Prog. Aerospace Sci. Vol. 25, pp. 297-328, 1988 .
111. Fielding, J.P. et al *'The aerodynamic and structural design of variable camber wing (VCW)'* ICAS 1992.
112. Hilbig, H. and Wagner, H. *'Variable wing camber control for civil transport aircraft'* ICAS-84-5.2.1, 1984 .
113. Szodruch, J. *'The influence of camber variation on the aerodynamics of civil transport aircraft'* AIAA 85-0353, 1985.
114. Renken, J.H. *'Mission adaptive wing camber control systems for transport aircraft'* AIAA Paper 85-5006, 1985 .
115. Stollery, J. and Fielding, J. *'Cranfield to work with British aerospace on variable camber wings'* AEROGRAM, Vol.5, No.4 May 1989 Cranfield Institute of Technology.
116. Jupp, J.P. *Wing Developments,* Airbus Industrie Advanced Technology Symposium, June 1990. (ECATA Lecture).
117. Feazel, M. *'MBB studies variable camber wings to improve lift, Expand Fleet Uniformity'* Aviation Week & Space Technology/April 29, 1985.
118. Renken, J.H. *'Integration of a variable wing camber function into an EFCS of a transport aircraft'* AIAA-87-2879, Aircraft Design and Operations Meeting Sep. 14-16, 1987/St. Louis, Missouri .
119. Towell, K.J. *S-80 variable camber wing : mainbox*, M.Sc. Project Thesis, Cranfield Institute of Technology, 1981.
120. Landry, J. G. N. *A90 500 passenger short range airliner variable camber outer flaps*, M.Sc. Project Thesis, Cranfield Institute of Technology, 1991.
121. Larrive, L. *A90, 500 seater short haul airliner : design of variable camber inner flaps*, M.Sc. Project Thesis, Cranfield Institute of Technology, 1991.
122. Carboon, Jonathan P. *F93/A WOMBAT variable camber flap design*, M.Sc. Project Thesis, Cranfield University, 1994.
123. Edi, Prasetyo. *A feasibility study on the application of variable camber wings on a military tactical transport aircraft*, M.Sc. Project Thesis, Cranfield University, 1994.
124. Verghese, P.K. *S80 Variable camber wing moving surfaces* / P.K. Verghese, M.Sc. Project Thesis, Cranfield Institute of Technology, 1981.
125. Nettleton, T.R. *Amethod of estimating the effects of rear fuselage up sweep and fuselage cross flow sectional shape on fuselage drag.* Unpublished report of De Haviland Canada, Nov. 1964.
126. Kapteijn, P. *Design charts for the aerodynamic characteristics of straight and swept, tapered, twisted wings at subsonic speeds.* Delft University of Technology, Dept. of Aeron. Engng., Memurandum M-180, May 1972.
127. Wolfram, S. *Mathematica a system for doing mathematics by computer.* Second Edition. Addison - Wesley Publishing Company Inc., 1991.
128. Garner, H.C. *Some remarks on Vortex drag and its spanwise distribution in incompressible flow.* The Aeronautical Journal, p.623, July 1968.
129. Howe, D. *The prediction of aircraft wing mass.* Professor of Aircraft

Design, Cranfield University, Proc. Instn. Mech. Engrs. Vol 210, I Mech E, 1996.

130. Collyer, M.R., and Lock, R.C. *Improvement to Viscous Garabedian and Korn (VGK) method for calculating transonic flow past an airfoil.* RAE TR 78039, 1978.

131. Williams, B. *The prediction of separated flow using a viscouse-inviscid interaction method* RAE TM AERO 2010, 1984.

132. MIL-HDBK-217C, *Reliability prediction of electronics equipment*, 9April 1976.

133 Fielding J.P. *Internal debate within Conceptual design research group*, College of Aeronautics, Department of Aerospace Technology, 1993 to 1996.

134. Wilson, R.A.L. Jones, R.I. *Project design studies on aircraft employing natural and assisted laminar flow technologies,* SAE Technical paer series 952038, Aertech '95, Los Angeles, California, Sept. 18-21, 1995.

135. Anonymous, *"Subsonic aerodynamic loading distributions"* DAeT 9147 lecture notes, College of Aeronautics, Cranfield University.

136. Greff, E. The private communication with Aerodynamic department, Daimler Benz Aerospace Airbus, 1995.

137. Hoerner, S.F. *Fluid-dynamic Drag,* published by the author, 1965.

138. Berger, R.L. *A Systems Approach Minimising Life Cucle Cost* US Airforce System Command, SAE 831107.

139 Buckingham, R.D. *Helicopter cooling, air cycle/ vapor cycle trade-offs*, SAE 840942, 14th Intersociety Conference on Environmental Systems, California July, 1984.

140. ARINC 408A, *Air Transport Indicator Cases and Mounting*, Aernautical Radio Inc., Annapolis, Maryland 1975.

Appendix A

Nomenclature / Notation / Abbreviation

* : Input Value, ** : Mission Input Value, IV : Independent Variable,
DV : Dependent Variable, OB : Objective Function

No.	Abbreviation	Notation	Definition	Unit	Value	Type
1		C_{Lmax}	Maximum Aircraft Lift Coefficient (Trimmed)	-	-	DV
2		C_L	Aircraft Lift Coefficient	-	-	-
3		γ	Ratio of specific heats	-	1.4	*
4		β	Fuselage upsweep angle	deg	7.5	*
5		$\varepsilon(\eta)$	Twist value at any spanwise location	-	-	DV
6		ε_t	Angle of twist			
7		η_{CP}	Wing centre of pressure from wing root	-	-	DV
8		ΔC_{design}	VCW extra developemnt cost, design	$	-	DV
9		$\Delta_e C_{DV}$	Induced drag coefficient due to twist	-	-	DV
10		$\Delta_{\alpha\beta}(C_D S)$	Drag increment due to aft body upsweep	-	-	DV
11		$\lambda_{avionics}$	Avionics failure rate per 1000 FH	<	-	DV
12		ΔC_{ci}	Decrease in fillet circumference length	m	-	DV
13		$\Delta_i(C_D S)_p$	Drag increment due to wing fuselage viscous interference	-	-	DV
14		ηicomp	Isentropic efficiency of compressor of ACAU	-	0.7	*
15		ηitur	Isentropic efficiency of turbine of ACAU	-	0.8	*
16		ηmech	Mechanical efficiency of ACAU, and its prime mover	-	0.95	*
17		Δsfc	sfc rise due to bleed	N/g/s	-	DV
18		ΔT	Thrust fall due to power off take from engines	N	-	DV
19		t_r	Thickness to chord ratio at wing root	-	-	DV
20	-	T_{SL}	Standard ambient temperature at sea level	"	-	DV
21	A	A	MIL-HDBK-472 category A criteria	-	-	-
22	A/C	a/c	Aircraft	-	-	-
23	A03D	$C_{L\alpha}$	Slope of the C_L vs α of the wing	1/rad	-	DV
24	AC	ac	Aerodynamic centre	-	-	-
25	ACAU	-	Auxiliary cool air unit	-	-	-
26	ACLIFE	A_{clife}	Service life of airframe, and engine	year	20	*
27	ACLMD	-	Maximum C_L of basic wing and LE devices at AP	-	-	DV
28	ACSYNT	-	AirCraft SYNThesis	-	-	-
29	ADAS	-	Aircraft Design & Analysis System	-	-	-
30	ADCLMSO	A_{DCLMSO}	Additional lift due to LE devices during Approach	-	-	DV
31	AEA	-	Association of Europian Airlines	-	-	-
32	A_I	-	Fuselage planform areas of forebody	m2	-	-
33	A_{II}	-	Fuselage planform areas of aft swept body	m2	-	-
34	AISLES	A_{ISLES}	Number of aisles	-	-	**
35	ALFA0L	$\alpha_{0\ell}$	Change in zero-lift angle of the wing per degree of the positive twist at the tip	deg	-0.4	*
36	ALFAF	α_f	Body angle of attack	deg	-	-

37	ALFAL0R	$(\alpha_{\ell 0})_r$	Zero lift angle of the root section	deg	-2.0	*
38	ALFMIN	$\alpha_{f\,min}$	Body angle of attack for minimum upsweep drag	deg	-	DV
39	AMAX	-	Maximum value of aspect ratio	-	-	DV
40	AMC	AMC	Aerodynamic mean chord	-	-	DV
41	AMCETA	AMC_{eta}	Spanwise location of AMC	-	-	DV
42	AMFUS	A_{mfus}	Variable in the definition of fuslage mass	-	-	DV
43	AMP	A_{mp}	Airplane market price	$	-	DV
44	AP	-	Approach	-	-	-
45	ASRATD	A_{sratd}	Area ratio parameter of datum wing and LE devices at AP	-	-	DV
46	ASRE	-	Avionics System Reliability Enhancement	-	-	-
47	ASWPLT	A_{SWPLT}	A constraint for sweep and aspect ratio	-	8.1	*
48	ATA	ATA	Air Transport Association	-	-	-
49	B	B	MIL-HDBK-472 category B criteria	-	-	-
50	BANGLL	-	Body angle on landing	deg	-	DV
51	BIZJET	-	Bussiness Jet Design Synthesis	-	-	-
52	BPR	BPR	By pass ratio	-	-	-
53	BTAA	β_A	Approach value of flap angle of deflection	deg	-	IV
54	BTAMX	β_{Tmax}	Maximum deflection of flap β	-	40	*
55	BTATO	β_T	Take off value of flap angle of deflection	deg	-	IV
56	C	C	MIL-HDBK-472 category C criteria	-	-	-
57	C	-	Number of spares assigned to remote stations	-	-	-
58	C	c	Wing chord at any location from the root	-	-	DV
59	C_ℓ	-	Section lift coefficient	-	-	-
60	c(η)	-	Chord value at any spanwise location	-	-	DV
61	$C_{\ell 0S}$		Basic lift coefficient	-	-	DV
62	$C_{\ell S}$		Additional lift coefficient	-	-	DV
63	C01,2	$C_{01,2}$	Coefficient in the expression for drag due to twist, 1.2623E-05, 1.070E-04	-	<	*
64	CABIN	C_{ABIN}	Number of cabin crew (air hostesses)	-	-	DV
65	CACAD	-	Computer Assisted Conceptual Aircraft Design	-	-	-
66	CAD	-	Computer Aided Design	-	-	-
67	CAMM5	C_{amm5}	Coefficients in expression for airframe maintenance material cost	-	7.5E-06	*
68	CAPDA	-	A Computer Assisted Aircraft Design System Developed by Berlin Technical University	-	-	-
69	CBLOC	C_{bloc}	Taxing time per flight	hr	0.3	*
70	C_{ci}	-	Circumferential length for both wing halves of the wing fuselage intersection	m	-	DV
71	CD0	C_{D0}	Lift independent drag coefficient	-	-	DV
72	CD0EW	C_{D0EW}	Lift independent drag coefficient other than wing	-	-	DV
73	CD0W	C_{D0W}	Lift independent drag coefficient wing	-	-	DV
74	CDA		Drag coefficient at approach			
75	CDCLRA	-	CDA/CLA			
76	CDCR	C_{dcr}	Drag coefficient cruise	-	-	DV
77	CDCRB	-	Drag coefficient at start of cruise climb, due to CLCRB			
78	CDCRB1,2,3,4,5	-	Drag coefficient at the start of every cruise sector due to CLCRB1,2,3,4,5	-	-	DV
79	CDDIV	C_{ddiv}	Drag coefficient at diversion	-	-	DV
80	CDDIV	-	Drag coefficient at diversion phase	-	-	DV
81	C_{design}	-	Cost of design of an aircraft	$	-	DV
82	CDETA1	$\Delta_e C_{DV}$	Increment in induced drag due to twist	-	-	DV
83	CDK2,3	-	Coefficient in expression for DOCDK	100,	-	*

				2.0		
84	CDPFA,TO	-	Profile drag coefficient due to flaps at AP, and TO	-	-	DV
85	CDT0	$C_{D\,t0}$	Lift independent drag coefficient at take-off			
86	CDUC	-	Drag coefficient due to undercarriage at low speed			
87	CDVFA,TO	-	Vortex drag coefficient due to flaps at AP, and TO	-	-	DV
88	CDWDR	C_{DWDR}	Compressibility drag coefficient	-	.001 to 0.002	*
89	CDWDR	$C_{D\,comp}$	Compressibility drag ranging from 0.001 to 0.002	-	<	*
90	CDYEFH	-	Yawing drag coefficient at single engine fialed height	-	-	DV
91	CEF1	C_{pi}	Cost index factor	-	-	-
92	CEML1,5	$C_{emL1,5}$	Coefficients in expression for engine maintenance time	-	0.6, .0006	*
93	CEMM3	C_{emm}	Coefficient in DOCEM	-	4.5E-05	*
94	CERT,A	-	Wing chord ratio, TO, and AP	-	-	DV
95	CF	C_F	Skin friction drag coefficient of smooth flat plate	-	-	DV
96	CFC	sfc_{cruise}	Engine specific fuel consumption for cruise (this value is fed into CACAD from an existing engine near to aircraft's requirement)	1/h	-	**
97	CFDIV	sfc_{div}	Engine specific fuel consumption for diversion	1/h	-	**
98	CFH	sfc_{hold}	Engine specific fuel consumption for hold	1/h	-	DV
99	CGIENG	CG_{IENG}	Distance of inboard wing mounted engines from a/c CG / FUSL	-	-	DV
100	CGOENG	CG_{OENG}	Distance of outboard wing mounted engines from a/c CG / FUSL	-	-	DV
101	CGPOSN	Cg_{posn}	CG position from nose of fuselage / FUSL	-	-	DV
102	CGPOSN	cg	Aircraft centre of gravity location fron nose of a/c / FUSL	-	-	-
103	CGWING	CG_{WING}	Distance of wing group from a/c CG / FUSL	-	-	DV
104	$C_{L\alpha}$	A03D	Slope of the C_L vs α of the wing	1/rad	-	DV
105	CLA	-	Lift coefficient at approach	-	-	DV
106	CLA1,2,3	$C_{la1,2,3}$	Coefficients in definition of GSCLOM, 1.445, -1.7, 2.1	-	<	*
107	CLB1,2	$C_{lb1,2}$	", 0.0131, -0.025	-	<	*
108	CLBOA	C_{Lboa}	Lift coefficient buffet onset required	-	-	DV
109	CLBOR	C_{Lbor}	Lift coefficient buffet onset "is required from wing"			
110	CLCR	C_{Lcr}	Coefficient of lift at cruise	-	-	DV
111	CLCRB	-	Lift coefficient at the start of cruise climb due to MSSB	-	-	DV
112	CLCRB1,2,3,4,5	$C_{L\,crb1\,to\,5}$	Lift coefficients at the start of cruise climb due to MSSB1,2,3,4,5	-	-	DV
113	CLCRBB	-	Lift coefficient at the start of cruise climb due to MSSBB	-	-	DV
114	CLDES	$C_{L\,des}$	Design lift coefficient	-	-	DV
115	CLDIV	C_{Ldiv}	Lift coefficient diversion	-	-	DV
116	CLF1,2,3,4	$C_{lft,2,3,4}$	Coefficients in the definition of TE devices additional lift, 0.7675,-0.163,-0.0415,-6.63	-	<	*
117	CLMA,TO	-	Maximum available trimmed C_L at AP, and TO	-	-	DV
118	CLMB	C_{LMB}	Basic wing C_{lmax} (no t/c influence)	-	1.61	*
119	CLMFA,TO	-	Increment in C_{Lmax} due to flap deflection at AP, TO	-	-	DV
120	CLMTO	-	Maximum lift coefficient trimmed at take-off condition	-	-	DV

121	CLS1,2	$C_{Ls1,2}$	Coefficients in the definition of LE devices additional lift	-	8.3, -15.0	*
122	CLTO	$C_{L\,to}$	Lift coefficient at the take-off condition	-	-	DV
123	CONFLL	-	Contigency fuel mass	hg	-	DV
124	CP	C_p	Specific heat capacity of air at constant pressure	J/kg/ kW	1.005	*
125	CPDS	-	A Very Advance Aircraft Design System Developed by Boeing	-	-	-
126	CPR	CPR	Compressor pressure ratio	-	-	-
127	CPR	-	Compressor pressure ratio of ACAU	-	2	*
128	C_R	-	Average cost of avionics maintenance labour & material per every removal	-	-	-
129	CR	C_r	Wing root chord	m	-	DV
130	CRT	-	Cathod ray tube	-	-	-
131	CRXTA	C_{rxta}	Required rate of climb at true start of the cruise	m/s	1.016	*
132	CT	C_t	Wing tip chord	m	-	DV
133	DCLDA	$dC_l/d\alpha$	Lift curve slope for critical gust case	1/rad	-	DV
134	DCLDAA	-	Lift curve slope at field operation condition	-	-	DV
135	DCLDAC	-	Lift curve slope at cruise	-	-	DV
136	DCLFA,TO	-	Increment in C_L due to flaps, at constant incident, AP & TO	-	-	DV
137	DCLMFT,A	$D_{clmfT,A}$	Additional lift due to TE flaps at Take-off, and Approach	-	-	DV
138	DCR	D_{CR}	Drag cruise	N	-	DV
139	DECK	D_{ECK}	Number of deck crew	-	-	**
140	deg	-	degree	-	-	-
141	DEL					
142	DELTA	δ	Induced drag factor deviation from unity	-	-	DV
143	DFLP	D_{flp}	Distance from flap LE to rear spar / wing chord	-	0.05	*
144	DHTEN	D_{thten}	Energy hieght for cruise	km	-	DV
145	DHTEND	D_{htend}	Energy hieght for diversion	km	-	DV
146	DIV	D_{iv}	Diversion stage length	km	-	**
147	DMAR	dM_{AR}				
148	DMAR	$D_{M\,aspect\ ratio}$	Correction for aspect ratio to M_{2D}	-	-	DV
149	DMCCL	dMc_{CL}	Increment in critical Mach number due to lift	-	-	DV
150	DMCCL	dMc_{CL}	Increment in zero lift Mach number due to lift resulting in Mach critical drag	-	-	DV
151	DMCR	dM_{cr}	Critical increment in Mach number	-	-	DV
152	DMCR	dM_{cr}	Increment in Mch number resulting in Mach critical drag	-	-	Dv
153	DMDES	D_{mdes}	Design Mach number	-	-	DV
154	DMSWP	$D_{M\,sweep}$	Correction for sweep to M_{2D}	-	-	DV
155	DOC	-	Direct Operating Cost either £ or $/Flight, or Block Hour; or Penc or Cent/ Seat Kilometer	<	-	OB
156	DOCAFLM 0,1,2	DOC_{aflm}	Airframe maintenance cost, base, approach1, approach2	£/flt	-	DV
157	DOCAFLMR		Airframe maint. cost excluding APU	£/flt	-	DV
158	DOCAFLR	-	Airframe maint. labour cost excluding APU	£/flt	-	DV
159	DOCAFLT0 ,1,2	DOC_{aflt}	Airframe labour maintenance cost, base, approach 1, approach 2	£/flt	-	DV
160	DOCAFMT		DOCAFMT excluding APU	£/flt	-	DV
161	DOCAFMT 0,1,2	DOC_{afmt}	Airframe material maintenance cost, base, approach 1, approach 2	£/flt	-	DV
162	DOCDK	-	Deck cost per flight	£/flt	-	DV

163	DOCEL	DOC_{el}	Labour maintenance cost of engines	£/flt	-	DV
164	DOCEM	DOC_{em}	Material maintenance cost of engines	£/flt	-	DV
165	DOCF	DOC_f	Fuel cost part of DOC	£/flt	-	OF
166	DOCLAPU1,2	-	Maintenance labour for APU approach 1 & 2	£/flt	-	DV
167	DOCLEL1,2	-	Maint. labour for electronics approach 1 & 2	£/flt	-	DV
168	DOCLELS1,2	-	Maint. labour for electrical system approach 1& 2	£/flt	-	DV
169	DOCLF	DOC_{lf}	Landing fee part od DOC	£/flt	-	OF
170	DOCLFIN1,2	-	Maintenance labour for fin approach 1 & 2	£/flt	-	DV
171	DOCLFS1,2	-	Maint. labour for fuel system approach 1&2	£/flt	-	DV
172	DOCLFUR1,2	-	Maintenance labour for furnishing approach 1&2	£/flt	-	DV
173	DOCLFUS1,2	-	Maintenance labour for fuselage approach 1 & 2	£/flt	-	DV
174	DOCLHYD1,2	-	Maint. labour for hydraulic system approach 1&2	£/flt	-	DV
175	DOCLIAE1,2	-	Maint. labour for Instrument, Avionics and Electronics approach 1 & 2	£/flt	-	DV
176	DOCLMM1,2	-	Maint. labour for Miscellaneous items such as oxygen, ballast etc. approach 1 & 2	£/flt	-	DV
177	DOCLSTR	DOC_{lSTR}	Maintenance labour cost of structure per flight	£/flt	-	DV
178	DOCLTER1,2	-	Maint. labour for wing TE rest approach 1 & 2	£/flt	-	DV
179	DOCLTP1,2	-	Maintenance labour for tail plane approach 1 & 2	£/flt	-	DV
180	DOCLUC1,2	-	Maint. labour for landing gear approach 1 & 2	£/flt	-	DV
181	DOCLWBX1,2	-	Maintenance labour for wing box approach 1 & 2	£/flt	-	DV
182	DOCLWLE1,2	-	Maintenance labour for wing LE approach 1 & 2	£/flt	-	DV
183	DOCLWTF1,2	-	Maint. labour for wing TE flap approach 1 & 2	£/flt	-	DV
184	DOCM	DOC_m	Maintenance cost part of DOC	£/flt	-	OF
185	DOCMAPU1,2	-	Maintenance material for APU approach 1 & 2	£/flt	-	DV
186	DOCMEL1,2	-	Maint. material for electronics approach 1 & 2	£/flt	-	DV
187	DOCMELS1,2	-	Maint. material for electrical system approach 1& 2	£/flt	-	DV
188	DOCMFIN1,2	-	Maintenance material for fin approach 1 & 2	£/flt	-	DV
189	DOCMFS1,2	-	Maint. material for fuel system approach 1&2	£/flt	-	DV
190	DOCMFUR1,2	-	Maintenance material for furnishing approach 1&2	£/flt	-	DV
191	DOCMFUS1,2	-	Maintenance material for fuselage approach 1 & 2	£/flt	-	DV
192	DOCMHYD1,2	-	Maint. material for hydraulic system approach 1&2 -	£/flt	-	DV
193	DOCMIAE1,2	-	Maint. material for Instrument, Avionics and Electronics approach 1 & 2	£/flt	-	DV
194	DOCMMM1,2	-	Maint. material for Miscellaneous items such as oxygen, ballast etc. approach 1 & 2	£/flt	-	DV
195	DOCMTER1,2	-	Maint. material for wing TE rest approach 1 & 2	£/flt	-	DV
196	DOCMTP1,2	-	Maintenance material for tail plane approach 1 & 2	£/flt	-	DV
197	DOCMUC1,2	-	Maint. material for landing gear approach 1 & 2	£/flt	-	DV
198	DOCMWBX1,2	-	Maintenance material for wing box approach 1 & 2	£/flt	-	DV
199	DOCMWLE1,2	-	Maintenance material for wing LE approach 1 & 2	£/flt	-	DV
200	DOCMWTF1,2	-	Maint. material for wing TE flap approach 1 & 2	£/flt	-	DV
201	DOCSCAFT	-	Standing charge for airframe	£/flt	-	DV
202	DRTDIV	$D_{rt\text{-}div}$	Coefficient for expression MRTDIV	-	-	DV
203	DTD	D_{TD}	Temperature fall in avionics in deck due to cooling	deg F	-	DV
204	DTO	-	Take-off distance	m	-	**
205	E	E	Index of empannage mass expression	-	1.2	*
206	E, or EC	ε_t	Twist angle	-	4	*
207	ECS	ECS	Environmental control unit	-	-	-
208	EFCS	-	Electronic Flight Control System	-	-	-
209	EFH	E_{fh}	Engine failed height requirement	m	-	**

210	EFH0,1,2,3	-	Coefficient in definition of JTEFH,1.3672,-1.3493,1.245,-0.4167			
211	EFHKWM	-	Allowance for windmilling, and spillage drag at single engine failure height	-	-	DV
212	EFHM	Efhm	Mach number for engine-failed height case	-	-	DV
213	EFTKWM	-	Allowance for windmilling, and spillage drag engine failed height case	-	-	DV
214	ELE	Ele	Ratio of wing chord ahead of spar to wing chord	-	-	IV
215	ELEC	E_{lec}	Parameter defining LE chord extension at AP	-	0.7	*
216	ELESE	E_{elese}	Chord extension of the wing LE at AP	-	-	DV
217	ENGIND	E_{ngind}	Exponent in definition of ENGPOS	-	0.40	*
218	ENGPOS	E_{engpos}	Distance of wing mounted engine's cg from wing leading edge	m	-	DV
219	ETA	Eta	Ratio of gross flap span to wing span	-	-	IV
220	ETA	η	Station number across the wing span	-	-	-
221	ETAFS	E_{tafs}	Ratio of spanwise extend of fuselage to wing span	-	-	DV
222	ETE	Ete	Ratio of wing chord to aft of the rear spar to wing chord	-	-	IV
223	ETEF	Etef	Effective flap chord ratio	-	-	DV
224	ETEFB	E_{tefb}	Unextended flap chord ratio	-	-	DV
225	ETEFET,A	$E_{tefeT,A}$	Rearward translation of wing TE at TO, and AP	-	-	DV
226	ETEFRT,A	$E_{etefrT,A}$	Extended flap chord ratio for approach and take-off	-	-	DV
227	ETEFT,A	-	ETEF at TO, & AP	-	-	DV
228	ETOPS	-	Extended range Twin OPerationS	-	-	-
229	EURT	-	Electronic Unit average Repair Time	days	-	-
230	EXCEL	-	A computer software for spreat sheet, and graphical work	-	-	-
231	FA1		The average allowable direct stress level assumed to be constant everywhere in MWBCOV2	N/m2	352E06	*
232	f_{amc}		?			
233	FATF	f_{atf}	A factor relating to military advance technology features	-	-	-
234	f_{atf}		Factor to represent the effect of advance tecchnology fighter	-	-	-
235	FB	F_b	Financial Burden	-	2	*
236	FBTAA,TO	Fβto,a	Flap deflection parameter affecting flap additional lift at AP, and TO	-		DV
237	FCAD	f_{cad}	Factor to represent the effect of CAD	-	0.8	*
238	FCER	F_{cer}	Ratio of ETEF to ETEFB when BTA is BTAMX	-	-	DV
239	FCW	-	Fixed Camber Wings	-	-	-
240	FD0,1	$F_{D1,0}$	Constants in definition of the fuselage diameter	-	1.14,.5	*
241	FD2	F_{D2}	Extra constant in definition of the fuselage diameter, only used for UHCA	m	-	*
242	FDIF	f_{diff}	A factor relating to advance technology feature	-	-	-
243	FDIFD	$[(f_{diff})_{VCW}]_{design}$	Extra developement cost factor, design of VCW	-	-	DV
244	FDIFFT	$[(f_{diff})_{VCW}]_{flight}$	Extra developement cost factor, flight testing of VCW aircraft prototype	-	-	DV
245	FDIFM	f_{difm}	A factor relating to extra maintenance cost due to introduction of new technology	-	-	-
246	FDIFMA	$[(f_{diff})_{VCW}]_{manufacturing}$	Extra developement cost factor, manufacturing of VCW aircraft prototype	-	-	DV
247	FDIFML	f_{difml}	Factors relating to extra MH due to introduction of new technology	-	-	-

248	FDIFMLFC	$f_{difmlFC}$	The value of f_{difml} for flight control system	-	-	-
249	FDIFMLHYD	$f_{difmlHYD}$	The value of f_{difml} for hydraulic system	-	-	-
250	FDIFMLVC	$f_{difmlVC}$	The value of f_{difml} for VCD	-	-	-
251	FDIFMM	f_{difmm}	Factors relating to extra maintenance material due to introduction of new technology	-	-	-
252	FDIFMMFC	$f_{difmmFC}$	The value of f_{difmm} for flight control system	-	-	-
253	FDIFMMHYD	$f_{difmmHYD}$	The value of f_{difmm} for hydraulic system	-	-	-
254	FDIFMMVC	$f_{difmmVC}$	The value of f_{difmm} for VCD	-	-	-
255	FDIFMT	$(f_{material})_{VCW}$	Extra developement cost factor, material of VCW aircraft prototype	-	-	DV
256	FDIFT	$[(f_{diff})vcw]_{support}$	Extra developement cost factor, support and testing of VCW	-	-	DV
257	FDIFTL	$[(f_{diff})_{VCW}]_{tooling}$	Extra developement cost factor, tooling of VCW aircraft prototype	-	-	DV
258	FETFRT,.A	$F_{etfrT,A}$	Coefficients in the definition of trimmed maximum lift coefficient	-	-	DV
259	FF	ff	power index in Pekham's formula for MFUS	-	1.56	*
260	FF1	F_{f1}	Fuel fraction fo start	-	0.99	*
261	FF2	F_{f2}	Fuel fraction for Taxi	-	0.99	*
262	FF3	F_{f3}	Fuel fraction for take-off	-	0.995	*
263	FF4	F_{f4}	Fuel fraction for climb	-	0.98	*
264	FF5	F_{f5}	Cruise fuel fraction for cruise	-	-	DV
265	FF6	F_{f6}	Fuel fraction during hold	-	-	DV
266	FF7	F_{f7}	Fuel fraction for descent	-	0.99	*
267	FF8	F_{f8}	Fuel fraction for land	-	0.992	*
268	FF9	F_{f9}	Fuel fraction fo diversion	-	-	DV
269	FFM	F_{fm}	Mission fuel fraction	-	-	DV
270	FH	FH	Flying hours	hrs	-	DV
271	FINAC	F_{inac}	Distance of ac of fin from nose of fuselage / FUSL	-	0.94	*
272	FL1,2,3	$F_{L3,2,1}$		-		*
273	FLPC	F_{lpc}	Flap complexity coefficient	-	1.15	*
274	FLT	flt	Flight	-	-	-
275	FMS	FMS	Flight management system	-	-	-
276	FPANGL	-	Flight path angle on approach	deg	3	*
277	FPNGLR	F_{pnglr}	Flight path angle in radians	rad	0.0523	*
278	FPR	-	Fan Pressure Ratio	-	-	-
279	FR1,2,3	$F_{r1,2,3}$	Coefficients in the definition of trimmed C_{lmax} , 0.4083,5.391,-10.39	-	<	*
280	FRF	-	Failure rate factor	-	-	-
281	FRF	F_{RF}	Failure rate factor	-	-	-
282	FRFC	F_{RFc}	Failure rate factor change in avionics compartment	-	-	DV
283	FRFD	F_{RFD}	Failure rate factor change in avionics compartment	-	-	DV
284	$f_{security}$	-	Factor to reperesent the effect of secret project	-	-	-
285	FSWPB,S,F	$F_{swpB,S,F}$	Functions of SWP in evaluation of the effects of sweep in C_{Lmax} Module	-	-	DV
286	FTRETA	F_{TRETA}	Planform parameter for flap geometry	-	-	DV
287	FUR1,2,3,4	$F_{UR1,2,3,4}$	Coefficients in definition of MFUR, 16.75, 24.1, 50.0, 18.0, 86.2	-	<	*
288	FUSD	F_{USD}	Fuselage outside diameter	m	-	DV
289	FUSL	F_{USL}	Total length of fuselage	m	-	DV
290	G	g	Acceleration due to gravity	m/s2	9.81	*
291	GAF	G_{AF}	Gust alleviation factor	-	-	DV
292	GAL	G_{AL}	Number of gallies	-	-	DV
293	GAMMA	-	Value of GAMMA2 at other number of engines	-	-	DV
294	GAMMA2	-	Climb-out gradient requirement on TO for twin	rad	0.024	*

295	GATEP	-	A Computer Program to Design Propeller Driven Aircraft	-	-	-
296	GD	GD	General Dynamics	-	-	-
297	GENG	G_{eng}	Coefficient in definition of ENGPOS	-	0.015	*
298	GMAEFH	G_{maefh}	Climb gradient requirement for engine failed height condition	rad	0.01	*
299	GMC	GMC	Geometric mean chord : $(S_g / AR)^{0.5}$	m	-	DV
300	GSCLOM	G_{sclom}	Planform factor in definition of trimmed and untrimmed maximum lift coefficient	-	-	DV
301	H	H	Aircraft height	m	-	DV
302	h	h	Section camber -typical value for h/c	1.2	-	*
303	HC	H_C	Cabin height	m	-	DV
304	HMLDG	H_{MLDG}	Highest permissible landing mass	-	-	DV
305	HMLDGF	H_{mldgf}	Maximum landing mass factor	-	0.05	*
306	HOC	-	-			
307	HOLD	Hold	Duration of hold	h	-	**
308	HP	HP	High pressure compressor		-	-
309	HPAYF	H_{payf}	Factor defining maximum permissible payload	-	1.47	*
310	HPAYF	H_{payf}	Factor defining maximum permissible pay load	-	1.47	*
311	hr	-	Hour	-	-	-
312	HTMCR	H_{tmcr}	Altitude at cruise	m	-	**
313	HTMDIV	H_{tmdiv}	Altitude for diversion	km	-	DV
314	HTMTO	H_{tmto}	Hieght for TO	m	0.0	*
315	IP	IP	Intermediate compressor	-	-	-
316	IV	-	Independent Variable	-	-	-
317	IW1	$(i_W)_{VCW}$	Wing root setting angle without twist angle	rad	-	DV
318	IW2	$(i_W)_{FCW}$	Wing root setting angle with twist	rad	-	DV
319	IY	I_y	Yawing moment of inertia	lb-ft2	-	DV
320	JBXCOV	J_{BXcov}	Coefficient in the expression of wing box mass, cover	-	3.7E-07	*
321	JBXJNT	J_{BXjnt}	Coefficient in the expression of wing box mass, joint	-	95.6 E-08	*
322	JBXPP	J_{BXpp}	Coefficient in the expression of wing box mass, powerplant supports	-	0.02	*
323	JBXRB	$J_{BXrib1,2,3,4,5}$	Coefficients in the expression of wing box mass ribs, 15.4, 88.1, 4.08E-05, 2.76E-06, 3.6E-06	-	<	*
324	JBXSP1,2,3	$J_{BXsp1,2,3}$	Coefficient in the expression of wing box mass, spar. 14.7, 5.2E-06 , 2.37E-06	-	<	*
325	JBXUC	J_{BXuc}	Coefficients in the expression of wing box mass undercrriage attachments	-	0.585E -03	*
326	JFLP	J_{FLP}	Mass density of flap system	kg/m 2	-	DV
327	JFLP0	J_{FLP0}	Coefficient in expression for JFLP	-	0.005	*
328	JFUS	J_{fus}	Coefficient in the Expression of MFUS	-		*
329	JFUS1,2	$J_{fus1,2}$	Coefficient in definition of Pekham's MFUS formula	-	0.494, 1.0	*
330	JLE	J_{le}	Wing LE mass density	kg/m 2	-	DV
331	JSYS1,2,3,4, 5,6	$J_{sys1,2,3,4,5,6}$	Coefficient in expression for MSYS405, 0.176, 0.0105, 76, 47, 19	-		*
332	JT	-	Specific mass of installed engines	-	-	DV
333	JTCR	J_{tcr}	Value of JT at cruise condition	-	-	DV
334	JTCRD	-	Value of JTCR for datum cruise condition	-	-	DV
335	JTCRD0	-	Value of JTCRD when Rating=1, varies for different engines	-	-	**

336	JTEFD0		Specific mass of engines at datum Mach number engine failed height case	-	-	**
337	JTEFD0	-	Mass thrust ratio of installed engines at datum Mach number at single engine failure height	kg/N	-	**
338	JTEFH	-	Engine mass thrust ratio at single engine failure height	kg/N		
339	JTSTA0	J_{tsta0}	Re rated specific mass of installed engines for static conditions at Rating=1	-	-	DV
340	JTSTAT	J_{tstat}				
341	JTT0A	-	Mass thrust ratio at approach	-	-	DV
342	JTT0D,G	J_{TTOD}	Specific installed mass of engines at take-off run, and climb	-	-	DV
343	JUC	J_{UC}	Coefficient in expression of undercrriage mass	-	-	DV
344	JVCD	J_{VCD}	Specific mass of VCD	-	-	DV
345	K		The mission file numbering, e.g. 1 corresponds to Fokker F100	-	-	**
346	KCR	K_{cr}	Induced drag factor (Lift dependent drag coefficient)	-	-	DV
347	KCR1,2,3	$K_{cr1,2,3}$	Coefficient in expression KCR	-	-	DV
348	KDOOR	-	Wie factor for cargo door	-	1.0	*
349	KENG	K_{eng}	Distance of CG of rear mounted engine from the nose of fuselage / FUSL	-	0.80	*
350	KFA0	K_{fa0}	Fuel allowance for taxing as fraction of MTO	-	0.004	*
351	KFA1	K_{fa1}	Fuel allowance at take-off and initial climb as fraction of MTO	-	0.006	*
352	KFA1	K_{fa1}	Fuel allowance for take-off and initial climb as fraction of MTO	-	0.006	*
353	KFA2	K_{fa2}	Fuel allowance for landing as fraction of MLDG,or MSSY	-	0.006	*
354	KFCL	K_{fcl}	Coefficient for contingency fuel	-	0.001	*
355	KFIN	K_{fin}	Distance of CG of fin from the nose of fuselage / FUSL	-	0.94	*
356	KFINA	K_{fina}	Distance of ac of fin from a/c cg / FUSL	-	-	DV
357	KFSP	K_{fsp}	Fuel density aviation gasoline, lb/US gallon		5.87	*
358	KFUSC	K_{fusc}	Distance of CG of fuselage group from the nose of fuselage / FUSL	-	0.45	*
359	KFUSW	K_{fusw}	Coefficient in definition of MFUS	-	0.0125	*
360	KNAC	K_{nac}	Coefficient in expression SNAC	-	.00021	*
361	KPAY	K_{pay}	Fuel tankage coefficient	0.0	-	*
362	KPEL	K_{pel}	Cost coefficient for electronics	£/kg	2700	*
363	KPENG	K_{peng}	Cost coefficient for engine	£/kg	46444	*
364	KPFUR	K_{pfur}	Cost coefficient for furnishing	£/kg	972	*
365	KPFUS	K_{pfus}	Cost coefficient for fuselage	£/kg	411	*
366	KPPEN	K_{ppen}	Cost coefficient for empennage	£/kg	411	*
367	KPSYS	K_{psys}	Cost coefficient for systems	£/kg	1188	*
368	KPWBX	K_{pwbx}	Cost coefficient for wing box	£/kg	476	*
369	KPWLE	K_{pwle}	Cost coefficient for wing LE	£/kg	810	*
370	KPWTE	K_{pwte}	Cost coefficient for wing TE	£/kg	810	*
371	KSFEMP	$K_{sf\text{-}emp}$	Drag coefficient based on wetted area empennage	-	0.0033	*
372	KSFFUS	$K_{sf\text{-}fus}$	Drag coefficient based on wetted area fuselage	-	0.002	*
373	KSFNAC	$K_{sf\text{-}nac}$	Drag coefficient based on wetted area nacelles	-	.00346	*
374	KT0D	-	A constant in the expression for MENG1	-	1.0	*
375	KTA	K_{ta}	Distance of CG of ampennage from nose of fuslage/FUSL	-	0.45	*
376	KTCS	K_{tcs}	Coefficient in expression of TCS	-	0.90	*

377	KTP	K_{tp}	Distance of CG of tail plane from the nose of fuselage / FUSL	-	0.96	*
378	KUC	-	Weight factor for undercarriage in MFUS3	-	1.0	*
379	KWS	-	A coefficient in the expression of MFUS3	-	-	DV
380	L		see ACLIFE	-	-	-
381	LDIV	L_{div}	Lost range in diversion	km	-	DV
382	LDRCR	$(L/D)_{cruise}$	Lift drag ratio at cruise for class 1 MTO	-	18	*
383	LDRCR1,2, 3,4,5	-	Lift drag ratio at start of every cruise segment	-	-	DV
384	LDRCRB	-	CLCRB/CDCRB	-	-	DV
385	LDRDIV	(L/D)div	Lift drag ratio at diversion for class 1 MTO	-	18	*
386	LDRHOLD	$(L/D)_{hold}$	Lift drag ratio at hold for class 1 MTO	-	10	*
387	LE	-	Leading Edge	-	-	-
388	LMF	L_{mf}	Landing mass factor	-	-	DV
389	LP	LP	Low pressure compressor	-	-	-
390	LRGE		Lost range in design cruise	km	-	DV
391	LRU	LRU	Line replacable unit	-	-	-
392	LTIME	L_{time}	It is conceptually equivalent to lost range, equal to time taken to climb, and descent	hr	-	DV
393	m	-	Average number of avionics units being repaired per day	-	-	-
394	M2D	M_{2D}	Two dimensional drag divergence Mach number	-	-	DV
395	MAF	M_{AF}	Mass of airframe	kg	-	DV
396	MAPI	M_{API}	Mass of airconditioning, pressurisation, and ice protection	kg	-	DV
397	MAPI3	-	see MCAU			
398	MAPU	M_{APU}	Mass of auxiliary power unit	kg	-	DV
399	MAUX	M_{AUX}	Mass of	kg	-	DV
400	MB	M_b	Mass bled from engines	lb/min/kW	-	**
401	MBB	-	Messerschmitt-Bolkow-Blohm, presently Daimler Benz Aerospace Airbus	-	-	-
402	MBC	M_{BC}	Mass of	kg	-	DV
403	MBPKAC	M_{bpkac}	Pounds of mass bled from engine per minute per KW of avionics compartment power consumption	lb/min/kW	-	DV
404	MBPKAD	M_{bpkad}	Pounds of mass bled from engine per minute per KW of avionics deck power consumption	lb/min/kW	-	DV
405	MBS	M_{bsi}	Mass bled from engines lb/sec/kW	lb/s/kW	-	DV
406	MC	MC	Symbolic maintenance time merit for removal and replacement by application of MIL-HDBK-472	min	-	DV
407	MCAU	M_{cau}	Mass of cold air unit	kg	-	DV
408	MCFUS, WBX, WLE	$MC_{FUS, WBX, WLE}$	Symbolic maintenance time merit for removal and replacement of fuselage, wing box, wing LE by application of MIL-HDBK-472	min	-	DV
409	MCR	M_{cr}	Mach number at cruise	-	-	**
410	MCREW	M_{crew}	Mass of Crew	kg	-	DV
411	MCRIT0	M_{crit0}	Mach critical drag at zero lift	-	-	DV
412	MCU	MCU	Modular concept unit	-	-	-
413	MCVT,WTEF,HT,WTER	$MC_{VT,WTE,HT,WTER}$	Symbolic maintenance time merit for removal and replacement of vertical tail, wing TE flap, TE rest, Horizontal tail by application of MIL-HDBK-472	min	-	DV
414	MDES	M_{des}				
415	ME	M_e	Empty mass	kg	-	DV
416	ME	M_E	Empty mass	kg	-	DV
417	M_{ecs}		Mass of ECS	kg	-	DV

418	MECS	m_{ecs}	Output flow rate of ECS	kg/min	-	DV
419	M_{ECS}	MAPI2	Mass of ECS system	kg	-	DV
420	MEFF	M_{EFF}	Effective mass of the wing for stressing case	kg	-	DV
421	MEFH	-	Mach number at single engine failure height			
422	MELS	M_{ELS}	Mass of electric system	kg	-	DV
423	MEMP	M_{EMP}	Mass of empennage	kg	-	DV
424	MENG	Meng	Mass of installed engine	kg	-	IV
425	MENG1,2,3, 4,5	Meng1, to 5	Mass of installed engines appropriate for, take-off run; climb-out one engine cut, cruise, engine failed height, miss approach	kg	-	DV
426	MFC1	M_{FC}	Mass of flight control system, from Raymer	kg	-	DV
427	MFC2	M_{FC}	Mass of flight control system, from Roskam	kg	-	DV
428	MFIN	M_{FIN}	Mass of fin	kg	-	DV
429	MFLAL	-	Mass fuel allowance	kg	-	DV
430	MFRES	M_{fres}	Mass of fuel for reserve	kg	-	DV
431	MFRT	M_{FRT}	Mass of freight	kg	-	DV
432	MFS	M_{FS}	Mass of fuel system	kg	-	DV
433	MFUEL	M_{fuel}	Mass of fuel load for the design mission	kg	-	DV
434	MFUELC	M_{fuelc}	Mass of fuel for cruise phase	kg	-	DV
435	MFUELC1,2 ,3,4,5	-	Mass of fuel consumed in every cruise sector	kg	-	DV
436	MFUELC6	-	Sum of MFUELC1,2,3,4,5	kg	-	DV
437	MFUELC7	-	Mass of fuel for cruise without segmenting the cruise phase	kg	-	DV
438	MFUELD	-	Mass of fuel diversion	kg	-	DV
439	MFUELH	-	Mass of fuel hold	kg	-	DV
440	MFUELU	M_{fuelu}	Mass of fuel used in a typical fuel mission	kg	-	DV
441	MFUR	M_{FUR}	Mass of furnishing	-	-	DV
442	MFUS	M_{FUS}	Mass of the fuselage	kg	-	DV
443	MFUS1,2,3	-	Mass of fuselage using, Collingbourn, Pekham, Raymour references	kg	-	DV
444	MFUSC	M_{FUSC}	Mass of fuselage group	kg	-	DV
445	MFUSED	M_{fused}	Mass of fuel consumed during mission, a term in class 1 Roskam take-off mass estimate	kg	-	DV
446	MG	M_G	Mach number for critical gust loading case	-	-	DV
447	MH	MH	Maintenance manhours	-	-	-
448	MHPF	-	Total MH per flight	hr	-	DV
449	MHPFH		Total MH per FH	hr	-	DV
450	MHPFHR		Total MH per FH excluding APU	hr	-	DV
451	MHYD1	M_{HYD}	Mass of hydraulic system from Raymer	kg	-	DV
452	MHYD2	M_{HYD}	Mass of hydraulic system, from Roskam	kg	-	DV
453	MIAE	M_{IAE}	Mass of aircraft instrumentation, avionics, electronics	kg	-	DV
454	MIENG	M_{IENG}	Mass of inboard engines	kg	-	DV
455	MLDG	M_{LDG}	Mass of aircraft at start of diversion	kg	-	DV
456	MLE	M_{LE}	Mass of wing LE	kg	-	DV
457	MMO	-	Maximum allowable Mach number	-	-	DV
458	MOENG	M_{OENG}	Mass of outboard engines	kg	-	DV
459	MOX	M_{OX}	Mass of oxygen system	kg	-	DV
460	MPAX	M_{PAX}	Mass of passenegers	kg	-	DV
461	MPAY	M_{pl}	Mass of payload, design mission	kg	-	DV
462	MPF	-	Reduction factor due to absence of pipes	-	.2 to .3	*
463	MPFAF		Airframe maintenance manhours per flight	hr	-	DV
464	MPFAFR		Airframe maintenance manhours per flight excluding APU	hr	-	DV

465	MPFENG	M_{pfeng}	Engine maintenance manhours per flight	hr	-	DV
466	MPFFIN	M_{pfFIN}	MH per flight fin	h	-	DV
467	MPFFUS	M_{pfFUS}	MH per flight fuselage	h	-	DV
468	MPFHAF		Airframe MH per block hour of flight	hr	-	DV
469	MPFHAFR		Airframe MH per block hour of flight excluding APU	hr	-	DV
470	MPFHENG	-	Engine MH per block hour of flight	hr	-	DV
471	MPFTP	M_{pfTP}	MH per flight tail plane	h	-	DV
472	MPFWBX	M_{pfWBX}	MH per flight wing box	h	-	DV
473	MPFWLE	M_{pfWLE}	MH per flight wing LE	h	-	DV
474	MPFWTEF	M_{pfWTEF}	MH per flight wing TE flap	h	-	DV
475	MPFWTER	M_{pfWTER}	MH per flight wing TE rest	h	-	DV
476	MPH	-	Total MH per 1000 FH	hr	-	DV
477	MPHAIR	-	MH per 1000 FH for airconditioning system	hr	-	DV
478	MPHAIR	M_{phAIR}	MH per 1000 FH, airconditioning system	hrs	-	DV
479	MPHAPI	-	MH per 1000 FH for airconditioning, pressurisation, ice protection system	hr	-	DV
480	MPHAV	-	MH per 1000 FH for avionics	hr	-	DV
481	MPHAV	M_{phAV}	MH per 1000 FH, avionics system	hrs	-	DV
482	MPHELS	-	MH per 1000 FH for electrical system	hr	-	DV
483	MPHELS	M_{phELS}	MH per 1000 FH, electrical system	hrs	-	DV
484	MPHFC	-	MH per 1000 FH for flight control system	hr	-	DV
485	MPHFC	M_{phFC}	MH per 1000 FH, flight control system	hrs	-	DV
486	MPHFIR	-	MH per 1000 FH for fire system	hr	-	DV
487	MPHFIR	M_{phFIR}	MH per 1000 FH, fire system	hrs	-	DV
488	MPHFS	-	MH per 1000 FH for fuel system	hr	-	DV
489	MPHFS	M_{phFS}	MH per 1000 FH, fuel system	hrs	-	DV
490	MPHFUR	-	MH per 1000 FH for furnishing	hr	-	DV
491	MPHFUR	M_{phFUR}	MH per 1000 FH, Furnishing	hrs	-	DV
492	MPHHYD	-	MH per 1000 FH for hydraulic system	hr	-	DV
493	MPHICE	-	MH per 1000 FH for ice protection system	hr	-	DV
494	MPHICE	M_{phice}	MH per 1000 FH, ice protection system	hrs	-	DV
495	MPHLI	-	MH per 1000 FH for light system	hr	-	DV
496	MPHLI	M_{phLI}	MH per 1000 FH, light system	hrs	-	DV
497	MPHOX	-	MH per 1000 FH for oxygen system	hr	-	DV
498	MPHOX	M_{phOX}	MH per 1000 FH, oxygen system	hrs	-	DV
499	MPHPEN	M_{phPEN}	MH per 1000 FH, pneumatic system	hrs	-	DV
500	MPHPRE	-	MH per 1000 FH for pressurisation system	hr	-	DV
501	MPHSTR	-	MH per 1000 FH for structure system	hr	-	DV
502	MPHSTR	M_{phSTR}	MH per 1000 FH, structure	hrs	-	DV
503	MPHUC	-	MH per 1000 FH for undercrriage system	hr	-	DV
504	MPHUC	M_{phUC}	MH per 1000 FH, undercarriage system	hrs	-	DV
505	MPHWW	-	MH per 1000 FH for water waste system	hr	-	DV
506	MPHWW	M_{phWW}	MH per 1000 FH, water waste system	hrs	-	DV
507	MPT	M_{PT}	Mass of the a/c external paint	kg	-	DV
508	MRAT1,2,3, 4,5	-	Mass ratio over equivalent design cruise segment1, 2,3 ,4 , 5, no contigency allowance	kg	-	DV
509	MRENG	M_{RENG}	Mass of all engines	kg	-	DV
510	MRTDIV	M_{RTdiv}	Fuel fraction for diversion	-	-	DV
511	MSSB	M_{SSB}	Mass of aircraft at start of cruise climb	kg	-	DV
512	MSSB1,2,3, 4,5	-	Mass of the aircraft at the start of every cruise sector	kg	-	DV
513	MSSBB	-	Mass of aircraft at the start of cruise for MTO initialisation	kg	-	DV
514	MSSCR	M_{SSCR}	Mass of aircraft at the end of cruise climb	kg	-	DV

515	MSSEC	-	Mass of aircraft at the end of descent no contigency fuel allowance	kg	-	DV
516	MSSY	M_{SSY}	Mass of aircraft at start of approach after diversion & hold	kg	-	DV
517	MSTR	-	Mass of structure	kg	-	DV
518	MSYS	M_{SYS}	Mass of aircraft total system	kg	-	DV
519	MTBF	MTBF	Mean time between failure	-	-	-
520	MTBMF	-	Mean time between maintenance failure rate	-	-	-
521	MTBUR	-	Mean time between unscheduled removal	-	-	-
522	MTFO	M_{tfo}	?	kg	-	DV
523	MTO	M_{to}	Take-off Mass	kg	-	DV
524	MTP	M_{TP}	Mass of tail plane	kg	-	DV
525	MU	M_U	Aircraft mass ratio for critical gust case	-	-	DV
526	MUAV	M_{uav}	Mass of un-installed avionics system	kg	-	DV
527	MUC	M_{UC}	Mass of undercarriage	kg	-	DV
528	MVO	-	Multi-Variate Optimisation in Conceptual Design of Aircraft	-	-	-
529	MWBCOV1	M_{WBcov}	Mass of wing box cover, Collingbourn's relation	kg	-	DV
530	MWBCOV2	M_{WBcov}	Mass of wing box cover, Howe's relation	kg	-	DV
531	MWBJNT	M_{WBjnt}	Mass of wing box joint	kg	-	DV
532	MWBRB	M_{WBrib}	Mass of wing box ribs	kg	-	DV
533	MWBSP	M_{WBsp}	Mass of wing box spar	kg	-	DV
534	MWBTIP	M_{WBtip}	Mass of wing box tip	kg	-	DV
535	MWBUC	M_{WBuc}	Mass of wing box undercarriage fittings	kg	-	DV
536	MWBX	M_{WBX}	Mass of wing box	kg	-	DV
537	MWINGC	M_{WINGC}	Mass of wing group	kg	-	DV
538	MWTE	M_{WTE}	Mass of wing trailing edge	kg	-	DV
539	MWTEF	M_{WTEF}	Mass of wing TE flap	kg	-	DV
540	MWTER	M_{WTER}	Mass of wing TE rest	kg	-	DV
541	N	-	Fleet size	-	-	-
542	NBAR	N	Effective design ultimate acceleration factor			
543	ND	N_{rdte}	Number of aircraft produced for RDT&E	-	2	*
544	NE	N_e	Number of wing mounted engines	-		**
545	NEIW	N_{eiw}	Number of inboard wing mounted engines	-		**
546	NEOW	N_{eow}	Number of outboard wing mounted engines	-		**
547	NF	N_f	Number of functions performed by controls (4 to 7)	-	7	*
548	NM	N_m	Number of mechnical functions (typically 0-2)	-	1	*
549	NN	N	Aircraft normal load factor	-	-	DV
550	NN	N	Effective design ultimate acceleration factor	-	-	DV
551	NP	N_p	Number of people onboard, crew, deck, passenger	-	-	DV
552	NT	N_t	Number of separate fuel tanks	-	-	DV
553	NUCR	μcr	Kinematic viscosity of air for cruise conditions	m2/s	-	DV
554	NWAF	N_{waf}	Net wing area factor	-	-	DV
555	PAB	P_{AB}	Number of seats abreast the cabin	-	-	**
556	PAC	P_{AC}	Price of aircraft	£	-	DV
557	PAF	P_{af}	Price of airframe	£	-	DV
558	PAPI	-	price of pressurisation, airconditioning, and ice protection			
559	PAPU	-	Price auxiliary power unit			
560	PAV	P_{av}	Typical price of avionics system	-	-	-
561	PAX	P_{AX}	Number of passengers, design mission	-		**
562	PAX	pax	number of passengers	-	-	-
563	PAX1	P_{AXmax}	Maximum number of passenger for a fuselage length	-	-	**

564	PAXCBR	P_{AXCBR}	Ratio of passenegrs to number of cabin crew	-	50	*
565	PCH	P_{CH}	Seat pitch	m	0.815	*
566	PCL	P_{CL}	Length of the pressurised cabin	m	-	DV
567	PEL	P_{el}	Price of electronics (avionics)	£	-	DV
568	PELS	-	Price of electrical system			
569	PENG	P_{eng}	Price of engine	£	-	DV
570	PFC	-	Price of flight control system			
571	PFIN	-	Price fin			
572	PFS	-	Price of fuel system			
573	PFUEL	P_{fuel}	Price of fuel per kg	£/kg	0.19	*
574	PFUR	P_{fur}	Price of furnishing	£	-	DV
575	PFUS	P_{fus}	Price of fuselage	£	-	DV
576	PHYD	-	Price of hydraulic system			
577	PIAE	-	Price of instrument, electronics, and avionics	£	-	Dv
578	PIREPS	PIREPS	Pilot reports	-	-	-
579	PMM	-	Price of miscellaneous items			
580	POFT	P_{net}	Power consumption of ACAU equivalent of off take	Watt	-	DV
581	PPEN	-	Price of empennage			
582	PPEN	P_{pen}	Price of emmpennage	£	-	DV
583	PRSDIF	P_{rsdif}	Cabin differential pressure	kPa	57.0	*
584	PSYS	P_{sys}	Price of system	£	-	DV
585	PTP	-	Price tail plane			
586	PTR	P_{TR}	Number of passengers per toilet	-	50	*
587	PUC	P_{uc}	Price of undercarriage	£	-	DV
588	PWBX	P_{wbx}	Price of wing box	£	-	DV
589	PWLE	P_{wle}	Price of wing LE	£	-	DV
590	PWTE	P_{wte}	Price of wing TE	£	-	DV
591	Q	-	Spares inventory, as fraction of item price	-	-	-
592	QCR	-	Dynamic pressure, design cruise	Pa	-	DV
593	QEFH	-	Dynamic pressure single engine failure height	Pa	-	DV
594	R	r	Wing relief effect due to inertia	-	-	DV
595	R	-	see RESVAL	-	-	-
596	R&M	-	Reliability and Maintainability	-	-	-
597	R&ME	R&ME	Reliability and maintainability enhancement measure	-	-	-
598	R1	N_r	Rate of production of prototype aircraft per month	-	0.33	*
599	RAE	-	Royal Aeronautical Establishment	-	-	-
600	RATING	R_{ating}	Factor on datum static thrust and cruise thrust	-	-	DV
601	RDCR	R_{dcr}	Relative density of air at cruise	-	-	DV
602	RDDIV	R_{ddiv}	Relative density at diversion	-	-	DV
603	RDIV	R_{div}	Equivalent range, diversion	km	-	DV
604	RDT&E	-	Rsearch, Developemnt, Testing, and Evaluation	-	-	-
605	RE	RE	Reliability enhancement	-	-	-
606	RE1	$\Re_{er}$	Design engineer salary rate	$/hr	64	*
607	REM	REM	Reliability enhancement measure	-	-	-
608	RESVAL	R_{esval}	Residual value factor	-	0.1	*
609	RGE	Range	Equivalent range for design mission	km	-	DV
610	RHS	-	Right hand side	-	-	-
611	RL1	R_L	Laboure rate	£/hr	27.3	*
612	RL2	$\Re_{mr}$	Labour salary rated	$/hr	35	
613	RMCS	-	Royal Military College, Shrivenham UK	-	-	-
614	RN	RN	Cruise Raynold's number	-	-	DV
615	ROA	ρa	Value of air density at approach	m3/kg	-	DV

616	ROBOX	ρbox	Mass density of the wing skin	kg/m3	2550	*
617	ROCR	ρcr	Value of air density at cruise altitude	m3/kg	-	DV
618	RODIV	ρdiv	Value of air density at diversion altitude	m3/kg	-	DV
619	ROEFH	ρefh	Density at single engine failure height	kg/m3	-	DV
620	ROTO	ρto	Value of air density at take-off altitude	m3/kg	-	DV
621	R_R	-	Removal rate	-	-	-
622	RT1	$\Re_{tr}$	Tooling engineer salary rate	$/hr	45	
623	S/L	s/l	Sea level	-	-	-
624	SB1,2,3	$S_{b1,2,3}$	Coefficients in expression of sweep effect in C_{Lmax}, 1.023,-0.00254, -0.000187	-	<	*
625	SC1,2,2	$S_{c1,2,3}$	Coefficient in standing charge	-	-	DV
626	SCPAF	S_{cpAF}	Value of spares holding for airframe as fraction of airframe price	-	0.06	*
627	SCPAV	S_{cpAV}	Value of spares holding for avionics as function of airframe spares holding	-		DV
628	SCPENG	S_{cpENG}	Value of spares holding for engine as fraction of engine price	-	0.3	*
629	SCPFC	S_{cpFC}	Value of spares holding for flight control system as function of airframe spares holding	-		DV
630	SCPM	S_{cpM}	Value of spares holding for miscellaneous sections as function of airframe spares holding	-		DV
631	SCPPAS	S_{cpAF}	Value of spares holding for passenger section as function of airframe spares holding	-		DV
632	SCPPOW	S_{cpPOW}	Value of spares holding for power section as function of airframe spares holding	-		DV
633	SCPSTR	S_{cpSTR}	Value of spares holding for structure section as function of airframe spares holding	-		DV
634	SCPUC	S_{cpUC}	Value of spares holding for undercarriage as function of airframe spares holding	-		DV
635	SCS	S_{CS}	Total area of control surfaces	m2	-	DV
636	SDC	S_{do}	Spillage drag constant	-	1.0E-06	*
637	SEMP	S_{EMP}	Surface area of empennage	m2	-	DV
638	SF1,2,3	$S_{f1,2,3}$	“, 1.0175, -0.00436, -0.000224	-	<	*
639	sfc_{cruise}	CFC	Engine specific fuel consumption for cruise (this value is fed into CACAD from an existing engine near to aircraft’s requirement)	1/h	-	DV
640	sfc_{div}	CFDIV	Engine specific fuel consumption for diversion	1/h	-	**
641	sfc_{hold}	CFH	Engine specific fuel consumption for hold	1/h	-	DV
642	SFNJT	S_{fnjt}	Specific mass of engines for critical engine failure condition	-	-	DV
643	SFNKWM	S_{fnkwm}	Value of KWM for engine-failed take-off	-	-	DV
644	SFTE	S_{FTE}	Surface area of flap system	m2	-	DV
645	SFUSW	S_{fusw}	External fuselage surface	m2	-	DV
646	S_g	X(4)	Wing gross area	m2	-	IV
647	SIGMAEF	-	Density ratio at single engine failure height	-	-	Dv
648	SLE	S_{LE}	Surface area of wing LE	m2	-	DV
649	SME	-	School of Mechanical Engineering	-	-	-
650	SNAC	S_{NAC}	Surface area of nacelles	m2	-	DV
651	SOFA, T		Rearward translation of flap TE at AP,and TO/ETEF	-	-	DV
652	SOFB	S_{ofb}	Fraction of unextended flap shielded by shroud	-	0.4	*
653	SPAN	Span	Aircraft span : $(AR \times S_g)^{0.5}$	m	-	DV
654	SPIENG	S_{pieng}	Distance of inboard wing mounted engines from a/c centre-line/(span/2)	-	0	*

655	SPOENG	S_{poeng}	Distance of outboard wing mounted engines from a/c centre-line/(span/2)	-	0.3	*
656	SRATT,A	$S_{ratT,A}$	Area ratio parameter for flaps, at TO and Approach	-	-	DV
657	SRTE	S_{RTE}	Surface area of aileron system	m2	-	DV
658	SS1,2,3	$S_{s1,2,3}$	“, 1.015, 0.0, -0.000238	-	<	*
659	SSDEFH	S_{sdefh}	Speed of sound at single engine failure height	m/s	-	DV
660	SSPDC	SV_{sound}	Speed of sound	m/s	-	DV
661	SSPDVM	-	Speed of sound at critical altitude HCR	m/s	-	DV
662	ST	-	Total aircraft surface area	m	-	DV
663	ST0DWT	S_{T0DWT}	Static thrust to weight ratio diversion	-	-	DV
664	STAGE	Stage	Stage length for design mission	km	-	**
665	SWBX	-	Surface area of wing box	m2	-	DV
666	SWPF	Λ_f	Average sweep back of flap structure	deg	-	DV
667	SWPH	$\Lambda_{1/2}$	Sweep of wing at half chord	deg	-	DV
668	t_r	-	Thickness ratio of wing root	-	-	IV
669	T01	T_{01}	Cabin total temperature entering ACAU	degK	308	*
670	TA	-	Thrust requirement at approach	N	-	DV
671	TBLOC	T_{BLOC}	Block time for mission	hr	-	DV
672	TBO	-	Time between overhaul	-	-	-
673	TC	t/c	Wing Thickness to Chord Ratio	-	-	IV
674	TC1	-	Ambient temperature at critical height	deg K	-	DV
675	TCLMD	-	Maximum C_L of basic wing and LE devices at TO	-	-	DV
676	TCMNC	-	Constraint on thichness and sweep angle	0.1	-	*
677	TCR	T_{cr}	Ambient temperature at cruise altitude	deg K	-	DV
678	TCS	T_{cs}	Critical take-off speed	m/s	-	DV
679	TDCLMSO	T_{DCLMSO}	Additional lift due to LE devices during TO	-	-	DV
680	TDIV	-	Ambient temperature at diversion altitude	deg K	-	DV
681	TE	-	Trailing Edge	-	-	-
682	TEFH	-	Thrust required at single engine failure height	N	-	DV
683	TELEC	T_{elec}	Parameter defining LE chord extension at TO	-	0.8	*
684	TELESE	T_{elese}	Chord extension of the wing LE at TO	-	-	DV
685	TET	TET	Turbine entry temprature	degK	-	-
686	TFLT	T_{flt}	Total flight duration	hr	-	DV
687	THETADI	-	Temperature ratio at diversion	-	-	DV
688	THETAEF	-	Temperature ratio at engine failure hieght	-	-	DV
689	TJAV	T_{jav}	Avionics average junction temperature	deg C	-	DV
690	TJMAX	T_{jmax}	Avionics maximum junction temperature	deg C	-	DV
691	TO	-	Take-off	-	-	-
692	TPAC	T_{pac}	Distance of ac of tail plane from nose of fuselage / FUSL	-	-	DV
693	TPR	-	Turbine pressure ratio of ACAU	-	1.5	*
694	TR	TR	Taper ratio	-	-	IV
695	TREQ	-	Thrust required at the start of cruise	N	-	DV
696	TSRATD	T_{sratd}	Area ratio parameter of datum wing and LE devices at TO	-	-	DV
697	TST	-	Thrust produced by each engine at standard s/l	lbf	-	IV
698	TSTAT	T_{STAT}	Static thrust of installed engines	N	-	DV
699	TT	TT	Number of toilets	-	-	DV
700	TTEFH	-	see TPEFH	-	-	-
701	U	-	Aircraft utilisation per year	hr	-	DV
702	UCLMA,TO	-	Untrimmed maximum lift coefficient at AP, TO	-	-	DV
703	UHCA	-	Ultra High Capacity Aircraft	-	-	-
704	VA	V_A	Approach speed	m/s	-	**
705	VC	-	Variable Camber	-	-	-

706	VCD	-	Variable Camber Device	-	-	-
707	VCR	V_{cruise}	Aircraft forward speed, cruise	km/h	-	DV
708	VCREAS	-	Equivalent airspeed at cruise codition	km/h	-	DV
709	VCW	-	Variable Camber Wing	-	-	-
710	VCW	-	Variable Camber Wings	-	-	-
711	VDIV	V_{div}	Aircraft forward speed, diversion	km/h	-	DV
712	VDIVES	-	Equivalent forward speed at diversion	-	-	DV
713	VEFH	-	Aircraft forward speed single engine failure height	m/s	-	DV
714	VFIN1	V_{fin1}	Fin volume in definition of SFIN	-	0.05	*
715	VFUEL	-	Total fuel volume permissible	m3	-	DV
716	VG	V_G	Aircraft forward speed (EAS) for critical gust condition	m/s	-	DV
717	VMC	-	Either of VA, or TCS whichever is the bigger	m/s	-	DV
718	VPAX	V_{pax}	Volume of passenger cabin	m3	-	DV
719	VRD	V_{RD}	Vertical rate of descent approach	m/s	-	DV
720	VSA	V_{sa}	Stall speed at approach	m/s	-	DV
721	VTA	-	Total fuel tank volume	m3	-	DV
722	VTL1,2	$V_{tl1,2}$	Inboard and outboard limits on fuel tank, 0 to +1, and 0 to -1 respectively		-	**
723	VTO	V_{TO}	Take-off speed	m/s	-	DV
724	VTP	V_{tp}	Tail plane Volume	-	-	DV
725	WAMPR	W_{ampr}	Aeronautical manufacturer's planning report	lb	-	DV
726	WB	W_B	Wheel base	m	-	DV
727	WBANGL	-	Wing setting relative to fuselage			
728	WDC	W_{dc}	Wnd milling drag constant	-	2.6E-06	*
729	WMF	W_{MF}	Empirical factor on effective loading on wing	-	-	DV
730	WT	W_T	Wheel track	m	-	DV
731	WUNENG	$W_{un\text{-}eng}$	Mass of one installed engine	kg	-	DV
732	X(1)	AR	Aspect Ratio	-	-	IV
733	X(3)	TR	Taper Ratio	-	-	IV
734	X(4)	S_g	Wing gross area	m2	-	IV
735	X(5)	$\Lambda_{1/4}$	Sweep Angle at Quarter Chord	deg	-	IV
736	YR	Y_r	The difference of year between 1959, and first flight	year		**
737	Z	Z	Factor allowing for wing taper, and location of root attachment	-	-	DV
738	ZAPX	-	It is an approximate term in Howe's MWBCOV expression for wing taper, and wing fuselage attachment	-	-	DV
739	ZFM	Z_{FM}	Zero fuel mass	kg	-	DV
740	ZFMMAX	Z_{FMmax}	Maximum zero fuel mass	kg	-	DV
741	ZM	Z_m	"	-	-	DV
742	ZM1	Z_{m1}	" for aircraft with aft fuselage mounted engines	-	-	DV

Appendix B

CACAD Formulation And Results

B1. Introduction

In this Appendix the detailed formulation of CACAD with a brief description for each formula is presented. The DOC, and its maintenance cost breakdown is dealt with in detail. The results of CACAD designing 9 types of passenger aircraft are also included.

B2. Aircraft Design Relations in CACAD

The following relations are presented in the same sequence as is presented in the CACAD flow diagram of Figure 2-3. This makes the tracking of the code more user friendly. All notations and abbreviations in the formulae were made to look most similar to what is in CACAD listing. They are defined and their values are included (if they are input data) in Appendix A. If the unit of an item is not mentioned, Appendix A gives all units. There are some constant values in the relations for converting units. These are 2.205 for lb. to kg, 3.281 for meter to foot, 10.765 for square meter to square foot, 1.852 for knot to kmph, 3.6 for kmph to m/s, 12.96 for square kmph to square m/s. Most of the references of the following equations are mentioned as they appear, but for obvious relations no reference in mentioned.

B2.1 Class 1 Take-off Mass Determination

The following relations establish a module in CACAD, and are based on Volume 1 [15]. Because a detailed take-off mass estimation will be presented later in the Appendix, some of the parameters in this module is treated with approximation. This module at the beginning of the program helps to initialise more accurate wing area and thrust values, so that the iteration in the downstream of the program converges quickly. The module itself operates through an iteration.

$$M_{to} = M_e + M_{tfo} + M_{crew} + M_{pl} + M_{fueli} \qquad \text{B1}$$

$$M_e = \frac{10^{((\log_{10} M_{to} \times 2.2 - 0.0833)/1.0383)}}{2.2} \qquad \text{B2}$$

$$M_{crew} = 2.0 \times (175 + 30.0)/2.2 \qquad \text{B3}$$

$$M_{pl} = (175. + 40.) \times P_{AX}/2.2 + (175. + 30.) \times (P_{AX}/P_{AXCBR})/2.2 \qquad \text{B4}$$

$$M_{fueli} = M_{fused} + M_{fres} \qquad \text{B5}$$

$$M_{fused} = (1 - F_{fm}) \times M_{to} \qquad \text{B6}$$

$$F_{fm} = F_{f1} \times F_{f2} \times F_{f3} \times F_{f4} \times F_{f5} \times F_{f6} \times F_{f7} \times F_{f8} \times F_{f9} \qquad \text{B7}$$

$$F_{f9} = \frac{1}{e^{\left\{\frac{Div \times sfc_{div}}{(L/D)_{div} \times V_{div}}\right\}}} \qquad \text{B8}$$

$$F_{f6} = \frac{1}{e^{\left\{\frac{Hold \times sfc_{hold}}{(L/D)_{hold}}\right\}}} \qquad \text{B9}$$

$$F_{f5} = \frac{1}{e^{\left\{\frac{Stage \times sfc_{cruise}}{(L/D)_{cruise} \times V_{cruise}}\right\}}} \qquad \text{B10}$$

F_{f1} , F_{f2} , F_{f3} , F_{f4}, F_{f7} , and F_{f8} are assumed *0.99, 0.99, 0.995, 0.98, 0.99, 0.992* respectively. V_{div} is assumed 250 knots, and $(L/D)_{div}$, $(L/D)_{hold}$, $(L/D)_{cruise}$ are *10, 18,18* repectively. P_{AXCBR} is an input data. *Stage, Div, Hold,* V_{cruise} , sfc_{cruise}, , sfc_{div} , sfc_{hold} , P_{AX} are special mission input data.

B2.2 Initialisation of Independent Variables

Using existing transport aircraft data [43,26], the following correlation equations were developed to give a reasonable value for the gross wing area, and the engine mass.

The engine mass in CACAD is converted into engine thrust through known engine thrust mass ratio [26].

$$S_g = 10^{-9} \times (1.3893 \times M_{to}^2 + 0.0011 \times M_{to} + 36.916) \qquad \text{B11}$$

$$Meng = 55 \times P_{AX} + 0.0245 \times (P_{AX})^2 \qquad \text{B12}$$

For other independent variables (IV), the following reasonable ranges are defined. The optimiser uses these ranges to search for optimum values of IV.

Ete	*0.2*	*to*	*0.3*
Eta	*0.5*	*to*	*0.7*
β_{to}	*10*	*to*	*20 deg*
β_{app}	*25*	*to*	*35 deg*
AR	*7.5*	*to*	*10*
t_c *or TC*	*0.08*	*to*	*0.12*
Ele	*0.15*	*to*	*0.20*

Sweep angle, and taper ratio are quasi-dependent variables. The cruise Mach number is an input value, from which CACAD determines Mach critical drag at zero lift (M_{crit0}). This shall be dealt with later. When optimiser chooses a value for *TC*, sweep angle at *1/4* chord is automatically derived from the following equation developed from a three dimensional graph presented in Corning (Fig. D-7).

$$\Lambda_{1/4} = -180.345 + 211.415 \times M_{crit0} + 298.207 \times TC - 149.599 \times TC^2 \qquad \text{B13}$$

M_{crit0} shall be derived in the later section. Taper ratio is also determined, once the value of sweep is derived from above relation. This is an equation fit to match the curve in Torenbeek for transport aircraft, see Fig. B-1.

$$TR = 0.32278 + 0.004626 \times \Lambda_{1/4} + 0.000030357 \times (\Lambda_{1/4})^2 \qquad \text{B14}$$

B2.3 Mach Critical Drag Module

In this module, effort is made to establish the relationships that produces Mach critical drag at zero lift from cruise Mach number. This then shall be used to predict wing sweep angle (B13) suitable to the selected thickness to chord ratio of the supercritical modern wings of present transport aircraft. According to Corning, M_{crit0} is found from adding cruise Mach number to Mach number rise that causes compressibility drag, subtracting Mach number rise due to lift coefficient.

$$M_{crit0} = M_{cr} + dM_{cr} - dMc_{CL} \qquad \text{B15}$$

For permissible compressibility drag of 0.002, dM_{cr} is zero, see Fig. D-5 [25]. For dMc_{CL} the following equation is a fit to the curve of Fig. D-6 [25].

$$dMc_{CL} = -0.005714 + 0.0321143 \times C_{Lcr} - 0.1 \times (C_{Lcr})^2 \qquad \text{B16}$$

C_{Lcr} is the lift coefficient at the start of cruise.

$$C_{Lcr} = 12.96 \times M_{SSB} \times g / \{ 0.5 \times \rho_{cr} \; S_g \times (V_{CR})^2 \} \qquad \text{B17}$$

$$M_{SSB} = (1 - Kfa1) \times M_{to} \qquad \text{B18}$$

ρ_{cr} & V_{CR} is found from atmospheric module. *Kfa1* is an input value, and relation B18 is from [14].

B2.4 Atmospheric Module

Following relations establish ambient temperature and density at the required altitude from [16].

$$T_{cruise\ or\ diersion\ or\ hold} = T_{SL}\ (which\ is\ 288.2\ deg\ K\ ) - 0.0065 \times H_{tmcr\ or\ diversion\ or\ hold}$$

deg K B19

$$V_{sound-at-any-altitude} = \sqrt{\gamma \times R \times T} = \sqrt{1.4 \times 287 \times T_{same-daltitude}} \quad \text{m/sec} \qquad \text{B20}$$

$$V_{cr} = M_{cr} \times (3.6 \times V_{sound}) \quad \text{kmph} \qquad \text{B21}$$

$$\theta_{\ cruise\ or\ diversion\ or\ hold} = T_{\ cruise\ or\ diversion\ or\ hold} / 288.2 \qquad \text{B22}$$

$$R_{dcr} = \rho_{\ cruise\ or\ diversion\ or\ hold} / \rho_{\ sea\ level} = (\theta_{\ cruise\ or\ diversion\ or\ hold})^{4.2561} \qquad \text{B23}$$

$$\rho_{\ cruise\ or\ diversion\ or\ hold} = (\rho_{\ cruise\ or\ diversion\ or\ hold} / \rho_{\ sea\ level}) \times 1.225052$$

kg/m^3 B24

Altitude for cruise and diversion is in meter.

B2.5 Aircraft Parameters independent of IVs

In this section the methods of determining aircraft parameters (geometry, or mass), which are independent of IVs are presented. They are fuselage pressurised length, fuselage diameters, fuselage length, outside surface area of fuselage, pay load, number of cabin attendant, number of crew, number of toilets, number of galleys, and mass of cabin furnishing. All units are in SI.

$$P_{CL} = (P_{CH} + F_{L1}) \times P_{AXmax} / P_{AB} + F_{L3} \qquad \text{B25}$$

$$F_{USD} = F_{D0} + F_{D1} \times (P_{AB} + A_{ISLES}) + F_{D2} \quad \text{B26}$$

$$F_{USL} = P_{CL} + F_{L2} \times F_{USD} \quad \text{B26-1}$$

$$M_{PAX} = J_{PAX} \times P_{AX} \quad \text{B27}$$

$$M_{PAY} = M_{PAX} + M_{FRT} \quad \text{B28}$$

$$C_{ABIN} = P_{AX} / P_{AXCBR} \quad \text{B29}$$

$$C_{REW} = D_{ECK} + C_{ABIN} \quad \text{B30}$$

$$TT = P_{AX1} / P_{TR} \quad \text{B31}$$

$$G_{AL} = 0.5 \times (P_{AX1} / P_{TR}) \quad \text{B32}$$

$$M_{FUR} = F_{UR1} \times (P_{CL} - F_{L3}) \times F_{USD} + F_{UR2} \times P_{AX1} + F_{UR3} \times D_{ECK} + F_{UR4} + F_{UR5} \times TT \quad \text{B33}$$

The coefficients F_{L1} , F_{L3} , F_{D0} , F_{D1} , F_{D2} , J_{PAX} , P_{AXCBR} , P_{TR} , F_{UR1} , F_{UR2} , F_{UR3} , F_{UR4} , F_{UR5} are general input values. P_{AB} , A_{ISLES} , P_{AX1} , M_{FRT} , D_{ECK} , P_{CH} are mission input values.

B2.6 Mass of Fuselage & Wing LE Devices

From [14], empirical equation for the mass of fuselage is more detailed, and takes into account the amount of cabin pressurisation, as well as allowances for material technology. It also accounts for the rear fuselage mounted engine extra mass if user chooses so.

$$M_{FUS} = J_{fus} \{ A_{mfus} + 0.01377[(F_{USL} \times Z_m) / F_{USD}^{\,2}]^{0.4665} + K_{fusw} \times M_{to} + 8.956 M_{to}^{\,1.8} (P_{rsdif} - 13.789) F_{USD} \times 10^{-10} \} \quad \text{B34}$$

$$A_{mfus} = 0.8287 S_{fusw} (P_{rsdif} \times F_{USD})^{0.4995} + 4.8825 (S_{fusw} - 18.58) + 0.64752 F_{USD} (P_{rsdif} - 13.789) + F_{USL} \times P_{AB} [2.6043 + 2.3924 (F_{USD} / P_{AB}) + 0.03738 F_{USD}^{\,2}) \quad \text{B35}$$

$$S_{fusw} = 2\, F_{USD} \times F_{USL} \quad \text{B36}$$

$$Z_m = 108.95 \{ P_{AB} [F_{USL} - 0.9144 (5 + P_{AB})] \}^{1.1675} \quad \text{B37}$$

$$Z_m = Z_m + 0.9 M_{to} \quad \text{B38}$$

J_{fus} is usually one, but can be reduced if lighter material than present state-of-the-art is used. K_{fusw} is increased from *0.0125* to *0.015* if engines are mounted at the rear of fuselage. P_{rsdif} and P_{AB} are mission input data.

For quicker result but rather heavier mass, an out of date, but simple relation from Pekham [13] is as follows :

$$M_{FUS} = J_{fus1} \times (S_{FUS})^{ff} \qquad \text{Pekham [13]} \qquad \text{B39}$$

$$S_{FUS} = \pi \times F_{USD} \times F_{USL} - 4.71 F_{USD}^{2} \qquad \text{Howe [129]} \qquad \text{B40}$$

$$S_{FUS} = \pi \times F_{USD} \times F_{USL} - 4.5 F_{USD}^{2} \qquad \text{Collingbourn [14]} \qquad \text{B41}$$

J_{fus1} and *ff* are general input data.

Reference [14] gives the most reasonably detailed empirical equation for wing LE mass estimation as a function of the surface of the leading edge. The relation for LE surface is standard for swept tapered wings.

$$M_{WLE} = J_{le} \times S_{LE} + J_{les} \times (Eles/Ele) \times S_{LE} \qquad \text{B42}$$

$$S_{LE} = Ele \times S_g - \frac{Ele \times F_{USD} \times GMC}{1+TR}\left[2 - \frac{F_{USD}(1-TR)}{Span}\right] \qquad \text{B43}$$

$$Span = \sqrt{AR \times S_g}$$

$$GMC = \sqrt{\frac{S_g}{AR}} \qquad \text{B44}$$

J_{le} is the specific mass of LE devices, and J_{les} is additional specific mass if the leading edge devices are mounted in full span. *Eles* is LE device width chord ratio and is typically 5 % less than LE spar fraction of the chord *Ele*.

B2.7 C_{LMAX} at Take-off, and Approach Module

Collingbourne is the only source that proposes a set of empirical relations that are functions of wing aspect ratio, taper ratio, sweep angle, LE devices' geometry, TE flap's geometry, deflection angle of LE, and TE devices. Some modification to her module was necessary and shall be explained later in the section. The most important feature of this module is the influence of the variations of each IV on C_{Lmax} that influences the whole aircraft sizing, making optimisation quite an effective tool. According to [14] the trimmed maximum lift coefficient is given as below:

$$(C_{LMAX})_{trimmed} = (C_{LMAX})_{untrimmed\ with\ flap} - 0.15\,[2AR/(2+AR)]\,[(C_{LMAX})_{untrimmed\ with\ flap} - (C_{LMAX})_{untrimmed\ without\ flap}] - 0.05 \qquad \text{B45}$$

$$(C_{LMAX})_{untrimmed\ with\ flap} = \{ Basic\ wing\ Clmax \times effect\ of\ sweep + Additional\ lift\ due\ to\ LE\ devices \times effect\ of\ sweep + Additional\ lift\ due\ to\ TE\ devices \times effect\ of\ sweep \times (geometry\ of\ flap)^{0.5} \}\ (effect\ of\ flap\ geometry\ \&\ wing\ taper\ /\ Effect\ of\ wing\ taper)$$

Note : wherever "or" appear in the relationships below, it distinguishes between the take-off, and the approach phase of the flight.

$$(C_{LMAX})_{untrimmed\ with\ flap} = \{ C_{LMB} \times F_{swpB} + (T_{DCLMSO}\ or\ A_{DCLMSO})F_{swpS} + (D_{clmfT}\ or\ D_{clmfA})\,F_{swpF}\,\sqrt{F_{TRETA}}\,\}\,[\,(S_{ratT}\ or\ S_{ratA})/G_{sclom}\,] \qquad \text{B46}$$

$$(C_{LMAX})_{untrimmed\ without\ flap} = \{ C_{LMB} \times F_{swpB} + (T_{DCLMSO}\ or\ A_{DCLMSO})F_{swpS}\,\} \times [\,(T_{sratd}\ or\ A_{sratd})/G_{sclom}\,] \qquad \text{B47}$$

$$F_{swpB} = Sb1 + Sb2 \times \Lambda_{1/4} + Sb3 \times (\Lambda_{1/4})^2 \qquad \text{B48}$$

$$F_{swpS} = Ss1 + Ss2 \times \Lambda_{1/4} + Ss3 \times (\Lambda_{1/4})^2 \qquad \text{B49}$$

$$F_{swpT} = St1 + St2 \times \Lambda_{1/4} + St3 \times (\Lambda_{1/4})^2 \qquad \text{B50}$$

$$G_{sclom} = C_{la1} + C_{la2} \times TR + C_{la3} \times TR^2 - AR(\,C_{lb1} + C_{lb2} \times TR) \qquad \text{B51}$$

$$S_{ratA}\ or\ S_{ratT} = 1 + (T_{elese}\ or\ E_{lese}) \times (E_{tefeT}\ or\ E_{tefeA}) \times F_{TRETA} \qquad \text{B52}$$

$$F_{TRETA} = \frac{\{2-(1-TR)Eta\}Eta - \{2-(1-TR)E_{tafs}\}E_{tafs}}{(1+TR) - \{2-(1-TR)E_{tafs}\}E_{tafs}} \qquad \text{B53}$$

$$T_{elese} = E_{elec}\,(\,T_{elec} \times Eles\,) \qquad \text{B54}$$

Note : $T_{eles} = T_{elec} \times Eles$

$$E_{lese} = E_{elec} \times Eles \qquad \text{B55}$$

$$E_{tefeT}\ or\ E_{tefeA} = (\,S_{ofT}\ or\ S_{ofA}) \times (\,E_{tefT}\ or\ E_{tefA}\,) \qquad \text{B56}$$

Rear spar location fraction of the chord *Ete* B57

Flap chord fraction $Etefb = Ete - D_{flp}$ B58

D_{flp} is usually 5%, and is an input data.

Flap chord un-extended & unshielded $Etef = Etefb(1 - S_{ofb})$ B59

S_{ofb} is the shielded percentage of the flap, and is an item of the input data.

Flap chord fully extended but not deflected $Etef = Etefb \times Fcer$ B60

Fcer is an input data.

Flap chord partly extended, and partly deflected (β_T for take-off, β_A for approach), with maximum deflection at take-off and approach being, β_{Tmax} , β_{Amax} respectively :

$$E_{tefT}\text{"or"}E_{tefA} = Etefb\{1 - S_{ofb} + (Fcer - 1 + S_{ofb})(\frac{\beta_T\text{"or"}\beta_A}{\beta_{Tmax}\text{"or"}\beta_{Amax}})^{fdin}\} \quad \text{B61}$$

The rearward translation of the flap at TE as fraction of the chord :

$$E_{tefeT}\text{"or"}E_{tefeA} = (Fcer - 1 + S_{ofb})(\frac{\beta_T\text{"or"}\beta_A}{\beta_{Tmax}\text{"or"}\beta_{Amax}})^{fdin} \quad \text{B62}$$

The rise of C_{LMAX} due to LE extension T_{DCLMSO} *or* A_{DCLMSO} at take-off and approach respectively :

$$T_{DCLMSO} \text{ or } A_{DCLMSO} = C_{ls1} \times (T_{eles} \text{ or } Eles) + C_{ls2} \times (T_{eles} \text{ or } Eles)^2 \quad \text{B63}$$

The rise of C_{LMAX} due to TE extension D_{clmfT} *or* D_{clmfA} at take-off and approach :

$$D_{clmfT} \text{ or } D_{clmfA} = C_{lf1} \times (F_{\beta to} \text{ or } F_{\beta a}) \times (F_{etfrT} \text{ or } F_{etfrA}) +$$

$$C_{lf2}[1 + C_{lf3} \times (\beta_T \text{ or } \beta_A)][1 + C_{lf4}(E_{tefrT} \text{ or } E_{tefrA})] \quad \text{B64}$$

The following relationships describe the terms used in above equations :

$$F_{\beta to} \text{ or } F_{\beta a} = \beta_1 + \beta_2 \times (\beta_T \text{ or } \beta_A) + \beta_3 \times (\beta_T \text{ or } \beta_A)^2 \quad \text{B65}$$

$$F_{etfrT} \text{ or } F_{etfrA} = F_{r1} + F_{r2} \times (E_{tefrT} \text{ or } E_{tefrA}) + F_{r3} \times (E_{tefrT} \text{ or } E_{tefrA})^2 \quad \text{B66}$$

$$E_{tefrT} \text{ or } E_{tefrA} = (E_{tefT} \text{ or } E_{tefA})/(C_{erT} \text{ or } C_{erA}) \quad \text{B67}$$

$$C_{erT} \text{ or } C_{erA} = 1 + (T_{elese} \text{ or } E_{lese}) \times (E_{tefeT} \text{ or } E_{tefeA}) \quad \text{B68}$$

$$T_{sratd} \text{ or } A_{sratd} = 1 + T_{elese} \text{ or } E_{lese} \quad \text{B69}$$

$$E_{tafs} = F_{USD} / Span \quad \text{B70}$$

The coefficients *Sb1, Sb2, Sb3, Ss1, Ss2, Ss3, St1, St2, St3,* C_{la1}, C_{la2}, C_{la3}, C_{lb1}, C_{lb2}, T_{elec}, E_{elec}, C_{lf1}, C_{lf2}, C_{lf3}, C_{lf4}, β_1, β_2, β_3, F_{r1}, F_{r2}, and F_{r3} are general input data.

C_{LMB} is maximum wing lift coefficient (without high lift devices), and according to [14] it can be assumes as 1.61. This has caused certain problem in CACAD optimiser. The variation of thickness to chord ratio from 0.07 to 0.12 must have some impact on C_{LMB}. Corning [25] has shown the variation of C_{LMB} with thickness to chord ratio, and sweep angle for supercritical wing in the form of curves. These curves have been converted into a three dimensional equation as below:

$$C_{LMB} = [\, 5. \times TC \times (\, 0.008 \times \Lambda_{1/4} + 0.875\,) + 0.65\,] + 0.53 \qquad \text{B71}$$

B2.8 Wing TE Mass Estimate

The coefficient of lift at take-off (C_{LTO}) is taken as 0.694 fraction of C_{LMAX} and shall be used in this module to estimate take-off speed of the aircraft. Flap mass density is function of approach speed, and its deflection at approach. It is also function of take-off speed and deflection at take-off. Which ever is bigger shall be selected by CACAD. Collingbourne offers the most IV dependent and detailed approach to mass estimation, although [129] is equally applicable. Relations for surface areas of flap, and ailerons of a tapered swept wing are standard.

$$M_{WTE} = M_{WTEF} + M_{WTER} \qquad \text{B72}$$

$$M_{WTEF} = J_{FLP} \times S_{FTE} \qquad \text{B73}$$

$$M_{WTER} = J_{RTE} \times S_{RTE} \qquad \text{B74}$$

$$S_{FTE} = \frac{S_g \times Eta \times Ete}{1+TR}[2 - Eta(1-TR)] - \frac{Ete \times F_{USD} \times GMC}{1+TR}[2 - \frac{F_{USD}(1-TR)}{Span}] \qquad \text{B75}$$

$$S_{RTE} = Ete \times S_g[1 - \frac{Eta\{2 - Eta(1-TR)\}}{1+TR}] \qquad \text{B76}$$

$$J_{FLP} = J_{FLP0} \times F_{lpc}\,(S_{FTE} \times E_{taf} \times Span\,)^{0.1875}\,[\,(\,V_A \text{ or } V_{TO}\,) \times \sin(\beta_a \text{ or } \beta_{to}) \times \cos(\Lambda_f) / TC\,]^{0.75} \qquad \text{B77}$$

$$\tan(\Lambda_f) = \tan(\Lambda_{1/4}) - \frac{(1-TR)(3-4E_{tefb})}{A(1+TR)} \qquad \text{B78}$$

$$V_{TO} = \sqrt{\frac{M_{to} \times g}{\frac{1}{2}\rho_{cr} \times C_{LTO} \times S_g}} \qquad \text{B79}$$

$$E_{taf} = Eta - F_{USD} / Span \qquad \text{B80}$$

J_{FLP0} is a coefficient to represent the type of flap and is 0.006 for current transport aircraft. F_{lpc} is a complexity factor and is 1.2 for fowler flap. They are both general input data.

B2.9 Zero Lift Drag Coefficient

This is made of two part, zero lift drag coefficient due to wing and due to other than the wing (fuselage, and empennage).

$$C_{D0} = C_{D0W} + C_{D0EW} \qquad \text{B81}$$

The following expression for zero lift coefficient of the wing though not unique is the work of Edwards in [31] :

$$C_{D0W} = \frac{1.15 N_{waf}[(1 + 3TC \times \cos^2(\Lambda_A)]}{(\log_{10} RN)^{21/8}} \qquad \text{B82}$$

It is an impirical relation constructed upon a fundamental relation as below:

$C_{D0W} = f$ (*skin friction effect, thickness ratio and shape factor effect,* S_{wet} / S_{net})

Note : *skin friction effect* $= f$ (*some constant / Reynolds Number*)

N_{waf} is the ratio of net wing area to twice the gross wing area :

$$N_{waf} = 1 - \frac{2F_{USD} \times Span - F_{USD}^2(1 - TR)}{A \times S_g(1 + TR)} \qquad \text{B83}$$

Λ_A is an effective aerodynamic sweep of the wing, intermediate between 0.3 and chord-wise position where the roof top pressure (RTP) distribution ends. In the same reference a long procedure is proposed to find the above angle. The investigation shows that the approximate location of the RTP is 0.7 to 0.8 fraction of the chord This makes the intermediate location nearly at 0.5 chord.

$$\Lambda_A \cong \Lambda_{1/2} = tan^{-1} \{tan(\Lambda_{1/4}) + (4/AR) \times [(1-TR)/(1+TR)](1/4 - 1/2) \qquad \text{B84}$$

RN is the cruise Reynolds Number based on *GMC*

$$RN = V_{CR} \times GMC / (3.6 \times \mu_{cr}) \qquad \text{B85}$$

where μ_{cr} is the kinematics viscosity of air at cruise conditions, which is a mission input data. The following empirical expression for zero lift coefficient of the fuselage, the engine nacelle, and the empennage is from [14] :

$$C_{D0EW} = (K_{sf\text{-}fus} \times S_{FUS} + K_{sf\text{-}nac} \times S_{NAC} + 2\, K_{sf\text{-}emp} \times S_{EMP}) / S_g \qquad \text{B86}$$

S_{NAC} is the wetted area of the engine nacelles and is related to engine thrust through the following empirical relation [14]:

$$S_{NAC} = K_{nac} \times Meng / J_{tsta0} \qquad \text{B87}$$

S_{EMP} is the wetted area of the empennage and is derived by using the simple relationship from [13] :

$$S_{EMP} = \frac{V \times GMC \times S_g}{K_{ta} \times F_{USL}} \qquad \text{B88}$$

where V is tail volume ratio and K_{ta} is tail arm as fraction of fuselage length and are input data. $K_{sf\text{-}fus}$, $K_{sf\text{-}nac}$, and $K_{sf\text{-}emp}$ are zero lift drag coefficient factors based on wetted area for the fuselage, nacelle, and empennage respectively. They are specified in the input data.

B2.10 Drag Coefficient at Cruise

There are different approaches to determine C_{Dcr} but [14] was chosen due to an empirical but very useful relation for induced drag factor. An initial value for C_{dcr} is assumed and through an iteration the final value is computed.

$$C_{Dcr} = C_{D0} + C_{DWDR} + K_{cr} (C_{Lcr})^2 / \pi\, AR \qquad \text{B89}$$

$$C_{Lcr} = 12.96 \times M_{SSCR} \times g / \{ 0.5 \times \rho_{cr} \times S_g \times (V_{CR})^2 \} \qquad \text{B90}$$

$$K_{cr} = K_{cr1} + K_{cr2} (F_{USD} / Span)^2 + K_{cr3} \times AR \times sec (\Lambda_{1/4}) \qquad \text{B91}$$

M_{SSCR} is found through an empirical relation that allowes fuel fraction for climb to cruise.

$$M_{SSCR} = M_{to} (1 - fuel\, fraction\, for\, climb) \qquad \text{B92}$$

$$M_{SSCR} = M_{to} \left(1 - \frac{D_{hten} \times sfc_{cr}}{V_{cr}} \times \frac{1.15 \times T_{STAT} + 6 D_{CR}}{T_{STAT} - D_{CR}}\right) \qquad \text{B93}$$

$$D_{CR} = 0.5 \times \rho_{cr} \times C_{Dcr} \times S_g \times (V_{CR})^2 \quad \text{B94}$$

$$T_{STAT} = R_{ating} \times Meng / J_{tsta0} \quad \text{B95}$$

According to the same reference D_{hten} is the energy height increase in climb and decrease in descent which are assumed to be the same. This is given by following standard relation.

D_{hten} = *(Potential energy & kinetic energy at cruise altitude - Potenyial energy & kinetic energy at sea level altitude)*

$$D_{hten} = \{H_{tmcr} - H_{tmto} + \frac{V_{CR}^2}{12.96 \times 2g}(1 - R_{dcr})\}\frac{1}{1000} \quad \text{B96}$$

R_{ating} and J_{tsta0} are both input data.

B2.11 Cruise Fuel Mass Module

In order to estimate the fuel used during climb, cruise, and descent, the lost range technique [14] is used. In this approach the range covered during climb and descent is found and is called lost rang *Lrge*, and is then added to the stage length *Stage* which is a mission input data. This is called equivalent cruise-range and is used to estimate the fuel consumption during cruise covering climb and descent too. A simple Breguet equation is used instead of a complicated relations in the same reference.

$$M_{fuel-cr} = M_{SSB} \times (1 - \frac{1}{e^{\frac{Range \times sfc_{cr}}{V_{CR} \times (L/D)_{cr}}}}) \quad \text{B97}$$

$$Range = Stage + Lrge \quad \text{B98}$$

$$Lrge = D_{hten} \frac{C_{Lcr}}{C_{Dcr}} (\frac{1.15 S_{THOWT}}{S_{STHOWT} - C_{Dcr}/C_{Lcr}} - 0.8) \quad \text{B99}$$

S_{THOWT} is the maximum static thrust of engines to aircraft take-off mass, and is given as below:

$$S_{THOWT} = T_{STAT} / (M_{to} \times g) \quad \text{B100}$$

B2.12 Load Factor

The critical load factor is determined according to BCAR for a flight altitude of 20000ft, a gust of 15.24 m/s (U_{max}), during the descent phase when cruise is already

covered, at the maximum operating speed of the aircraft. The relationship is standard and is the same in most references :

$$N = 1.5[1 + \frac{\rho_0 \times G_{AF} \times V_G \times U_{max} \times \{d(C_L)/d(\alpha)\}}{2\frac{M_{LDG}}{S_g}}] \qquad \text{B101}$$

$$d(C_L)/d(\alpha) = D_{CLDA} = \frac{2\pi \cos(\Lambda_{1/4})(1+TC)}{2\cos(\Lambda_{1/4})/AR + \{1 - M_G^2 \times \cos^2(\Lambda_{1/4}) + [2\cos(\Lambda_{1/4})/AR]^2\}^{1/2}} \qquad \text{B102}$$

$$M_{LDG} = M_{SSB} - M_{fuel\text{-}cr}(1 + K_{fcl}) \qquad \text{B103}$$

$$V_G = (M_{cr} + dM)/V_{sound\ at\ 20000ft} \qquad \text{B104}$$

G_{AF} is gust alleviation factor and M_U is aircraft mass ratio. Both are given by the following expressions [14].

$$G_{AF} = \frac{0.88 \times M_U}{5.3 + M_U} \qquad \text{B105}$$

$$M_U = \frac{3.06 M_{LDG}}{D_{CLDA} \times S_g \times GMC} \qquad \text{B106}$$

K_{fcl} is the coefficient for contingency fuel.

B2.13 Diversion, Hold, Allowance, and Contingency Fuel Mass Module

The lost range technique and the fuel fraction estimation method associated with this technique elaborated in [14] is used in CACAD for the fuel mass estimation in diversion, and hold phase of the flight. Although the fuel fraction formula might look quite different from famous Breguet range equation, but by some mathematical manipulation (tangent and exponential series) they are exactly identical.

During diversion some range is covered while climbing to diversion altitude, and some during descent. These ranges are assumed as lost ranges L_{div}, and shall be derived from following expressions to be added to the diversion length D_{iv} to produce total diversion length R_{div}. This is used to compute the fuel fraction M_{RTdiv} during diversion.

$$M_{fuel\text{-}diversion} = M_{LDG}(1 - M_{RTdiv}) \qquad \text{B107}$$

$$M_{RTdiv} = tan\{tan^{-1}(D_{rt-div}) - \frac{R_{div} \times sfc_{div}}{V_{DIV}}(\frac{K_{cr} \times C_{D0}}{\pi \times AR})^{1/2}\} / D_{rt-div} \quad \text{B108}$$

$$D_{rt\text{-}div} = C_{ldiv}\,[\,K_{cr} / (\,\pi\, AR \times C_{D0}\,)\,]^{1/2} \quad \text{B109}$$

$$R_{div} = Div + L_{div} \quad \text{B110}$$

$$L_{div} = D_{hten-div}\frac{C_{L-div}}{C_{D-div}}(\frac{1.15S_{TODWT}}{S_{STODWT} - C_{D-div}/C_{L-div}} - 0.8) \quad \text{B111}$$

$$S_{STODWT} = T_{STAT} / (M_{LDG} \times g) \quad \text{B112}$$

$$D_{hten} = \{H_{tm-div} - H_{tmto} + \frac{V_{DIV}^2}{12.96 \times 2g}(1 - R_{d-div})\}\frac{1}{1000} \quad \text{B113}$$

$$M_{LDG} = M_{SSB} - M_{fuel\text{-}cruise}\,(\,1 + K_{fcl}) \quad \text{B114}$$

For the maximum diversion range, the diversion speed is equal to $3^{1/4}\times$(minimum drag speed) where the compressibility drag is ignored [14].

$$C_D = C_{D0} + K_{cr} \times (C_L)^2/(\pi AR) \quad \text{B115}$$

$$V_{DIV} = 5.033[\frac{M_{LDG} \times g}{S_g \times \rho_{div}}(\frac{K_{cr}}{AR \times C_{D0}})^{1/2}]^{1/2} \quad \text{B116}$$

$$C_{L\text{-}div} = 12.96 \times M_{LDG} \times g / \{\,0.5 \times \rho_{div} \times\ S_g \times (V_{DIV})^2\} \quad \text{B117}$$

$$C_{D\text{-}div} = C_{D0} + K_{cr}\,(C_{L\text{-}div})^2/(\pi \times AR) \quad \text{B118}$$

For the hold phase it is assumed that hold speed is *1.15* times the minimum drag speed. [14] proposes a relation for the lift drag ratio for hold , this is used in Breguet equation.

$$M_{fuel-hold} = \{M_{LDG} - M_{fuel-diversion}(1 + K_{fcl})\}\{1 - exp(-1.173Hold \times sfc_{hold}\sqrt{K_{cr} \times C_{D0} / AR} \quad \text{B119}$$

$$\frac{(L/D)_{max}}{(L/D)_{hold}} = \tfrac{1}{2}(1.15^2 + \frac{1}{1.15^2}) = 1.0393 \quad \text{B120}$$

$$(D/L)_{hold} = 1.173\sqrt{K_{cr} \times C_{D0} / AR} \quad \text{B121}$$

Div, and *Hold* are both mission input data.

Some fuel shall be consumed for taxing, take-off, and initial climb. Some for landing, and contingency. These are computed using empirical constant. Sum of all above fuel consumed is $M_{fuel\text{-}loaded}$, and is found according to following relations.

$$M_{fuel} = M_{fuel\text{-}cruise} + M_{fuel\text{-}diversion} + M_{fuel\text{-}hold} + M_{fuel\text{-}allowance} + M_{fuel\text{-}contingency} \quad \text{B122}$$

$$M_{fuel\text{-}allowance} = K_{fa0} \times M_{to} + K_{fa1} \times M_{to} + K_{fa2} \times M_{SSY} \quad \text{B123}$$

$$M_{SSY} = M_{SSB} - (M_{fuel\text{-}cruise} + M_{fuel\text{-}diversion} + M_{fuel\text{-}hold})(1 + K_{fcl}) \quad \text{B124}$$

$$M_{fuel\text{-}contingency} = (M_{fuel\text{-}cruise} + M_{fuel\text{-}diversion} + M_{fuel\text{-}hold})\, K_{fcl} \quad \text{B125}$$

K_{fa0}, K_{fa1}, and K_{fa2}, are empirical constant for taxi, take-off and initial climb, and landing respectively.

B2.14 Wing Box Mass Module

This section of the wing consists of wing box cover, ribs, spars, tips, joints, wing mounted engine support structure, undercarriage attachments. Reference [14] found to offer reasonably accurate empirical prediction equations for all sections of wing box. For wing box cover an alternative equation from Howe [129] is also included. This is used in Chapter 4 when VCW is integrated in CACAD. It requires an iteration i.e. an initial value for wing box mass must be assumed at the start of the module.

$$M_{WBX} = M_{WBtip} + M_{WBcov} + M_{WBjnt} + M_{WBsp} + M_{WBpp} + M_{WBuc} + M_{WBrb} \quad \text{B126}$$

$$M_{WBcov} = \frac{J_{WBcov} \times N \times M_{EFF} \times g \times W_{MF} \times AR(1 + 1.44TR)}{TC \times \cos^2(\Lambda_{1/4})}$$

$$\times \left\{ \frac{1 + 1.2(0.6 - Ete)^2}{1.075} \right\} \quad \text{B127}$$

$$M_{WBjnt} = \frac{J_{WBjnt} \times N \times M_{EFF} \times g \times W_{MF} \times AR(1 + 1.44TR)}{TC \times \cos^2(\Lambda_{1/4})} \quad \text{B128}$$

$$M_{WBsp} = \frac{\begin{array}{l} J_{BXsp1} \times S_g \times GMC \times TC^2 + J_{BXsp2} \times N \times M_{EFF} \times g \times W_{MF} \times Span \\ + J_{BXsp3} \times L_{mf} \times M_{to} \times g \times Span \end{array}}{\cos(\Lambda_{1/4})} \quad \text{B129}$$

$$M_{WBpp} = J_{BXpp} \times W_{un\text{-}eng}\,(N_{eiw} + N_{eow}) \quad \text{B130}$$

$$M_{WBrb} = \frac{J_{BXrb1} \times S_g \times GMC \times TC(1 - Ele + Ete)(1 + TR + TR^2)}{1 + TR^2}$$

$$+ \frac{J_{BXrb2} \times S_g \times GMC \times TC^2(1 - Ele + Ete)}{AR}$$

$$+ J_{BXrb3} \times L_{mf} \times M_{to} \times g \times GMC(1 - Ele + Ete)$$

$$+ \frac{J_{BXrb4} \times N \times M_{EFF} \times g \times W_{MF} \times GMC(1 - Ele + Ete)^2}{TC \times \cos(\Lambda_{1/4})}$$

$$+ J_{BXrb5} \times N \times M_{EFF} \times g \times W_{MF} \times Span(1 - Ele + Ete)\tan(\Lambda_{1/4}) \qquad \text{B131}$$

$$M_{WBuc} = J_{BXuc} \times L_{mf} \times M_{to} \times g \qquad \text{B132}$$

The terms $N \times M_{EFF} \times g \times W_{MF}$ is the effective load on the wing for the stressing case, after allowing for load relief from the wing mass, the fuel mass, and the weight of any wing mounted engines in Newton. W_{MF} is introduced to reduce the alleviating effect of aerodynamic twist when sweep becomes small.

$$W_{MF} = 1 + 0.3 \times exp\{-0.006(\Lambda_{1/4} - 2)^2\} \qquad \text{B133}$$

$$M_{EFF} = M_{to} - M_{fuel} + M_{PAY}(H_{payf} - 1) - 0.56(M_{WBX} + M_{WLE} + M_{WTE})$$

$$- 3.6\, W_{un\text{-}eng}(N_{eow} \times S_{poeng}^2 + N_{eiw} \times S_{pieng}^2) \qquad \text{B134}$$

$$W_{un\text{-}eng} = Meng / N_e \qquad \text{B135}$$

J_{BXcov}, J_{BXjnt}, J_{BXpp}, J_{BXuc}, J_{BXsp1}, J_{BXsp2}, J_{BXsp3}, J_{BXrb1}, J_{BXrb2}, J_{BXrb3}, J_{BXrb4}, J_{BXrb5}, and S_{poeng}, S_{pieng}, are general input data. N_e, N_{eow}, N_{eiw} are mission input data. Their value and definition are given in Appendix A.

For the estimation of the mass of the wing box cover the following alternative procedure is presented from latest theoretically based work of Professor Howe [129] :

$$M_{BXcov} = 6.4\,\bar{N} \times M_{to} \times r \times Span \times \sec \Lambda_{effective} \times \frac{\rho_{box}}{f_a}(Z) \qquad \text{B136}$$

(Z) is the factor allowing for wing taper, and location of root attachment, and is given by the following relation:

$$(Z) = 0.67 + 0.103(1 + TR)\frac{AR \times \sec \Lambda_{1/4}}{TC} \qquad \text{B137}$$

r is the relief effect due to inertia. It is given by the following options :

No engine under the wing :

$$r = 1 - [\, 0.12 + (\, 0.1 + Range \times 10^{-5}\,)] \qquad \text{B138}$$

Two engines on wing:

$$r = 1 - [\, 0.2 + (\, 0.1 + Range \times 10^{-5}\,)] \qquad \text{B139}$$

Four engines on wing:

$$r = 1 - [\, 0.22 + (\, 0.1 + Range \times 10^{-5}\,)] \qquad \text{B140}$$

$\bar{N}$ is the effective design ultimate acceleration factor and is given by the either of the following relationships, whichever yield bigger:

$$\bar{N} = 1.5\,(M_1 + 0.1) \qquad \text{B141}$$

$$\bar{N} = 1.65 + \frac{6.45 \times 1.25 \times (V_{cr} / 3.6)}{(M_{to} / S_g)(2 / AR + \sec \Lambda_{1/4})} \qquad \text{B142}$$

$M_1 = 3.8$ *for* $M_{to}<1882\ kg$

$M_1 = 2.1+[10900/(4530+M_{to})$ *for* $1882<M_{to}<22720\ kg$

$M_1 = 2.5$ *for* $M_{to}>22720\ kg$

f_a is the average allowable direct stress level, and ρ_{box} is the average density of the structural box. They are both given in input data file (App. A).

B2.15 CG Position Module

Location of *CG* position is fairly a standard practice. CG_{posn} is the location of aircraft *CG* from the nose of fuselage as fraction of the fuselage length. This is the same for the non-dimensional distances used in the following relations. The aerodynamic centre of the wing is assumed to be coincident with the aircraft *CG*, and the wing-group mass is taken as acting at a distance $C_{WING} \times A_{mc}$ aft of the wing aerodynamic centre and hence aircraft *CG* (see Fig. B-2).

The wing aerodynamic centre is assumed to be located by the quarter chord point of the aerodynamic mean chord *AMC*. For a trapezoidal wing *AMC* is located at $AMC_{eta} \times Span/2$ outboard of the centre line.

Note that the *CG* location is an iterative procedure in which mass of the tail plane and mass of the fin shall be assumed until *CG* is found. The program will then proceed into the next module in which the mass of these sections are accurately determined. They are then compared with the assumed value, until the iteration converges.

$$S_{emp}=V_{tp} \times GMC \times S_g / (K_{ta} \times F_{USL}) \qquad \text{B143}$$

$$M_{EMP} = J_{emp} \times (S_{emp})^E$$

Following empirical equations were developed from real transport aircraft using [43] and Torenbeek.

$$M_{TP} = 0.64\, M_{EMP} \qquad \text{B144}$$

$$M_{FIN} = 0.36\, M_{EMP}$$

$$CG_{posn} = \frac{M_{FUSC} \times K_{fusc} + M_{RENG} \times K_{eng} + M_{TP} \times K_{tp} + M_{FIN} \times K_{fin}}{M_{FUSC} + M_{RENG} + M_{FIN}}$$

$$- \frac{M_{IENG} \times CG_{IENG} + M_{OENG} \times CG_{OENG} + M_{WINGC} \times CG_{WING}}{M_{FUSC} + M_{RENG} + M_{FIN}} \qquad \text{B145}$$

$$M_{FUSC} = M_{FUS} + M_{PAX} + M_{FRT} + M_{CREW} + M_{FUR} + M_{EL} + 0.5\, M_{SYS} \qquad \text{B146}$$

$$M_{WINGC} = M_{WBX} + M_{WLE} + M_{WTE} + 0.5\, M_{SYS} \qquad \text{B147}$$

$$M_{RENG} = W_{un\text{-}eng} \times N_{er} \qquad \text{B148}$$

$$M_{IENG} = W_{un\text{-}eng} \times N_{eiw} \qquad \text{B149}$$

$$M_{OENG} = W_{un\text{-}eng} \times N_{eow} \qquad \text{B150}$$

CG_{WING} is the centre of gravity of the wing group and is taken to be positive if it is located ahead of the aircraft *CG*.

$$CG_{WING} = - C_{WING} \times AMC / F_{USL} \qquad \text{B151}$$

$$AMC = \frac{2S}{(1+TR)Span}\{1 - AMC_{eta}(1-TR)\} \qquad \text{B152}$$

$$AMC_{eta} = {(1+TR)}/{\{3(1+TR)\}} \qquad \text{B153}$$

$$CG_{IENG}\text{"or"}CG_{OENG} = \frac{AMC_{eta} - (S_{pieng}\text{"or"}S_{poeng})}{F_{USL}} \times \frac{Span}{2} tan(\Lambda_{1/4}) \times$$

$$\frac{S_g}{2Span \times F_{USL}} \times \frac{1}{1+TR}\{1-(S_{pieng}"or"S_{poeng})(1+TR)+\frac{E_{ngpos}}{F_{USL}}$$

B154

$$E_{ngpos} = G_{eng} \times W_{un-eng}^{Engind}$$ B155

The values and definition of the empirical coefficients K_{ta}, E, K_{fusc}, K_{eng}, K_{tp}, K_{fin}, C_{WING}, G_{eng}, and E_{ngind} as general input data are found in Appendix A.

B2.16 Tail Plane & Fin Mass Estimate Module

Once CG is located in the last module, following relations which are standard in most references, are used to estimate the tail and fin mass.

$$K_{tpa} = T_{pac} \times Cg_{posn}$$ B156

$$S_{TP}=V_{tp} \times GMC \times S_g / (K_{tpa} \times F_{USL})$$ B157

$$M_{TP} = J_{tp} \times S_{TP}^{E}(0.5+\frac{V_G}{270})$$ B158

$$M_{FIN} = J_{fin} \times S_{FIN}^{E}(0.5+\frac{V_G}{270})$$ B159

For the estimation of the area of the fin S_{FIN}, two requirements for fin sizing must be fulfilled. Whichever requires the higher value, it will be selected.

For fuselage stability:

$$S_{FIN} = V_{fin1} \times F_{USD} \times F_{USL} / K_{fina}$$ B160

The fin must be also powerful enough to cope with a failed outboard wing mounted engine in critical condition. An outboard failed engine not only does not balance the moment due to the thrust of the other engine, but intensifies it with a spillage, and windmilling drag.

$$S_{FIN} = \frac{V_{fin2}(0.5Span \times S_{poeng})(0.5N_{eow} \times W_{un-eng})(1+S_{fnkwm})}{0.5\rho_0 \times (V_{CTO}^2"or"V_A^2) \times S_{fnjt} \times F_{USL} \times K_{fina}}$$ B161

$$V_{CTO} = K_{tcs} \times V_{TO} / 1.1$$ B162

$$S_{fnkwm} = \frac{\rho_0 \times (V_{CTO}^2"or"V_A^2) \times S_{fnjt} \times (S_{dc} \times W_{dc})}{2J_{tsta0}}$$ B163

$$S_{fnjt} = J_{tstat} / [1\text{-}L_R \times (V_{CTO} \text{ or } V_A)] \quad \text{B164}$$

The values and definition of the empirical constants V_{tp} , T_{pac} , J_{tp} , K_{fina} , J_{tsta0} , S_{dc} , W_{dc} , and L_R as general input data are found in Appendix A.

B2.17 Undercarriage & System Mass Estimate Module

1) Undercarriage mass is found to be influenced with the vertical rate of descent at approach.

$$M_{UC} = J_{uc} \times M_{to} \quad \text{B165}$$

$$J_{uc} = 0.03 + 0.0008 (V_{RD})^2 \quad \text{B166}$$

$$V_{RD} = V_A \times F_{pnglr} \quad \text{B167}$$

F_{pnglr} is the flight path angle in radians, which is an input data.

System mass is presented according to each individual system.

$$M_{SYS} = M_{IAE} + M_{FC} + M_{HYD} + M_{ELS} + M_{FS} + M_{API} + M_{OX} + M_{BC} + M_{AUX} + M_{APU} \quad \text{B168}$$

They are mainly from Roskam [15] Raymer [1], Torenbeek [32]. Due to airframe mass being one of driving parameters, and shall be determined later, the whole process is iterative.

Following empirical equations were developed from actual flying transport aircraft using references [15], [32].

2) Electronic, and instrument system from Roskam :

$$M_{IAE} = \frac{0.575(\frac{M_E}{2.205})^{0.556} \times (\frac{Range}{1.852})}{2.205} \quad \text{B169}$$

$$M_E = M_{AF} + Meng \quad \text{B170}$$

According to Collingbourn the electronic, navigation, and instrument together as avionics system can be taken as 1200 kg, which is a good approximation for transport aircraft from 150 Pax to 350 Pax.

3) The empirical relation for the mass of flight control system from Raymor was checked against real values and found that with a small modification, it gives realistic

result. The benefits of Raymor relation is elaborated in Chapter 4 for VCW technology modelling.

$$M_{FC} = 2\frac{145.9N_f^{0.554} \times (S_{CS} \times 10.765)^{0.2} \times (I_Y \times 10^{-6})^{0.07}}{(1+\frac{N_m}{N_f}) \times 2.205} \qquad \text{B171}$$

S_{CS} is the sum of the area of the control surfaces. In CACAD there is no module to size these surfaces. This is due to the fact that R&M study did not require such modelling. Therefore simple but reasonably accurate relations were developed based on data from [43], and [32] to predict these surfaces as below:

$$S_{rudder} = 0.055 \times S_g \qquad \text{B172}$$

$$S_{elevator} = 0.07 \times S_g \qquad \text{B173}$$

$$S_{lift\ dumpers} = 0.08 \times S_g \qquad \text{B174}$$

$$S_{CS} = S_{rudder} + S_{elevator} + S_{lift\ dumpers} + S_{LE} + S_{TER} + S_{TEF} \qquad \text{B175}$$

I_Y which is the moment of inertia around Y-axis of aircraft is the sum of the product of the mass of each aircraft major section (wing group, fuselage group, tail plane, vertical fin, engine group) with the square of their respective distance from aircraft CG. This is given by following relation :

$$\begin{aligned} I_Y = \{ & M_{FUSC}(Cg_{posn} - K_{fusc})^2 + M_{WINGC}(CG_{WING})^2 + M_{FIN}(K_{fin} - Cg_{posn})^2 \\ & + M_{TP}(K_{tp} - Cg_{posn})^2 + M_{IENG}(CG_{IENG})^2 + M_{OENG}(CG_{OENG})^2 \\ & + M_{RENG}(K_{eng} - Cg_{posn})^2 \} \{(F_{FUSL} \times 3.281)^2\} \times 2.205 \end{aligned} \qquad \text{B176}$$

N_f is the number of functions the system performs, and N_m is the number of mechanical functions. Both are input data. The alternative formula from Torenbeek is also included in this module.

4) Hydraulic mass estimation is taken from Raymor due to the same reason as flight control system. But due to lack of accuracy, a correcting factor of 4.7 was found through correlation with real aircraft data.

$$M_{HYD} = 4.7 \times \frac{0.2673}{2.205} N_f [(F_{USL} + Span) \times 3.28]^{0.937} \qquad \text{B177}$$

5) Electrical system mass is estimated using General Dynamic relation:

$$M_{ELS} = \frac{1163}{2.205}[2.205(\frac{M_{FS} + M_{IAE}}{1000})]^{0.506} \quad \text{B178}$$

where M_{FS} is the mass of the fuel system as below:

$$M_{FS} = \frac{80(N_e + N_t - 1) + 15N_t^{0.5}(\frac{M_{fuel} \times 2.205}{K_{fsp}})^{0.333}}{2.205} \quad \text{B179}$$

N_t which is the number of separate fuel tanks is assumed to be

$$N_t = N_e + 3 \quad \text{B180}$$

6) Air-conditioning and pressurisation mass estimation is based on Torenbeek method:

$$M_{API} = \frac{6.75}{2.205}(P_{CL} / 3.281)^{1.28} \quad \text{B181}$$

7) Oxygen system M_{OX}, baggage & cargo handling system M_{BC}, auxiliary gear M_{AUX}, paint over the aircraft external body M_{PT}, and auxiliary power unit M_{APU} mass estimation are taken from Roskam as follows:

$$M_{OX} = (7/2.205)(C_{REW} + P_{AX})^{0.702} \quad \text{B182}$$

$$M_{BC} = [0.0646\ (P_{AXmax})^{1.456}] / 2.205 \quad \text{B183}$$

$$M_{AUX} = 0.01 \times M_E \quad \text{B184}$$

$$M_{APU} = 0.004 \times M_{to} \quad \text{B185}$$

$$M_{PT} = 0.0045 \times M_{to} \quad \text{B186}$$

According to [14] aircraft system mass can also be represented fairly accurately by the following single relationship. This is used in CACAD as an option for the confidence of the user.

$$M_{SYS} = J_{sys1} + J_{sys2} \times M_{PAX} + J_{sys3} \times M_{to} + J_{sys4}(\frac{S_{LE} \times Eles}{Ele} + S_{FTE})^{2/3}$$

$$+ J_{sys5}\ (S_{EMP})^{2/3} + J_{sys6} \times Span \times sec(\Lambda_{1/4}) \quad \text{B187}$$

Above relation does not include the mass of avionics system. J_{sys1} to J_{sys6} are empirical constants and are given in data file and also in Appendix A.

B2.18 Aircraft Take-off Mass Module

Aircraft major masses are fuselage group mass, wing group mass, airframe mass , empty mass, zero fuel mass, maximum zero fuel mass, landing mass, maximum landing mass, and take-off mass. They are formulated in CACAD as follows :

$$M_{WINGC} = M_{WING} + 1/2\, M_{SYS} \quad \text{B188}$$

$$M_{FUSC} = M_{FUS} + M_{FUR} + 1/2\, M_{SYS} + M_{PAX} + M_{CREW} + M_{EL} \quad \text{B189}$$

$$M_{AF} = M_{FUS} + M_{FUR} + M_{EL} + M_{SYS} + M_{PEN} + M_{UC} \quad \text{B190}$$

$$M_E = M_{AF} + Meng \quad \text{B191}$$

$$Z_{FM} = M_{AF} + M_{PAY} + M_{CREW} + Meng \quad \text{B192}$$

$$Z_{FMmax} = M_{to} - M_{FUEL} + M_{PAY}\,(H_{payf} - 1) \quad \text{B193}$$

$$M_{LDG} = M_{SSB} - M_{fuel\text{-}cruise}\,(1 + K_{fcl}) \quad \text{B194}$$

$$H_{MLDG} = Z_{FM} + H_{mldgf} \times M_{to} \quad \text{B195}$$

$$M_{to} = Z_{FMmax} + M_{FUEL} \quad \text{B196}$$

B2.19 Aircraft Pricing

There are number of approaches to this section. The simple Roskam empirical relation is as follows

$$A_{mp} = \log_{10}^{-1}[3.3191 + 0.8043 \log_{10}(M_{to} \times 2.205)] \quad \text{B197}$$

This relation must be multiplied with price index factor between 1989, and 1995. It is an appropriate relation for quick determination of airplane market price. A more detail approach consisting of RDT&E cost and production cost is used as VCW cost implication modelling in Chapter 4 (and App. D). For CACAD the most useful approach is a pricing system that distinguishes the share of each major component of aircraft in final pricing. This approach exists in [14] which was used in CACAD and is presented below:

$$P_{fus} = K_{pfus} \times M_{FUS} \quad \text{B198}$$

$$P_{wbx} = K_{pwbx} \times M_{WBX} \quad \text{B199}$$

$$P_{wle} = K_{pwle} \times M_{WLE} \quad \text{B200}$$

$$P_{wte} = K_{pwte} \times M_{WTE} \quad \text{B201}$$

$$P_{el} = K_{pel} \times M_{EL} \quad \text{B202}$$

$$P_{sys} = K_{psys} \times M_{SYS} \quad \text{B203}$$

$$P_{pen} = K_{ppen} \times M_{PEN} \quad \text{B204}$$

$$P_{fur} = K_{pfur} \times M_{FUR} \quad \text{B205}$$

$$P_{uc} = K_{puc} \times M_{UC} \quad \text{B206}$$

$$P_{eng} = K_{peng} \times Meng \quad \text{B207}$$

$$P_{af} = P_{uc} + P_{fur} + P_{pen} + P_{sys} + P_{el} + P_{wte} + P_{wle} + P_{wbx} + P_{fus} \quad \text{B208}$$

$$P_{AC} = P_{eng} + P_{uc} + P_{fur} + P_{pen} + P_{sys} + P_{el} + P_{wte} + P_{wle} + P_{wbx} + P_{fus} \quad \text{B209}$$

The cost coefficient (£/kg, 1993) used in the above relations are very useful to remember. They are purposely given below so that the cost implication of each aircraft major component become evident. They have strong interference with DOC, and hence an optimum aircraft.

K_{pfus}	K_{pwbx}	K_{pwle}	K_{pwte}	K_{pel}	K_{psys}	K_{ppen}	K_{pfur}	K_{puc}	K_{peng}
411	476	810	810	2700	1188	411	972	810	46444

B3. Constraint Module of CACAD

The following constraints are adequate to produce a reasonable aircraft, fulfilling safety, and regulatory enforced requirements. They will also help to include some implications of R&M modelling in next Appendices.

B3.1 Approach Conditions

This constraint ensures that the aircraft is designed to have stall speed adequately smaller than the prescribed approach speed (usually 70 m/s) :

$$V_{SA} \times 1.3 - V_A = 0 \quad \text{B210}$$

$$V_{SA} = \{H_{MLDG} \times g / [0.5 \times \rho_{app} \times S_g \times C_{Lmax\,app}]\}^{0.5} \qquad \text{B211}$$

All terms in RHS are already described in previous sections. When the constraint is not fulfilled, CACAD changes wing area.

B3.2 Take-off run Limitation

In order to take-off at a prescribed take-off distance D_{to} , following constraint must be fulfilled :

$$D_{to} - T_{od} \geq 0 \qquad \text{B212}$$

T_{od} is take-off distance produced by aircraft.

$$T_{od} = \frac{K_{tod} \times M_{to}^{2} \times g \times J_{TTOD}}{Meng1 \times C_{Lto} \times S_g \times \rho_{to}} \qquad \text{B213}$$

K_{tod} is an empirical constant derived from a correlation of take-off data for current transport aircraft (typical value is 1.556) [14]. *Meng1* is the mass of engine sufficient for this constraint. When the constraint is not fulfilled, CACAD changes aircraft engine mass.

B3.3 Climb-out Gradient with One Engine Cut

The regulatory enforced gradient varies with the number of engines :

$$G_{amma} = G_{amma2} + 0.003\,(N_e - 2) \qquad \text{B214}$$

where G_{amma2} is the required gradient for a twin engine aircraft. Its value is an input data. The required engine thrust required to fulfil above constraint is given below :

$$Meng2 = \frac{Ne \times Mto \times g \times J_{TTOD}\{(C_{Dto} + C_{Dyefh}) / C_{Lto} + Gamma\}}{Ne - 1 - Eftkwm} \qquad \text{B215}$$

E_{ftkwm} is an allowance for the windmilling, and the spillage drag and is given by the following empirical expression :

$$E_{ftkwm} = \{\rho_{to} \times (V_{TO})^2 \times J_{ttog} \times (W_{dc} + S_{dc})\} / (2 \times J_{tsta0}) \qquad \text{B216}$$

Drag coefficient at take-off :

$$C_{dto} = C_{D0} + K_{cr} \times (C_{Lto})^2 / (\pi \times AR) + C_{Dvfto} + C_{Dpfto} \qquad \text{B217}$$

C_{Dvflo} , , C_{Dpflo} , and C_{Dyefh} are drag coefficients associated with vortex drag due to flaps, incremental profile drag coefficient due to flap deflection, and yaw drag coefficient respectively. There are a chain of empirical expressions for deriving above coefficients [14, section 12.2.1]. They are included in the listing of CACAD.

B3.4 Thrust Requirement for Cruise

This constraint ensures, the engine sizing is sufficient to produce the required cruise thrust, plus a given rate of climb (climb gradient) at the beginning of cruise.

$$Meng3 = J_{tcr} \times T_{req} \qquad \text{B218}$$

$$T_{req} = Q_{cr} \times S_g \times C_{Dcr} + M_{SSCR} \times g \times C_{rxta} \times 3.6 / V_{cruise} \qquad \text{B219}$$

C_{rxta} is the required rate of climb at the beginning of cruise, and is given as input data.

B3.5 Engine-failed Height Requirement

This constraint ensures that there will be adequate thrust, i.e. engine size (mass) to maintain a small climb gradient in the event of an engine failure at some prescribed height E_{fh}, shortly after take-off.

$$Meng4 = J_{tefh} \times T_{efh} \qquad \text{B220}$$

$$T_{efh} = \frac{Ne}{Ne - 1 - Efhkwm} D_{rgefh} + G_{maefh} \times M_{to} \times g \qquad \text{B221}$$

$$E_{efhkwm} = \{ \rho_{efh} \times (V_{EFH})^2 \times J_{tefh} \times (W_{dc} + S_{dc}) \} / (2 \times J_{tsta0}) \qquad \text{B222}$$

$$J_{tefh} = J_{efd0} / \{ E_{fh0} + E_{fh1} \times E_{fhm} + E_{fh2} \times (E_{fhm})^2 + E_{fh3} \times (E_{fhm})^3 \qquad \text{B223}$$

$$E_{fhm} = V_{EFH} / S_{sdefh} \qquad \text{B224}$$

$$D_{rgefh} = 2 \{1/2 \, \rho_{efh} \times (V_{EFH})^2 \times S_g \times C_{D0} \} \quad \text{(for minimum drag case)} \qquad \text{B225}$$

$$V_{EFH} = \{ \frac{Kcr \times Mto^2 \times g^2}{S_g \times C_{D0} \times \pi \times b^2 \times 1/4 \times (\rho_{efh})^2} \}^{0.25} \qquad \text{B226}$$

G_{maefh} is the prescribed climb gradient, and $E_{fh0,1,2,3}$ are coefficients in the expression of engine mass thrust ratio. All are input values.

B3.6 Missed-approach Requirement

This constraint ensures that the aircraft while approaching is capable of climbing again, with one engine in-operative. This is equivalent to the throttle limit constraint

in collingbourne's methodology (the amount of the throttle back of the engines, which is permitted on the approach, so that they are capable of being opened up again in the event of an aborted landing). The following expression gives the required thrust, and includes the spillage, as well as windmilling effect :

$$Meng5 = \frac{Ne}{Ne - 1 - Efakwm} Hmldg \times g \times Jttoa(\frac{C_{DA} + C_{dya}}{C_{LA}} + \beta_a) \qquad \text{B227}$$

$$E_{fakwm} = \{ \rho_a \times (V_A)^2 \times J_{ttoa} \times (W_{dc} + S_{dc}) \} / (2 \times J_{tsta0}) \qquad \text{B228}$$

Special Note : In the constraint equation solving module of CACAD, the values of *Meng1 to 5* are determined using above expressions. Thereafter the highest among them is found. This is then compared with the engine mass assumed earlier in the program. An algorithm is built in the module to adjust engine mass to the highest value dictated by the constraints.

B3.7 Fuel Volume Limitation

This constraint ensures that there is enough space within the wing (and extended into wing / fuselage intersection) for the fuel tank to contain the mission fuel mass estimated in previous modules. Following geometrical relationships determine the fuel tank capacity within the wing, between the spars :

$$V_{t0} = 4. \times K_{vt} \times TC \times S_g \times GMC \times (1.\text{-}Ele\text{-}Ete)/(1 + S_g)^2 \qquad \text{B229}$$

$$V_{t1} = (1 - V_{tl2}) - (1 + V_{tl1}) \times F_{USD} / b \qquad \text{B230}$$

$$V_{t2} = (1 - S_g) \times \{(1 - V_{tl2})^2 - [(1 + V_{tl1}) \times F_{USD} / b]^2 \} \qquad \text{B231}$$

$$V_{t3} = (1 - S_g)^2 \times \{(1 - V_{tl2})^3 - [(1 + V_{tl1}) \times F_{USD} / b]^3 \} / 3 \qquad \text{B232}$$

$$V_{TA} = V_{t0} \times (V_{t1} - V_{t2} + V_{t3}) \qquad \text{(Tank Volume)} \qquad \text{B233}$$

$$M_{FUELT} = M_{FUEL} + K_{pay} \times M_{PAY} \qquad \text{B234}$$

$$V_{FUEL} = M_{FUELT} / 800. \qquad \text{B235}$$

According to this constraint, V_{FUEL} must be either equal to or less than V_{TA} . If there is a shortage of fuel tank capacity, CACAD allows the V_{tl1} , and V_{tl2} to change their values so that fuel tank is extended towards the tip of the wing, on one side, and towards the fuselage centre line on the other.

B3.8 Buffet Onset Limitation

A transport aircraft would require a lift coefficient at the beginning of the cruise, determined pre-dominantly by its payload,and range. This is termed as $C_{L\ crb1}$ in CACAD. This must be 1.3 times away from the $C_{L\ buffet}$ [32] that the wing is capable of producing.

$$C_{L\,buffet} - 1.3 \times C_{L\,crb1} \geq 0 \qquad \text{B236}$$

Delta Method [39] was used to establish the value of $C_{L\ buffet}$. A surface was made to fit with characteristic 3-D curve of Fig. 28 of the above reference with the help of Mathematica [127]. This produced the following correlation equation :

$$C_{L\,buffet} = C_{L\,des} + \{AR \times [1.+ 0.1(h/c)] / Cos(\Lambda_{1/4})\} \times$$

$$\{0.029522 - 0.5933 \times D_{mdes} - 5.01333 \times (D_{mdes})^2 - 0.139333 \times TC^{2/3} +$$

$$0.15 \times TC^{2/3}\} \qquad \text{B237}$$

$C_{L\ des}$ is the design lift coefficient and is given by the following equation fit to the curve of Fig.1 of [39]

$$C_{L\,des} = \{Cos(\Lambda_{1/4}) \times [1.+ 0.1(h/c)] / (AR)^{0.5}\} \times$$

$$\{0.14911 + 0.151345 \times AR + 0.002114 \times AR^2\} \qquad \text{B238}$$

$$D_{mdes} = M_{2D} + D_{M\,sweep} + D_{M\,aspect\ ratio} \qquad \text{B239}$$

M_{2D} , $D_{M\,sweep}$, and $D_{M\,aspect\ ratio}$ are found from the following equations developed by using Figs.3, and 4 of [39].

$$M_{2D} = \{1. + 0.241647 - 0.12416 \times C_{L\,crb1} - 2.7077 \times TC^{2/3} + 1.59765 \times TC^{4/3}\}^{0.5}$$

B240

$$D_{M\,sweep} = 0.00328985 - 0.0005 \times \Lambda_{1/4} + 0.00005971 \times (\Lambda_{1/4})^2 \qquad \text{B241}$$

$$D_{M\,aspect\ ratio} = -0.000527 + 0.1432 \times (1./AR) \qquad \text{B242}$$

B3.9 Aspect Ratio Sweep Requirement

This constraint prescribes a limit which restricts optimum solution to an aspect ratio / sweep range applicable to existing transport aircraft to prevent any stability and control problem.

$$A_{SWPLT} \geq AR \times [Tan\ (\Lambda_{1/4})^{0.378}] \qquad \text{B243}$$

A_{SWPLT} is the limiting value of aspect ratio-sweep constraint, and is an input value (App.A).

B4. Objective Function DOC and Maintenance Cost Module

The objective function in CACAD is DOC, which reflect aircraft performance, geometry, mass, and cost assembled together. The methodology for DOC in CACAD has been described in Chapter 2. Here the formulation of DOC module is presented. Maintenance cost breakdown, and number of approaches are also dealt with in detail along with standing charges cost breakdown. The coefficients of different empirical equations from [13], and [14] were developed from 1970 to 1993 values.

According to MVO method [13,14], DOC of a jet transport aircraft is composed of cost of fuel, deck (pilot, and co-pilot), landing fee, maintenance, and standing charges. Following formulations are for DOC per flight.

$$DOC = DOC_f + DOC_{lf} + DOC_m + DOC_{sc} \qquad \text{B243}$$

$$DOC_f = M_{fuelu} \times P_{fuel} \qquad \text{B244}$$

$$M_{fuelu} = M_{fuel\text{-}cr} + M_{fuel\text{-}allowance} + M_{fuel\text{-}contingency} \qquad \text{B245}$$

$$DOC_{lf} = 0.0028 \times M_{to} \qquad \text{B246}$$

The labour maintenance cost equations are functions of the article's maintenance man hours per flight, and include flight block hours. On the other hand the maintenance material equations are functions of article's market price.

$$DOC_m = DOC_{me} + DOC_{aflm} \qquad \text{B247}$$

$$DOC_{me} = DOC_{el} + DOC_{em} \qquad \text{B248}$$

$$DOC_{em} = C_{emm} \times P_{eng} \times (T_{BLOC})^{0.5} \qquad \text{B249}$$

$$T_{BLOC} = T_{flt} + C_{bloc} \qquad \text{B250}$$

$$T_{flt} = Stage / V_{CR} + L_{time} \qquad \text{B251}$$

$$L_{time} = \frac{D_{hten}}{V_{CR}} \left(\frac{1.2}{S_{thowt} - C_{Lcr}/C_{Dcr}} + \frac{C_{Lcr}}{3C_{Dcr}} \right) \qquad \text{B252}$$

$$DOC_{el} = N_e \times R_L \times F_b \times M_{pfeng} \quad \text{B253}$$

$$M_{pfeng} = C_{emL1} + C_{emL5} \times W_{uneng} \, (T_{BLOC})^{0.5} \quad \text{B254}$$

$$DOC_{aflm} = DOC_{afmt} + DOC_{aflt} \quad \text{B255}$$

$$DOC_{afmt} = C_{amm} \times P_{af} \times (T_{BLOC})^{0.5} \quad \text{B256}$$

$$DOC_{aflt} = R_L \times F_b \times M_{pfaf} \quad \text{B257}$$

$$M_{pfaf} = C_{amL1} + C_{amL5} \times M_{AF} \, (T_{BLOC})^{0.5} \quad \text{B258}$$

Further airframe maintenance breakdown shall be done separately in the next section. Standing cost is composed of airframe, and or engine which is the sum of residual value at the end of their life, interest rate of their prices, residual value of their spare parts, interest rate of their spare parts, and insurance. All are calculated per flight.

$$DOC_{sc} = DOC_{scAF} + DOC_{scEN} + DOC_{scINS} \quad \text{B259}$$

$$DOC_{scAF} = (S_{c1} \times P_{AF} \times T_{BLOC})/U \quad \text{B260}$$

$$DOC_{scEN} = (S_{c2} \times P_{EN} \times T_{BLOC})/U \quad \text{B261}$$

$$DOC_{scINS} = (S_{c3} \times P_{AC} \times T_{BLOC})/U \quad \text{B262}$$

$$S_{c1} = \frac{1 - R_{esval}}{A_{clife}} + \frac{X_{\text{int}}}{2} + S_{cpAF} \times \frac{1 - R_{esval}}{A_{clife}} + S_{cpAF} \times \frac{X_{\text{int}}}{2} \quad \text{B263}$$

$$S_{c1} = (1 + S_{cpAF})(\frac{1 - R_{esval}}{A_{clife}} + \frac{X_{\text{int}}}{2}) \quad \text{B264}$$

$$S_{c2} = (1 + S_{cpENG})(\frac{1 - R_{esval}}{A_{clife}} + \frac{X_{\text{int}}}{2}) \quad \text{B265}$$

$$S_{c3} = X_{INS} \quad \text{B266}$$

Further standing charges cost breakdown shall be done separately in the next section.

F_b is maintenance burden factor, and R_L is the labour rate and C_{emm} , C_{emL1} , C_{emL5} , C_{amm} , C_{amL1} , C_{amL5} are coefficients of equations. S_{cpAF} , S_{cpENG} are coefficient of spare part cost equation, and A_{clife} is the life of the article, X_{INS} , X_{int} are coefficient for insurance, and interest rate in standing charge cost. They are supplied in data file, and Appendix A.

For reasons elaborated in Chapter 2, the airframe maintenance cost and standing charge cost are required to be divided into different airframe subsections. Also structural elements of airframe must be further divided into major sub-sections. This shall be useful for the ASRE, and the VCW modelling integration into CACAD.

B4.1 Airframe Maintenance Cost Breakdown, Approach 1

This cost DOC_{aflm} is composed of labour DOC_{aflt} and material cost DOC_{afmt}. Each shall be dealt with separately. The labour cost is composed of two part. In the first part the maintenance labour cost of airframe major sections are determined using Serghides predicting equations [7]. In the second part the structural labour cost is further divided to its sub-sections based on merits obtained by application of MIL-HDBK-472 [93].

B4.1.1 Maintenance Labour Cost Major Sections

In this approach airframe maintenance man hours are divided proportionately based on Serghides equations [6,7]. This method is also supported by Professor P.G. Pugh. The aircraft parameters determined by CACAD are applied to the predicting equations of [7] to produce maintenance man-hours of each airframe major ATA chapter. These values are then added, and divided by each section. These results give the share of each ATA chapter with respect to the sum of airframe maintenance cost. These ratios are then applied to CACAD total airframe maintenance man-hours determined by MVO method to arrive at individual section.

For some aircraft parameters used in Sergheidis relations simple correlation equations were developed using the existing transport aircraft reported in [43] as follows

$W_T = 0.199\ Span$ (Wheel track)

$W_B = 0.368\ F_{USL}$ (Wheel base)

$H_C = 0.58\ F_{USD}$ (Cabin Height)

$H = Span / 2.7$ (Aircraft height)

$Y_r = 1994\text{-}1959$ (The base year in Sergheidis formulea)

Auto-flight (ATA-22), Communication (ATA-23), Instrument (ATA-31), Navigation (ATA-34) are assumed together as avionics systems.

$$M_{phAV} = (0.9254 - 0.7433E\text{-}04 \times Range + 0.571E\text{-}06 \times M_{to})(0.563 + 0.5391E\text{-}01\ Y_r)$$
$$+ (-0.1667E\text{-}01 + 0.1459E\text{-}02 \times P_{AXmax} - 0.1185E\text{-}01 \times H)\ (1.795 - 0.0683\ Y_r)$$
$$+ (-0.02723 - 0.5012E\text{-}05 \times H_{tmcr} + 0.125E\text{-}03\ V_{CR})\ (0.897 + 0.01345Y_r)$$
$$+ (0.09285 - 0.2451E\text{-}05\ M_{to} - 0.4544E\text{-}02 \times H)\ (1.167 - 0.0175\ Y_r)$$

B267

Electrical system : ATA-24 B268

$$M_{phELS} = (-0.3107 + 0.146\ F_{USD} - 0.1876E\text{-}06 \times T_{stav})\ (1.228 - 0.03082Y_r)$$

Lights : ATA-33 B269

$$M_{phLI} = exp(-0.4929 + 0.8752E\text{-}04 \times Range + 0.0813\ H)\ (1.522 - 0.02555Y_r)$$

Furnishing : ATA-25 B270

$$M_{phFUR} = exp(-1.393 + 0.6634E\text{-}04 \times Range + 0.002085\ P_{AXmax})\ (1.262 - 0.0199Y_r)$$

Flight controls system : ATA-27 B271

$$M_{phFC} = exp(-17.1 + 0.01612V_{CR} + 0.001059P_{CL} \times F_{USD} \times H_C)\ (1.302 + 0.02293Y_r)$$

Air-conditioning System :ATA-21 B272

$$M_{phAIR} = (-0.08355 + 0.5627E\text{-}06 \times M_{to} + 0.3966E\text{-}02 \times F_{USL})\ (1.431 - 0.05187 \times Y_r)$$

Pneumatic system :ATA-36 B273

$$M_{phPN} = (-0.1077 + 0.1742E\text{-}04 \times H_{tmcr} + 0.6617E\text{-}04 \times P_{AXmax})\ (1.956 - 0.0559 \times Y_r)$$

Ice and rain protection system : ATA-30 B274

$$M_{phICE} = exp(-6.256 + 0.9306 \times F_{USD} - 0.168E\text{-}04 \times M_E)\ (1.592 - 0.04256 \times Y_r)$$

Fuel system :ATA-28 B275

$$M_{phFS} = exp(-3.68 + 0.9513E\text{-}04 \times Range + 0.0051 \times Span)\ (1.47 - 0.0369 \times Y_r)$$

Under-carriage :ATA-32

$$M_{phUC} = exp(-0.4235 - 0.7232E\text{-}05 \times M_{PAY})\ (1.146 - 0.004462 \times Y_r)$$ B276

Oxygen system : ATA-35

$$M_{phOX} = exp(-9.35 + 2.788\ H_C - 0.006671 \times F_{USL})\ (2.586 - 0.0989 \times Y_r)$$ B277

Water waste system :ATA-38 B278

$$M_{phWW} = exp(-5 + 0.403 \times F_{USD} - 0.159E\text{-}05 \times M_E)\,(1.061 + 0.01364 \times Y_p)$$

Structure :ATA-52 to 57 B279

$$M_{phSTR} = (-0.7227 + 0.1705 \times W_T + 0.7411E\text{-}05 \times M_E)\,(1.151 - 0.01584 \times Y_p)$$

Fire protection system :ATA-26 B280

$$M_{phFIR} = (0.30E\text{-}02 + 0.88E\text{-}06 \times M_{PAY} - 0.205E\text{-}07 \times T_{stay})\,(1.11 - 0.0135 \times Y_p)$$

B4.*1.1.1 Breakdown of Maintenance Labour Cost for Structure*

It is essential to break down the maintenance cost of structure into its main constituents in order that, the VCW maintenance implications be investigated in Chapter 4. The main sub-sections of aircraft structure are fuselage, wing box, wing LE, wing TE flap, wing TE aileron, horizontal tail, vertical tail.

In this approach two criteria were considered. First, the mass of each section with respect to total structural mass is considered. The bigger the mass, the higher maintenance man-hours it would require. Second is the number of scores each section achieves when MIL-HDBK-472 is applied for it. The standard contains criteria that are reasonably appropriate for a merit analysis. The Table B-1 show the type of merit each major structural section obtained.

The formula below determines the amount of time for removal and replacement of the above major structural items. It is used a symbolic merit for allocating a reasonable share for each structural item within the total structural labour maintenance cost.

$$MC = \log^{-1}(3.54651 - 0.02512\,A - 0.03055\,B - 0.01093\,C) \quad \text{B281}$$

$MC_{FUS} = 962$, $MC_{WBX} = 230$, $MC_{WLE} = 227$, $MC_{VT} = 757.5$, $MC_{WTEF} = 305$

$MC_{HT} = 876$, $MC_{WTER} = 261$, Sum = 3619.5

The percentage merit of each section is then found with respect to the sum. Assuming that total maintenance man-hours per flight for structure is M_{pfSTR} , the following relationship determines the share of maintenance man-hours of each major structural sections, based on individual mass, and MIL hand book merits obtained above.

$$M_{pfWTER} = [(0.0722 + M_{WTER} / M_{STR}) \times M_{pfSTR}]/2 \quad \text{B282}$$

$$M_{pfWTEF} = [(0.0842+M_{WTEF}/M_{STR}) \times M_{pfSTR}]/2 \quad \text{B283}$$

$$M_{pfFUS} = [(0.2658+M_{FUS}/M_{STR}) \times M_{pfSTR}]/2 \quad \text{B284}$$

$$M_{pfWBX} = [(0.0635+M_{WBX}/M_{STR}) \times M_{pfSTR}]/2 \quad \text{B285}$$

$$M_{pfWLE} = [(0.0627+M_{WLE}/M_{STR}) \times M_{pfSTR}]/2 \quad \text{B286}$$

$$M_{pfTP} = [(0.2421+M_{TP}/M_{STR}) \times M_{pfSTR}]/2 \quad \text{B287}$$

$$M_{pfFIN} = [(0.209+M_{FIN}/M_{STR}) \times M_{pfSTR}]/2 \quad \text{B288}$$

B4.1.2 Maintenance Material

The maintenance material for airframe is divided according to the share of price each section is contributing to total aircraft price. Using table in section 16 of B2.1. A typical case for fuselage is presented below :

$$DOC_{mFUS} = (P_{fus} / P_{AC}) \times DOC_{afmt} \quad \text{B289}$$

This is extended to all airframe and even structural sub-sections having identical relations. The rest of the relations are found in CACAD listing.

B4.2 Airframe Maintenance Cost Breakdown, Approach 2

In this approach the maintenance cost of the airframe DOC_{aflm} which was determined in previous section B2.2 equations B220 to B223 shall be subjected to further breakdown using approach number 2. This approach is based on [38]. Table B-2 is based on the data supplied from maintenance divisions of airlines. These percentages were used to break the airframe maintenance cost.

The usefulness of this table is evident in its ability to help break the maintenance cost using above percentages. This shall be applied to derive the structure maintenance material and labour cost part of total airframe maintenance cost as below. For other airframe sections see the program listing in Appendix E.

$$DOC_{mlSTR} = 0.125 \times DOC_{aflm} \quad \text{B289}$$

$$DOC_{lSTR} = 0.65 \times DOC_{mlSTR} \quad \text{B290}$$

$$DOC_{mSTR} = 0.35 \times DOC_{mlSTR} \quad \text{B291}$$

Table B-1 : Merit allocation to major sections of structure using MIL-HDBK-472

Criteria	*Fuselage*	*Wing box*	*Wing LE*	*Wing TE flap*	*WingTE Aileron*	*Horizo-ntal Tail*	*Vertical Tail*
Access (external)	2	1	1	1	1	1	0
Latches&Fast. (ext.)	2	2	2	1	2	1	1
Latches&Fast. (int.)	1	0	0	0	0	0	0
Access internal	2	1	1	1	1	0	0
Package	2	2	1	1	1	1	0
Units - Parts	2	1	1	1	1	0	0
Visual displays	3	2	2	2	2	1	1
Fault indications	3	2	2	2	2	1	1
Test points	2	2	2	2	2	1	1
Test points Identifi.	2	1	1	1	1	1	0
Labelling	2	2	2	1	2	1	1
Adjustment	0	2	2	2	2	0	1
Testing	-	-	-	-	-	-	-
Protective devices	2	1	1	1	1	1	1
Safety	3	2	2	2	2	0	0
Total A	28	21	20	19	20	9	7
External Test Equip.	2	1	1	1	1	1	1
Connectors	3	2	2	2	2	1	1
Jiggs & Fixtures	3	2	2	2	2	1	1
Visual Contact	3	3	3	2	3	1	1
Assistant Operation	1	2	2	2	2	1	1
AssistantTechnical	0	2	2	1	1	1	2
Assistant Supervisory	0	2	2	2	2	1	2
Total B	12	14	15	12	13	7	10
Arm leg & back stre.	1	2	2	2	2	1	2
Endurance & energy	0	2	2	2	2	1	1
Eye & hand co-ord.	2	2	2	2	2	1	1
Visual acuity	2	2	2	2	2	2	1
Logical analysis	2	2	2	2	2	2	2
Memory, ideas	2	2	2	2	2	2	2
Planfulness, resouce.	1	2	2	2	2	1	2
Alertness, cautious	3	3	3	2	3	1	1
Concentration, persi.	2	2	2	2	2	2	2
Initiative	2	2	2	2	2	2	2
Total C	17	21	21	20	21	15	17

But two areas are necessary to be further divisioned to help CACAD for VCW implications in Chapter 4. One is hydraulics, that must be separated from electrical system, and the other is the structure. For such divisioning, a new approach was taken, which will be described for structure only.

Table B-2 : % share of maintenance cost (labour & material) of aircraft systems in the airframe.[38]

Airframe sections	*% with respect to total airframe maint. cost*	*% Material*	*% Labour*
Avionics	11.5	33	67
Passenger : ECS, Oxygen, Water waste, Furnishing	22	30	70
Power systems : Hydraulic and Electrical	15.5	54	46
Flight control system	7	60	40
Undercarriage	26	59	41
Structure	12.5	35	65
Miscellaneous : Fire, Fuel, Ice-Protection, Light	5.5	35	65

B4.2.1 Criteria for Structure Sub-division

Structural maintenance is primarily consists of repairing corrosion damages, cracks specially around fasteners, loosened fasteners, inspection and perhaps paint removal of number of parts, the LE, and TE devices shafts, rotating parts, hinges, bearings, etc. The higher exposed surfaces of the structural section would result in higher number of fasteners, and more cracks, and the deeper and extended corrosion. The labour man-hours derived from Serghides equations were also treated as on of the decisive factors. There are other factors that influence the structure maintenance cost. They have been classified as internal, and external. The internal factors are briefly described below:

- Stress, strain, and deflection : The wing is more under stress and strain, and deflection than the fuselage. This may be a major factor in causing cracks, and other damages.
- Fuel leakage : Presence of fuel tank and fuel lines increases the possibility of fuel leakage and hence higher maintenance work.
- Pressurisation : This is also another source that enhances structural failure, and helps to increase maintenance work.

- Sanitation : The existence of toilets, and toilet drainage has always caused neighbouring structure to corrode faster.
- Cut outs : The higher their number the more stress concentration, and stress corrosion.
- Piping, wiring, ducting, and cables, etc. : Their higher number causes more maintenance such as high pressure leakage, duct cracking, wire conductivity tests, and their chafing, nicks, and dents, etc.

The external factors are briefly described as below :

- Corrosion, friction etc. : Some structural sections of the airframe offer more chances of chemical damages than others. Either due to large number of sheet metal parts assembled, or large number of mechanism with un-similar material in close contact.
- FOD : Some structural assemblies offer higher chances of getting hit by foreign objet damage than others.
- Accessibility Potential : In some structural assemblies, accessibility provision is easier to incorporate. This is obvious for fuselage than wing.
- Number of sub-assemblies & Parts : The more the number of sub-assemblies the higher the chances of longer maintenance time. Also if the assembly is composed of numerous parts, bits, and pieces, they are more prone to failure, and dissimilar material corrosion, and failure propagation etc.
- GSE damage : Ground support equipment that are driven toward aircraft for all sorts of reasons have damaged structure according to experience of the Author. They damage fuselage much more than wing.

If we assign a highest merit of 4 to highest affected structural section, the following table may then represent a merit study of above criteria applied to major structural sections :

Table B-3 : External, and internal criteria for sub-dividing airframe structure maintenance cost.

Structural Items External & Internal Factors	*Fuselage*	*Wing Box*	*Wing L.E*	*Wing TEF*	*Tail Plane*	*Fin*	*Wing TER*
1. Corrosion & Friction Etc.	4	1	2	2	3	3	1
2. FOD	4	1	2	1	2	2	1
3. Accessibility Potential	2	2	2	3	4	4	2
4. Number of Assemblies & Parts	3	2	2	3.5	2	2	1.5
5. GSE damage	4	1	2.5	1.5	1.5	1	1.5
Sum	17	7	10.5	11	12.5	13	7
Total Sum	78						
1. Stressing	2	4	3	2	2	2	1
2. Fuel Leak	2	4	1	1	1.5	1.2	1
3. Pressurisation	4	1	1	1	1	1	1
4. Sanitation	4	1	1	1	1	1	1
5. Cut-outs	4	1.5	1	1	1.2	1.2	1
6. Piping, Ducting, Wiring, ect.	4	2	1.5	1.3	1.3	1.3	1
Sum	20	13.5	8.5	7.3	8	7.7	6
Total Sum	71.2						

The internal and external factor merits, external surface area as well as labour man-hours from Serghides equation shall be applied for divsioning of aircraft structure labour cost. The above factors but price to replace labour equations shall be also applied for divsioning of aircraft structure material cost. This is shown for fuselage part of aircraft structure below. For other structural sections see the program listing in Appendix E.

$$DOC_{mFUS} = \frac{\frac{S_{FUS}}{S_T} + \frac{17}{78} + \frac{20}{71.5} + \frac{P_{FUS}}{P_{STR}}}{4} \times DOC_{mSTR} \qquad \text{B292}$$

$$DOC_{lFUS} = \frac{\frac{S_{FUS}}{S_T} + \frac{17}{78} + \frac{20}{71.5} + \frac{M_{pfFUS}}{M_{pfSTR}}}{4} \times DOC_{lSTR} \qquad \text{B293}$$

B4.3 Standing Charges Cost Breakdown

The coefficients within empirical equation of standing charges in MVO can be reasonably classified so that this cost be sub-divided into airframe major sections, and even structural sub-sections.

$$DOC_{scAF} = (S_{c1} \times P_{AF} \times T_{BLOC})/U \qquad \text{B294}$$

$$S_{c1} = \frac{1 - R_{esval}}{A_{clife}} + \frac{X_{\text{int}}}{2} + S_{cpAF} \times \frac{1 - R_{esval}}{A_{clife}} + S_{cpAF} \times \frac{X_{\text{int}}}{2} \qquad \text{B295}$$

S_{cpAF} according to [14] is 0.06 i.e. 6% of the airframe price. This value of spares price holding shall be spent for maintenance of airframe in its whole life as fraction of airframe price . The cost of spares of each sub-division of airframe is reasonably decided according to the percentage of maintenance cost. These percentages are taken from the table in section B.2.2.2. Therefore the following relation are established :

$$S_{cpAV} = \{((P_{av}/P_{af}) + 0.115) \times S_{cpAF}\} / 2 \qquad \text{B296}$$

$$S_{cpPAS} = \{((P_{fur}/P_{af}) + 0.22) \times S_{cpAF}\} / 2 \qquad \text{B297}$$

$$S_{cpFC} = \{((P_{fc}/P_{af}) + 0.07) \times S_{cpAF}\} / 2 \qquad \text{B298}$$

$$S_{cpUC} = \{((P_{uc}/P_{af}) + 0.26) \times S_{cpAF}\} / 2 \qquad \text{B300}$$

$$S_{cpM} = \{((P_{sys}/P_{af}) + 0.055) \times S_{cpAF}\} / 2 \qquad \text{B301}$$

$$S_{cpSTR} = \{((P_{str}/P_{af}) + 0.125) \times S_{cpAF}\} / 2 \qquad \text{B302}$$

$$S_{cpPOW} = \{((P_{sys}/P_{af}) + 0.155) \times S_{cpAF}\} / 2 \qquad \text{B303}$$

R_{esval} is the residual value of the airframe at the end of its life as fraction of airframe price. It is the money the owner of the airframe obtains from the sale of her airframe due to perhaps good maintenance practices, and initial durable design of aircraft. Although for some aircraft some money has to be paid for its salvation. This value was zero 20 years ago, but from sources in RAE they assign 0.1 to R_{esval} .

By reasonable engineering judgement R_{esval} for sub-sections of airframe can be established.

If we assume airframe has residual value of 0.1 after 20 years life, then avionics which has shortest life of 5 years (Roskam) must be sold for nearly nothing. In following table the residual values are allocated according to the age of the airframe major sections :

Airframe sections	*Life (A_{obj})*	*Fraction*	*R_{esval}*
Avionics	5 (L_{AV})	(5/90)×0.1	0.0055 (R_{AV})
Passenger : ECS, Oxygen, Water waste, Furnishing	10 (L_{PAS})	(10/90)×0.1	0.011 (R_{PAS})
Power systems : Hydraulic and Electrical	15 (L_{POW})	(15/90)×0.1	0.0166 (R_{POW})
Flight control system	15 (L_{FC})	(15/90)×0.1	0.0166 (R_{FC})
Undercarriage	15 (L_{UC})	(15/90)×0.1	0.0166 (R_{UC})
Structure	20 (L_{STR})	(20/90)×0.1	0.0222 (R_{STR})
Miscellaneous : Fire, Fuel, Ice-Protection, Light	10 (L_M)	(10/90)×0.1	0.011 (R_M)

From the above table standing charge cost part of DOC will be sub-devided down to sub-section level. A typical relation for wing trailing edge, and flight control system is given below:

$$DOC_{scFC} = \frac{(\frac{1-R_{FC}}{L_{FC}} + \frac{X_{int}}{2} + S_{cpFC} \times \frac{1-R_{FC}}{L_{FC}} + S_{cpFC} \times \frac{X_{int}}{2}) \times P_{FC} \times T_{BLOC}}{U} \quad \text{B304}$$

$$DOC_{scTEF} = \frac{(\frac{1-R_{STR}}{L_{STR}} + \frac{X_{int}}{2} + S_{cpSTR} \times \frac{1-R_{STR}}{L_{STR}} + S_{cpSTR} \times \frac{X_{int}}{2}) \times P_{WTEF} \times T_{BLOC}}{U}$$

B305

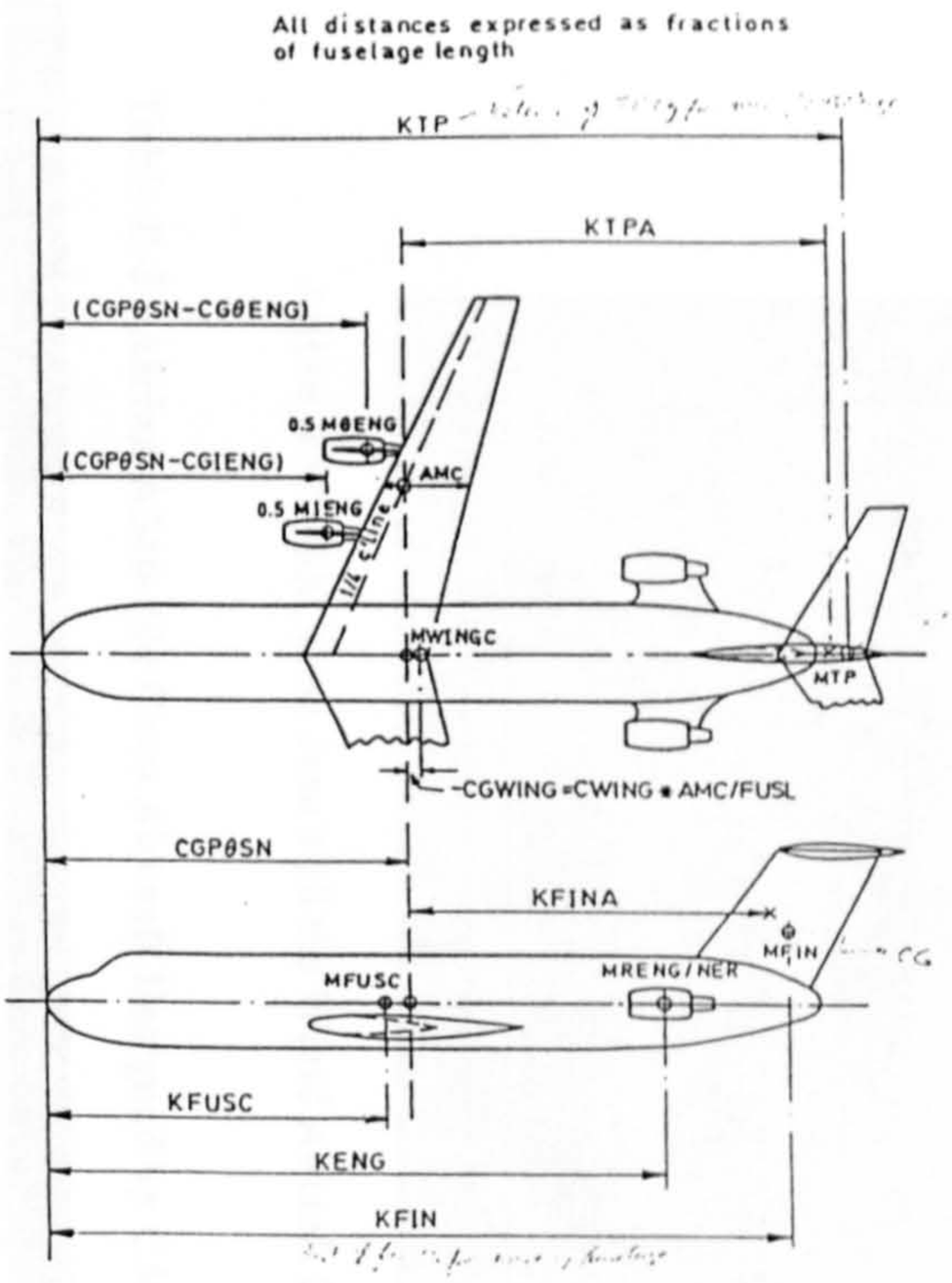

Figure B-1 Nomenclature for the balanced equation

(Note : All the parameters (70) in the Tables B-4 to B-12 are defined in Table B-9)

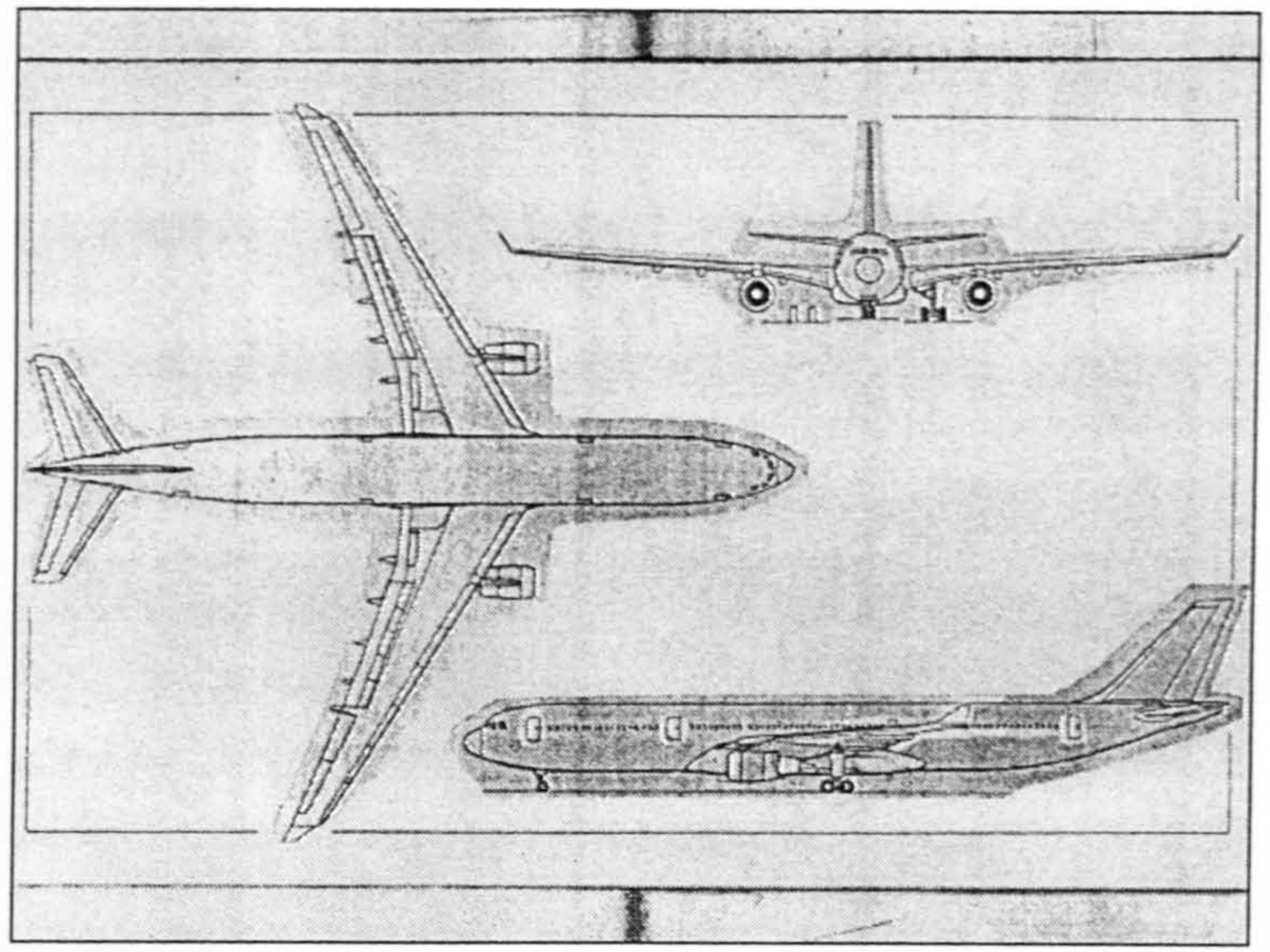

Airbus A330-200, from Jane's all the World Aircraft CD-ROM

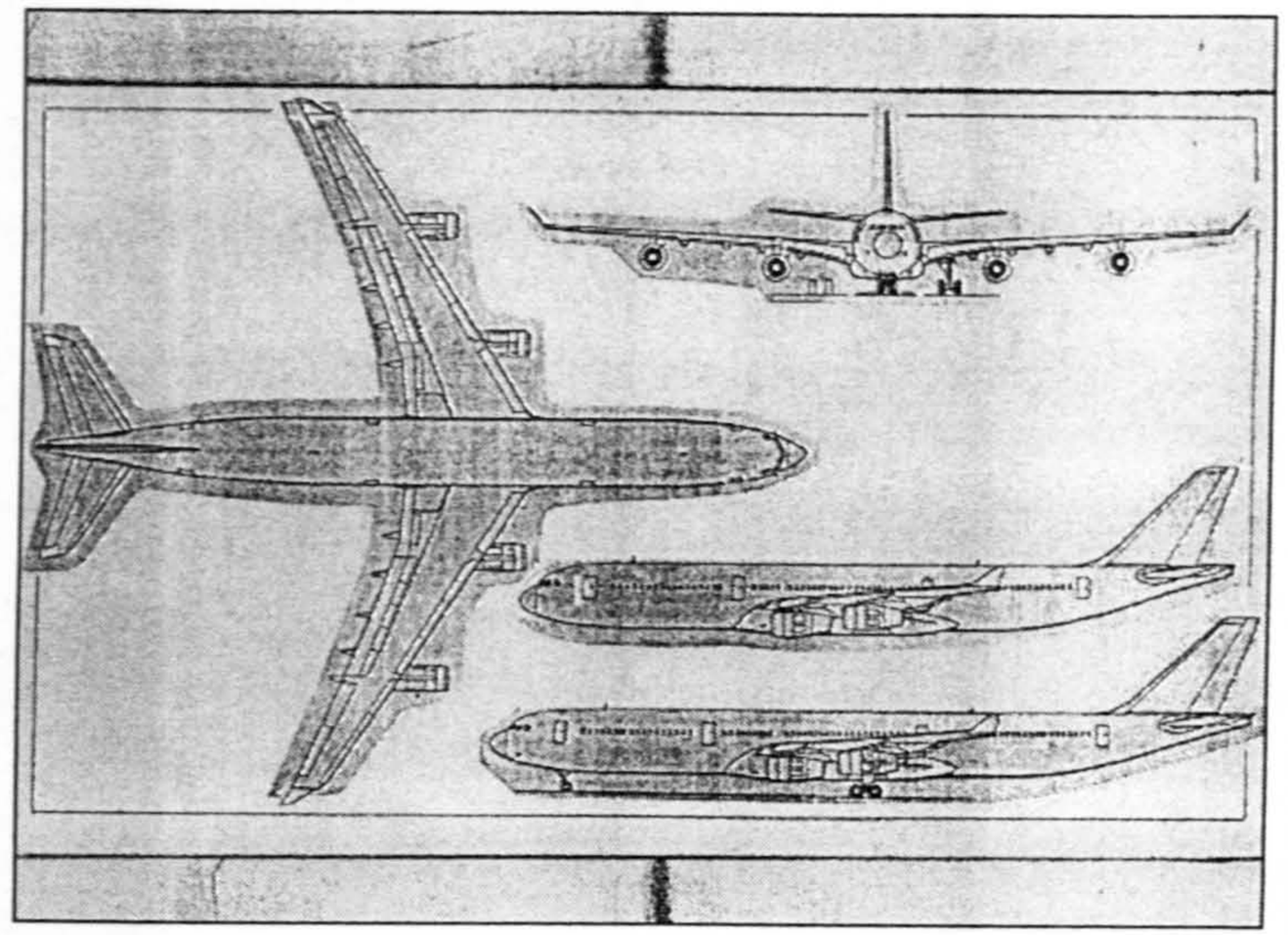

Airbus A340-200, from Jane's all the World Aircraft CD-ROM

Table B-4 : Airbus A330-200 Class Aircraft Designed by CACAD

No	Parameter	CACAD	A330-200	% Difference	Unit
1	PAX	336	335		
2	RGE	8481	8481		km
3	PAB	7	7		
4	AISLES	2	2		
5	MFRT	0	0		kg
6	HTMCR	10677	?		m
7	MCR	0.84	?		
8	ACLIFE	20			year
9	EFH	4573.0	?		m

Table B-5 : Airbus A340-200 Class Aircraft Designed by CACAD

Parameter	CACAD	A340-200	% Difference	Unit
PAX	263.00	263.00		
RGE	13973.94	13973.94		km
PAB	9	9		
AISLES	2	2		
MFRT	0	0		kg
HTMCR	10667	?		m
MCR	0.84	.82to.85		
ACLIFE	20	?		year
EFH	4573.0	?		m

10	DOCRAE2	45409.1			£/FL	DOCRAE2	80075.80			£/FL
11	DOCAFLM0	6324.40			£/FL	DOCAFLM0	8743.87			£/FL
12	ZFMMAX	159400.4	164000	2.8	kg	ZFMMAX	166697.95	160000	4	kg
13	TC	0.1000	?			TC	0.0950	?		
14	A	8.6000	10			A	9.7000	10	3	
15	S	342.130	363.1	14	m^2	S	378.365	363.1	4	m^2
16	MENG	0.675			kg	MENG	29974.64			kg
17	SWP	27.70	30	7	deg	SWP	27.70	30.0	7	deg
18	TR	0.2179				TR	0.2179	?		
19	ETA	0.600				ETA	0.600	?		
20	ETEFB	0.225				ETEFB	0.150	?		
21	ETE	0.275				ETE	0.200	?		
22	MTO	204768.50	212000	3	kg	MTO	254164.36	244000	4	kg
23	MWING	30497.16			kg	MWING	33890.88			kg
24	MFUEL	60372.55			kg	MFUEL	99220.62			kg
25	DOCMLHYD2	0.06				DOCMLHYD2	0.05			
26	MAF	90920.79			kg	MAF	99367.01			kg
27	ME	111735.89	119745	0.1	kg	ME	129345.05	122769	5	kg
28	DOCMLFC2	0.07				DOCMLFC2	0.07			
29	DOCMLWTE2	0.02				DOCMLWTE2	0.02			
30	CD0	0.01495				CD0	0.01405			
31	CDC	0.01695				CDC	0.01605			
32	CLCRB1	0.49569				CLCRB1	0.55636			
33	CLCRB2	0.46775				CLCRB2	0.51071			
34	CLCRB3	0.44101				CLCRB3	0.46817			
35	CLCRB4	0.41534				CLCRB4	0.42828			
36	CLCRB5	0.39065				CLCRB5	0.39069			
37	KCR	1.16831				KCR	1.17822			
38	PAC	73813832.			£	PAC	86061032	83000000	3.6	£
39	LMF1	0.8284				LMF1	0.7059			
40	JFLP	48.91			kg/m^2	JFLP	48.19			kg/m^2
41	MWTEF	3001.76			kg	MWTEF	2212.83			kg
42	SFTE	61.37			m^2	SFTE	45.92			m^2
43	GMC	6.31			m	GMC	6.25			m
44	MWTE	3520.48			kg	MWTE	2771.04			kg

45	CLMA	2.73767				CLMA	2.62142			
46	SRTE	17.29				SRTE	18.61			
47	MWTER	518.72284				MWTER	558.20496			
48	DOCPHR2	4651.894			£/hr	DOCPHR2	5039.6006			£/hr
49	CLMB	1.72993				CLMB	1.70088			
50	DOCPKS2	1.62162				DOCPKS2	2.20647			
51	LDRCR1	17.97498				LDRCR1	19.84999			
52	LDRCR2	17.70974				LDRCR2	19.53463			
53	LDRCR3	17.38944				LDRCR3	19.08318			
54	LDRCR4	17.01537				LDRCR4	18.50040			
55	LDRCR5	16.58900				LDRCR5	17.79197			
56	FUSD	5.64000	5.64	0	m	FUSD	5.64000	5.64	0	m
57	FUSL	64.53600	≅63.65	1	m	FUSL	59.70044	≅59.3	0	m
58	MSYS2	11251.59			kg	MSYS2	11857.78			kg
59	FVEC(7)	36.59251			m^3	FVEC(7)	10.80946			m^3
60	MHYD1	1069.49			kg	MHYD1	1082.17			kg
61	MFC1	2162.64			kg	MFC1	2165.97			kg
62	HMLDG	169638.84	174000.0	2.5	kg	HMLDG	179406.17	172000	4.3	kg
63	MLDG	150583.91			kg	MLDG	161166.23			kg
64	TST	62413.02			lbf	TST	31197.46	31200	0.2	lbf
65	FVEC(1)	-0.0059			m/s	FVEC(1)	0.0394			m/s
66	FVEC(8)	0.1177				FVEC(8)	0.1141			
67	VC	896.3464	856.0		kmph	VC	896.3464	?		kmph
68	SPAN	54.24	60.3	10	m	SPAN	60.58	60.3	0	m
69	DOCF	10618.492			£/FL	DOCF	18044.646			£/FL
70	DOCSCT1	19843.90			£/FL	DOCSCT1	36614.00			£/FL

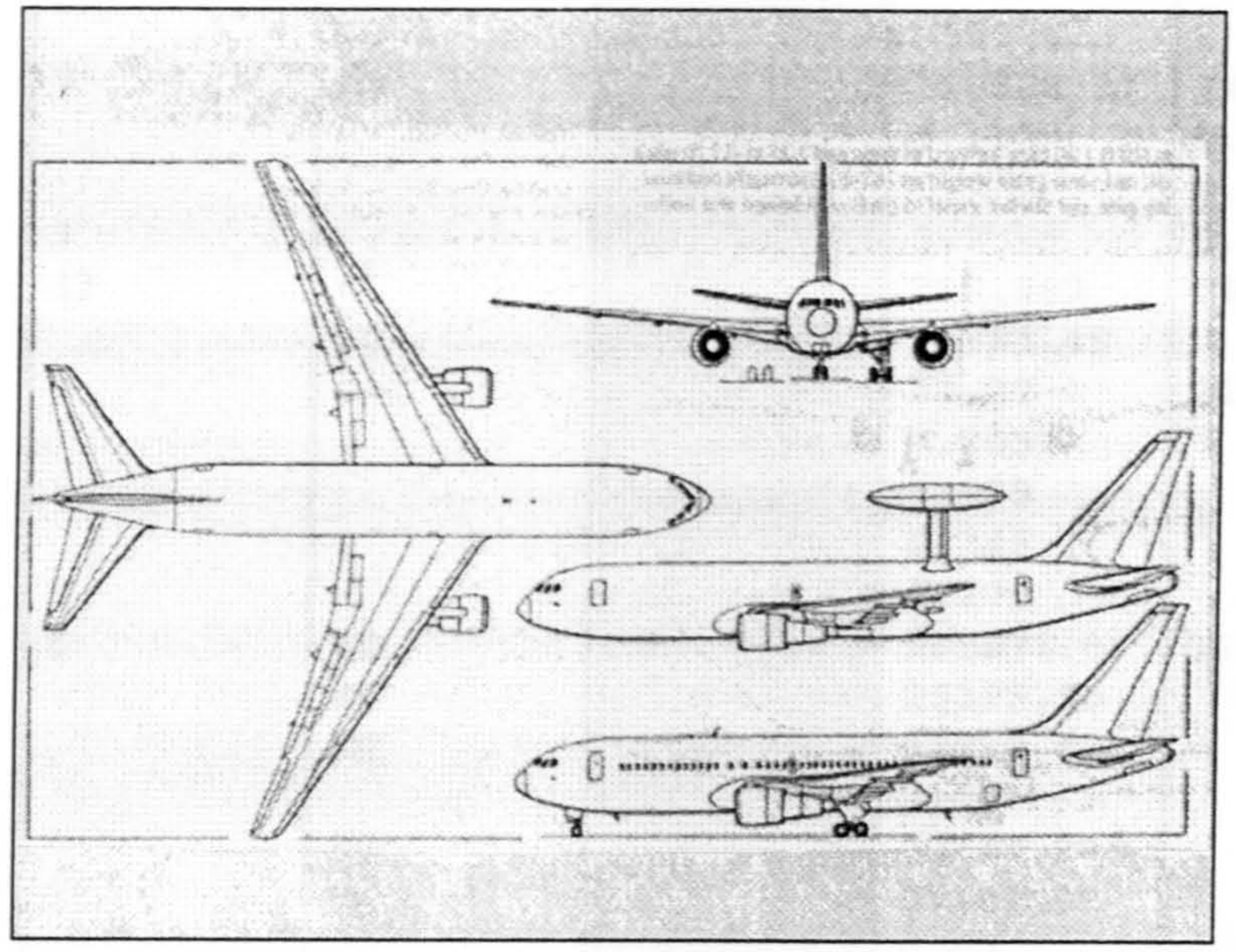

Boeing B767-200A, and Boeing B767-300Q, from Jane's all the World Aircraft CD-ROM

Table B-6 : Boeing B767-200A Class Aircraft Designed by CACAD

No	Parameter	CACAD	B767-200	% Difference	Unit
1	PAX	216.00	216.00		
2	RGE	6127.02	6127.02		km
3	PAB	8	8		
4	AISLES	2	2		
5	MFRT	0	?		kg
6	HTMCR	11581	11950		m
7	MCR	0.85	0.80		
8	ACLIFE	20			year
9	EFH	6705	?		m

Table B-7 : Boeing B767-300Q Class Aircraft Designed by CACAD

Parameter	CACAD	B767-200	% Difference	Unit
PAX	210.00	210.00		
RGE	11391.26	11391.26		km
PAB	7	7		
AISLES	2	2		
MFRT	0	0		kg
HTMCR	11581	10400		m
MCR	0.85	0.8		
ACLIFE	20			year
EFH	6705	?		m

10	DOCRAE2	25084.03			£/FL	DOCRAE2	47879.03			£/FL
11	DOCAFLM0	3775.86			£/FL	DOCAFLM0	5965.61			£/FL
12	ZFMMAX	103885.9	112491	7	kg	ZFMMAX	118328.22	145149	8	kg
13	TC	0.1000	0.151to 0.103			TC	0.1050	0.151to 0.103		
14	A	8.1000	8.0	1		A	9.7	8.0	21	
15	S	248.652	283.3	12	m^2	S	292.982	283.3	6	m^2
16	MENG	11676.07			kg	MENG	14783.45			kg
17	SWP	29.98	31	3	deg	SWP	32.27	31	4	deg
18	TR	0.2114				TR	0.2051			
19	ETA	0.675				ETA	0.675			
20	ETEFB	0.225				ETEFB	0.225			
21	ETE	0.275				ETE	0.275			
22	MTO	127180.80	136078	6	kg	MTO	169971.84	181437	6	kg
23	MWING	18894.23			kg	MWING	25323.50			kg
24	MFUEL	32941.00			kg	MFUEL	61022.17			kg
25	DOCMLHYD2	0.05				DOCMLHYD2	0.05			
26	MAF	61421.54			kg	MAF	73604.23			kg
27	ME	73092.72	74752	2	kg	ME	88389.02			kg
28	DOCMLFC2	0.07				DOCMLFC2	0.07			
29	DOCMLWTE2	0.02				DOCMLWTE2	0.02			
30	CD0	0.01455				CD0	0.01441			
31	CDC	0.01655				CDC	0.01641			
32	CLCRB1	0.47810				CLCRB1	0.54229			
33	CLCRB2	0.45558				CLCRB2	0.50282			
34	CLCRB3	0.43387				CLCRB3	0.46564			
35	CLCRB4	0.41290				CLCRB4	0.43048			
36	CLCRB5	0.39262				CLCRB5	0.39709			
37	KCR	1.16607				KCR	1.18362			
38	PAC	53090700.			mil£	PAC	61526652.			mil£
39	LMF1	0.8668				LMF1	0.7462			
40	JFLP	43.85			kg/m^2	JFLP	44.64			kg/m^2
41	MWTEF	1921.82			kg	MWTEF	2405.87			kg
42	SFTE	43.83			m^2	SFTE	53.90			m^2

43	GMC	5.54			m	GMC	5.50			m
44	MWTE	2295.54			kg	MWTE	2841.68			kg
45	CLMA	2.44734				CLMA	2.39013			
46	SRTE	12.46				SRTE	14.53			
47	MWTER	373.72818				MWTER	435.80923			
48	DOCPHR2	3509.3042			£/hr	DOCPHR2	3674.1211			£/hr
49	CLMB	1.51000				CLMB	1.56000			
50	DOCPKS2	1.94620				DOCPKS2	2.03024			
51	LDRCR1	17.68669				LDRCR1	19.47927			
52	LDRCR2	17.47685				LDRCR2	19.16504			
53	LDRCR3	17.22914				LDRCR3	18.74788			
54	LDRCR4	16.94425				LDRCR4	18.23099			
55	LDRCR5	16.62292				LDRCR5	17.61812			
56	FUSD	5.03000	5.		m	FUSD	5.03010			m
57	FUSL	48.86950	47.24	3.5	m	FUSL	53.68576	53.67	0	m
58	MSYS2	8761.46			kg	MSYS2	9899.45			kg
59	FVEC(7)	13.45948			m^3	FVEC(7)	13.35051			m^3
60	MHYD1	856.79			kg	MHYD1	969.75			kg
61	MFC1	1909.76			kg	MFC1	2031.30			kg
62	HMLDG	110244.93	122470.0	10	kg	HMLDG	126826.81	145149.0	12	kg
63	MLDG	98594.62			kg	MLDG	113746.43			kg
64	TST	37989.61			lbf	TST	54311.43			lbf
65	FVEC(1)	-0.0155			m/s	FVEC(1)	-0.0056			m/s
66	FVEC(8)	0.0999				FVEC(8)	0.0517			
67	VC	894.6108			kmph	VC	894.6108			kmph
68	SPAN	44.88	47.57	5	m	SPAN	53.31	47.57	12	m
69	DOCF	5637.6416			£/FL	DOCF	10938.788			£/FL
70	DOCSCT1	11111.35			£/FL	DOCSCT1	22086.02			£/FL

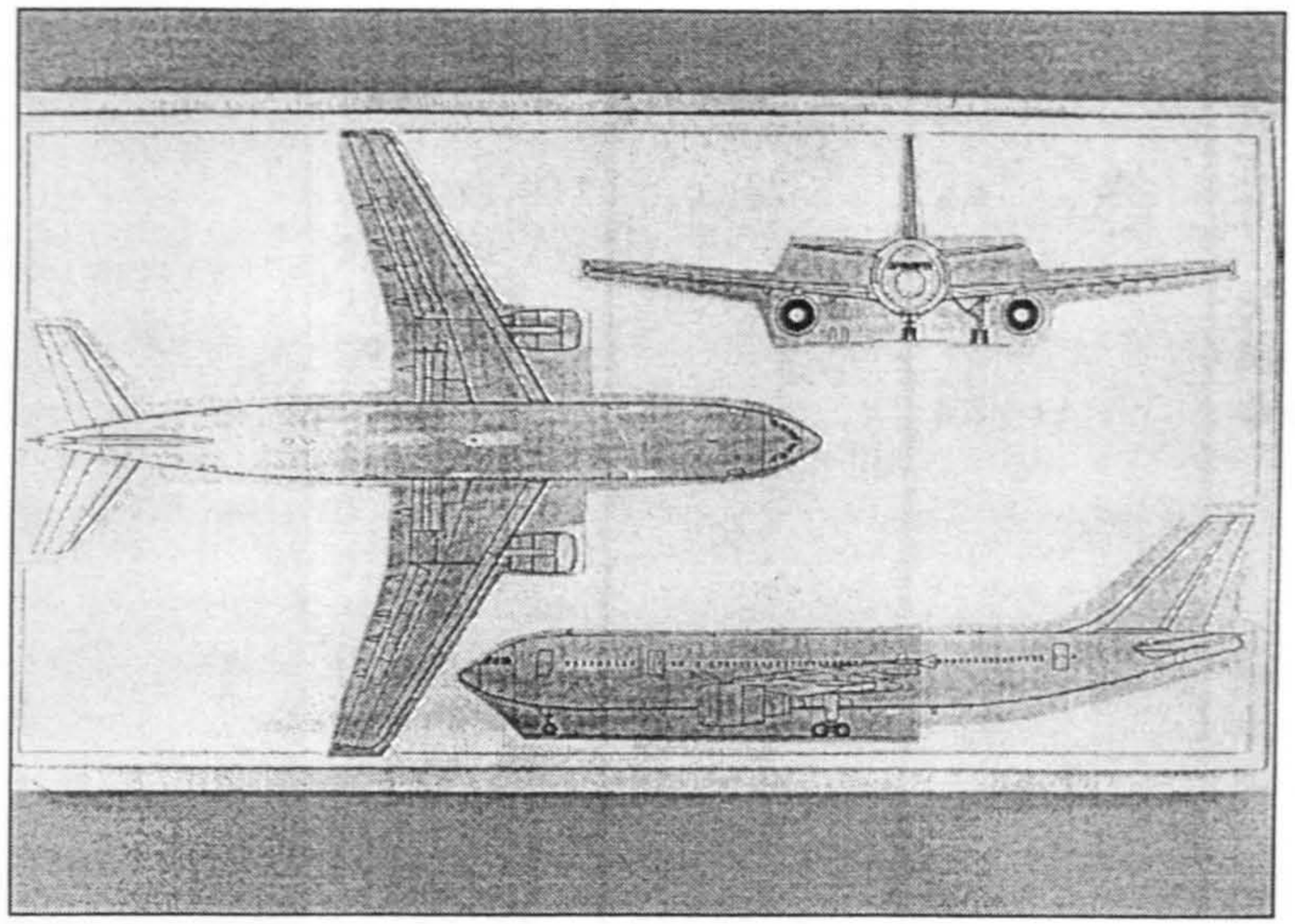

Airbus A300-600, from Jane's all the World Aircraft CD-ROM

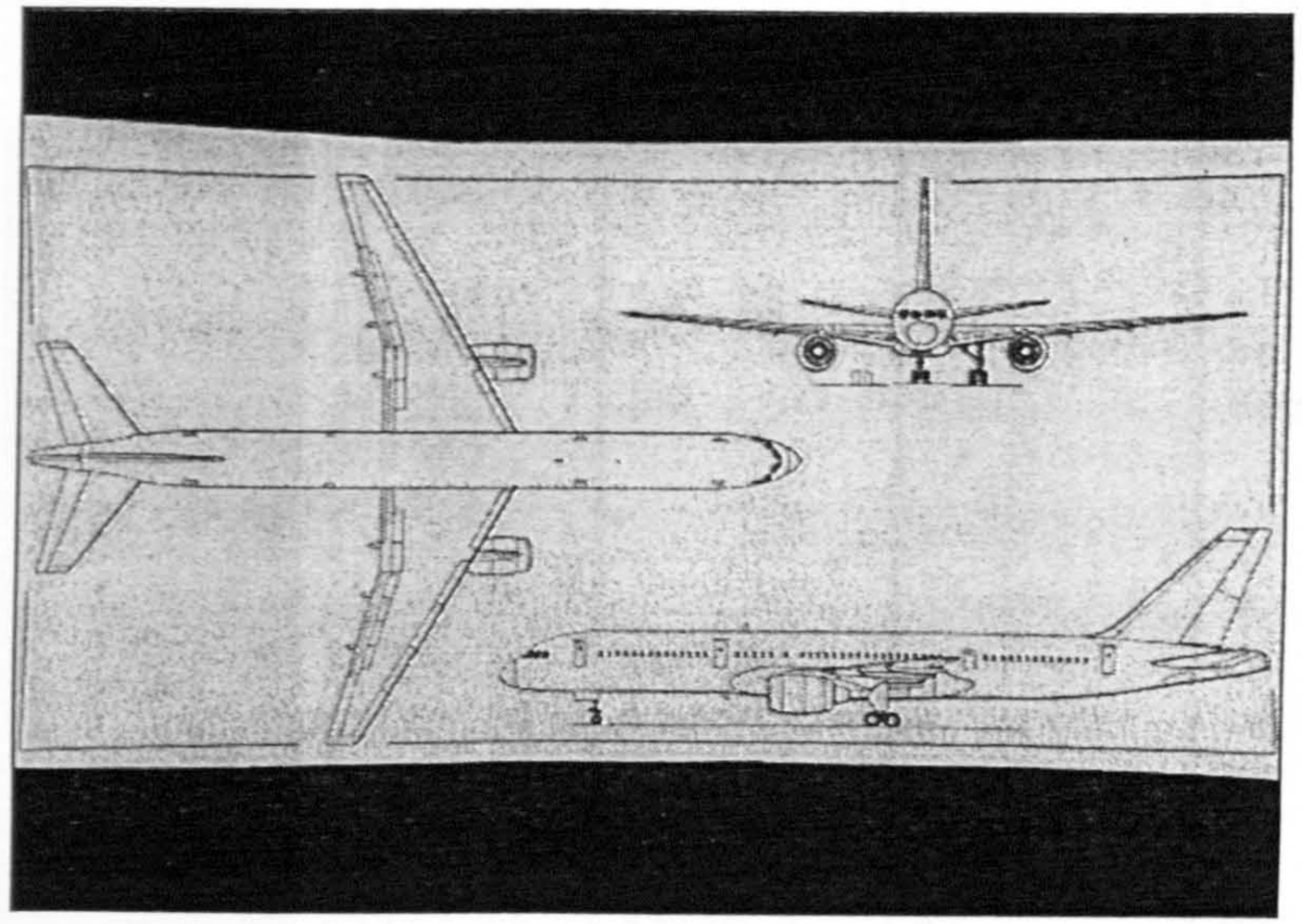

Boeing B757-200A, from Jane's all the World Aircraft CD-ROM

Table B-8 : Airbus A300-600 Class Aircraft Designed by CACAD

No	Parameter	CACAD	A300-600	% Difference	Unit
1	PAX	267.00	267.00		
2	RGE	6803.28	6803.28		km
3	PAB	9	9		
4	AISLES	2	2		
5	MFRT	0	?		kg
6	HTMCR	10667			m
7	MCR	0.82	0.82		
8	ACLIFE	20			year
9	EFH	6097	?		m

Table B-9 : Boeing B757-200A Class Aircraft Designed by CACAD

Parameter	CACAD	B757-200	% Difference	Unit
PAX	186.00	186.00		
RGE	5365.31	5365.31		km
PAB	6	6		
AISLES	1	1		
MFRT	0	0		kg
HTMCR	10667	11880		m
MCR	0.82	.80 to .86		
ACLIFE	20			year
EFH	6097	?		m

10	DOCRAE2	33833.15			£/FL	DOCRAE2	19059.16			£/FL
11	DOCAFLM0	4952.84			£/FL	DOCAFLM0	2878.91			£/FL
12	ZFMMAX	132673.969	130000	2	kg	ZFMMAX	85254.273	83460	2.1	kg
13	TC	0.1100	0.105	4.7		TC	0.1000	?		
14	A	9.8000	7.7			A	10.0	7.82		
15	S	271.305	260	4.2	m^2	S	167.406	185.25	9	m^2
16	MENG	17411.58			kg	MENG	10707.60			kg
17	SWP	27.02	28	3.5	deg	SWP	24.17	25	3	deg
18	TR	0.2199				TR	0.2287			
19	ETA	0.675				ETA	0.675			
20	ETEFB	0.225				ETEFB	0.225			
21	ETE	0.275				ETE	0.275			
22	MTO	164697.70	165000	0.2	kg	MTO	99288.83	104325.0	4.8	kg
23	MWING	24192.71			kg	MWING	13684.26			kg
24	MFUEL	43947.08			kg	MFUEL	22341.04			kg
25	DOCMLHYD2	0.05				DOCMLHYD2	0.06			
26	MAF	77265.14			kg	MAF	47998.99			kg
27	ME	94677.01	89672.0	5	kg	ME	58702.00	57180.0	2.6	kg
28	DOCMLFC2	0.07				DOCMLFC2	0.07			
29	DOCMLWTE2	0.02				DOCMLWTE2	0.02			
30	CD0	0.01560				CD0	0.01611			
31	CDC	0.01760				CDC	0.01811			
32	CLCRB1	0.52759				CLCRB1	0.51547			
33	CLCRB2	0.50164				CLCRB2	0.49528			
34	CLCRB3	0.47664				CLCRB3	0.47564			
35	CLCRB4	0.45251				CLCRB4	0.45653			
36	CLCRB5	0.42918				CLCRB5	0.43790			
37	KCR	1.18197				KCR	1.17837			
38	PAC	64652956.			milf	PAC	44729428.			milf
39	LMF1	0.8556				LMF1	0.8200			
40	JFLP	42.22			kg/m^2	JFLP	39.68			kg/m^2
41	MWTEF	2027.23			kg	MWTEF	1216.23			kg
42	SFTE	48.02			m^2	SFTE	30.65			m^2
43	GMC	5.26			m	GMC	4.09			m

44	MWTE	2440.70			kg	MWTE	1474.90			kg
45	CLMA	2.94286				CLMA	2.84943			
46	SRTE	13.78				SRTE	8.62			
47	MWTER	413.47153				MWTER	258.67737			
48	DOCPHR2	4190.84424			£/hr	DOCPHR2	2964.02466			£/hr
49	CLMB	1.88014				CLMB	1.61			
50	DOCPKS2	1.89979				DOCPKS2	1.96075			
51	LDRCR1	18.64659				LDRCR1	18.35356			
52	LDRCR2	18.39646				LDRCR2	18.12901			
53	LDRCR3	18.10331				LDRCR3	17.87849			
54	LDRCR4	17.76801				LDRCR4	17.60241			
55	LDRCR5	17.39151				LDRCR5	17.30125			
56	FUSD	5.640	5.64		m	FUSD	3.83060	3.53	8.5	m
57	FUSL	53.30	53.30		m	FUSL	52.40064	46.96	11.6	m
58	MSYS2	9818.63			kg	MSYS2	8341.74			kg
59	FVEC(7)	5.23815			m^3	FVEC(7)	-2.18901			m^3
60	MHYD1	951.64			kg	MHYD1	853.09			kg
61	MFC1	2000.17			kg	MFC1	1701.95			kg
62	HMLDG	140908.84	138000.0	2	kg	HMLDG	81416.84	89810.0/80636	1	kg
63	MLDG	126126.82			kg	MLDG	80344.58			kg
64	TST	62781.70	59000	6	lbf	TST	33846.01	40100	15	lbf
65	FVEC(1)	-0.0057			m/s	FVEC(1)	0.0403			m/s
66	FVEC(8)	0.1171				FVEC(8)	0.2013			
67	VC	875.0048	890		kmph	VC	875.0048			kmph
68	SPAN	51.56	44.84	13	m	SPAN	40.92	38.05		m
69	DOCF	7593.9810			£/FL	DOCF	3764.3567			£/FL
70	DOCSCT1	14920.25			£/FL	DOCSCT1	8692.67			£/FL

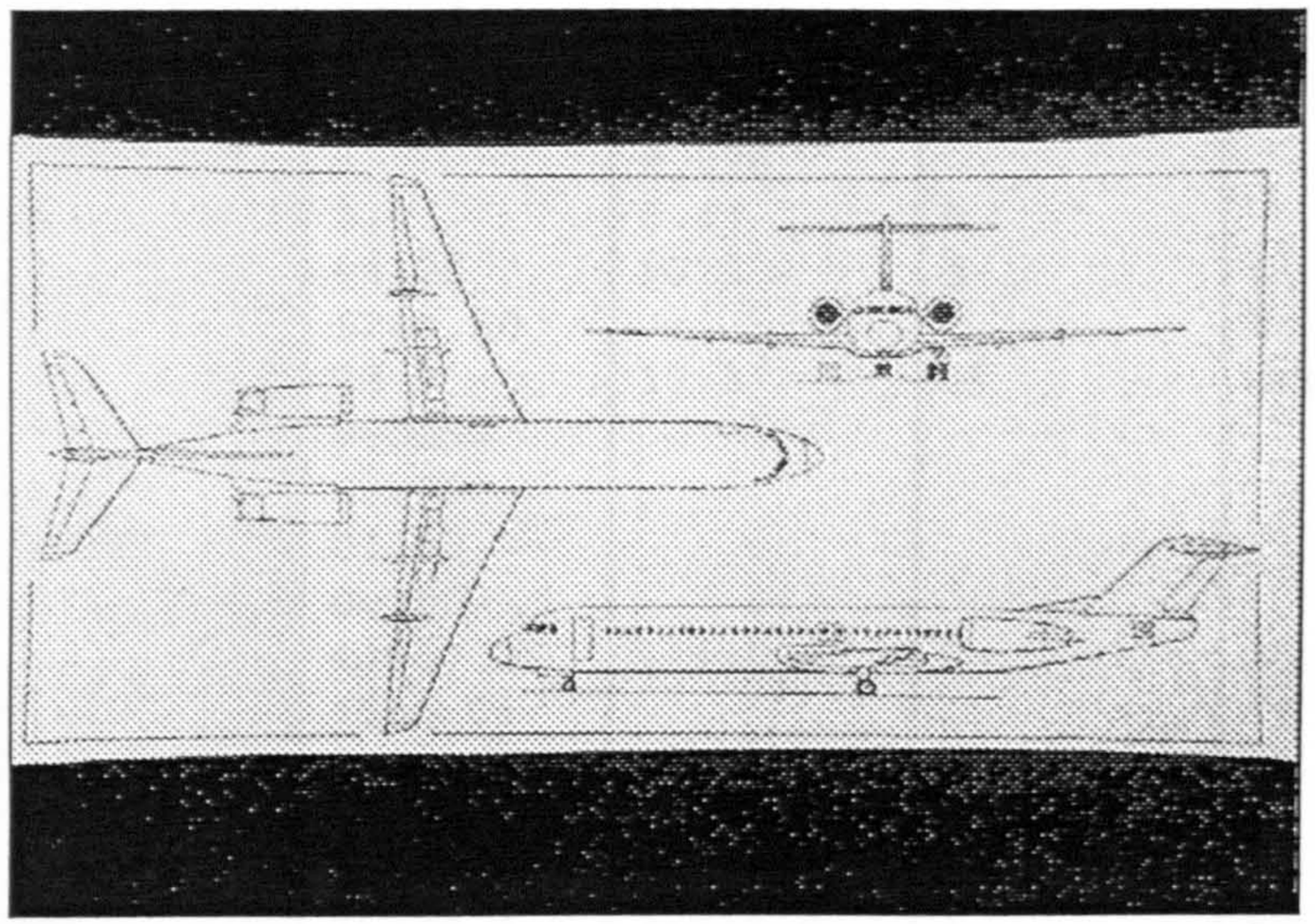

Fokker F-100, Courtesy of Jane's all the World Aircraft CD-ROM

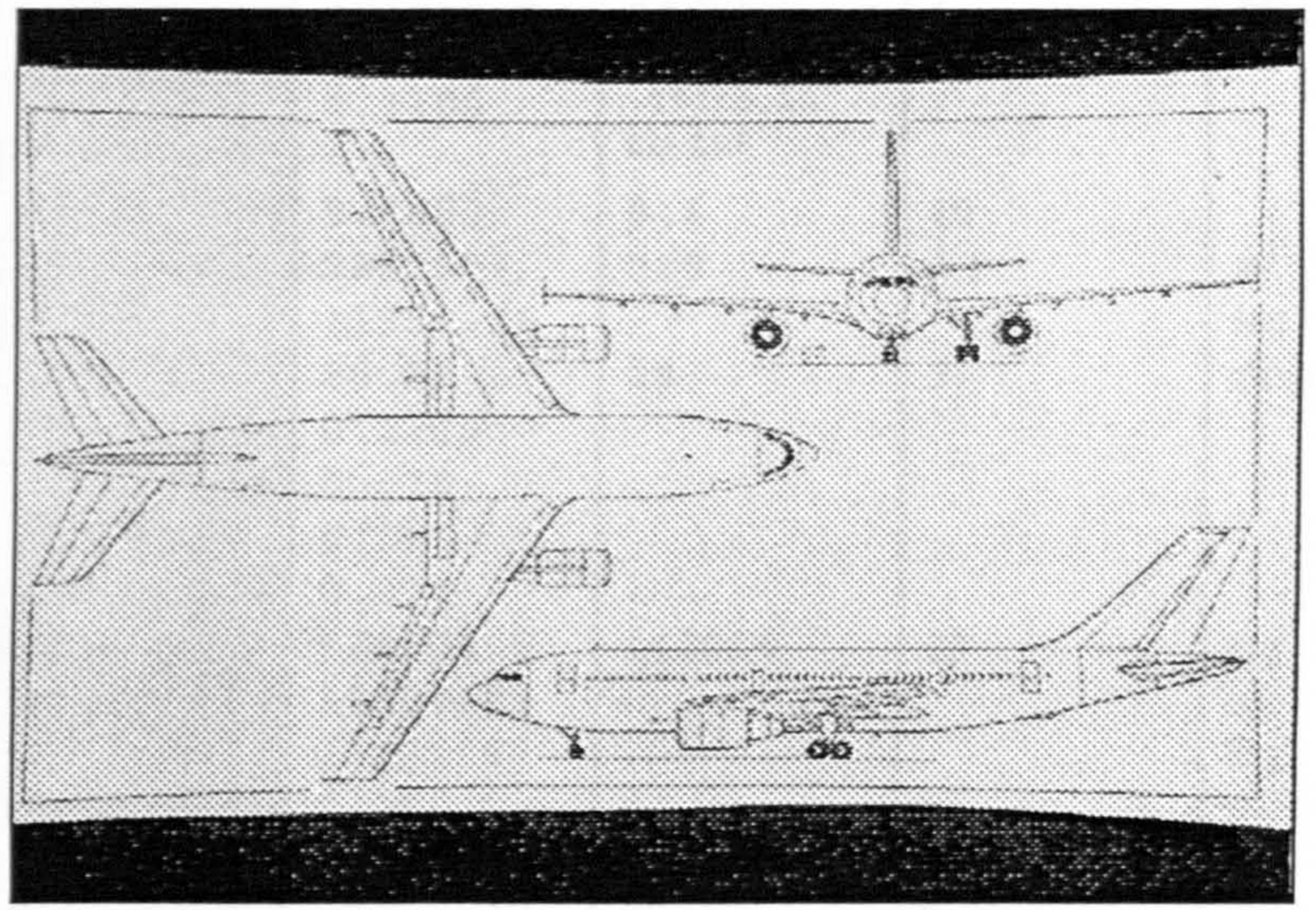

Airbus A310, from Jane's all the World Aircraft CD-ROM

Table B-10 : Fokker F-100 Class Aircraft Designed by CACAD

No	Parameter	CACAD	F100	% Difference	Unit
1	PAX	107.00	107.00		
2	RGE	2484.69	2484.69		km
3	PAB	5	5		
4	AISLES	1	1		
5	MFRT	943.0			kg
6	HTMCR	7770	7770		m
7	MCR	0.77	0.77		
8	ACLIFE	20			year
9	EFH	4573.0	?		m
10	DOCRAE2	6440.4			£/FL
11	DOCAFLM0	1019.9			£/FL

Table B-11 : Airbus A310 Class Aircraft Designed by CACAD

Parameter	CACAD	A310	% Difference	Unit
PAX	218.00	218.00		
RGE	6949.45	6949.45		km
PAB	9	9		
AISLES	2	2		
MFRT	0	0		kg
HTMCR	10667			m
MCR	0.82	0.82		
ACLIFE	20			year
EFH	6097.0	?		m
DOCRAE2	27571.42			£/FL
DOCAFLM0	4018.59			£/FL

12	ZFMMAX	42004	36740/ 40049.5	4.8	kg	ZFMMAX	104228.2	113000	7	kg
13	TC	0.1150	0.123to 0.096	4		TC	0.1100	.152to.11 to.108	?	
14	A	8.4	8.43	0		A	9.7000	8.8	10	
15	S	94.25	93.5	5	m^2	S	225.859	219	3.1	m^2
16	MENG	6244.50			kg	MENG	11954.34			kg
17	SWP	23.8	17.3	23	deg	SWP	26.52	28	5	deg
18	TR	0.2298				TR	0.2215			
19	ETA	0.625				ETA	0.675			
20	ETEFB	0.150				ETEFB	0.225			
21	ETE	0.200				ETE	0.275			
22	MTO	44857.60	44450.0	0	kg	MTO	128324.5	142000	10	kg
23	MWING	4550.63			kg	MWING	18107.01			kg
24	MFUEL	7632.59			kg	MFUEL	33831.67			kg
25	DOCMLHYD2	0.05				DOCMLHYD2	0.05			
26	MAF	20463.6			kg	MAF	61202.88			kg
27	ME	26724.4	24727.0	4	kg	ME	73162.39	80142	8	kg
28	DOCMLFC2	0.07				DOCMLFC2	0.07			
29	DOCMLWTE2	0.02				DOCMLWTE2	0.02			
30	CD0	0.01581				CD0	0.01541			
31	CDC	0.01681				CDC	0.01741			
32	CLCRB1	0.30396				CLCRB1	0.49379			
33	CLCRB2	0.29614				CLCRB2	0.46980			
34	CLCRB3	0.28840				CLCRB3	0.44661			
35	CLCRB4	0.28073				CLCRB4	0.42417			
36	CLCRB5	0.27314				CLCRB5	0.40242			
37	KCR	1.16557				KCR	1.18293			
38	PAC	24.313			milf	PAC	52553004. 0			milf
39	LMF1	0.9100				LMF1	0.8622			
40	JFLP	25.84			kg/m^2	JFLP	40.09			kg/m^2
41	MWTEF	330.0			kg	MWTEF	1560.55			kg
42	SFTE	11.12			m^2	SFTE	38.93			m^2

43	GMC	3.35			m	GMC	4.83			m
44	MWTE	416.27			kg	MWTE	1905.59			kg
45	CLMA	2.704				CLMA	2.75071			
46	SRTE	4.30				SRTE	11.50			
47	MWTER	129.07				MWTER	345.03638			
48	DOCPHR2	2012.73			£/hr	DOCPHR2	3345.59888			£/hr
49	CLMB	1.610				CLMB	1.63694			
50	DOCPKS2	2.51949				DOCPKS2	1.85992			
51	LDRCR1	14.55056				LDRCR1	18.36720			
52	LDRCR2	14.31837				LDRCR2	18.07853			
53	LDRCR3	14.08025				LDRCR3	17.74999			
54	LDRCR4	13.83629				LDRCR4	17.38246			
55	LDRCR5	13.58661				LDRCR5	16.97695			
56	FUSD	3.30000	3.30		m	FUSD	5.64	5.64		m
57	FUSL	31.76100	32.50	2	m	FUSL	46.54933	45.13	3	m
58	MSYS2	5581.07			kg	MSYS2	8534.23			kg
59	FVEC(7)	4.504			m^3	FVEC(7)	1.85249			m^3
60	MHYD1	563.11			kg	MHYD1	853.43			kg
61	MFC1	1446.79			kg	MFC1	1843.11			kg
62	HMLDG	40820.42	39915.0	1	kg	HMLDG	110644.44	123000.	10	kg
63	MLDG	38961.02			kg	MLDG	98471.22			kg
64	TST	14826.01	15100	2	lbf	TST	38355.08	53500		lbf
65	FVEC(1)	-0.0319			m/s	FVEC(1)	-0.0196			m/s
66	FVEC(8)	0.3693				FVEC(8)	0.1628			
67	VC	856.3	856.0		kmph	VC	875.0048			kmph
68	SPAN	28.14	28.08	0.8	m	SPAN	46.81	43.89	6	m
69	DOCF	1197.84			£/FL	DOCF	5879.4814			£/FL
70	DOCSCT1	2714.4			£/FL	DOCSCT1	12545.20			£/FL

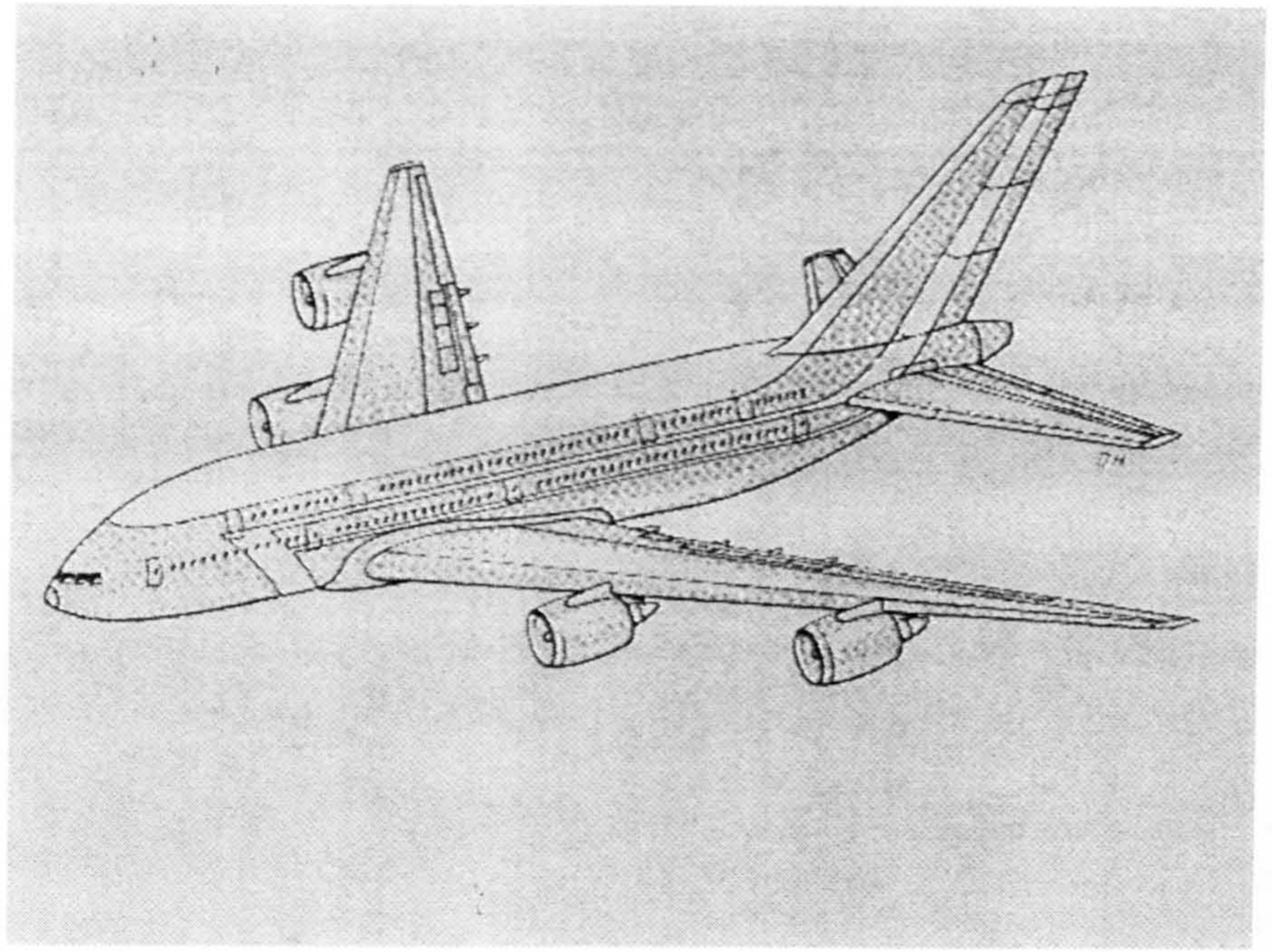

UHCA, from Jane's all the World Aircraft CD-ROM

Table B-9 Ultra High Capacity Aircraft Class Aircraft Designed by CACAD

No	Parameter	CACAD	UHCA	%d	Unit	Description
1	PAX	660	660			P_{AX} is number of passenger considered as payload (not P_{AXmax})
2	RGE	13653.83	13653.83		km	Range
3	PAB					P_{ab} Number of seats abreast
4	AISLES					A_{isles} Number of aisles
5	MFRT				kg	M_{FRT} Mass of Freight

6	HTMCR		m	H_{tmcr} Cruise altitude
7	MCR			M_{cr} Cruise Mach number
8	ACLIFE	20	year	A_{clife} Life of the aircraft
9	EFH		m	E_{fh} Engine (single engine) failed hieght requirement
10	DOCRAE2	162741.62	£/FL	DOC £ per flight
11	DOCAFLM0	20048.76	£/FL	DOC_{AFlm0} Cost of maintenance £/flight (part of DOC)
12	ZFMMAX	382541.250	kg	$Z_{fuel-max}$ Maximum zero fuel mass
13	TC	0.0975		TC Thichness to chord ratio
14	A	8.60		AR Aspect Ratio
15	S	751.0	m^2	S_g Gross wing area
16	MENG	52956.71	kg	Meng Sum of all engine mass
17	SWP	29.86	deg	$\Lambda_{1/4}$ Sweep angle at quater chord
18	TR	0.2117		TR Taper ratio
19	ETA	0.675		Eta Ratio of gross flap span to wing span
20	ETEFB	0.225		Etefb Unextended Flap chord ratio
21	ETE	0.275		Ete Ratio of wing chord aft of rear spar to wing chord
22	MTO	577542.19	kg	M_{to} Take-off Mass
23	MWING	86691.55	kg	M_{WING} Wing mass
24	MFUEL	224474.34	kg	M_{fuel} Total fuel mass loaded
25	DOCMLHYD2	0.06		%of hydraulic system maint. cost wrt total maint. cost
26	MAF	235949.16	kg	M_{AF} Mass of the airframe(fuse.,furn.,emp.,Ldgear.,Systems)
27	ME	288911.13	kg	M_E Empty mass (Airfram, and engines mass)
28	DOCMLFC2	0.07		%of flight control system maint. cost w.r.t. total maint. cost
29	DOCMLWTE2	0.02		%of wing TE system maint. cost w.r.t. total maint. cost
30	CD0	0.01414		C_{D0} Zero lift drag coefficient
31	CDC	0.01614		C_{DC} total lift independent drag coefficient
32	CLCRB1	0.63692		C_{Lcr-1} Lift coefficient at cruise first sector
33	CLCRB2	0.58333		C_{Lcr-2} Lift coefficient at cruise second sector
34	CLCRB3	0.53424		C_{Lcr-3} Lift coefficient at cruise third sector
35	CLCRB4	0.48895		C_{Lcr-4} Lift coefficient at cruise forth sector
36	CLCRB5	0.44688		C_{Lcr-5} Lift coefficient at cruise fiveth sector
37	KCR	1.17009		K_{cr} induced drag factor
38	PAC	178815600.	milf	P_{rice} price of the aircraft
39	LMF1	0.7124		L_{mf1} Landing mass factor

40	JFLP	68.28	kg/m^2	J_{FLP} Flap mass density
41	MWTEF	9198.93	kg	M_{WTEF} Wing TE flap mass
42	SFTE	134.72	m^2	S_{FTE} Surface area of wing TE flap
43	GMC	9.34	m	GMC Geometric mean chord
44	MWTE	10328.21	kg	M_{WTE} Wing TE mass including flap and aileron
45	CLMA	2.63737		C_{LMAX} trimmed at approach
46	SRTE	37.64		S_{RTE} Surface area of wing TE rest (aileron)
47	MWTER	1129.28		M_{WTER} Wing TE rest mass (aileron)
48	DOCPHR2	10478.10	£/hr	DOC £ per flying hour
49	CLMB	1.72301		C_{LMAX} for the base airfoil
50	DOCPKS2	1.82651		DOC Penny per seat per km
51	LDRCR1	18.89194		$(L/D)_{cr1}$ lift drag ratio required at cruise sector 1
52	LDRCR2	18.89000		$(L/D)_{cr2}$ lift drag ratio required at cruise sector 2
53	LDRCR3	18.74318		$(L/D)_{cr3}$ lift drag ratio required at cruise sector 3
54	LDRCR4	18.45426		$(L/D)_{cr4}$ lift drag ratio required at cruise sector 4
55	LDRCR5	18.02712		$(L/D)_{cr5}$ lift drag ratio required at cruise sector 5
56	FUSD	8.40	m	F_{USD} External diameter of fuselage
57	FUSL	77.235	m	F_{USL} Toatl length of fuselage
58	MSYS2	22333.62	kg	M_{SYS} Sum of all system masses
59	FVEC(7)	85.35023	m^3	The amount of aircraft tank volume in excess of fuel volume
60	MHYD1	1394.75	kg	M_{HYD} Hydraulic System Mass
61	MFC1	2824.43	kg	M_{FC} Flight control system mass
62	HMLDG	411418.34	kg	M_{HLDG} Highest landing mass
63	MLDG	367146.81	kg	M_{LDG} Landing mass of aircraft
64	TST	85113.61	lbf	T_{st} Maximum thrust of the each engine at static sea level
65	FVEC(1)	0.0287	m/s	Difference between aircraft approach, and 1.3×stall speed
66	FVEC(8)	-0.0716		Difference between C_L buffet on set and C_L buffet produced
67	VC	896.3464	kmph	V_{CR} Cruise true velocity
68	SPAN	80.37	m	Span
69	DOCF	40824.2969	£/FL	Fuel cost £ per flight
70	DOCSCT1	71407.27	£/FL	Standing charges (Depreciation cost) £ per flight

APPENDIX C

Avionics Reliability Enhancement

Modelling Formulation And Results

C 1 . Introduction

In this appendix the detailed formulation and further description of ASRE modelling are presented in the following order :

Engine performance simulation with bleed, ECS mass modelling, modelling of avionics systems cooling by ECS, avionics systems reliability modelling, avionics maintenance cost modelling, and ACAU modelling for UHCA. At the end of this appendix, the tables and figures of results are presented.

C 2 . Engine Performance Simulation with Bleed

Four classes of transport aircraft were defined for CACAD, the details of which are given in Chapter 3. Four turbofan engine classes were selected for bleed investigation suitable for those classes of aircraft. They are, 15000 lbf, 30000 lbf, 52000 lbf, and 75000 lbf class of engines. In order to make a realistic performance simulation of such engines, to match the real life engines, it was necessary to choose certain real engine types so that Turbomatch can be guided to arrive at the nearest possible engine. Hence TAY 650, CFM56C2, CF6-80C2, and TRENT775 engines were chosen for performance validation .

Turbomatch mass flow, CPR, BPR, etc., are chosen to match the above engines, and TET was varied to arrive at the published S/L static thrust value (TST) . Turbomatch was set up to fly the engines to 35000 ft, 0.82 Mach, after which the throttle setting was varied to arrive at the published engine thrust. If the sfc at cruise matched the published value the simulation was complete, and the bleed operation simulation could be commenced. Otherwise, the component efficiency and fan pressure ratio (FPR) guess values were modified. The whole process of simulation was repeated until cruise sfc, and thrust were very close to published values.

C 2 .1 Bleed Effect Modelling

In order to develop empirical equations to demonstrate bleed effects on turbofan engines, the four selected engines described in the last section were bled using Turbomatch performance simulation. Table C-1 shows the specification of 4 real engine [26,43] and the specification of the equivalent engines designed by using Turbomatch Code [72] to the nearest possible matching.

The effect of bleed from intermediate compressor on thrust and sfc at typical cruise altitude (35000 ft) and Mach number (0.82), where the throttle setting is equivalent to real engines described in Tables C-1 are tabulated in Tables C-2. Table C-3 puts the actual SFC penalty in mg/s/N and the actual thrust penalty in N against actual amount of bleed in kg/s for all 4 types of engines at 100% cruise condition. Fig. C-1, C-2, and C-3 show sfc increase, thrust fall, and % sfc increase of the named engines.

The data in Table C-3 were fed into Mathematica [127] for curve fitting to find the appropriate equation of the variation of thrust fall and SFC rise with bleed flow rate for each class of engine. Below are the said equations and Figs. C-4, and C-5 show how closely equation of the curves made by these equations run closely with the points .

m_{bs} = Mass bled from mid compressor (IPC) in kg/sec

ΔT = Thrust fall in N

Δsfc = Specific fuel consumption rise in mg/sec/N

T_{STAT} = Static sea level thrust

$$\Delta T_{TAY} / T_{STAT} = 1010.89 \times m_{bs} - 101.13 \times m_{bs}^{2} + 32.1321 \times m_{bs}^{3} \qquad \text{C1}$$

$$\Delta T_{CFM} / T_{STAT} = 1151.84 \times m_{bs} + 76.5757 \times m_{bs}^{2} \quad \text{C2}$$

$$\Delta T_{CF6} / T_{STAT} = 963.056 \times m_{bs} + 24.1611 \times m_{bs}^{2} \quad \text{C3}$$

$$\Delta T_{TRENT} / T_{STAT} = 1352.03 \times m_{bs} - 44.7204 \times m_{bs}^{2} + 5.37266 \times m_{bs}^{3} \quad \text{C4}$$

$$\Delta sfc_{TAY} = 0.8902 \times m_{bs} + 0.16224 \times m_{bs} \quad \text{C5}$$

$$\Delta sfc_{CFM} = 0.2997 \times m_{bs} + 0.02357 \times m_{bs}^{2} \quad \text{C6}$$

$$\Delta sfc_{CF6} = 963.056 \times m_{bs} + 24.1611 \times m_{bs}^{2} \quad \text{C7}$$

$$\Delta sfc_{TRENT} = 0.22234 \times m_{bs} - 0.00406154 \times m_{bs}^{2} + 0.00108035 \times m_{bs}^{3} \quad \text{C8}$$

C 3 . ECS Mass Modelling

Based on an ECS design study [73], the major portion of bleed requirement from aircraft engines is allocated to ECS. This system supply air-conditioned air to (a) the cabin for passengers, galleys, and toilets, and (b) the flight deck for crew, avionics instruments, and (c) the avionics equipment bays at all locations in aircraft. Any extra cooling supply to avionics equipment not only requires higher bleed from the engines, but may compel ECS capacity to increase, causing a rise in its mass. This section is an attempt to develop an empirical relation to show ECS mass as a function of its output flow rate. The present ECS empirical mass equations in lbs for jet transport aircraft are presented from different source . General Dynamics Method [15]:

$$M_{ecs} = (469/2.205) \{ V_{pax} \times 35.32 \times (C_{REW} + P_{AX}) / 10000 \}^{0.419} \quad \text{C9}$$

where V_{pax} is the volume of passenger cabin (approximately the pressurised cabin volume including flight deck as well). Torenbeek Method [32,15]:

$$M_{ecs} = (6.75/2.205) (P_{CL} / 3.281)^{1.28} \quad \text{C10}$$

Raymer Method [1]:

$$M_{ecs} = (62.36/2.205) (N_p)^{0.25} (V_{pr} \times 35.32 / 1000)^{0.604} (M_{uav} \times 2.205)^{0.10} \quad \text{C11}$$

$$N_p = C_{REW} + P_{AX} \quad \text{C12}$$

where N_p is the number of people on board (crew and passenger), V_{pr} is the volume of the pressurised cabin, and M_{uav} is the mass of un-installed avionics system

equipment. Howe's [129] method suggest 5 kg per passenger as mass density for ECS. He also proposes the following simple relation.

$$M_{ecs} = 0.035\,(M_{to})^{0.88}$$

From above relations, it was found that the General Dynamic equation is more realistic with respect to actual ECS mass values of transport aircraft given in [15]. Therefore C9 was selected and applied to predict ECS mass of transport aircraft. The output of ECS in all passenger aircraft are mainly the air-conditioned air which is supplied according to the following requirement :

Average fresh air to every passenger ($m_{fresh/pax}$)	0.545 kg/min
Average sufficient fresh air to toilets ($m_{fresh/toilet}$)	1.0 kg/min
Average fresh air to galleys ($m_{fresh/gallies}$)	0.7 to 1.0 kg/min
Arinc 600 minimum cooling air to avionics bay ($m_{avionics}$)	5.0 lb/min/kW
Arinc 408 cooling air to avionics in flight deck ($m_{avionics}$)	8.0 lb/min/kW

The above requirements were used to derive the following general relation for ECS output flow supply :

$$m_{ecs} = m_{fresh/pax} \times P_{AX} + m_{fresh/toilet} \times TT + m_{fresh/gallies} \times G_{AL} + m_{avionics} \times P_A \qquad \text{C13}$$

An Excel table was developed for aircraft ranging from 100 to 450 pax in which the mass of ECS was determined using GD equation . Also the output flow rate necessary for each aircraft was found using equation C13 . The numbers of crew was assumed 2 for 100 pax, and 4 for 450 pax, and 3 for the rest. The number of aisles are 1 for narrow body 100 and 150 pax, and 2 for the rest. Seat pitch is assumed 0.815m for all the ranges. Equations B25, and B26 were used to find pressurised cabin length, and fuselage diameter respectively. Finally assuming one crew and one toilet for 50 pax, and applying GD equation for ECS mass, the table became complete. The detailed results are included in Table C-4. Mathematica was used to correlate ECS mass with its output flow rate. This relation is given below, and Fig. C-6 shows the characteristics:

$$M_{ECS} = 15.35 \times m_{ecs} + 0.000757 \times m_{ecs}^{\,2} \qquad \text{C14}$$

C 4 . Avionics Cooling Modelling

In this section, the cooling modelling for avionics equipment in compartments, and flight deck is described. The procedure, and formulation, with related figures, and tables are presented.

C 4 .1 Avionics Compartment Cooling

In this section an equation is developed to correlate junction temperature (degree C) of MCUs in Avionics compartments as function of ECS cooling bleed flow rate (lb/min/kW of Avionics power consumption), and ECS cooling flow temperature (degree C). It is based on the method and experimental results in [79] elaborated in Chapter 3. Fig. C-6 show the characteristic surface developed using Mathematica to fit the 3-D points of Table C-5 . The equation of the surface fit is given below :

$$T_{jav} = 97.965 - 42.679 \times M_{bpkac} + 7.943 \times (M_{bpkac})^2 + 1.01008 \times T_{ecs} \qquad \text{C15}$$

C 4 .2 Deck Avionics Cooling

In this section the procedure and formulation developed for avionics deck case temperature as function of ECS output cooling flow rate is presented. According to the selected method and experimental results [82] discussed in chapter 3, case temperature rise (degree F) of avionics in aircraft deck is shown in Fig. C-7, redrawn based on Figure 3-47b (back exhaust), and the associated Table C-6 is established against ECS cooling bleed flow rate (lb/min/kW of Avionics power consumption). To the said table of points a curve fit was performed, using Mathematica, the accuracy of which is shown in Figure C-8. The equation corresponding to above figure is given below :

$$D_{TD} = 93.839 - 7.63476 \times M_{bpkad} + 0.204245 \times M_{bpkad} \qquad \text{C16}$$

C 5 . Avionics Reliability Modelling

Here, the reliability modelling for avionics equipment in compartments, and flight deck is described. The procedure, and formulation, with related figures, and tables are presented.

C 5 .1 Avionics Compartment Failure Rate

In this section the procedure for the development of a relation for failure rate variation of avionics in compartment bay against its junction temperature is presented.

Figure C-9 is the failure rate of a typical electronic equipment whose average reliability is sensitive to temperature, and it is originally based on Figure 3-49 of [83]. From the said figure, Table C-7 is established for average junction temperature. Mathematica was used to fit a curve to the above table of points the accuracy of which is shown in the Figure C-10. The equation of fit is given below :

$$F_{FRc} = 0.06058 + 0.00322 \times T_{jav} - 0.00007575 \times (T_{jav})^2 + 6.5713 \times 10^{-7} \times (T_{jav})^3 \quad \text{C17}$$

C 5 .2 Avionics Deck Failure Rate

In this section the development of a relation for failure rate variation of avionics equipment in flight deck with its case temperature rise is presented .

Based on the curve produced by reliability group in one of UK Defence Establishment shown in Figure 3-50 [84] the Excel Figure C-11 was drawn. It shows the relative failure rate rise with case temperature. It has been derived from published failure rate data for the component parts and is representative of a component population typical of many avionics equipment. Experimental and service experience has largely substantiated this characteristic pattern. The points of this figure helped to establish Table C-8. Mathematica was used to fit a curve to the said table of points, the accuracy of which is shown in Figure C-12. The equation of fit is given as below :

$$F_{RFd} = 1.09133 + 4.811 \times 10^{-8} \times (T_{case})^4 \quad \text{C18}$$

C 6 . Maintenance Cost Modelling

In this section the procedure and the formulation necessary to include the effects of failure rate improvement of avionics system in CACAD maintenance labour, material, spare part, and depreciation cost module are presented.

C 6 .1 Avionics Maintenance Labour, and Material Cost

The average maintenance man-hours of any system per flying hour is the product of system failure rate per flying hour and average maintenance man-hours per visit to

repair station each time system fails. Any improvement in reliability must be accompanied by a reduction in failure rate factor. For the avionics system in the flight deck, a reduction in failure rate factor takes place every time an extra cooling flow is supplied to this area.

$$F_{RFc} = F_{RFc\ after\ REM} / F_{RFc\ before\ REM} \qquad \text{C19}$$

$MHR_{avionics\ before\ REM}$ is a known quantity elaborated in Appendix B for the base aircraft.

$$MHR_{avionics\ after\ REM} = F_{RFc} \times MHR_{avionics\ before\ REM} \qquad \text{C20}$$

This relation is valid if the type of REM applied to avionics system has not caused any side effect either in system complexity, or system accessibility. Otherwise the rise in MHR per visit should also be modelled. Note that F_{RFc} is less than 1.

The same methodology and formulation was applied to the avionics in the compartment. Effect of failure rate improvement on maintenance material cost is definitely toward reducing it, but the rate of reduction is not clear. According to reference [85] MTBUR of avionics system directly influences the total maintenance cost of avionics (material & labour) by following relation :

$$DOC_{maint.\ avionics} = R_R \times C_R \qquad \text{C21}$$

where C_R is the cost of avionics maintenance labour and material per every removal, and R_R is the removal rate. It is assumed that C_R remains the same when ASRE is applied. Then :

$$DOC_{maint.\ avionics\ after\ REM} = DOC_{maint.\ avionics\ before\ REM} \times (R_{R\ after\ REM} / R_{R\ before\ REM})$$

C22

$$F_{RF} = (R_{R\ after\ REM} / R_{R\ before\ REM}) \qquad \text{C23}$$

From above relation it is evident that total maintenance cost improvement is also dependent on F_{RF} which was found in previous section. When the maintenance labour cost share of DOC was proved to be F_{RF} dependent, the material part of it is also seen to be F_{RF} dependent.

$$DOC_{maint.\ material\ avionics\ after\ REM} = DOC_{maint.\ material\ avionics\ before\ REM} \times F_{RF} \qquad \text{C24}$$

C 6 .2 Avionics Spare Parts Holding Cost

Based on spares provisioning equation derived by SABENA, presented in [85], the total cost of avionics spares is as follows :

$$C_{av.\,spare} = P_{av} \times Q \qquad \text{C25}$$

where P_{av} is the price of avionics equipment, and Q being the spares inventory, defined as below :

$$Q = m + \frac{1.6 \times \sqrt{m}}{\sqrt{N}} + C \qquad \text{C26}$$

where m is the average number of avionics units being repaired per day and therefore is the number of units needed to fill the pipe line, C is the number of spares assigned to remote stations, $\frac{1.6 \times \sqrt{m}}{\sqrt{N}}$ is the term that accounts for random fluctuation in failure rate, in which N is the fleet size, which signifies the fact that the bigger the fleet size, the less the cost of spares holding . The value of m is given by the following relation :

$$m = EURT \times FH/_{MTBUR} \qquad \text{C27}$$

where $EURT$ is the electronic unit repair time in days, and FH is the average aircraft utilisation rate in flight hours per day, $MTBUR$ is the mean time between unscheduled removal .

If we ignore the spares deployed in remote stations, and also let no fluctuation in avionics failure rate be considered at conceptual design phase, then the cost of spare parts will be as below :

$$C_{av.spare} = P_{av} \times \frac{EURT \times FH}{MTBUR} \qquad \text{C28}$$

Any improvement in failure rate factor i.e. being reduced, may increase $MTBUR$ directly, and therefore reduces the cost of spares .

$$MTBUR_{after\ RE\ measure} = MTBUR_{before\ RE\ measure} \div FRF \qquad \text{C29}$$

where *FRF* is failure rate factor . As ASRE were selected such that it did not affect the maintainability of the avionics system, *EURT* remains unchanged before and after *RE* modelling . This is the same for *FH*, hence the following relation is concluded :

$$C_{av.spare\ after\ RE\ measure} = C_{av.\ spare\ before\ RE\ measure} \times Failure\ Rate\ Factor \qquad C30$$

C 6 .3 Avionics Depreciation Cost

Depreciation of avionics as part of aircraft DOC standing charges per flight is given by the following relation, as used in CACAD, and also approved by [14,15] :

$$C_{standing/avionics} = \frac{1-R}{L} \times P_{av} \times \frac{T_{block}}{U} \qquad C31$$

where T_{block} is the flight block time, U is annual utilisation (hours of flight per year), R is the residual value of the avionics system at the end of its service life. L is the service life of the avionics equipment in years and is the only parameter that is affected by REM. The following is a maintenance approach to the value of L :

$$L = No.\ of\ Overhaul \times \ TBO \qquad C32$$

where *TBO* is the system time between overhaul and is so selected not to exceed *MTBF* of the avionics which is given as below :

$$MTBF = 1/\lambda_{avionics} \qquad C33$$

therefore the life of avionics also are related inversely to avionics failure rate factor as below :

$$L_{avionics\ after\ RE\ measure} = L_{avionics\ before\ RE\ measure} \times \ FRF \qquad C34$$

C 7 . ACAU Modelling for UHCA

The following modelling was made to enable design proposal 2 (elaborated in Chapter 3 section 3.15) to be implemented for ASRE integration into UHCA.

- **Mass Modelling** : The ECS mass estimation modelling presented in C3 was used to predict the mass of the ACAU. Due to absence of considerable piping, a mass pipe reduction factor (*MPF)* of 20 to 35% is defined to account for such mass reduction as below.

$$M_{cau} = (15.3482 \times m_b + 0.00075698 \times m_b{}^2) \times (1. - MPF) \qquad C36$$

The above relation gives a reasonable mass estimate, to a higher value than perhaps real cold air units would weigh .

- Cold Air Unit Power Consumption : The first law of thermodynamics was used to establish the following relationship to predict the ACAU power consumption as function of its out-put flow rate.

$$P_{net} = m_{bsi} \times C_p \times T_{01} \times \{ (CPR^{\gamma-1/\gamma} - 1) / \eta_{icomp} - \eta_{itur} \times \eta_{mech} \times [1 - (1/ TPR)^{\gamma-1/\gamma}] \times [1 + (CPR^{\gamma-1/\gamma} - 1) / \eta_{icomp}] \} \quad C37$$

in which the compressor pressure ratio (CPR), and turbine pressure drop ratio (TPR) was assumed as 2, and 1.5 respectively together with conservative values for isentropic efficiency of compressor 0.7 (η_{icomp}), turbine 0.8 (η_{itur}), and mechanical efficiency of transmission 0.95 (η_{mech}).

- ACAU Power-off Take Effects : The TURBOMATCH code was again used to simulate engine performance, subjected to power-off take during cruise at 35000 ft, and 0.82 Mach number for 75150 lbf TRENT class engine. The empirical relation developed from the data was validated fairly well with actual data supplied from a prominent manufacturer [76]. The TRENT class power-off take penalty characteristics is shown in Figure C-23, and the correlation equations are given as below:

$$\Delta T / T_{st} = [-1.05732 + 0.0104147 \times (P_{net} - 100)] / 334.145 \quad C38$$

$$\Delta SFC = [- 52.522 + 0.51722 \times (P_{net} - 100)] / 1000 \quad C39$$

C 8 . Results of ASRE Integration with CACAD

Figures C-13 to C-21 show the program result of ASRE in CACAD for conventional aircraft resembling Fokker F100, Airbus A340, A310, and A330. Figure C-22 shows the program result of design proposal 1, and 2 integration in UHCA. A complete discussion and analysis of the results are provided in section 3.17 of Chapter 3.

Engine	Thrust static	Mass Flow	CPR	BPR	TET	SFC	ALT.cr	Mcr	TETcr	Mass Flow cruise	Thrust cruise	SFC cruise
unit → type ↓	N	kg/sec			deg K	mg/s/N	foot		deg K	in kg/s	in N	in mg/s/N
TAY650	61604.8	186.36	15.8	3.04	?	?	35000	0.8	?	?	11342.4	19.5
Turbo-tay	61463.4	186.36	15.8	3.04	1430	12.98	35000	0.8	1225	75.32	11499.8	21.36
CFM56 -C2	138777.	466.8	37.4	6.6	?	?	35000	0.8	?	?	30740	16.06
Turbo CFM	138634.	466.8	37.6	6.6	1680	8.735	35000	0.8	1610	195.256	30641.7	16.63
CF6-80 -C2	233342.	802.1	30.4	5.05	?	?	35000	0.85	?	?	50396	16.372
Turbo CF6	233584.	802	30.384	5.05	1500	9.124	35000	0.85	1410	348.3	50267	17.53
TRENT -775	334267.	919.81	39.03	4.77	?	?	35000	0.82	?	?	51152	16.031
Turbo Trent	334145.	919.81	39.027	4.77	1748	10.262	35000	0.82	1390	333.32	50817	16.42
IAE-V2525	111250	355.62	27.7	4.8	?	?	35000	0.80	?	?	25689.85	16.258
Turbo IAE	111246.9	355.62	27.683	4.79	1578	10.2	35000	0.8	1530	149.811	25661.21	18.983

Table C-1 : Comparison of real life engine specification with the one designed by Turbomatch

	TurboTay (Engine designed by Turbomatch for Fokker F100)								TurboCFM (Engine designed by Turbomatch for Airbus A340)							
% Bleed	m core	m bleed	Thrust cruise	SFC cruise	Thrus t fall	SFC rise	% SFC	% Thrust	m core	m bleed	Thrus t cr.	SFC	Thrus t fall	SFC rise	% SFC	% Thrust
Unit	kg/sec	kg/sec	in N	mg/s/N	dT	dSFC	rise	fall	kg/sec	kg/sec	in N	mg/s/N	dT	dSFC	rise	fall
0	17.198	0	11500.	21.366	0	0	0	0	26.534	0	30642	16.632	0	0	0	0
0.01	17.219	0.1722	11308.	21.567	192.3	0.2011	0.0094	0.0170	25.586	0.2559	30306	16.718	336	0.086	0.0052	0.0111
0.02	17.256	0.3451	11145	21.751	354.9	0.3848	0.0180	0.0318	26.641	0.5328	29969	16.806	673	0.174	0.0105	0.0225
0.03	17.299	0.5190	10988	21.934	511.9	0.5678	0.0266	0.0466	26.695	0.8009	29631	16.896	1011	0.264	0.0159	0.0341
0.04	17.341	0.6936	10828	22.125	671.9	0.7588	0.0355	0.0621	26.751	1.0700	29292	16.989	1350	0.357	0.0215	0.0461
0.05	17.384	0.8692	10671	22.318	828.9	0.9518	0.0445	0.0777	26.807	1.3403	28951	17.084	1691	0.452	0.0272	0.0584
0.06	17.43	1.0458	10512	22.519	987.9	1.1528	0.0540	0.0940	26.865	1.6119	28609	17.181	2033	0.549	0.0330	0.0711
0.07	17.476	1.2233	10355	22.722	1144.9	1.3558	0.0635	0.1106	26.914	1.8840	28249	17.278	2393	0.646	0.0388	0.0847
0.08	17.526	1.4021	10202.	22.926	1298.3	1.5598	0.0730	0.1273	26.895	2.1516	27830	17.383	2812	0.751	0.0452	0.1010
0.09	17.578	1.5820	10052	23.128	1447.9	1.7618	0.0825	0.144	26.898	2.4208	27427	17.488	3215	0.856	0.0515	0.1172
0.1	17.615	1.7615	9882	23.361	1617.9	1.9948	0.0934	0.1637	26.898	2.6898	27020	17.596	3622	0.964	0.0580	0.1340
0.15	17.626	2.6439	8900	24.765	2599.9	3.3988	0.1591	0.2921	26.644	3.9966	24721	18.199	5921	1.567	0.0942	0.2395
0.2	17.466	3.4932	7845	26.523	3654.9	5.1568	0.2414	0.4659	26.343	5.2686	22481	18.872	8161	2.24	0.1347	0.3630

Table C-2a : the effect of bleed at 35000 ft and Mach 0.82, and at Intermediate Compressor port on Thrust and SFC of the specified engines at 100% throttle setting..

	Turbo CF6 (Engine designed by Turbomatch for Airbus A310)								Turbo TRENT (Engine designed by Turbomatch for Airbus A330)							
% Bleed	m core	m bleed	Thrust cruise	SFC cruise	Thrus t fall	SFC rise	% SFC	% Thrust	m core	m bleed	Thrus t cr.	SFC	Thrus t fall	SFC rise	% SFC	% Thrust
Unit	kg/sec	kg/sec	in N	mg/s/N	dT	dSFC	rise	fall	kg/sec	kg/sec	in N	mg/s/N	dT	dSFC	rise	fall
0	58.174	0	50268	17.53	0	0	0	0	53.579	0	50817	16.417	0	0	0	0
0.01	58.316	0.5832	49646	17.656	622	0.126	0.0072	0.0125	53.605	0.5361	50125	16.529	692	0.112	0.0069	0.0138
0.02	58.467	1.1693	49026	17.784	1242	0.254	0.0145	0.0253	53.645	1.0729	49446	16.643	1371	0.226	0.0138	0.0277
0.03	58.624	1.7587	48405	17.916	1863	0.386	0.0220	0.0385	53.685	1.6106	48763	16.76	2054	0.343	0.0209	0.0421
0.04	58.784	2.3513	47784	18.051	2484	0.521	0.0297	0.0520	53.725	2.149	48079	16.881	2738	0.464	0.0283	0.0569
0.05	58.948	2.9474	47159	18.191	3109	0.661	0.0377	0.0659	53.775	2.6887	47399	17.004	3418	0.587	0.0358	0.0721
0.06	59.117	3.5470	46536	18.333	3732	0.803	0.0458	0.0802	53.823	3.2294	46719	17.131	4098	0.714	0.0435	0.0877
0.07	59.276	4.1493	45894	18.479	4374	0.949	0.0541	0.0953	53.873	3.7711	46037	17.261	4780	0.844	0.0514	0.1038
0.08	59.35	4.748	45185	18.636	5083	1.106	0.0631	0.1125	53.929	4.3143	45357	17.395	5460	0.978	0.0596	0.1204
0.09	59.445	5.3500	44485	18.795	5783	1.265	0.0722	0.1300	53.984	4.8586	44673	17.533	6144	1.116	0.0680	0.1375
0.1	59.542	5.9542	43782	18.96	6486	1.43	0.0816	0.1481	54.05	5.405	43993	17.675	6824	1.258	0.0766	0.1551
0.15	59.351	8.9027	39706	19.906	10562	2.376	0.1355	0.2660	53.794	8.0691	40020	18.498	10797	2.081	0.1267	0.2698
0.2	59.066	11.813	35523	21.088	14745	3.558	0.2030	0.4151	52.649	10.530	35256	19.574	15561	3.157	0.1923	0.4414

Table C.2b show the effect of bleed at 35000 ft and Mach 0.82, and at Intermediate Compressor port on Thrust and SFC of mentioned engines where the throttle setting is 100% .

TAY		CFM		CF6		TRENT	
m	SFC	m	SFC	m	SFC	m	SFC
bleed	rise	bleed	rise	bleed	rise	bleed	rise
kg/sec	mg/s/N	kg/sec	dSFC	kg/sec	dSFC	kg/sec	dSFC
0	0	0	0	0	0	0	0
0.1722	0.2011	0.2559	0.086	0.5832	0.126	0.5361	0.112
0.3451	0.3848	0.5328	0.174	1.1693	0.254	1.0729	0.226
0.5190	0.5678	0.8008	0.264	1.7587	0.386	1.6106	0.343
0.6936	0.7588	1.0700	0.357	2.3514	0.521	2.149	0.464
0.8692	0.9518	1.3403	0.452	2.9474	0.661	2.6888	0.587
1.0458	1.1528	1.6119	0.549	3.5470	0.803	3.2294	0.714
1.2233	1.3558	1.8840	0.646	4.1493	0.949	3.7711	0.844
1.4021	1.5598	2.1516	0.751	4.748	1.106	4.3143	0.978
1.5820	1.7618	2.4208	0.856	5.3500	1.265	4.8586	1.116
1.7615	1.9948	2.6898	0.97	5.9542	1.43	5.405	1.258
2.6439	3.3988	3.9966	1.567	8.9027	2.376	8.0691	2.081
3.4932	5.1568	5.2686	2.24	11.813	3.558	10.530	3.157

TAY		CFM		CF6		TRENT	
m	Thrust	m	Thrust	m	Thrust	m	Thrust
bleed	fall	bleed	fall	bleed	fall	bleed	fall
kg/sec	in N	kg/sec	in N	kg/sec	in N	kg/sec	in N
0	0	0	0	0	0	0	0
0.1722	192.3	0.2559	336	0.5832	622	0.5360	692
0.3451	354.9	0.5328	673	1.1693	1242	1.0729	1371
0.5190	511.9	0.8008	1011	1.7587	1863	1.6105	2054
0.6936	671.9	1.0700	1350	2.3514	2484	2.149	2738
0.8692	828.9	1.3403	1691	2.9474	3109	2.6887	3418
1.0458	987.9	1.6119	2033	3.5470	3732	3.2294	4098
1.2233	1144.9	1.8840	2393	4.1493	4374	3.7711	4780
1.4021	1298.3	2.1516	2812	4.748	5083	4.3143	5460
1.5820	1447.9	2.4208	3215	5.3500	5783	4.8586	6144
1.7615	1617.9	2.6898	3622	5.9542	6486	5.405	6824
2.6439	2599.9	3.9966	5921	8.9026	10562	8.0691	10797
3.4932	3654.9	5.2686	8161	11.813	14745	10.530	15561

Table C-3 : The actual SFC penalty and the actual thrust penalty, against actual amount of bleed in kg/s for all 4 types engine at 100% cruise condition .

P_{AXmax}	C_{ABIN}	P_{AB}	F_{USD} m	P_{CL}	Vpax in m^3	M_{ECS} in kg	P_A	m_{ccx} in kg/min
100	2	4	2.81	29.325	90.8846	926.7189	7	65.26364
150	3	6	3.81	29.325	167.0812	1417.521	8	106.0227
200	4	7	4.81	33.12857	300.8379	2041.815	8	134.2727
250	5	8	5.31	35.98125	398.2034	2518.351	9	165.9318
300	6	8	5.31	42.6375	471.8679	2916.265	9	194.1818
350	7	8	5.31	49.29375	545.5324	3303.864	9	222.4318
400	8	9	5.81	50.03333	662.9051	3789.583	10	254.0909
450	9	10	6.31	50.625	791.1583	4289.971	10	282.3409

Table C-4 : ECS mass modelling converting cabin particular dependency to cabin airconditioning and pressurisation flow dependency .

ECS flow in lb/min/kW	T_{ecs} *in deg. C*	$T_{j\,av.}$ *in deg. C*
1.364	5.55	60
1.45	7.22	60
1.82	13.17	60
2.05	15.56	60
2.27	17.94	60
1.364	25	80
1.45	26.6	80
1.57	29.44	80
1.73	32.22	80
1.82	33.33	80
1.98	35	80
2.27	37.78	80
1.364	45	100
1.56	48.89	100
1.73	51.67	100
1.82	52.78	100
1.98	54.44	100
2.27	57.44	100

Table C-5 : Data extracted from experimental results of Figure 3-29.

ECS Flow Rate in lb/min/kW	*Case Temperature Rise in deg F*
8	46
10	37
12	32
14	28
16	25
18	23

Table C-6 This table is developed from experimental results of Figure 3.47b (back exhaust) [82].

Junction Temperature deg. C	*Failures Per 10^6 Hr*
20	0.1
50	0.115
60	0.121
67	0.1335
72	0.147
77	0.161
81	0.174
85	0.19
88	0.207
91	0.221
96	0.249
98	0.272

Table C-7 This table was developed from average failure rate demonstrated from typical two extreme group of avionics components i.e. highly and poorly temperature dependent components [83] .

Case Temperature in deg C (TCASE)	*Relative Failure Rate*
20	1.1
40	1.2
60	1.74
80	2.9
90	4.15
100	5.8

Table C-8 This table was developed from the a curve widely accepted by industry. It is failure rate factor of avionics equipment variation with thier case temperature [84].

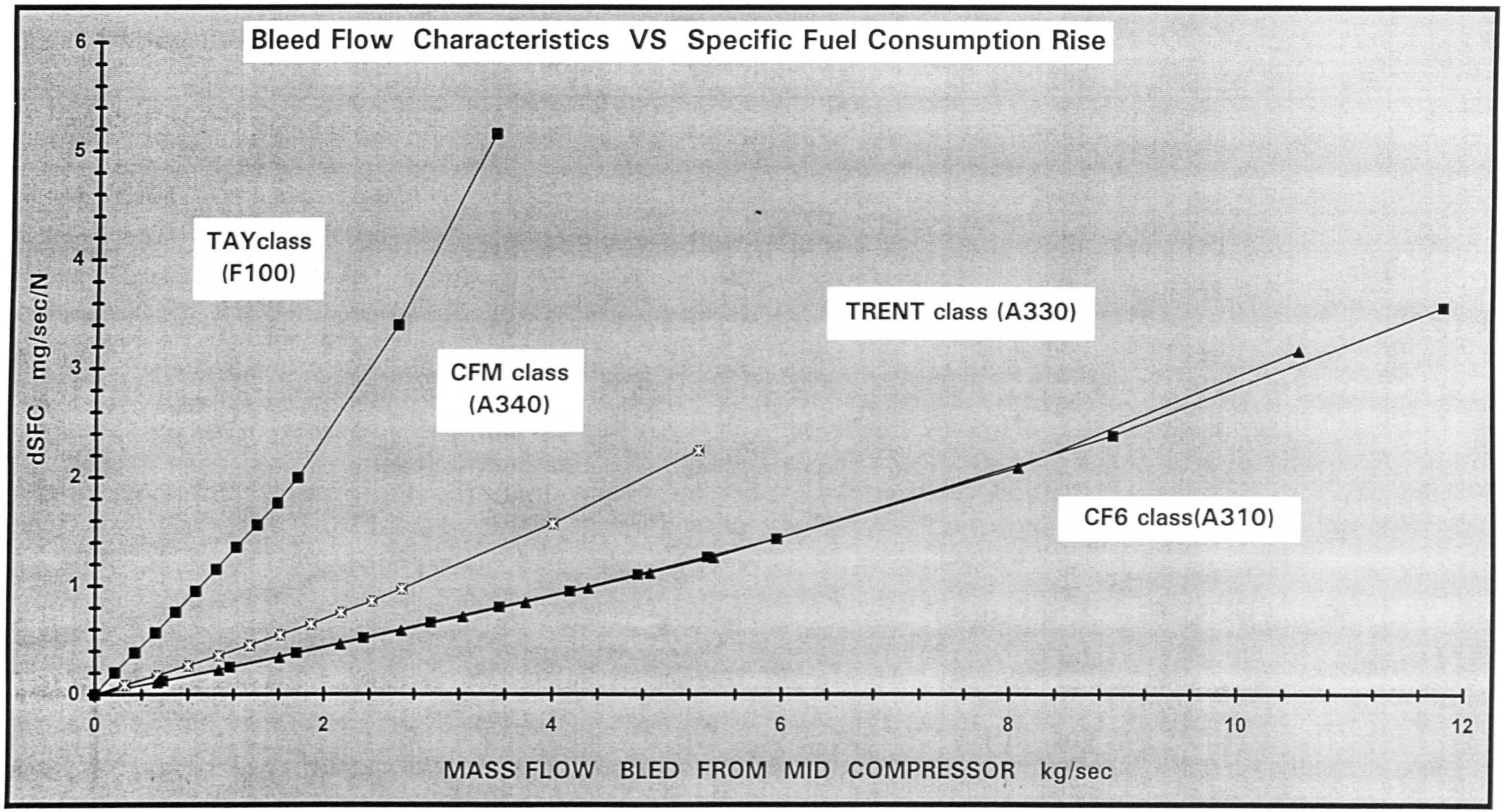

Figure C-1 : sfc rise due to bleed during 35000 ft, 0.82 Mach cruise of above simulated engines by Turbomatch

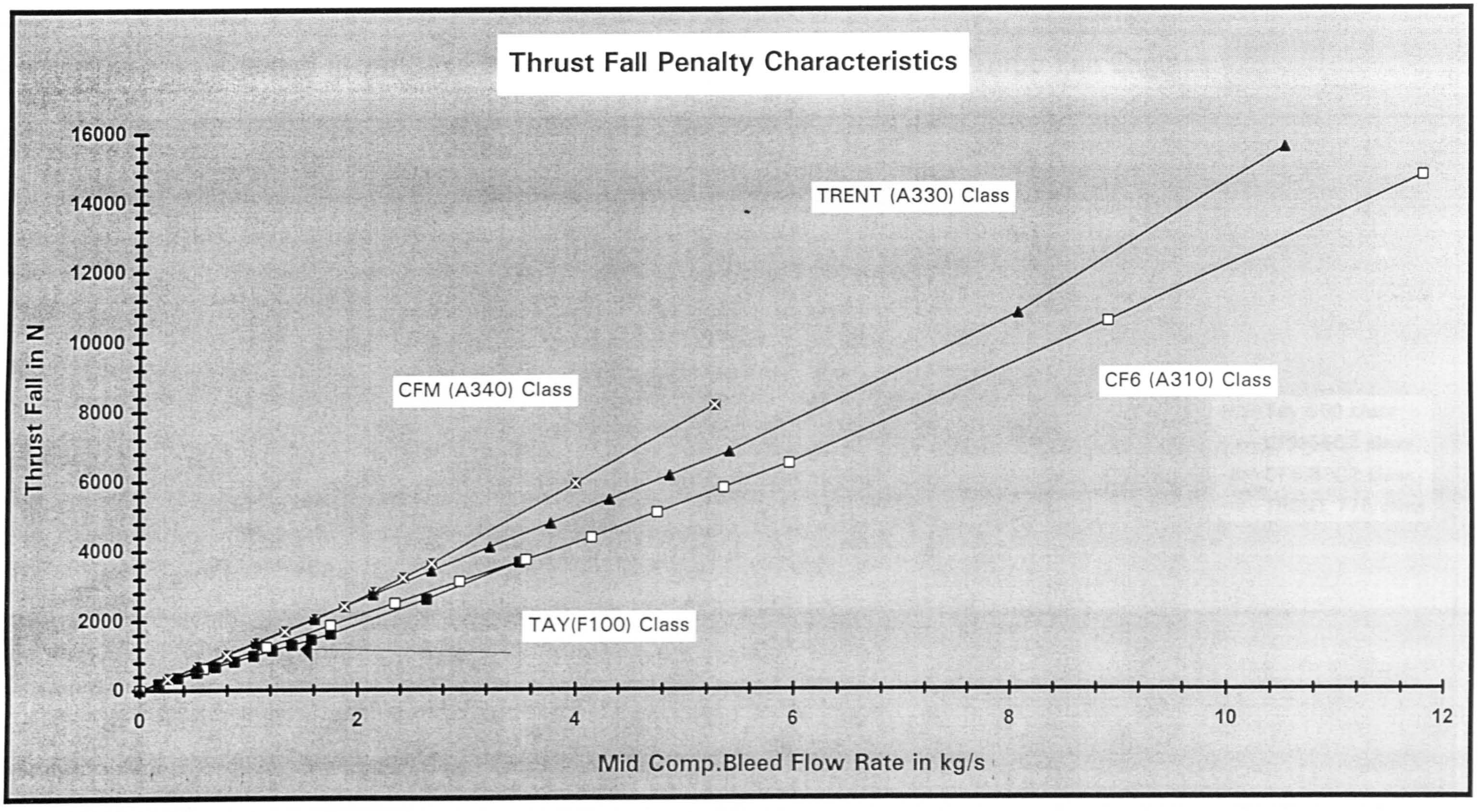

Figure C-2 : Thrust fall due to bleed during 35000 ft, 0.82 Mach cruise of above simulated engines by Turbomatch Code .

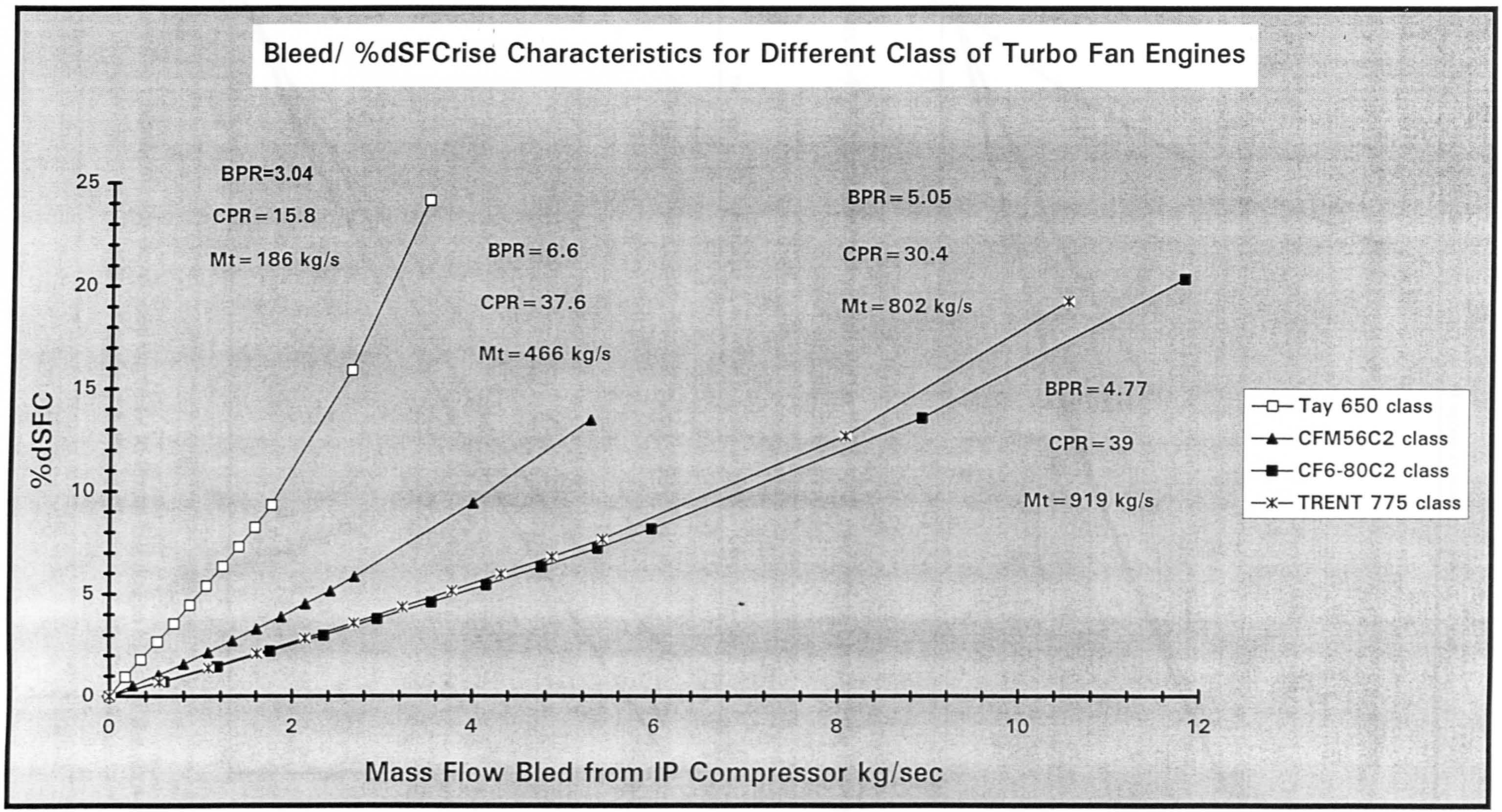

Figure C-3, % sfc rise due to bled . Tay 650 : 15100 lbf s/l, 2950 lbf cr., 0.69 SFCcr; CFM56C2 : 31200 lbf s/l, 7370 lbf cr., 0.545 SFCcr; CF6-80C2 : 52460 lbf s/l, 11330 lbf cr., 0.578 SFCcr; TRENT 775 : 75150 lbf s/l, 11500 lbf cr., 0.565 SFCcr

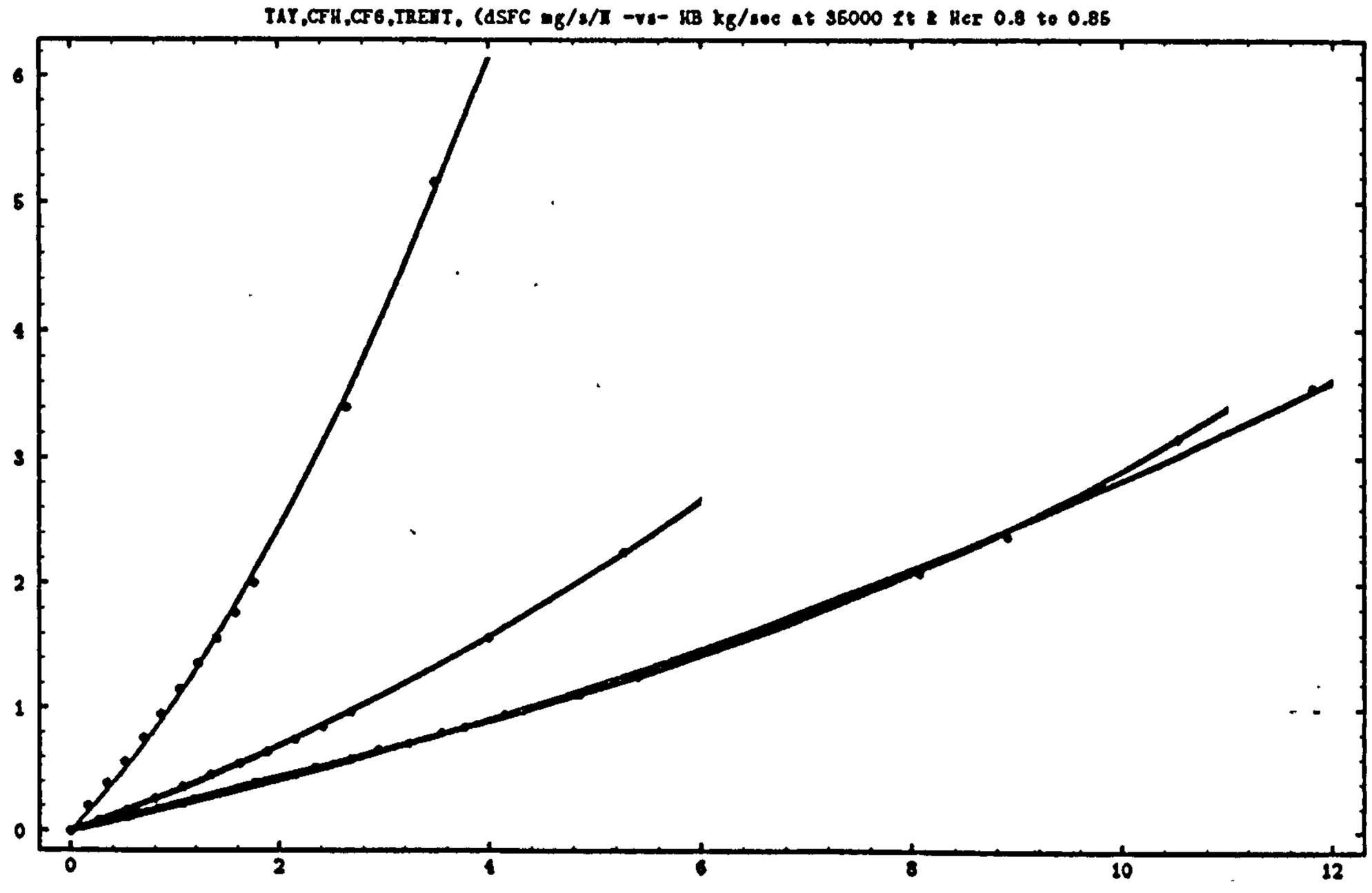

Figure C-4 : Mathematica developed curve fit to %sfc rise due to bleed of the above class of engines during cruise.

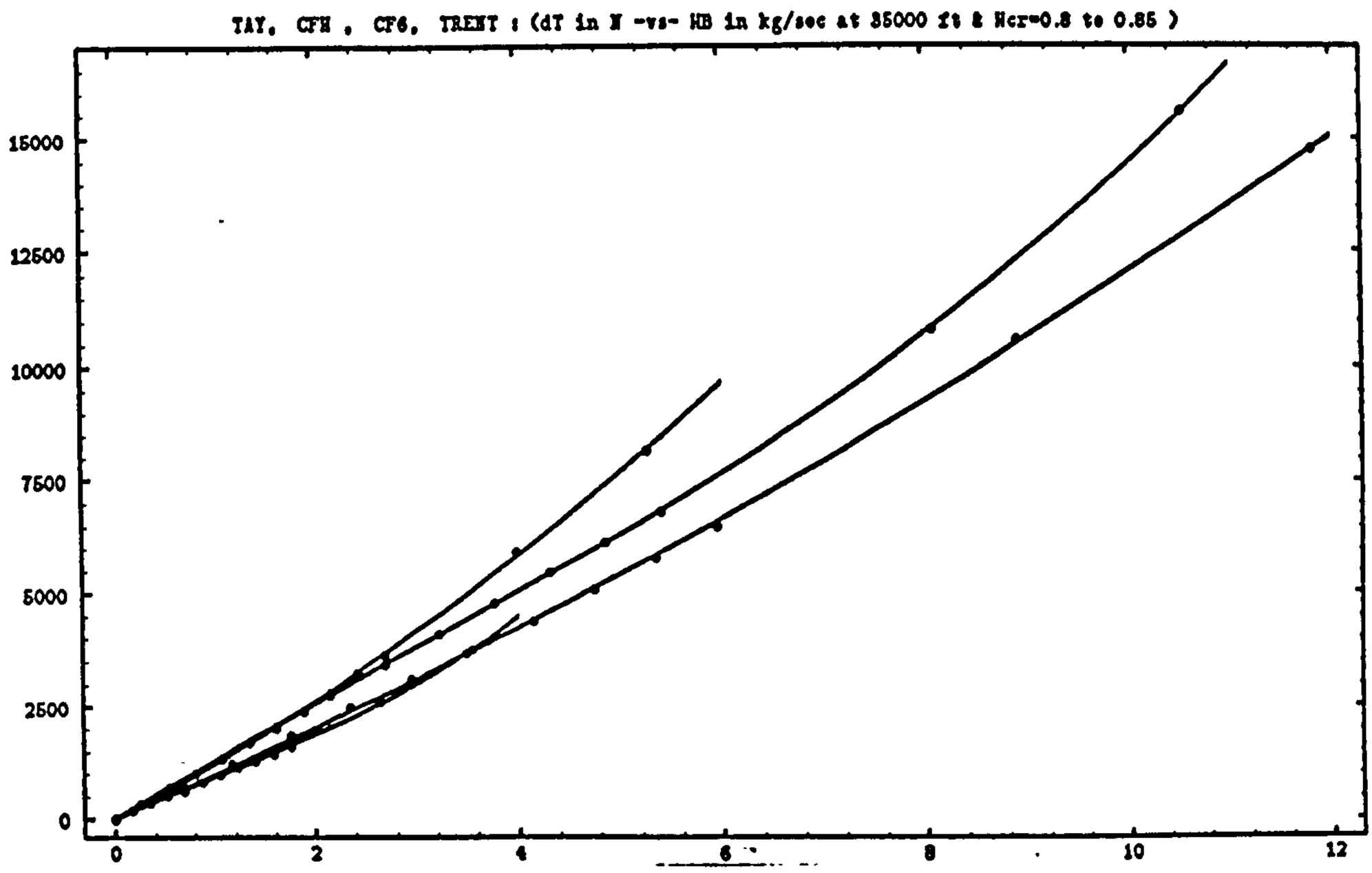

Figure C-5 : Mathematica developed curve fit to thrust fall due to bleed of the above class of engines during cruise.

T_{jav} in degree C

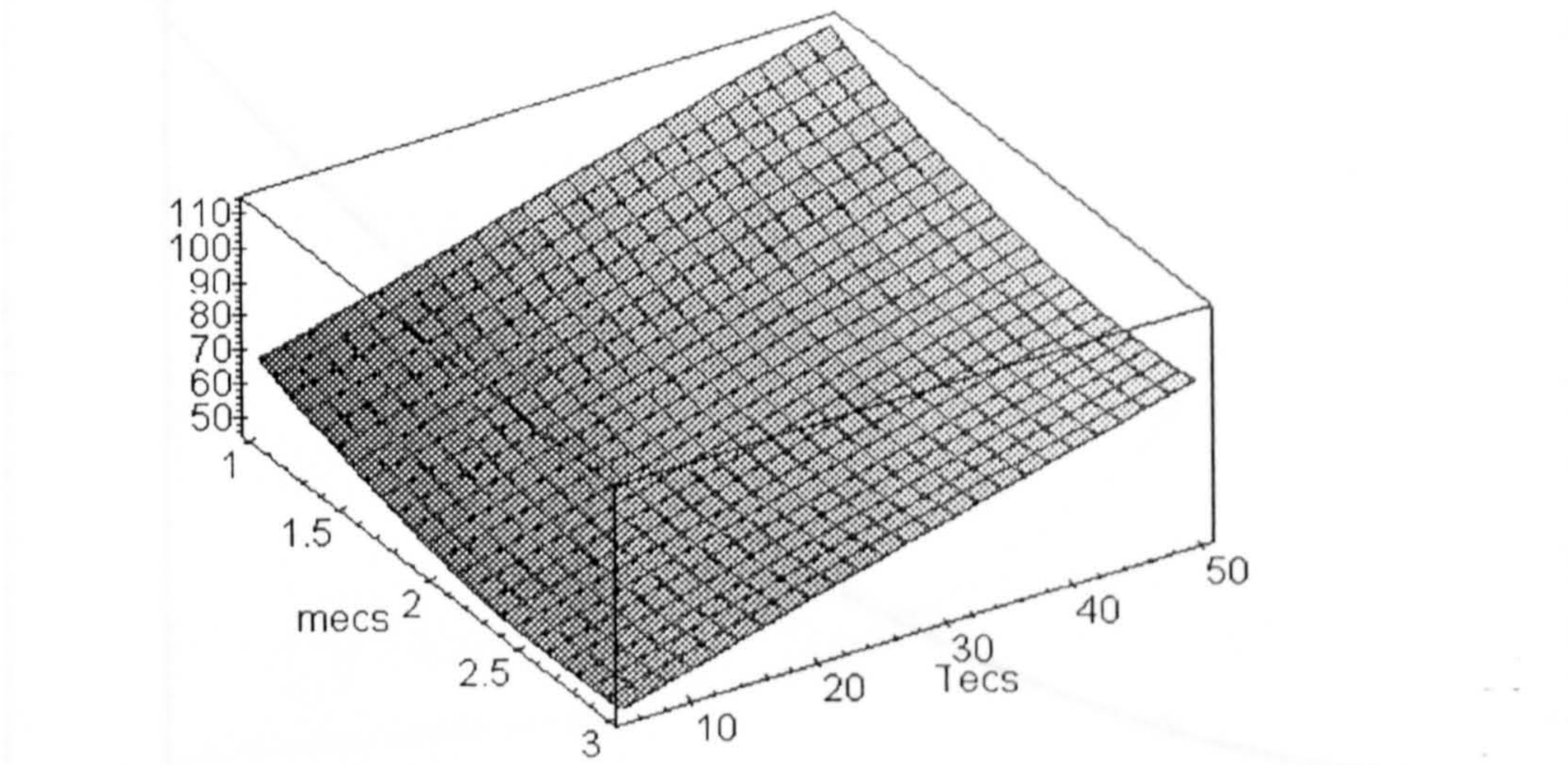

Figure C-6 : Cooling flow surface characteristics in air-rail cooled racks made by Mathematica, drawn by Maple.

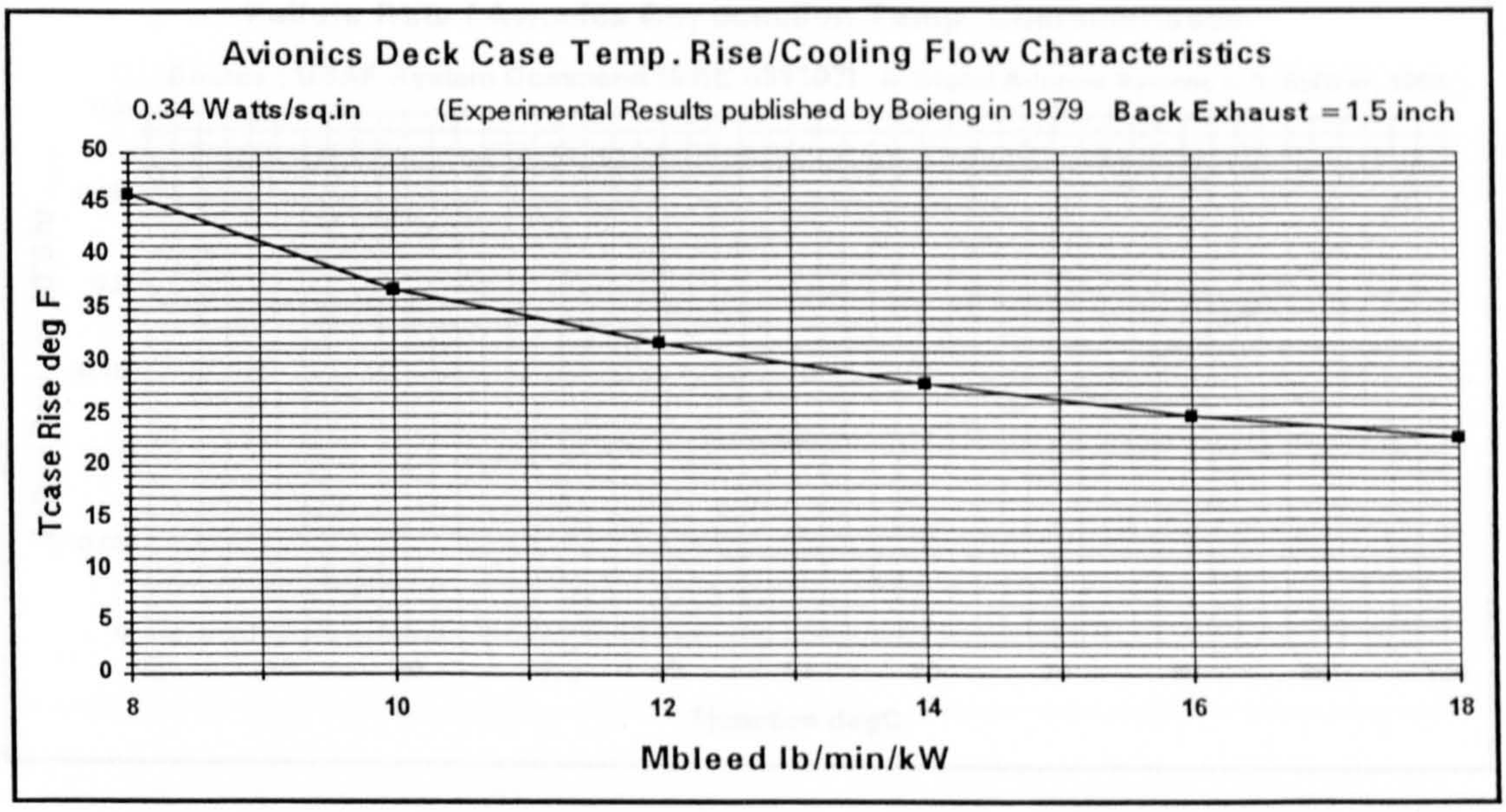

Figure C-7 : Case temperature rise of avionics in flight deck as function of ECS output flow rate extracted from experimental results published in AGARD-CP-196.

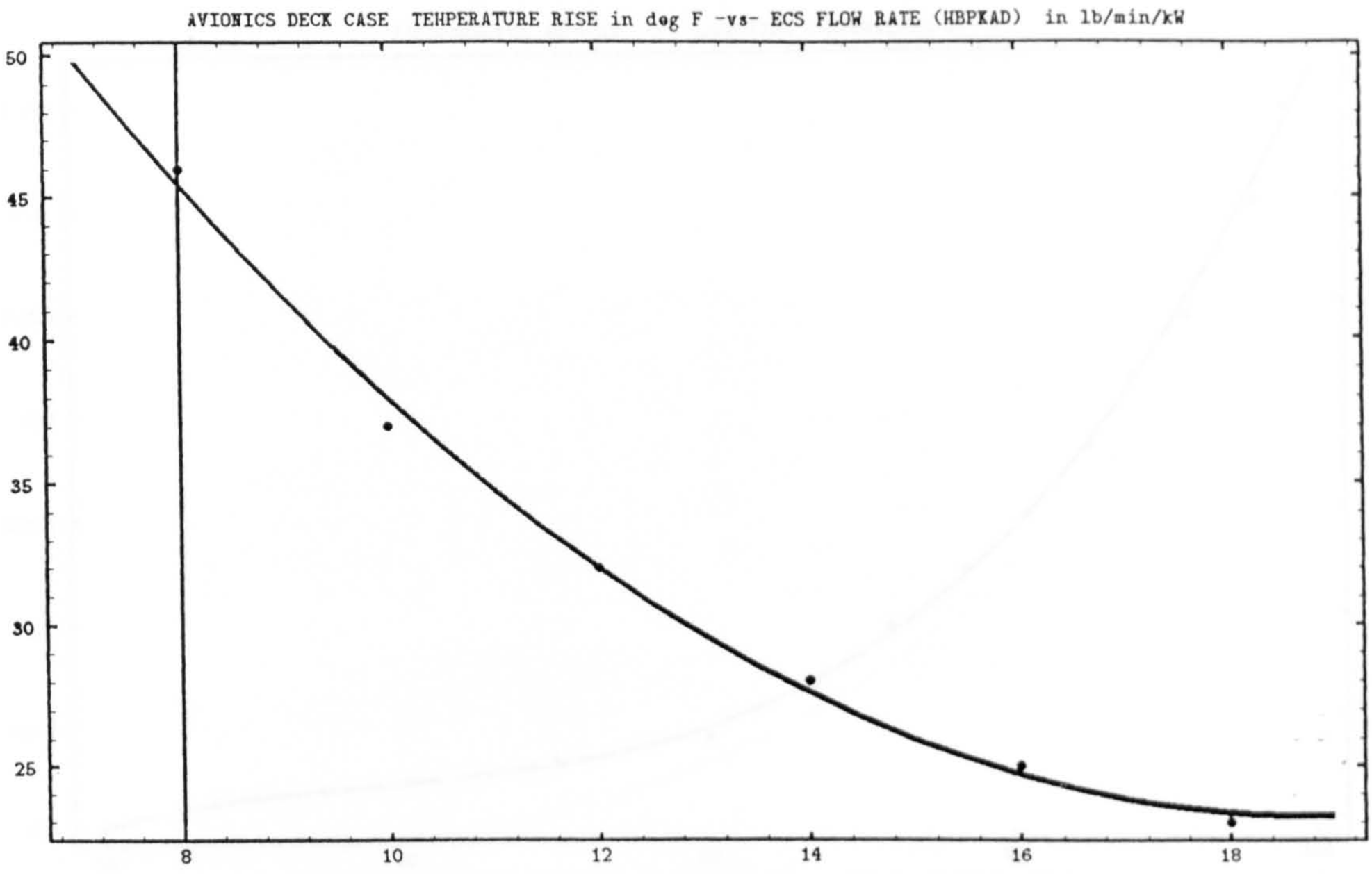

Figure C-8 : Mathematica developed curve fit to avionics flight deck case temperature rise versus ECS flow rate.

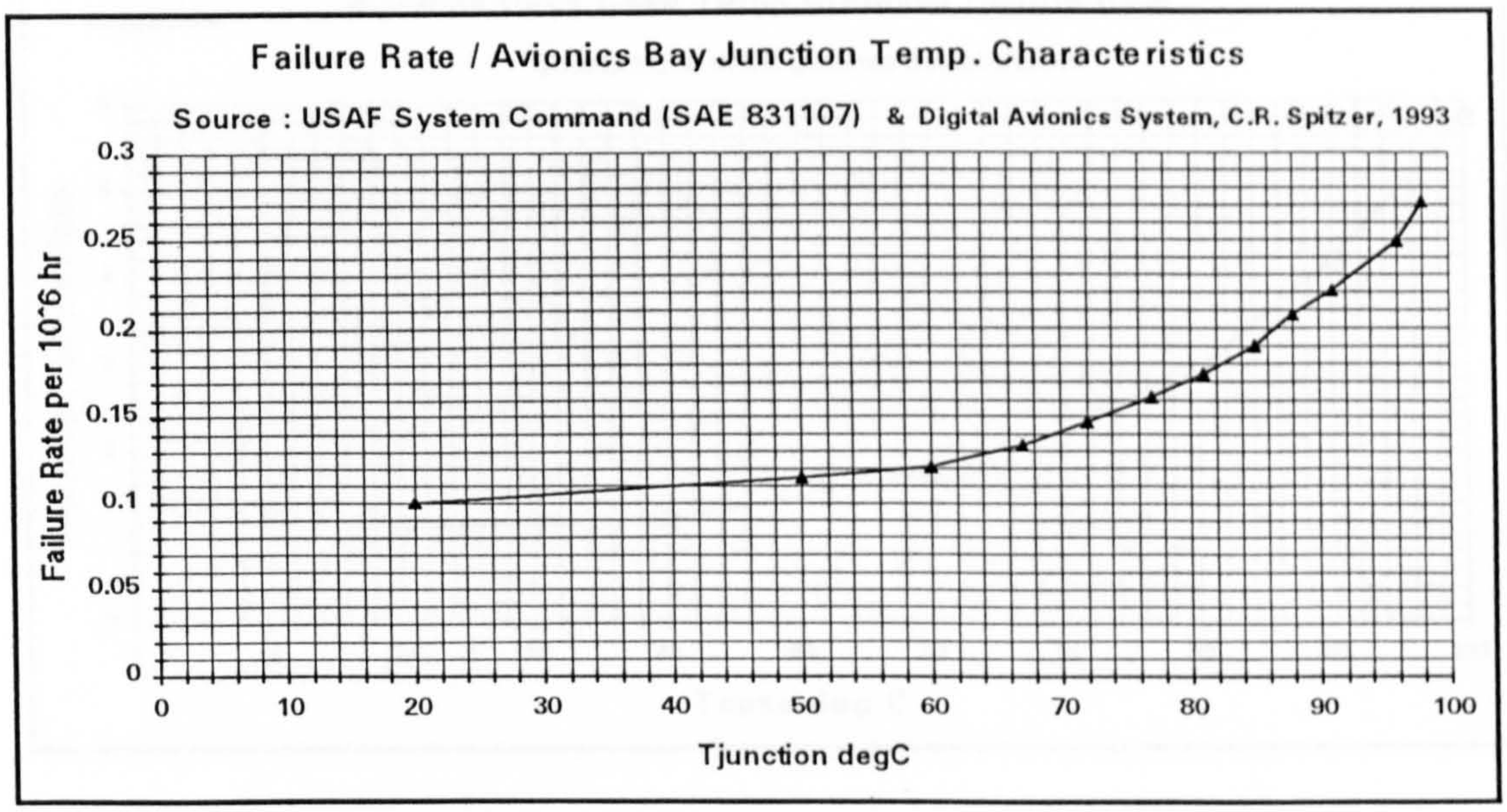

Figure C-9 : Average failure rate variation with avionics equipment bay junction temperature from [83].

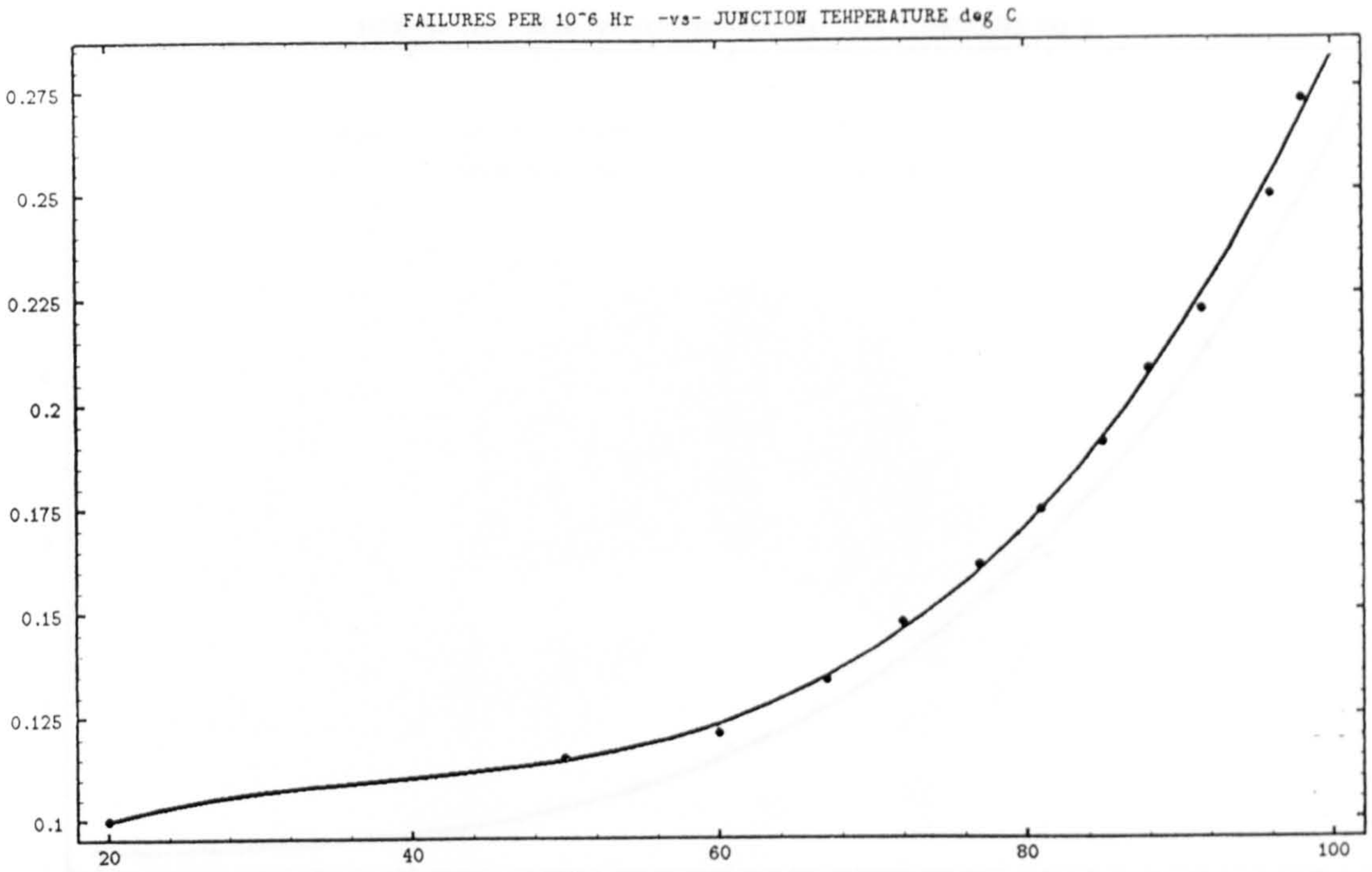

Figure C-10 : Mathematica developed curve fit to avionics average failure rate variation with its component junction temperature.

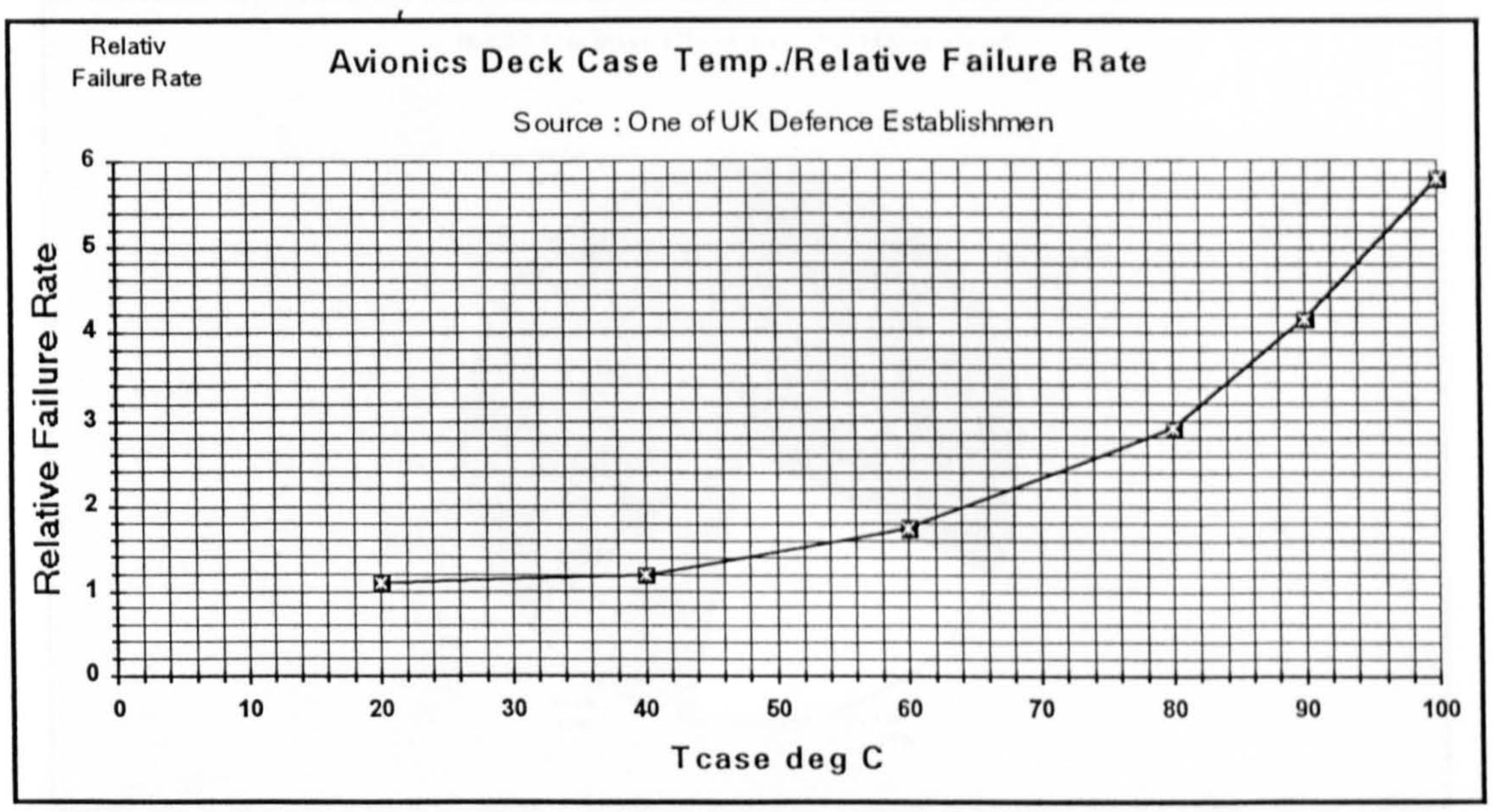

Figure C-11 : Relative failure rate variation with case temperature rise of typical avionics equipment in flight deck, generally accepted by Industry [84].

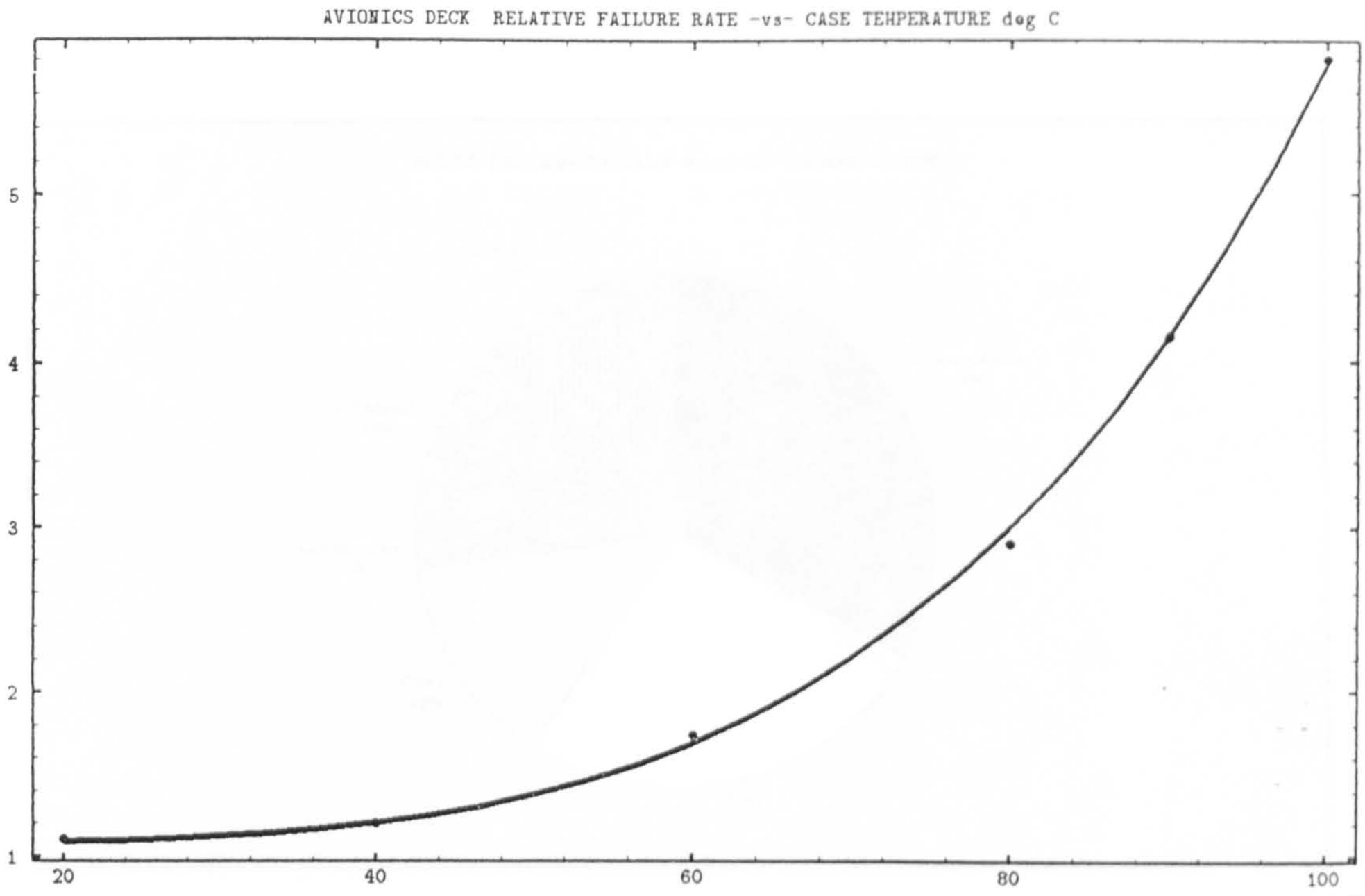

Figure C-12 : Mathematica developed curve fit to typical avionics equipment in flight deck failure rate variation with case temperature rise.

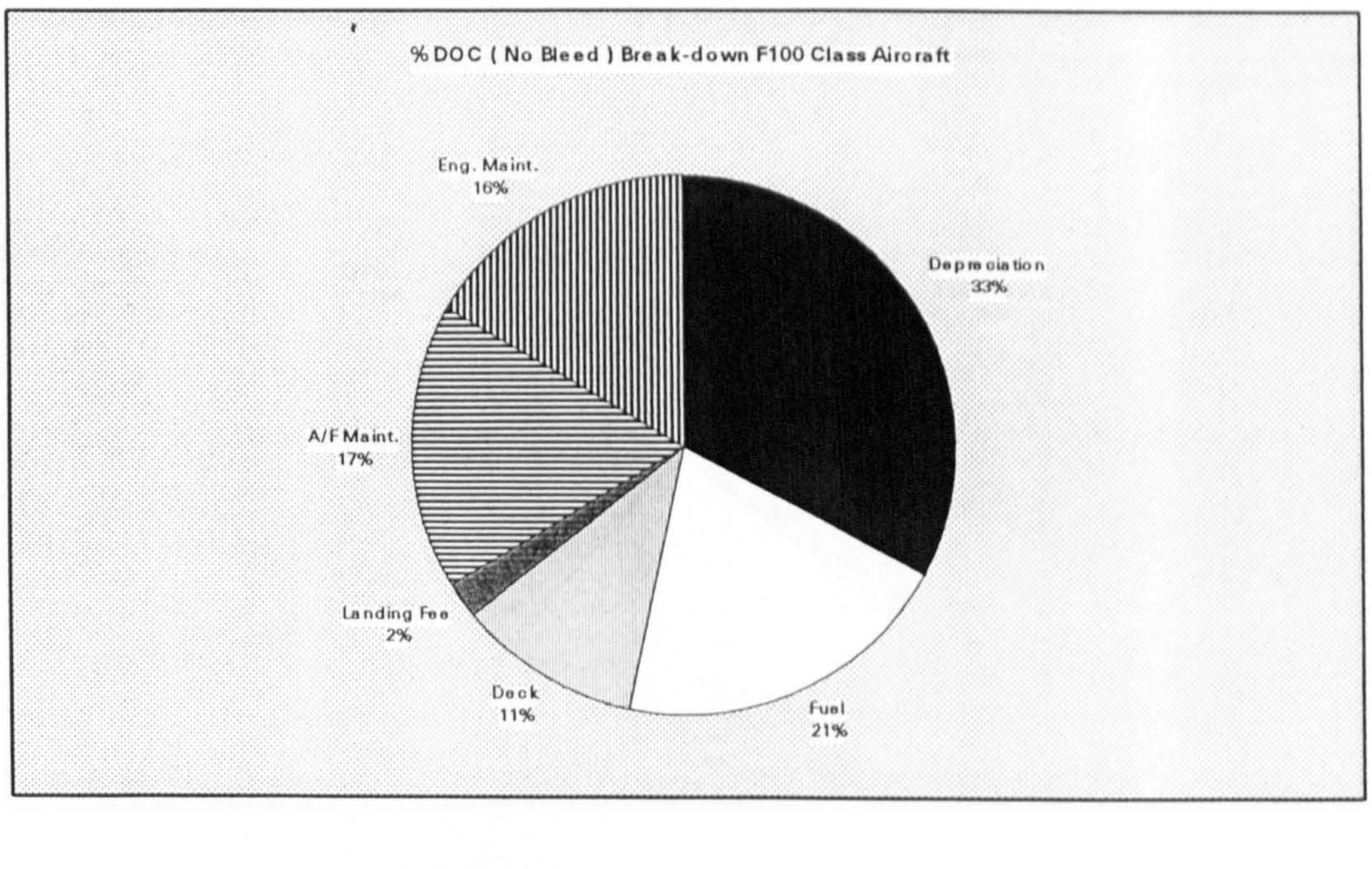

Figure C-13 : DOC major break-down for defined mission before REM
a) Twin aft engines, 107 PAX, 2400 km range

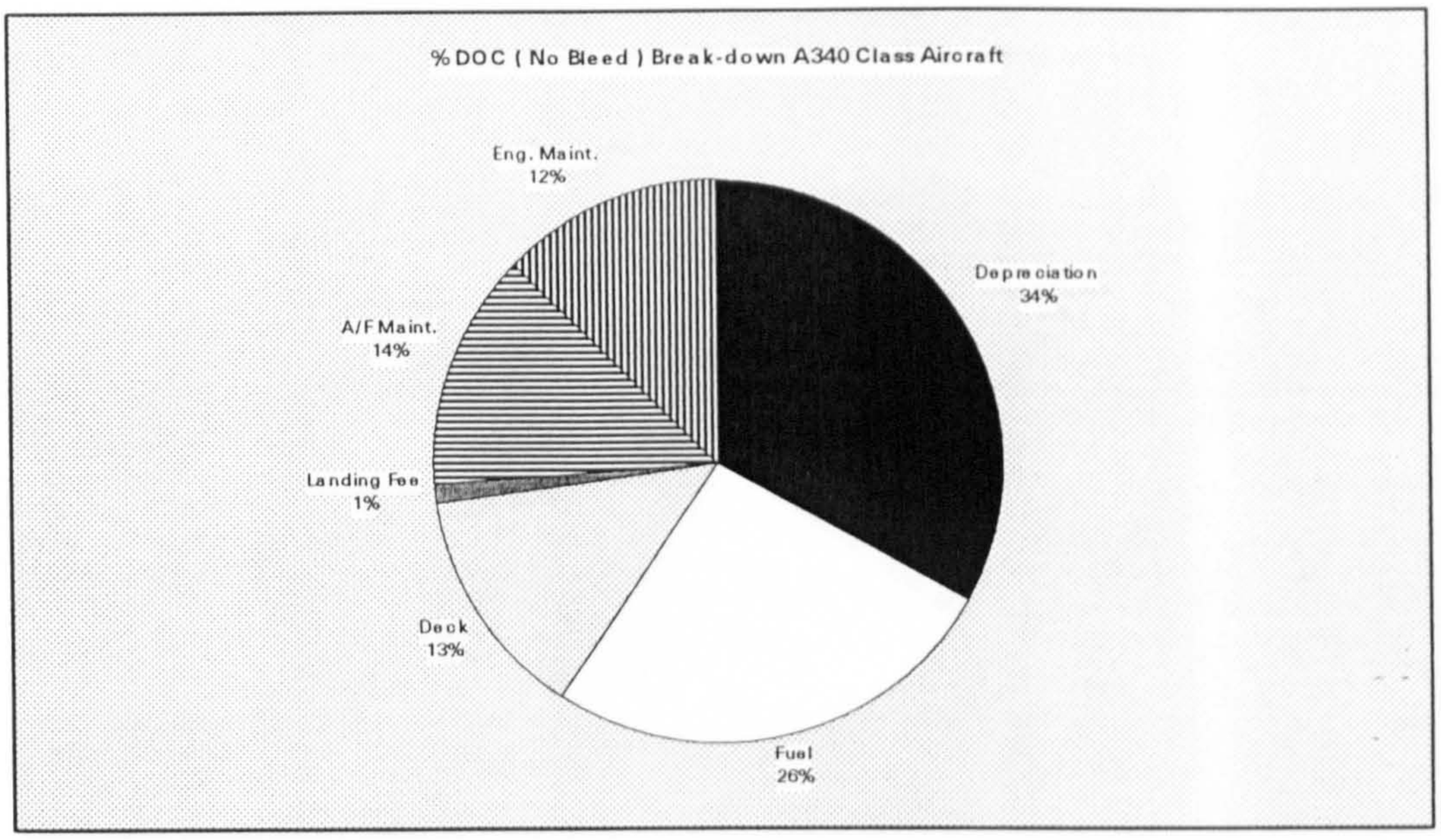

Figure C.13- DOC major break-down for defined mission before REM
b) 4 Engines, 440 PAX, 10200 km

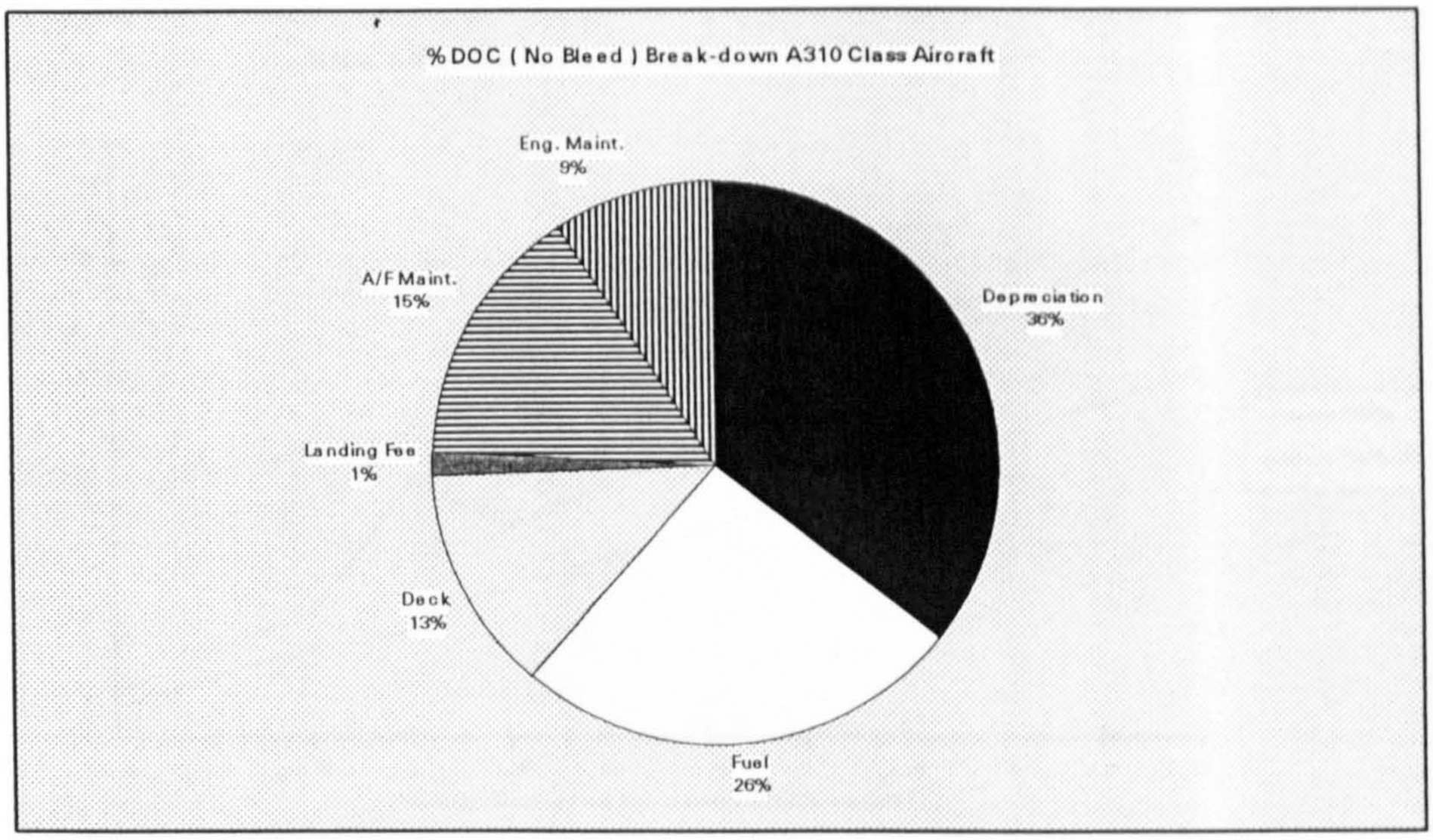

Figure C-13 : DOC major break-down for defined mission before REM
c) Twin engines, 280 PAX, 7982 km

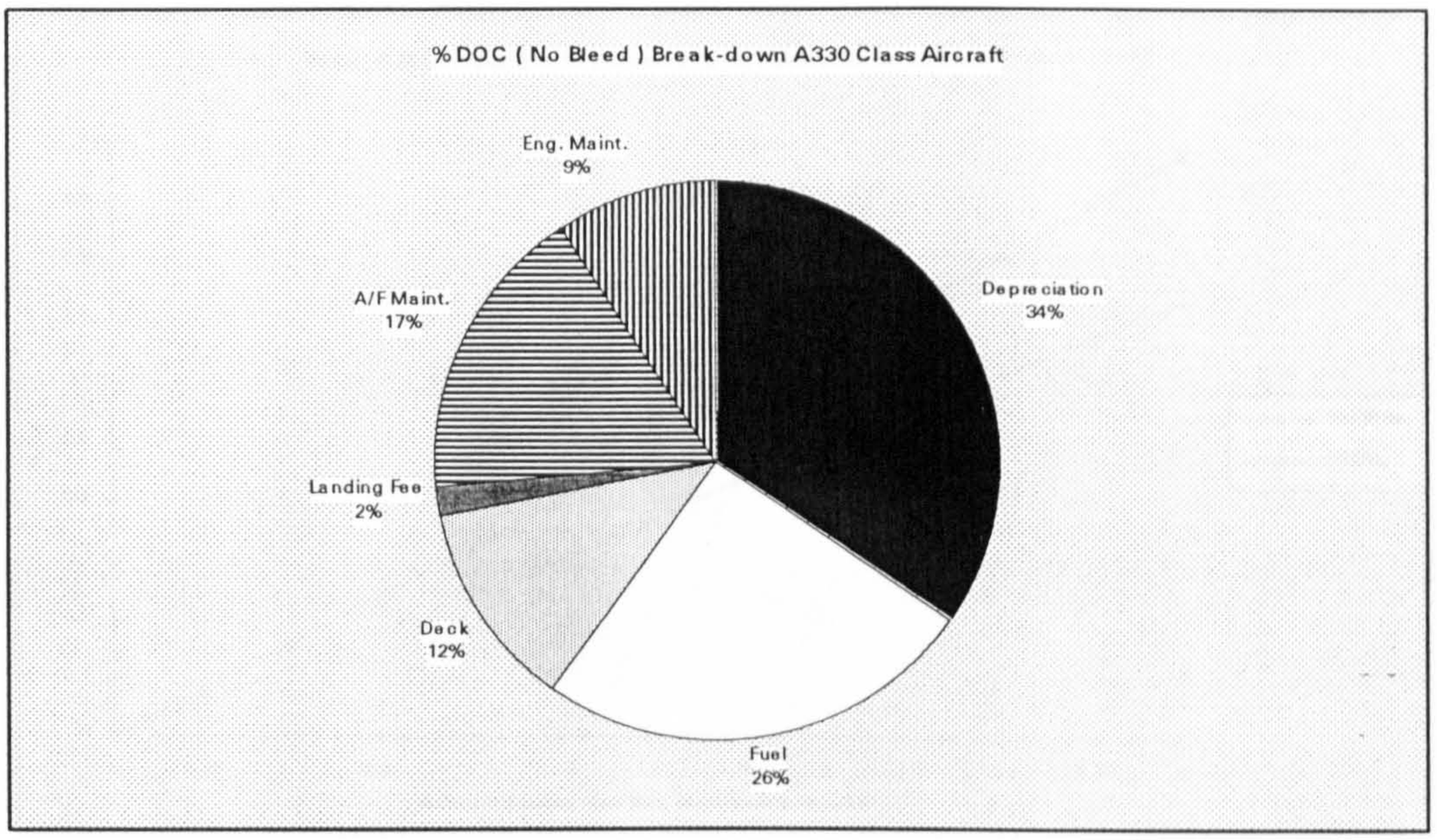

Figure C-13 : DOC major break-down for defined mission before REM
d) Twin engines, 440 PAX, 6483 km

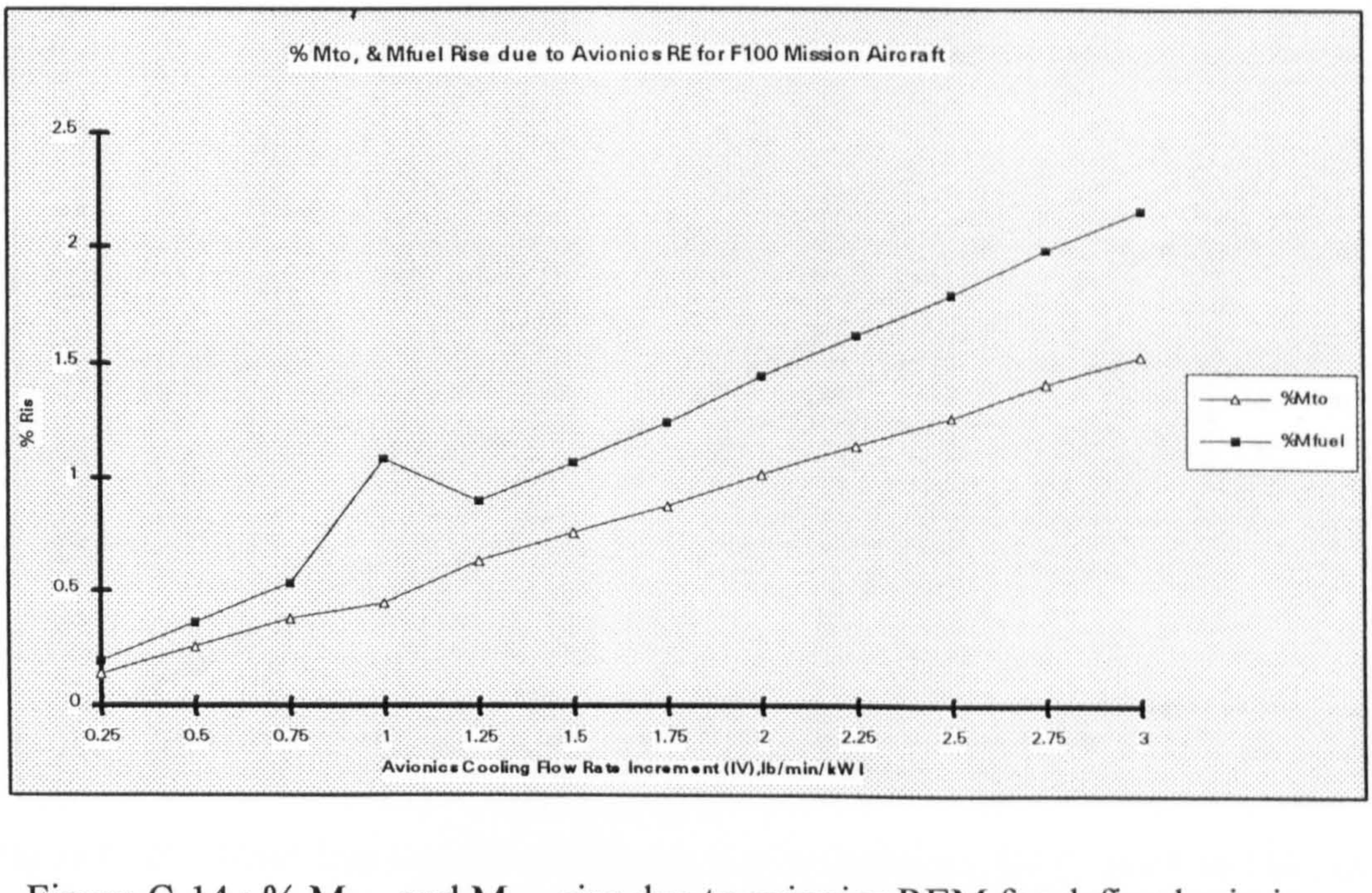

Figure C-14 : % M_{to} , and M_{fuel} rise due to avionics REM for defined missions.
a) Twin aft engines, 107 PAX, 2400 km

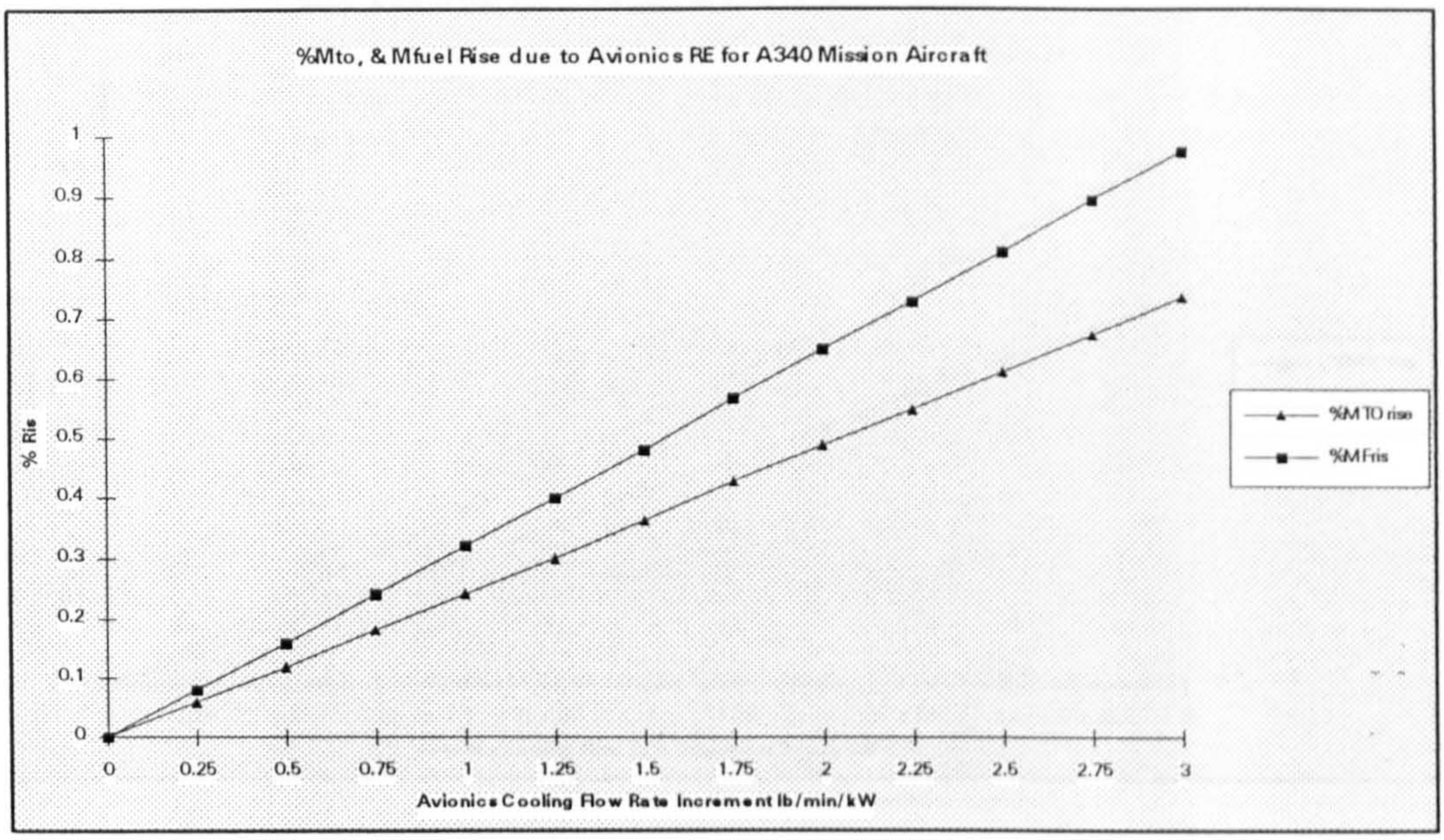

Figure C-14 : % M_{to} , and M_{fuel} rise due to avionics REM for defined missions.
b) 4 Engines, 440 PAX, 10200 km

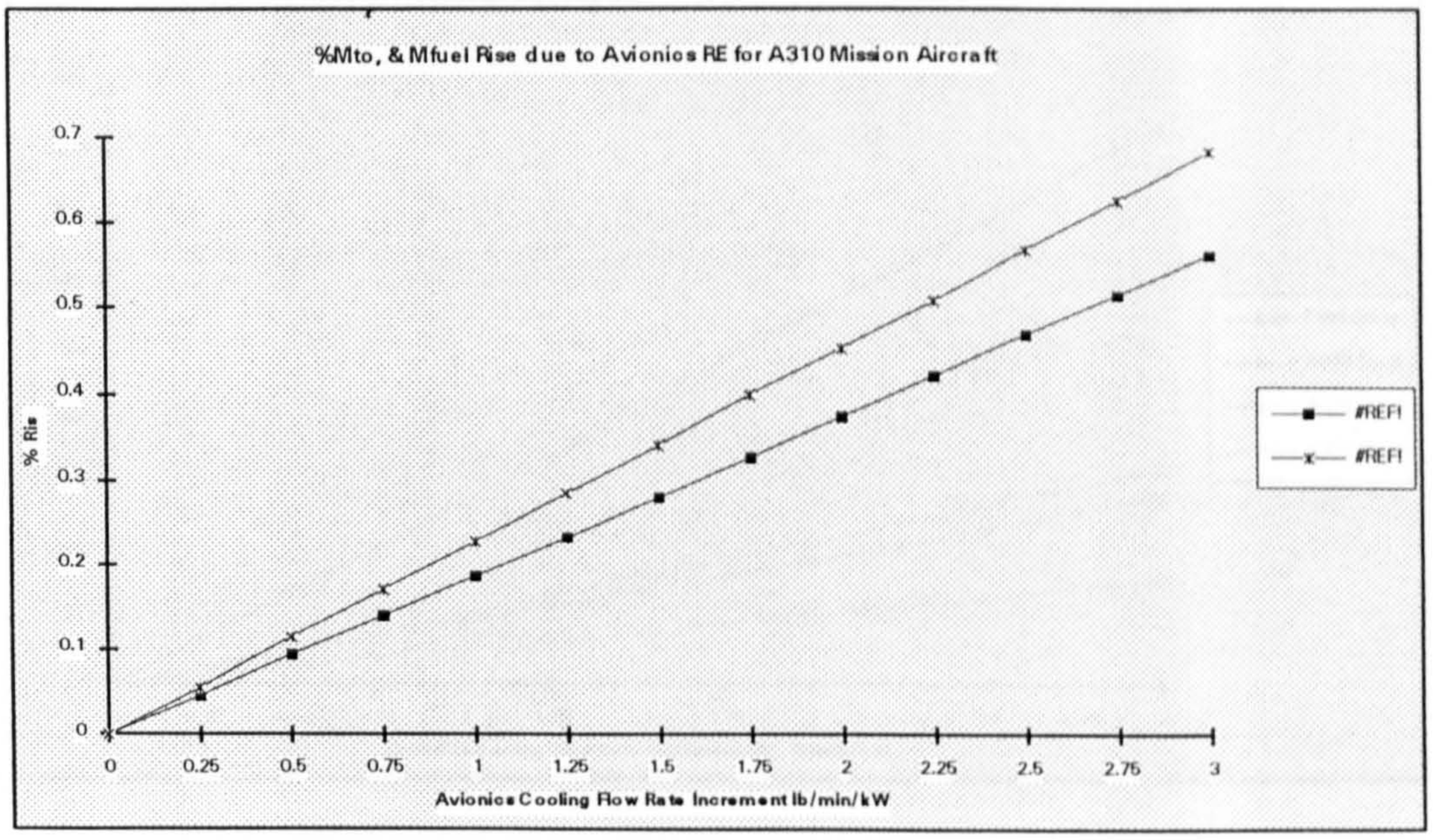

Figure C-14 : % M_{to} , and M_{fuel} rise due to avionics REM for defined missions.
c) Twin engines, 280 PAX, 7982 km

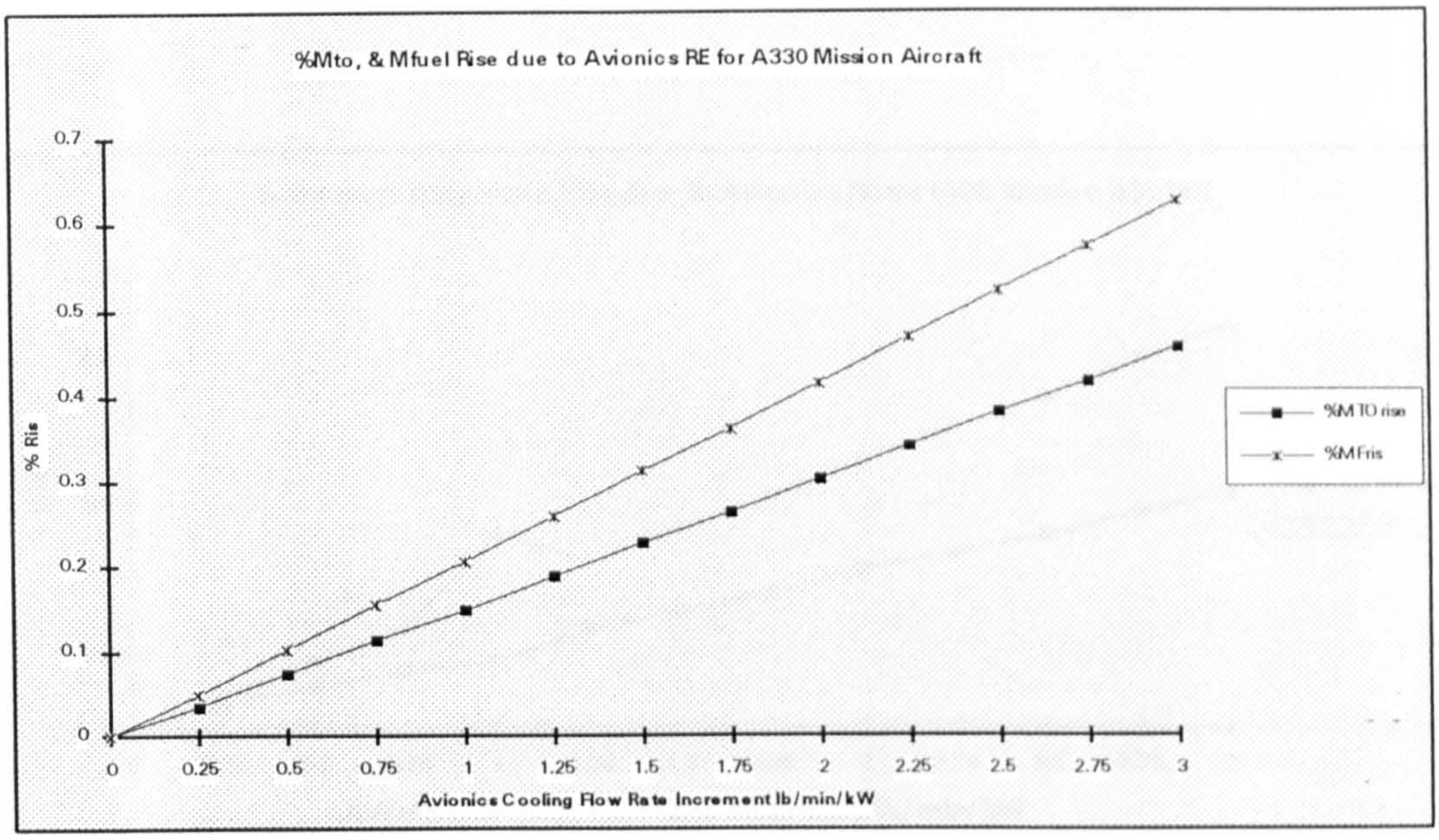

Figure C-14 : % M_{to} , and M_{fuel} rise due to avionics REM for defined missions.
d) Twin engines, 440 PAX, 6483 km

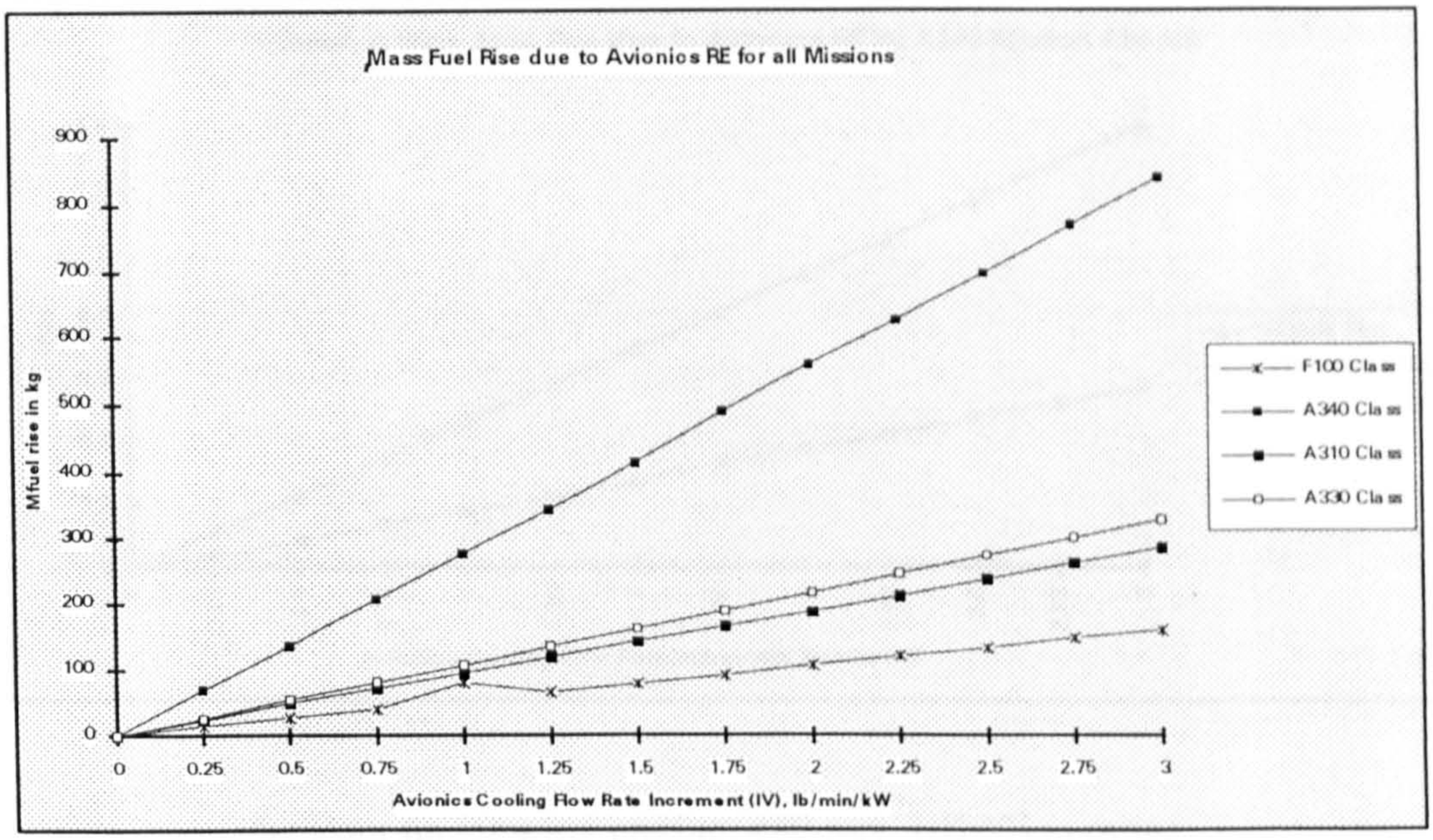

Figure C-15 : Mass fuel rise for all mission shown together, Every ponit in this figure corresponds to an optimised airplane at the particular avionics RE cooling increment .

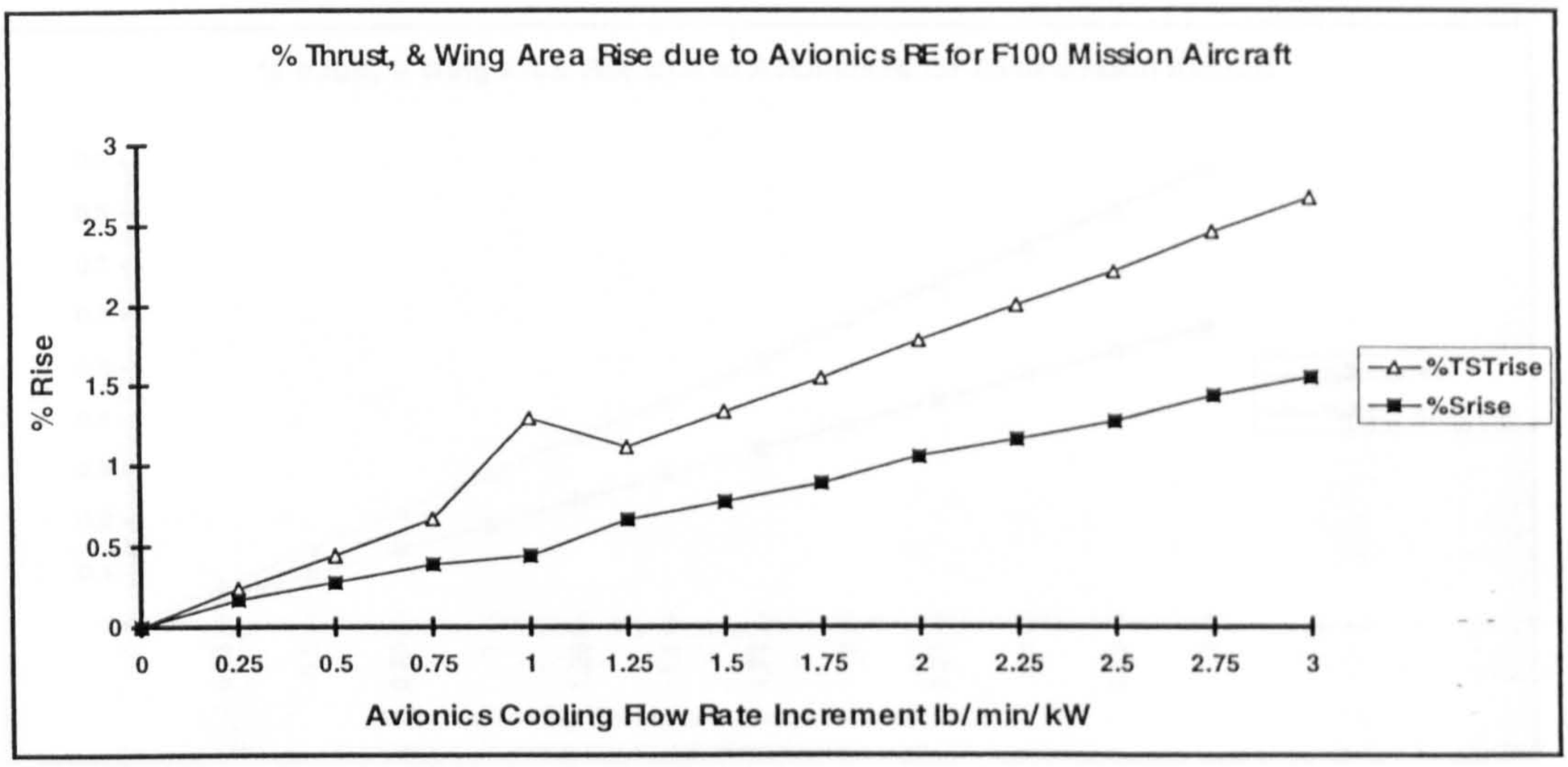

a : Twin aft engine, 107 pax, 2400km range.

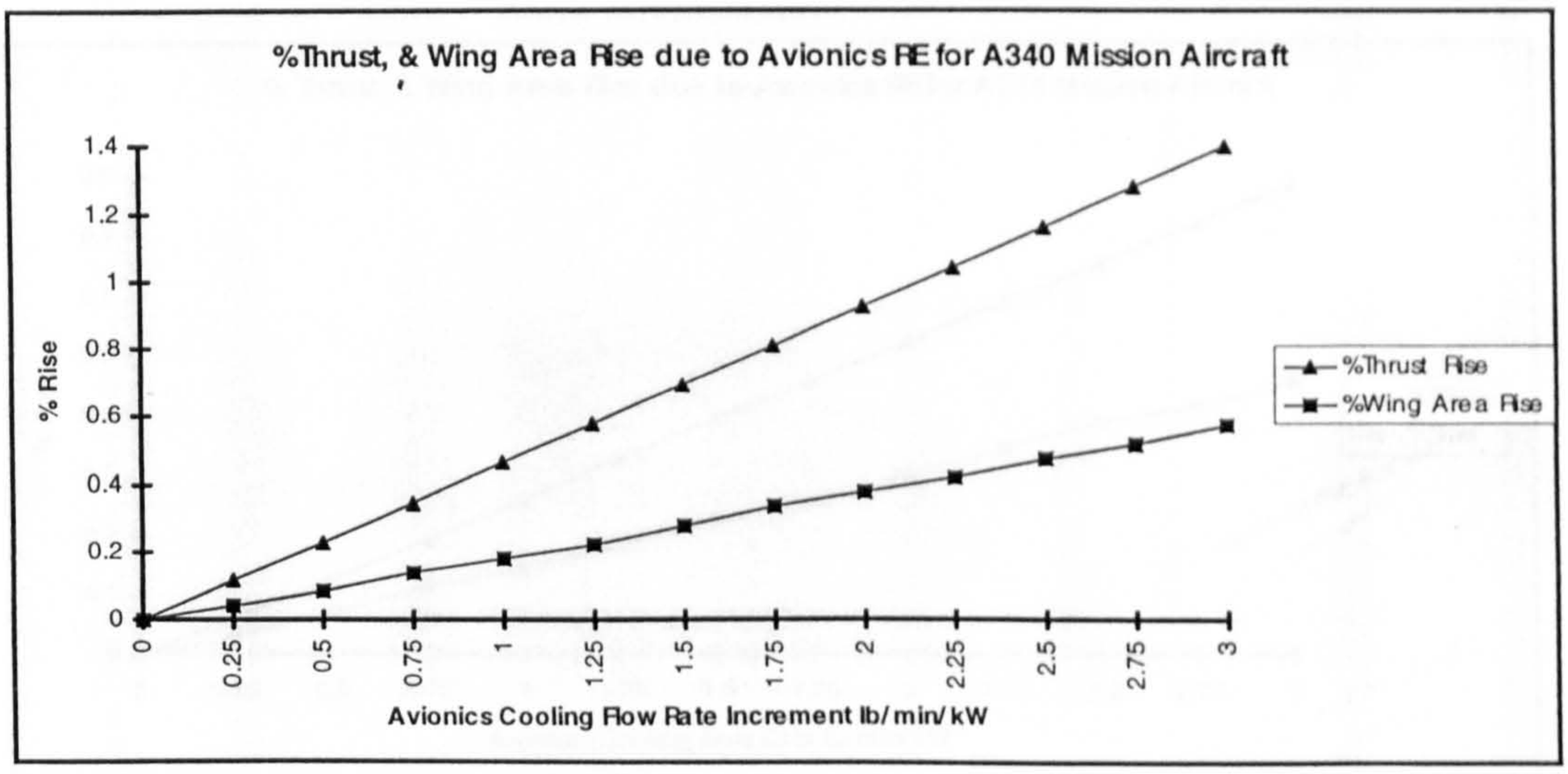

b : Four under wing engine, 440 pax, 10200km range.

Figure C-16 % Thrust and wing area rise due to avionics RE modelling for every mission

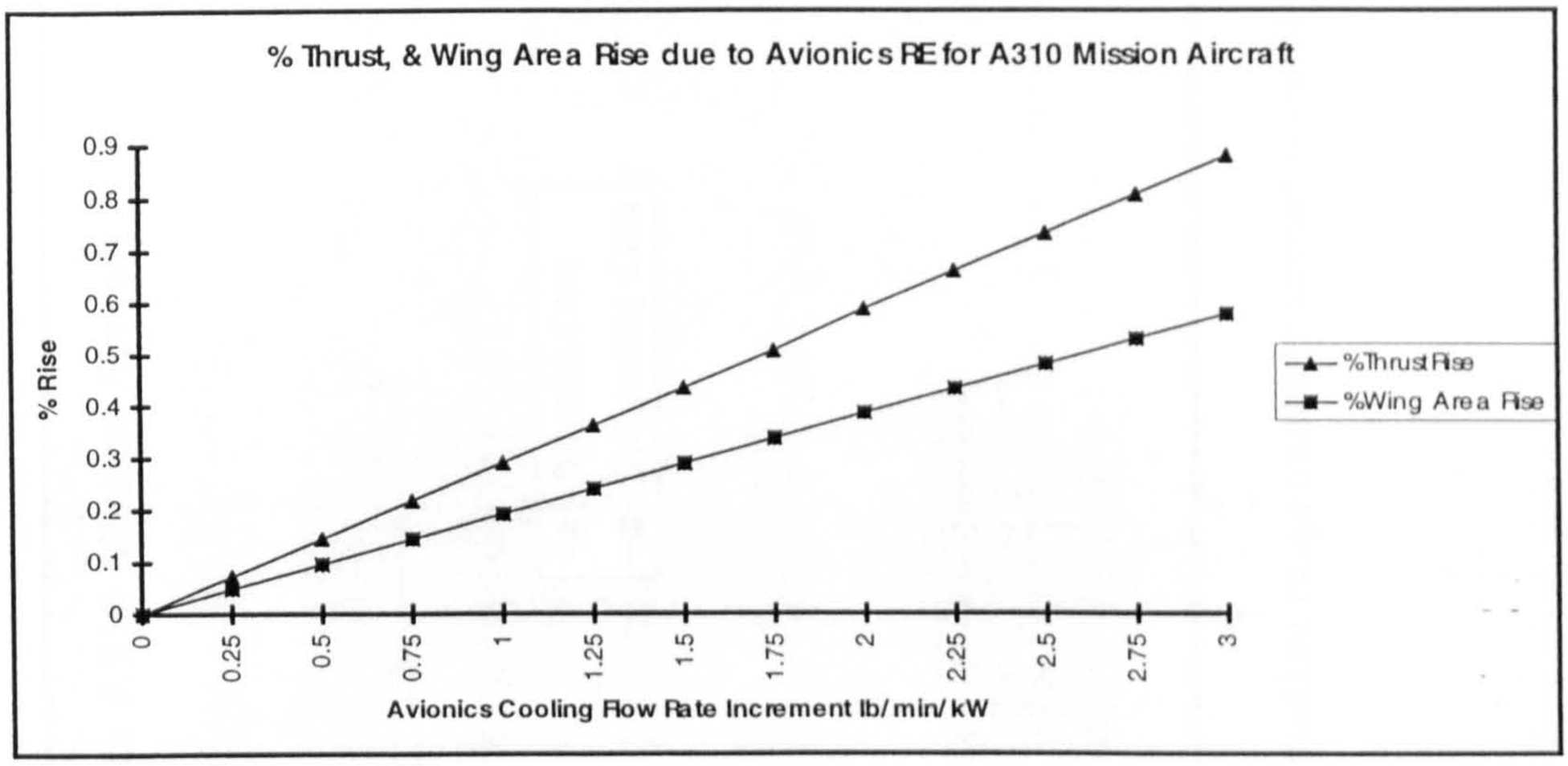

c : Twin , 280 pax, 7982 km range.

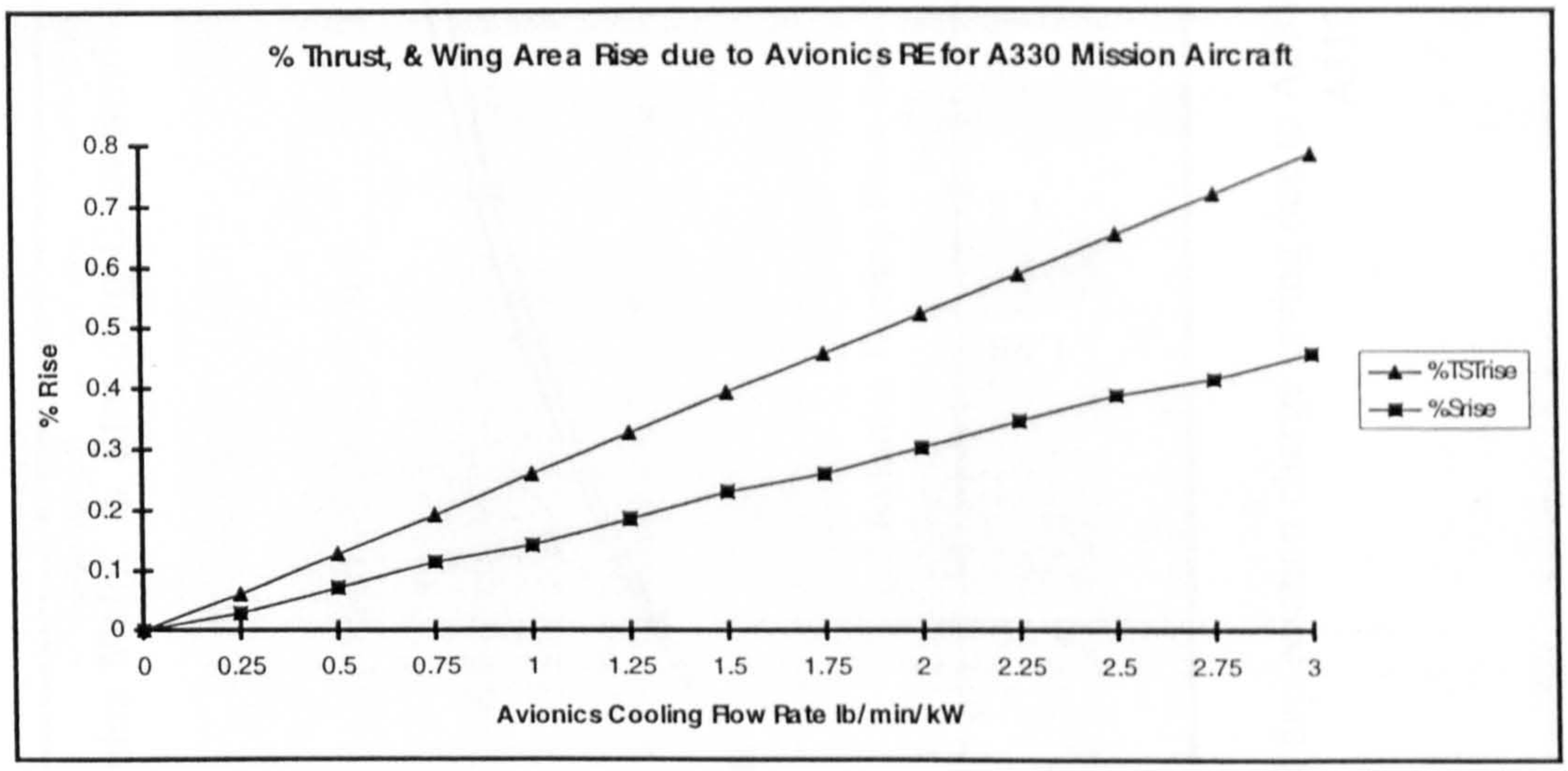

d : Twin engine, 440 pax, 6432 km range.

Figure C-16 Continued.

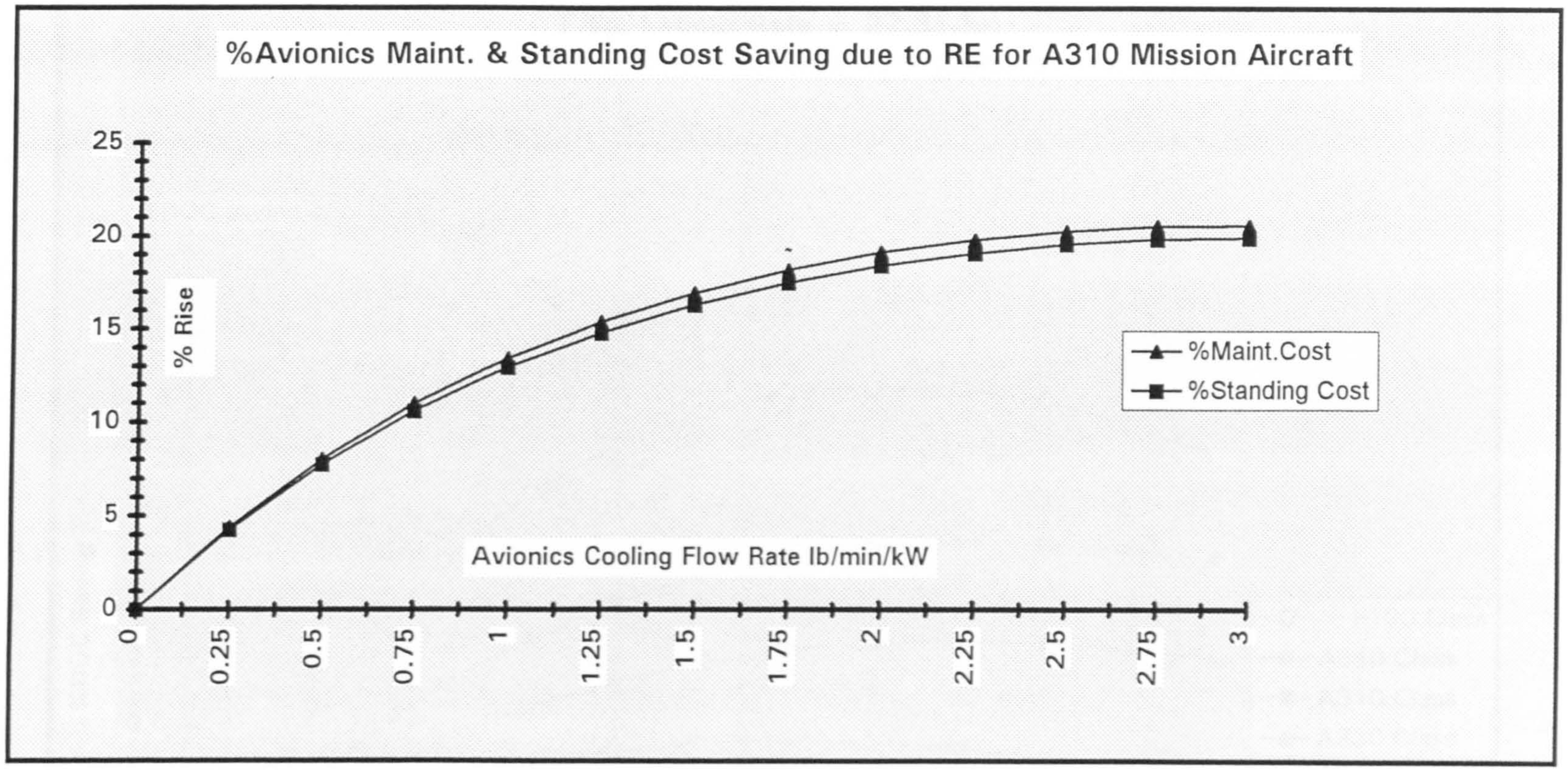

Figure C-17 : % Maintenance and depreciation charge saving due to ASRE for a typical medium range transport aircraft resembling the Airbus A310.

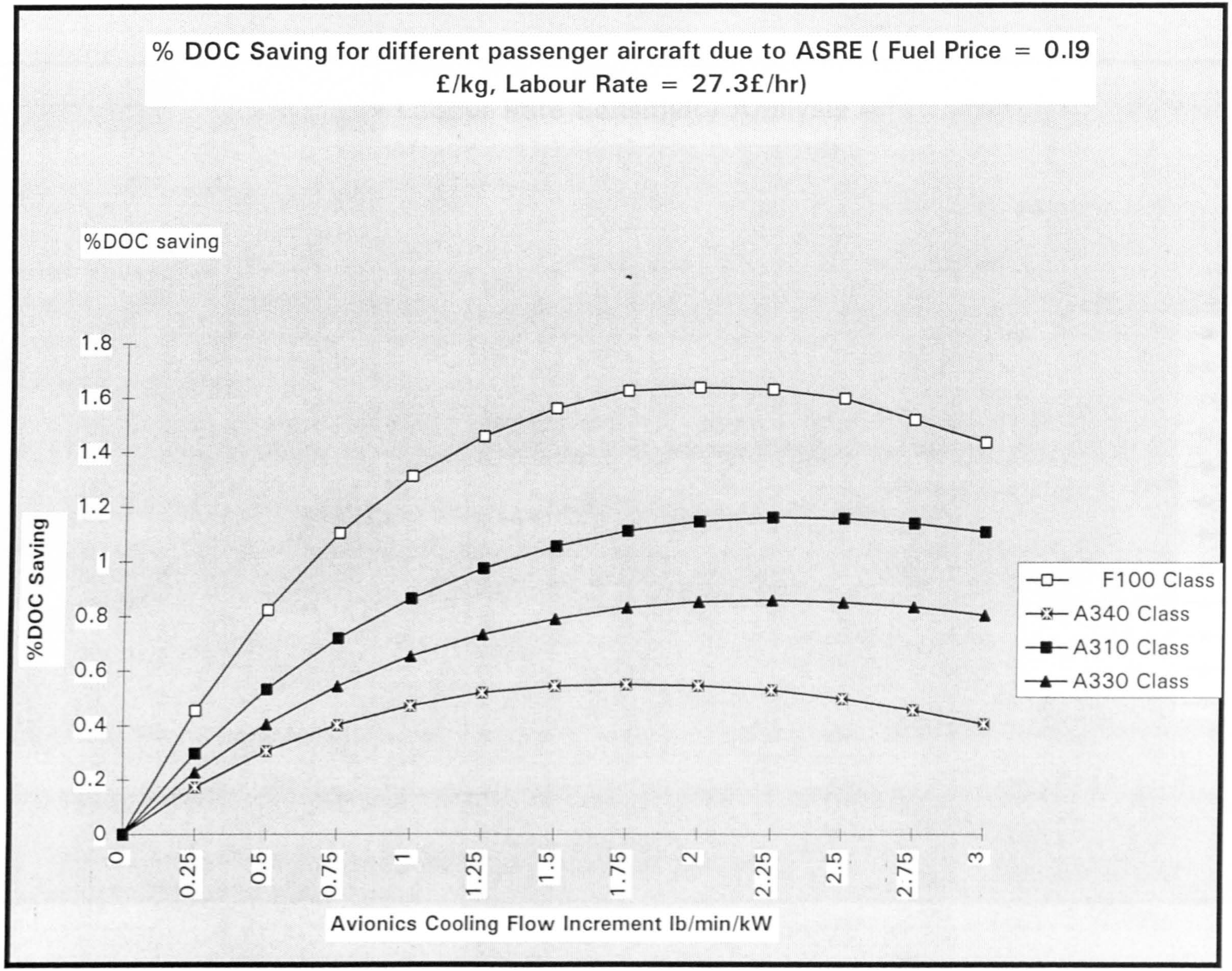

Figure C-18 % DOC saving due to avionics RE modelling for a range of passenger aircraft . Each point corresponds to an optimised aeroplane at the particular avionics cooling increment .

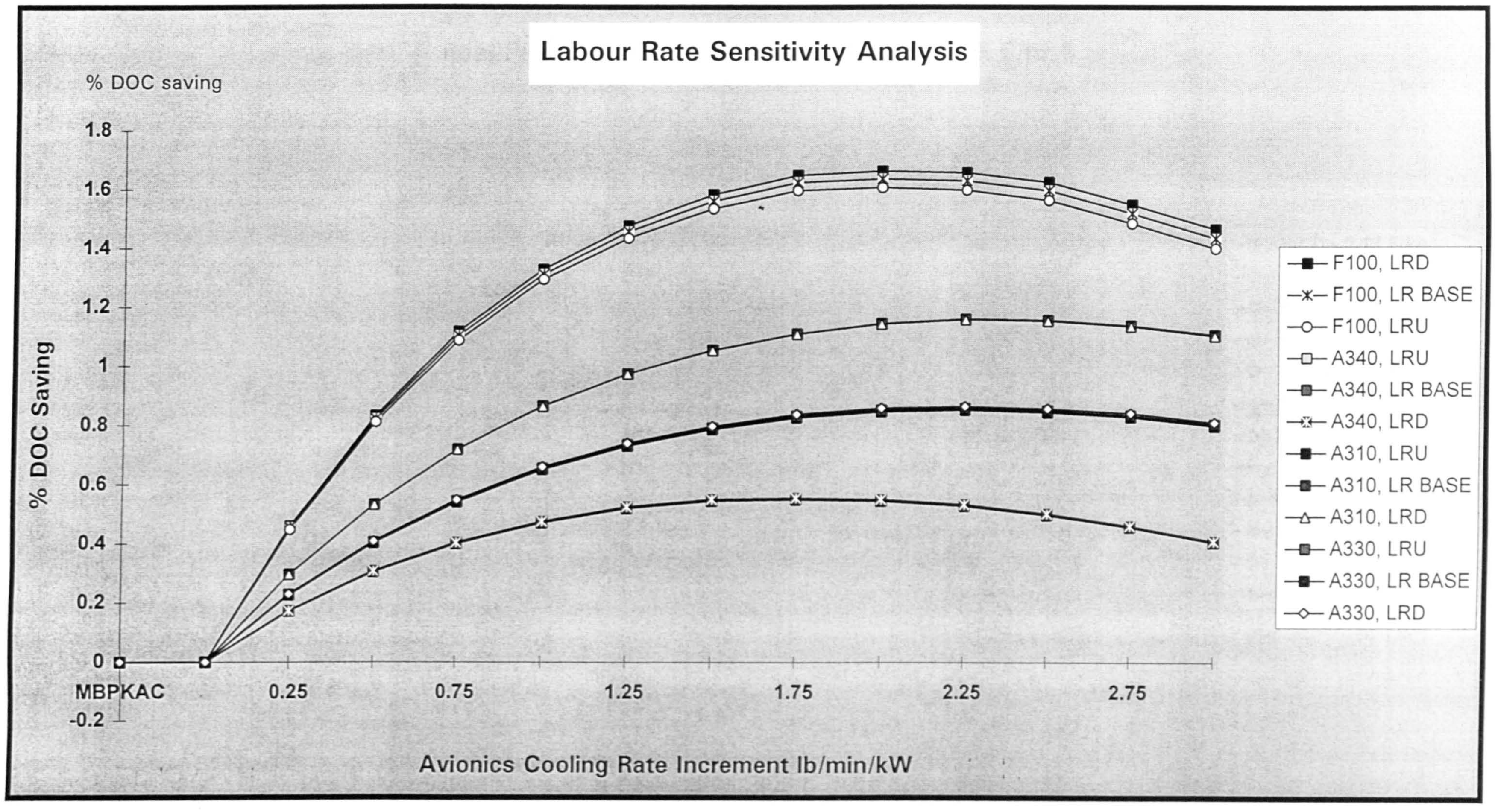

Figure C-19 : Sensitivity analysis with labour rate variation, for all class of aircraft together .

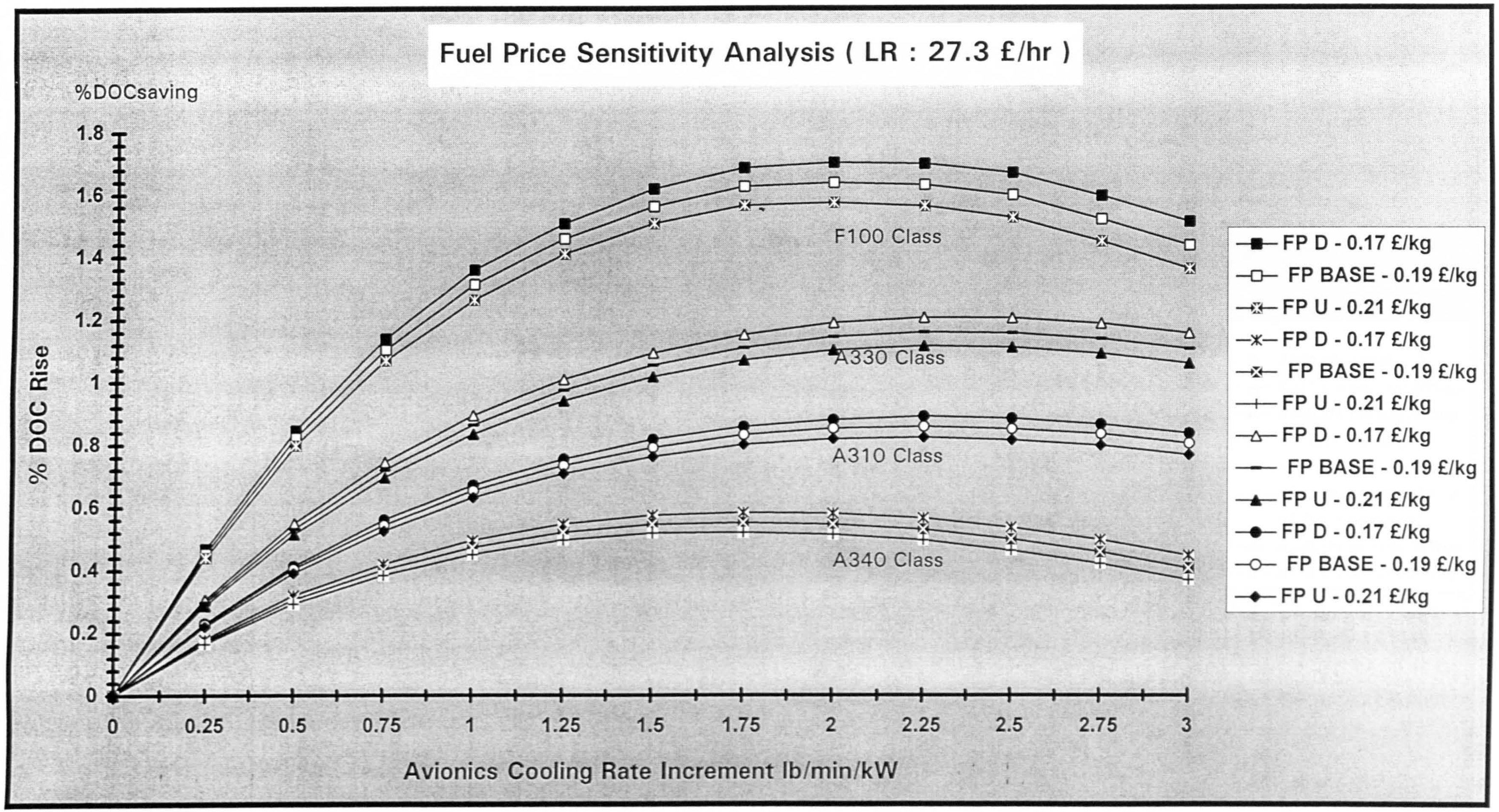

Figure C-20 Sensitivity analysis with fuel price variation, for all class of aircraft together

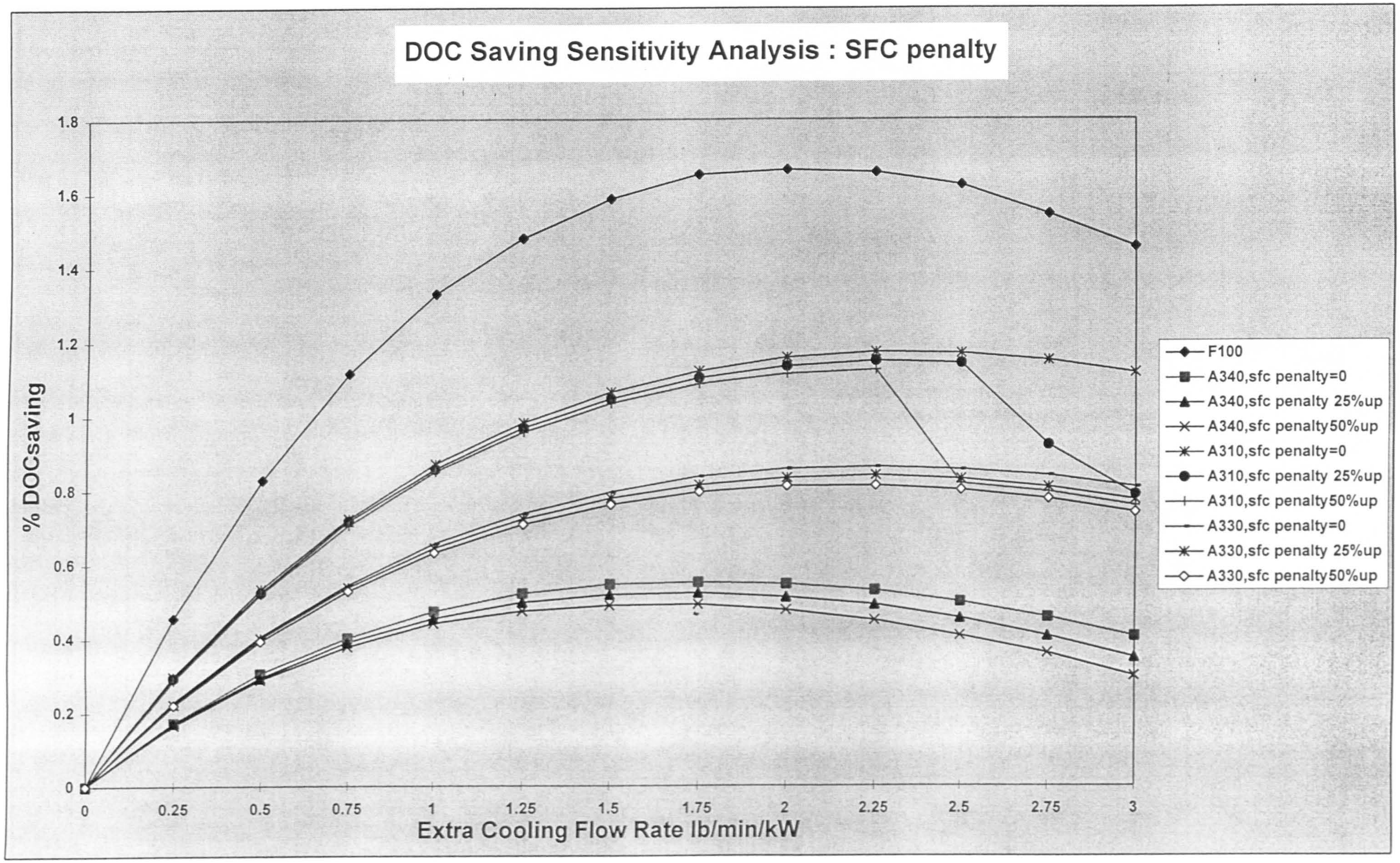

Figure C-21 : Sensitivity analysis with sfc penalty variation for base value, 25%, and 50% higher

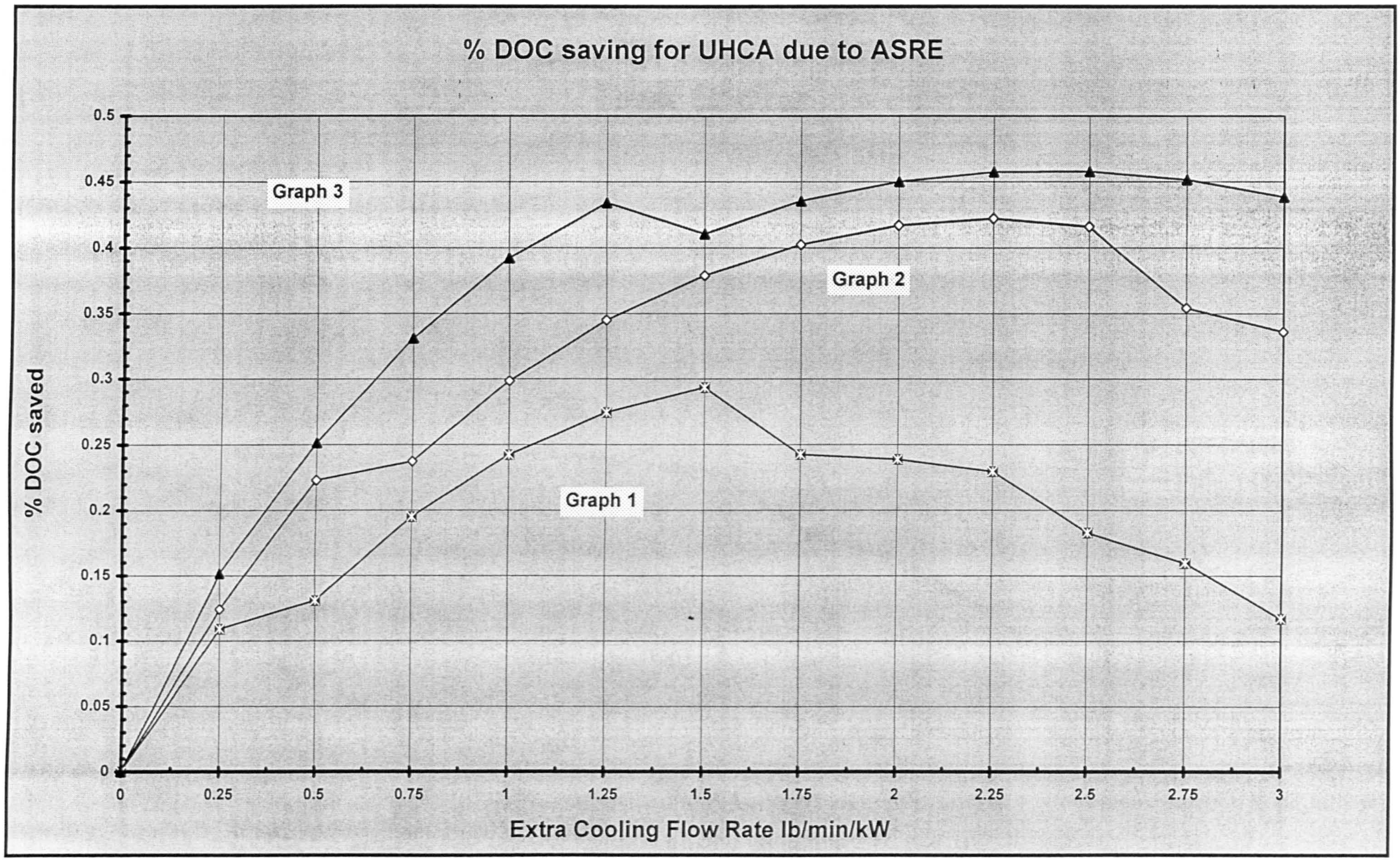

Figure C-22 % DOC saving due to ASRE in UHCA : Graph 1 corresponds to design proposal 1 when bleed burden is equally for all engine, Graph 2 correspond for bleed burden equally shared by engines, Graph 3 for design proposal 2.

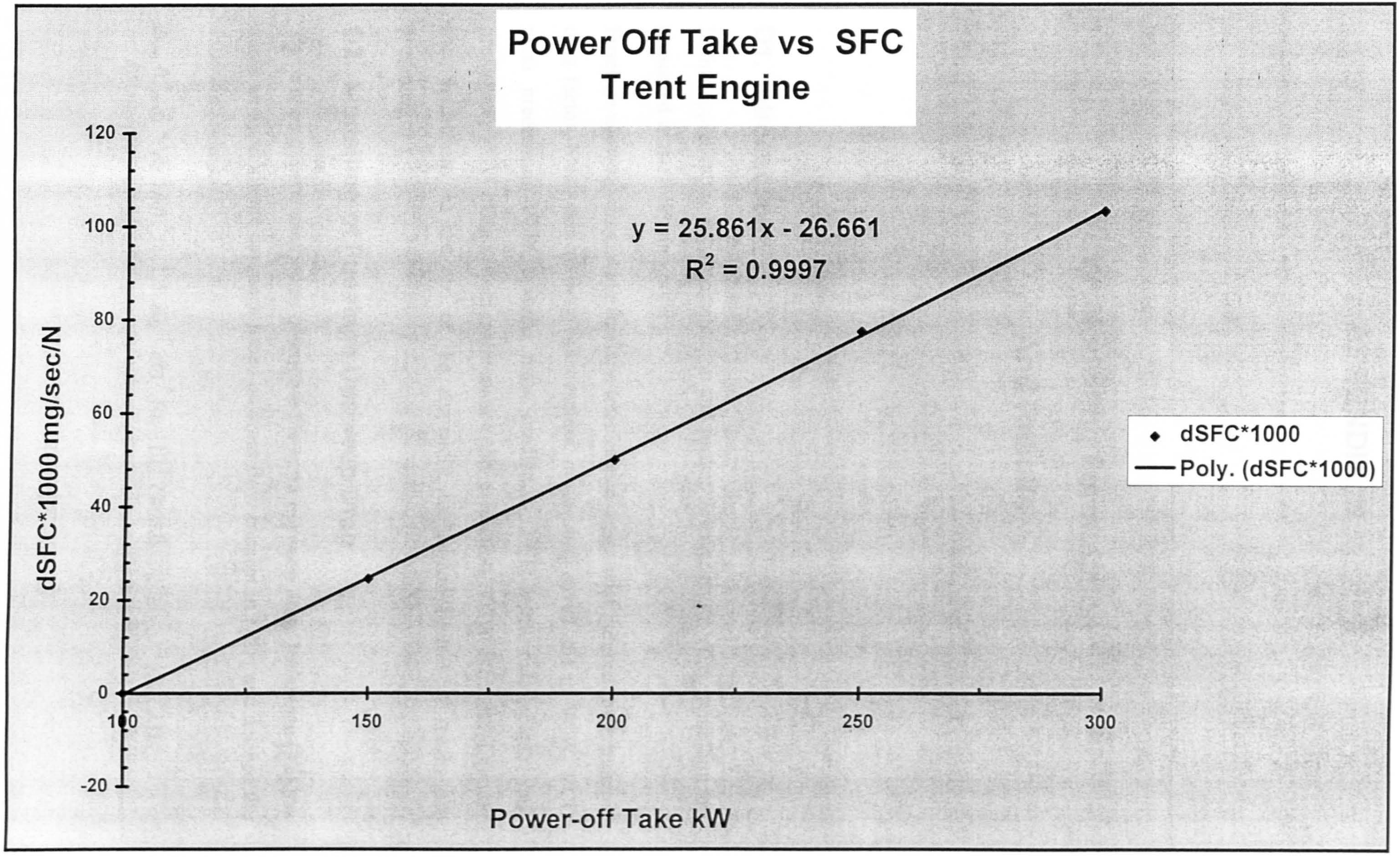

Figure C-23 : Power-off take characteristics of a turbofan engine resembling TRENT, at 35000 ft, and Mach 0.82, at 100% cruise setting

APPENDIX D

VCW Modelling Formulation

And Results

D1. Introduction

In this appendix the detail formulation and further description of VCW modelling are presented in the following order :

Fuselage upsweep drag, wing fuselage interference drag, twist induced drag, induced drag factor, Mach critical drag enhancement, cruise drag saved due to VCW, VCD mass prediction, VCW systems mass prediction, VCD extra maintenance cost prediction, VCW extra system maintenance cost prediction, VCW extra development cost prediction. At the end of the Appendix, tables and figures of results are presented.

D2. Modelling of Fuselage Upsweep Drag

There is no general method to determine the extra upsweep drag. Reference [32] has made an approximate approach based on cross flow concept in [125] and derived the following relation :

$$\Delta_{\alpha\beta}(C_D S) = A_I \left| \sin^3 \alpha_f \right| + A_{II} \left| \sin^3 (\alpha_f - \beta) \right| / \cos \beta \qquad \text{D1}$$

The graphs of Fig. D-1 developed by [32] conforms to the experimental results in [125]. The ratio of fuselage length to its diameter being 8, and the ratio of A_I/A_{II} being 1.85 is fairly applicable to present modern transport aircraft.

For an upsweep angle of 7.5 degree, which is a typical value for present modern transport aircraft, the points extracted from Fig. D-1 were included in Table D-1. An Excel curve of Fig. D-2 was drawn using the said table. Mathematica was used to fit the following equation to Fig. D-2.

$$\Delta_{\alpha\beta}(C_D S) = 0.008976 - 0.00276 \times \alpha_f + 0.00041771 \times \alpha_f^2$$
$$-2.6209 \times 10^{-6} \times \alpha_f^3 + 6.00962 \times 10^{-7} \times \alpha_f^4 \qquad \text{D2}$$

Above expression is corrected with fuselage frontal area with respect to wing gross area. The differentiation of the above equation renders the flight angle for minimum upsweep drag (a typical value of 2.421 degree). It is assumed that aircraft commences the cruise at nearly the same flight angle.

In the cruise sector, fuel consumption in every sector is computed, and is used to determine the change in aircraft mass, and hence change in aircraft C_L is found. Using the following relation from [32], wing lift curve slope is determined. For simplicity and computational limitation in CACAD, the complex aircraft C_L/α relation is avoided .

$$C_{L\alpha} = 2\pi / \{ 2/A + [(1/\cos^2 \Lambda_{1/2}) - M_{cr}^2 + (2/A)^2]^{0.5} \} \qquad \text{D3}$$

The above slope together with the known aircraft C_L are used by CACAD to determine the required angle of attack at the end of each cruise sector . Such a difference from the angle associated with minimum drag is then used in relation D2 to estimate the drag saving in VCW aircraft .

D3. Wing Fuselage Viscous Interference Drag Modelling

Wing fuselage viscous interference drag, according to Hoerner is given by the following relation :

$$\Delta_i (C_D S)_p = 1.5\, C_F\, t_r\, C_{ci} \cos^2 \Lambda_{1/2} \qquad \text{D-4}$$

C_F is determined in drag estimate module of CACAD, and t_r , $\Lambda_{1/2}$ are both independent variables. C_{ci} is the total circumferential length for both wing halves of

the wing / fuselage intersection line at which the boundary layers intersect. The value of C_{ci} is decided by the circumference of the fillet size. It is approximately 4.5 times the root chord [32], which is equivalent to the circumference of two rectangles i.e. wing fillets on both side of the fuselage. The length of each rectangle is the root chord and the width being one eighth of the root chord. The wing root setting angle in a FCW, and VCW is given by the following relations [32] respectively :

$$(i_W)_{FCW} = C_L / C_{L\alpha} + \alpha_{0\ell} \times \varepsilon_t + (\alpha_{\ell 0})_r \qquad \text{D5}$$

$$(i_W)_{VCW} = C_L / C_{L\alpha} + (\alpha_{\ell 0})_r \qquad \text{D6}$$

$\alpha_{0\ell}$ is the change in zero-lift angle of the wing per degree of the positive twist at the tip, and its value is approximately -0.4, and $(\alpha_{\ell 0})_r$ is the zero lift angle of the root section, and it is approximately -2.0 degree [103].

The difference are used in determining the reduction in value C_{ci} as follows :

$$\Delta C_{ci} = 4 \times C_r \times \{ [\cos((i_W)_{FCW} - \alpha_{f\,min}) + \sin((i_W)_{FCW} - \alpha_{f\,min})] - [\cos((i_W)_{VCW} - \alpha_{f\,min}) + \sin((i_W)_{VCW} - \alpha_{f\,min})] \} \qquad \text{D7}$$

The above drag saving is found when D7 is substituted in following expression :

$$d\{\Delta_i (C_D S)_p\} = 1.5\, C_F\, t_r\, \Delta C_{ci} \cos^2 \Lambda_{1/2} \qquad \text{D8}$$

D4. Twist Induced Drag Modelling

During the cruise phase of the flight, the basic lift distribution of a twisted wing causes a vortex induced drag at zero lift. This extra induced drag due to twist for a straight and swept wings with linear lofted twist is given in [32] as below :

$$\Delta_\varepsilon C_{DV} = \varepsilon_t^2\, C_{01} + \varepsilon_t\, C_L\, C_{11} \qquad \text{D9}$$

In the drag estimate module of CACAD for VCW, such drag is computed at every cruise sector when the related C_L is known . This drag is then treated as an induced drag saving, and thereby deducted from total induced drag .

Values of C_{01} and C_{11} are computed from lifting surface theory and are shown in the Fig. D-3, and D-4 [32] respectively. It is not easy to convert such graphs into mathematical equations nor it is essential and necessary. The current transport aircraft

usually possess a typical range of aspect ratio between 8.5 to 10, and taper ratio between 0.2 to 0.3, and flight Mach number between 0.82 to 0.84. For such typical values, the values of C_{01} and C_{11} are approximately 1.2623×10^{-5} & 1.070×10^{-4} respectively.

The value of ε_t can be assumed between 3 and 4 degree. Higher value will result in unacceptably large induced drag of the order of 5 to 10 counts, and the lower values beside being not effective, are not practical on existing transport aircraft.

At every cruise sector, CACAD computes the fuel fraction, the aircraft existing all up mass, and hence the current cruise C_L , relation D-8 is used to determine the induced drag due to twist .

D5. Induced Drag Factor Modelling

This is the modelling of drag saving in VCW due to the absence of gradual induced drag increment. It is resulted from elliptical lift distribution deterioration, through the cruise stage in fixed camber wing aircraft. The induced drag factor which is used in the drag estimate module of CACAD is given by an empirical equation B91 from [14]. It is the function of sweep angle, aspect ratio, span, and fuselage diameter. It is adequately accurate, because it produces reasonable engine sizing for most classes of aircraft.

$$1 + \delta = K_{cr1} + K_{cr2} \left(F_{USD} / Span \right)^2 + K_{cr3} \times AR \times sec\left(\Lambda_{1/4}\right) \qquad \text{D10}$$

The above relation produces a good average value for induced drag factor. Hence it is kept as a base value in CACAD.

On the other hand an analytical determination of induced drag factor by Garners' method [128] offers an expression which is the function of the location of wing centre of pressure (η_{CP}) from the wing root.

$$\delta = 46.264 \times \left[\eta_{CP} - (4/3)\,\pi \right]^2 \qquad \text{D11}$$

Relation D11 was used to establish induced drag factor variation with cruise lift coefficient, so that its increase at every cruise sector may be used in the form of a drag saving to reduce induced drag in VCW aircraft. In the following, an analytical approach is used to establish the wing centre of pressure change to determine the

induced drag factor change as function of lift coefficient. This will then be used to compute induced drag saving in VCW aircraft. Referring to equation D11, where :

$$\eta_{CP} = \int_0^1 [(C_\ell \times c)/(C_L \times GMC)]\,\eta\, d\eta \qquad \text{D12}$$

c is the local section chord, *GMC* is the geometric mean chord, and C_ℓ is the section lift. C_L is aircraft lift at any cruise sector, and η is the non-dimensional span-wise co-ordinate being 0 at the wing root and 1 at the tip. Using references [103], and [135] the above relation is expanded into the set of following relationships .

$$GMC = \sqrt{(S_g/A)} \qquad \text{D13}$$

$$c(\eta) = C_R \times [1 - (1-\lambda)\,\eta] \qquad \text{D14}$$

$$\varepsilon(\eta) = EC \times \eta \qquad \text{D15}$$

$$C_\ell = C_{\ell 0S} + C_{\ell \delta} \qquad \text{D16}$$

$C_{\ell 0S}$ and $C_{\ell \delta}$ are the basic and the additional lift coefficient respectively. y' is the span-wise location of centre of pressure of the additional lift. Assuming linear distribution of twist :

$$C_{\ell 0S} = 0.5 \times [\alpha_0 + \varepsilon(\eta)] \times C_{L\alpha} \qquad \text{D17}$$

$$\alpha_0 = -\{\int_0^1 \varepsilon(\eta) \times c(\eta) \times d(\eta)\} / \{\int_0^1 c(\eta) \times d(\eta)\} \qquad \text{D18}$$

α_0 is the overall zero lift angle at which there is no overall lift. Due to the presence of twist, however there will be local lift across the wing, some up and some down giving zero net lift .

$$y' = 0.42 + 0.001 \times AR \times (1-M_{cr}^2) \times [(4.4 + 5\,TR)Tan(\Lambda_{1/2})/(1-M_{cr}^2) + 10.4\,TR^{1/2} - 6.7] \qquad \text{D19}$$

$$C_{\ell \delta} = [1.28(1-\eta^2)^{1/2} + (14.13\,\eta - 6.35)(y' - 0.425)]\{GMC \times C_L / c(\eta)\} \quad (\text{for } \eta \le 0.7) \qquad \text{D20}$$

$$C_{\ell \delta} = \{1.28(1-\eta^2)^{1/2} + [4.25 - 53.8(\eta - 0.815)^2](y' - 0.425)\} \times$$

$$\{ GMC \times C_L / c(\eta) \}$$

$$(\text{for } \eta > 0.7) \qquad \text{D21}$$

Relations D-11 to D-19 are assembled into a FORTRAN algorithm so that all the integration are carried out, and finally an equation linking $1 + \delta$ with aircraft C_L is established from which the rate of change of induced drag factor $(1 + \delta)$, *or* k with C_L is found :

$$d(k) / d(C_L) = (-0.109027+0.070752 \times C_L) \qquad \text{D22}$$

$$k = k' - (C_{L\,2nd\,sector} - C_{L\,1st\,sector}) \times (-0.109027+0.070752 \times C_L) \qquad \text{D23}$$

where k' is the base induced drag factor determined by the equation B91. The reason for subtracting the second term from the first term of RHS of D23 lies with the fact that such an increment in induced drag in FCW is simulated in the VCW modelling in the form of a benefit.

D6. Critical Mach Number Enhancement Modelling for VCW

In this section effort is made to model the benefit of VCW lower section C_l than aircraft C_L resulted from span-wise deployment of VCD. When a cruise flight Mach number is decided, the following relations may help in determining critical Mach number at zero lift, which in turn helps to decide a reasonable combination of sweep and thickness to chord ratio [25]. Recalling relation B15:

$$M_{crit0} = M_{cr} + dM_{cr} - dMc_{CL} \qquad \text{D24}$$

$(M_{cr} + dM_{cr})$ is Mach critical drag. The value of dM_{cr} is decided by the amount of increment in drag due to compressibility, which is usually between 0.001 and 0.002. The graph in Fig. D-5 [25] will then give the corresponding value of dM_{cr}. The value of dMc_{CL} (Mach number increment due to C_L) is extracted from Fig. D-6, for the highest value of C_L , *or* C_l at the cruise start. Hence the value of M_{crit0} may be found from D24. For any reasonable selection of thickness to chord ratio the above values together with the complex graph of Fig. D-7 gives a sweep angle that is a compromise with respect to flight Mach number, buffet onset Mach number (Mach critical lift), aircraft C_L , Mach critical drag, and aspect ratio. Now the whole of the above argument was modelled into the Mach critical module of CACAD.

An algorithm was placed within the induced drag factor module of CACAD, i.e. within the integration module of expression D12 to determine the highest value of C_l . The difference with aircraft C_L is then computed. Such difference is then accounted for in Mach critical module as a reducing parameter for C_L in VCW aircraft.. The following relation which is an equation fit to Fig. D-6 will result in higher dMc_{CL} for VCW aircraft.

$$dMc_{CL} = -0.005714 + 0.0321143 \times C_{Lcr} - 0.1 \times (C_{Lcr})^2 \qquad \text{D25}$$

Assuming compressibility drag value, from 0.001 for long range to 0.002 for short range aircraft, [32,25], the following relationship was fitted to the experimentally developed curve of Fig. D-5 [25] to determine the compressibility drag .

$$dM_{cr} = 0.135729 - 178.953 \times C_{D\,comp} + 109791.37 \times (C_{D\,comp})^2 + 3.3221 \times 10^7 \times (C_{D\,comp})^3 + 3.76453 \times 10^9 \times (C_{D\,comp})^4 \qquad \text{D26}$$

With M_{cr} as an input value in CACAD, and the higher value of dMc_{CL} together with above findings, equation D24 will yield lower M_{crit0} for VCW aircraft. This may enable the optimisor to choose higher value of TC for still lower sweep angle .This is decided by following equation which was fitted with the help of Mathematica to the Fig. D-7 [25].

$$\Lambda_{1/4} = -180.345 + 211.415 \times M_{crit0} + 298.207 \times TC - 149.599 \times TC^2 \qquad \text{D27}$$

Above procedure enables CACAD to design a transport aircraft with rationally decided sweep and thickness to chord ratio which ensures a reasonable margin between flight Mach number and Mach critical drag. It also enables a VCW aircraft to be benefited from its drag divergence margin in its entire configuration sizing, contributing toward a lower DOC.

D7. Cruise Drag Saved by Camber Change

Cruise phase of flight is accompanied by fuel mass reduction, hence aircraft all up mass is continuously reduced. This makes the wing produced lift to be more than aircraft required lift. FCW aircraft either increases the flight altitude or reduces the flight angle of attack to balance the lift. The prime purpose of VCW is to establish

such balance by way of reducing camber chordwise. This not only balances the lift, but produces some drag saving as compared with FCW aircraft.

In the following, the aerodynamic achievement of theoretical, and experimental work of MBB, and Cranfield is presented so that, an average but confident degree of drag saving to be incorporated into drag estimate module of CACAD.

1. Rao's 2-D airfoil undergoes camber change by computational method, using Powell & Horton code , from 0 to 2 to 4 degree TE deflection achieved 6.7 % drag saving, section 2.3.2 of [105].

2. Rao's Experimental work on a 25.3 cm chord, 60 cm span 2-D wing placed in a 33 m/s, 1/2 million Reynolds number Cranfield Weybridge wind tunnel, with variable camber deflection, at LE up to 2 and TE up to 7 deg , achieved 6 to 9 % drag saving for C_L between 0.55 to 0.45, and nearly 13% at C_L=0.7.

3. Rao's Experimental work on 3-D wing of 23 cm chord and the same size span in the same wind tunnel with the same conditions achieved no drag saving.

4. Mackinnon's work [106] on the Rao's 3-D wing, with tunnel being re-calibrated , and modified experimental apparatus, achieved approximately 6 % drag saving for C_L between 0.6 to 0.7, at 2, and 4 degree TE deflection.

5. Mackinnon's work on a specially designed supercritical airfoil using EJ-61 code in consultation with British Aerospace for cruise Mach number of 0.74. He used BVGK computational code [130], to predict the 2-D camber deflection performance, varying camber at TE from -2 to +2, achieved nearly 7 to 8 % drag saving at usual cruise lift coefficients. He also used William's RAE code [131], which takes into account viscous effects but not compressibility effect to predict the camber deflection performance, achieving 6.2 % drag saving at the typical cruise lift coefficients.

6. Mackinnon's 3-D work with the same airfoil but incorporated into a 160 cm span, and 60 cm chord wing, placed in 50 m/s flow at Reynolds number of nearly 2 million in an 8 ft x 6 ft closed return tunnel . He achieved a drag saving of 3 to 5 % but at the C_L values much higher than cruise condition .

The cross over point in the drag polar (even corrected for real Reynolds number of 40 million) was 0.65 for 5 deg and 0.85 for 10 deg deflection of TE camber device .

7. From all the references published for MBB work [109,110,112to114,118] the one reported by [110] contain the required data. In this, the experimental results obtained in transonic tunnel with Reynolds number around 6 million and from the Figure 33 of the same reference, it is evident that, a drag saving of 5 to 6 % is achieved at the usual cruise lift.

In the following the drag polar diagram achieved computationally and experimentally by the aerodynamic research in Cranfield and MBB for airfoils (2-D), and wings (3-D) may be presented as evidence of variable camber performance in drag saving chosen by the Author .

1. It is understood from section 2.3.2 of Rao's work [105] on 2-D drag polar, developed computationally, an approximately 6 to 9 % drag saving at usual cruise C_L range. Figure 2-14 of [105] is misprinted, instead an equivalent figure is presented to depict her work; see Fig. D-8.

2. Fig. D-9 shows Rao's 2-D drag polar developed experimentally. From the figure, there is an approximately 9 % drag saving at usual cruise C_L range.

3. Fig. D-10 shows Rao's 3-D drag polar developed experimentally. From the figure, it is evident that there is no drag saving.

4. Fig. D-11 shows Mackinnon's work on Rao's 3-D wing. The drag polar was developed experimentally by re-calibrating the Weybridge wind tunnel. From the same figure, it can be seen approximately 6 % drag saving at cruise C_L, higher than the usual range.

5. Fig. D-12 shows Mackinnon's 2-D drag polar developed computationally on a specially developed airfoil for variable camber operation. From the same figure a drag saving of approximately 7 to 8 % at usual cruise C_L range is observed. He also used William's RAE Code and produced the drag polar of Fig. D-13, from which an approximately 6.2 % drag saving is observed at usual cruise C_L range .

6. Fig. D-14 shows Mackinnon's 3-D drag polar developed experimentally. From the figure, Author extracted approximately 3 to 5 % drag saving, but at cruise C_L, higher than the usual range.

7. Fig. D-15 shows MBB's 3-D drag polar developed experimentally on a specially designed airfoil for variable camber operation. From the figure, an approximately 5 to 6 % drag saving is possible at usual cruise C_L range.

With the above computational, and experimental achievements, it is possible that a camber deflection during cruise stage would result in 5 % drag saving for a transonic wing carefully designed for variable camber operation chordwise.

In CACAD the cruise range is segmented into 5 sectors. Drag saving takes place at all sectors, distributing 5 % equally to each sector i.e. 1 % per sector .

D8. VCD Mass Prediction Modelling

In this section, the method of establishing VCD mass prediction is presented. Raymer, Corning, Nickolai, and Roskam have treated the wing a complete body, without any reference to the trailing edge devices. Torenbeek is the main source for [14] from which the following relation for flap specific mass is presented :

$$J_{FLP} = J_{FLP0} \times F_{lpc} \, (S_{FTE} \times E_{taf} \times Span)^{0.1875} \, [\, (V_A \; or \; V_{TO}) \times \sin(\beta_a \; or \; \beta_{to}) \times \cos(\Lambda_f) / TC \,]^{0.75} \qquad \text{D28}$$

where V is either approach or take-off speed (m/s), whichever is the bigger, and also J_{FLP} may not be less than 30 kg/m^2, or otherwise it is 30 kg/m^2. J_{FLP0} is a constant coefficient and is of the order of 0.006 for the flap systems in use in current transport aircraft . F_{lpc} is the flap complexity coefficient which is 1.2 for the fowler flaps .

Should a flap system operate as a VCD, it must have extra mass to enable it to deflect as VCD before it deflects as fully extended flap. Therefore this extra mass can be assumed as a function of VCD deflection angle. Above relation was applied to the A340-200 class of aircraft and made to vary with deflection angle. The graph of Fig. D-16 shows that at deflections around 15 to 17 ° (the usual aileron deflection at cruise), the flap mass density is 30 kg/m^2. The same value is proposed by [14] for aileron, which enhances the confidence for the following methodology. The

following differentiation determines the rate of change of flap specific mass with deflection angle :

$$d(J_{FLAP})/d(\beta_{flap}) = 0.75 \times \{J_{FLP0} \times F_{lpc} \times (S_{flap} \times Span_{flap} \times Span)^{0.1875} \times V^2 \times \cos(\Lambda_{flap}) / TC]^{0.75}\} \times \cos(\beta_{flap}) \times [\sin(\beta_{flap})]^{-0.25} \quad \text{D29}$$

This is about .8 to 1 kg/m^2/deg of deflection for the same class of aircraft. Thus the specific mass of VCD may be given by the following expression :

$$J_{VCD} = J_{FLAP} + \{d(J_{FLAP})/d(\beta_{flap}) \times \beta_{VCD}\} \quad \text{D30}$$

The above relation was used to predict the specific mass of VCD in an A340-200 class aircraft which produced the value of 56 kg/m^2 , and consequently the increase over FCW flap without the effect of other VCW benefits, and snow ball effect which reduce the flap area, etc. is 16%.

D9. VCW Hydraulic System Mass Modelling

Raymour proposes a reasonable equation for mass estimation of the hydraulic and flight control system. It includes the number of system functions and the square of the area of the control surfaces as amongst the variables. This is found most suitable for the prediction of hydraulic system mass increment due to VCW in CACAD. It has an additional advantage of being suitable for design proposals put forward by MBB. The equation is as follows :

$$M_{HYD} = 4.7 \times \frac{0.2673}{2.205} N_f [(F_{USL} + Span) \times 3.28]^{0.937} \quad \text{D31}$$

N_f is the number of functions performed by hydraulics system that are located in different corners of aircraft with independent piping . For FCW, it is assumed as 7 (elevator, rudder, aileron, flaps, brakes, main, and nose landing gear). For VCW, N_f is assumed to be 8, the eighth function is VCD operation . Note that although fuselage length remains the same, the span of VCW will slightly reduce, retarding hydraulics system mass increment.

Table D-2 shows different aircraft, and their hydraulics system mass, along with mass predicted with different formula. It is apparent from the said table that the Raymer formula underestimates, the hydraulics system mass, although it offers very related

parameters. A correlation factor of 4.7 for Raymer equation as default factor to match its results with the A330 aircraft (considered base aircraft for CACAD) hydraulics system mass was found reasonably applicable to other types of transport aircraft treated in CACAD.

D10. VCD Maintenance Cost Prediction Modelling

Trailing edge system maintenance cost of FCW aircraft can be determined by the two approaches discussed in Appendix B. In the following section the Airbus comparison method is used to predict extra maintenance cost difficulty factors for VCD when substituted for wing TE system.

D10.1 Comparison method

VCW trailing edge system is assumed to replace the conventional TE system of FCW aircraft (excluding the hydraulics system elements in its vicinity) . This will allow the Airbus methodology to be used, [92] to predict, the extra maintenance material cost coefficient F_{difmm} and labour F_{difml}. Table D-3 lists such factors and determines the required coefficients.

The above coefficients may be used to predict VCW maintenance cost of trailing edge system from that of FCW :

$$VCD_{maintenace\ material\ cost} = FCW_{flap\ maintenance\ material\ cost} \times F_{difmm} \qquad \text{D32}$$

Assuming the maintenance man-hours spent on the aircraft be approximately a quarter of man-hours spent off aircraft, then the following relation holds :

$$VCD_{\ maintenance\ labour\ cost} = F_{difml} \times FCW_{flap\ maintenance\ labour\ cost} \qquad \text{D33}$$

D10.2 Approach 2 method

In the second approach method described in B4.2.1 were used to predict the influence of VCD extra maintenance cost against FCW.

a) The surface area contribution

VCW aircraft due to drag reduction and overall better performance has lower wing area and hence lower VCD (TE surface) area. This criteria helps to reduce VCW maintenance cost.

b) The mass proportioning

Although surface area reduction of VCD contributed to a lower mass, the increase in its specific mass may lead to an overall rise in VCD mass. This will cause higher maintenance cost.

c) The price proportioning (used only for material cost)

The extra development cost of VCW that was described in subsequent sections may contribute to higher specific price of VCD. This is one of contributing factors in pushing the cost of maintenance material of VCD to a higher value.

d) Among the external and internal factors, Table D-4 differentiates wing TE flaps from VCD, the sum of the merits obtained will then be fed into the appropriating module to predict the extra cost of maintenance material and labour for VCD.

$$VCD_{maintenace\ material\ cost} = \{ (S_{VCD} / S_{total}) + (Internal\ factors\ Merit_{VCD} / Total\ Internal\ Merit) + (External\ Factors\ Merit_{VCD} / Total\ External\ Merit) + P_{VCD} / P_{STR} \} \times F_{difml} \times STR_{maintenance\ material\ cost} \quad \text{D34}$$

$$VCD_{maintenace\ labourl\ cost} = \{ (S_{VCD} / S_{total}) + (Internal\ factors\ Merit_{VCD} / Total\ Internal\ Merit) + (External\ Factors\ Merit_{VCD} / Total\ External\ Merit) + M_{VCD} / M_{STR} \} \times F_{difml} \times STR_{maintenance\ labour\ cost} \quad \text{D35}$$

The second approach increased the trailing edge maintenance cost by 1.45 times. This value was analysed for validation in 4.8.1. It fell within reasonably range of 1.25 to 1.75, adapted generally by the experts of the field in the form of maintenance difficulty factor F_{difm}.

D11. Extra Maintenance Cost Prediction of VCW System

Hydraulic system, and flight control system of FCW aircraft are assumed to have been replaced by a hydraulic, and flight control systems that fulfils the functions of

VCW too, then Airbus scheme for prediction of maintenance cost can be applied. For this Table D-5, and D-6 are established to predict those factors that enables the prediction of extra maintenance cost of the said systems from that of the known value of FCW aircraft.

Maintenance material cost of VCW hydraulics system =

$$(F_{difmm})_{HYD} \times \textit{Maintenance material cost of FCW hydraulics system}$$

Maintenance labour cost of VCW hydraulics system =

$$(F_{difml})_{HYD} \times \textit{Maintenance labour cost of FCW hydraulics system}$$

Maintenance material cost of VCW flight control system =

$$(F_{difmm})_{FC} \times \textit{Maintenance material cost of FCW flight control system}$$

Maintenance labour cost of VCW flight control system =

$$(F_{difml})_{FC} \times \textit{Maintenance labour cost of FCW flight control system}$$

D12. VCW Extra Development Cost Modelling

The methodology to predict VCW extra development cost consists in breaking down all areas of development cost as classified in [15] and examine an appropriate $(f_{diff})_{VCW}$ to each section. This is down as below in major and minor sections.

D12.1 Airframe engineering and design cost

It consist of the following tasks :

(a) Planning & conceptual design

(b) Preliminary design and system integration

(c) Design of wind tunnel models and mock-ups

(d) Design of dedicated test facilities

(e) Design and construction of development tests, static tests, system tests

(f) Design for detail and development

(g) Preparation, release and maintenance of drawings and specifications

(h) Liaison engineering with aircraft manufacturer, and operator, and vendors .

(i) Design of modifications

(j) Determination of required specifications for materials, and processes

(k) Development of specifications for items purchased from vendors

(l) Design analysis for reliability

(m) Design analysis for maintainability and accessibility

Formulae used by Roskam is as follow :

$$C_{design} = \{ 0.0396 \, (M_{ampr})^{0.791} (V_{max})^{1.526} (N_{rdte})^{0.183} \} \times f_{diff} \times f_{cad} \times \Re_{er} \qquad \text{D36}$$

and the equation used by Wayne Burnes (given here for reference only) :

$$C_{design} = \{ 0.066 \, (M_{ampr})^{0.796} (V_{max})^{1.538} (N_{rdte})^{0.183} \} \times f_{atf} \times f_{amc} \times f_{security} \times \Re_{er} \qquad \text{D37}$$

Analysis of above relation shows that the latter relation is approximately predicting twice as much the cost of design part of development phase. Design tasks has been investigated in Table D-7 for the most realistic value of $[(f_{diff})_{VCW}]_{design}$.

Note that due to lack of detail man-hours contribution of each sub-division of design phase or for other phases of development cost, the Author had to assume that each sub-division weighs the same in terms of cost. Extra design cost of VCW is given by following relationship .

$$\Delta C_{design} = \{ 0.0396 \, (V_{max})^{1.526} (N_{rdte})^{0.183} \} \times \{ [(M_{ampr})^{0.791}]_{VCW} \times [(f_{diff})_{VCW}]_{design} - [(M_{ampr})^{0.791}]_{FCW} \} \times f_{cad} \times \Re_{er} \qquad \text{D38}$$

D12.2 Development support and testing cost

It is the cost of the following works for which a comparative study was conducted to find the extra cost for VCW aircraft included in Table D-8 :

- Wind tunnel testing
- System testing
- Structural testing

- Propulsion testing
- Simulation & development support

Formulae used by Roskam is as follow:

$$C_{support\&test} = \{ 0.008325 \, (M_{ampr})^{0.873} (V_{max})^{1.890} (N_{rdte})^{0.346} \} \times C_{pi} \times f_{diff} \qquad \text{D39}$$

and the equation used by Wayne Burnes which is produces 4 times higher value is presented below for reference only :

$$C_{support\&test} = \{ 0.0356 \, (M_{ampr})^{0.903} (V_{max})^{1.93} (N_{rdte})^{0.346} \} \times f_{atf} \times C_{pi} \times f_{security} \qquad \text{D40}$$

Extra support and testing cost of VCW is given by the following relationship. Development support tasks has been investigated in Table D-8 for the most realistic value of $[(f_{diff})_{VCW}]_{support}$.

$$\Delta C_{support\&test} = \{0.008325 \, (V_{max})^{1.890} (N_{rdte})^{0.346} \} \times \{ [(M_{ampr})^{0.873}]_{VCW} \times [(f_{diff})_{VCW}]_{support} - [(M_{ampr})^{0.873}]_{FCW} \} \times C_{pi} \qquad \text{D41}$$

D12.3 Prototype cost of flight test aeroplanes

Cost of construction of prototype flight test aeroplanes with VCW technology may be higher only in the airframe subdivision. Propulsion, and the avionics systems may be unaffected and is out of our comparison. Airframe cost consists of :

D12.3.1 *Structural construction labour cost*

This cost also includes installation of fixed equipment, and may be higher for VCW primarily in TE of wing section, including equipping of this area with extra VCD related articles.

Assuming the labour cost is equally divided between fuselage and the wing (wing contributes to more than 50% of the aircraft development cost, about 45% of the structural weight, and more than 60% of the total drag). Wing trailing edge should take roughly quarter of the wing construction time (wing leading edge, wing box, wing tip, wing engine pylon, and engine housing), it is possible to allocate 25 to 50% man-hours cost increase (a factor of 1.375) to this section as a result of VCW introduction . This may result in following value:

$$[(f_{diff})_{VCW}]_{manufacture} = 1.375 \times 0.5 \times 0.25 + 1 = 1.1718 \qquad \text{D42}$$

This is used in Roskam prediction equation D43 as in D45 :

$$C_{manufacture} = \{ 28.984 (M_{ampr})^{0.740} (V_{max})^{0.543} (N_{rdte})^{0.524} \} \times f_{diff} \times \Re_{mr} \qquad \text{D43}$$

and the equation used by Wayne Burnes (given here for reference only) :

$$C_{manufacture} = \{ 43.61 (M_{ampr})^{0.76} (V_{max})^{0.549} (N_{rdte})^{0.554} \} \times f_{amc} \times f_{security} \times \Re_{mr}$$

D44

Extra manufacturing man-hours cost of VCW is given by following relationship .

$$\Delta C_{manufacture} = \{28.984 (V_{max})^{0.543} (N_{rdte})^{0.524} \} \times \{[(M_{ampr})^{0.740}]_{VCW}$$

$$\times [(f_{diff})_{VCW}]_{manufacture} - [(M_{ampr})^{0.740}]_{FCW} \} \times \Re_{mr} \qquad \text{D45}$$

D12.3.2 *Tooling fabrication labour cost*

This cost may be higher for VCW aircraft, but primarily in the wing trailing edge system. Tools can be divided into the following category :

(a) Jigs and fixture used in aircraft sub-assembly, major assembly and final assembly

(b) Parts fabrication special tools : such as flat patterns, calibration tools, dies, templates, etc. used in machining, welding stretching, press forming, casting, etc.

(c) System tests jigs, and fixtures, and special tools etc.

(d) Aircraft operation trolleys, carts and special system testers and peculiar equipment for ground testing (other than general GSE)

If we assume half of the above cost is invested in the wing, 30% of which for trailing edge system (structural parts, assembly, equipping, and rigging). It is possible even with a conservative view to predict that this cost may be 50% higher for VCW, which yields the following value for f_{diff} :

$$[(f_{diff})_{VCW}]_{tooling} = 1.50 \times 0.5 \times 0.30 + 1 = 1.225 \qquad \text{D46}$$

This is used in Roskam prediction equation D47 as in D49 below :

$$C_{tooling} = \{ 4.0127 (M_{ampr})^{0.764} (V_{max})^{0.899} (N_{rdte})^{0.178} (N_r)^{0.066} \} \times f_{diff} \times \Re_{tr} \quad \text{D-47}$$

and the equation used by Wayne Burnes (given here for reference only) :

$$C_{tooling} = \{ 5.083 \, (M_{ampr})^{0.768} \, (V_{max})^{0.899} \, (N_{rdte})^{0.180} \, (N_r)^{0.066} \} \times f_{amc} \times f_{security} \times \Re_{tr}$$

D48

Extra tooling man-hours cost of VCW is given by following relationship .

$$\Delta C_{tooling} = \{4.0127 \, (V_{max})^{0.899} \, (N_{rdte})^{0.178} \, (N_r)^{0.066} \} \times$$

$$\{[(M_{ampr})^{0.764}]_{VCW} \times [(f_{diff})_{VCW}]_{tooling} - [(M_{ampr})^{0.764}]_{FCW}\} \times \Re_{tr} \qquad \text{D49}$$

D12.3.3 *Material Cost for Prototype*

This cost may also be higher for VCW prototype aircraft primarily in area of trailing edge system . Fortunately the extra material and equipment required for variable camber operation are such that would be supplied off the shelf and they don't require special development cost by the vendors . The methodology for best possible judgement for the value of $(f_{material})_{VCW}$ is similar to previous argument though trailing edge extra material cost in view of the Author may not be higher than 25% of the conventional flap/aileron system of FCW :

$$(f_{material})_{VCW} = 1.250 \times 0.5 \times 0.30 + 1 = 1.1875 \qquad \text{D50}$$

This is used in Roskam prediction equation D51 as in D53 :

$$C_{material} = \{ 37.632 \, (M_{ampr})^{0.689} (V_{max})^{0.624} (N_{rdte})^{0.792} \} \times C_{pi} \times f_{material} \qquad \text{D51}$$

and the equation used by Wayne Burnes (given here for reference only) :

$$C_{material} = \{ 96.677 \, (M_{ampr})^{0.692} (V_{max})^{0.639} (N_{rdte})^{0.803} \} \times C_{pi} \times f_{material} \times f_{low\ obs}$$

D52

Extra manufacturing man-hours cost of VCW is given by following relationship .

$$\Delta C_{material} = \{37.632 (V_{max})^{0.624} (N_{rdte})^{0.792} \} \times \{[(M_{ampr})^{0.689}]_{VCW} \times (f_{material})_{VCW} -$$

$$[(M_{ampr})^{0.689}]_{FCW} \} \times C_{pi} \qquad \text{D53}$$

D12.4 Flight test operations cost

It is the cost of the following works listed in Table D-9 for which a comparative study was conducted to find the extra cost for VCW aircraft :

- Routine flight testing

- Associated simulation work
- For stealth and other peculiar flight tests

Formulae used by Roskam is as below:

$$C_{flight\ test} = \{ 0.001244\ (M_{ampr})^{1.16}\ (V_{max})^{1.371}\ (N_{rdte} - N_{prod.})^{1.281} \} \times C_{pl} \times f_{diff} \times f_{att} \qquad \text{D54}$$

and the equation used by Wayne Burnes is also given for comparison (nearly 4 times bigger) :

$$C_{flight\ test} = \{ 0.00558\ (M_{ampr})^{1.19}\ (V_{max})^{1.401} (N_{rdte} - N_{prod.})^{1.281} \} \times f_{att} \times C_{pl} \times f_{security} \qquad \text{D55}$$

The extra flight test operation cost of VCW is given by substituting the factor derived in Table D-9 in the following relationship .

$$\Delta C_{flight\ test} = \{ 0.001244\ (V_{max})^{1.371}\ (N_{rdte} - N_{prod.})^{1.281} \} \times \{ [(M_{ampr})^{1.16}]_{VCW} \times [(f_{diff})_{VCW}]_{flight} - [(M_{ampr})^{1.16}]_{FCW} \} \times C_{pl} \qquad \text{D56}$$

D12.5 Total Extra Development Cost of VCW

Adding all the above derived extra costs will render the total extra development cost of VCW against FCW. It is reasonable to assume N_{prod} for passenger aircraft as 600 which would guaranty the return of investment. Therefore the extra development cost per aircraft per unit mass of wing trailing edge for VCW is as follows :

$$(\Delta C_{development})_{VCW} = (\Delta C_{design} + \Delta C_{support\&test} + \Delta C_{manufacture} + \Delta C_{tooling} + \Delta C_{material} + \Delta C_{flight\ test}) / [N_{prod} \times M_{TER}] \qquad \text{D57}$$

The term $(\Delta C_{development})_{VCW}$ may be added to the price density of the wing trailing edge of VCW aircraft in price module of CACAD to account for extra development cost .

Table D-1 : Points extracted from 7.5 degree upsweep drag increment from [32].

α_f	10	9	8	7	6	5	4	3	2	1	0	-1	-2	-3	-4	-5
$\Delta_{\alpha\beta}C_{Df}$	0.026	0.021	0.015	0.010	0.007	0.006	0.005	0.0045	0.005	0.0065	0.009	0.0125	0.016	0.021	0.027	0.034

Table D-2 : Hydraulic system mass, real and predicted ones for different passenegr aircraft

Aircraft Type	*Take-off Mass*	*Take-off Mass*	*Hyd. Mass*	*Hyd. Mass*	*Hyd. mass Roskam*	*Span*	*Fuselage Length*	*Number Function*	*Hyd. mass Raymor*	*Hyd. mass Ray.×4.7*
Unit	lb	kg	lb	kg	lb	ft	ft	N_f	lb	lb
DC-9-30	108000	48979.59	480	217.7	972	28.47	32.74	7	269.6	1264.6
MD-80	140000	63492.06	540	244.9	1260	32.86	41.3	7	322.1	1513.7
DC-10-10	430000	195011.3	2330	1056.7	3870	47.37	51.97	7	423.5	1990.7
DC-10-30	555000	251700.7	2587	1173.2	4995	50.39	51.97	7	435.6	2047.3
B737-200	115500	52380.95	873	395.9	1039.5	28.35	29.54	7	255.4	1200.2
B727-100	160000	72562.36	1418	643.1	1440	32.92	35.41	7	298.3	1401.9
B747-100	710000	321995.5	4471	2027.7	6390	59.64	68.63	7	538.2	2529.3
A300 B2	302000	136961.5	3701	1678.5	2718	44.84	52.03	7	413.7	1944.3

Table D-3 Application of Airbus methodology

for prediction of extra maintenance cost of VCD trailing edge system

Code	*Comparison area*	*1 ± %change*	*Justification*
D1	Complexity	1.05	VCD changes in spanwise, imparts complexity to the wing trailing edge system
D2	Stage of Development	1.1	?
D3	Environment	1	
D4	Flight hour per flight	1	
D5	Operation time per flight	1	
D	**Design**	**1.155**	**D1×D2×D3×D4×D5**
R1	Overhaul and inspection rate	1.05	Due to sliding of VCD underneath lift dumpers a rise in this rate in inevitable
R2	Removal	1.05	due to higher complexity and inspection rate this rise is also unavoidable
R	**Reliability**	**1.1025**	**R1×R2**
M1	Reachability	1	
M2	Accessibility	1	
M3	Diagnostic capability	1	
M4	Manageability	1	
M	**Maintainability**	**1**	**M1×M2×M3×M4**
O	Overhaul and repair time	1	Due to added function this should rise, but due to lower in size of the VCD it should fall
E	Material cost	1.05	New track system and fittings etc. together with the rise in cost of procurement make E to rise, but due to lower in size of VCD it should fall
S	Skill	1.05	VCD requires some new skill acquiring
F_{difmm}	**Material cost factor**	**1.3371**	**E×R×D**
F_{difml}	**Labour cost factor**	**1.2734**	**(1/4)×M×R×D+(3/4) ×M3×O×R×D**

Table D-4 Factors affecting VCD maintenance cost as compared with FCW one.

Item of criteria	*Wing TE flap*	*Wing TE VCD*	*Justification*
Internal factors			
Corrosion & friction	2	3	VCD rubs against lift dumpers when operated
FOD	1	2	There are higher chances that an FO item stickes between rubbing surfaces
Accesibility	3	3	
Number of parts ..	3.5	4	There are more parts, bits, and complication and subassemblies in VCW
Chances of people causing damage	1.5	1.5	
Sum	11	13.5	
External factor			
Stressing	2	2	
fuel contaminent	1	1	
Pressurisation	1	1	
Sanitation	1	1	
Cut outs	1	1	
Piping and wiring in the area	1.3	1.7	For obvious reasons VCD requires more wiring, and piping in wing TE
Sum	7.3	7.7	

Table D-5 Application of Airbus methodology
for prediction of extra maintenance cost of VCD hydraulics system

Code	*Comparison area*	*1 ± %change*	*Justification*
D1	Complexity	1.03	VCD changes in spanwise imparts complexity to the hydraulics system ?
D2	Stage of Development	1	
D3	Environment	1	
D4	Flight hour per flight	1	
D5	Operation time per flight	1	
D	**Design**	**1.03**	**D1×D2×D3×D4×D5**
R1	Overhaul and inspection rate	1	
R2	Removal	1.05	Due to higher complexity and addition of more equipment this rise is unavoidable
R	**Reliability**	**1.05**	**R1×R2**
M1	Reachability	1.05	VC actuators shall be placed in the vicinity of high lift device actuators, with extra piping and wiring
M2	Accessibility	1	
M3	Diagnostic capability	1	
M4	Manageability	1	
M	Maintainability	1.05	M1×M2×M3×M4
O	Overhaul and repair time	1.15	Due to addition of more actuators, relays, piping, etc. to the system, increasing the fuctions from 7 to 8
E	Material cost	1.05	Due to increase in equipment within the system
S	Skill	1	
F_{difmm}	Material cost factor	1.1356	E×R×D
F_{difml}	Labour cost factor	1.2032	(1/4)×M×R×D+(3/4) ×M3×O×R×D

Table D-6 : Application of Airbus methodology
for prediction of extra maintenance cost of VCD flight control system.

Code	*Comparison area*	*1 ± %change*	*Justification*
D1	Complexity	1.05	VCD changes in spanwise and chordwise imparts complexity to the flight control system ?
D2	Stage of Development	1.02	
D3	Environment	1	
D4	Flight hour per flight	1	
D5	Operation time per flight	1	
D	**Design**	**1.071**	**D1×D2×D3×D4×D5**
R1	Overhaul and inspection rate	1	
R2	Removal	1.05	Due to higher complexity this rise is unavoidable
R	**Reliability**	**1.05**	**R1×R2**
M1	Reachability	1	
M2	Accessibility	1	
M3	Diagnostic capability	1	
M4	Manageability	1	
M	**Maintainability**	**1**	**M1×M2×M3×M4**
O	Overhaul and repair time	1.05	Due to addition complexity to the system, and increasing the fuctions from 7 to 8
E	Material cost	1.05	Due to increase in the cost of system software
S	Skill	1	
F_{difmm}	Material cost factor	1.1808	E×R×D
F_{difml}	Labour cost factor	1.1667	(1/4)×M×R×D+(3/4) ×M3×O×R×D

Table D-7 : VCW design and engineering tasks compared with FCW.

Item	*Rise factor*	*Justification*
(a)	1.02	slight extra cost and MHR envisaged at conceptual phase
(b)	1.05	VCD, Hydraulic, and flight control software
(c)	1.10	wing with VCD deployed
(d)	1.03	to test the integrity of VCD operation during cruise
(e)	1.05	extra system test for VCD
(f)	1	detail design shall treat VCW as any other system once it is finalised in previous design stages
(g)	1	drawing activity shall treat VCW as any other system
(h)	1	liaisonning is also indifferent to VCW
(i)	1.05	there are extra chances for issuing modifications for VCW
(j)	1	same as (h) & (g)
(k)	1	as above
(l)	1.03	extra design work for prediction VCW reliability
(m)	1.05	sliding of VCD underneath lift dumpers, & camber variation across span
	$[(f_{diff})_{VCW}]$ design	(a) ×..× (m) = 1.4468

Table D-8 : VCW development support cost compared with FCW

Item	*Item Name*	*Rise Factor*	*Justification*
(a)	Wind tunnel testing	1.75	great extra work, needed to design the airfoil, wing, deployed VCD
(b)	System testing	1.1	extra flight control, and hydraulic testing
(c)	Structural testing	1.05	extra testing of trailing edge of the wing
(d)	Propulsion testing	1	irrelevant to VCW
(e)	Simulation & development support	1.02	some extra simulation work for cruise VCD deployment
	$[(f_{diff})_{VCW}]_{support}$	1.384	(a)× (b)× (c)×(d)×(e)

Table D-9 : VCW flight test operation compared with FCW.

Item	*Item Name*	*Rise Factor*	*Justification*
(a)	Routine flight testing	1.1	VC operation in all phases of flight
(b)	Associated simulation work	1.03	extra work toward VC operation in all phases of the flight
(c)	For stealth and other peculiar flight tests	1	no relation with VCW
	$[(f_{diff})_{VCW}]_{flight}$	1.133	(a)×(d)×(c)

Table D-10 : FCW vs VCW Rsults
Aircraft : A340-200 Class

FCW aircraft Results :

DESIGN MISSION :

1. PAX	=	263.0	2. STAGE	=	13799.0
3. DIV	=	370.0	4. HOLD	=	0.5
5. MFRT	=	0.00	6. PAB	=	9.0
7. AISLES	=	2.0	8. VCR	=	896.3
9. HTMCR	=	10667.0	10.HTMDIV	=	6096.0
11.DTO	=	2000.0	12.VA	=	70.0
13.EFH	=	6095.0			

INDEPENDENT VARIABLES :

1.X(1),A	=	9.7	2.X(2),BTAA	=	35.00
3.X(3),TR	=	0.2223	4.X(4),S	=	377.07
5.X(5),SWP	=	27.73	6.X(6)MENG	=	30050.64
7.X(7)BTATO	=	10.0	8. ELE	=	0.150
9. ETE	=	0.200	10.ETEFB	=	0.150
11.ETA	=	0.600	12.TC	=	0.0950

AIRCRAFT SIZES:

1. AMC	=	7.076	2. GMC	=	6.235
3. FUSL	=	59.700	4. FUSD	=	5.640
5. CR	=	10.202	6. CT	=	2.268
7. PCL	=	48.984	8. ENGPOS	=	0.533
9. SPIENG	=	0.300	10.SPOENG	=	0.639
11.SPAN	=	60.478	12.TBLOC	=	15.899
13.SFTE	=	45.673	14.SFIN	=	54.766
15.STP	=	92.557	16.SFUS	=	914.128
17.SLE	=	48.242	18.VTA	=	140.045
19.RGE	=	13973.67	20.VFUEL	=	130.272
21.SRUD	=	20.739	22.SELV	=	26.395
23.SABR	=	30.165	24.SCS	=	189.863
25.CGPOSN	=	0.4820	26.IY	=	101033477.157
27.VPAX	=	611.58			

MASS EST. DETAIL :

23.MTO	=	254221.15	24.MFUS1	=	20554.07
25.MFUS2	=	23509.88	26.MPEN	=	4654.72
27.MFIN	=	1740.93	28.MTP	=	2913.80
29.MWING	=	33890.06	30.MWINGC	=	39692.00
31.MWLE	=	2883.27	32.MWTEF	=	2196.78
33.MWTEFVC	=	0.00	34.MWBCOV2	=	18622.44
35.MWBTIP	=	1274.48	36.MWBJNT	=	910.17
37.MWBSP	=	2603.46	38.MWBPP	=	601.01
40.MWBRB	=	3209.39			
41.MWBX	=	28250.52	42.MSYS1	=	11603.88
43.MSYS2	=	11856.04	44.MUC	=	10358.83
45.MFUR	=	15078.33	46.MEL	=	1200.00
47.MIAE	=	2625.96	48.MFS	=	963.64
49.MFC1	=	2164.01	49.1.MHYD1	=	1081.29
49.3.MFC2	=	2181.36	49.2.MHYD2	=	472.73
50.MELS	=	1504.10			
51.MAPI1	=	2044.77	52.MOX	=	219.89
53.MAPU	=	1016.89	54.MBC	=	187.08
55.MAUX	=	1294.02	56.ME	=	129401.92
57.MPAY	=	24985.00	58.MSSCR	=	250836.00
59.MSSEC	=	161306.22	60.MAF	=	99347.87
61.ZFM	=	155000.61	62.MFUELC6	=	91391.77
63.MFUELC1	=	20737.45	64.MFUELC2	=	19325.31
65.MFUELC3	=	18111.81	66.MFUELC4	=	17063.52
67.MFUELC5	=	16153.67	68.MFUELD	=	2584.47
69.MFUELH	=	1664.65	70.MFLAL	=	3484.00
71.CONFLL	=	95.64	72.MFUELU	=	94971.41
73.MFUEL	=	99220.53	75.MPT	=	1144.00

LIFT & DRAG,AND RELATED ITEMS :

1. CDA	=	0.131933	2. CDCR	=	0.027960
3. CDWDR	=	0.002000	4. CD0W	=	0.005690
5. CD0EW	=	0.008386	6. CD0	=	0.014076
7. CDTO	=	0.090931	8. CDFMIN	=	0.000000
9. DCDVI2	=	0.000000	10.DCDVI1	=	0.000000
11.DCDVI	=	0.000000	12.CDC	=	0.016076
13.CDETA1	=	0.000000	14.CDETA2	=	0.000000
15.CDETA3	=	0.000000	16.CDETA4	=	0.000000
17.CDETA5	=	0.000000	18.CDI1	=	0.000000
19.CDI2	=	0.000000	20.CDI3	=	0.000000
21.CDI4	=	0.000000	22.CDI5	=	0.000000
23.DCDF1	=	0.000000	24.DCDF2	=	0.000000
25.DCDF3	=	0.000000	26.DCDF4	=	0.000000
27.DCDF5	=	0.000000	28.CDC1	=	0.000000
29.CDC2	=	0.000000	30.CDC3	=	0.000000
31.CDC4	=	0.000000	32.CDC5	=	0.000000
33.CDT1	=	0.000000			
34.CDT2	=	0.000000	35.CDT3	=	0.000000
36.CDT4	=	0.000000	37.CDT5	=	0.000000
38.CLMTO	=	2.092550	39.CLTO	=	1.452230
40.CLCR	=	0.554270			
42.CLDIV	=	0.348318	43.CLCRB1	=	0.558384
44.CLCRB2	=	0.512561	45.CLCRB3	=	0.469858
46.CLCRB4	=	0.429837	47.CLCRB5	=	0.392131
48.KCR	=	1.178286	49.K1CR	=	0.000000
50.K2CR	=	0.000000	51.K3CR	=	0.000000
52.K4CR	=	0.000000	53.K5CR	=	0.000000

DOC BREAKDOWN :

1. DOCRAE0	=	73798.83	2. DOCRAE1	=	80600.72
3. DOCRAE2	=	80090.91			
5. DOCF	=	18044.57	6. DOCDK	=	9667.54
7. DOCLF	=	711.82	8. DOCEM	=	2888.33
9. DOCEL	=	4055.19	10.DOCME	=	6943.53
11.DOCAFMT	=	1966.09	12.DOCAFLT0	=	6650.45
13.DOCAFLM0	=	8742.04	14.DOCSCAFT	=	21836.28
15.DOCSCENT	=	6163.62	16.DOCSCINS	=	1689.43
17.DOCSCT0	=	29689.34			

DOC MATERIAL :

18.DOCMFUS1	= 288.87	19.DOCMFUS2	= 184.77
20.DOCMWBX1	= 402.02	21.DOCMWBX2	= 81.48
22.DOCMWLE1	= 69.82	23.DOCMWLE2	= 32.98
24.DOCMTER1	= 13.55	25.DOCMTER2	= 18.20
26.DOCMWTF1	= 53.20	27.DOCMWTF2	= 30.44
28.DOCMTP1	= 35.80	29.DOCMTP2	= 34.00
30.DOCMFIN1	= 21.39	31.DOCMFIN2	= 30.30
32.DOCMFUR1	= 438.16	33.DOCMFUR2	= 282.97
34.DOCMUC1	= 250.84	35.DOCMUC2	= 1260.57
36.DOCMEL1	= 96.86	37.DOCMIAE1	= 93.26
38.DOCMAV2	= 311.85	39.DOCMAPU1	= 36.12
40.DOCMELS1	= 53.42	41.DOCMELS2	= 400.14
42.DOCMFS1	= 34.22	43.DOCMFS2	= -
44.DOCMAPI1	= 72.62	45.DOCMAPI2	= 141.48
46.DOCMHYD1	= 287.66	47.DOCMHYD2	= 287.66
48.DOCMFC1	= 76.86	49.DOCMFC2	= 345.14
50.DOCMM1	= 60.41	51.DOCMOX2	= 47.16
52.DOCMWW2	= 28.30	53.DOCAFMT1	= 2042.56
54.DOCAFMT2	= 3653.02		

DOC LABOUR :

1. DOCLAV1	= 659.07	2. DOCLAV2	= 633.16
3. DOCLLI1	= 164.29	4. DOCLLI2	= 181.51
5. DOCLELS1	= 219.81	6. DOCLELS2	= 212.83
7. DOCLFUR1	= 1386.84	8. DOCLFUR2	= 1087.06
9. DOCLFC1	= 440.18	10.DOCLFC2	= 230.09
11.DOCLAPI1	= 122.72	12.DOCLAPI2	= 96.19
13.DOCLICE1	= 25.43	14.DOCLICE2	= 28.10
15.DOCLPRE1	= 66.49	16.DOCLAIR1	= 30.79
17.DOCLFS1	= 83.57	18.DOCLFS2	= 92.33
19.DOCLHYD1	= 212.93	20.DOCLHYD2	= 177.78
21.DOCLUC1	= 710.16	22.DOCLUC2	= 875.99
23.DOCLOX1	= 9.83	24.DOCLOX2	= 7.70
25.DOCLWW1	= 95.10	26.DOCLWW2	= 74.54
27.DOCLFIR1	= 13.06	28.DOCLFIR2	= 14.43
29.DOCLSTR1	= 2133.86	30.DOCLSTR2	= 667.67
31.DOCLFUS1	= 636.98	32.DOCLFUS2	= 314.14

33.DOCLWBX1=	553.47	34.DOCLWBX2=	119.82
35.DOCLWLE1=	116.47	36.DOCLWLE2=	57.41
38.DOCLVTR2=	41.46		
39.DOCLWTF1=	127.61	40.DOCLWTF2=	56.72
41.DOCLTP1 =	308.40	42.DOCLTP2 =	81.11
43.DOCLFIN1=	252.92	44.DOCLFIN2=	72.51
45.DOCAFLT1=	6575.16	46.DOCAFLT2=	4454.89
47.DOCLAPU1=	375.09		

DOC MAINTENANCE MATERIAL & LABOUR:

1.DOCMLUC1 =	0.110	2.DOCMLUC2 =	0.244
3.DOCMLFUR1=	0.209	4.DOCMLFUR2=	0.157
5.DOCMLAV1 =	0.086	6.DOCMLAV2 =	0.108
7.DOCMLFC1 =	0.059	8.DOCMLFC2 =	0.066
9.DOCMLAPI1=	0.022	10.DOCMLAP2=	0.027
11.DOCMLFG1=	0.177	12.DOCMLFG2=	0.082
13.DOCMLWG1=	0.163	14.DOCMLWG2=	0.050
15.DOCMLEL1=	0.031	16.DOCMLEL2=	0.070
17.DOCMLHY1=	0.029	18.DOCMLHY2=	0.053
19.DOCMLFS1=	0.013	20.DOCMLAPU1=	0.047
21.DOCMLMI1=	0.020	22.DOCMLMI2=	
23.DOCMLOX1=		24.DOCMLOX2=	0.006
25. =		26.DOCMLWW2=	0.012

DOC STANDING AND INSURANCE :

0. DCSCAFT1=	28762.49		
1. DOCSCT1 =	36615.55	2. DOCSFUS =	3015.81
3. DOCSWBX =	4197.06	4. DOCSWLE =	728.93
5. DOCSVCD =	0.00	6. DOCSWTEF=	555.37
7. DOCSTP =	373.78	8. DOCSFIN =	223.32
9. DOCSFUR =	8228.12	10.DOCSUC =	2618.83
11.DOCSAV =	3218.18	12.DOCSFS =	434.84
13.DOCSFC =	1302.00	14.DOCSHYD =	487.93
15.DOCSELS =	942.66	16.DOCSAPI =	922.69
17.DOCSMM =	756.85	17.DOCSAPU =	614.67

MAINT. MAN HOURS :

1. MPFAV =	12.07	2. MPFHYD =	3.90
3. MPFUC =	13.01	4. MPFOX =	0.18
5. MPFWW =	1.74	6. MPFELS =	4.03
7. MPFLI =	3.01	8. MPFFUR =	25.40
9. MPFFC =	8.06	10.MPFAPI =	2.25
11.MPFFS =	1.53	12.MPFSTRV =	38.14
13.MPFFIR =	0.24	14.MPFAFVR =	113.55
15.MPFENG =	18.57	16.MHPF =	140.37
17.MPFHENG =	1.17	18.MPFHAFR =	7.21
19.MPFAFR =	114.49	20.MHPFHR =	8.37
21.TFLT =	15.59	22.TBLOC =	15.89
23.MPFHAV =	0.76	24.MPFHELS =	0.25
25.MPFHLI =	0.19	26.MPFHFUR =	1.60
27.MPFHFC =	0.51	28.MPFHAPI =	0.14
29.MPFHFS =	0.10	30.MPFHHYD =	0.25
31.MPFHUC =	0.82	32.MPFHOX =	0.01
33.MPFHWW =	0.11	34.MPFHSTR =	0.00
35.MPFHFIR =	0.02	36.MPFHAFVR=	6.75
37.MHPFVR =	132.12	38.MHPFHVR =	7.91

AIRCRAFT PRICES :

1. PAC =	86064946.57	2. PFUS =	9662562.39
3. PWING =	18015277.50	4. PEL =	3240000.00
5. PAF =	69962699.78	6. PSYS =	14084980.92
7. PENG =	16102246.79	8. PWBX =	13447246.95
9. PWLE =	2335450.95	10.PWTE =	2232579.60
11.PWTEF =	1779392.77	12.PIAE =	3119643.74
13.PFS =	1144808.09	14.PFC =	2570839.96
15.PELS =	1786870.21	16.PAPI =	2429181.57
17.PMM =	2020770.22	18.PPEN =	1913091.87
19.PTP =	1197570.01	20.PFIN =	715521.86
21.PFUR =	14656138.19	22.PUC =	8390648.91
23.DEVVCW1 =	0.00	24.DEVVCW2 =	0.00
25.DEVVCW3 =	0.00	26.KPWTEVC =	0.00

VCW aircraft Results :

DESIGN MISSION :

1. PAX	=	263.0	2. STAGE	=	13799.0
3. DIV	=	370.0	4. HOLD	=	0.5
5. MFRT	=	0.00	6. PAB	=	9.0
7. AISLES	=	2.0	8. VCR	=	896.3
9. HTMCR	=	10667.0	10.HTMDIV	=	6096.0
11.DTO	=	2000.0	12.VA	=	70.0
13.EFH	=	6095.0			

INDEPENDENT VARIABLES :

1.X(1),A	=	10.0	2.X(2),BTAA	=	35.00
3.X(3),TR	=	0.2183	4.X(4),S	=	352.77
5.X(5),SWP	=	27.54	6.X(6)MENG	=	28582.64
7.X(7)BTATO	=	10.0	8. ELE	=	0.150
9. ETE	=	0.225	10.ETEFB	=	0.175
11.ETA	=	0.675	12.TC	=	0.1000

AIRCRAFT SIZES:

1. AMC	=	6.755	2. GMC	=	5.939
3. FUSL	=	59.700	4. FUSD	=	5.640
5. CR	=	9.750	6. CT	=	2.128
7. PCL	=	48.984	8. ENGPOS	=	0.522
9. SPIENG	=	0.300	10.SPOENG	=	0.639
11.SPAN	=	59.394	11.TBLOC	=	15.890
13.SFTE	=	52.835	14.SFIN	=	50.799
15.STP	=	81.924	16.SFUS	=	914.128
17.SLE	=	44.972	18.VTA	=	126.584
19.RGE	=	13974.36	20.VFUEL	=	121.628
21.SRUD	=	19.402	22.SELV	=	24.694
23.SABR	=	28.221	24.SCS	=	184.747
25.CGPOSN	=	0.4788	26.IY	=	89708725.400
27.VPAX	=	611.58			

MASS EST. DETAIL :

23.MTO	=	242802.17	24.MFUS1	=	20554.07
25.MFUS2	=	23274.21	26.MPEN	=	4107.59
27.MFIN	=	1590.72	28.MTP	=	2516.87
29.MWING	=	32143.77	30.MWINGC	=	37847.85
31.MWLE	=	2687.83	32.MWTEF	=	2565.36
33.MWTEFVC	=	2954.00	34.MWBCOV2	=	17020.16
35.MWBTIP	=	1146.49	36.MWBJNT	=	861.39
37.MWBSP	=	2496.29	38.MWBPP	=	571.65
40.MWBRB	=	2859.25			
41.MWBX	=	25955.68	42.MSYS1	=	11408.15
43.MSYS2	=	11814.40	44.MUC	=	9893.54
45.MFUR	=	15078.33	46.MEL	=	1200.00
47.MIAE	=	2574.77	48.MFS	=	949.38
49.MFC1	=	2134.38	49.1.MHYD1	=	1225.32
49.3.MFC2	=	2122.51	49.2.MHYD2	=	451.50
50.MELS	=	1490.16			
51.MAPI1	=	2044.77	52.MOX	=	219.89
53.MAPU	=	971.22	54.MBC	=	187.08
55.MAUX	=	1248.98	56.ME	=	124897.55
57.MPAY	=	24985.00	58.MSSCR	=	239564.97
59.MSSEC	=	156576.97	60.MAF	=	96311.84
61.ZFM	=	150496.58	62.MFUELC6	=	84770.52
63.MFUELC1	=	19254.53	64.MFUELC2	=	17891.59
65.MFUELC3	=	16787.67	66.MFUELC4	=	15831.88
67.MFUELC5	=	15004.85	68.MFUELD	=	2492.05
69.MFUELH	=	1611.79	70.MFLAL	=	3342.35
71.CONFLL	=	88.87	72.MFUELU	=	88201.74
73.MFUEL	=	92305.58	75.MPT	=	1092.62

LIFT & DRAG,AND RELATED ITEMS :

1. CDA	=	0.151025	2. CDCR	=	0.028441
3. CDWDR	=	0.002000	4. CD0W	=	0.005769
5. CD0EW	=	0.008622	6. CD0	=	0.014391
7. CDTO	=	0.093833	8. CDFMIN	=	0.004742
9. DCDVI2	=	0.000325	10.DCDVI1	=	0.000317
11.DCDVI	=	0.000009	12.CDC	=	0.016383
13.CDETA1	=	0.000446	14.CDETA2	=	0.000426
15.CDETA3	=	0.000408	16.CDETA4	=	0.000391

17.CDETA5	=	0.000375	18.CDI1	=	0.011784		
19.CDI2	=	0.009901	20.CDI3	=	0.008299		
21.CDI4	=	0.006924	22.CDI5	=	0.005740		
23.DCDF1	=	-0.000005	24.DCDF2	=	0.000096		
25.DCDF3	=	0.000087	26.DCDF4	=	0.000084		
27.DCDF5	=	0.000079	28.CDC1	=	0.016387		
29.CDC2	=	0.016287	30.CDC3	=	0.016295		
31.CDC4	=	0.016298	32.CDC5	=	0.016304		
33.CDT1	=	0.027890					
34.CDT2	=	0.025926	35.CDT3	=	0.024348		
36.CDT4	=	0.022990	37.CDT5	=	0.021824		
38.CLMTO	=	2.144347	39.CLTO	=	1.488177		
40.CLCR	=	0.565829					
42.CLDIV	=	0.357075	43.CLCRB1	=	0.570039		
44.CLCRB2	=	0.524562	45.CLCRB3	=	0.482304		
46.CLCRB4	=	0.442653	47.CLCRB5	=	0.405260		
48.KCR	=	1.181792	49.K1CR	=	1.181792		
50.K2CR	=	1.178522	51.K3CR	=	1.175356		
52.K4CR	=	1.172275	53.K5CR	=	1.169271		

DOC BREAKDOWN :

1. DOCRAE0	=	71333.59	2. DOCRAE1	=	78301.39
3. DOCRAE2	=	77823.66			
5. DOCF	=	16758.33	6. DOCDK	=	9305.12
7. DOCLF	=	679.85	8. DOCEM	=	2816.97
9. DOCEL	=	3863.58	10.DOCME	=	6680.55
11.DOCAFMT	=	1953.34	12.DOCAFLT0	=	6452.38
13.DOCAFLM0	=	8530.40	14.DOCSCAFT	=	21695.12
15.DOCSCENT	=	6011.47	16.DOCSCINS	=	1672.75
17.DOCSCT0	=	29379.35			

DOC MATERIAL :

18.DOCMFUS1	=	285.98	19.DOCMFUS2	=	180.57
20.DOCMWBX1	=	369.37	21.DOCMWBX2	=	74.56
22.DOCMWLE1	=	65.09	23.DOCMWLE2	=	30.80
24.DOCMTER1	=	27.29	25.DOCMTER2	=	27.37
26.DOCMWTF1	=	85.59	27.DOCMWTF2	=	45.23
28.DOCMTP1	=	30.93	29.DOCMTP2	=	31.26
30.DOCMFIN1	=	19.55	31.DOCMFIN2	=	28.31
32.DOCMFUR1	=	438.17	33.DOCMFUR2	=	276.12
34.DOCMUC1	=	239.58	35.DOCMUC2	=	1230.05
36.DOCMEL1	=	96.86	37.DOCMIAE1	=	91.45
38.DOCMAV2	=	304.30	39.DOCMAPU1	=	34.49
40.DOCMELS1	=	52.93	41.DOCMELS2	=	368.31
42.DOCMFS1	=	33.72	43.DOCMFS2	=	-
44.DOCMAPI1	=	72.62	45.DOCMAPI2	=	138.06
46.DOCMHYD1	=	302.85	47.DOCMHYD2	=	302.85
48.DOCMFC1	=	75.81	49.DOCMFC2	=	397.67
50.DOCMM1	=	58.81	51.DOCMOX2	=	46.02
52.DOCMWW2	=	27.61	53.DOCAFMT1	=	2030.31
54.DOCAFMT2	=	3641.39			

DOC LABOUR :

1. DOCLAV1	=	611.25	2. DOCLAV2	=	617.83
3. DOCLLI1	=	156.94	4. DOCLLI2	=	173.37
5. DOCLELS1	=	219.63	6. DOCLELS2	=	201.97
7. DOCLFUR1	=	1368.69	8. DOCLFUR2	=	1059.43
9. DOCLFC1	=	506.82	10.DOCLFC2	=	261.95
11.DOCLAPI1	=	122.42	12.DOCLAPI2	=	94.76
13.DOCLICE1	=	27.07	14.DOCLICE2	=	29.91
15.DOCLPRE1	=	65.62	16.DOCLAIR1	=	29.73
17.DOCLFS1	=	82.03	18.DOCLFS2	=	90.61
19.DOCLHYD1	=	252.83	20.DOCLHYD2	=	215.58
21.DOCLUC1	=	700.83	22.DOCLUC2	=	854.78
23.DOCLOX1	=	9.70	24.DOCLOX2	=	7.51
25.DOCLWW1	=	94.52	26.DOCLWW2	=	73.16
27.DOCLFIR1	=	13.41	28.DOCLFIR2	=	14.82
29.DOCLSTR1	=	2041.28	30.DOCLSTR2	=	651.51
31.DOCLFUS1	=	623.71	32.DOCLFUS2	=	307.66
33.DOCLWBX1	=	509.85	34.DOCLWBX2	=	111.12
35.DOCLWLE1	=	110.08	36.DOCLWLE2	=	53.99
38.DOCLVTR2	=	60.55			
39.DOCLWTF1	=	158.33	40.DOCLWTF2	=	80.03
41.DOCLTP1	=	290.25	42.DOCLTP2	=	75.54
43.DOCLFIN1	=	240.59	44.DOCLFIN2	=	68.20
45.DOCAFLT1	=	6541.57	46.DOCAFLT2	=	4452.77
47.DOCLAPU1	=	363.91			

DOC MAINTENANCE MATERIAL & LABOUR:

1.DOCMLUC1 =	0.110	2.DOCMLUC2 =	0.244
3.DOCMLFUR1=	0.212	4.DOCMLFUR2=	0.157
5.DOCMLAV1 =	0.082	6.DOCMLAV2 =	0.108
7.DOCMLFC1 =	0.068	8.DOCMLFC2 =	0.077
9.DOCMLAPI1=	0.023	10.DOCMLAP2=	0.027
11.DOCMLFG1=	0.175	12.DOCMLFG2=	0.081
13.DOCMLWG1=	0.168	14.DOCMLWG2=	0.057
15.DOCMLEL1=	0.032	16.DOCMLEL2=	0.067
17.DOCMLHY1=	0.035	18.DOCMLHY2=	0.061
19.DOCMLFS1=	0.014	20.DOCMLAPU1=	0.047
21.DOCMLMI1=	0.021	22.DOCMLMI2=	
23.DOCMLOX1=		24.DOCMLOX2=	0.006
25. =		26.DOCMLWW2=	0.012

DOC STANDING AND INSURANCE :

0. DCSCAFT1=	28621.44		
1. DOCSCT1 =	36305.66	2. DOCSFUS =	2985.72
3. DOCSWBX =	3856.31	4. DOCSWLE =	679.55
5. DOCSVCD =	0.00	6. DOCSWTEF=	893.64
7. DOCSTP =	322.88	8. DOCSFIN =	204.06
9. DOCSFUR =	8228.50	10.DOCSUC =	2501.32
11.DOCSAV =	3218.33	12.DOCSFS =	428.42
13.DOCSFC =	1284.23	14.DOCSHYD =	552.94
15.DOCSELS =	933.97	16.DOCSAPI =	922.73
17.DOCSMM =	736.84	17.DOCSAPU =	587.09

MAINT. MAN HOURS :

1. MPFAV =	11.19	2. MPFHYD =	4.63
3. MPFUC =	12.84	4. MPFOX =	0.18
5. MPFWW =	1.73	6. MPFELS =	4.02
7. MPFLI =	2.87	8. MPFFUR =	25.07
9. MPFFC =	9.28	10.MPFAPI =	2.24
11.MPFFS =	1.50	12.MPFSTRV =	37.34
13.MPFFIR =	0.25	14.MPFAFVR =	113.14
15.MPFENG =	17.69	16.MHPF =	135.87
17.MPFHENG =	1.11	18.MPFHAFR =	6.99
19.MPFAFR =	111.08	20.MHPFHR =	8.10
21.TFLT =	15.59	22.TBLOC =	15.89
23.MPFHAV =	0.70	24.MPFHELS =	0.25
25.MPFHLI =	0.18	26.MPFHFUR =	1.58
27.MPFHFC =	0.58	28.MPFHAPI =	0.14
29.MPFHFS =	0.09	30.MPFHHYD =	0.29
31.MPFHUC =	0.81	32.MPFHOX =	0.01
33.MPFHWW =	0.11	34.MPFHSTR =	0.00
35.MPFHFIR =	0.02	36.MPFHAFVR=	6.77
37.MHPFVR =	130.83	38.MHPFHVR =	7.88

AIRCRAFT PRICES :

1. PAC =	85211213.10	2. PFUS =	9565702.35
3. PWING =	18307865.32	4. PEL =	3240000.00
5. PAF =	69507195.06	6. PSYS =	14035506.88
7. PENG =	15704018.04	8. PWBX =	12354902.08
9. PWLE =	2177143.59	10.PWTE =	3775819.65
11.PWTEF =	2863043.96	12.PIAE =	3058829.68
13.PFS =	1127865.36	14.PFC =	2535643.34
15.PELS =	1770309.15	16.PAPI =	2429181.57
17.PMM =	1967258.35	18.PPEN =	1688218.36
19.PTP =	1034432.78	20.PFIN =	653785.58
21.PFUR =	14656138.19	22.PUC =	8013763.96
23.DEVVCW1 =	44127.61	24.DEVVCW2 =	940604.14
25.DEVVCW3 =	3774821.75	26.KPWTEVC =	0.00

Table D-11 : Comparison of the FCW version of B767-300Q class of aircraft, the under sized wing member of the B767 family, designed by CACAD, with VCW version.

FXED CAMBER WING BOEING 767-300Q (Under sized wing) RESULTS						VARIABLE CAMBER WING BOEING 767-300Q (Under sized wing) RESULTS					
A1. RUN	=	553.00	E. CLBOEF	=	1.1200	A1. RUN	=	452.00	E. CLBOEF	=	1.1200
A. NF	=	7.00	B. FDIF	=	1.00	A. NF	=	7.00	B. FDIF	=	1.00
C. PAX	=	210.00	D. STAGE	=	11360.94	C. PAX	=	210.00	D. STAGE	=	11375.23
1. DOCRAE0	=	45019.10	2. ZFMMAX	=	118904.66	1. DOCRAE0	=	43901.81	2. ZFMMAX	=	117492.78
3. ZFM	=	109513.516	4. TC	=	0.1100	3. ZFM	=	108102.070	4. TC	=	0.1100
5. A	=	7.9900	6. S	=	283.300	5. A	=	7.9900	6. S	=	283.300
7. MENG	=	17610.45	8. SWP	=	31.50	7. MENG	=	16780.45	8. SWP	=	31.50
9. TR	=	0.2000	10.ETA	=	0.650	9. TR	=	0.2000	10.ETA	=	0.650
11.ETEFB	=	0.225	12.ETE	=	0.275	11.ETEFB	=	0.225	12.ETE	=	0.275
13.MTO	=	179715.28	14.MWING	=	20571.62	13.MTO	=	172860.33	14.MWING	=	20413.29
15.MFUEL	=	70201.77	16.MFUELC1	=	14363.78	15.MFUEL	=	64758.25	16.MFUELC1	=	13433.96
17.MFUELC2	=	13469.57	18.MFUELC3	=	12694.70	17.MFUELC2	=	12425.06	18.MFUELC3	=	11606.70
19.MFUELC4	=	12020.22	20.MFUELC5	=	11430.71	19.MFUELC4	=	10900.47	20.MFUELC5	=	10290.50
21.MFUELC6	=	63978.98	22.IW2	=	0.0000	21.MFUELC6	=	58656.70	22.IW2	=	4.9991
23.IW1	=	0.0000	24.CD0	=	0.01493	23.IW1	=	3.3991	24.CD0	=	0.01487
25.DCDVI	=	0.00000	26.CDC	=	0.01741	25.DCDVI	=	0.00001	26.CDC	=	0.01726
27.CLCRB1	=	0.49803	28.CLCRB2	=	0.45799	27.CLCRB1	=	0.56985	28.CLCRB2	=	0.52530
29.CLCRB3	=	0.42044	30.CLCRB4	=	0.38505	29.CLCRB3	=	0.48410	30.CLCRB4	=	0.44561
31.CLCRB5	=	0.35154	32.KCR	=	1.16489	31.CLCRB5	=	0.40946	32.KCR	=	1.16489
33.K1CR	=	0.00000	34.K2CR	=	0.00000	33.K1CR	=	1.16489	34.K2CR	=	1.16168
35.K3CR	=	0.00000	36.K4CR	=	0.00000	35.K3CR	=	1.15860	36.K4CR	=	1.15562
E. K5CR	=	0.00000				E. K5CR	=	1.15273			

37.CDI1 =	0.00000	38.CDI2 =	0.00000	37.CDI1 =	0.01463	38.CDI2 =	0.01235
39.CDI3 =	0.00000	40.CDI4 =	0.00000	39.CDI3 =	0.01041	40.CDI4 =	0.00875
41.CDI5 =	0.00000	42.DALFAF1 =	0.00000	41.CDI5 =	0.00733	42.DALFAF1 =	0.00000
43.DALFAF2 =	0.00000	44.DALFAF3 =	0.00000	43.DALFAF2 =	0.42189	44.DALFAF3 =	0.39020
45.DALFAF4 =	0.00000	46.DALFAF5 =	0.00000	45.DALFAF4 =	0.36450	46.DALFAF5 =	0.34232
47.DCDF1 =	0.00000	48.DCDF2 =	0.00000	47.DCDF1 =	0.00000	48.DCDF2 =	0.00010
49.DCDF3 =	0.00000	50.DCDF4 =	0.00000	49.DCDF3 =	0.00010	50.DCDF4 =	0.00009
51.DCDF5 =	0.00000	52.LMF1 =	0.7116	51.DCDF5 =	0.00008	52.LMF1 =	0.7297
53.JFLP =	42.45	54.JVCD =	0.00	53.JFLP =	42.05	54.JVCD =	40.16
55.MWTEF =	2093.06	56.MVCD =	0.00	55.MWTEF =	2073.18	56.MVCD =	563.21
57.SFTE =	49.31	58.SVCD =	0.00	57.SFTE =	49.31	58.SVCD =	63.33
59.DEVVCW1 =	43810.79	60.DEVVCW2 =	-93656.80	59.DEVVCW1 =	43806.45	60.DEVVCW2 =	-89334.19
61.DEVVCW3 =	2663817.75	62.CLMA =	2.42572	61.DEVVCW3 =	2642194.75	62.CLMA =	2.42572
63.SRTE =	15.45	64.MWTER =	463.54962	63.SRTE =	15.45	64.MWTER =	42.84912
65.MWBX =	15903.83594	66.MFUELC7 =	64946.43750	65.MWBX =	15622.88477	66.MFUELC7 =	64946.43750
67.LDRCRB =	17.21972	68.LDRCR1 =	17.21972	67.LDRCRB =	17.61781	68.LDRCR1 =	18.04832
69.LDRCR2 =	16.87213	70.LDRCR3 =	16.41495	69.LDRCR2 =	17.98574	70.LDRCR3 =	17.73345
71.LDRCR4 =	15.85244	72.LDRCR5 =	15.18955	71.LDRCR4 =	17.36602	72.LDRCR5 =	16.88298
73.FUSL =	53.68576	74.FUSD =	5.03010	73.FUSL =	53.68576	74.FUSD =	5.03010
75.DTO =	2000.00000	76.VA =	70.95000	75.DTO =	2000.00000	76.VA =	70.50000
77.EFH =	6545.00000	78.MSYS2 =	9893.41992	77.EFH =	6545.00000	78.MSYS2 =	9961.99414
79.FVEC(7) =	11.38981	80.MFUELC8 =	61162.04297	79.FVEC(7) =	18.19421	80.MFUELC8 =	61162.04297
81.MWBCOV1 =	9685.07	82.MWBCOV2 =	9280.04	81.MWBCOV1 =	9658.04	82.MWBCOV2 =	9037.28
83.HMLDG =	127890.42	84.MLDG =	114608.59	83.HMLDG =	126135.80	84.MLDG =	113121.93
85.TST =	64697.26	86.FVEC(1) =	-0.0134	85.TST =	61648.01	86.FVEC(1) =	0.0251
87.FVEC(8) =	-0.0076	88.HTMCR =	10481.0000	87.FVEC(8) =	0.0258	88.HTMCR =	11581.0000
89.MENG1 =	12657.4951	90.MENG2 =	13209.5625	89.MENG1 =	11669.2725	90.MENG2 =	12618.4658
89.MENG3 =	17186.2832	90.MENG4 =	17610.4102	89.MENG3 =	16176.0283	90.MENG4 =	16778.9434
89.MENG5 =	9693.7461			89.MENG5 =	9537.9502		

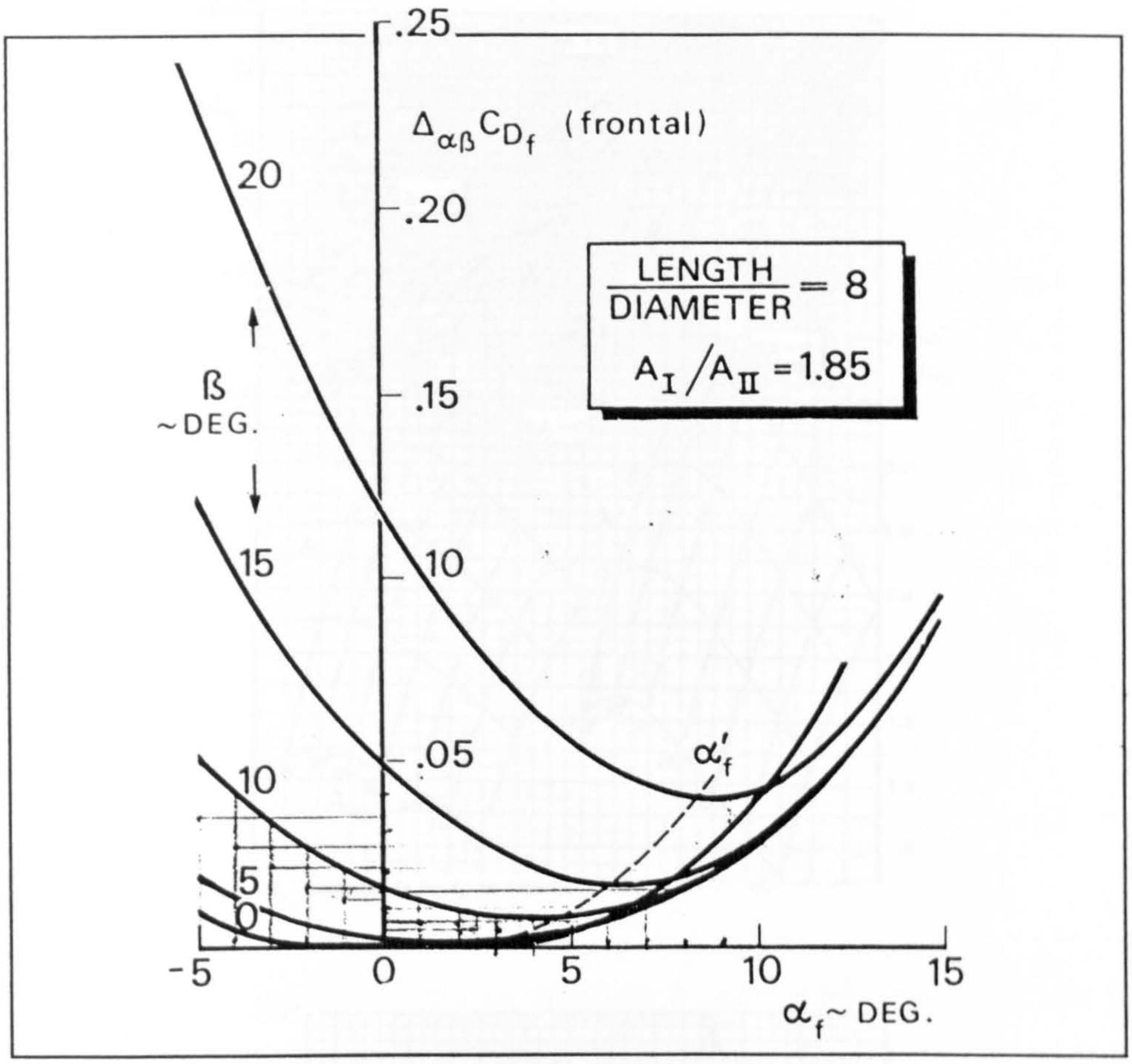

Figure D-1 Estimated fuselage profile drag increment due to angle of attack and rear fuselage upsweep [32]

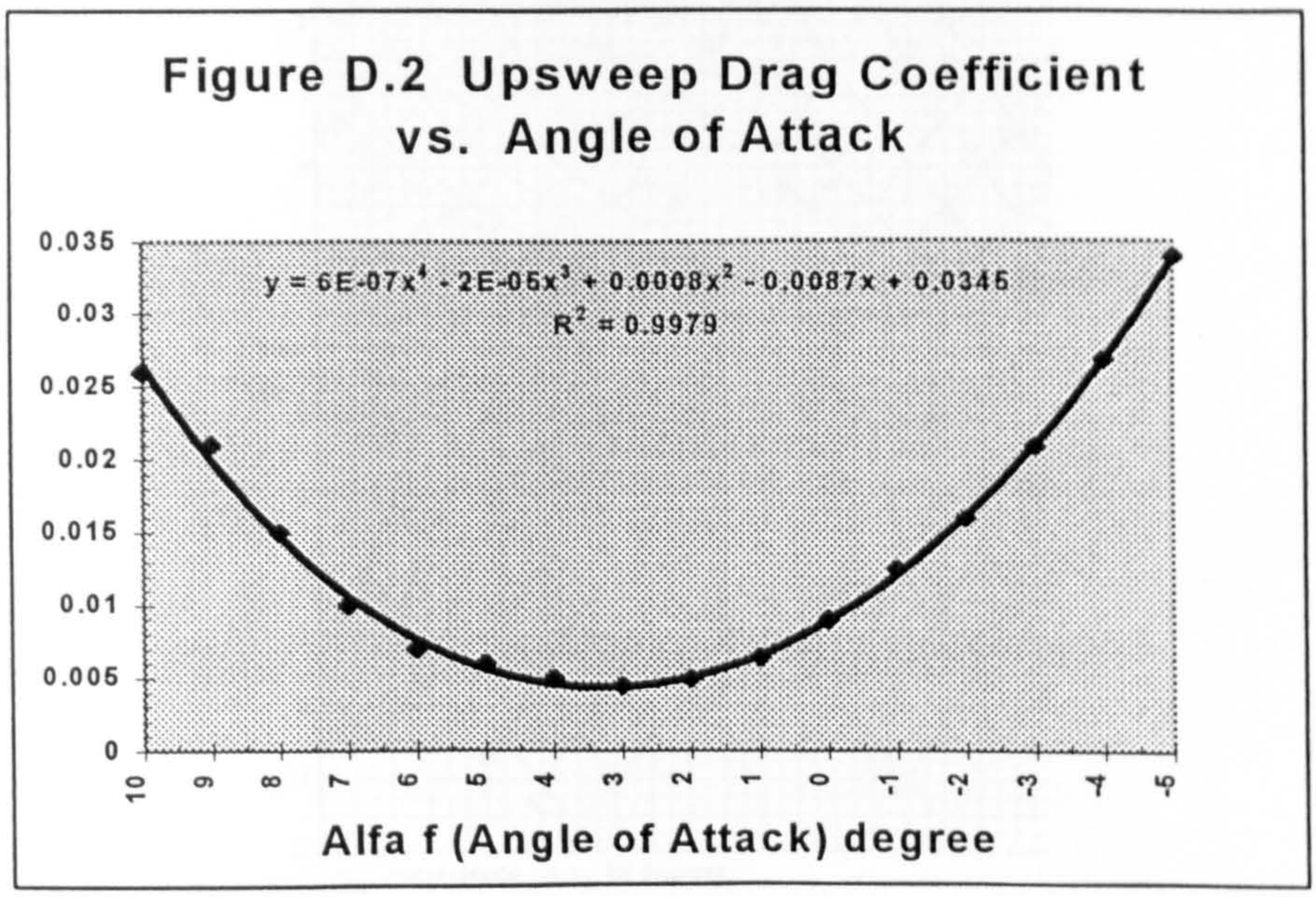

Figure D-2 : Estimated fuselage profile drag increment due to angle of attack and rear fuselage upsweep.

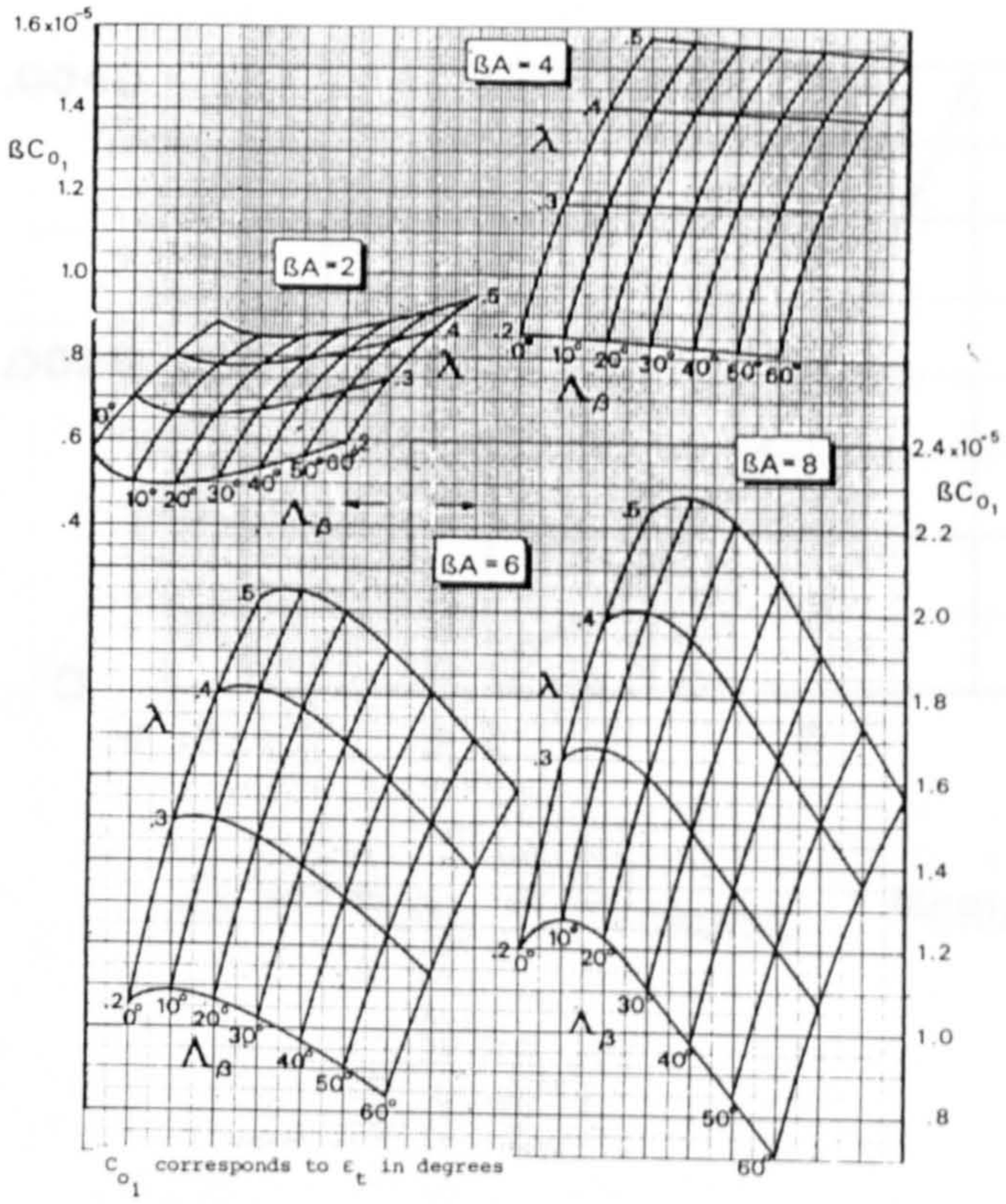

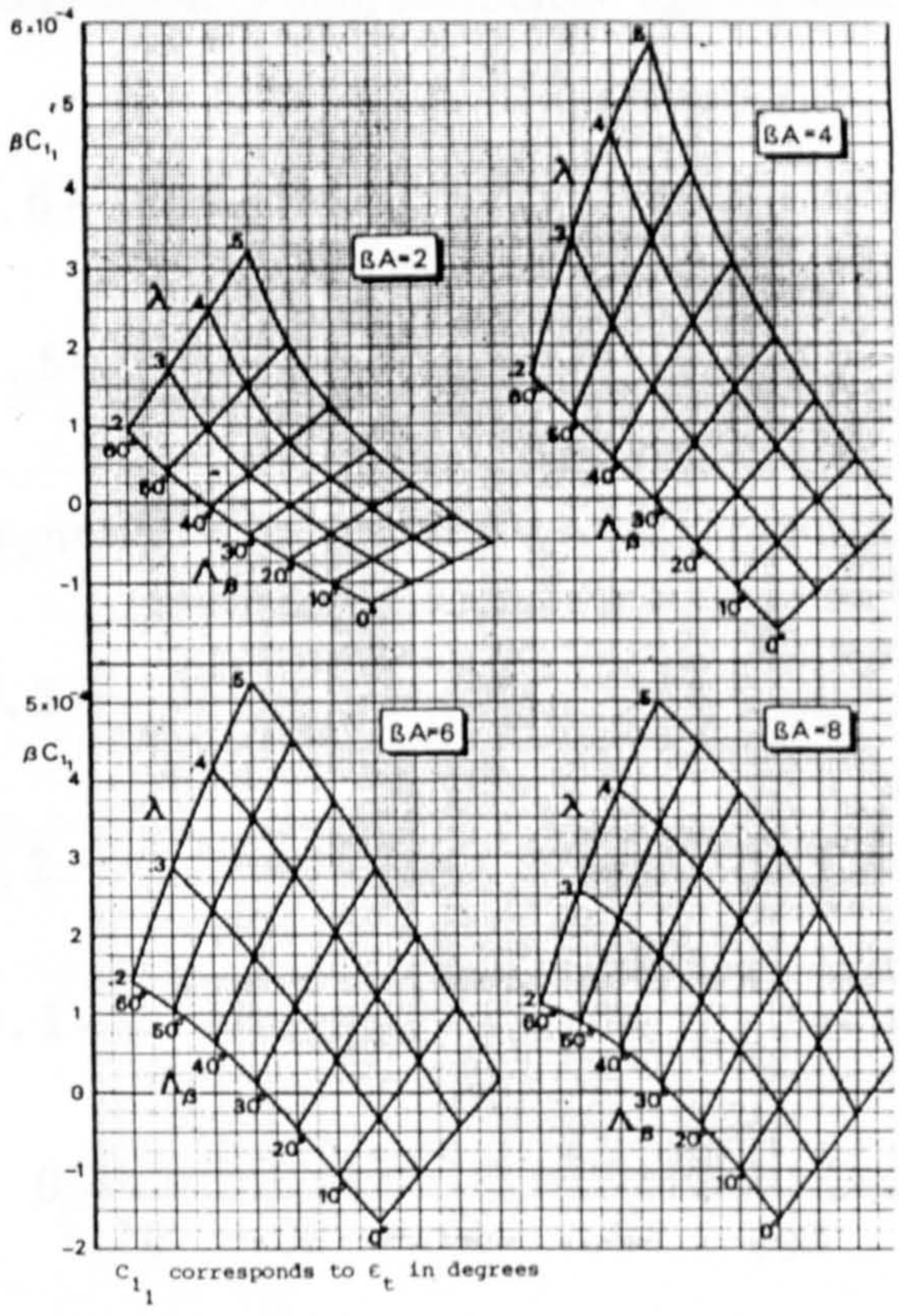

Figure D-3, and D-4 The factor C_{01} , C_{11} for the computation of vortex-induced drag due to twist[32]

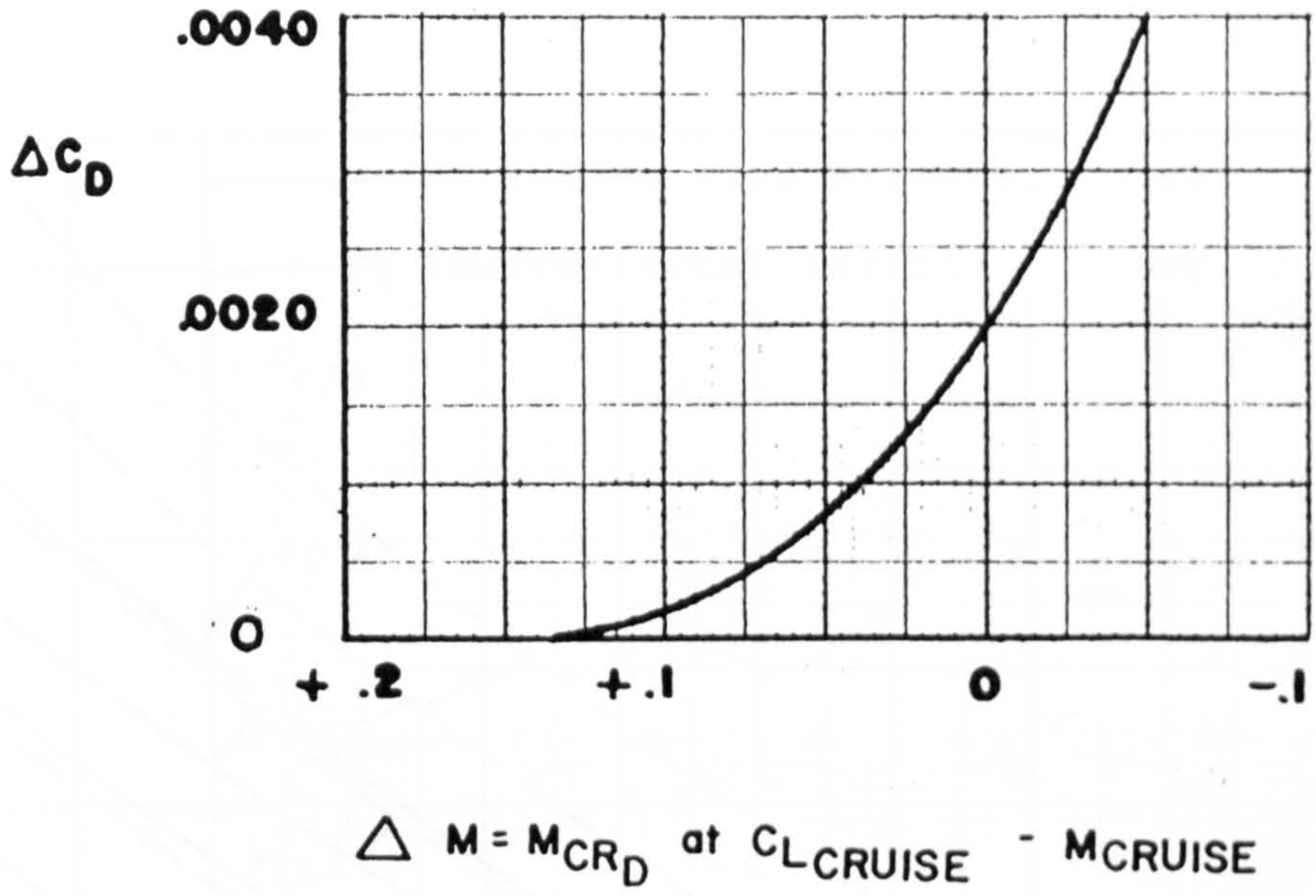

Figure D-5 : Compressibility drag coefficient against Mach number rise [25]

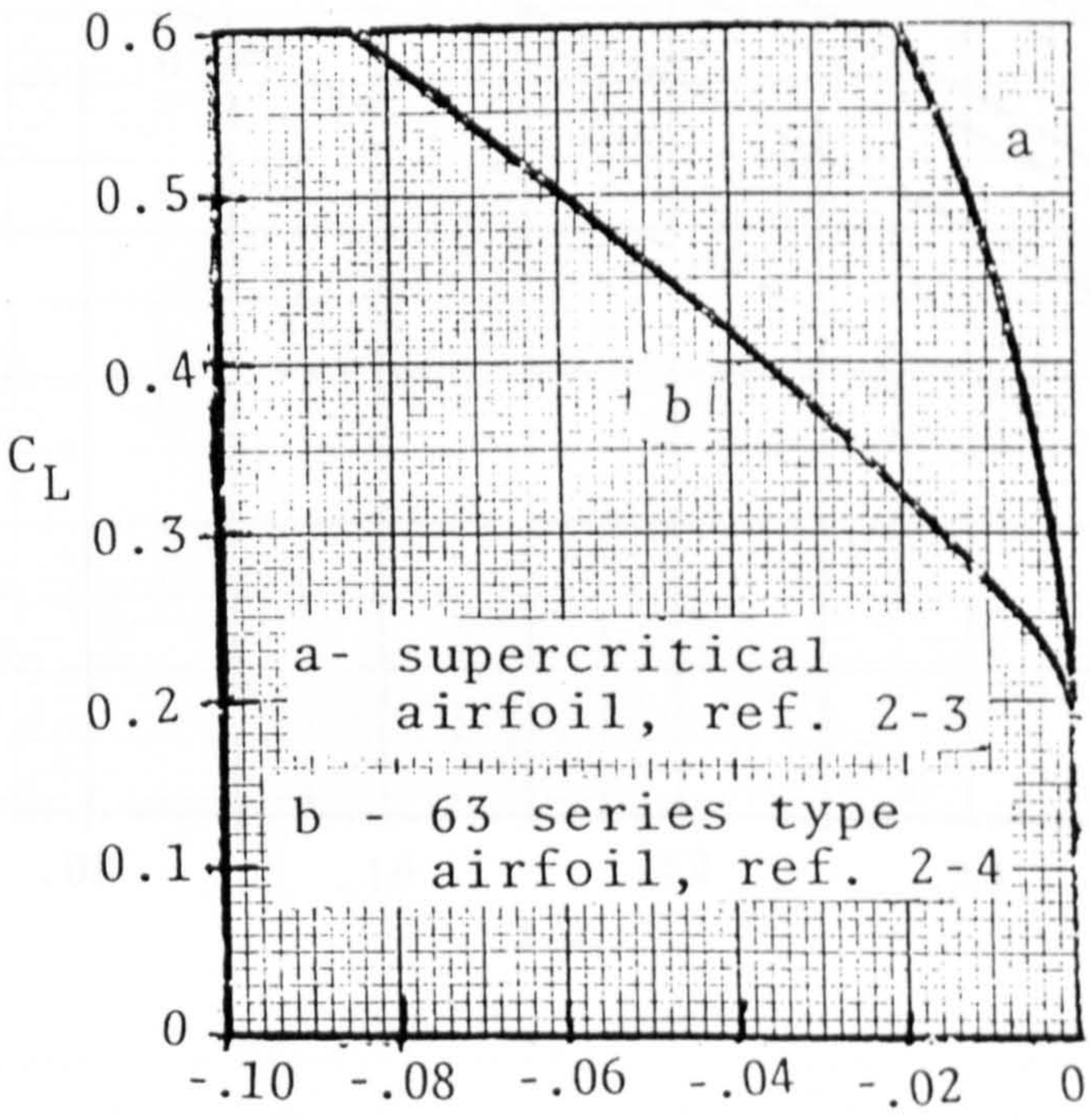

Figure D-6 : Mach critical drag rise due to lift coefficient for two types of airfoil [25].

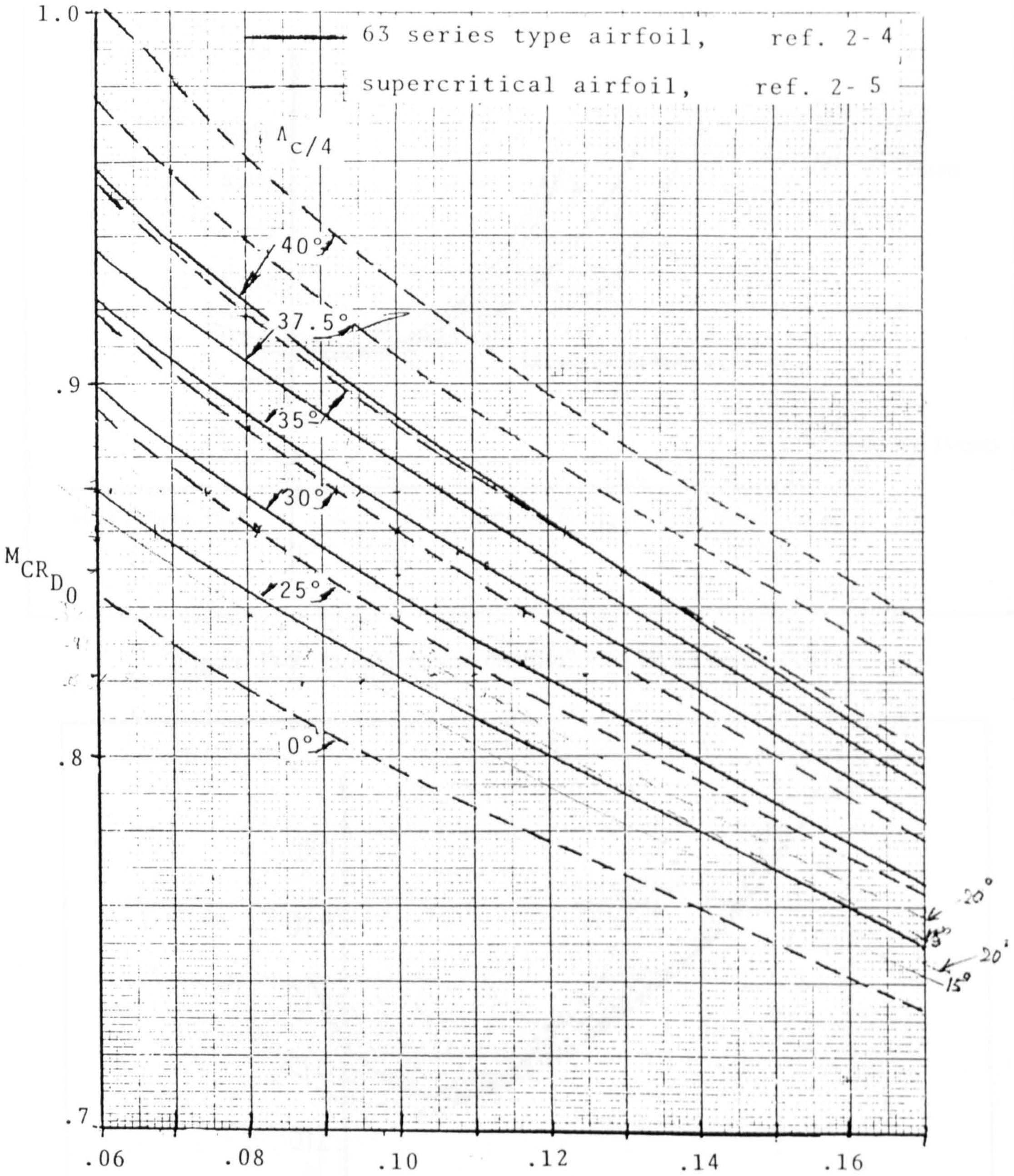

Figure D-7 : Mach critical drag at zero lift variation agianst thichness to chord ratio, and sweep angle at quarter chord [20].

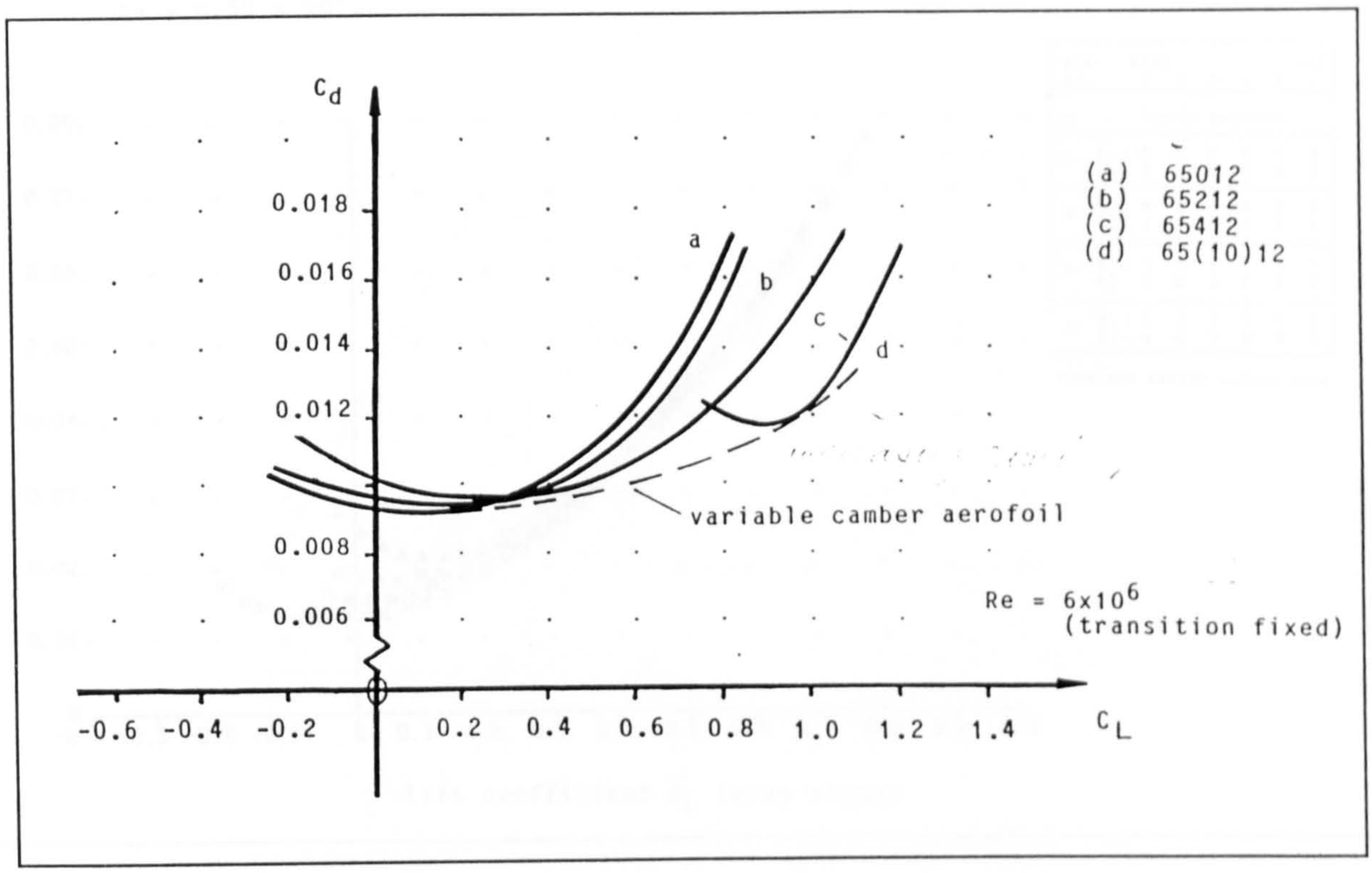

Figure D-8 : Drag polars of the NACA 65 series family [105].

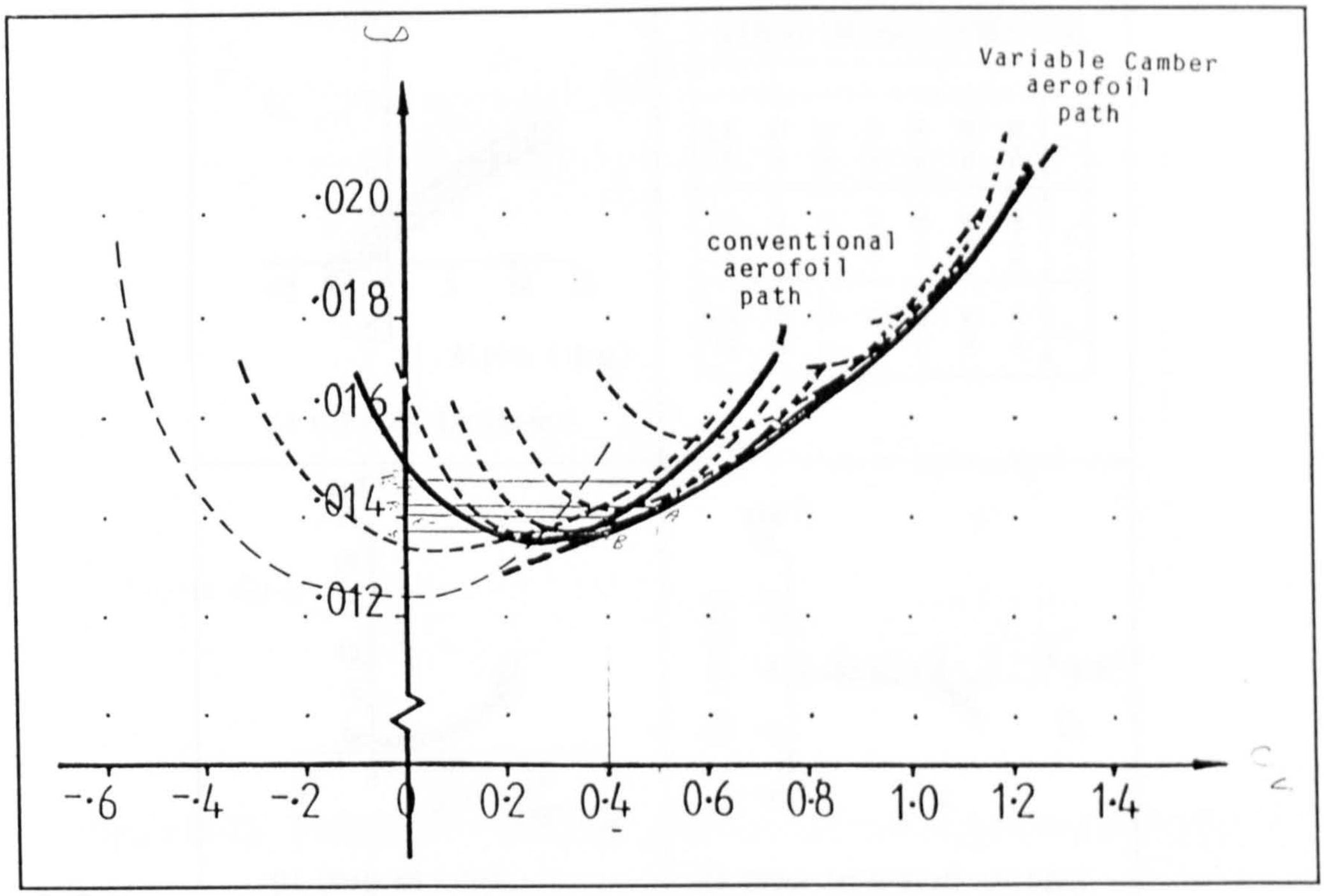

Figure D-9 : Comparison of variable camber and conventional airfoil operation [105].

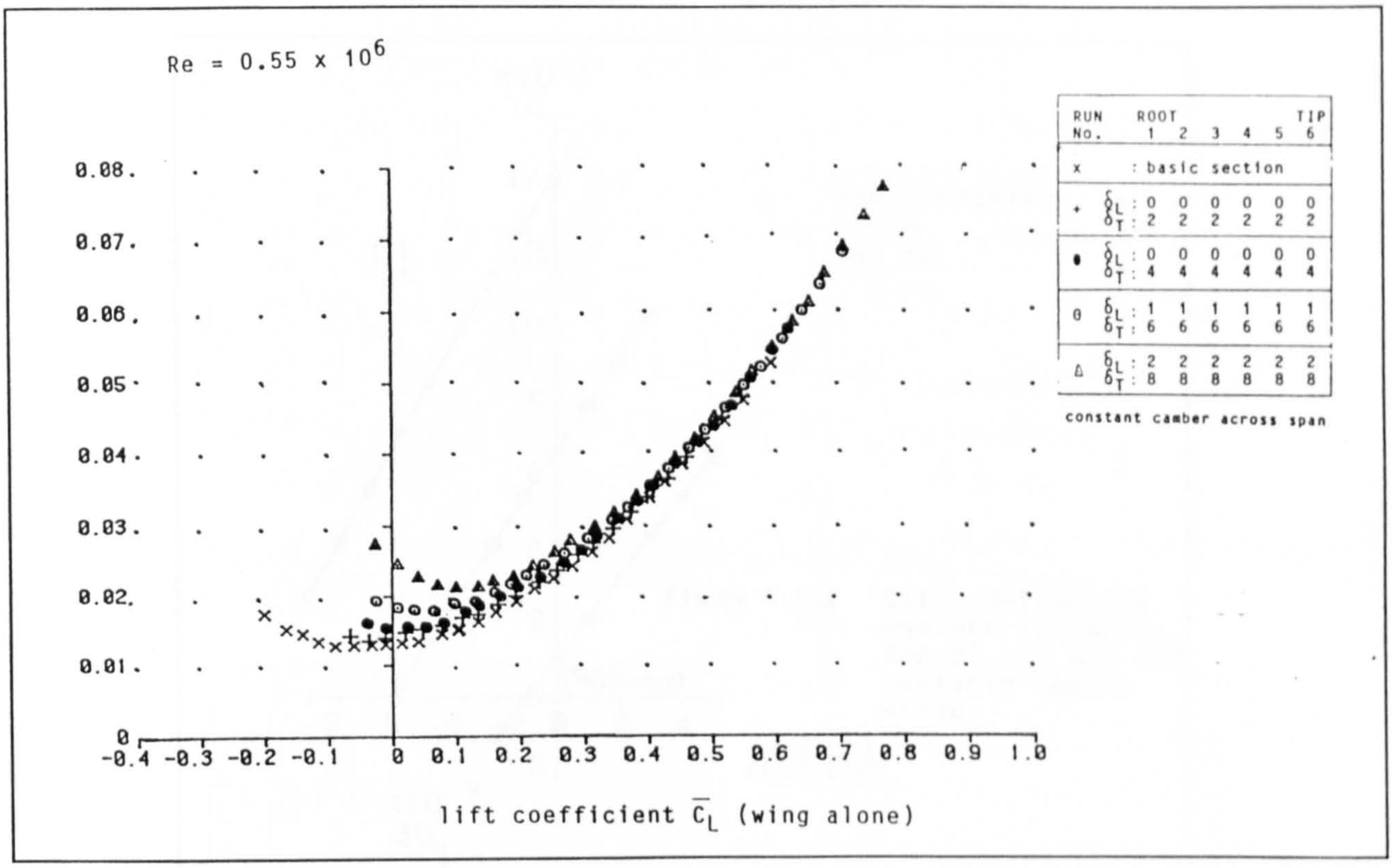

Figure D-10 : Variation of C_D with C_L for several cruise wing configuration. [105]

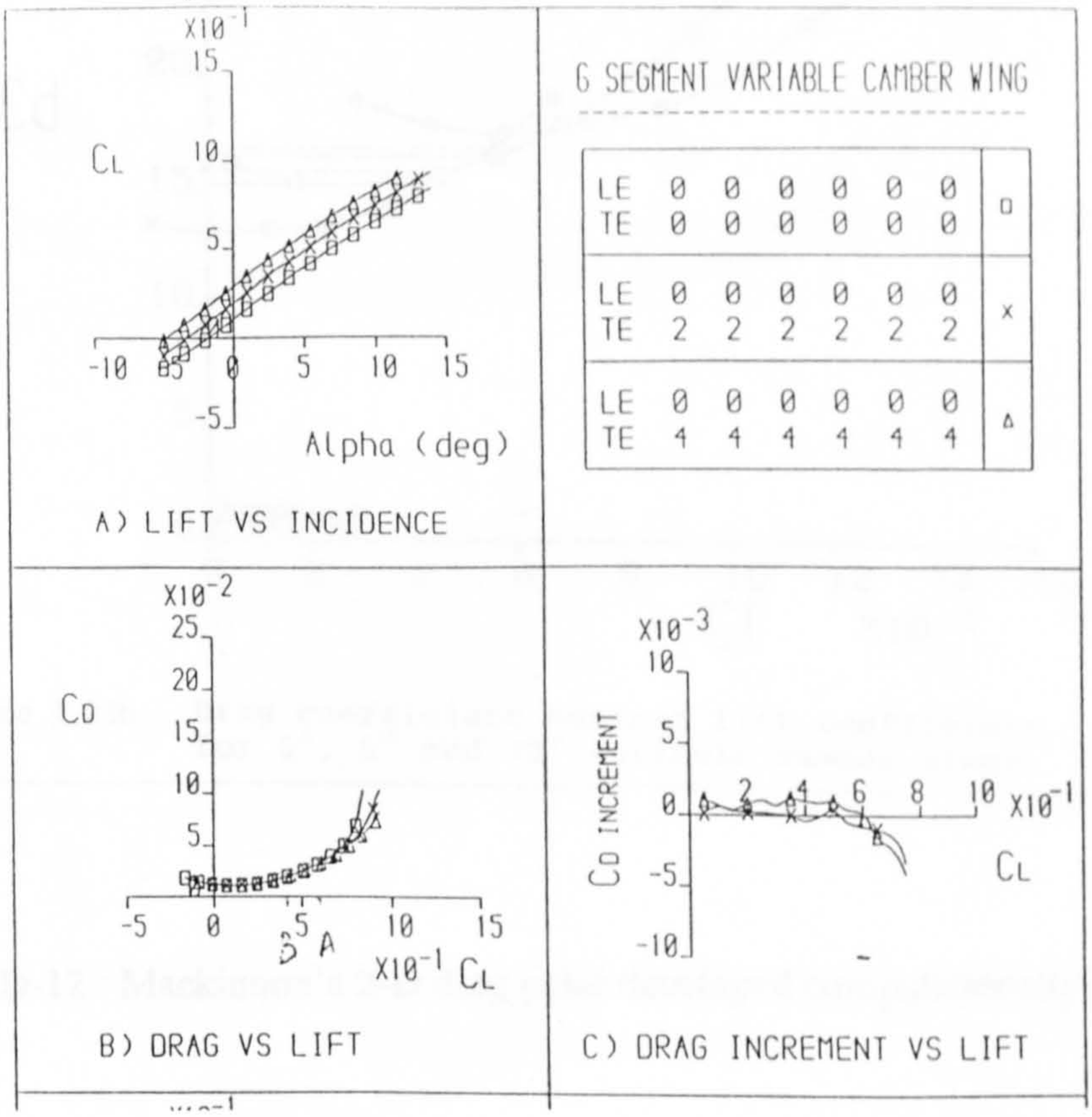

Figure D-11 : Mackinon work on Rao,s wing. Experimentally developed drag polar [107].

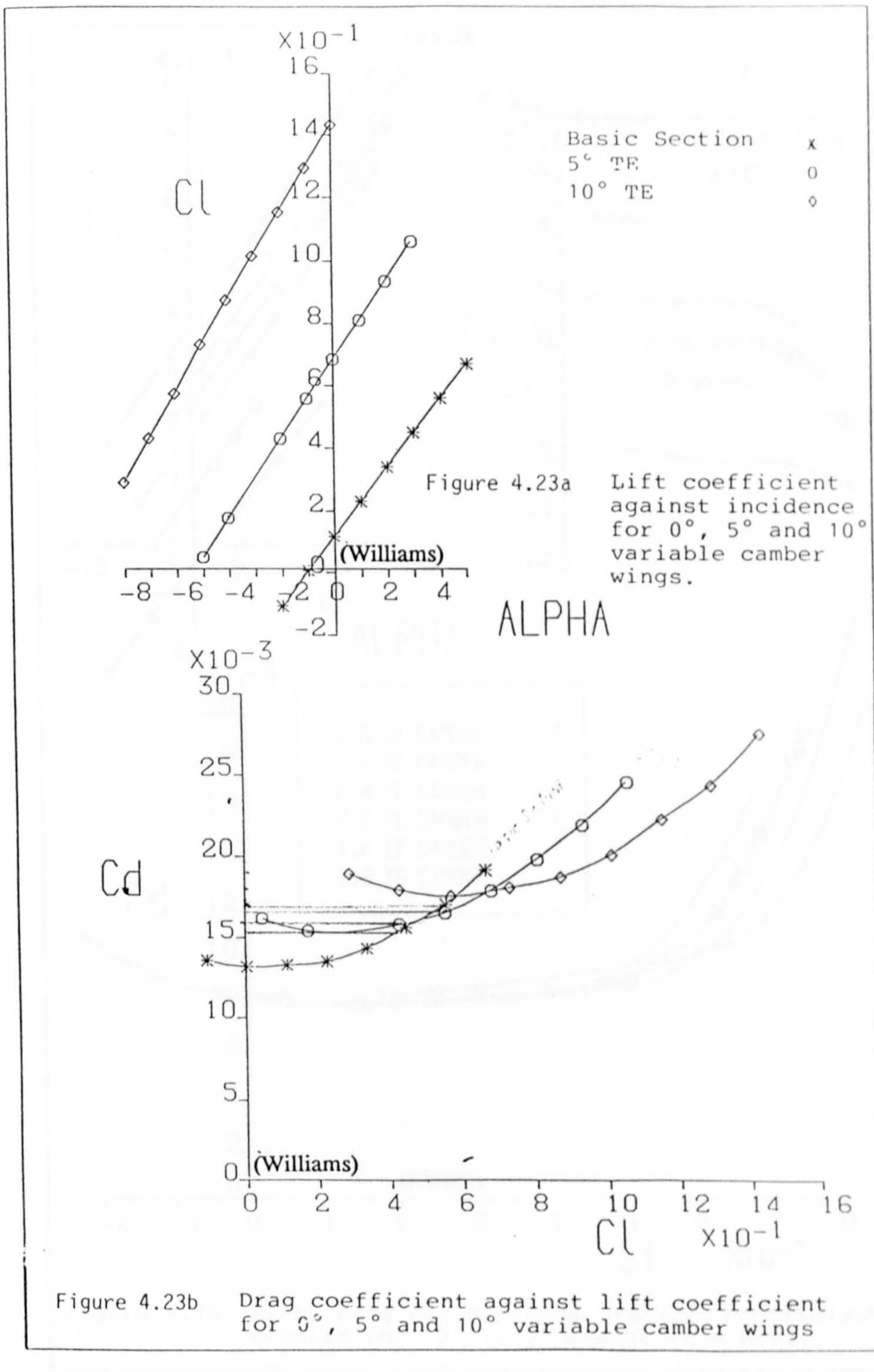

Figure 4.23a Lift coefficient against incidence for 0°, 5° and 10° variable camber wings.

Figure 4.23b Drag coefficient against lift coefficient for 0°, 5° and 10° variable camber wings

Figure D-12 : Mackinnon's 2-D drag polar developed computationally [107].

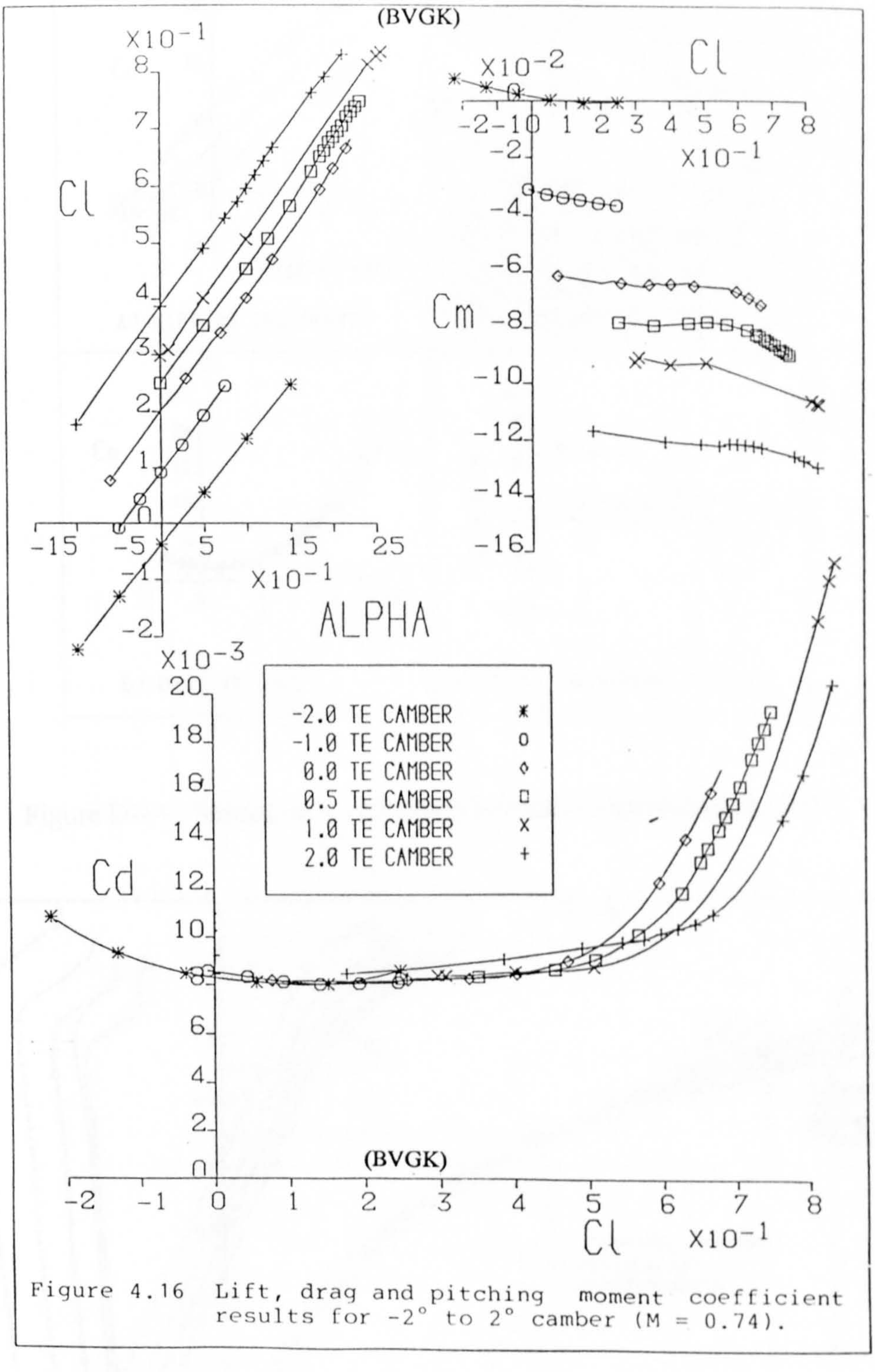

Figure 4.16 Lift, drag and pitching moment coefficient results for -2° to 2° camber (M = 0.74).

Figure D-13 : Mackinnon's 2-D drag polar developed computationally , using William's RAE Code [107].

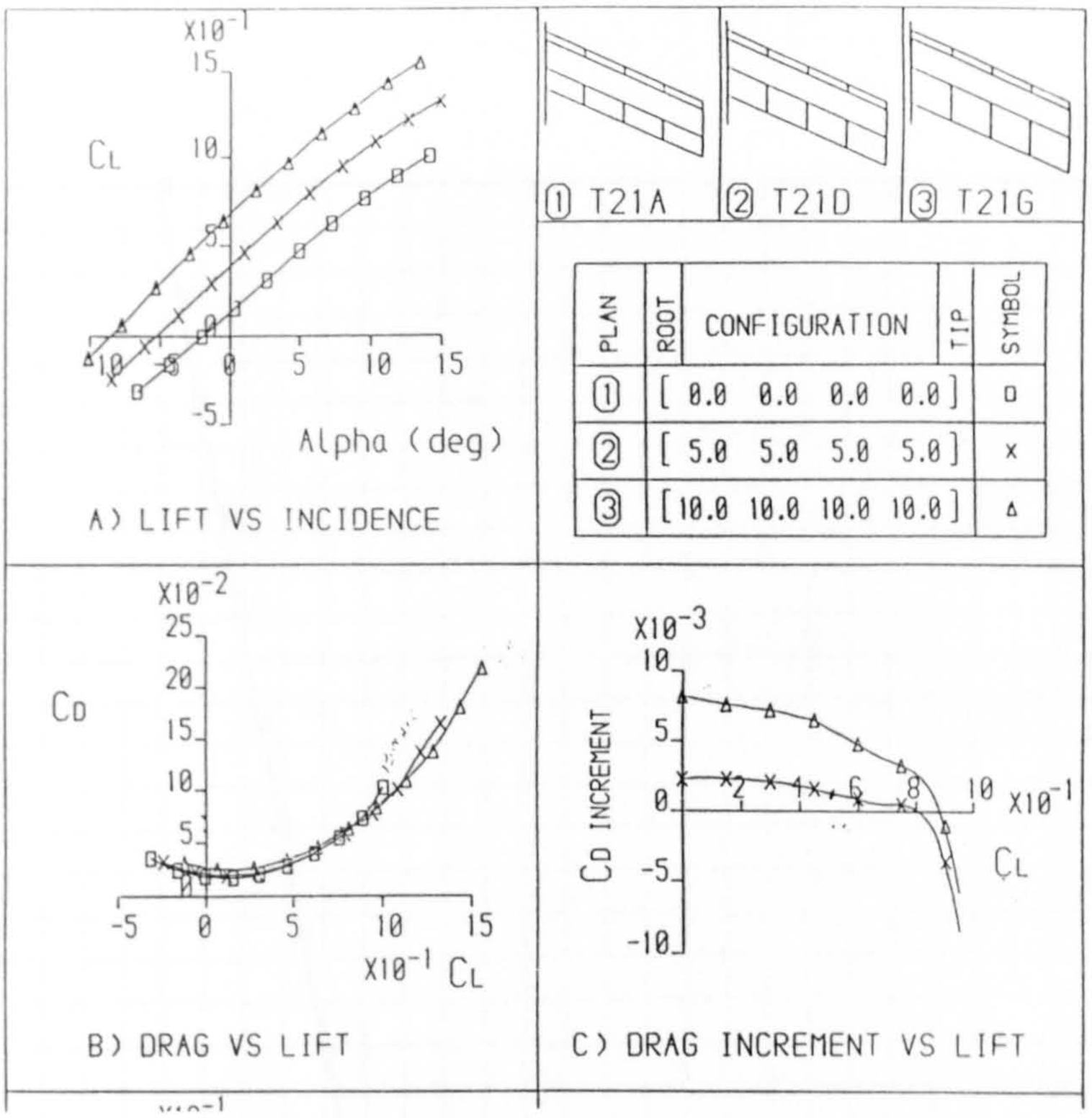

Figure D-14 : Mackinon's 3-D polar developed experimentally [107].

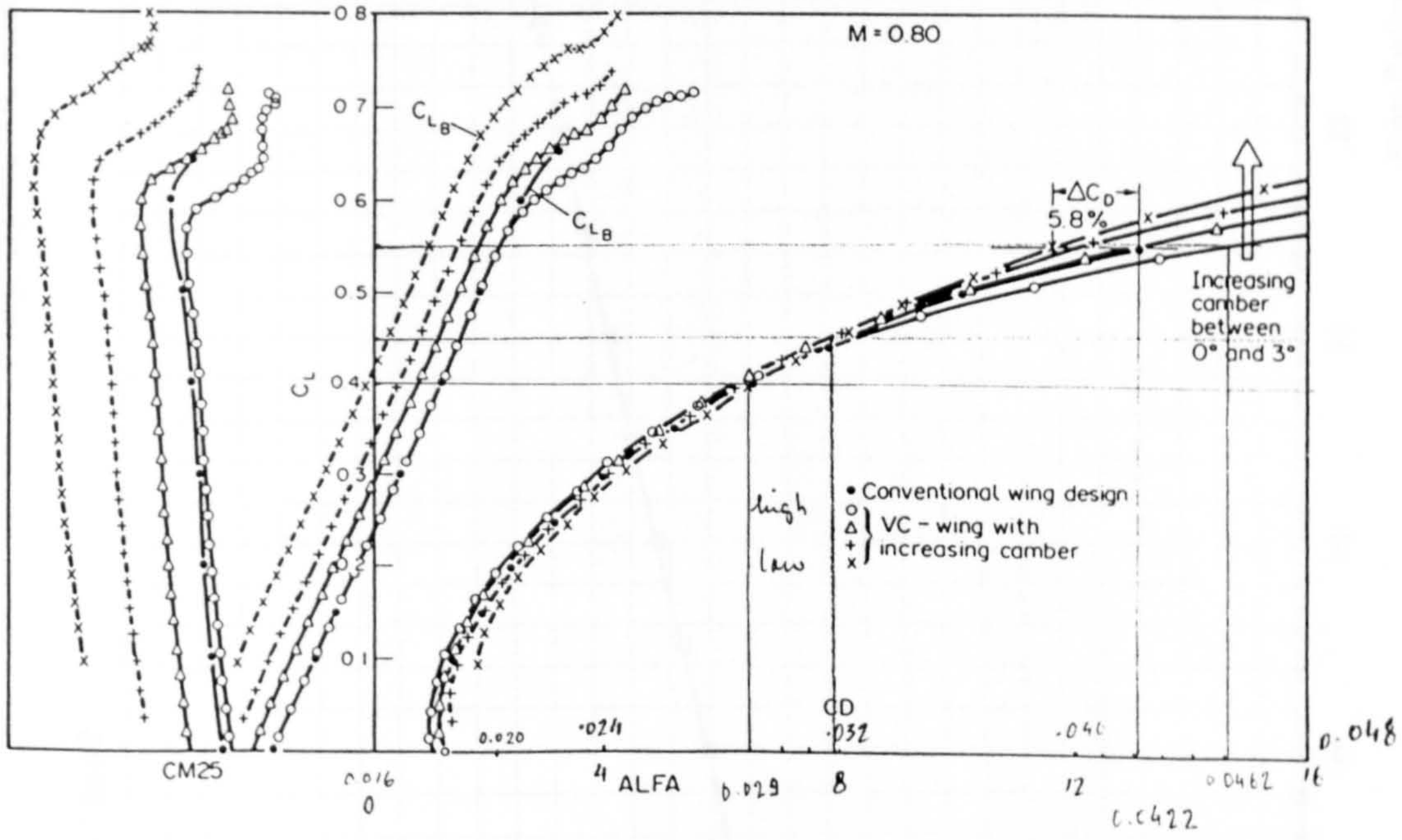

Figure D-15 : MBB's VCW design - Experimental results [109].

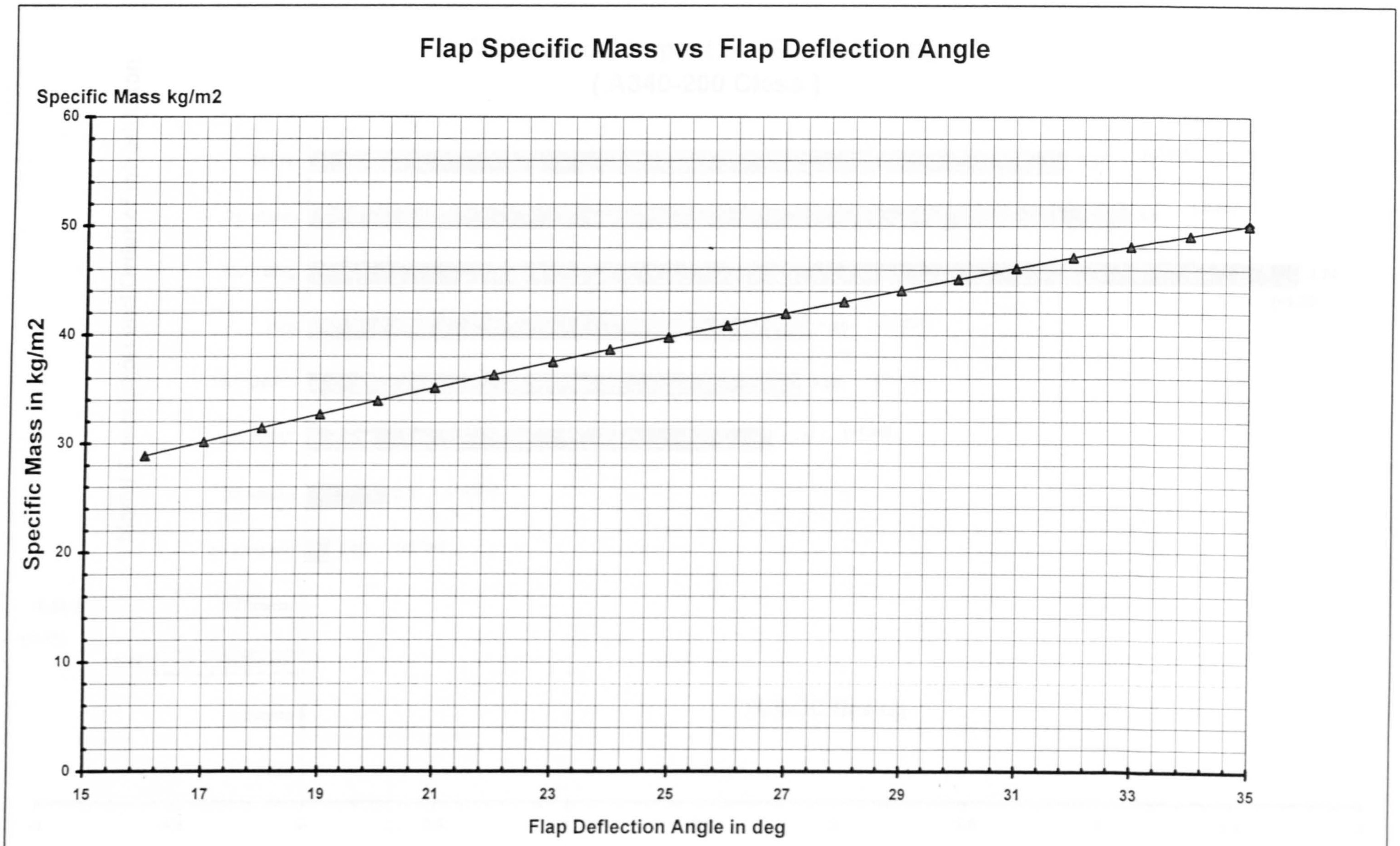

Figure D.16 : Flap specific mass vs flap deflection angle

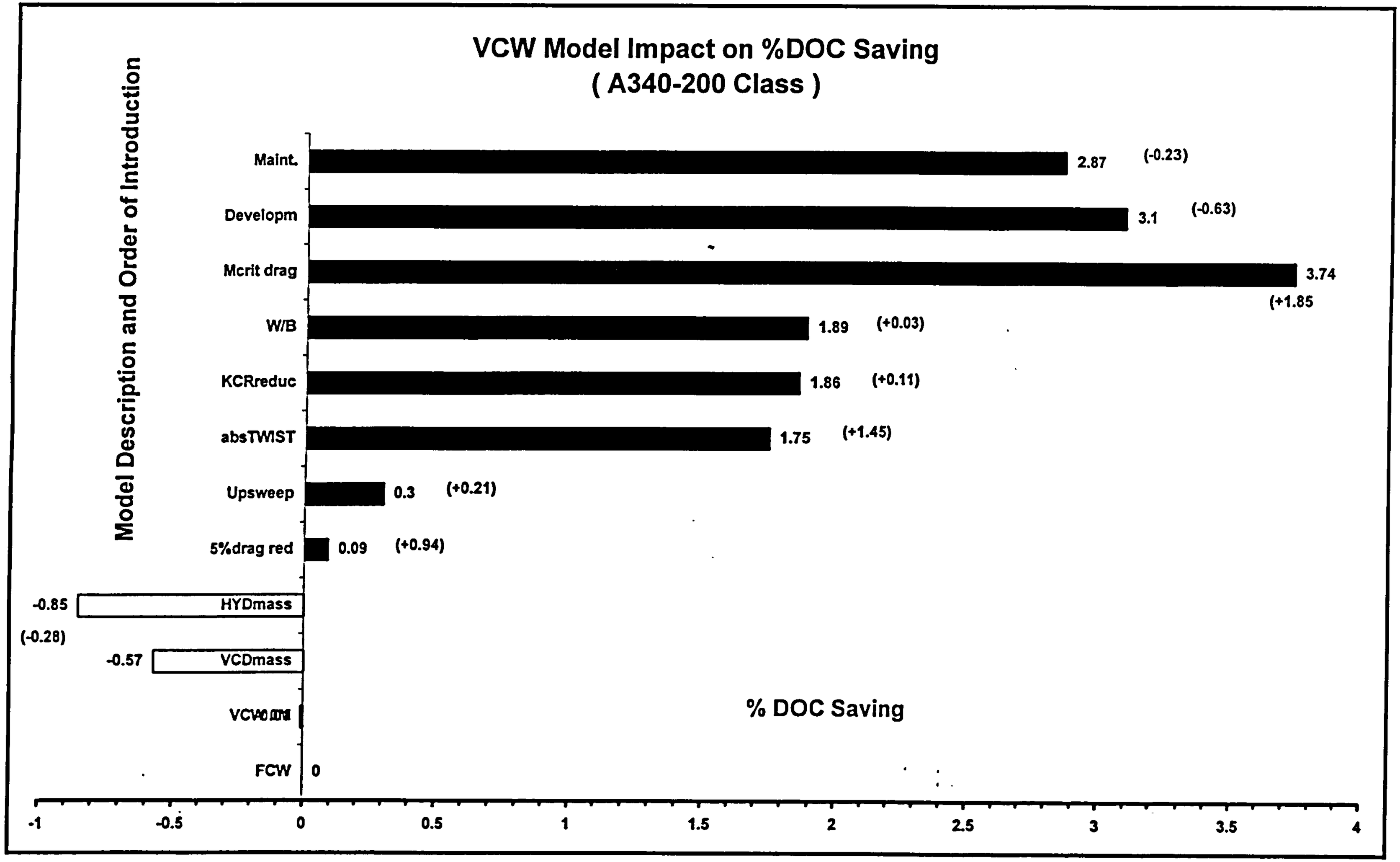

Figure D-17 : Impact of each VCW model on the A340-200 class aircraft DOC.

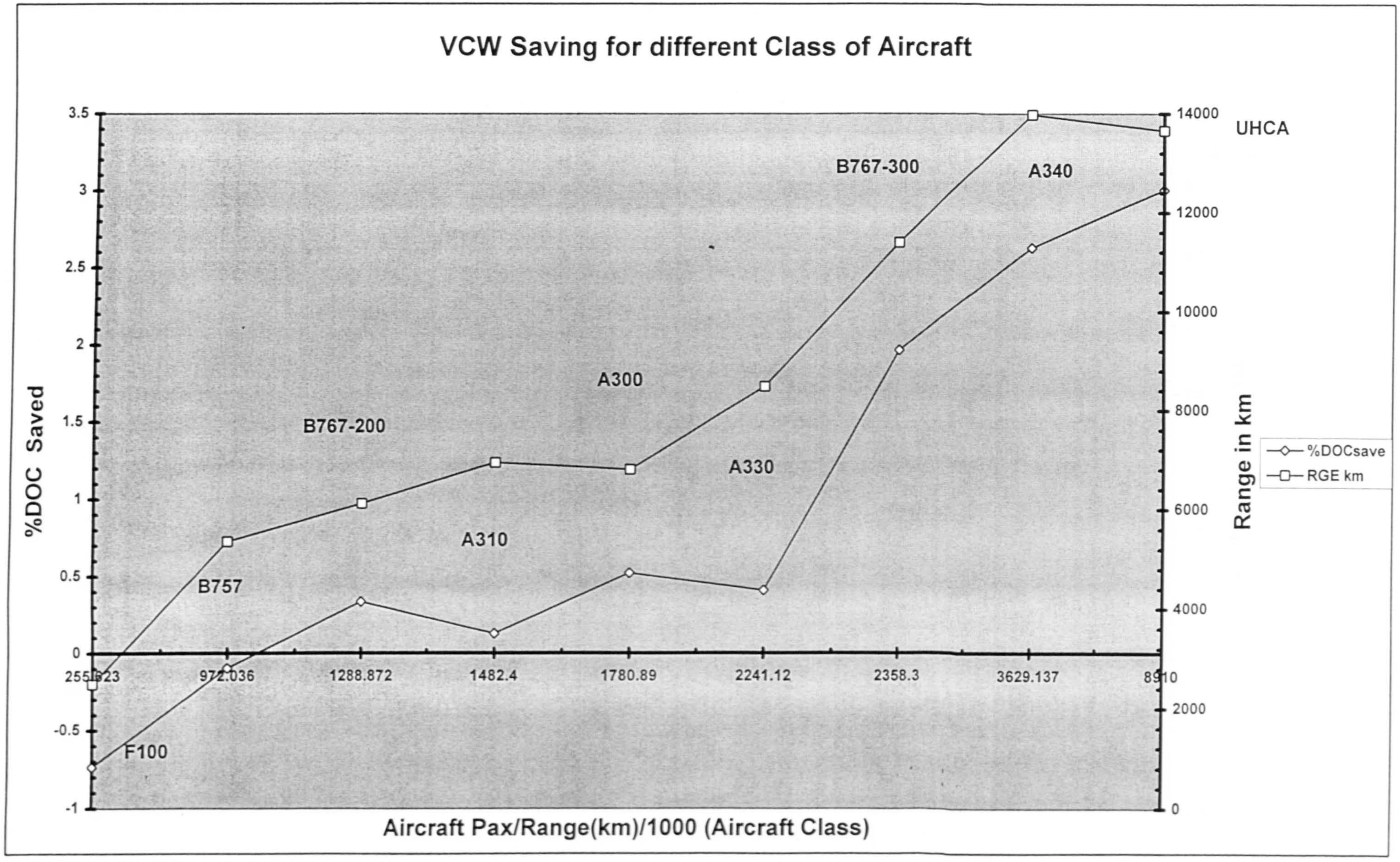

Figure D-18 : %DOC saved for different classes of transport aircraft with respect to range variation with VCW technology.

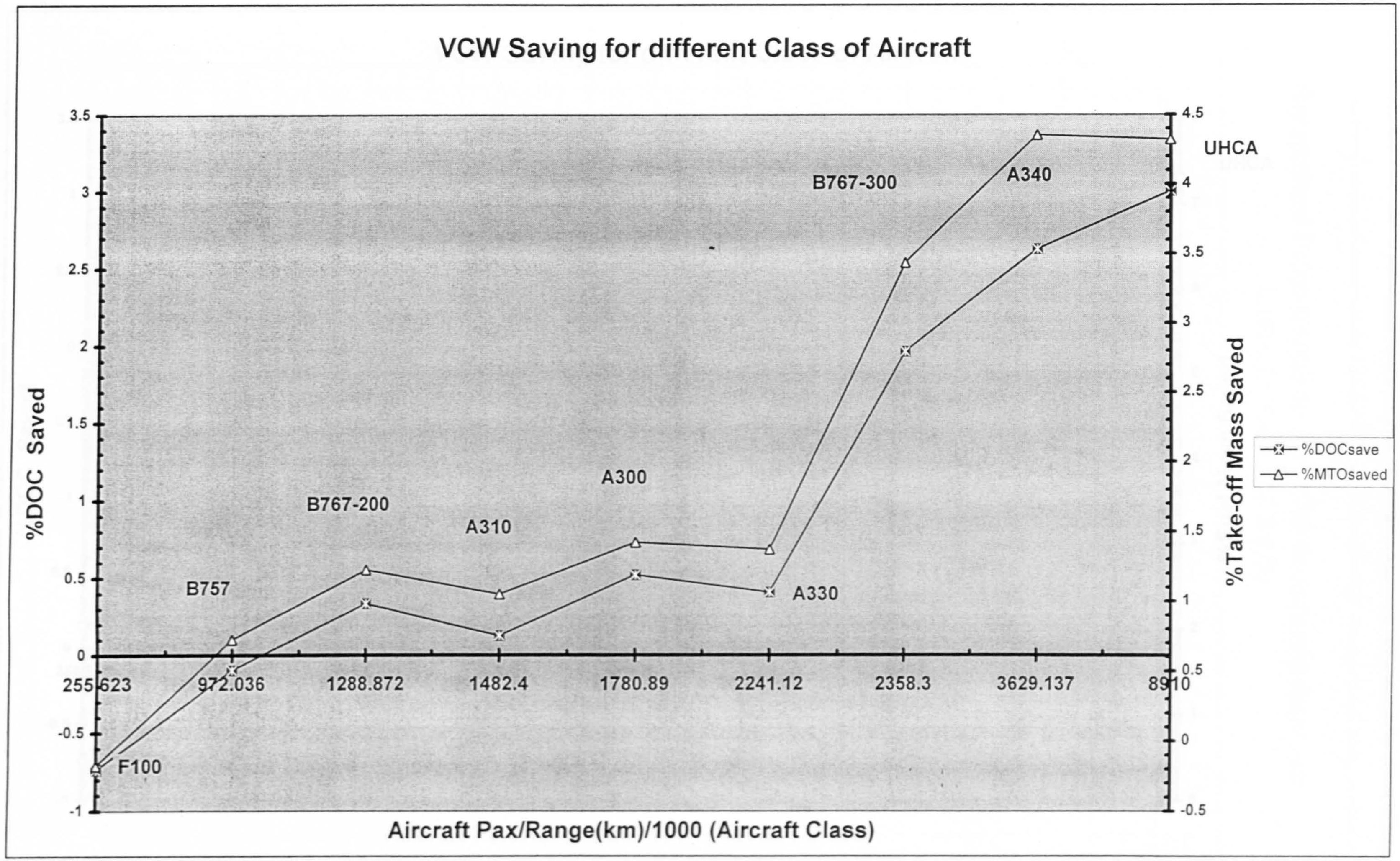

Figure D-19 : The trend of DOC saving of different classes of aircraft with respect to % reduction of their take-off mass.

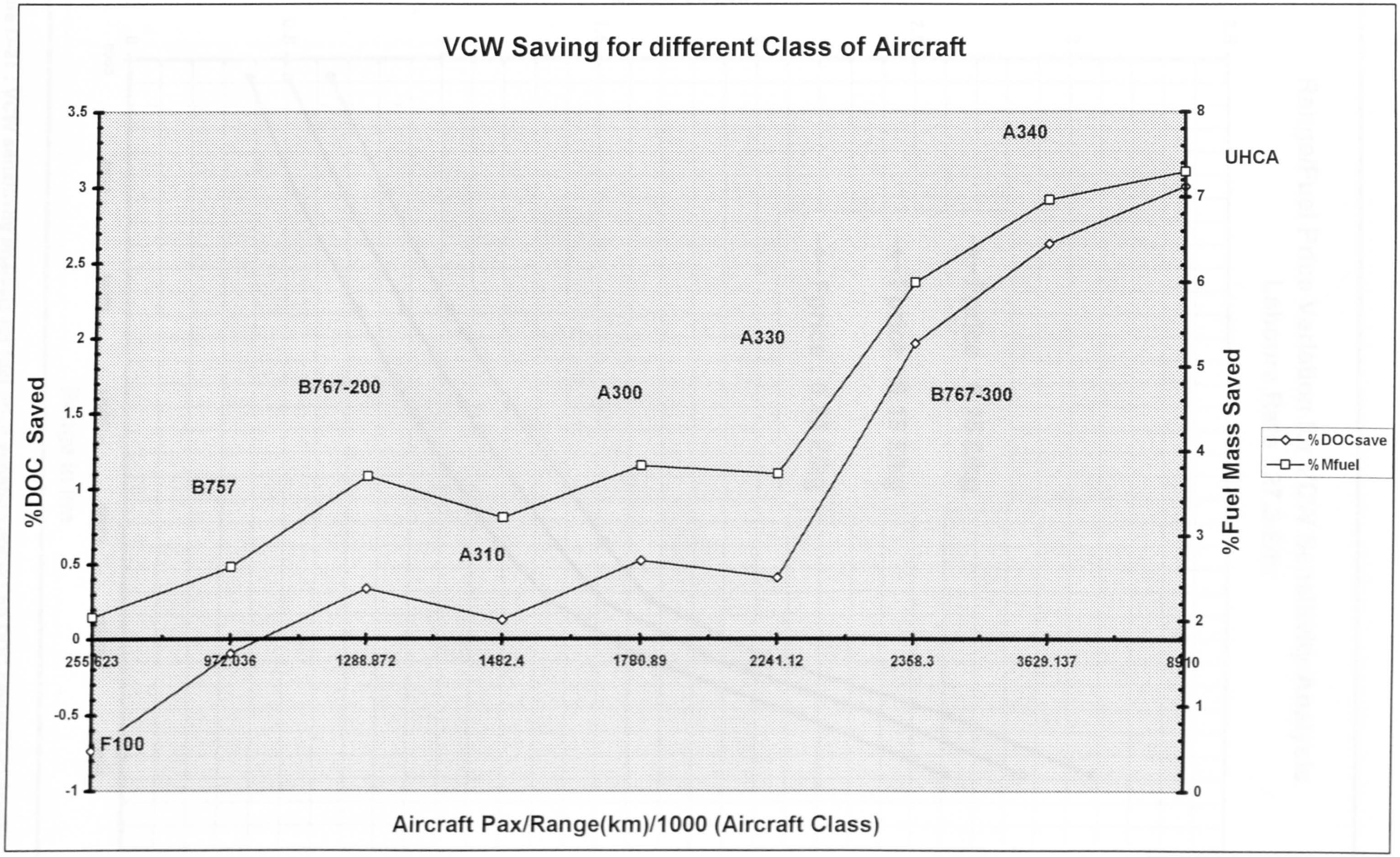

Figure D-20 : The trend of DOC saving of different classes of aircraft with respect to %reduction in their mission fuel mass due VCW

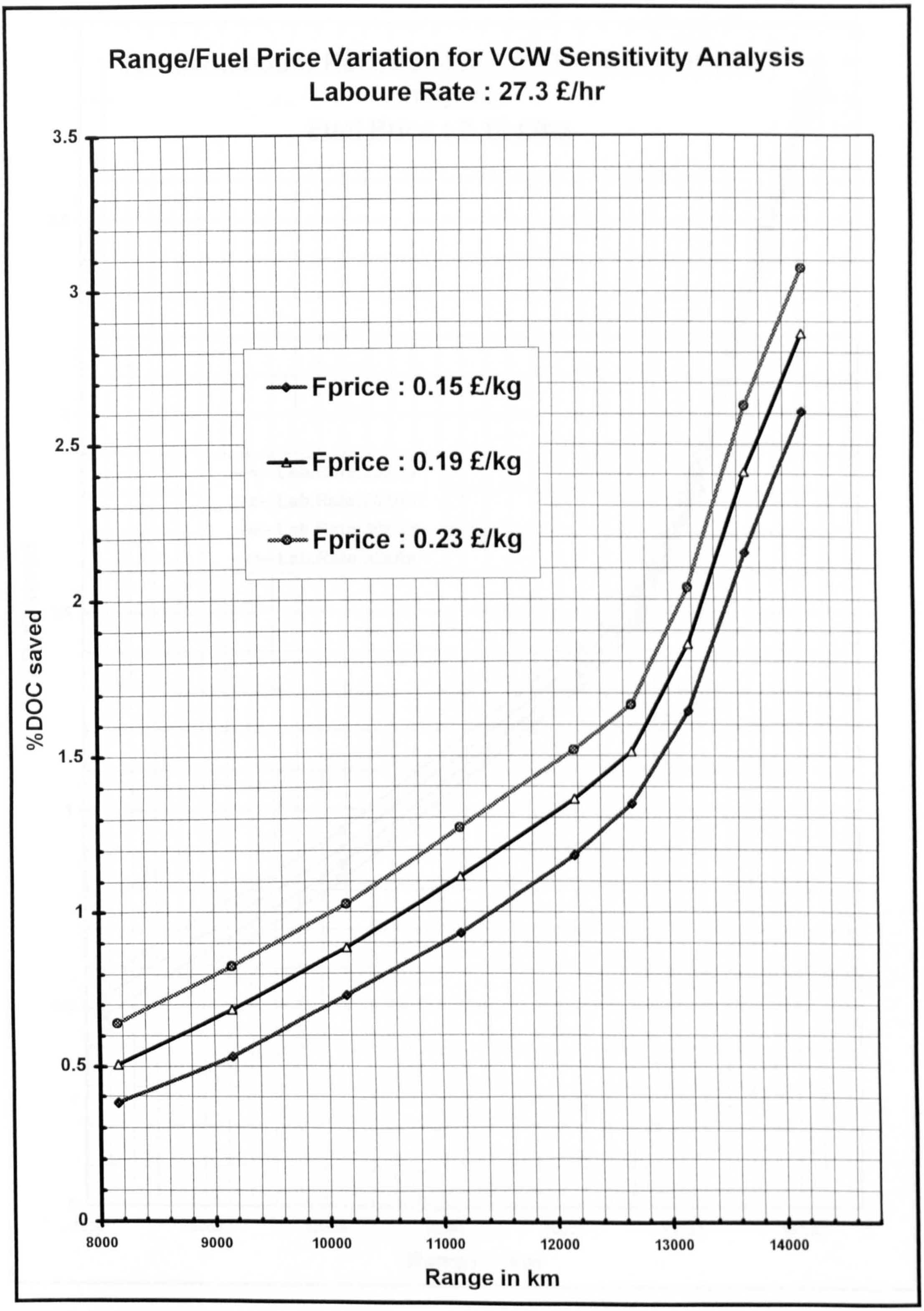

Figure D-21 : VCW sensitivity analysis for fuel price variation impact on DOC saving for various range classes.

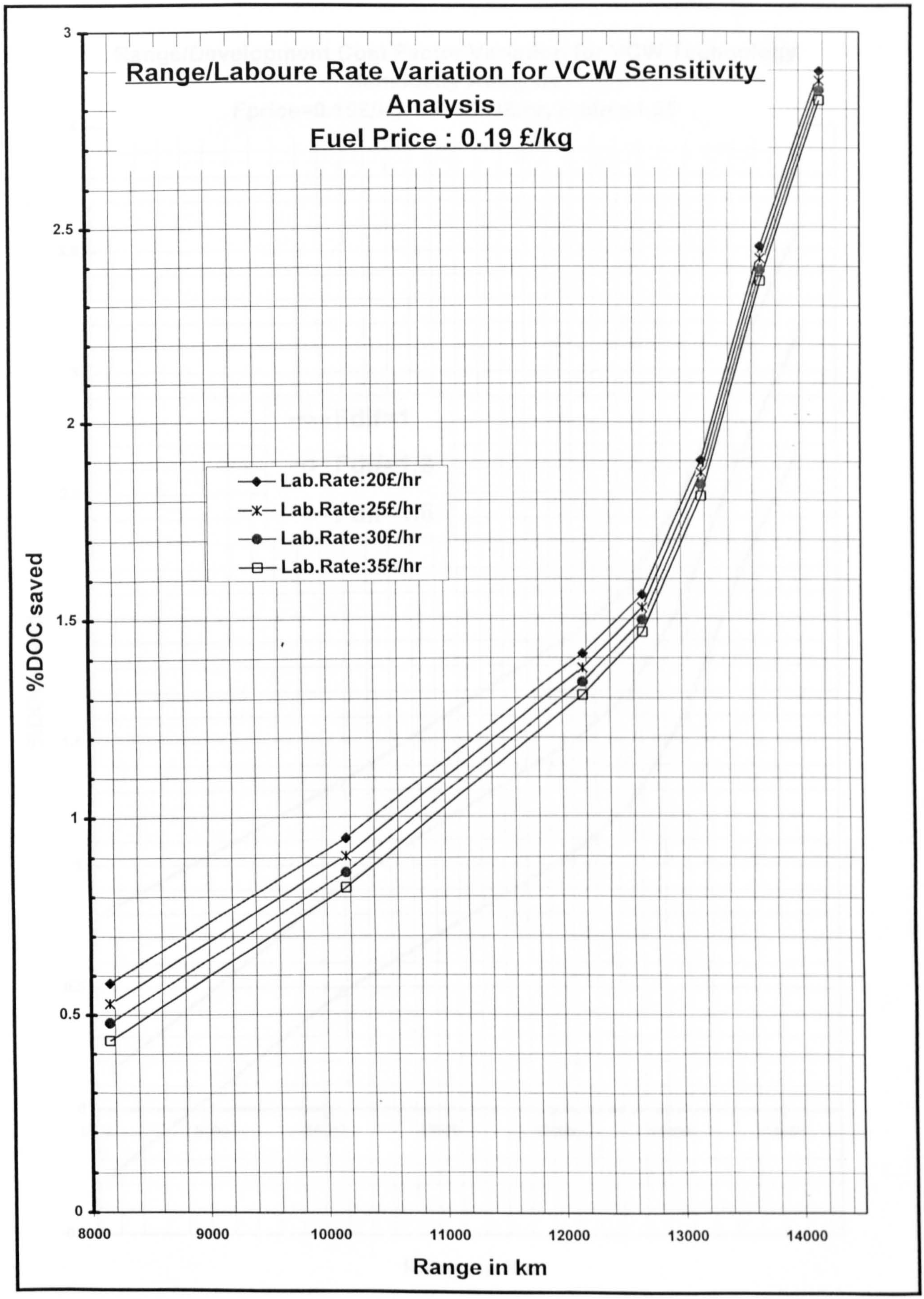

Figure D-22 : VCW sensitivity analysis for fuel price variation impact on DOC saving for various range classes.

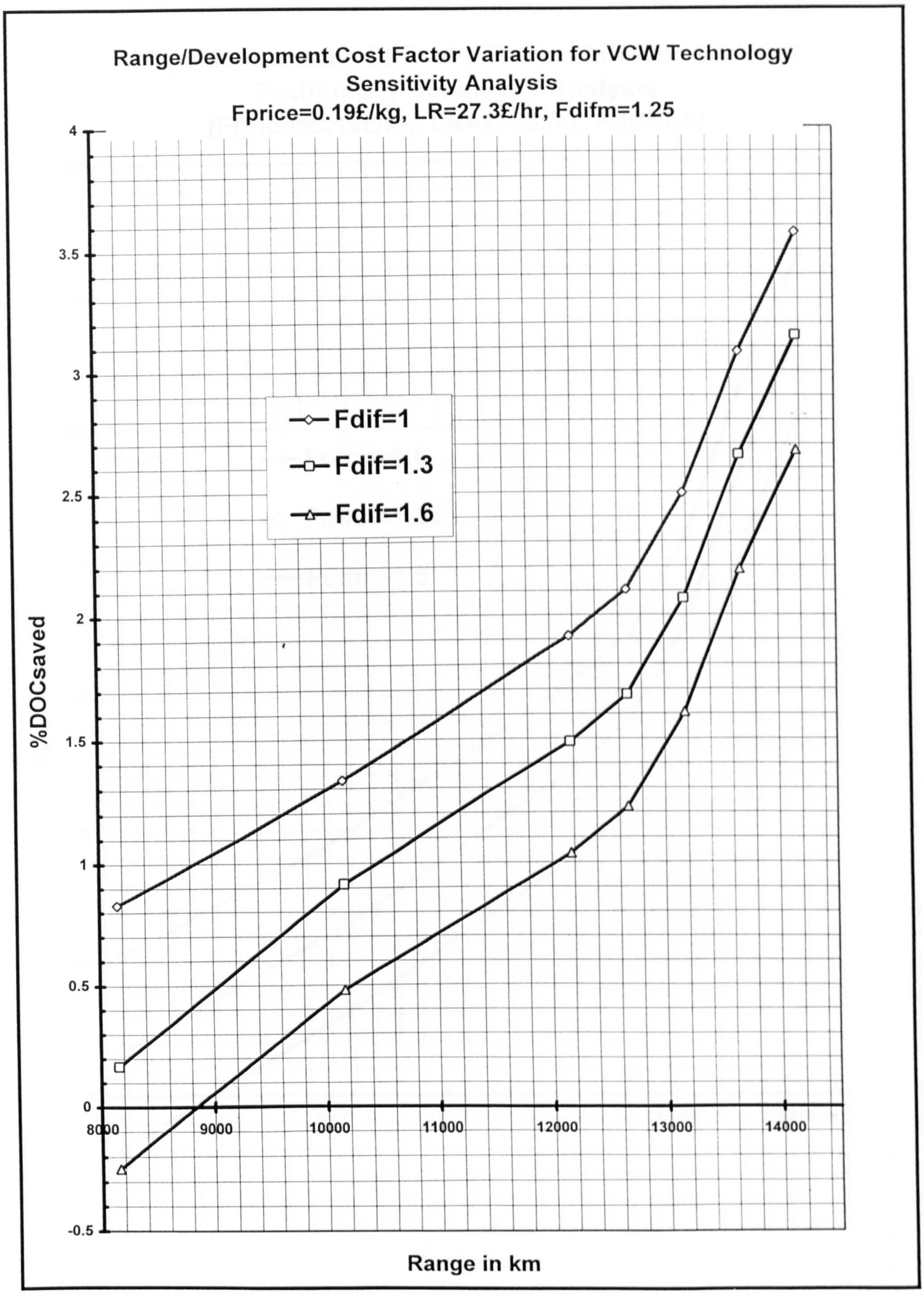

Figure D-23 : VCW sensitivity analysis for development cost variation impact on DOC saving for various range classes.

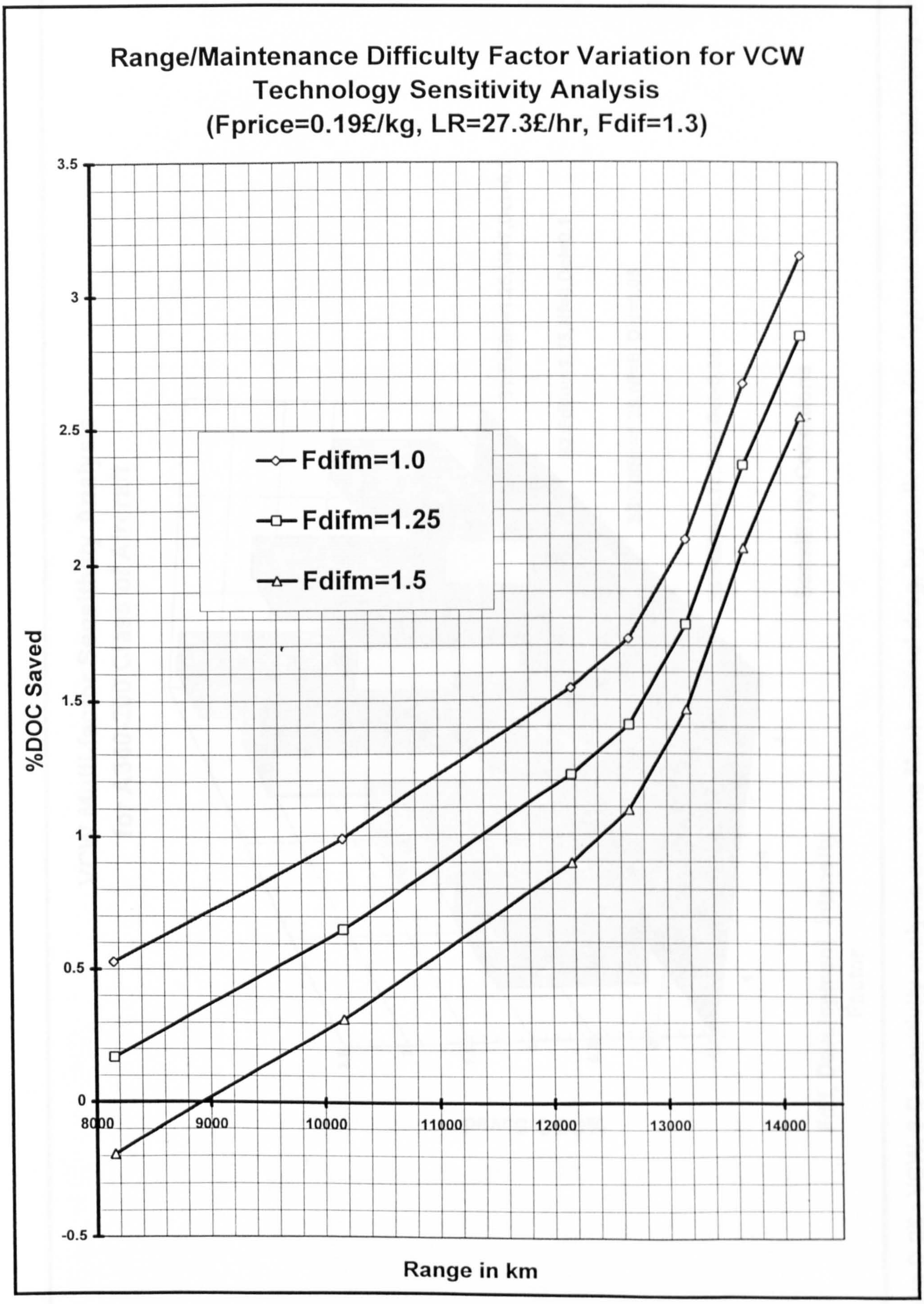

Figure D-24 : VCW sensitivity analysis for maintenance cost variation impact on DOC saving for various range classes.

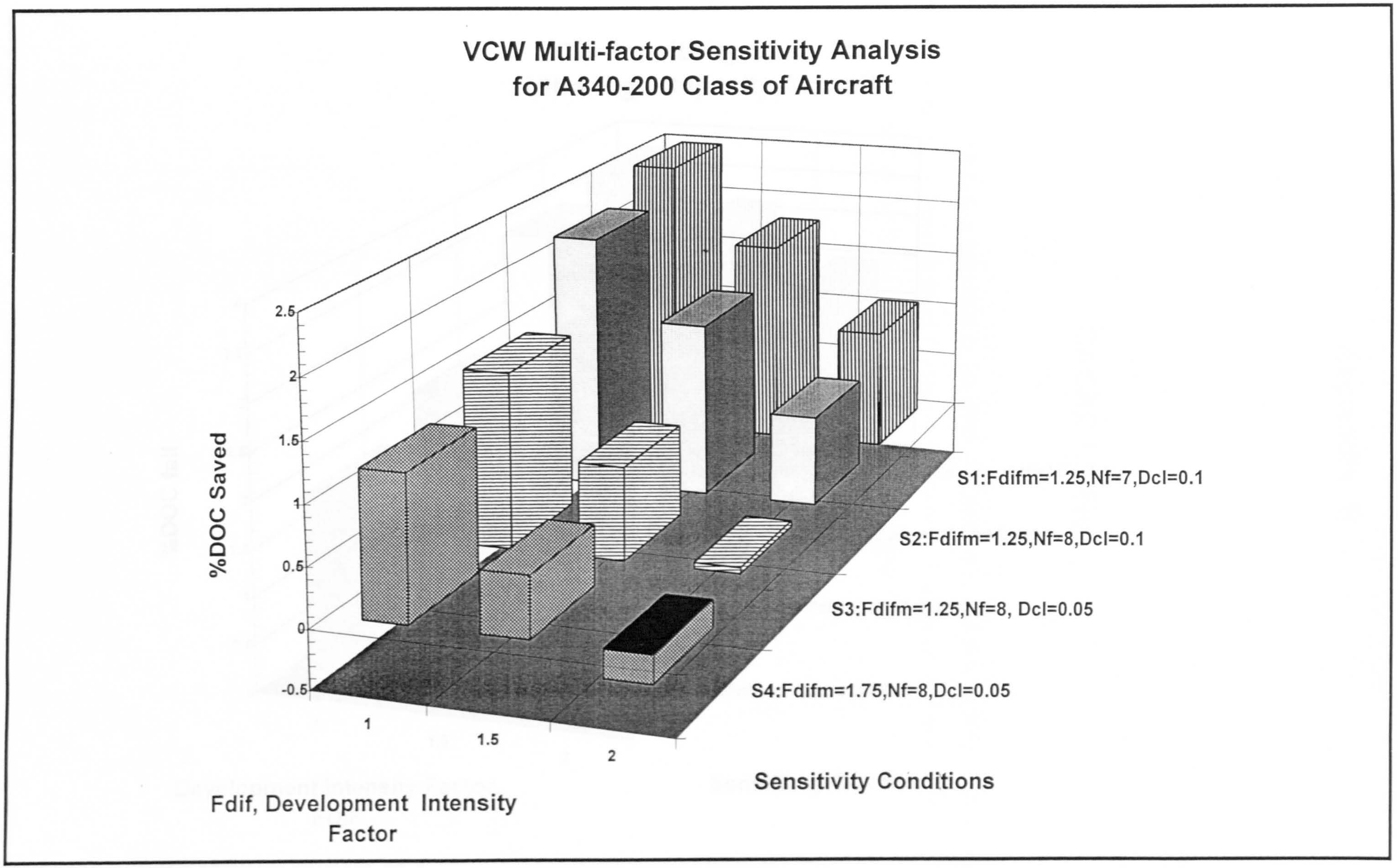

Figure D-25 : VCW, 3-D sensitivity analysis covering Mach critical drag, hydraulic mass, developemnt cost, maintainability cost variation.

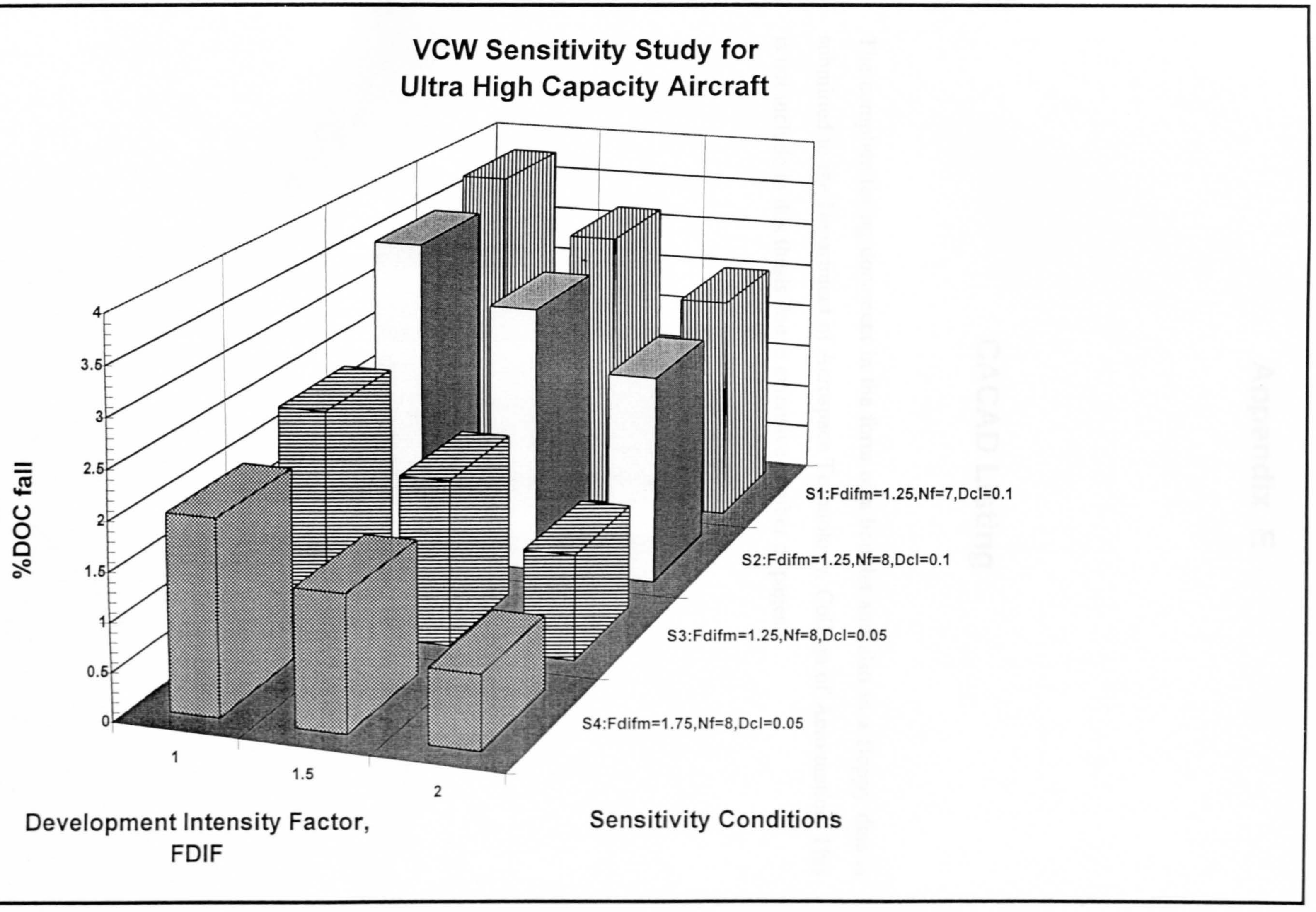

Figure D-26 : VCW, 3-D sensitivity analysis covering Mach critical drag, hydraulic mass, developement cost, maintainability cost variation.

Appendix E

CACAD Listing

The complete listing document in the form of a booklet and also in a floppy disc is submitted to the Department of Aerospace Technology, College of Aeronautics. This is not include in this thesis due to extensive number of pages.